Forschungszentrum Jülich

Institut für Festkörperforschung

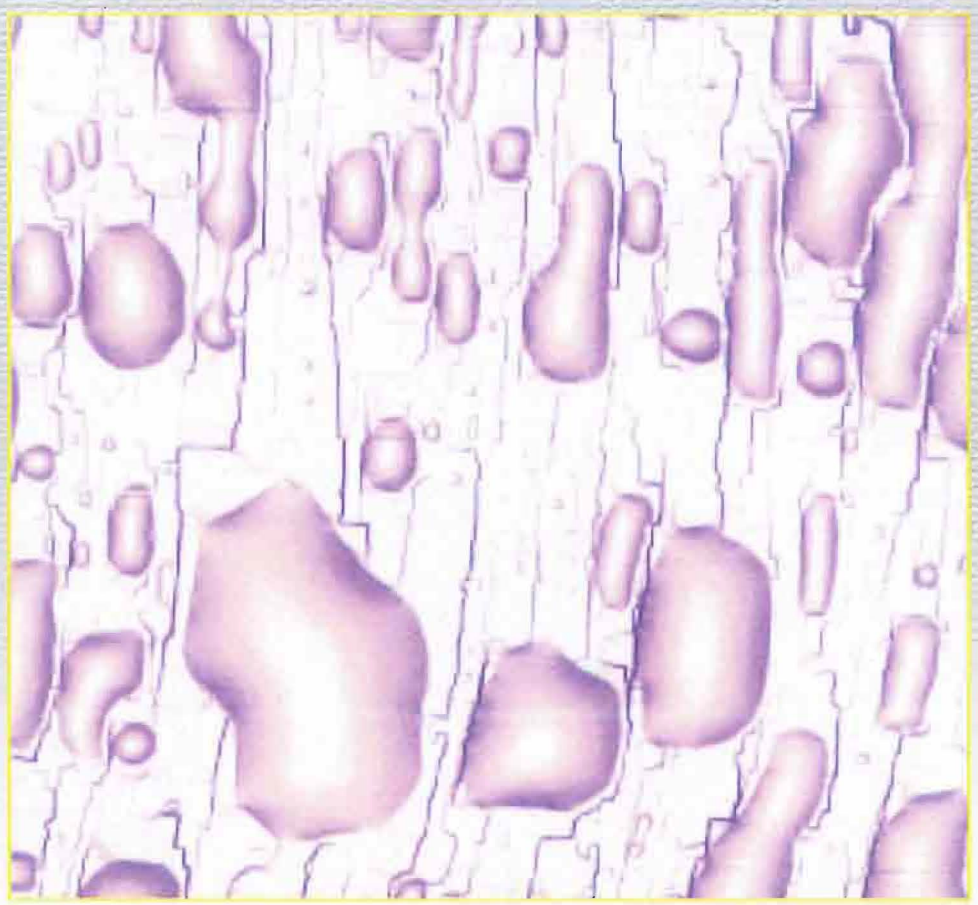

Scientific Report 1999/2000

Institut für Festkörperforschung

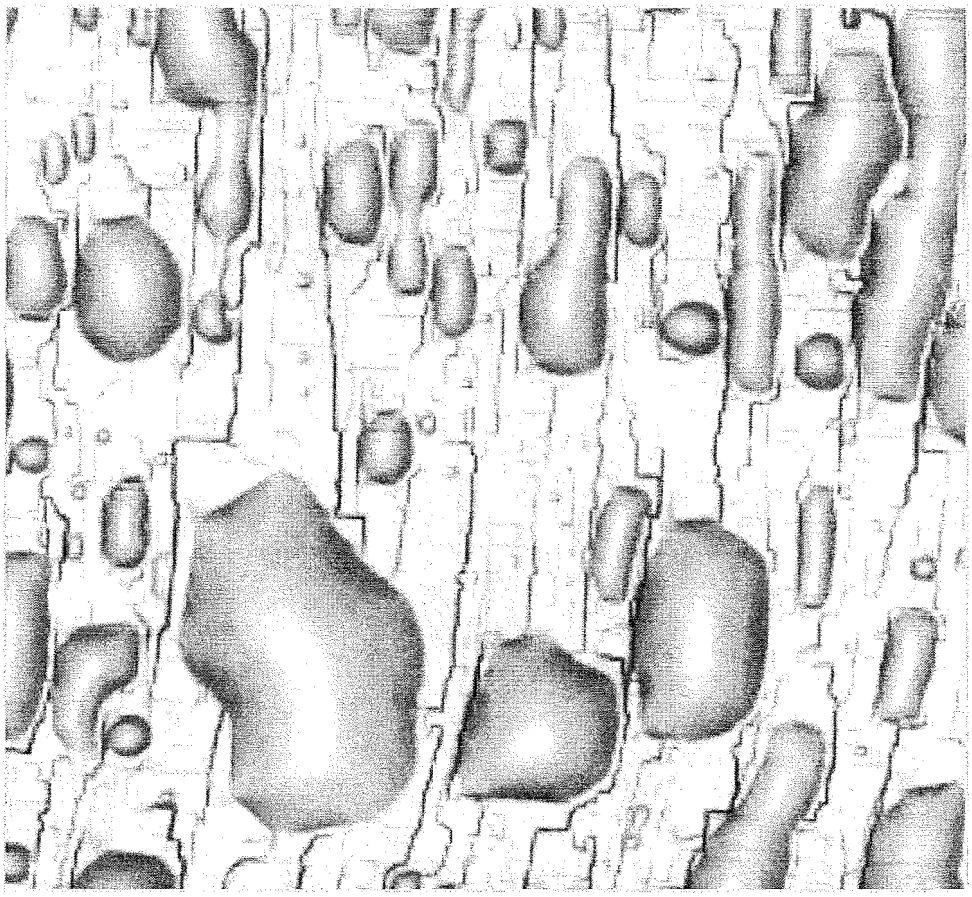

Scientific Report 1999/2000

Published by Forschungszentrum Jülich GmbH
D-52425 Jülich
Telephone: +49 2461 61-0 – Telex: 833556-0 kfa d
Responsible for content: the Managing Director of the IFF
tel: +49 2461 614465, fax: +49 2461 612410, e-mail: h.geisler@fz-juelich.de
Wholly set-up by BD-SG, Grafische Betriebe, Forschungszentrum Jülich GmbH
Time of going to press: 29th February 2000

Introduction

This is the second IFF annual report now published in English. We have chosen to make this report and thus our scientific results and accomplishments over the past year available to the world wide scientific community. Additionally, this report also serves as the main base of communication to our international scientific advisory board. The articles in this report represent only a partial selection of the numerous projects and collaborations the scientists of the IFF are engaged in. We hope that all of you find it interesting and worthwhile to read through this selection.

In the IFF we again can look back at a scientifically quite successful year. In terms of the number of publications, patents, and invited talks at international conferences we could still keep up the pace of our scientific accomplishments. Furthermore, we are also especially proud that B. Kessler was appointed as a professor at the "Fachhochschule Koblenz" keeping up the leading role of the IFF in providing superior candidates for faculty appointments worldwide. Other outstanding achievements include the award of the Gustav-Hertz prize (2000) of the DPG to G. Schütz and the "Heyn-Denkmünze" of the "Deutsche Gesellschaft für Materialkunde" received by K. Urban.

We are also very happy that we are again complete in terms of having all the chairs of the department filled. As of January 2000 Prof. Jan Dhont actually joined our department to set up his activities in soft matter physics and concentrating on phase transitions and shear flow in colloids.

With this report we want to communicate our results and accomplishments in a general overview and closed form to the scientific community at large. Additionally, we acknowledge our responsibility to the tax payers who are funding our research. These results and the past successes of the IFF have been and are accounted for in terms of actual scientific discoveries and publications, patents and licenses to industry, or training of people and their transfer to high level positions in industry and at universities. However we want to clearly state and reiterate here that most of these accomplishments are a product of the scientific freedom and stimulating environment at the IFF, but not due to strategic planning at some government agency or ministry. At times, when the federal government is threatening to curb our scientific freedom by introducing socialistic planning structures, this is a grave concern of all of us at the IFF. Technological advances can be planned, and then implemented at a huge cost of capital and manpower, as the semiconductor and computer industry has demonstrated with their road maps. True innovation and inventions as well as novel scientific discoveries are not plannable, rather they are the result of a stimulating and nurturing atmosphere where creativity wins over long term planning. Incidentally, the discovery of the GMR sensors has obliterated and significantly changed the carefully and strategically planned advances in magnetic data storage. These are the true innovations that only basic science and the curious minds of creative scientists can deliver, thus enabling our society to face the social, environmental, and technological challenges of the future and to compete in the global marketplace in the long term.

" He whose generals are able and not interfered with by the sovereign will be victorious"
Sun Tzu, "The Art of War", China 500 B.C.

Wolfgang Eberhardt
IFF Managing Director, 2000

Contents

Institute for Solid State Research (IFF)

1. Management and Structure

Institutes:

Prof. G. Eilenberger,
Institute 'Theory I'

Prof. G. Gompper
Institute 'Theory II'

Prof. H. Mueller-Krumbhaar,
Institute 'Theory III'

Prof. Th. Brückel,
Institute 'Scattering Methods'

Prof. D. Richter,
Institute 'Neutron Scattering'

Prof. R. Waser,
Institute 'Electroceramic Materials'

Prof. J. Dhont
Institute 'Soft Matter'
(since 01.01.2000)

Prof. K. Urban,
Institute 'Microstructural Research'

Prof. W. Eberhardt,
Institute 'Electronic Properties'
(IFF Managing Director for 2000)

Special Group:

'Materials under high doses of radiation'.
Prof. H. Ullmaier

Central Facilities:

'Electronics Laboratory'
Dr. G. Durcansky

'Numerical Methods and Data Processing'
Prof. G. Eilenberger

'Accelerator'
Dl. R. Hoelzle,

'Construction'
H. Feilbach

'Workshop'
K.Hirtz

'Administration'
H.Geisler (Permanent Deputy of the Managing Director)

2. Overview

The Institute of Solid State Research (IFF) pursues research on condensed materials in the solid or liquid state. In addition to studies of bulk properties of condensed phases, the IFF is concerned with inhomogenous systems and with the consequences of low dimensionality. This refers in particular to the physics of clusters, surfaces, thin films and membranes. With regard to both theory and experiment, the institute's research can be understood in terms of three strategically distinct categories:-

- Phenomena oriented research: The search for, discovery of and research on an explanation for general phenomena and behaviour in condensed matter systems, including the mathematical and physical concepts and structure underlying this behaviour.

- Materials oriented research: The investigation of specific materials or classes of materials with a view to gaining an understanding of their special properties and, where appropriate, exploring their potential for practical application.

- Method oriented research: Development of new methods and the improvement of existing methods, both in the experimental and the theoretical/numerical sectors.

The general physical basis for these components is provided by statistical physics and quantum mechanics, which describe on a microscopic scale the behaviour and the reaction to external influences of electrons and atoms, the building blocks whose aggregation and cooperation is responsible for the formation of condensed phases. The issues to which these connections give rise in the context of current research form the basis of the work of theoretical and experimental groups within the institute.

Alongside this work is an increasing experimental effort in the development of systems and components that show promise of interesting and outstanding characteristics. This effort grew naturally as a consequence of past work on special materials and methods of preparation.

In pursuing a research strategy oriented towards the future, the IFF has extended its sphere of activity substantially by founding Institutes focused on ceramics and on scattering methods. This establishes new areas in the Department with strong potential for the future, and extends and builds on its core activities. Similarly, the research sector 'Soft Materials' has been strengthened by the founding of a new Institute with this focus, by the choice of a Director of the Institute Theory II whose research focuses in this area, by coordinating work in other institutes to impact on soft materials research and by providing wide-ranging and attractive possibilities for cooperation within the Jülich Research Centre in general.

The following specific foci of work in the IFF are symptomatic of the nature and purpose of a Helmholtz-Research-Centre:

- Contributing to the construction and operation of new experimental equipment and measuring facilities for international sources of neutron and synchrotron radiation. In addition to the Jülich Research Reactor 'DIDO', the sources at Argonne, Berlin, Brookhaven, Gaithersburg, Grenoble, München, Risø, Saclay and Appleton are used. The Jülich Research Centre contributes to the FE-Programme for the European Spallation Source (ESS), the prototype for which involves the participation of 11 European countries. The IFF is primarily involved in the ESS project via research into shock-wave effects in the liquid mercury target, the optimisation of the target and the moderators, and in the development of instrumentation. Experiments with synchrotron radiation are carried out at BESSY, DELTA and HASYLAB in Germany, and internationally at Argonne (APS), Berkeley (ALS), Brookhaven (NSLS), ESRF (Grenoble) and ELETTRA (Trieste).

- Using the Jülich Computer Centre, mainly for theoretical investigation and large-scale numerical simulations.

- Projects that require high levels of investment and/or the continuity of a highly qualified team of staff (in most cases in the context of national and international cooperative projects and services). Examples are the Centre for High-resolution Microscopy, the operation of accelerators, the Electro-ceramics

laboratory, superconductor technology and the development of sophisticated numerical algorithms and programs.

Over the long term, the research effort of the IFF has achieved a broad-based and internationally recognized status. Special technical excellence was achieved in the following areas: application of synchrotron-radiation and neutron scattering, electron-microscopy, electron-spectroscopy, high-temperature superconductivity, magneto-electronics, the physics of clusters, electronic structure theory, dynamical features of phase-transitions, quasi-crystals and polymers.

A prerequisite for the focal areas of research in the IFF mentioned above and its position in the international community as a valued partner for cooperation is its strong position in basic research. The IFF carries out basic research in areas where interesting developments having potential for the future occur, especially when this research provides the underpinnings of more applied research projects.

Genuine innovation (as distinct from continuous development) occurs typically as a by-product of curiosity-driven research. This is exemplified particularly well by the discovery of the 'giant-magneto-resistance' effect, which over the past years has become a very active area in solid state research. The effect has attractive applications for magnetic sensors eg. as read heads for data storage and for control of moving parts. The license revenue from the patents which were take out as a result of early work in the IFF on this effect represents the largest contribution to the total patent revenue of the Jülich Research Centre devolving from a single application!

The IFF participates along with ISI and IGV in the Jülich's program 'Basic Research in Information Technology' (PGI). With its strong basic research infrastructure as foundation, the IFF has in recent years in the context of PGI extended its facilities for technical development and component-design substantially. This has led to the acceptance of the IFF's research program within the the framework of the HGF-Strategic-Fund Project 'Microtechnological High-Performance Components –Microinductors'. In 1999, a further Strategy Fund Project for development and characterization of film systems for magneto-electronics was granted. The development over many years in IFF of the program 'High-temperature Superconductors in Communications Technology' was to a large part integrated with the superconductivity research in ISI. The areas 'Squid-microscopy' and 'Hilbert-Transformation Spectroscopy' in IFF will be strengthened.

In 1999, the scientific work of the IFF generated 244 publications 8 patents and 20 patent applications. IFF scientists gave 308 seminars at universities, institutes, conferernces of worksops of which 183 were invited. In addition IFF staff carried out of 47 courses or educational seminars at universities. 27 are represented in the formal lecture schedules of teaching institutions.

The traditional IFF-Spring School was held in 1999 with the topic 'Magnetic Film Systems' and attracted 250 participants.

In 1999, 17 diploma students and 52 doctoral students worked at IFF. 12 Diploma students and 19 doctoral students completed their programs during the year.

3. Scientific and Technical Infrastructure

In the past years, the IFF has tightened its technical infrastructure in order to retain optimal efficiency of the Department's internal service groups. This has been achieved through organisatorial and strategic measures in the context of dwindling resources, the loss of the technical know-how of retiring staff who could not be replaced and the need to close down some technical facilities. These measures have now reached a critical boundary.

Research 'at the cutting-edge' requires the capability to build and maintain experimental facilities in high-tech areas. In this regard, the basic research performed by the IFF at national and international sources as well as applied research is equally affected. Equipment must meet high international standards, and especially so when the work performed is to be 'industry relevant'. A basic requirement for the work of the Department is an infrastructure, within the IFF and the Research Centre itself, that supplies the necessary expertise, effectiveness and facilities.

The *Electronic-Laboratory* of the IFF maintains and services the workstation cluster and networks, and supports scientific staff in the design and performance of experiments as well as via the networking and usage of workstations and PC's. In the context of its limited staffing possibilities, the EL supplies expert assistance in hard- and software and in the supply and repair of components. Hardware and software units are developed and automatization of exprimental systems facilitated.

The *Numerical Methods and Dataprocessing* group is responsible for issues relating to information and data-evaluation. Together with the Electronics Laboratory, the group maintains the IFF-workstation cluster, provides programming advice and participates in the training of mathematical-technical assistants.

The *Accelerator Group* is responsible for the running of the Compact-Cyclotron and the Tandetron.

Construction and Workshop propose and build equipment for the IFF over a wide range, from simple mechanics to sophisticated modern technology. The facility works closely together with the scientists and engineers of the Institute to achieve the ambitious quality and tolerance goals set by the experimentalists.

Staff members

K. v. Ameln, N. Bayer, S. Berger, H.P. Esser, A. Bremen, H. Cremer, G. Durcansky, P. Eickenberg, M. Emmerich, H. Feilbach, U. Funk-Kath, R. Gehlhaar, G. Grimm, E. Gundt, R. Heckmann, J. Heinen, D. Henkel, K. Hirtz, R. Hölzle, K.H. Johnen, S. Krahe, J. Lingenbach, T. Matulewski, W. Noack, T. Nguyen-Vu, P. Pickartz, M. Pohl, B. Radermacher, H. Sachsenhausen, L. Schätzler, H. Schnitzler, J. Schramm, T. Starc, P. Stefelmanns, W. Stellmacher, H. Terberger, E. Westphal, K. Wingerath, A. Zens.

4. Other Scientific Activities: Collaborations with Universities, Institutions and Industry.

The productivity of a Research Institute depends strongly on its capacity for scientific exchange and for scientific and technical collaboration. In this regard, the Jülich Research Centre offers excellent possibilities. The Centre's exemplary infrastructure offers efficient assistance, facilitating extended or short-term visits by external guests. Many guest scientists were able to utilize the infrastructure and facilities. Modern neutron scattering instrumentation appropriate for cutting-edge studies are available to many IFF guest scientists in the DIDO building and in the measuring laboratory ELLA (?). The wide variety of collaborations in which the neutron studies institutes of the IFF are involved leads to optimal usage of the potential of the relevant equipment. Concomitantly, the availablity of complementary facilities at other Institutions is important for the IFF. In particular, by building and developing measuring capabilities, the IFF contributed to the development and improved usage of external facilities such as ILL and CEN (Grenoble), FELTA (Dortmund), HASYLAB (Hamburg), BESSY (Berlin), NSLS (Brookhaven), NIST (Gaithersburg ?).

Bilateral agreements as regards the use of the Jülich centre for high-resolution microscopy for specialized studies in the area of quantitative and high-resolution microscopy, and as regards use of the Jülich microscope with correction of the spherical abberation have been concluded with the Paul-Drude Institute, Berlin, RWTH Aachen, IBM Rüshlikon, and the universities Bonn, Göttingen and Kiel.

In the past year, the IFF has expanded its activities as a sub-contractor to large companies (eg. Bosch, Siemens, Daimler-Benz, Thompson, Philips) and contract work has become the main focus of the scientific work of several groups. This is in particular the case with regard to attracting large-scale national (German) and international external funding. Of special importance is the IFF's participation in the BMBF-Project 'Magnetoelectronics'. Under the auspices of the Technology Transfer Bureau of the Jülich Research Centre, the IFF leases equipment to companies that have established themselves in the Jülich Technology Centre. In addition, the IFF has designed and built pilot equipment for industrial concerns.

Amongst the most important roles of a large Research Centre is making its facilities and equipment available to universities and other research organisations for research projects that need not necessarily

have a direct connection with active research programs of te Centre. In this regard, the Jülich Research Centre with its exemplary infrastructure, supports the individual Institutes of the IFF in regard to the Department's Guest Program in solid state research (see 23.06.0).

Many staff members of the IFF serve in scientific committees (eg. advisory boards for institutes and scientific societies, program committees for international meetings, editors of proceedings, journals and databases, referees for the scientific community, special research areas and prize committees.) Collaborations with other Institutes of the Research Centre were especially fruitful and the common utilization of equipment and facilities lead as usual to frequent consultations in areas of common interest.

On 25th June 1999, the Heyn-Denkmünze of the German Society for Materials Science was awarded to Prof. K. Urban, Director if the Institute for Microstructural Research of the IFF.

On 22nd March 2000, in Dresden, the Gustav-Hertz prize of the German Physical Society was awarded to Dr. Gunter Schütz.

Alexander von Humboldt Research Prizes were awarded to Prof. M. A. Olmstead, University of Washington, Seattle (Guest of the Institute Electronic Properties) and Prof. T. Burkhardt, Temple University, Philadelphia, USA (Guest of Institute Theory II),

Alexander von Humbolt Stipendia were awarded to:

Dr D. Caprion, University Montpellier II, Montpellier, France
Dr H. Ishida. University of Yokyo, Tokyo, Japan
Dr W. Ma, Southwest University, Nanying, China.
Dr K. Maiti, IISC Bangalore, Bangalore, India.
Dr J. Wu, Institute National Polytechnic, de Lorraine, Nancy, France
Dr S.-S. Yan Physics department, Shandong University, Jinan, China.

Personal Honours, Awards, and Distinctions

Prof. Dr. W. Eberhardt was appointed for six additional years to the Advisory Board at the "Max-Plank-Institut for Solid State Physiks" in Stuttgart.

Prof. Dr. W. Eberhardt was selected to serve as Member of the national committee „Forschung mit Synchrotronstrahlung".

Prof. Dr. R. Waser was appointed to serve in the International Advisory Committee of the ISIF(International Symposium on Integrated Ferroelectrics) and as Chairman of the ISIF 2000 in Aachen (Together with Dr.D.Wouters,

Prof. Dr. R. Waser was appointed to serve at the FZJ-ISI Advisory Board.

Dr. B. Kessler was appointed as a C3 professor position at the Fachhochschule Koblenz in Laser Physics and Materials Science.

Prof. Dr. K. Urban was rewarded the "Heyn-Denkmünze" of the "Gesellschaft für Materialkunde".

Prof. Dr. Th. Brückel was selected as Proxy Chairman to the Committee "Forschung mit Neutronen"(KFN)".

Dr. A. Wischnewski received the Young Scientists Award for his lecture "Reptation in polyethylene with different molecular weights" at the 2nd European Conference on Neutron Scattering 1999 in Budapest.

Dr. G. Schütz received the "Gustav-Hertz-Award 2000" of the "Deutsche Physikalische Gesellschaft"

Institute Reports with Selected Research Results 1999

Institute Theory I

General Overview

Research Areas

The main focus in the Institute is on gaining an understanding of electronic structure and atomic-scale processes and, wherever realistically possible, performing quantitative calculations. The term 'quantitative' is used here to draw a distinction to the other important 'qualitative' aspect of theory, which considers characteristic elements of physical reality in the abstract and represents these using the simplest possible theoretical or numerical representation. The individual themes that constitute this area of activity will be described in more detail below.

For a given collection of nuclei, the structure and properties of the resulting atomic assemblies are determined in the last analysis by the electrons. Thus the main focus of the Institute's work programme, referred to above, in fact spans the entire physics of condensed materials! The institute's choice of relevant problems in this area, which is addressed by a virtual army of theorists worldwide, is made according to the following aspects:

- current issues of a methodological or thematic nature,
- the expertise of staff members,
- the availability of computer programme-packages that have evolved over many years (and so can be compared to moderately expensive experimental equipment),
- special capabilities of the Jülich computer facility,
- status of competition and possibilities for collaboration, local, national and international.

In this sense, a central feature is the ongoing development and application of current density-functional/ab initio molecular dynamics programmes, especially in conjunction with the powerful computational facility in ZAM. Work in this area has been performed by Dr. Jones, Dr. Lichtenstein and Dr. Ballone. A new example of work in this research area can be found below.

The computer programmes run currently on the T3E. On-going development includes the testing of new, non-local approximations for the exchange-correlation energy functional. Such approximations are essentially empirical and not the result of ab initio theory. This leads to systematic deviations with respect to measured values and with values calculated for small systems by more reliable, but much more resource intensive quantum methods. Combining accuracy with ease of computation will remain a challenge into the future. The focus of applications has been to atomic clusters, especially those with light atoms (organic molecules, carbon-aggregates, systems containing water), which require 'hard' pseudopotentials and so represent difficult numerical problems. Other applications include energy surfaces and phonons in glasses.

A further area of research concerns the interaction of electrons and electromagnetic fields in bulk materials (Prof. Sturm) and on sufaces (Dr. Liebsch). A perennial challenge to the condensed matter theorist is the problem of interactions and correlations among electrons. Whereas for s- and p-electron systems these effects are satisfactorily taken into account by density functionals, d- and f-electron systems show phenomena which are beyond the scope of LDA. Methods like dynamical mean field theory, quantum Monte Carlo calculations and exact diagonalization will be applied for those systems by Dr. Liebsch. Work in this direction is reported below.

Dr. Harris returned to the institute after a five years leave of absence during which he worked in a US company providing scientific software. He builds on the experience of many years by applying density functional theory to materials problems, and together with Dr. Bringer is establishing a programme to apply data mining methods for materials research at the institute, as described below.

An important research topic in the Institute is the atomic theory of friction and the related issue of crack propagation. A new result is presented below as an example of the general area of research. Over the past years, Dr. Persson had pioneered work in this area (much of which is summarized in his 1997 monograph on this topic). This remains an area whose development is just breaking out of infancy, and has broad-based ramifications and many open questions and applications.

Another research area of the Institute, the theory of non-linear systems, had been transferred for the period 1997-99 to the 'Modelling Forum', where Dr Lustfeld, co-opted as a member of the Forum, was applying his know-how to environmental problems. This multi-institutional approach to interdisciplinary tasks will retain support from theory, in line with the research policy of our research center.

The research area of Prof. Eisenriegler - 'Geometric Effects in Complex Fluids' - bears a close relationship to the theory of soft-matter. At the end of this year, Prof. Eisenriegler will join the Institute Theory II and take this activity along with him. The work studies the forces that operate between geometric objects - walls, spheres (colloids) and cylinders having dimensions in the mesoscopic range - which arise as a result of thermodynamic effects in the surrounding fluid. Examples are critical fluid mixtures and dilute polymer solutions. The methods employed in these studies include analytical, field-theoretical approaches as well as numerical simulations in collaboration with Dr. Bringer, who contributed methodologies and programmes.

External Funding and Collaborative Projects

- Between 1994 and 1999, Dr. Persson was granted support by the DFG to cover annual 3-month guest visits to IFF by Prof. Volokitin, University of Samara, Russia.
- As a participant on a 5-year BMBF(German Research Ministry)-supported German-Israeli Cooperative Project, Dr. Persson receives from 1998 annual funding of 50,000 DM to cover guest visits and travel expenses.
- As a contributor in a collaboration between institutes from Jülich, Mainz and Heidelberg, Dr. Jones received for the years 1996-98 from the MaTech Programme of the BMBF funding of in total 1,141,000DM. An extension of this funding for the years 2000-2002 is pending.

Gert Eilenberger

Personnel 1999/2000 and areas of activity

Staff members

Dr. A. Bringer	Problems of electron correlation, genetic algorithms for materials research	23.20.0
Prof. G. Eilenberger, Institute Director	Applications of supersymmetry in solid state problems, nonlinear dynamics	23.20.0 23.15.0
Prof. E. Eisenriegler	Geometric effects in complex fluids	23.30.0
Dr. J. Harris	Practical applications of computational and informational methods to materials research	23.20.0
Dr. R.O. Jones	Structure and dynamics of clusters and amorphous and liquid systems; Project: "Chemistry-Laboratory Computer"	23.20.0
Dr. A. Liebsch	Linear and non-linear response, electronic correlation with quantum impurity methods	23.20.0
Dr. H. Lustfeld	Theory of nonlinear systems and its applications in atmospheric chemistry	23.15.0
Dr. B.N.J. Persson	Electronic response at surfaces, atomic friction, adsorbate modes, crack propagation	23.20.0
Prof. K. Sturm	Electronic response; dielectric properties of metals and semi-conductors	23.20.0
Mrs Ch. Hake	Secretary	

Guests 1999

Prof. P. Ballone	(University of Messina, Italy) Development and applications of the DF/DM method	23.20.0
Dr. J. Bene	(Eötvös University, Budapest, Hungary) Theory of non-linear systems	23.15.0
Prof. O. Braun	(University of Kiev, Ukraina) Aspects of atomic friction	23.20.0
Prof. K.H. Fischer	(FZ Jülich, retired) Vortices in d-wave and high T_c super-conductors	23.20.0
Dr. Z. Kaufmann	(Eötvös University, Budapest, Hungary) Theory of non-linear systems	23.15.0
Prof. A. Lichtenstein	(Catholic University Nijmegen, The Netherlands) Correlation problems in d-electron systems	23.20.0
Dr. C. Lopez	(Cuernavaca, Mexico) Optical phenomena at Ag surfaces	23.20.0
Dr. J. Maytorena	(Cuernavaca, Mexico) Optical phenomena at Ag surfaces	23.20.0
Prof. V.L. Popov	(Russian Academy of Sciences, Tomsk, Russia) Aspects of atomic friction	23.20.0
Prof. A. Volokitin	(Samara University, Samara, Russia) Adsorbates at surfaces	23.20.0

Graduate students

Ms S. Biermann	(Univ. Cologne) Application of supersymmetric methods to interacting particles	23.20.0
R. Maaßen	(Univ. Cologne) Geometric effects in complex fluids	23.30.0

Density functional study of reactions in polycarbonate

R. O. Jones and P. Ballone†
Institute Theory I

Density functional calculations have been used to study the reactions of small molecules [phenol, lithium phenoxide (LiOPh), and sodium phenoxide (NaOPh)] with the cyclic tetramer of bisphenol-A polycarbonate (BPA-PC), which should represent very well a part of a polycarbonate chain. Both LiOPh and NaOPh catalyze ring opening with small energy barriers ($\Delta E = 4.0, 2.5$ kcal/mol, respectively) to a chain with a phenyl carbonate at one end and a phenoxide at the other, a "living polymer". The barrier is large for phenol ($\Delta E > 40$ kcal/mol), but the total energy differences between the reactants and the chain are very small in all three molecules. This demonstrates the usefulness of DF calculations in the study of complex chemical reactions.

F&E-Nr: 23.20.0

The density functional (DF) method is now well-established as a means of performing calculations on the geometrical and electronic properties of molecules. When combined with molecular dynamics (the "Car-Parrinello method"), it can also be used to simulate the behaviour of bulk systems including disordered materials. While such calculations avoid the use of parametrized force fields common in the study of, for example, polymer systems, they are very demanding of computing resources. This has meant that they are currently restricted to systems with fewer than 200 atoms, and there have been few - if any - attempts to follow complex chemical reactions with this method. We describe here our first attempts to follow the path of such reactions in the context of bisphenol-A polycarbonate (BPA-PC), the remarkable mechanical and optical properties of which make it one of the most important polymers in industrial production.

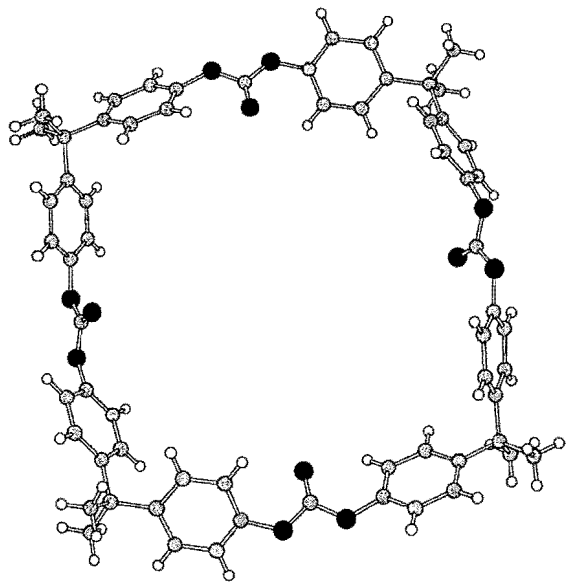

FIG. 1. Cyclic tetramer of BPA-PC. Carbon atoms are grey, oxygen atoms black, hydrogen atoms white.

The structural unit of BPA-PC contains 33 atoms. It is quite remarkable that cyclic oligomers can be formed with many such units, and the dimer and tetramer [1,2] can even be prepared as single crystals for which x-ray diffraction studies can be performed [3]. The tetramer [see Fig. 1], which is strain-free and shows the *cis-trans* isomerization also found in polycarbonate chains, then provides an ideal model for PC. We have used it to study the reaction of phenol and phenoxide molecules approaching the carbonate group from both inside and outside the ring. The reactions with the phenoxide molecules are representative of "nucleophilic attack", which often leads to the rupture of ring systems (ring-opening polymerization) [2].

The energetics of these reactions are calculated using a single reaction coordinate R_C, namely the distance between the C atom of a carbonate group and the O atom of the attacking molecule. This coordinate is reduced progressively from large values (> 5 Å) in steps of 0.2 to 0.4 Å until a structural transformation or a large energy increase occurs. For each value of R_C we relax *all* other degrees of freedom until the energy gradients along the unconstrained directions are less than 10^{-5} a.u. The calculations employ the Car-Parrinello scheme (plane wave basis, large unit cell, pseudopotential description of the electron-ion interaction, Perdew-Burke-Ernzerhof gradient-corrected functional) used in our earlier work on organic molecules [4].

In Fig. 2 we show six snapshots of the trajectory for the reaction of LiOPh outside the cyclic tetramer, and the corresponding energy changes as a function of R_C are shown in Fig. 3(a). The two molecules react very weakly for $R_C \sim 4$ Å, with minor relaxations and energy changes of less than 1 kcal/mol. For shorter separations, the Li-O attraction produces a rotation of the carbonyl group, and bond formation leads to a rapid decrease in total energy. In this configuration the C atom of the original carbonate has a large positive charge and approximately tetrahedral coordination. The configuration (4) provides a threefold axis for rotations of the Li-O bond that give

rise to variations in total energy of less than 1 kcal/mol. The energy of structure (6) is 6 kcal/mol below the combined energy of the reactants. At room temperature the Li-O bond should break easily, leading to an open chain with an active -C-O-Li termination. This in turn can attack another chain, i.e. initiating a catalytic reaction that could result in the breaking of all ring structures present and the formation of long chain segments.

This mechanism is not only possible, but it forms the basis of a process that is used to produce the polymer BPA-PC. The reaction proceeds in a similar fashion if the phenoxide molecule is initially *inside* the ring, and if the initiating molecule is NaOPh. The different sizes of the Li and Na ions lead, of course, to differences in detail between the mechanisms, but the variation in the energy found for NaOPh [Fig. 3(b)] is very similar. Strikingly different, however, is the change of energy as a phenol molecule approaches the carbonate group [Fig. 3(c)]. The interaction is repulsive for approach from both outside an inside the ring, confirming a well-known fact that phenol and BPA-PC do not react with each other. Further details are provided in Ref. [5].

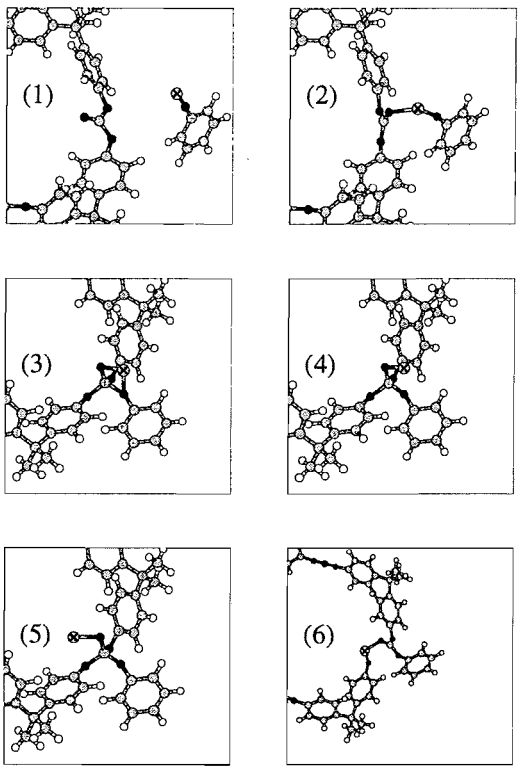

FIG. 2. Reaction of LiOPh with cyclic tetramer of BPA-PC. Only part of the ring is shown.

The DF calculations described here have provided a clear picture of the mechanism of a complex, well-studied reaction of industrial importance. Such calculations should provide valuable insight into other reactions for which mechanisms are either unknown or very difficult to study experimentally.

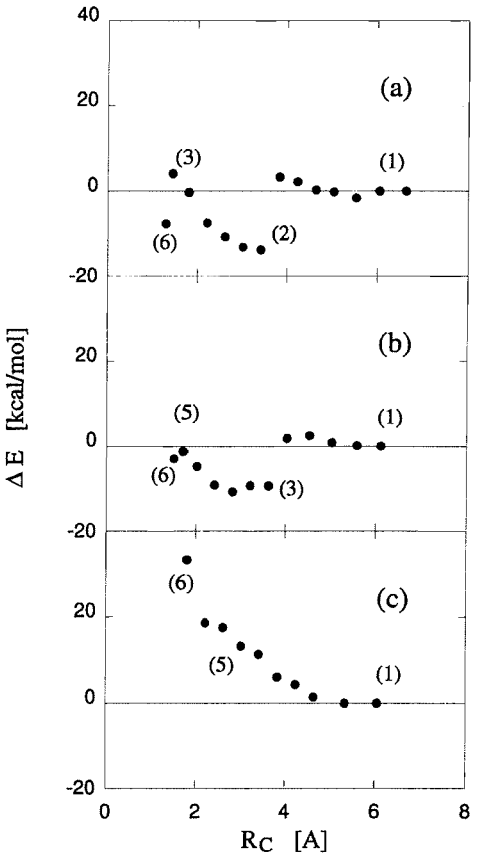

FIG. 3. Variation of total potential energy with reaction coordinate R_C during reactions of (a) LiOPh, (b) NaOPh, (c) phenol. $\Delta E = 0$ corresponds to the sum of the energies of the isolated molecules. Numbers denote the related structure in Fig. 2 and for NaOPh and phenol.

† Present address: Università degli Studi di Messina, Dipartimento di Fisica, I-98166 Messina, Italy.

[1] H. Schnell and L. Bottenbruch, Makromol. Chem. **57**, 1 (1962).

[2] D. J. Brunelle, In *Ring-Opening Polymerization: Mechanisms, Catalysis, Structure, Utility*; Edited by D. J. Brunelle, (Hanser, München, 1993), p. 1, p. 309.

[3] D. J. Brunelle and M. F. Garbauskas, Macromolecules **26**, 2724 (1993).

[4] See B. Montanari, P. Ballone, and R.O. Jones, Macromolecules **32**, 3396 (1999), and references therein.

[5] P. Ballone, B. Montanari, and R. O. Jones (submitted).

Deformation of Sr_2RuO_4 Fermi Surface Observed in Photoemission

A. Liebsch and A. Liechtenstein
Institute Theory I

Multi-band quasi-particle calculations based on perturbation theory and dynamical mean field methods show that the creation of a photoemission hole state in Sr_2RuO_4 is associated with a highly anisotropic self-energy. Since the narrow Ru-derived $d_{xz,yz}$ bands are more strongly distorted by Coulomb correlations than the wide d_{xy} band, charge is partially transferred from $d_{xz,yz}$ to d_{xy}, thereby shifting the d_{xy} van Hove singularity close to the Fermi level.

F&E-Nr. 23.20.0

Angle-resolved photoemission spectroscopy is one of the key techniques providing information on the Fermi surface of high temperature superconductors. To verify the reliability of these data, the detection of superconductivity in Sr_2RuO_4 is of great importance since this system is the only layered perovskite compound known so far that is superconducting in the absence of doping. Surprisingly, dHvA and photoemission studies yield contradictory Fermi surfaces [1]. This discrepancy raises serious questions concerning the interpretation of photoemission data also in cuprate superconductors.

In order to determine the effect of Coulomb correlations on the shape of the Fermi surface, we have calculated the quasi-particle spectral function for a two-dimensional multi-band Hubbard model using both perturbation theory and dynamical mean field methods [2]. Because of the layered structure of Sr_2RuO_4, the electronic bands close to the Fermi level may be qualitatively understood in terms of a simple tight-binding picture for the Ru t_{2g} states (see Fig. 1). The wide xy band exhibits two-dimensional character, while the narrow xz, yz bands are nearly one-dimensional. Density functional calculations based on the local density approximation (LDA) place the xy van Hove singularity at M about 50 meV *above* the Fermi energy. Whereas the dHvA data are consistent with these results, photoemission spectra reveal a different topology: the xy van Hove singularity appears *below* the Fermi level, converting the γ sheet from electron-like to hole-like.

According to the reduced dimensionality of Sr_2RuO_4, creation of a photohole should be associated with highly anisotropic screening processes reflecting the nature of the electronic states involved. Since the local Coulomb energy is believed to be about $U = 1.5$ eV, we have the peculiar relation $W_{xz,yz} < U < W_{xy}$, where $W_{xz,yz} = 1.4$ eV and $W_{xy} = 3.5$ eV are the widths of the t_{2g} bands. Thus, intra-atomic correlations have a much larger effect on the xz, yz bands than on the xy band. Because of the $\sim 2/3$ filling of the xz, yz bands, their narrowing, combined with Luttinger's theorem, must lead to a charge flow from the xz, yz bands to the xy band. As we have found, for reasonable values of U this charge transfer is large enough to push the xy singularity close to or even below the Fermi level.

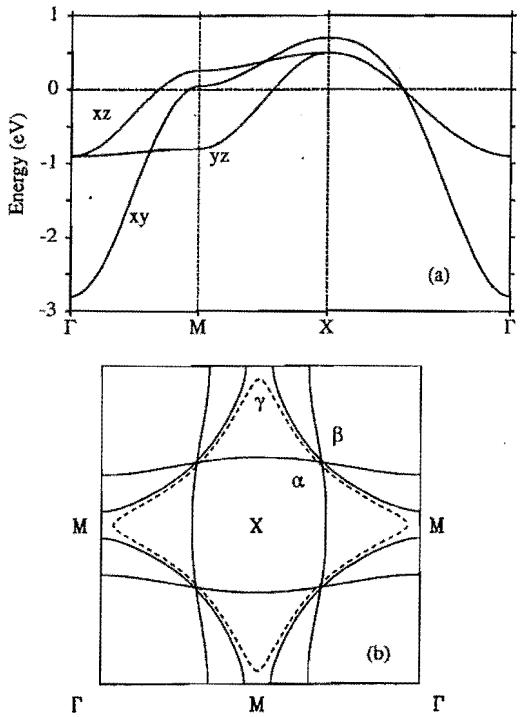

FIG. 1. (a) Dispersion of t_{2g} bands of Sr_2RuO_4 in simplified two-dimensional Brillouin Zone ($E_F = 0$). (b) Solid lines: Fermi surface consistent with LDA band structure and dHvA measurements. Dashed line: approximate xy Fermi surface derived from photoemission.

We have calculated the local self-energy using a two-dimensional next-nearest-neighbor tight-binding model for the t_{2g} bands. The on-site Coulomb and exchange integrals are given by ($i \neq j$): $U = \langle ii||ii\rangle$, $U' = \langle ij||ij\rangle$, and $J = (U - U')/2$, where $i = 1 \ldots 3$ refers to xy, xz, yz. Since the t_{2g} bands do not hybridize, the self-energy has no off-diagonal elements. Self-consistency is included in the spirit of dynamical mean-field theory [3]. In this scheme, $\Sigma_i(\omega)$ is a functional of the effective bath Green's function $\mathcal{G}_i^{-1} = G_i^{-1} + \Sigma_i$, where the local G_i is given by $G_i(\omega) = \int d\omega' \rho_i(\omega')/[\omega + \mu - \Sigma_i(\omega) - \omega']$. A typical frequency variation of Σ_i obtained within second-order perturbation theory is shown in Fig. 2. Near E_F,

the imaginary parts vary quadratically with frequency and the real parts satisfy $\Sigma_{xz,yz} \gg \Sigma_{xy}$, i.e., the energy shift of the narrow xz, yz bands is much larger than for the wide xy band.

Qualitatively similar results are derived from more refined treatments of on-site Coulomb correlations using multi-band self-consistent Quantum Monte Carlo (QMC) methods [3]. The temperature of the simulation was 15 meV with 128 imaginary time slices and $\sim$ 300 000 Monte Carlo sweeps. Fig. 3 shows the quasi-particle density of states $N_i(\omega) = -\frac{1}{\pi} \operatorname{Im} G_i(\omega)$, obtained via maximum entropy reconstruction, together with the bare density of states $\rho_i(\omega)$. The van Hove singularities near the edges of the xz, yz bands are shifted towards E_F, causing a sizeable band narrowing. Because of the $\sim 2/3$ filling of these bands, this effect is not symmetric, giving a stronger relaxation shift of the occupied bands than for the unoccupied bands. There is also some band narrowing of the xy bands, but since $U < W_{xy}$ this effect is much smaller than for the xz, yz bands.

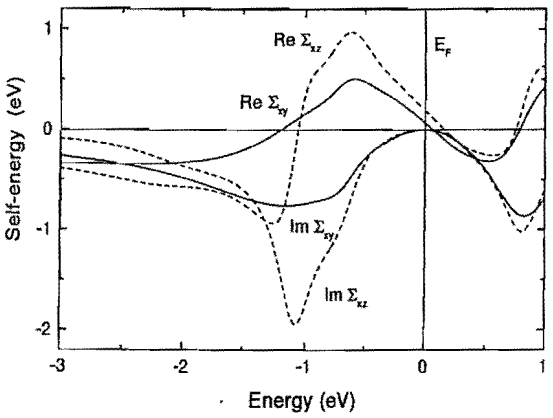

FIG. 2. Real and imaginary parts of self-consistent second-order self-energy for $U = 1.2$ eV, $J = 0.2$ eV. Solid curves: xy, dashed curves: xz.

A crucial point is now that in order to satisfy the Luttinger theorem the more pronounced band narrowing of the xz, yz bands requires a transfer of spectral weight to the xy bands. Thus, the xy van Hove singularity is pushed towards the Fermi level. In the example shown in Fig. 3, it lies about 10 meV above E_F, compared to 50 meV in the single-particle spectrum. We note that this result is a genuine multi-band effect where the filling of a relatively wide quasi-particle band is modified by correlations within narrow bands of a different symmetry. Although the approximate nature of our model does not permit a quantitative prediction of the frequency of the xy singularity, it is evident that its near-degeneracy with E_F makes it extremely difficult using angle-resolved photoemission to determine the k-point at which the xy band crosses the Fermi energy. Photoemission data taken with better energy and angle resolution might provide a more conclusive answer. Fig. 3 also shows that due to the narrowing of the xz, yz bands, the weakly dispersive band is shifted from -0.8 eV to about -0.4 eV, in agreement with photoemission data. For $k_\parallel$ between M and X, this band is observed to cross E_F at about $(\pi, 0.6\pi)$, in good accord with our calculations. Also, the calculations indicate a satellite below the xz, yz bands which might be related to the spectral feature observed near 2.5 eV binding energy using resonant photoemission.

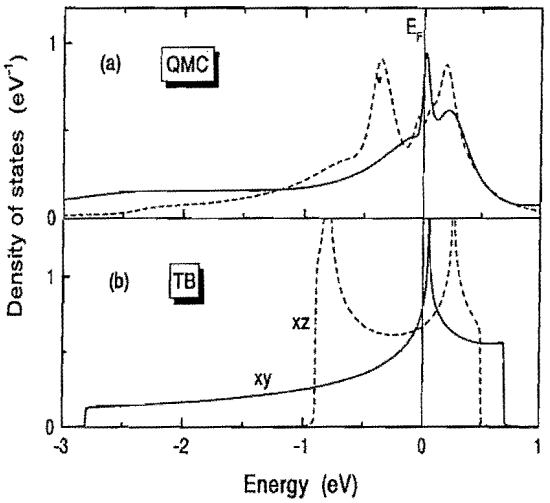

FIG. 3. (a) Quasi-particle density of states $N_i(\omega)$ derived from self-consistent QMC scheme for $U = 1.2$ eV, $J = 0.2$ eV. (b) Single-particle density of states $\rho_i(\omega)$ derived from tight binding bands. Solid curves: xy, dashed curves: xz.

In summary, multi-band quasi-particle calculations for Sr_2RuO_4 show that the simultaneous existence of nearly one- and two-dimensional t_{2g} bands near E_F leads to a highly anisotropic self-energy of the photoemission hole state. Because of Luttinger's theorem, this anisotropy gives rise to a charge flow from the narrow xz, yz bands to the wide xy band, thereby shifting the xy van Hove singularity very close to E_F. As a result, in the vicinity of M considerable spectral weight appears below E_F. These results might explain the controversial nature of recent photoemission data which have difficulty in determining whether or not the xy band at M is occupied.

[1] For discussions, see: A.V. Puchkov, Z.X. Shen, T. Kimura, and Y. Tokura, Phys. Rev. B **58**, R13322 (1998); A.P. Mackenzie, S. Ikeda, Y. Maeno, T. Fujita, R. Julian, and G.G. Lonzarich, J. Phys. Soc. Japan **67**, 385 (1998), and references herein.

[2] A. Liebsch and A. Liechtenstein, submitted to Phys. Rev. Lett.

[3] A. Georges, G. Kotliar, W. Kraut, and M.J. Rozenberg, Rev. Mod. Phys. **68**, 13 (1996).

Application of Data-Mining Techniques in Materials Research

Andreas Bringer and John Harris
Institute Theory I

The use of statistical modeling methods is widespread in organic- and bio-chemistry. In materials research, on the other hand, such methods have been used sparsely. One reason for this is the absence of a single highly focused application such as rational drug design (that has essentially spawned the discipline of bioinformatics). Another is the strong focus of condensed matter theorists on "law-based" rather than "statistically-based" methodologies. In this note we outline how statistical methods may contribute to materials research.

F&E-Nr: 23.20.0

I. INTRODUCTION

Theoretical physicists are trained to seek out the fundamental laws that govern behaviour and to employ law-based methods to solve problems. The focus is on the understanding of a class of behaviour in a broad sense. Physicists are trained to ask and to answer the question "Why?", whereas a technological advance often requires answering the question "How?". For example, the question as to why ceramic materials exhibit superconductivity has received fairly massive attention from the community of theoretical condensed matter physicists. The question "How can we prepare wires of these materials that can be used in general applications?" is considered to be a technological one.

Statistically-based methods involving *data-mining* may provide the basis for developing an understanding of an issue, but are more focused on providing an answer to a practical question. In life science areas, the value of these methods is widely recognized and has resulted in a new discipline - bioinformatics. A rather interesting spin-off of the use of such techniques is described in a recent issue of Chemical and Engineering News [1]. Since 1984, Proctor and Gamble has eliminated 80% of its animal toxicology testing largely by using instead data-mining, analysis and modeling (thereby earning accolades from environmental and animal rights groups!).

In condensed matter physics and materials science, theory is generally restricted to ideal conditions (perfect crystals, flat surfaces etc.). Many questions remain untreatable by law-based methods because, for example, they refer to systems that are not "well-characterized". Non-characterized materials are important because they are cheap and easy to manufacture, whereas in general characterized materials are expensive and difficult to manufacture.

A training in theoretical physics can be valuable in connection with non-law-based methodologies, especially those which possess the characteristics of an acceptable theory. These are that the method should be:

i) Predictive, ii) Practical iii) Transparent,
iv) Falsifiable

We will consider a methodology based on statistical analysis of data that can satisfy these criteria.

II. DATA-MINING AND STATISTICAL METHODS

The development of predictive methods based on data-mining assumes that data contain patterns and correlations that are hidden, but that the application of statistical methods can extract. Methods for uncovering correlations within data can be classified as "structure mapping" [2] and "mathematical modeling" which are, respectively, graphical and algebraic in nature. Algebraic methods (QSAR and derivatives) are in widespread use in bioinformatics.

Perhaps the best known example of the use of data-mining in materials science is Pettifor's classification of the crystal structures of binary alloys [3]. On arranging the elements of the periodic table in a certain order along the axes of an x-y plot (structure map), Pettifor found that A_nB_m alloys having the same crystal structure tended to cluster in certain regions of the plot. The Pettifor ordering of the elements (see, for example, Fig 6. of ref. [2]) corresponds basically to a "string" running up and down the columns of the Periodic Table. By locating a given alloy on the plot, its structure can be predicted with some degree of likelihood as being that of the alloys within the surrounding cluster whose structures are known. Structure maps have been used in several connections, e.g. the stability of quasicrystals [4], high-T_c superconductors [5], weldability of AB intermetallics [6].

A more general methodology is to attempt to derive a mathematical model based on data for some property, X, of a system belonging to a certain class of systems. This property is conventionally expressed as a series

$$X_n = X_0 + \sum_i c_{i,n} d_i, \qquad (1)$$

where the d_i are so-called *descriptors* or *basis functions* and the c_i are coefficients. The descriptors are characteristics of the system whose values are known or easily measured or calculated. They may be simply numbers

(defining a given property such as the work function of a metal, or its bulk modulus), or they may be functions of such numbers (non-linear models). It is assumed that within the class of systems under study there is a subclass, referred to as the "*training set*", where the values of X and of all the descriptors are known. The coefficients c_i are determined by least squares fitting using these known data. The value of the method lies in its ability to extrapolate out of the training set of data and to predict values of X for systems for which this quantity has not been measured.

As is well known, the ability of a model to *extrapolate* from known data is not necessarily related to the ability of the model to *reproduce* values within the training set. For example, suppose there are N data points. Then a model with N descriptors - assume for the sake of argument these are linearly independent - will reproduce the data exactly. However, it may do this (as a high-order spline does) by developing an "oscillatory character" which means that "points" outside the training set may be very poorly represented. Thus the predictive value of a model must contain an element that is not related simply to the ability of the model to reproduce data within the training set.

A reasonable measure for the ability of a model to extrapolate from a given training set is the Friedman "lack-of-fit" measure, F, defined by [7]

$$F = \frac{E}{1-(c+d\,p)/n}, \tag{2}$$

where E is the least squares error for a given model, n is the number of data samples used in the least squares fit, c is the number of (non-constant) basis functions in the model, p the total number of fit parameters in the model, and d is a control parameter of order unity. The number of fit parameters, p, will in general be different from the number of basis functions, c, because many of these will contain two or more parameters (e.g. coefficients and exponents). This measure discriminates in favour of low-order models ($c, p \ll n$) and penalizes models that are "overfit" (see the "Flare Brilliance" example outlined below).

The key to a successful model is to find the "right" set of descriptors, or basis functions and this is the heart of the methodology. Several methods are available including neural-net modeling, but the potentially most powerful method for problems in materials science involves the construction of a family of models and the application of a "genetic algorithm"[8] to generate from this family successively better models. The genetic algorithm (**GA**) (or recipe, if one will) amounts to the following procedure. Step 1 is the construction of a series of models containing different basis functions. A population of k models can be characterized via the basis functions they contain

$$X_1 = \{a_1, a_2, a_3, a_4 \cdots\}$$

$$X_2 = \{b_1, b_2, b_3, b_4 \cdots\}$$

$$\cdots$$

$$X_k = \{p_1, p_2, p_3, p_4 \cdots\}$$

Each model is now fit to the data within the training set using standard least squares, and is evaluated using the Friedman measure F. From the set of models so constructed, two "good models" are selected probabilistically (using the set of Friedman measures as a definition of "goodness"). The two models are randomly cut into two sections which are then joined to generate a new model. Viz.

$$\begin{aligned} X_k &= \{p_1, p_2, p_3, p_4 \cdots p_n\} && \text{(Parent model 1)} \\ X_l &= \{q_1, q_2, q_3, q_4 \cdots q_m\} && \text{(Parent model 2)} \\ X_c &= \{p_1, p_2, p_3, q_4 \cdots q_m\} && \text{(New model)} \end{aligned}$$

This model is then added to the set and evaluated using the Friedman measure. The set now contains $k+1$ models, and the one having the worst value of F is discarded, restoring the population to k. This procedure is continued until the average value of F for the models stabilizes. Optionally, a "mutation" may be applied to a new model (e.g. replacing one of the basis functions by a randomly chosen basis function from another model).

This genetic recipe for optimizing models has the important advantage of flexibility. There is almost no restriction on the basis functions. They can be analytic functions (sines, exponentials, etc) or non-analytic. For example, a basis function that has been found useful in describing threshold behaviour is $(x-a)\Theta(x-a)$. In addition, the model can be run for long periods without the problem of overfitting because the complexity of the model is determined by the Friedman parameter, not by a "training process" such as is used in methods based on neural networks. A standard test for the predictive capacity of an algorithm for generating a model is to subject it to a process known as "cross-validation". The training set is reduced sequentially by one member, the algorithm applied to the $N-1$ remaining members, and the value of the Nth predicted. This provides N examples of the predictability of the algorithm, which is expressed in terms of a "cross-validation" score in the range $0 < s < 1$. A score of $s < 0.3$ means very poor predictability, a score $s > 0.7$ implies high predictability.

An example of the use of the GA in chemistry is the study of flare brilliance by Rogers [9]. The problem of flare brilliance, involving highly complex, transient chemical reactions and the requirement that the energy liberated be focussed in the visible portion of the spectrum, is not particularly tractable using standard methods in theoretical physics and chemistry. The flares in question were composed of mixtures of magnesium, sodium nitrate, and strontium nitrate together with a binder. Measurements of the illumination for specific sets of concentrations of the ingredients provided a training set. Possible descriptors for this problem are the individual concentrations of the ingredients and cross-products

of these concentrations. A standard analysis using a 10-term model containing these ingredients generated a "best model" which, when subject to "cross-validation", showed essentially zero predictability. A GA analysis assuming linear basis functions produced a surprising result. The genetic procedure generated as "best model" one which involved only the concentrations of magnesium and the cross-product of the magnesium and binder concentrations. This model was clearly superior to the standard models, but still did not score well enough on the "cross-validation" test to be regarded as truly predictive. Allowing non-linear basis functions to represent threshold processes, however, changed this situation radically. The leading model had 4 basis functions, one of them non-linear, and scored 0.9 on the "cross-validation" test, indicating a high degree of predictability.

A key factor in obtaining this predictability was found to be the product of the concentrations of sodium and strontium nitrate. If this product fell below a certain value the illumination was strongly reduced. Whether this finding has any meaning in terms of a critical mixing process, or co-crystallization is not known. However, this is in any event not the purpose of the genetic analysis, which is to generate a model that has predictive value in a statistical sense. If information results that points towards certain physical processes and suggests a possible way to understand what is happening at the microscopic level, this is an added bonus.

III. GA IN MATERIAL RESEARCH

In solid state theory statistical methods have been applied, somewhat sporadically, in a number of areas. These include: i) *Thermal properties of materials.* The standard problem is to determine the partition function of a physical system by "Monte-Carlo" simulations, which can be done with modern computers for fairly large and complicated systems. ii) The *determination of spectra.* The **M**aximum **E**ntropy algorithm has been used to extract real spectra from simulated thermodynamic data. iii) *Pattern Recognition.* The same algorithm can be used to recover information of blurred images [10]. iv) *Complex Structures.* The determination of the structure of minimal energy of a collection of particles (cluster-structures) is a "**N**on-**P**olynomial-hard" problem. That means, the necessary effort to find the structure of globally minimal energy increases exponentially with the number of particles, mainly because the number of side minima in energy increases exponentially and any analytical search routine will become trapped with certainty in a local minimum. To avoid this, a "thermal-annealing" process, by which experimentally purification of imperfect crystalls is achieved, is simulated and a larger part of the configuration space is checked.

This type of problem, to determine simultaneously both local and global properties of a system should be very suitable for a GA. It has been demonstrated that for a system of 60 carbon atoms the "bucky-ball" structure forms after a few thousend genetic operations [11]. In this study the positions of the particles were taken as the genes of a member of the population and this genetic information was manipulated as outlined in the preceeding paragraph. The "fitness"-function in this case is the energy directly.

The reconstruction of the electron wave function in a **T**ransmission **E**lectron **M**icroscope from micrographs taken at different distances from the object has been studied by both thermal annealing and GA [12]. The comparison of both methods indicates that GA results are as reliable as those of thermal annealing and GA might have a wider range of applicability (larger systems).

There are many applications of datamining in materials research of relevance to current work in the IFF. We are working directly on two: 1. Electrical conductivity of ceramics: Here the task would be to prepare a model that describes reasonably the electrical conductivity in terms of readily measurable or calculable descriptors in order to predict new ceramics with optimized properties. 2. The structure of quasi-crystals: Several groups [2] [4] have used structure map techniques to predict new quasi-crystals. A related problem is the recovery of atomic positions from electron transmision microscopy data. This is in essence a pattern recognition problem that can be treated by maximum entropy, neural networks or GA methods.

---

[1] Article by Gary Anthes, C&E News 06.12.1999.
[2] J.K. Burdett and J.R. Rodgers, in "Encyclopedia of Inorganic Chemistry", ed. R. Bruce-King, Publishers: John Wiley & Sons, Vol. 7, 3934 (1994)
[3] D. G. Pettifor J. Phys. C. 19, 285 (1986)
[4] K.M. Rabe, A.R. Kortan, J.C. Phillips and P. Villars, Phys. Rev. B43, 6280 (1991)
[5] P. Villars and J.C. Phillips, Phys. Rev. B37, 2345 (1987)
[6] D. G. Pettifor J. Mater. Sci. Technol. 4, 674 (1988)
[7] J. Friedman, Technical Report No.102, Lab. for Computational Statistics, Stanford University, Nov 1988.
[8] See, for example, D. Rodgers and A.J. Hopfinger, Journal of Chemical Information and Computer Science 34, 854 (1994).
[9] D. Rogers (unpublished)
[10] R.N. Silver, D.S. Sivia, J.E. Gubernatis, Phys. Rev. B41, 2380 (1990)
[11] D.M. Deaven, K.M. Ho, Phys. Rev. Lett. 75, 288 (1995)
[12] A. Thust, M. Lentzen, K. Urban, Ultramicrosopy 53, 101 (1994)

Boundary lubrication: layering transition for curved solid surfaces with long-range elasticity

B.N.J. Persson
Institute Theory I

The properties of an atomic lubricant confined between two approaching surfaces are investigated by molecular dynamics. In the limit of thin interfaces, the lubricant atoms form well defined layers, whose number decreases in discontinuous steps with increasing applied pressure. These transitions occur easily and completely for unpinned lubricant films, while they are sluggish and incomplete in the case of strong pinning. Before the transition, an intermediate phase arises, which facilitates the thinning of the lubricant. Lateral sliding of the surfaces enhances the thinning rate.

F&E-Nr: 23.20.0

Sliding friction is one of the oldest problems in physics, and has undoubtedly a huge practical importance [1]. In recent years, the ability to produce durable low-friction surfaces and lubricant fluids has become an important factor in the miniaturization of moving components in technologically advanced devices. For those applications, the interest is focused on the stability under pressure of thin lubricant films, since the complete squeeze out of the lubricant from an interface may give rise to cold-welded junctions, resulting in high friction and catastrophically large wear.

We have investigated the late stages of the approach of two elastic solids limited by two curved surfaces, wetted by an atomic lubricant film of microscopic thickness [2]. Under these conditions, the behavior of the lubricant is mainly determined by its interaction with the solids, that induces a 2D order along the surfaces, and layering in the perpendicular direction. We focus on the atomic processes by which the thickness of the interface decreases by discontinuous steps, corresponding to the decrease in the number n of lubricant layers. For solid surfaces that approach without lateral sliding, separated by unpinned or weakly pinned (incommensurate) lubrication layers, fast and complete layering transitions occur. Commensurate or strongly pinned incommensurate layers lead to sluggish and incomplete transitions, often leaving islands trapped in the contact region. In fact, for commensurate layers we observe that it is nearly impossible to squeeze out the last few layers simply by increasing the perpendicular pressure. However, the squeeze-out rate is greatly enhanced by lateral sliding, since, in this case, the lubricant film can turn into a fluidized or disordered state, facilitating the ejection of one layer.

We have performed simulations for three different cases. In all cases the lubricant is Xe, but we have varied the Xe-substrate interaction potential so that a monolayer film of lubrication atoms forms unpinned (case A) or pinned (case B) incommensurate layers, or a commensurate layer (case C). The block is 100Å thick, with the same elastic modulus as of steel. The upper surface of the block is "glued" to a rigid surface profile with a cosine corrugation in the x-direction, and constant in the y-direction, and periodic boundary conditions are used in the xy-plane. The amplitude of the cosine corrugation is large enough that during all stages in the squeeze out, there is "empty" space in some regions between the block and the substrate, into which the lubrication fluid can be squeezed without building up a hydrostatic pressure. The substrate is only one atomic layer thick, and is "glued" onto a flat rigid surface, which is kept fix in space. In all the computer simulations, the upper rigid surface profile moves with a constant velocity towards the substrate, and the distance displayed in Fig. 1 is the displacement of the upper rigid surface profile towards the substrate rigid surface, where $d = 0$ correspond to an (arbitrary) starting point where the two elastic solids with lubrication layers are nearly in contact.

A. Incommensurate layer (unpinned)

Fig. 1A shows the average perpendicular stress acting on the substrate as a function of the displacement of the block towards the substrate, for two different temperatures, $T = 50$K and 300K, where (for clarity) the latter curve is displaced towards negative pressure by 0.2GPa. The block and the substrate are initially separated by about four Xe-monolayers. The three "bumps" on the curves correspond to the layering transitions (with increasing pressure) $n = 4 \rightarrow 3$, $3 \rightarrow 2$ and $2 \rightarrow 1$. We observe that these transitions, in particular the $n = 2 \rightarrow 1$ transition, are rather abrupt, and are marked by a significant pressure drop. The latter implies that the squeeze-out occur so rapidly that during the transition, the upper surface has moved only a small fraction of the diameter of the Xe-monolayer. Note that the layering transitions occur at higher pressures at low temperature, indicating that they are thermally activated.

Fig. 2(top) shows a sequence of snapshot pictures of the central interface region during squeeze at $T = 300$K. The time (in natural units $\tau \approx 2.9$ps) of each snapshot picture is indicated. The open circles denote the bottom layer of block atoms and top layer of substrate atoms.

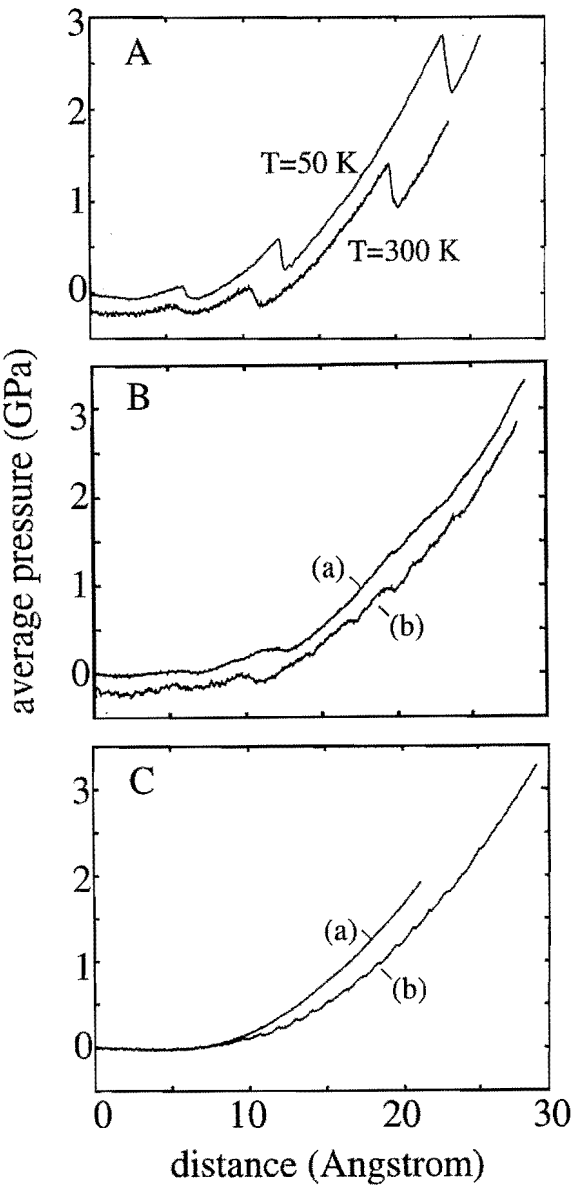

FIG. 1. The dependence of the average pressure on the distance the upper surface of the block has moved towards the bottom surface of the substrate. (A) Results for model A for two different temperatures, $T = 50$K and $T = 300$K, and with the squeeze velocity $v_z = 3$m/s. (B) Results for model B at $T = 200$K and for (a) squeezing with $v_z = 4.4$m/s and (b) squeezing ($v_z = 4.4$m/s) and sliding at $v_x = 17.7$m/s. (C) Results for model C at $T = 80$K and for (a) squeeze with $v_z = 4.6$m/s and (b) squeezing ($v_z = 4.6$m/s) and sliding at $v_x = 18.3$m/s.

Fig. 2(bottom) shows snapshot pictures of the lubrication film during the nucleation of the squeeze out $n = 2 \rightarrow 1$. Immediately before the nucleation of the layering transition the lubrication film in the central region has undergone a phase transformation and now exhibits fcc(100)-layers parallel to the solid surfaces. Since the fcc(100)-layers have a lower concentration of Xe atoms than the hexagonal layers (assuming the same nearest neighbor Xe-Xe distance), a fraction of the Xe-solid binding energy is lost during this transformation. On the other hand the solid surfaces can now move closer to each other (since the distance between the fcc(100)-layers is smaller than between the hexagonal layers) and in this way elastic energy is released. After the phase transformation, the layering transition $n = 2 \rightarrow 1$ can occur much more easily since density fluctuations (opening up of a "hole") require less energy in the more dilute fcc(100) layers than in the higher density hexagonal layers.

B. Incommensurate layer (pinned)

Fig. 1B shows the average perpendicular stress acting on the substrate (or block) as a function of the displacement of the block towards the substrate. The upper curve (a) is without lateral sliding ($v_x = 0$) while the lower curve (b) is for $v_x > 0$. For clarity the latter curve is displaced towards negative pressure by 0.2GPa. Note that in contrast to case A, in the present case, where the lateral atomic corrugation experienced by the lubrication atoms is much higher, the squeeze out is more sluggish, and only very weak bumps corresponding to the $n = 4 \rightarrow 3$ and $n = 3 \rightarrow 2$ transitions can be detected in the upper curve.

In case (a) it is found that at the end of squeezing in Fig. 1B, a trapped $n = 2$ island occurs, surrounded by a single Xe-monolayer. Fig. 3 shows snapshot pictures of the trapped island. Trapped islands have recently been observed experimentally [3]. During squeezing *and* sliding the $n = 2 \rightarrow 1$ transition is complete, i.e., no $n = 2$ island remains trapped.

C. Commensurate layer

Fig. 1C shows the average perpendicular stress acting on the substrate (or block) as a function of the displacement of the block towards the substrate. The upper curve (a) is without lateral sliding ($v_x = 0$) while the lower curve (b) is for $v_x > 0$. Note that the commensurate adsorbate layers are strongly pinned, and even though the Xe-substrate binding energy in the present case is much smaller than for case A, it is (if no lateral sliding occurs) difficult to squeeze out the lubrication film. Thus at the end of the squeeze-out process in Fig. 1C (no sliding) the surfaces are still separated by four Xe-layers, just as at the beginning of squeeze-out. However, lateral sliding tends to break up the pinning (e.g., fluidization of the adsorbate layer may occur), and during sliding it is much easier to squeeze out the lubrication layer, and at the end of squeeze-out [curve (b)] only one Xe-layer remains between the surfaces in the high-pressure region.

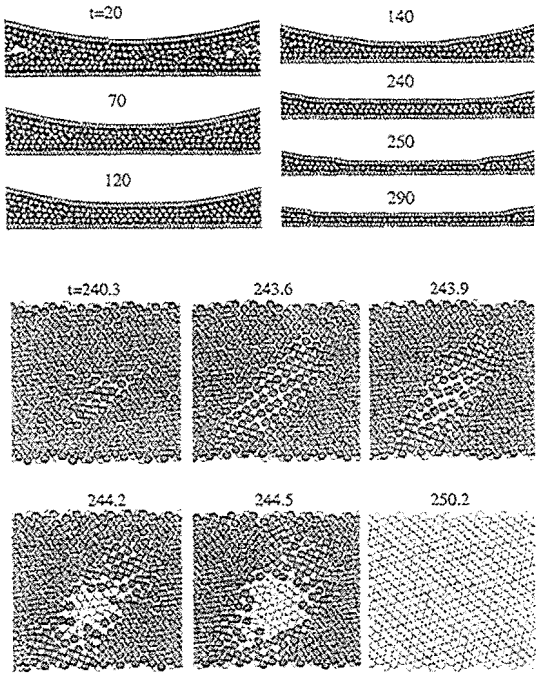

FIG. 2. Top: Snapshot pictures during squeeze-out. The time of each snapshot is indicated. Bottom: Snapshot pictures of the lubricant layer for times close to the point where the $n = 2 \rightarrow 1$ squeeze out transition occur. The first and second monolayer atoms are indicated with different grey-scale. For model A at $T = 300$K.

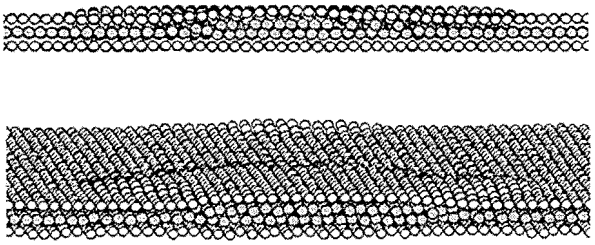

FIG. 3. Snapshot pictures, at two different view angles, of the trapped island. For model B at $T = 200$K.

[1] B.N.J. Persson, *Sliding Friction: Physical Principles and Applications*, Springer (Heidelberg) 1998; Surf. Sci. Rep. **33** 83 (1999).

[2] B.N.J. Persson and P. Ballone, submitted to prl; B.N.J. Persson and E. Tosatti, Phys. Rev. B**50** 5590 (1994).

[3] F. Mugele, and M. Salmeron, submitted to prl.

Chemical dynamics of pollutants in the atmosphere

H. Lustfeld
Institute Theory I

By modelling chemical reaction equations of the troposphere with 10 particularly important pollutants it is shown that these equations contain real or hidden instabilities. These occur for certain output strengths of pollutant sources like NO and CO and lead to fluctuations of pollutant concentrations by a factor of 10 in a few days. The instabilities are all of the Hopf type and a generalized time dependent Ginzburg Landau equation can explain the mechanism behind the huge fluctuations occuring in the chemical equations. The meaning of the results for pollutants in atmospheric flows is briefly discussed.

F&E-Nr: 23.15.0

The chemical reaction equations of pollutants in the troposphere are relatively well known[1]. Until recently it was believed that they always converge to a stationary state due to their dissipative character.

As is known from the theory of dynamical systems, however, dissipative systems may have periodic or even chaotic attractors. After periodic solutions [2] had been found in a simple model we investigated solutions of a model containing ten pollutants (NO, NO_2, O_3, CO, OH, HO_2, H_2O_2, $HCHO$, MO_2[2], CH_4) and the corresponding 32 chemical reactions that occur among them in the troposphere. The aim was to look for possible instabilities of this system and to elucidate the mechanism behind the nonstationary solutions. These have a characteristic structure: The concentrations vary slowly over a large time interval but suddenly undergo a drastic fluctuation on a time scale of a few days, (cf Fig. 1). *All* fixed points of the system (including the complex ones) could be detected by applying the Groebner basis scheme[3] [6]. It turns out that there is only one single physical fixed point which can become unstable and we concentrated on this fixed point. The onset of its instability depends on the strength of the pollutant sources NO_{source}, CO_{source} and the CH_4 concentration[4] that act as control parameters of the system. In a typical scenario beyond the instability threshould a slow variable, (the CO concentration,) starts moving away from the fixed point driving the subsystem to an instability. At this stage the slow variable acts as a control parameter of the subsystem. Finally the subsystem undergoes a subcritical Hopf bifurcation. After that it changes faster than exponentially. The hitherto slow variable (CO) becomes dynamic because of the coupling to the subsystem and returns to the vicinity of the (unstable) fixed point in which the subsystem becomes stable again. The fast motion of the subsystem stops and the slow motion described above starts again.

This phenomenon can be modeled by coupling a time dependent Ginzburg Landau equation to a further quantity. The result beyond the point of instability is shown in Fig. 2. The qualitative agreement between the model and the complicated chemical system is good indeed for the aforementioned scenario.

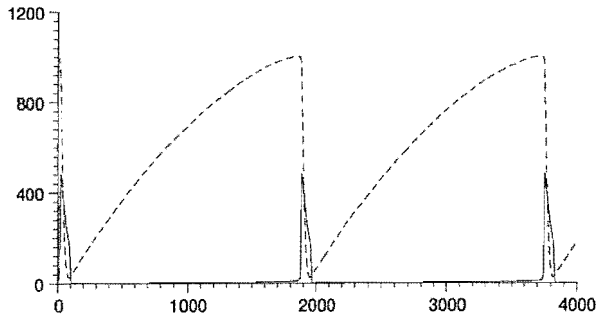

FIG. 1. pollutant concentrations of O_3 (solid line, in ppb) and CO (dashed line, in 0.1ppb) versus time (in days). concentration of CH_4: 1700 ppb. pollutant source strengths: $CO_{source} = 2.75 \cdot 10^6 cm^{-3} sec^{-1}$, $NO_{source} = 4.5 \cdot 10^6 cm^{-3} sec^{-1}$.

[1]The equations were first established by F. Stockwell [1] and part of various computer codes.

[2]MO_2 is a methyl peroxy radical.

[3]The Groebner basis scheme was successfully applied to a simpler model [5] and to the present one [3]. It failed when applied to a model with 14 pollutants [4].

[4]Because of their slow variation we keep CH_4 as a parameter here.

When incorporating the transport by the atmospheric flows the chemical dynamics of the pollutants will change, of course. First of all very long periods of the chemical dynamics cannot be detected. However, the strong fluctuations of the trajectories should remain important because they lead to changes of the pollutant concentrations witin a few days.

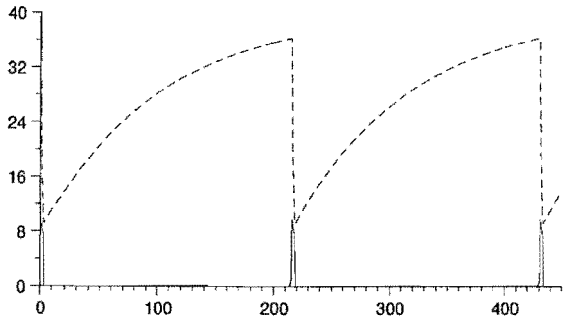

FIG. 2. result of model equations simulating the abrupt change of the real system, shown in Fig. 1. The units are arbitrary.

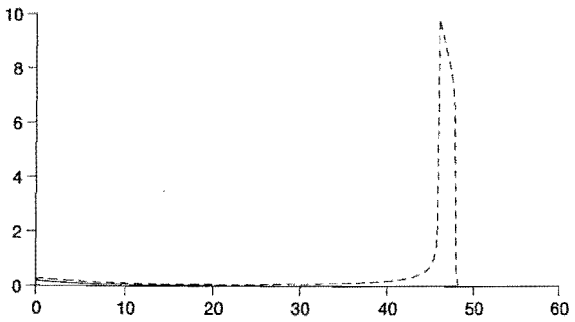

FIG. 3. Hidden instabilities occur in the real as well as in the model system. Here a hidden instability of the model system is shown. Solid line: a small perturbation decays exponentially. Dashed line: a slightly larger perturbation gives rise to a strong peak as in Fig. 2 before the system returns to the (globally) stationary state.

Note that even *globally stable* fixed points can give rise to these fluctuations: A perturbation driving the subsystem beyond the subcritical Hopf bifurcation leads to such an effect. We call this a hidden instability. In this case the region of stability of a stable fixed point is not identical to the basin of attraction. It is smaller and given by the neighborhood that excludes an instability of the subsystem. This is shown in Fig. 3.

The detection - even of long - periodic solutions in the chemical system can have a real meaning in that at least one Lyapunov exponent becomes nonnegative. If diffusion within the flow is neglected, the concentrations of pollutants become discontinuous. Such an effect has been demonstrated for a model consisting of one isolated vortex plus the reaction equations of the Brusselator and a point source located in the vortex stream [7]. The results demonstrate the much more important role of diffusion in such situations.

In summary, we have gained a relatively clear understanding of chemical dynamics in a model containing essential pollutants of the troposphere. Next we plan to investigate the full chemical system (RADM2) of pollutants in a similar manner as described here. Furthermore we have developed an approximation for 2 dimensional flows [8] and plan to incorporate transport in the chemical reaction equations.

---

[1] W.R. Stockwell J. Geophys. Res. **95**, 16334 (1990).

[2] D. Poppe and H. Lustfeld. J. Geophys. Res. **101**, 14373 (1996).

[3] S. Bröcheler, private communication.

[4] A. Dolzmann and T. Sturm, private communication.

[5] H. Lustfeld:
Instabilities of pollutant concentrations in the atmosphere due to chemical reactions in: A perspective look at nonlinear media in physics, chemistry and biology, editors: J. Parisi, S.C. Mller und W. Zimmermann, Springer 1998

[6] T. Becker and V. Weispfennig, Gröbner bases - a computational approach to commutative algebra, Springer, Berlin (1993).

[7] H. Lustfeld, Z. Neufeld, J.Phys. A (Math),**32**, 3717 (1999).

[8] J. Bene, S. Bröcheler, H. Lustfeld, preprint (1999).

Publications in refereed journals

Ballone P.; Marchi M.1
1CECAM, ENS Lyon and DBCM, CEA Saclay, France
Density Functional Study of a New Family of Anticaner Drugs: Paclitaxel, Taxotere, Epothilone, and Discodermolide
J. Phys. Chem. A, 103, 3097-3102, 1999
23.20.0

Ballone P.; Montanari B.; Jones R.; Hahn O.1
1MPI für Polymerforschung, Mainz
Polycarbonate Simulations with a Density Functional Based Force Field
J. Phys. Chem. A, 103, 5387-5398, 1999
23.20.0

Bringer A.; Eisenriegler E.; Schlesener, F.1; Hanke A.1
1FB Physik, Universität Wuppertal
Polymer Depletion Interaction between a Particle and a Wall
Eur. Phys. J. B11, 101-119, 1999
23.30.0

Dumas, P.1; Hein, M.2; Otto, A.2; Persson, B.; Rudolf, P.3; Raval, R.4; Williams, G.P.5
1LURE and LASIR, Orsay, France
2Universität Düsseldorf
3LISE, Namur, Belgium
4University of Liverpool
5NSLS, BNL, Upton, USA
Vibrational Spectroscopy in the far- to mid-Infrared Range Using Synchrotron Radiation
Surface Science, 433-435, 797-805, 1999
23.20.0

Hanke A.1; Eisenriegler E.; Dietrich S.1
1FB Physik, Universität Wuppertal
Polymer Depletion Effects near Mesoscopic Particles
Phys. Rev. E, 59, 6853-6878, 1999
23.30.0

Jones R.
Cluster Geometries from Density Functional Calculations - Prospects and Limitations
Euro. Phys. J. D, 9, 1-4, 1999
23.20.0

Jones R.
Density Functional Study of Carbon Clusters C2n (2(n (16): I. Structure and Bonding in the Neutral Clusters
J. Chem. Phys., 101, 5189-5200, 1999
23.20.0

Liebsch A.
Theory of Sum Frequency Generation from Metal Surfaces
Appl. Phys. B, 68, 301-304, 1999
23.20.0

Liebsch A.; Goncalves S.1; Kiwi M.2
1Universidad Federal, Porto Alegre
2Universidad Catolica, Santiago de Chile
Electronic vs Phononic Friction of Xenon on Silver
Phys. Rev. B, 60, 5034-5043, 1999
23.20.0

Lustfeld H.; Neufeld Z.1
1Eötvös University, Budapest
Chemical Dynamics vs Transport Dynamics in a Simple Model
J. Phys. A, 32, 3717-3731, 1999
23.15.0

Montanari B.; Ballone P.; Jones R.
Density Functional Study of Polycarbonate. 2. Crystaline Analogs, Cyclic Oligomers, and Their Fragments
Macromolecules, 32, 3396-3404, 1999
23.20.0

Ortiz G.1; Harris M.2; Ballone P.
1Los Alamos National Laboratory, USA
2MPI für Festkörperforschung, Stuttgart
Zero Temperature Phases of the Electron Gas
Phys. Rev. Lett., 82, 5317-5320, 1999
23.20.0

Persson B.
Brittle Fracture of Polymers
J. Chem. Phys., 110, 9713- 9724, 1999
23.20.0

Persson B.
Sliding Friction
Surface Science Reports, 33, 83-120, 1999
23.20.0

Persson, B; Tosatti, E.1; Fuhrmann, D.2; Witte, G.2; Wöll, Ch.2
1ICTP/SISSA, Trieste, Italy
2Ruhr Universität Bochum
Low-Frequency Adsorbate Vibrational Relaxation and Sliding Friction
Phys. Rev. B, 59, 11777-11791, 1999
23.20.0

Volokitin, A.I.1; Persson, B.
1Samara University, Samara, Russia
Theory of Friction: Contribution from Fluctuating Electromagnetic Field
J. Phys. C, 11, 345-359, 1999
23.20.0

Other publications

Ballone P.; Andreone W.1
1IBM Research Division, Zürich
Density Functional Theory and Car-Parrinello Molecular Dynamics for Metal Clusters
In Metal Clusters, Ed. W. Ekardt, pp. 71-144, Wiley, New York, 1999
23.20.0

Invited talks

Eisenriegler E.
Colloids in polymer solution
Klausurtagung des SFB 513 "Nanostrukturen an Grenzflächen", 14.10.1999, Tschagguns, Austria
23.30.0

Eisenriegler E.
Polymers interacting with colloids
International Conference on Liquid Matter, 03-07.07.1999, Granada
23.30.0

Harris J.
The Seven Pillars of Wisdom: How shall we construct the house?
Materials Modelling Laboratory Workshop, 03.09.1999, University of Oxford
23.20.0

Jones R.
Dichtefunktional mit Molekulardynamik - Neue Anwendungen, neue Perspektiven
Graduierter Kolleg der Universität Regensburg, 22.07.1999
23.20.0

Jones R.
Structure, energies, and reactions in model polycarbonates
Tagung Arbeitsgruppe Parrinello, 19.01.1999, Schloss Ringberg

23.20.0

Liebsch A,
Linear and nonlinear time dependent response of metal surfaces
Workshop on Time Dependent Density Functional Theory, 15.04.1999, Institute of Theoretical Physics, Santa Barbara, USA
23.20.0

Liebsch A.
Electronic Excitations at Metals Surfaces
07.09.1999, Academy of Sciences, Prag
3.20.0

Liebsch A.
Elektronische Anregungen an Metalloberflächen: von der Reibung zur nichtlinearen Optik
04.05.1999, RWTH Aachen
3.20.0

Liebsch A.
Elektronische Anregungen an Metalloberflächen: von der Reibung zur nichtlinearen Optik
09.12.1999, Universität Würzburg
3.20.0

Liebsch A.
Elektronische Anregungen an Metalloberflächen: von der Reibung zur nichtlinearen Optik
19.05.1999, TU München
3.20.0

Liebsch A.; Liechtenstein A.1
1University of Nijmegen
Photoemission quasi-particle spectra of Sr2RuO4
Symposium on Surface Physics, 28.06-02.07.1999, Trest, Czech Repubic
23.20.0

Lustfeld H.
Reaktionsgleichungen in der Atmosphärenchemie und Groebner Basen
19.01.1999, Universität Passau
3.15.0

Persson B.
Brittle Fracture
International Meeting on the Dynamics of Fracture, 25-27.10.1999, Austin, USA
23.20.0

Persson B.
Dynamical processes at surfaces
XIV International School Seminar "Spectroscopy of Molecules and Crystals", 7-12.06.1999, Odessa, Ukraine
23.20.0

Persson B.
Sliding Friction
Annual Meeting on Condensed Matter Physics of the Brazilian Physical Society, 11-15.05.1999, Sao Lourenco, Brazil
23.20.0

Persson B.
Sliding Friction
GAMM, 12-16.04.1999, Metz, France
23.20.0

Persson B.
Sliding Friction
Gordon Research Conference on "Dynamics at Surfaces", 08-13.08.1999, Andover, USA
23.20.0

Persson B.
Sliding Friction
International Meeting on Wetting, 15-18.06.1999, Trieste, Italy
23.20.0

Other talks

Harris J.
Computational Methods in Materials Science
Seminar, 16.04.1999, National Research Council of Canada, Ottawa, Canada
23.20.0

Harris J.
Computational Methods in Materials Science: Advances and Limitations
Seminar, 08.07.1999, National Center of High-Speed Computing, Shinsu, Taiwan
23.20.0

Harris J.
Dichte-Funktional-Theorie: Aspekte zur Anwendung
Seminar, 15.12.1999, Ringvorlesung Rechenverfahren in der Quantenchemie, FB Chemie, TU Darmstadt
23.20.0

Jones R.
Density functional studies of organic systems - Structure, vibration frequencies, and reactions in polycarbonates
Kolloquium, 19.05.1999, Dept. of Chemistry, Rutgers University, Piscataway, USA
23.20.0

Jones R.
Density functional studies of organic systems - Structure, vibration frequencies, and reactions in polycarbonates
Kolloquium, 20.05.1999, Dept. of Chemistry, Princeton University, Princeton, USA
23.20.0

Jones R.
Density functional studies of polycarbonate systems - Structure, vibration frequencies, and reactions
Kolloquium, 17.05.1999, Dept. of Chemistry, University of Pennsylvania, Philadelphia, USA
23.20.0

Jones R.
Density functional studies of polycarbonate systems - Structure, vibration frequencies, and reactions
Seminar, 26.05.1999, General Electric Research and Development Laboratories, Schenectady, USA
23.20.0

Jones R.
Geometrie und Spektroskopie von atomaren Clustern - Möglichkeiten und Grenzen von Dichtefunktionalrechnungen
Seminar, 02.07.1999, Physikalisches Institut, Universität Hamburg
23.20.0

Jones R.
Simulations of polycarbonate systems - Density functional studies of structure, vibration frequencies, and reactions
Kolloquium, 08.12.1999, Dept. of Polymer Science and Engineering, University of Massachusetts, Amherst, USA
23.20.0

Jones R.
Struktur und Spektroskopie von Kohlenstoffclustern - Möglichkeiten und Grenzen der Theorie
Seminar, 14.06.1999, I. Physikalisches Institut, Universität zu Köln
23.20.0

Jones R.

Thermal expansion of anisotropic materials - density functional study of high quartz systems
01.12.1999, Materials and Research Society Symposium, Boston, USA
3.20.0

Liebsch A.; Liechtenstein A.1
1University of Nijmegen
Photoemission quasi-particle spectra of Sr2RuO4
Workshop on Strong Correlations in Solids, 02-06.10.1999, Prag
23.20.0

Lustfeld H.
Dynamical flows and Poincaré maps of simple repellers
Seminar, 07.09.1999, Eötvös University, Budapest
23.15.0

Persson B.
Brittle Fracture
APS Meeting, 21-25.3.1999, Atlanta, USA
23.20.0

Persson B.
Layering transition in molecular thin lubrication films
APS Meeting, 21-25.3.1999, Atlanta, USA
23.20.0

Lecture courses

Eisenriegler E.
Kritisches Verhalten begrenzter Systeme
SS 99, Universität Düsseldorf, V 2

Lustfeld H.
Wavelets in der Physik mit Beispielen in C++
WS 99/00, Universität Duisburg, V 2, Ü 1

Sturm K.
Elektronentheorie
WS 98/99, 30. IFF-Ferienkurs "Magnetische Schichtsysteme", 01-12.03.1999

Sturm K.
Elektronische Anregungen im Festkörper
SS 99, Universität Düsseldorf, V 2

Institute Theory II

General Overview

Introduction: Soft Matter Research

The main research topic of the Institute is the theory of "complex fluids" and "soft matter" systems. Soft matter physics is an interdisciplinary research area encompasing statistical physics, material science, chemistry, and biology. The systems are characterized by

- Supramolecular structure and self-assembly
- Typical length scales ranging from nano- to micro-meters
- Typical energy scales comparable to the thermal energy k_BT.

Classical examples of complex fluids are

- Polymer solutions, mixtures, and melts
- Mixtures of block copolymers and homopolymers
- Lyotropic liquid crystals
- Amphiphilic systems, i.e. mixtures of oil, water and amphiphiles
- Colloidal suspensions.

While these areas remain active fields of research, the focus has recently shifted to more complex systems which are obtained by combining two or more of the components listed above. A few examples are

- Colloidal particles in polymer solutions
- Mixtures of surfactants and amphiphilic block-copolymers
- Mixtures of several surfactants or lipids
- Colloids in liquid crystals

This brings the systems which are studied in physics closer to applications in material science or biology.

Since the structures in soft matter systems often contain a large numer of molecules, *mesoscale modelling* is typically required to bridge the length- and time-scale gap between the microscopic domain — of atoms and their interactions — and the emerging properties of supramolecular assemblies on meso- or macroscopic scales. Microscopic models are employed to study properties of complex systems on the molecular scale, and to provide a link of mesoscale models to molecular architecture.

A large variety of methods is used to study soft matter systems. In fact, a combination of analytical and numerical methods is often needed to successfully characterize these complex systems. In particular, simulation methods (Monte Carlo, molecular dynamics), computational hydrodynamics, field theory, perturbation theory, and exact solutions are employed in our institute.

A characteristic feature of soft-matter research is the fruitful interaction between theory and experiment. With a third of the IFF institutes [Neutron Scattering (Richter), Theory II and (starting January 2000) Soft Matter (Dhont)] now focusing on soft matter research, many of the essential aspects of these systems are investigated here.

Some Remarks:

1999 has been a year of change in the group. Prof. Kehr, who was the acting director of the group for several years (1994-1999) until my arrival in March '99, retired last summer. I would like to use this opportunity to thank him for his leadership during this period. I hope that he will be a regular visitor in the institute for years to come.

Prof. Baumgärtner, who was a member of the "Forum Modellierung" from 1997 to 1999, has returned to the group at the beginning of this year. He will strengthen the research activity on biological systems.

Prof. Eisenriegler is currently a member of the Institute Theory I. Since his work is part of soft matter research, his research projects are described here as part of the "Theory II" research activities. It is intended that he will formally become a member of "Theory II" this year.

Research projects and results:

(in alphabetic order)

1. *Polymer-induced depletion interaction between a particle and a wall:*
   The motivation to study this geometry comes from experiments which can measure the interaction of an *individual* colloidal particle with a wall. For ideal, flexible polymers we obtain the potential of mean force for *arbitrary* distance and particle-to-polymer size ratio. While for large particles the force decreases monotonically with increasing distance, for small particles we find a force-*maximum*. (Eisenriegler, Bringer, Schlesener, Hanke)

2. *Small particles in solution of nonadsorbing polymers:*
   For colloidal particles much smaller than the polymer size and screening length a number of new exact results is derived. These encompass the depletion profile of the monomer density and the force between two particles in case of ideal chains, and the influence of the excluded volume interaction between chain monomers for the density distribution around one particle. Beyond their contribution to the understanding of polymer depletion the results provide a check for more versatile but approximate methods. (Eisenriegler)

3. *Influence of inter-chain overlap on depletion effects in polymer solutions:*
   We investigate a boundary wall of and a spherical particle in a polymer solution with concentration up to and beyond the overlap concentration. This is relevant for experiments which in general operate in between the dilute and semidilute limits. (Eisenriegler, Maassen, Bringer)

4. *Cubic bicontinuous phases in ternary amphiphilic systems:*
   Interfaces in amphiphilic systems can often be well described by elastic sheets with bending rigidity κ, saddle-splay modulus $\bar{\kappa}$, and spontaneous curvature c_0. The amphiphilic monolayers in ternary mixtures with water and oil can arrange in different ways to form micellar, hexagonal, lamellar and various triply periodic, bicontinuous cubic phases. The relative stability of the latter phases can be explained by the way in which their universal geometrical properties conspire with the concentration constraints. (Gompper, Schwarz)

5. *Freezing of planar membranes:*
   The thermal behavior of membranes on mesoscopic scales can be modelled very successfully by dynamically triangulated surfaces, which consist of hard spheres connected by tethers. We study the transition form the fluid to the crystalline phase by reducing the tether length and thereby increasing the in-plane density. For planar systems, a two-stage freezing transition is observed, with a very narrow region of stability of the hexatic phase. (Gompper, Kroll)

6. *Dynamics of swollen lamellar phases:*
   Among the large variety of phases, which appear in amphiphilic systems, the lamellar phase plays a key role for the understanding of the physical properties of these systems, since its simple geometry allows for detailed theoretical and experimental investigations. We study the relaxation rates of lamellar phase in a ternary system of water, oil and amphiphile, which are governed by the hydrodynamics of the fluid layers. A direct comparison with light scattering and neutron-spin-echo experiments is possible. (Gompper, Theissen)

7. *Wetting behavior in amphiphilic systems:*
   Due to the strong reduction of the interfacial tension of water-oil and water-air interfaces in the presence of amphiphilic molecules, the wetting behavior of these systems is very interesting. We calculate the contact angles of a microemulsion drop at the water-air interface, as a function of amphiphile chain lengths and temperature. [Supported by DFG priority program "Wetting and Structure Formation at Interfaces".] (Gompper, Schilling)

8. *Multidimensional NMR and the dynamics of complex molecules*
   The effect of the slow dynamics of polymers in melts — which is due to entanglements and repulsive inter-chain interactions — on two-dimensional NMR spectra is investigated. The motion of the polymers is simulated by the bond-fluctuation model, and the correlation functions which yield the 2-D NMR spectra are estimated. Differences in the dynamics of mid- and end-segments are predicted to be clearly visible. (Kehr, Krenzlin)

9. *Diffusion in glasses*
   The diffusion of interstitial particles in disordered systems without lattice translational invariance is investigated by a novel Monte Carlo approach. Experimental and simulated structures of silicate and alkali-silicate glasses are used to calculate the positions and energies of the minima and saddle points for the interstitials. The resulting transition rates are then utilized in Monte Carlo simulations, which can be extended to sufficiently long times to extract asymptotic diffusion coefficients. These show approximate Arrhenian behavior as functions of inverse temperature. (Kehr, Mussawisade)

10. *Reptation dynamics in polymer melts:*
    The dynamics of polymer melts and concentrated solutions can be described by the reptation model of Edwards, de Gennes and Doi. We have developed a lattice gas model for reptation which incorporates the collective effects of the entanglement network on the dynamics of a single polymer. It turns out that the predictions of the model are in very good agreement with experimental data for the tube length relaxation. (Schütz)

11. *Phase transitions in driven diffusive systems:*
    Shocks in driven particle systems are analogous to domain walls in equilibrium systems. We have found a heuristic criterion for the stability of a shock which follows from the macroscopic current-density relation. Investigation of a specific model has given further evidence that in homogeneous low-dimensional non-equilibrium systems phase transitions occur only for vanishing local hopping rates. (Schütz, Popkov, Helbing, Mukamel)

12. *Quantum spin chains far from equilibrium:*
    Non-stationary initial states of the XY quantum chain at T=0 are shown to evolve into a stationary current-carrying state selected by an extremal principle obtained through a Lagrange multiplier method. In the presence of a local conservation law one observes quantum aging phenomena even though no coarsening takes place. (Schütz, Antal, Rákas, Rácz, Trimper)

Awards etc.:

- G. Schütz spent the summer semester 1999 as visiting professor at the Universität Essen.
- G. Schütz has received a *Heisenberg-Stipendium* by the Deutsche Forschungsgemeinschaft, which is intended for the support of highly qualified young scientists.
- G. Schütz will be awarded the *Gustav-Hertz Preis 2000* by the Deutsche Physikalische Gesellschaft, in recognition of an excellent recently completed research project from the group of young scientists.
- Prof. Ted Burkhardt (Temple University, Philadelphia, USA) has received an award from the *Alexander von Humboldt Stiftung*, which he used to spend half a year (Sept. 1999 to Febr. 2000) as a visiting scientist at the IFF.

Gerhard Gompper

Personnel 1999/2000 and areas of activity

Scientific Staff

Dr. A. Baumgärtner	Statistical mechanics of proteins and membranes; Member of Forum Modellierung until Dec.1999	23.30.0
Dr. G. Gompper Institute Director	Statistical mechanics of amphiphilic systems	23.30.0
Prof. K. Kehr	Diffusion and relaxation in disordered systems	23.30.0
Dr. G. Schütz	Driven diffuse systems, reptation models	23.30.0

Technical Staff

H. Paffen	Secretary	

Graduate Students

M. Krenzlin	Dynamics of complex molecules by multi-dimensional NMR	23.30.0
K. Mussawisade	Diffusion in disordered materials	23.30.0
J.-H. Lin	Membrane proteins	23.30.0
T. Schilling	Wetting in amphiphilic systems	23.30.0

Guests

Prof. T. Burkhardt	(Temple University, Philadelphia, USA) Statistical mechanics of polymers; stochastic processes (Sept. 1999 - Febr. 2000)	23.30.0
Dr. Z. Koza	(University of Wroclaw, Poland) Driven lattice gas models (Mar. - May 1999)	23.15.0
Dr. D.M. Kroll	(University of Minnesota, Minneapolis, USA) Statistical mechanics of membranes (Oct. 1999)	23.30.0
Dr. K.P.N. Murthy	(IGCAR, Kalpakkam, India) Relaxation processes in glasses (July - Oct. 1999)	23.30.0
C. Pigorsch	(Universität Halle) Driven many-body systems (Nov. - Dec. 1999)	23.15.0
Dr. V. Popkov	(Inst. for Low-Temperature Physics, Kharkov, Ukraine) Reptation models; driven many-body systems (Sept. 1998 - Sept. 1999)	23.15.0
Dr. J. Santos	(TU München) Reptation models (Mar. 1999)	23.30.0

Colloid-polymer entropic interaction for small particle-to-polymer size ratio

E. Eisenriegler
Institutes Theory I and II

We consider the interaction between mesoscopic colloidal particles and nonadsorbing polymer chains in solution. In particular we show how the polymer-induced force between two particles is related to the local monomer density near the surface of one of the particles. The bulk-normalized density profile is independent of the Flory radius and Edwards screening length for particles much smaller than these lengths. For the case of the density profile around a single particle the influence of the excluded volume interaction between chain monomers is also studied.

F&E-Nr.: 23.30.0

Colloid science covers a broad class of substances encompassing milk, blood, and paints. A major goal is to understand the effective interactions between the mesoscopic colloidal particles such as the casein micelles in skim milk, the red cells in blood, etc. We concentrate on effective interactions induced by the solvent which in general is a complex fluid by itself and may contain several constituents. On varying their concentration, the effective interactions can be *tuned*, e.g. to provide in case of a solution of globular proteins conditions favorable for crystallization.

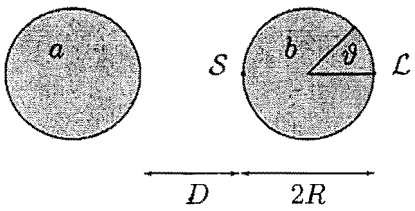

FIG. 1. Two spherical particles: The chains avoid the space between the particles and the density is smaller near the surface point S than near the surface point $\mathcal{L}$. The angle ϑ is introduced for later use in Eq. (1).

One important case is the interaction induced between rigid particles by adding nonadsorbing free polymer chains. For entropic reasons nonadsorbing chains avoid the space between two particles (see Fig. 1), leading to an unbalanced pressure from outside which pushes the two particles towards each other. Detailed information about the entropic polymer depletion near the colloidal particles is contained in the density profile $\mathcal{M}(\mathbf{r})$ describing the spatial distribution of chain material around them . Recent experiments were able to measure polymer depletion forces for an isolated pair of immersed particles.

The polymer depletion effect near a single immersed spherical particle crucially depends on the ratios of its radius R and the mesoscopic lengths such as the unperturbed chain size (Flory radius) $\mathcal{R}$ or the mesh size (screening length) ξ [1] of the embedding dilute or semidilute polymer solution. For large particle size $R \gg \mathcal{R}, \xi$ the depletion closely resembles that for a planar wall. Here we consider the other extreme of *small particle size* $R \ll \mathcal{R}, \xi$ –sometimes referred to as the 'protein limit'– and study the depletion of $\mathcal{M}(\mathbf{r})$ near one and two particles in the solution. We normalize $\mathcal{M}$ so that it approaches 1 in the bulk solution. The small particle case is dominated by configurations where the chain coils around the particle(s), see Fig. 2.

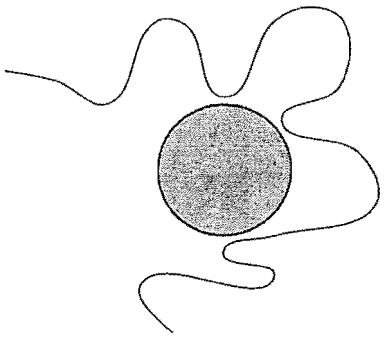

FIG. 2. A long chain coiling around a small mesoscopic particle.

Therefore, a single small spherical particle significantly perturbs the bulk density only within a distance of order R from its surface, and the normalized density profile is independent of $\mathcal{R}$ or ξ. In particular, the profile is the same for a dilute and a semidilute embedding polymer solution. Interpenetration effects of different chains in a semidilute solution do not show up on length scales R much smaller than ξ. This should be compared with the case of a *large* particle or a planar wall, in which the corresponding 'healing' distance of the profile is of order $\mathcal{R}$ for a dilute and of order ξ for a semidilute solution. We note that the widely used Asakura-Oosawa approximation, which treats the chains as non-deformable, fails completely in the case of small particles, even for a dilute polymer solution.

Consider first the simple case of ideal, random-walk like, chains without self avoidance, which is realized for a solution in three dimensions at the theta point. Besides the density $\mathcal{M}(\mathbf{r})$ of chain monomers we also consider the bulk-normalized density $\mathcal{E}(\mathbf{r})$ of chain ends. The $\mathcal{R}$-independent densities $\mathcal{M}$ and $\mathcal{E}$ around a small particle can be easily calculated if the chains are ideal. In this

case $\mathcal{M} = \mathcal{E}^2$, where $\mathcal{E}$ is a harmonic function [1] given by [2,3] $\mathcal{E} = 1 - \rho^{-(d-2)}$ with $\rho = r/R$, r being the distance from the center of the sphere, and d the spatial dimension.

For ideal chains interacting with *two* particles (Fig. 1) of equal radius R, closest surface-to-surface distance D, and $R, D \ll \mathcal{R}$, the harmonic function $\mathcal{E}(\mathbf{r})$ which vanishes at the particle surfaces, and $\mathcal{M} = \mathcal{E}^2$ can also be calculated. In particular, one may evaluate $\mathcal{M}$ near the surface of one of the particles, say particle b, in which case $\mathcal{M}(\mathbf{r}) \to (r_b - R)^2 (\partial_\perp \mathcal{E})^2$. Here $\partial_\perp$ is a normal derivative at the surface S_b, and r_b is the distance of $\mathbf{r}$ from the center of particle b.

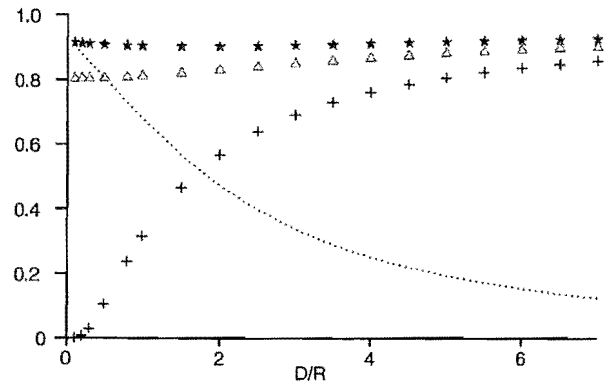

FIG. 3. Density-force relation for two spherical particles a and b in a solution of ideal chains in three dimensions (see Eq. (1) and Fig. 1). The monomer density and the local pressure along the surface S_b of particle b are proportional to $(\partial_\perp \mathcal{E})^2$, see text. Results for $R\,\partial_\perp \mathcal{E}$ at surface points with $\cos\vartheta = 1$ (point $\mathcal{L}$ in Fig. 1), $\cos\vartheta = 0$ and $\cos\vartheta = -1$ (point $\mathcal{S}$ in Fig. 1) are denoted, respectively, by asterisks, triangles, and crosses. The magnitude of the scaled total force $f/(k_B T n \mathcal{R}^2/3)$ acting on particle b is given by the dotted line.

Since the number of monomers per ideal chain is proportional to the mean square end-to-end distance $\mathcal{R}^2$ of the unperturbed chain, $\mathcal{R}^2 n \mathcal{M}$ is a convenient measure for the monomer density in terms of the bulk-normalized density $\mathcal{M}$ of the monomers and the bulk density n of the chains. The local pressure which the polymers exert on a surface element dS_b of particle b is proportional to the local monomer density. This is the basis of the density-force relation [3,4], which for our long ideal chains reads

$$\frac{1}{2d}\,\mathcal{R}^2\, n \int dS_b\, (\partial_\perp \mathcal{E})^2\, \cos\vartheta = f/k_B T\,. \qquad (1)$$

Here f is the magnitude of the total force pushing particle b towards particle a, and $\cos\vartheta$ is the projection of the inward pointing surface normal onto the direction of the total force (see Fig. 1). The quantity $R\,\partial_\perp \mathcal{E}$ is a function of D/R and the angle ϑ which can be expressed in closed analytic form [4]. Results are shown in Fig. 3: The monomer density and local pressure is larger near the surface point $\mathcal{L}$ with $\eta = \cos\vartheta = 1$ than near the surface point $\mathcal{S}$ with $\eta = \cos\vartheta = -1$. After substituting the expression for $\partial_\perp \mathcal{E}$ into (1), the integration over the surface of particle b can be done analytically and leads to a scaled force $f/(k_B T n \mathcal{R}^2/3)$, which is also shown in Fig. 3.

Finally we discuss the effect of the excluded volume interaction (EVI) between chain-monomers in a good solvent in which a single small spherical colloidal particle is immersed. In this case $\mathcal{M}$ has a form *different* from the result for ideal chains given above. In the limit in which $\mathbf{r}$ is far away from the sphere, one finds that

$$\mathcal{M} \to 1 - \alpha\, \rho^{-x} \quad , \quad R \ll r\,. \qquad (2)$$

Here $x = d - 1/\nu$, with ν the Flory exponent [1], and α is a universal amplitude. Table I shows that x and α are larger and smaller, respectively, than the results $x_{\rm id} = d - 2$ and $\alpha_{\rm id} = 2$ for ideal chains. Thus the EVI leads to a *smaller* depletion effect. In the other limit in which $\mathbf{r}$ is close to the surface of the sphere,

$$\mathcal{M} \to \beta\, (\rho - 1)^{1/\nu} \quad , \quad r - R \ll R\,. \qquad (3)$$

Here β is another universal amplitude. In this limit the EVI also leads to a decrease in the depletion effect, compare the values of $1/\nu$ and β in Table I which are smaller and larger, respectively, than the values $1/\nu_{\rm id} = 2$ and $\beta_{\rm id} = (d-2)^2$ for ideal chains.

TABLE I. Exponents and amplitudes in the power law behavior for $r/R \to \infty$ and $r/R \to 1$ of the monomer density profile around a single spherical particle in spatial dimension d.

d	x	$x_{\rm id}$	α	$\alpha_{\rm id}$	$1/\nu$	$1/\nu_{\rm id}$	β	$\beta_{\rm id}$
4	2	2	2	2	2	2	4	4
3	1.33	1	≈ 1.3	2	1.67	2	≈ 1.3	1
2	2/3	-	1.061	-	4/3	-	0.812	-

For the case of two dimensions ($d = 2$), i.e. for a solution of self-repelling chains in a *plane* outside a circular disc, $\mathcal{M}$ can be obtained in closed form for *arbitrary* r/R [4].

The decrease of the depletion effect around a small particle due to the excluded volume interaction between chain monomers was overlooked in previous work [2].

[1] P.G. de Gennes, *Scaling Concepts in Polymer Physics* (Cornell University, Ithaca, 1979).

[2] T. Odijk, Macromolecules **29**, 1842 (1996); J. Chem. Phys. **106**, 3402 (1996).

[3] See A. Hanke et al., Phys. Rev. E **59**, 6853 (1999), A. Bringer et al., Eur. Phys. J. B **11**, 101 (1999), and references cited therein.

[4] E. Eisenriegler, invited lecture at the 4th EPS Liquid Matter Conference, Granada 3-7 July 1999; to appear in J. Physics: Condensed Matter.

Stability of bicontinuous cubic phases in ternary amphiphilic systems with spontaneous curvature

U. S. Schwarz[1,2] and G. Gompper[1,3]
[1]MPI für Kolloid- und Grenzflächenforschung, 14476 Golm
[2]The Weizmann Institute of Science, Rehovot 76100, Israel
[3]Institute Theory II

Interfaces in amphiphilic systems can often be well described by elastic sheets with bending rigidity κ, saddle-splay modulus $\bar{\kappa}$, and spontaneous curvature c_0. The amphiphilic monolayers in ternary mixtures with water and oil can form micellar, hexagonal, lamellar and various bicontinuous cubic phases. For the latter case, we consider triply periodic surfaces of constant mean curvature of the families G, D, P, C(P), I-WP and F-RD. The relativ stability of these phases can be explained by the way in which their universal geometrical properties conspire with the concentration constraints. The most stable bicontinuous cubic phases with decreasing $\bar{\kappa} < 0$ are the single and double gyroid (G) structures since they combine favorable topological properties with extreme volume fractions.

F&E-Nr: 23.30.0

When a soap film is suspended in a closed wire frame, its shape is determined by its desire to minimize the surface area under the action of the surface tension. It is a straight-forward application of variational calculus to show that the minimization of surface area is equivalent to the requirement that the mean curvature

$$H = \frac{1}{2}\left(\frac{1}{R_1} + \frac{1}{R_2}\right) \tag{1}$$

vanishes at very point on the surface. Here R_1 and R_2 are the two principal radii of curvature. Therefore, surfaces with vanishing mean curvature are called minimal surfaces. A more general situation can also be considered, in which a pressure jump Δp occurs across the surface. In this case, the shape is determined by the Laplace equation

$$H = \frac{\Delta p}{\sigma} . \tag{2}$$

where σ is the surface tension. Such surfaces are called constant-mean-curvature (CMC) surfaces. Since pressure is a Lagrange parameter for volume, CMC surfaces occur when surfaces have to minimize their area under volume constraints.

Surfaces of constant mean curvature do not only occur in soap films and foams, but also for mono- and bilayers in amphiphilic systems. In this case, the area of the interface is fixed by the number of surfactant molecules, so that surface tension is irrelevant and shape is now controlled by the bending energy

$$\mathcal{H} = \kappa \int dS(H - c_o)^2 \tag{3}$$

where c_0 is the spontaneous curvature, which describes the preferred mean curvature of the interface. Obviously, CMC-surfaces follow from minimizing Eq. (3).

However, there is one big difference between soap films and amphiphilic membranes. Since no surface tension is present in the latter case and the spontaneous curvature introduces a new length scale, no wire frames are necessary to stabilize the surface. This applies, in particular, to minimal or CMC surfaces, which are triply periodic and divide space into two intertwined, space-filling labyrinths [1]. Before 1970, only three cubic minimal surfaces have been known (D, P, C(P)), compare Fig. 1. Then Schoen described five more (G, F-RD, I-WP, O,C-TO and C(D)). Today, some more examples are known, but none of them seems to be of physical relevance.

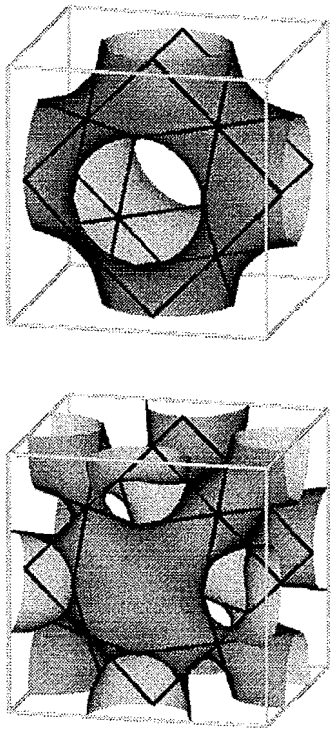

FIG. 1. Minimal surfaces P and C(P).

The aim of our work [2] is to study the stability of bicontinuous cubic phases in ternary amphiphilic systems as a function of the volume fractions ρ_O, ρ_W, and ρ_A of oil, water and amphiphilic, respectively, and of temperature - which determines the spontaneous curvature of the membrane. Our main assumption is that the membrane shape can be described by surfaces of constant mean curvature, as implied by the bending energy (3) without volume constraints. In this case, the curvature energy per unit volume takes the form

$$f(w,v,r) = wv\,[\Lambda(v)vw - 1]^2 + r\frac{(wv)^3}{\Gamma(v)^2} \qquad (4)$$

where $v = (\rho_O + \alpha\rho_A)$ is the hydrocarbon volume fraction, $w = \rho_A/[(\rho_O + \alpha\rho_A)c_0\ell]$ for amphiphiles of length ℓ and a hydrocarbon fraction $0 < \alpha < 1$, and $r = -\bar{\kappa}/2\kappa$ is the dimensionless saddle-splay modulus. All information about the geometry of the structure is contained in the dimensionless quantities

$$\Lambda(v) = \frac{HV}{A}\,, \quad \Gamma(v) = \frac{A^3}{2\pi|\chi_E|V^2} \qquad (5)$$

where A and χ_E are the area and Euler characteristic of the membrane within a unit cell, respectively, and V is the unit cell volume. It can be shown that both Λ and Γ are *independent* of the choice of the unit cell. In Eq. (4), the first contribution is the bending energy (3), the second derives from the Gaussian curvature (with the use of the Gauss-Bonnet theorem).

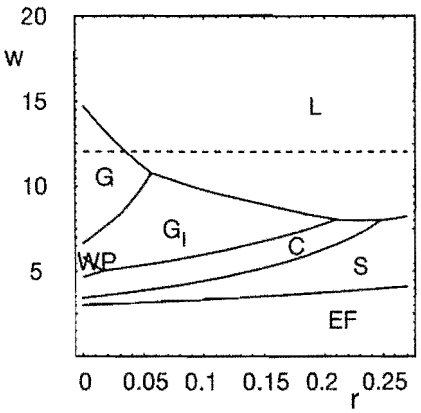

FIG. 2. Phase diagram as a function of w and r for $v = 0.2$. For $c_0\ell = 1/6$, only the area below the dashed line is mapped onto the Gibbs triangle. L: lamellar phase, S: spherical micelles, C: cylindrical micelles, EF: emulsification failure, G: single gyroid phase, G_I: double gyroid phase (water-filled bilayers).

We use data for $H(v)$ and $A(v)$ of Anderson [3] and Große-Brauckmann [4] for the D, P, C(P), I-WP, F-RD and G families of CMC surfaces to calculate the free energy (4) of the different cubic bicontinuous phases. For each family, we consider a *single* phase, where one monolayer separates an oil from a water labyrinth, and two *double* phases, where two monolayers form an water-filled (typ I) or an oil-filled (typ II) bilayer. The resulting phase diagram for fixed hydrocarbon volume fraction v is shown in Fig. 2. Note that w is proportional to the spontaneous radius of curvature, c_0^{-1}, and (for small ρ_A) to the amphiphile volume fraction ρ_A. Emulsification failure occurs at small w, i.e. not enough surfactant is present to solubilize all the oil. The most stable cubic bicontinuous phases are found to be the gyroid phases. As explained in detail in Ref. [2], this can be understood from the behavior of the geometrical quantities $\Lambda(v)$ and $\Gamma(v)$, which behave very characteristically for different CMC families and for single and double structures. In the phase diagram, cubic bicontinuous phases always occur between the lamellar and the cylindrical phases.

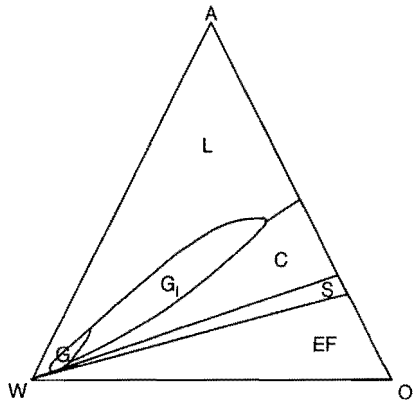

FIG. 3. Phase behavior in the Gibbs triangle for $r = 1/15$ and $c_0\ell = 1/12$.

The phase diagram of Fig. 2 can be mapped onto the Gibbs triangle, when a value for the spontaneous curvature is assumed, as shown in Fig. 3. In general, the predominance of the gyroid phases and their location in the phase diagram agrees well with experimental results; however, for a detailed comparison experimental data are still missing. We do not consider thermal fluctuations. They are expected to stabilize a disordered microemulsion as well as the double gyroid, which in fact can be considered to be a ordered microemulsion.

[1] U. S. Schwarz and G. Gompper, Phys. Rev. E **59**, 5528 (1999).

[2] U. S. Schwarz and G. Gompper, J. Chem. Phys. (to appear) (1999).

[3] D. M. Anderson, H. T. Davis, L. E. Scriven, and J. C. C. Nitsche, Adv. Chem. Phys. **77**, 337 (1990).

[4] K. Grosse-Brauckmann, J. Colloid Interface Sci. **187**, 418 (1997).

Relaxation of stretched DNA in concentrated solution

G.M. Schütz
Institute Theory II

We study the far-from-equilibrium relaxation of an initially stretched, entangled polymer by using an exactly solvable lattice gas model for reptation. Over a significant time range, including an initial universal power law regime, the predicted tube length relaxation is in very good agreement with experimental data for the relaxation of DNA. Experimental evidence and theoretical arguments suggest an observed systematic long-time deviation to be due to entanglement fluctuations. This view is confirmed by the analysis of an extension of the lattice gas model which appears to be a reliable foundation for further study of reptation dynamics.

F&E-Nr: 23.30.0

Polymers in concentrated solutions or melts are often compared with a spaghetti in a pasta dish. This analogy nicely demonstrates the obstacles a single polymer has to overcome in order to move. Indeed, the interactions between polymer chains in a concentrated solution of flexible polymers or in melts give rise to a rich variety of unusual properties, ranging from viscous flow on large time scales to glassy behaviour over short times. Various characteristic quantities such as the diffusion coefficient, mean entanglement distance etc. have been measured in the past, by and large confirming the reptation model which was developed by de Gennes, Edwards and Doi as a framework for understanding polymer dynamics on the level of topological interactions between polymer chains.

In the framework of reptation theory [1] one imagines the large-scale motion of an entangled polymer as being confined to a hypothetical tube. Loosely speaking, this is the sequence of pores in the entanglement network occupied by the polymer chain. The motion of the polymer segments transverse to the tube direction is strongly suppressed due to the topological constraints imposed by the surrounding network. However, mass transport along the tube is possible by diffusion of stored length (Fig. 1). The result of these dynamics is a snake-like random motion where polymer segments may retract into the existing tube at its ends (hence effectively shortening it) and subsequently diffuse into a new neighbouring pore (stretching the tube and changing the tube contour at the end), while the bulk of the tube does not change its shape.

The recent development in experimental techniques combining flourescence labelling, video imaging and the use of optical tweezers has made possible a rather detailed investigation of polymer dynamics. A few years ago, Perkins, Smith and Chu observed the relaxation of the visual contour of a single DNA molecule in a dense DNA solution, thus providing direct qualitative evidence for some of the key assumptions of reptation theory [2]. In order to understand the measured data – the relaxing visual contour length of an initially stretched DNA chain – *quantitatively* within the reptation picture we have studied reptation dynamics by an exactly solvable lattice gas model [3].

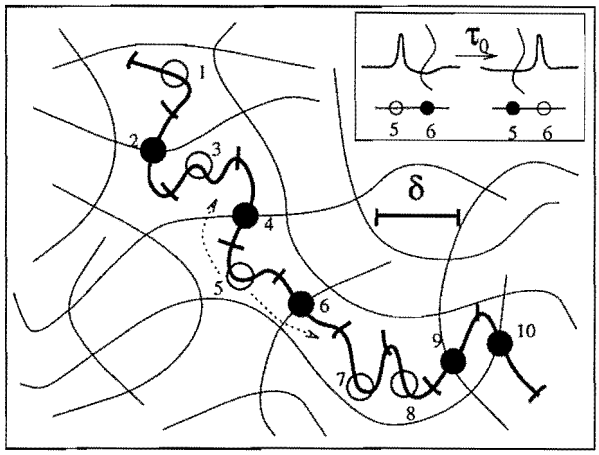

FIG. 1. Reptation of an entangled polymer in the confining tube and mapping to lattice gas dynamics. Polymer segments ('reptons') $1, \ldots, L = 10$ with a size of the mean entanglement distance δ move diffusively to neighboring pores. Segments connecting two consecutive 'pores' of the surrounding network correspond to particles (full circles), segments fully contained in a pore correspond to vacancies. Inset: Diffusion within the tube with rate $1/\tau_0$ to the right amounts to particle-hole exchange.

We obtain a lattice gas model by dividing the polymer into L virtual segments of the mean entanglements distance δ. Each segment fully contained within a pore of the network is called a vacancy, other segments are considered as particles. In order to describe the diffusion of stored length we consider the mean first passage time of the motion of a complete segment (unit of stored length) from one pore to the next along the tube. The first passage event translates into particle hopping in the bulk and particle exchange with a reservoir of fixed density (determined by the equilibrium tube length) at the boundary respectively. To complete the picture we model diffusion in standard manner by an exponential waiting time distribution with mean τ_0 for the hopping events. The experimentally accessible quantity – the visual con-

tour length – corresponds to the tube length and is therefore proportional to the number of particles in the lattice.

We study the relaxation function

$$R(t) \equiv \frac{\Lambda(t) - \Lambda^*}{\Lambda_0 - \Lambda^*} \tag{1}$$

of the experimentally measured visual tube length $\Lambda(t)$. Here Λ_0 and Λ^* are the initial and equilibrium tube length respectively. The results of our theoretical analysis of this model include a universal short-time relaxation law which can be reproduced from standard reptation theory and which is in good agreement with the experimental data over a significant time interval (Fig. 2). The only fitting parameter is a ratio involving the equilibrium tube length and the square root of the microscopic hopping time scale τ_0.

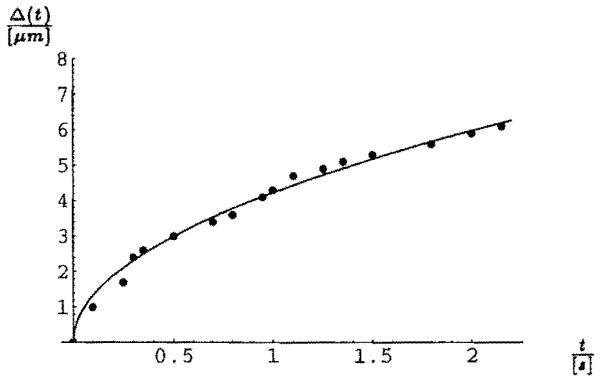

FIG. 2. Relaxation of the visual length $\Delta(t) = \Lambda(t) - \Lambda_0$ of an initially stretched DNA. The full curve shows a power law increase as predicted from the lattice gas model [3]. The dots are experimental data taken from Fig. 4 of Ref. [2].

For arbitrary times we obtain the exact relaxation function

$$R(t) = \frac{1}{L(2L+1)} \sum_{n=0}^{L-1} \cot^2\left(\frac{p_n}{2}\right) e^{-\epsilon_n t/\tau_0} \tag{2}$$

with $p_n = \pi(2n+1)/(2L+1)$ and the inverse relaxation times $\epsilon_n = 2(1 - \cos p_n)$. This function agrees with the experimental data up to times of approximately $5s$. After longer times a systematic deviation from the pure reptation result sets in. Perkins et al. have argued that at long times constraint release, the instability of the entanglement network due to fluctuations, starts playing a role in the dynamics. This conjecture may be supported by inspection of the video images which show tube deformation at times much less than the tube renewal time, but is difficult to verify from the usual reptation theory. Within the lattice gas model constraint release may be incorporated in the dynamics by introducing bulk particle-vacancy exchange which capture the effect of the disappearance and emergence of pores. An analytical treatment is of this model still possible in adiabatic approximation. The modified relaxation function (which has a second fitting parameter) reproduces the measured experimental data rather well (Fig. 3).

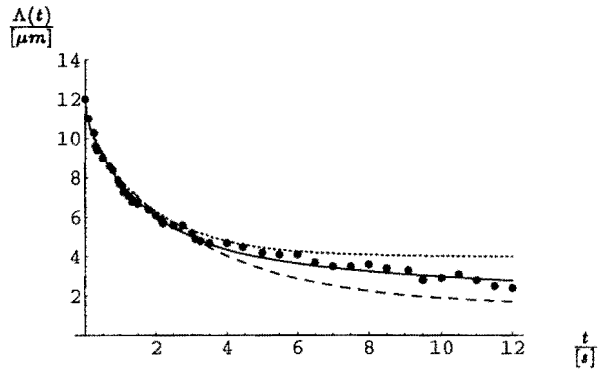

FIG. 3. Experimental relaxation data for the visual tube length $\Lambda(t)$ as a function of time taken from Fig. 4 of Ref. [2] in the range $0.6s \leq t \leq 12s$ (dots) and theoretical predictions from the lattice gas model. The pure reptation prediction (2) with two different values of an additional fitting parameter show a systematic deviation at long times. The full curve shows the modified relaxation function incorporating constraint release.

We conclude that relatively simple lattice gas models are suitable to describe the dynamical properties of single flexible polymers in concentrated solutions with satisfactory agreement with experimental results. We have obtained an understanding of the collective effects of the entanglement network beyond the predictions of standard reptation theory. This gives hope that some of the open questions of the reptation model, in particular the role of disorder and finite-size, can be settled within the lattice gas approach.

[1] P.G. de Gennes, J. Chem. Phys. **55**, 572 (1971); M. Doi and S.F. Edwards, *The Theory of Polymer Dynamics*, (Oxford University Press, Oxford, 1986).

[2] T.T. Perkins, D.E. Smith, S. Chu, Science **264**, 819 (1994).

[3] G.M. Schütz, Europhys. Lett. **48**, 623 (1999).

Publications in refereed journals

Ambaye, H., Kehr, K.
Toy Model for Molecular Motors
Physica A, 267 (1999) 111-123

Antal, T.1, Racz, Z. 1, Rakos, A.1, Schütz, G.M.:
1 Eötvös Univ. Budapest, Hungary
Transport in the XX-chain at zero temperature: Emergence of flat magnetization profiles
Phys. Rev. E59 (1999) 4912-4918

Helbing, D.1,2, Mukamel, D.2, Schütz, G.M.:
1 Univ. Stuttgart
2 Weizmann Institute, Rehovot, Israel
Global phase diagram of a one-dimensional driven lattice gas
Phys. Rev. Lett. 82 (1999) 10-13

Koza, Z.1
Univ. Wroclaw, Poland
General technique of calculating the drift velocity and diffusion coefficient in arbitrary periodic systems
J. Phys. A: Math. Gen. 32 (1999) 7637-7651

Popkov, V., Schütz, G.M.
Steady-state selection in driven diffusive systems with open boundaries
Europhys. Lett. 48 (1999) 257-263

Schütz, G.M.
Non-equilibrium relaxation law for entangled polymers
Europhys. Lett. 48 (1999)

Schütz, G.M., Trimper, S.1
1 Martin-Luther-Univ. Halle, Germany
Relaxation and Aging in Quantum Spin Systems
Europhys. Lett. 47 (1999) 164-170

Other publications

Schütz, G.M.
Rezension von Non-equilibrium Statistical Mechanics in One Dimension
V. Privman (ed.) (Cambridge University Press, Cambridge, 1997), in Contemporary Physics 40 (1999),159

Schütz, G.M.
Stochastic many-body systems and quantum spin chains
Proc. of the II Brazilian Probability School, Barra do Sahy 1998, Resenhas 4, 17-43 (1999)

Invited talks

Gompper, G.
Soft Matter: Amphiphile, Membranen, Mikroemulsionen
Institut für Computeranwendungen 1, Universität Stuttgart., 13.12.1999

Gompper, G.
Statistische Physik von Membranen und Vesikeln: Schmelzen, Ondulationen, Topologie-Fluktuationen",
RWTH Aachen, 21.06.1999

Kehr, K.
Toy Model for Molecular Motors
Theoretische Physik, Ludwig-Maximilian-Universitaet, München, 5. 3. 1999

Schütz, G.
Diffusion and Interaction of Shocker in the asymmetric exclusion process
Erwin-Schrödinger-Institut, Wien, 2. 3. 1999

Schütz, G.
Integrable Stochastic Processes for Biological and Chemical Systems
Universität Genf, 3. 5. 1999

Schütz, G.
Integrable Stochastic Processes for Biological and Chemical Systems
Universität Lausanne, 4. 5. 1999

Schütz, G.
Nonequilibrium Steady States of Quantum Spin Chains
Universidade Federal, Sao Carlos (Brasilien), 12. 8. 1999

Schütz, G.
Phasendiagramm von getriebenen diffusiven Systemen mit offenen Rändern
Universität Leipzig, 4. 7. 1999

Schütz, G.
Phasendiagramm von getriebenen diffusiven Systemen mit offenen Rändern
Universität Saarbrücken, 2. 2. 1999

Schütz, G.
Stationäre Nichtgleichgewichtszustände von integrablen Quantenspinketten
Freie Universität Berlin, 12. 7. 1999

Schütz, G.
Steady-State Selection in Driven Diffusive Systems with Open Boundaries
Erwin-Schrödinger-Institut, Wien, 25. 2. 1999

Schütz, G.
Relaxationsgesetz für gestreckte Polymere in Polymernetzwerken
DPG Frühjahrstagung, Münster, 26. 3. 1999

Other talks

Kehr, K.
Muon Spin Relaxation by Random Walks of Electrons
Workshop "Application of Low-Energy Muons", Paul-Scherrer Institute,
Villigen, Schweiz,
17. 2. 1999

Schütz, G.
Lattice gas approach to the relaxation of entangled DNA
III Escola Brasileira de Probabilidade, Mambucaba (Brasilien), Konferenzbeitrag
5. 8. 1999

Schütz, G.
Relaxation of entangled DNA
Renoutre de Physique Statistique, Paris, Konferenzbeitrag
27. 1. 1999

Posters

Schütz, G.
Dynamical Theory of Steady-State Selection in Open Driven Diffusive Systems
Traffic and Granular Flow, Konferenzbeitrag, 28. 9. 1999

Lecture courses

Schütz, G.
Stochastische Vielteilchensysteme
Universität/Gesamthochschule Essen, Sommersemester 1999

Institute Theory III

General Overview

Research Areas

The institute *Theory III* investigates the mechanisms of the formation of structures and their consequences in condensed matter. The research starts from electronic properties which define the shortest length and time scales, but it also encompasses the macroscopic consequences in mind. The analytical and numerical investigations are in many ways closely connected with experimental studies performed in other groups of IFF, but also with activities in other institutes of the Research Center Jülich.

Central points of interest for the research in *Theory III* are in the field of electronic structure of solids (F&E-Nr. 23.20.0). Materials classes under considerations are metals and semiconductors, specifically with respect to their importance for information technology (F&E-Nr. 23.42.0). A second mainstream is formed by cooperative phenomena in condensed matter (F&E-Nr. 23.15.0). Questions here aim at dynamics of structure and pattern formation and the statistical mechanics of order and disorder processes. Specific activities in the field of complex fluids (F&E-Nr. 23.30.0) are concerned with structure and dynamics of soft matter. The research of *Theory III* employs all analytical and numerical techniques applicable to many-body problems in condensed matter. In addition the development of new methodological concepts and numerical procedures is part of our research interest. The development of parallel program codes adapted to massively parallel computers has received special attention in recent years.

The explanation of the microstructure and dynamics of real solids requires the understanding of the electronic properties. One of the most important methods for the calculation of the electronic structure of real solids is the density functional theory in connection with appropriate numerical procedures. While in recent years bulk properties of metals and semiconductors have been at the center of our research a main concern now is directed towards the understanding of surface and interface properties.

In recent years, metals and semiconductors have been treated with different computational methods. In order to crosscheck our methods for investigation of semiconductor properties, a method usually employed for metals, the KKR-Green's function technique, and a typical procedure used for semiconductor properties, the pseudopotential method, have been compared. The electronic and geometrical structures of complexes of Cd or In acceptors with P, As, or Sb donors in Si and Ge have been analyzed. Behind this problem there is some technological interest, since the Coulomb attraction between oppositely charged defect atoms in Silicon or Germanium leads to the formation of stable acceptor-donor complexes, which can cause serious technological problems like uncontrolled annihilation or creation of charge carriers. Observables which are accessible to both methods agree well, for example the lattice relaxations around defect pairs in Silicon. In addition to the physical and technological interest in this problem, the results increase confidence in our numerical methods.

The properties of semiconductor crystals depend sensitively on their growth mechanism. One tries to avoid island-growth of the crystals because of the increased probability of impurity absorption at the step-edges around islands. Instead one would like to have layer-growth as far as possible. It is known since some time that the use of group-V elements like As or Sb on Silicon or Germanium surfaces act as surfactants favoring layer growth of the underlying crystal. A first principles pseudopotential study of surface steps of As terminated Silicon or Germanium crystals has been performed. Many details of structure and energetics of the step-edge and the activation barriers for the growth processes have been obtained.

The dynamics of glasses and other amorphous materials still pose a significant number of open questions. During the last year the isotope effect upon diffusion in a monatomic Lennard-Jones liquid has been calculated by molecular dynamics simulations. The isotope effect is the most direct measure of collectivity of motion. It was found for example, that the isotope effect depends rather sensitively upon the density and temperature of the material. These results are in good agreement with experiment.

Another class of related problems of disordered materials concerns the dynamics of polymers. A specifically difficult problem is the influence of long range forces between the individual parts of a long polymer chain. Such long range forces occur for example through hydrodynamic effects in polymer solutions. Viscoelasticity and turbulent drag reduction are examples for macroscopic consequences. Detailed numerical and analytical model studies of a strongly deformed polymer in solutions have led to a deeper understanding of correlation effects in the system.

A completely different source of a long range effective interaction in condensed matter physics is due to elastic deformations of solids. A particularly difficult problem hereby is the transition from coherent elastic deformation to incoherent deformations through production of dislocations. A puzzling experiment on SiC under helium gas implantation showed the formation of cracks and the sudden expulsion of dislocation loops near the crack tips. This complex phenomenon was analyzed theoretically in some detail and gave new insights in collective effects in crack propagation and loop formation.

A fundamental assumption in the theory of elasticity is that sufficiently far away from a point or line dislocation the elastic strain field can be described by linear theory of elasticity. In contrast it was now discovered that there are systems, where the strain field of an edge dislocation must be described in a nonlinear theory even far away from the core of the dislocation. In addition an exact analytical solution to this specific problem was found. This is one more example for the observation that elasticity problems even today are still full of surprises.

H. Müller-Krumbhaar

Personnel 1999/2000 and areas of activity

Scientific Staff

Dr. E. Brener	Kinetics of phase transformations	23.150
Prof. P.H. Dederichs	Electronic properties, interfaces and layered systems	23.200
Dr. K. Mika	Structure maps for binary systems	23.150
Prof. H. Müller-Krumbhaar, Institute Director	Non-linear dynamics of dissipative systems	23.150
Dr. H. Schober	Statics and dynamics of glasses, defects and phonons	23.300
Prof. K. Schroeder	Electronic and atomic structure of defects in semiconductors	23.420
Dr. H. Trinkaus	Dissipative structure formation, reaction-diffusion problems	23.150,23.805, 23.420
Dr. R. Zeller	Electronic structure and magnetic properties of metals	23.200
S. Oubenkhir	Secretary	
M. Ulbrich	Secretary	

Visitors

Dr. I.A. Cabria (SP)	Relativistic KKR-Green's function methods	23.200
Dr. D. Caprion (F)	Dynamic of amorphous and liquid Se	23.300
Dr. H. Emmerich	Hydrodynamics of wetting	23.150
Dr. M. Freyss (F)	Surface magnetism	23.200
Dr. J. Matsui (JP)	Dynamics at the glass transition	23.300
Prof. V. Kozub	Phonons in amorphous materials	23.300
Dr. V. Luchnikov	Voronoi analysis of glasses	23.300
Prof. V. Marchenko (GUS)	Elastic effects during phase transformations	23.150
Dr. Ph. Mavropoulos (GR)	Complex bandstructure and transport	23.200
Prof. C. Misbah (F)	Solidification processes, non-linear dynamics	23.150
Dr. N. Papanikolaou (GR)	Ab-initio calculations of forces and lattice relaxations	23.200
Prof. N. Stefanou (GR)	Mesoscopic transport	23.200
Dr. D. Temkin (GUS)	Pattern formation at interfaces	23.150

PhD and Diploma Students (University = RWTH Aachen)

Dipl.-Phys. M. Alaga-Bogdanovic	Phase field calculations of surface-wetting	23.150
Dipl.-Phys. A. Antons	Ab-initio calculations on surface reconstruction	23.420
Dipl.-Phys. A. Baranov (GUS)	Magnetic adatoms of surfaces	23.200
Dipl.-Phys. V. Bellini (I)	Electron structure of magnetic layered systems	23.200
Dipl.-Phys. R. Berger	Polar surfaces of III-V-semiconductors	23.420
Dipl.-Phys. F. Gutheim	Cluster growth on surfaces	23.150
Dipl.-Phys. M. Hartmann	Collective effects of cracks and dislocations	23.150
H. Höhler	Defects in semiconductors	23.420
Dipl.-Phys. D. Kienle	Transport coefficients in polymer solutions	23.150
Dipl.-Phys. M. Kluge	Binary metallic glasses	23.300
Dipl.-Phys. Wi. Kromen	Point defects and interfaces in Nitride-semiconductors	23.420
Dipl.-Phys. B. Nonas	Fully relativistic band structure methods	23.200
Dipl.-Phys. R. Rzehak	Polymer dynamics and hydrodynamic flow	23.150
Dipl.-Phys. A. Settels	Electronic structure of point defects in semiconductors	23.200
Dipl.-Phys. R. Spatschek	Collective effects of cracks in solids	23.150

Ab Initio Study of Acceptor-Donor Complexes in Silicon and Germanium

A. Settels, T. Korhonen, N. Papanikolaou, K. Schroeder, M. Aretz, R. Zeller, and P. H. Dederichs
Institute Theory III

The electronic and geometrical structures of complexes of Cd or In acceptors with P, As, or Sb donors in Si and Ge are studied by two independent ab initio electronic structure methods, the Korringa-Kohn-Rostoker (KKR) Green's-function method and the pseudopotential ab initio molecular dynamics method. The atomic equilibrium configurations are characterized by large defect-induced lattice relaxations which are calculated in good agreement by both methods. The electric field gradients (EFGs) calculated by the all-electron KKR method depend very sensitively on the relaxations and in the theoretically determined equilibrium positions they agree well with EFGs measured by the $\gamma\gamma$ perturbed angular correlation (PAC) technique. From the calculations a simple understanding of the EFGs emerges.

F&E-Nr: 23.20.0

If semiconductors are intentionally or unintentionally doped with both acceptor and donor atoms, the Coulomb attraction between the oppositely charged defect atoms lead to the formation of stable acceptor-donor complexes which can cause serious technological problems such as an uncontrolled annihilation or creation of charge carriers. Unfortunately very little microscopic information exists about these complexes since they are normally neither electrically nor magnetically active. One exception is the $\gamma\gamma$ perturbed angular correlation (PAC) technique using ^{111}In/^{111}Cd probe atoms. In these experiments an initial dimer complex consisting of the In acceptor and a donor atom such as P, As, or Sb is formed and after the decay of ^{111}In into ^{111}Cd the EFG at the Cd atom is measured. Whereas the measured symmetry of the EFG tensor gives important information about the symmetry of the defects, a fundamental understanding of the measured size of the EFG strongly needs the help of ab initio electronic structure calculations.

Lattice relaxations: The EFG depends very sensitively on the size of the defect-induced lattice relaxations as discussed below, which requires rather accurate calculations for these relaxations. Using the In-donor pairs as test cases we have applied two independent density-functional electronic-structure methods, the Korringa-Kohn-Rostoker (KKR) Green's-function method and the pseudopotential ab initio molecular dynamics method. Within the KKR calculations the solid is divided by a Voronoi construction into non-overlapping and space-filling cells around the shifted atomic positions. We use a finite region of 76 perturbed cells with C_{3v} symmetry, which by the Green's function approach is exactly embedded in the otherwise unperturbed host. 38 cells contain atoms and 38 are empty which ensures compact cells and a good convergence of angular momentum expansion (used up to $l_{max} = 4$). Forces are calculated by an ionic Hellman-Feynman theorem and lattice relaxations are treated by transforming host quantities such as Green's function and potentials relative to the displaced positions [1]. Within the pseudopotential calculations we use norm-conserving pseudopotentials of the Kleinman-Bylander form, a plane-wave basis set (used up to $E_{max} = 11.56$ Ry) and an iterative diagonalization scheme for the eigenvalues. We use supercells of 64 or 108 atoms, which are centered around the defect pair, and a **k**-point set equivalent to 6 x 6 x 6 **k**-points in the BZ of the bulk.

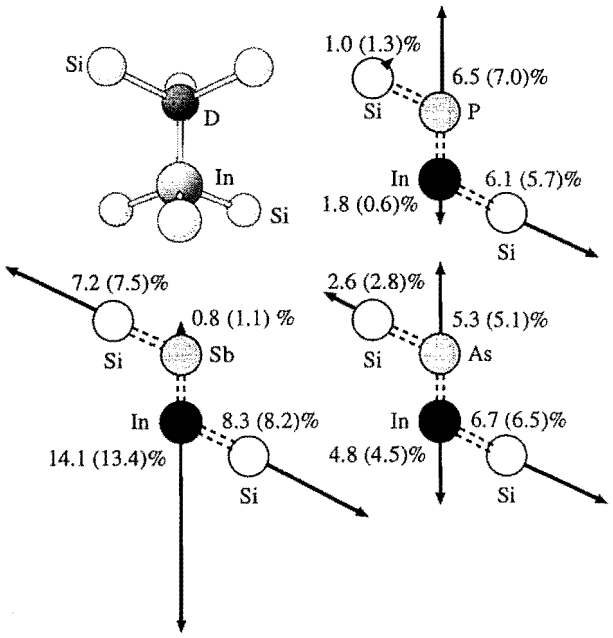

FIG. 1. Lattice relaxations around $[InD]^0$ (D=P, As, Sb) defect pairs in Si. Shown are the three-dimensional arrangement of the pairs (top, left-hand) and the (110) planes containing the InD pairs and two representative Si neighbors. Relaxations in percent of the nearest neighbor distance are given for the KKR and (in brackets) for the pseudopotential method.

The calculated equilibrium structures are shown in Fig. 1 for the InP, InAs, and InSb complexes in Si. The pictures illustrate the relaxations of the pair atoms and

the two representative Si neighbors in the (110) plane. The arrows indicate size and direction of the relaxations and the numbers give the size in percent of the Si nearest neighbor distance. The relaxations calculated by the KKR method are typically slightly larger than the ones calculated by the pseudopotential method, but always in good agreement showing the reliability and accuracy of both methods. The geometric arrangement of the pairs is dictated by the sizes of the In and the donor atoms. For instance, the In atom pushes the small P atom outwards by 6.5 %, while the larger Sb atom is shifted only slightly, but pushes the In atom away by 14 %.

$[CdD]^-$ complexes in Si and Ge: The calculated EFGs for the negatively charged $[CdD]^-$ complexes in Si and Ge and for neutral $[CdD]^0$ pairs in Si are displayed in Table I for the ideal (non-relaxed) and the relaxed configurations in comparison with experimental results. The results show that the EFG depends very sensitively on the relaxations of the atoms. Without lattice relaxations the calculated EFG values (EFG_{ideal} in Table I) even show the wrong trend and are more or less meaningless. On the other hand, for the relaxed positions the agreement between theory and experiment is good for both Si and Ge and in particular the trend with changing sizes of the donor atoms is correctly represented. The relaxations for the $[CdD]^-$ complexes in Si and Ge are quite similar to the relaxations for the $[InD]^0$ complexes in the corresponding hosts (see Fig.1). The main difference is that the CdD distance is slightly smaller than the InD distance and the relaxations of the Si or Ge neighbor atoms are somewhat reduced, both reflecting the somewhat smaller size of the Cd atom. A detailed analysis of the electronic structure gives direct insight into the origin of the EFG. The main contribution to the EFG is given by the quadrupole component of the charge density, which is proportional to the anisotropy of the p charge of the Cd-atom: $V_{zz} \propto \int^{E_F} \{\rho_{pz}(E) - \frac{1}{2}[\rho_{px}(E) + \rho_{py}(E)]\} dE$, where we have assumed the z-axis to point into the [111] dimer direction. The basic feature is that the p_z orbital of the Cd atom strongly hybridizes with the A_1 state of the single donor atoms, while the Cd p_x and p_y levels are orthogonal to this state. By hybridization p_z charge is transferred to the donor site, while the p_x and p_y charges are practically unaffected. The loss of the p_z charge leads to an anisotropic p charge distribution at the Cd site, which determines the Cd EFG.

$[CdD]^0$ complexes in Si: In PAC experiments with different donor concentrations and very high annealing temperatures, Achtziger and Witthuhn [2] found strong evidence that the CdD pairs in silicon form electrically deep centers with two different charge states, i.e., $[CdD]^-$ and $[CdD]^0$, leading to two different EFGs. Though the sign of the EFG cannot be determined by the experiments, by assuming the same sign for both charge states the resulting change in the EFG, Δ_{EFG}, turned out to be more or less independent of the donor type (about 145 MHz). These results are unequivocally confirmed by our calculations. For this we have performed spin polarized calculations, with the majority E level of the complex filled by two electrons and the minority level by only one electron, without reducing the C_{3v} symmetry. This leads for all three donor types to a small magnetic moment of 0.07 μ_B and a small hyperfine field of 8 kG at the Cd site. The resulting EFGs for both the ideal and the relaxed positions are shown in Table I. In the relaxed geometry the sign of the EFGs V_{zz} remains the same (compared to $[CdD]^-$) and the differences, Δ_{EFG}, are 135, 160, and 159 MHz for CdP, CdAs, and CdSb pairs, respectively, which is in good agreement with the experimental data. These reductions of the EFGs have two sources, the different charge states and the change of the forces on the atoms. The reduced charge mainly affects the relaxations of the Cd atom. For instance, in the $[CdSb]^0$ complex in Si the Cd atom relaxes by only 10.2% outwards as compared to 14.6% in the $[CdSb]^-$ complex. The reduction of the charge also leads to a simple understanding of the reduced EFGs, with the changes Δ_{EFG} being more or less independent of the donor atom. We have also performed calculations for $[CdD_2]^0$ trimers in Si, which show up in the PAC spectra for higher doping. Our results are in good agreement with the experiment, and again a simple picture for the EFG of the complexes emerges.

	EFG_{ideal}	$EFG_{relaxed}$	EFG_{exp} [2]
	Si-Host		
$[CdP]^-$	-189	-191	± 179
$[CdAs]^-$	-174	-249	± 229
$[CdSb]^-$	-85	-294	± 271
$[CdP]^0$	-79	-56	± 36
$[CdAs]^0$	-73	-89	± 83
$[CdSb]^0$	+6	-135	± 129
	Ge-Host		
$[CdP]^-$	-135	-124	± 86
$[CdAs]^-$	-118	-182	± 148
$[CdSb]^-$	+2	-235	± 201

TABLE I. The largest component, V_{zz}, of the EFG tensor.

[1] N. Papanikolaou, R. Zeller, P.H. Dederichs, and N. Stefanou, Phys. Rev. B **55**, 4157 (1997).

[2] A. Settels, T. Korhonen, N. Papanikolaou, R. Zeller, and P.H. Dederichs, Phys. Rev. Lett. **83**, 4369 (1999).

[3] A. Settels, K. Schroeder, T. Korhonen, N. Papanikolaou, M. Aretz, R. Zeller, and P.H. Dederichs, accepted in Solid State Commun.

ab initio investigations of the step structure on As covered Si(111)

A. Antons, R. Berger, S. Blügel, Wi. Kromen and K. Schroeder
Institute Theory III

The structures of $(11\bar{2})$ and $(\bar{1}\bar{1}2)$ oriented steps on As terminated Si(111) are determined using first-principles molecular statics calculations based on total energy and force. All calculations are carried out within the density functional formalism in the local-density approximation, using norm-conserving separable pseudo-potentials and a plane wave basis set. For both steps the energetically most favorable structure is the As passivated step with As atoms replacing the exposed second layer Si-atoms at the step edge. At the $(\bar{1}\bar{1}2)$ step edge this leads to the formation of As dimers. The energy difference between the two steps considered is $\approx$ 0.1eV per unit length. We also discuss a possible reaction sequence for step flow.

F&E-Nr: 23.42.0

The often observed Stranski-Krastanov growth mode in strained heteroepitaxial systems can be changed to layer-by-layer growth by the use of surfactants, an example is the use of group-V elements (As, Sb) on Si or Ge. Due to the extra electron the group-V layer passivates the (111) surface. It modifies the surface reconstruction, has a lower surface free energy and floats on top of the growing crystal. In our previous investigations we concentrated on the microscopic understanding of the kinetics of single group-IV adatoms (Si, Ge) on the unreconstructed (1x1) As terminated Si(111) surface. The competition between diffusion on top of the As layer and incorporation into the layer by exchange with an As atom is decisive for the growth mode.
From our results we suggest that Si and Ge behave differently: While both adatom species diffuse along the same path (H3 equilibrium site, T4 saddle point) with very similar activation energies ($E_D \approx 0.25$ eV), the energy profiles along the exchange path are very different. Si has about the same activation energy for exchange as for diffusion ($E_{EX} \approx 0.27$ eV) and is readily incorporated to a substitutional site in the As layer. It gains an energy of $E_B \approx 0.8$ eV upon exchange [1]. On the other hand, Ge has to overcome a much larger exchange barrier ($E_{EX} \approx 0.7$ eV) and gains only $E_B \approx 0.2$ eV. The reason is the smaller bond strength of Ge compared to Si: When an adatom approaches the substitutional site in the As layer on the Si substrate, bonds of the replaced As atoms to Si are replaced by bonds of the approaching adatom (Ge or Si) to Si. Since the energy gain due to the newly formed Ge-Si bonds is much lower than for Si-Si bonds the exchange barrier of a Ge atom is much higher than of a Si atom and the energy gain on the substitutional site much lower.

These energy relations have consequences for the growth process on As–covered Si(111). Si adatoms make only very few diffusion jumps before they are incorporated substitutionally. This results in a large nucleation rate for Si islands on terraces as is observed experimentally for homoepitaxy on Si(111):As [2]. On the other hand, Ge atoms perform many diffusion jumps on Si(111):As before they are incorporated (at T = 580 K the average number of jumps is $\approx 10^4$). Thus, most Ge atoms can reach the terrace steps. If they are readily incorporated there, growth would proceed by step flow which is not observed experimentally. Thus, an idea put forward by Kaxiras *et al.* [3] has to be checked, that the step edges are very effectively passivated by surfactant atoms and the Ge atoms are repelled from the steps. Then, in spite of the large diffusion length, one would expect Ge island nucleation on the terraces, as is observed. Thus, the reaction path and activation energy for incorporation of Ge adatoms at steps is an important quantity.

The determination of the microscopic structure of steps is a prerequisite for the understanding of the incorporation of adatoms. STM images show always double layer steps and irregularly shaped islands for Si homoepitaxy on As passivated Si(111) with mainly two kinds of steps: $(11\bar{2})$ and $(\bar{1}\bar{1}2)$.
Using our parallelized *ab initio* code EStCoMPP [4] we have investigated a wide variety of possible step structures for both kinds of steps. The calculations were performed using a 2x4 surface supercell with a ten-layer-thick slab in repeated slab geometry in which a core of 12 atoms were kept fixed to simulate bulk crystal termination. The lateral translation vectors of the supercell are chosen to connect an atom on the upper terrace to an equivalent atom a double layer down. Thus one can generate a supercell which contains only one type of step. The vertical length of the supercell was 9 times the double-layer spacing of the Si unit cell. The calculations were performed with three k-points in the irreducible wedge of the Brillouin zone. The electronic wave functions were expanded in a plane-wave basis set with an energy cutoff of 9 Ry. The calculations were terminated when the forces on all ions were smaller than 0.1 mRy/au.

The lowest energy structures are the As passivated steps as shown in Fig.1. The exposed second layer Si atoms at the step edges are replaced by As atoms. At

the $(11\bar{2})$ step this leads to a stable configuration since the As atoms are in a naturally three fold coordinated position, i.e. the As atoms at the step edge are in equivalent positions as on the (111) oriented terraces. At the $(\bar{1}\bar{1}2)$ step the As atoms are only two fold coordinated in the unrelaxed positions. Thus, they form dimers to saturate their bonds. The energy difference between these step edges is only $\approx$ 0.1 eV per unit length. At both step edges the replacement of Si with As atoms requires an additional As atom per unit length compared to the monolayer coverage.
At the $(11\bar{2})$ step edge the As atoms are in a very similar positions as on the (111) surface (and nearly so at the $(\bar{1}\bar{1}2)$ step). Thus, the exchange of these As atoms with Si/Ge adatoms approaching the step edge from the lower terrace will likely show the same behavior as on the terrace, i.e. we expect that Si atoms are easily incorporated at the step while Ge atoms have to overcome a larger activation barrier.

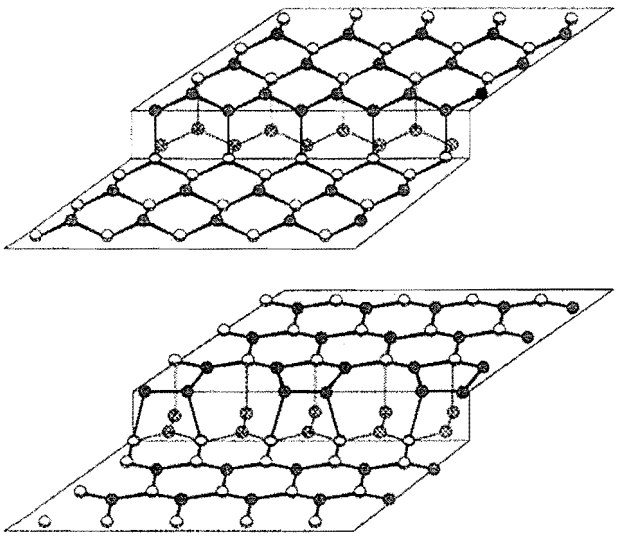

FIG. 1. Schematic picture of the $(11\bar{2})$ and $(\bar{1}\bar{1}2)$ steps. White circles indicate Si atoms, dark circles As atoms. On the terraces the As atoms are shown in the tetragonal positions above the Si atoms. At the terrace edge the Si atoms of the second layer are replaced by As. This leads to a stable configuration at the $(11\bar{2})$ step due to the naturally three fold coordinated position of the As atoms. At the $(\bar{1}\bar{1}2)$ step the As atoms form dimers to saturate their bonds.

We found a second metastable configuration for the $(11\bar{2})$ step edge with an overhanging As (Fig.2 b). Taking into account two step configurations one can imagine the following mechanism for stepflow on Si(111):As shown in Fig.2 which considers only double layer steps as experimentally observed: Starting with the stable configuration (a) an approaching Si atoms on the lower terrace exchanges with the extra As atoms at the step edge of the second layer, and pushes the As atoms to the metastable position (b). The next Si atom can exchange with an As atom on the lower terrace in front of the step edge pushing up the As atom into the stable configuration at step edge in the second layer (c). This extends the step edge by one unit. We think that the activation barriers for these two processes determine the incorporation probability for Si and Ge adatoms, and thus the balance of step flow versus island nucleation on terraces for Ge heteroepitaxy.

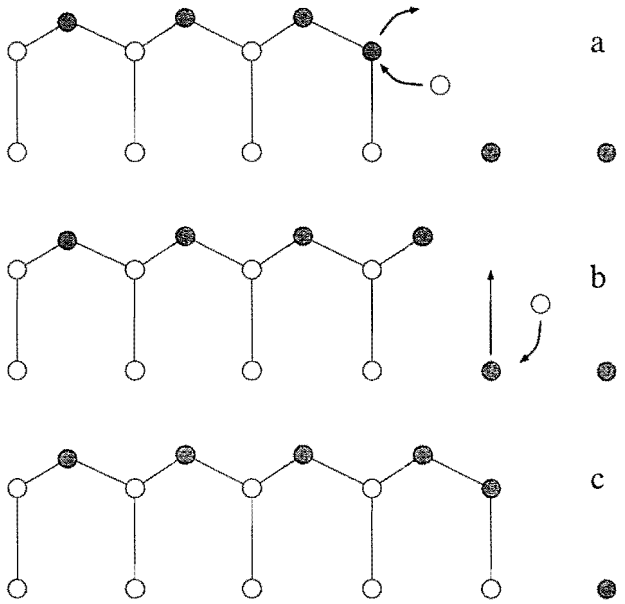

FIG. 2. Schematic sideview of the stepflow mechanism at $(11\bar{2})$ step edges on Si(111):As. White circles indicate Si atoms, dark circles As atoms. The upper picture (a) shows the stable configuration of As at the exposed second layer position with an approaching Si atoms on the lower terrace. After the exchange the metastable configuration is shown (b). The next exchange of Si with the As atom in front of the step edge on the lower terrace will lead again to a stable configuration (c).

[1] K. Schroeder *et al.*, Phys. Rev. Lett. **80**, 2873 (1998)
[2] B. Voigtländer *et al.*, Phys. Rev. **B 51**, 7583 (1995)
[3] D. Kandel and E. Kaxiras, Phys. Rev. Lett. **75**, 175 (1996)
[4] EStCoMPP, Electronic Structure Code for Materials Properties and Processes, Forschungszentrum Jülich, 1999. R.Berger *et al.*, Proceedings of the NIC-Workshop "Molecular Dynamics on parallel Computers", held at Jülich, 08.-10. Februar 1999 (World Scientific 1999)

Isotope effect of diffusion in a simple liquid

M. Kluge and H. R. Schober
Theorie III

The diffusional isotope effect of a monatomic Lennard Jones liquid is calculated by molecular dynamics simulation. Mass differences of 10% to 40% were used. At equilibrium density, with decreasing temperature a strong reduction of the isotope effect is found which indicates a marked increase of the collectivity of motion. Changing the density at constant temperature the same effect is seen which shows that the density change is the main driving force behind the reduction of the isotope effect.

F&E Nr.: 23.30.0

The atomic nature of transport in liquids has been the subject of numerous studies. Of particular interest is the possible change of mechanism upon cooling to melting point and beyond to the glass transition. In a monatomic liquid the diffusion constant can be written as

$$D = D_0 f(T,\rho) = D_0^* f(T,\rho)/\sqrt{m} \qquad (1)$$

where T is the temperature, ρ the atomic density and m is the mass of the diffusing particle. The temperature dependence of D can be described over a large temperature interval down into the undercooled regime by a Vogel – Fulcher – Tamman law (VFT)

$$D = D_0 \exp \frac{E_0}{k_B(T - T_0)} \qquad (2)$$

where the phenomenological VFT temperature T_0 is well below the glass transition temperature T_g. This empirical description reproduces the sharp drop of D upon undercooling. The inverse proportionality to the root of the mass is quite general, independent of the molecular aggregation, as long as only one species is present.

Already in the simple case of different isotopes, considered here, the situation is more complicated. At low densities and high temperatures when diffusion is dominated by binary collisions the kinetic approximation should hold and Eq. 1 should apply approximately for each component. Lowering the temperature or increasing the density effects of collective motion will gain importance. This cooperativity can be accounted for simply by replacing the particle mass in Eq. 1 by an effective mass for diffusion of isotope α

$$m^\alpha_{\text{eff}} = m^\alpha + (N_D - 1)\overline{m} \qquad (3)$$

with $\overline{m}$ the average particle mass and N_D the number of particles moving cooperatively. Eq. 1 is then modified to

$$D = F(T,\rho)/\sqrt{m_{\text{eff}}}. \qquad (4)$$

One can define an isotope effect parameter E [1]

$$E_{\alpha\beta} = \frac{D_\alpha/D_\beta - 1}{\sqrt{m^\beta/m^\alpha} - 1} \approx \frac{1}{N_D}. \qquad (5)$$

The isotope effect can thus be used as a quantitative measure of collectivity. Due to the small differences in isotopic masses it necessitates, however, very accurate measurements of the diffusion. Early measurements, therefore, often lead to conflicting evidence.

Progress was made by simultaneously measuring the diffusion of the tracer atoms ^{57}Co and ^{60}Co [2]. Using this technique for diffusion of Co in amorphous $Co_{76.7}Fe_2Nb_{14.3}B_7$ a value $E = 0.1$ was found indicating a high degree of collectivity. In contrast for self diffusion in crystalline Co the isotope effect is $E = 0.7$. There diffusion is by a vacancy mechanism which involves essentially single particle jumps with not too large displacements of the neighbors. The technique was applied to a supercooled melt of $Zr_{46.7}Ti_{8.3}Cu_{7.5}Ni_{10}Be_{27.5}$, and again a very low isotope effect was observed [3].

We present a systematic study of the diffusional isotope effect in a simple liquid as function of temperature and pressure. In order for the observed isotope effect to reflect the motion in the pure material we study the effect of small mass changes, 10% to 40%. The calculations are done for a monatomic Lennard-Jones (LJ) system. In the following we will use LJ units $\epsilon = \sigma = m = 1$. The glass transition is then at $T_g \approx 0.4$. Two series of calculations were done. For the first set the equilibrium densities $\rho(T)$ were determined and used to calculate the zero pressure diffusion constants as function of temperature in the range $0.44 \leq T \leq 0.96$. In a second calculation the temperature was kept constant at $T = 0.88$ and the density was varied $0.46 \leq \rho \leq 0.855$. In all runs pressure and energy were monitored to ensure stability of the configurations. The diffusion constant was calculated from the asymptotic slope of the atomic mean square displacements.

The mass dependence of D was then used to determine the isotope effect, Eq. 5. Taking the values for the zero pressure samples in Fig. 1 one sees first that all the values are relatively low in the whole temperature range investigated and secondly that E drops more or less linearly upon cooling towards the glass transition temperature. This clearly shows a marked increase of motional collectivity upon cooling. Taking the approximate relation

between E and the number of particles moving collectively we find that the latter increases from $N_D \approx 4$ at $T = 0.96$ to $N_D \approx 16$ at $T = 0.48$. This high collectivity is in agreement with the experimental findings of Ehmler *et al.* [3]. It is similar to the values found in the monatomic soft sphere glass at low temperatures [5].

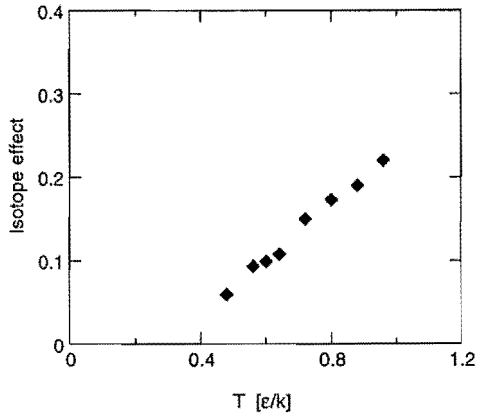

FIG. 1. Isotope effect as function of temperature at equilibrium density.

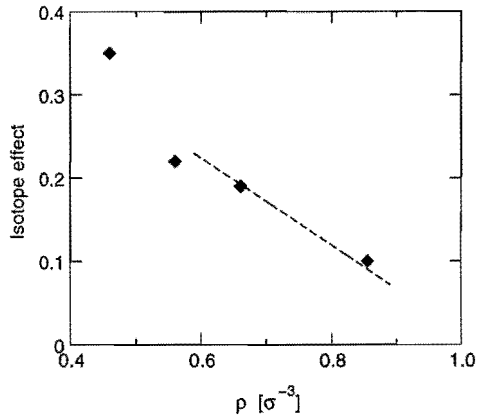

FIG. 2. Isotope effect as function of density for costant temperature $T = 0.88$ (solid diamonds). The broken line is a least square fit to the data of Fig. 1 using the temperature dependent equilibrium densities.

To check to what extent the drop of isotope effect is connected with the increase in density, the calculations were repeated at constant temperature $T = 0.88$ for different densities ρ. Fig. 2 (solid diamonds) shows an approximate proportionality between the decrease of isotope effect and the increase of density. Moreover the values at fixed temperature coincide within the limits of accuracy with those of the equilibrium samples (Fig. 1) at the same density but at a different temperature. This shows that the isotope effect is predominantly determined by the density. The diffusion constant itself depends strongly on both temperature and density.

Varying the mass increment δm between 0.1 and 0.4 we found no significant deviations from the simple square-root dependence of Eq. 4. Previous computer experiments on LJ liquids were done with much larger mass differences and different mass dependencies were deduced, e.g. $D(m_1)/D(m_2) = (m_2/m_1)^{-\mu}$ where $\mu < 0.1$ [4]. From our results we find that such a fit would require strongly temperature dependent coefficients.

In experiments on metallic glasses significantly larger isotope effects have been observed in rapidly quenched samples which decreases to about a fifth upon aging [6]. In our simulation of a liquid LJ system we observed a similar but less pronounced effect when using insufficiently equilibrated samples.

In summary, we studied the isotope effect of diffusion in a simple Lennard Jones liquid at equilibrium density as function of temperature and for constant temperature as function of density. The isotope effect drops strongly upon cooling towards the melting and glass transition temperatures and is strongly dependent on the densities. This indicates a strong increase in cooperativity of the atomic motion. The calculations were done for small mass differences and the results are in agreement with recent experiments. Incompletely equilibrated samples show an increased isotope effect, a less cooperative motion. Changing the mass ratio no deviation from the simple description in terms of effective masses was found.

[1] R. W. Keyes, J. Chem. Phys. **29**, 467 (1958).
[2] F. Faupel, P. W. Hüppe, and K. Rätzke, Phys. Rev. Lett. **65**, 1219 (1990).
[3] H. Ehmler *et al.*, Phys. Rev. Lett. **80**, 4919 (1998).
[4] R. J. Bearman and D. L. Jolly, Mol. Phys. **44**, 665 (1981).
[5] H. R. Schober, C. Oligschleger, and B. B. Laird, J. Non-Cryst. Sol. **156**, 965 (1993); C. Oligschleger and H. R. Schober, Phys. Rev. B **59**, 811 (1999).
[6] K. Rätzke, P. W. Hüppe, and F. Faupel, Phys. Rev. Lett. **68**, 2347 (1992).

Dynamics of Strongly Deformed Polymers in Solution

R. Rzehak, D. Kienle, W. Zimmermann
Institute Theory III

Bead spring models for polymers in solution are nonlinear when either the finite extensibility of the polymer, excluded volume effects or hydrodynamic interactions between polymer segments are taken into account. For such models we introduce a powerful method for the determination of the relaxation spectrum and modes from simulation data based on the Karhunen–Loève technique. Both spectrum and modes differ significantly from the linear Rouse modes and -times, whereby the various nonlinear interactions are most relevant in different parameter ranges. The precise relaxation spectrum and the relevant parameter ranges for each interaction may be a guideline for the development of more coarse–grained models of flowing polymer solutions. Apart from fluctuations around a *steady state* we also investigate the nonlinear response of the polymer to a *large sudden change* in the flow parameters. This response exhibits several different regimes with characteristic decay laws and shows features which are beyond the scope of single mode theories such as the dumbbell model.

F&E-Nr: 23.30.0

The dynamics of polymers causes the viscoelasticity of polymer solutions which manifests in such spectacular effects as turbulent drag reduction. In spite of active research for over 60 years already, the understanding of these phenomena is still incomplete. Progress towards a microscopically founded rather than empirical description of flowing polymer solutions can be made only by a thorough analysis of the interplay between the dynamics of single polymers and the flow. However, only recent experiments on individual DNA molecules allow to observe the molecular conformations and computer simulations facilitate a treatment of the nonlinear interactions within the polymer-solvent system.

The dynamics of a polymer in flow is commonly characterized by its relaxation modes and spectrum. These quantities determine the linear viscoelastic solution properties but they are known analytically only for the linear Rouse and Zimm models. Questions arising are: Is there an effective method for determining the complete relaxation spectrum and corresponding modes also for realistic polymer models which are nonlinear in general? What is their dependence on the polymer deformation and which decay laws describe the whole relaxation process from a strongly stretched polymer to equilibrium?

We give answers for the model problem of a tethered polymer in uniform flow which has been much investigated recently both experimentally [1,2] and theoretically using blob [3] and bead spring models [4–6]. By means of simulations we determine the relative importance for polymer dynamics of various nonlinear interactions such as the finite extensibility of a polymer, excluded volume (**EVI**), and hydrodynamic interactions (**HI**).

Polymer fluctuations at steady state are analyzed with the Karhunen–Loève (KL–) technique [7] as a generalization of the normal mode analysis used to solve the linear models of Rouse and Zimm. This new method in polymer dynamics overcomes weaknesses of other common approaches to the relaxation dynamics of nonlinear polymer models. Often, the *linear* Rouse modes have been used also to analyze *nonlinear* polymer models. In this approach the mode amplitudes are obtained by projecting the polymer dynamics on the respective Rouse mode and the relaxation times τ_p are determined by an exponential fit to a time series of the amplitudes. The determination of τ_p in this way is tedious and error-prone so that in practice only the few longest relaxation times can be obtained. In addition, independently relaxing modes do not exist for nonlinear systems; therefore, the significance of the Rouse modes for the relaxation process is unclear. Another approach aims at the relaxation spectrum directly, without referring to corresponding modes, by applying an inverse Laplace transform to a single time series of some observable like the end–to–end distance. Due to the presence of noise in the data this requires the use of special regularization techniques and the results depend strongly on the regularization parameter.

The approach we suggest [8] uses the KL–method to determine a set of uncorrelated modes from simulation data. Since these modes form a basis in the space of all polymer conformations, the method yields the complete relaxation spectrum rather than only the longest relaxation time considered in previous works. Furthermore, it also provides numeric values for the relaxation times which cannot be obtained from scaling arguments. From a practical viewpoint the KL–method is fast, easy to use, and needs no adjustments of parameters or additional assumptions.

The assumption that the polymer is always in a steady state requires variations in the flow field experienced by the polymer to be slow – an assumption which is probably not valid in flows as they occur *e.g.* in turbulent drag reduction. An interesting model for such rapidly varying flows is the immediate start-up and cessation of simple flows as considered here. The resulting average dynamics coincides with the relaxation of fluctuations in the steady state only in the linear regime of polymer dynamics where

the Rouse–Zimm model is valid.

Among the nonlinear effects considered, finite extensibility of the springs has the deepest impact on the polymer relaxation far from equilibrium. As shown in Fig. 1, the modes are very different from the Rouse form and the relaxation times decrease strongly with increasing flow velocity. This latter phenomenon has been reported recently also for a chain which is pulled at *the ends* [5]. That problem, however, is special in that the tension along the polymer is everywhere the same. In contrast, when the polymer is stretched by a flow such that drag forces are exerted on *each bead*, the tension in general is inhomogeneous [6]. A comparison of the modes calculated for both cases reveals that it is just this inhomogeneity that causes the strong deviation of the modes from the Rouse form observed in Fig. 1. A similar situation also holds for the effects of HI [6]. Again, the experimental finding that the relaxation of an elongated polymer is described well by the Rouse modes [9] is special to the case of a polymer pulled at the ends where there is no variation of the HI along the contour. For a tethered polymer in uniform flow, the relaxation times as calculated with the KL–method for a model with harmonic springs and both EVI and HI reveals the following: At first, the relaxation times decrease because EVI, which slow the relaxation process down, becomes weaker when the polymer is elongated. Then, in a certain range of flow velocities, HI lead to relaxation times that increase with v. A final crossover to Rouse behavior occurs only at very large flow velocities. For the chain lengths available in the present study, the combination of FENE springs with EVI and HI results in a monotonic decrease of the longest relaxation time. However, for much longer chains it is possible that a regime of increasing relaxation times as required for the coil stretch transition [10] might occur.

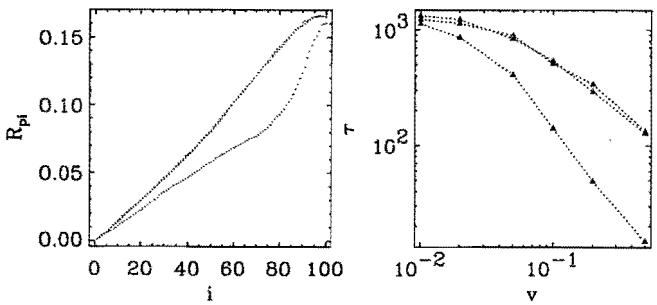

FIG. 1. First triplet ($p = 1$) of relaxation modes for $v = 0.2$ (left) and relaxation times (right) for a pure FENE chain.

For the average dynamics the most interesting behavior is found for the Rouse model with EVI added. After cessation of the flow we observe three distinct regimes as shown in Fig. 2. Initially, $X_E(t)$ decays exponentially with the longest Rouse time τ_1^R as time constant. This regime is dominated by the relaxation of the stretched part of the chain close to the tether-point where EVI are negligible. Then, one finds a stretched exponential decay $X_E(t) \propto \exp(-(t/\tau_1^R)^\beta)$ with stretching exponent $\beta \simeq 0.5$. During this stage the relaxation is increasingly slowed down because self-avoidance constraints become more important. Stretched exponential relaxation is commonly explained by a superposition of single exponential decays with time constants that obey a power law. It is thus unlikely that this complex behavior can be captured by a single mode theory like the dumbbell model. In a third regime finally, the entangling process is completed and the equilibrium value of $X_E = 0$ is approached by only local rearrangements within the coil. This process is again described by a single exponential law where the time constant is now given by the longest equilibrium KL relaxation time. After starting the flow the response of the chain is dominated by self-entanglements. These are resolved on a time scale of the longest relaxation time rather then the shortest one which corresponds to a stretching of individual springs.

These investigations are currently extended to more realistic flow fields like simple shear and elongational flows.

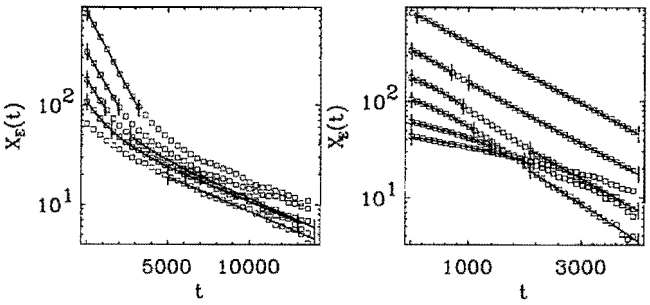

FIG. 2. Evolution of the x–component of the end–to–end vector $X_E(t)$ for a Rouse chain with EVI after cessation (left) and start-up (right) of the flow. Flow velocities are $v = 0.5, 0.2, 0.1, 0.05, 0.02$ and $v = 2.0, 1.0, 0.5, 0.2$ from top to bottom. $X_E(t)$ is calculated from an ensemble average over 100 independent simulation runs. Only a fraction of the data used for the fits (solid lines) is shown.

[1] T. T. Perkins, S. R. Quake, D. E. Smith, and S. Chu, Science **264**, 822 (1994).

[2] S. Manneville *et al.*, Europhys. Lett. **36**, 413 (1996).

[3] *e.g.* Y. Marciano and F. Brochard-Wyart, Macromolecules **28**, 985 (1985).

[4] R. G. Larson, T. T. Perkins, D. E. Smith, and S. Chu, Phys. Rev. E **55**, 1794 (1997).

[5] J. W. Hatfield and S. R. Quake, Phys. Rev. Lett. **82**, 3548 (1999).

[6] R. Rzehak, D. Kienle, T. Kawakatsu, and W. Zimmermann, Europhys. Lett. **46**, 821 (1999). R. Rzehak, W. Kromen, T. Kawakatsu, and W. Zimmermann, Euro. Phys. J. B. to appear

[7] M. Loève, *Probability Theory* (van Nostrand, Princeton, 1955).

[8] R. Rzehak and W. Zimmermann, submitted to Phys. Rev. Lett.

[9] S. R. Quake, H. Babcock, and S. Chu, Nature **388**, 151 (1997).

[10] P.-G. deGennes, J. Chem. Phys. **60**, 5030 (1974).

Evolution of gas-filled nano-cracks in crystalline solids

M. Hartmann and H. Trinkaus
Institute Theory III

The evolution of gas-filled cracks under gas implantation and subsequent annealing is studied on the basis of an elastic continuum approach. The observed growth limitation of He-filled nano-cracks in SiC is attributed to their stabilization by the formation of circular dislocations dipoles. The formation and Ostwald ripening of bubble-loop complexes at elevated temperatures is modeled in terms of gas atom exchange between bubbles coupled with matrix atom exchange between bubbles and associated loops. Scaling laws derived for the time dependence of bubble and loop sizes are in good agreement with experimental data. The idea of loop formation by gas-filled cracks is applied to model strain relaxation in GeSi on Si heterostructures by H implantation and subsequent annealing.

F&E-Nr: 23.15.0/23.42.0/23.80.5

By ion beam implantation, solid-gas systems far from thermodynamic equilibrium can be formed where the driving force for the precipitation of the gas atoms into bubbles is very high. For bubble formation, generally both gas and matrix atom diffusion are required. In a crystalline matrix, light gas atoms such as H and He commonly diffuse as interstitial atoms. At medium temperatures where such interstitial gas atoms are already mobile while matrix atom are still immobile, a process for which no matrix atom transport is required is the precipitation of the mobile gas atoms between atomic layers of the matrix lattice thus forming gas-filled Griffith cracks.

The present work was motivated by the observation of penny-shaped crack-like He platelets in SiC after He implantation and subsequent thermal annealing [1,2], experiments performed to simulate effects of He expected to be produced by (n,α) reactions in SiC in fusion reactor environments. It has turned out meanwhile that the formation of gas-filled nano-cracks is a general phenomenon in non-metallic systems. Thus, it has been shown recently that H ion implantation into Si results in H-filled nano-cracks which may be used to trigger strain relaxation in GeSi on Si heterostructures [3].

We have used the isotropic elastic continuum approach to study the evolution of such nano-cracks [4] and applied the basic idea of dislocation loop formation by such cracks to model strain relaxation in SiGe/Si heterostructures by H implantation [3]. For the case of He-implanted SiC, the following puzzling experimental observations had to be rationalized: (1) the uniform size of the observed nano-cracks forming during He implantation at RT and its maintenance upon annealing up to about 1300 K without any indication of further growth, and (2) the formation of complexes of bubbles and dislocation loops and their coarsening at higher temperatures.

For the observed diameters of 9nm, the pressure in the crack-like He platelets is estimated to be around 24GPa where He is expected to be solid even up to 470K. The maximum shear stress at the rim of the cracks is estimated to be around or even above the theoretical shear strength - independent of the crack size.

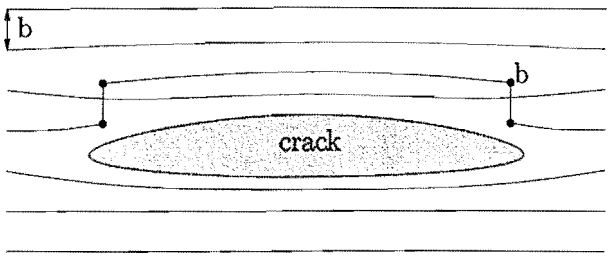

FIG. 1. Illustration of a gas-filled crack partially relaxed by the formation of a dislocation dipole.

Thus, we may assume partial pressure relaxation by the spontaneous formation of circular dislocation dipoles. Because of the large resistance against both dislocation glide and climb in non-metallic structures, a once formed dislocation dipole will stay in its original configuration of minimum separation as illustrated in Fig.1. An analysis of the free energy subject to this kinetic constraint shows that the crack is strongly bound to its dislocation dipole. After dipole formation, the crack tends to grow slightly to a size where, in contrast to the Griffith crack, further

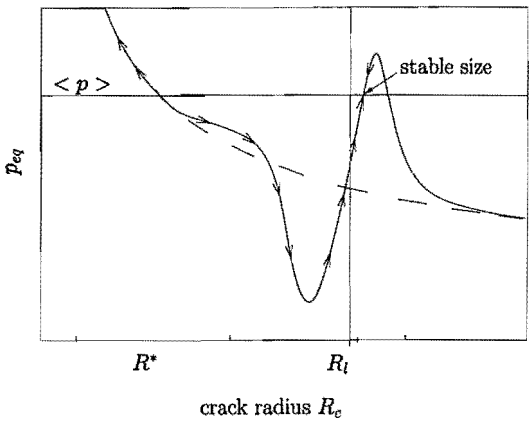

FIG. 2. Equilibrium gas pressure, peq, in the vicinity of a Griffith crack (dashed line) and a crack with a dislocation dipole (full line) as a function of the crack radius Rc; ¡p¿ is the average pressure defined by the background of small Griffith cracks (schematic).

growth would lead to an increase of the gas pressure and the local He concentration in its environment, resulting in a net emission of gas, thus stabilizing the crack at the size of vanishing net absorption/emission as illustrated in Fig. 2.

There remains, however, the question why a threshold value for the crack size is needed for the formation of a dislocation dipoles - even though the maximum shear stress resolved by an imaginary nascent dipole at the tip of a Griffith crack is independent of crack size. The answer is that the dipole formation process up to its completion depends indeed on crack size since the relative volume increase and, accordingly, the relaxation of the gas pressure in the crack upon dipole formation decreases with increasing crack size. Thus, for too small cracks, the gas pressure as the driving force for dipole formation exhausts before the dipole is completed. A quantitative estimate of the threshold size for dipole formation is difficult because of the complicated elastic boundary value problem.

At elevated temperature ($1300K < T < 2200K$) where at least local matrix atom transport along crack surfaces and dislocation cores becomes operative the so far metastable cracks transform into complexes of now three-dimensional (spherical) bubbles and dislocation loops which coarsen upon annealing (see Fig.3). The assumed restriction of matrix atom transport to internal surfaces and dislocation cores is confirmed by the experimental observation that the total volumes of the bubble and loop components in such complexes are equal. According to this, the kinetic interaction of complexes must be due to He atom exchange between them. Thus, we are confronted with a new type of two-component Ostwald ripening process where one component, the He atoms, perform long ranging bulk diffusion while the diffusional transport of the other component, the matrix atoms, is restricted to the environment of the growing/shrinking structure.

To analyse this coupled Ostwald ripening process the chemical potential of the gas atoms at the bubbles as well as that of the matrix atoms at the bubbles and along the dislocation loops must be considered. The analyses shows that three stages in the evolution of coupled bubble-loop complexes may be distinguished: a short transition stage where the high pressure is partially relaxed at constant density of the objects, and two coarsening stages where the chemical potential of the matrix atoms is dominated by the line tension of the loops and the surface tension, respectively. Taking global gas atom and local matrix atom conservation into account we have derived the following approximate scaling laws for the time dependence of the average bubble radius in the first and the second coarsening stages, respectively:

$$R_b \sim t^x, \text{ with } x = 1/6 \approx 0.167 \text{ and } x = 2/11 \approx 0.182.$$

According to this, the exponents of the power law time dependencies for the two coarsening stages differ only slightly and are, moreover, in good agreement with the value of 0.17 obtained from fitting experimental data [2].

Generally, the Burgers vector of the interstitial type dislocation loop forming at a gas-filled crack has a component in the loop plane. This is a property crucial for strain relaxation in GeSi on Si heterostructures by H^+ ion implantation with energies such that H-filled nanocracks are formed in Si well below the interface to the GeSi layer. Upon annealing, a loop formed at a nanocrack becomes glissile and glides, repelled by the crack and attracted by interfacial image forces, to the GeSi layer where the plane stress associated with the misfit strain exerts an asymmetric force on the loop, holding one side of it in the interface where it forms a misfit dislocations segment and pulling the other side to the surface where it forms a step. At sufficiently high nanocrack density, virtually all threading dislocations extending between the interface and the surface find partners for mutual annihilation within there interaction range. The desired low residual density of threading dislocation contrasts with the substantially higher density remaining in conventional strain relaxation. On the basis of this picture, the conditions for efficient and healthy strain relaxation to be imposed on the relevant parameters have been derived and found to be in good agreement with experiments. Thus, the model provides a basis for improving and extending this promising technique in microelectronic material processing.

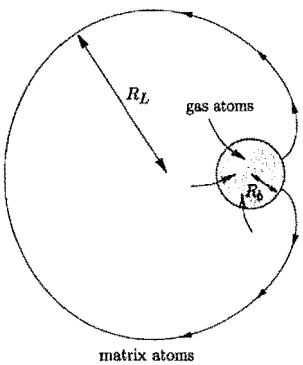

FIG. 3. Growth of a bubble-loop complex by the absorption of He atoms from the environment and the concurrent transfer of matrix atoms to the dislocation loop.

[1] J. Chen, P. Jung and H. Trinkaus, *Phys. Rev. Lett.*, **82**, 2709 (1999).

[2] J. Chen, P. Jung and H. Trinkaus, accepted by *Phys. Rev.B.*

[3] H. Trinkaus, B. Holländer, St. Rongen, S. Mantl, H.-J Herzog, J. Kuchenbecker, and T. Hackbarth, submitted to *Appl. Phys.Lett.*

[4] M. Hartmann, Diploma thesis, Aachen 1999.

Nonlinear theory of dislocations in smectics - an exact solution

Efim A. Brener and V.I. Marchenko
Institute Theory III

It is shown that the strain field of an edge dislocation in a smectic must be described in the framework of nonlinear theory even far away from the core region. We present an exact solution of this nonlinear problem. The result of the linear theory is recovered in the limit of large bending rigidity.

F & E-Nr: 23.15.0

The strain field of point and linear defects in crystals decays with the distance from the defect, so that the long range distortion around the defects can be described within the framework of the linear theory of elasticity. The same approach has been used by de Gennes to describe edge dislocations in a smectic [1]. This linear theory is believed to be exact far from the dislocation core and it is presented in text books on physics of liquid crystals and also in the more general context of the theory of elasticity (see for example [2,3]). The intrinsic anisotropy of smectics, however, means that nonlinear effects can be important even for small strains, and the Helfrich instability [4], the corrugation of smectic layers in a stretched smectic film, is a well-known example.

We show that the linear theory of edge dislocations in smectics [1] is valid only in the limit $b \ll \lambda$, where b is the Burgers vector and λ is the length scale in the elastic energy functional. In the general case where $b \sim \lambda$ nonlinearities must be taken into account to describe the asymptotic behavior even at large distances from the core. To the best of our knowledge this is the first instance where the asymptotic distortion field induced by the defect in a three-dimensional object must be treated by nonlinear theory. Moreover, we give an exact solution of the nonlinear equation for the displacement field around a dislocation.

For small strains the distortion energy of a smectic is [2]

$$F = \frac{1}{2}\int dxdz\left[A[\partial_z u - \frac{1}{2}(\partial_x u)^2]^2 + B(\partial_x^2 u)^2\right]. \quad (1)$$

Here $u(x,z)$ is the smectic displacement field, A is the elastic modulus and B is the bending modulus; the dislocation lies along the y axis. The intrinsic length scale λ is given by $\lambda = (B/A)^{1/2}$. In linear approximation the strain field for the edge dislocation is obtained [1] (see also [2]) as

$$\partial_z u = -\frac{bx}{8(\pi\lambda)^{1/2}z^{3/2}}\exp\left[-\frac{x^2}{4\lambda z}\right] \quad (2)$$

and

$$\partial_x u = \frac{b}{4(\pi\lambda z)^{1/2}}\exp\left[-\frac{x^2}{4\lambda z}\right] \quad (3)$$

for $z > 0$. The most significant change of the displacement field occurs in the region $x \sim \sqrt{\lambda z}$. The linear approximation is valid for $(\partial_x u)^2/|\partial_z u| \ll 1$. However, this ratio is of order b/λ and independent of z in the important region. Thus a nonlinear theory must be applied to describe the general case $b \sim \lambda$.

The full nonlinear equation is obtained by variation of the energy, Eq. (1), and reads

$$\lambda^2\partial_x^4 u - \partial_z^2 u$$
$$+2(\partial_x u)\partial_z\partial_x u + (\partial_x^2 u)\partial_z u - \frac{3}{2}(\partial_x u)^2\partial_x^2 u = 0. \quad (4)$$

Let us measure all the lengths (u, x, z, b) in units of λ. If we assume that, as in the linear approximation, the displacement field $u(x,z)$ depends only on the variable $v = x/\sqrt{z}$ the problem reduces to the solution of a third order ordinary differential equation for the strain field $\phi = du/dv = u'$:

$$\phi''' = \frac{v^2}{4}\phi' + \frac{3v}{4}\phi + \phi^2 + \frac{3v}{2}\phi\phi' + \frac{3}{2}\phi^2\phi' \quad (5)$$

subject to the constraint

$$u(+\infty) - u(-\infty) = \int_{-\infty}^{\infty}\phi dv = b/2. \quad (6)$$

Fortunately an exact solution of Eq. (5) exists which meets all physical requirements. Indeed, it is easily checked that under the condition

$$\phi' = -\frac{1}{2}\left(\phi^2 + v\phi\right) \quad (7)$$

Eq. (5) is automatically satisfied. The general solution of Eq. (7) is

$$\phi = \frac{2e^{-v^2/4}}{\int_{-\infty}^{v} e^{-t^2/4}dt + C} \quad (8)$$

where C is a constant of integration to be determined by Eq. (6). Finally, in the original, dimensioned variables the displacement field u is given by

$$u = 2\lambda\ln\left[1 + \frac{e^{b/4\lambda} - 1}{2\sqrt{\pi}}\int_{-\infty}^{x/\sqrt{\lambda z}} e^{-t^2/4}dt\right]. \quad (9)$$

In the limit $b \ll \lambda$ the result of the linear theory [1] is recovered,

$$u \approx \frac{b}{4\sqrt{\pi}} \int_{-\infty}^{x/\sqrt{\lambda z}} e^{-t^2/4} dt. \qquad (10)$$

We note that the field ϕ is an even function of v in the linear theory, whereas nonlinear effects destroy this symmetry. Fig. 1 presents the distortion field induced by a dislocation which we plot according to the exact result, Eq. (9). Fig. 1a corresponds to the small ratio $b/4\lambda = 1/8$ and the result of linear theory, Eq. (10), is a good approximation. The displacement field changes mainly in the range of positive and negative x, $|x| \sim \sqrt{\lambda z}$. Fig. 1b corresponds to the strongly nonlinear case, $b/4\lambda = 5$. In this case the asymmetry becomes very pronounced: the displacement field changes mainly in the range of negative x and $|x| \sim \sqrt{bz} > \sqrt{\lambda z}$ (linear theory still predicts symmetric range $|x| \sim \sqrt{\lambda z}$).

Normally λ is several times larger than the interlayer distance. Together with the fact that the actual expansion parameter is $b/4\lambda$ this makes the linear theory a good approximation in many experimental situations. However, for a finite density of dislocations in some localized region the effective Burgers vector can be large enough to make the nonlinear effects observable.

We now discuss another structure that appears as a limiting case of our exact solution. Eq. (8) gives for $C = 0$ the displacement field

$$u = 2\lambda \ln \left[\frac{1}{2\sqrt{\pi}} \int_{-\infty}^{x/\sqrt{\lambda z}} e^{-t^2/4} dt \right] \qquad (11)$$

(where we have chosen $u(+\infty) = 0$) which describes the following texture. For $x \gg \sqrt{\lambda z}$ there are almost flat smectic layers and for negative x ($|x| \gg \sqrt{\lambda z}$) the displacement field, $u = -x^2/2z$, corresponds to parabolic layers where z is the radius of curvature. This parabolic structure is the beginning of a circular structure. The smooth matching between the structures with zero and finite curvatures is in the region $|x| \sim \sqrt{\lambda z}$.

To conclude, we have found that even for a small strain, $\partial_z u \ll 1$ and $\partial_x u \ll 1$, the asymptotic distortion field around the edge dislocation in smectics *must* be treated in the framework of nonlinear theory using the elastic energy functional, Eq. (1). We have found an exact solution of this problem where the displacement field depends only on a scaling variable. Dislocations in smectics lie somewhere in between point defects, which can still be treated by linear theory, and cases with a localized force or linear distribution of forces. The angle $\partial_x u$ is of order unity in the latter, requiring the use of a fully nonlinear theory beyond the functional in Eq. (1). Such work is in progress.

Our findings should also be applicable to those systems which have common features with smectics such as block copolymer films, charge density waves, spin density waves, the vortex lattices in superconductors, and in superfluid He^3 and He^4.

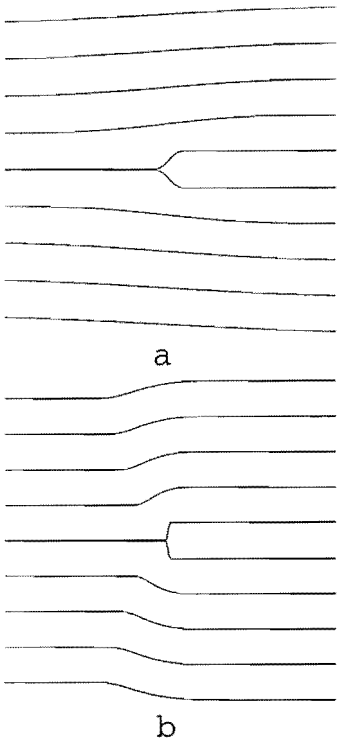

FIG. 1. The distortions induced by a dislocation in a smectic: a) $\lambda = 2b$; b) $\lambda = 0.05b$.

[1] P.G. de Gennes, C.r., Acad. Sci. (Paris) **275B**, 939 (1972).

[2] L.D. Landau and E.M. Lifshitz, *Theory of Elasticity*, Pergamon Press, Oxford, 1987.

[3] M. Kléman, *Points, Lines, and Walls in liquid crystals, magnetic systems and various ordered media*, Wiley-Interscience, New York, 1983.

[4] W. Helfrich, J. Chem. Phys. **55**, 839 (1971).

Publications in refereed journals

Asato M.1; Settels A.; Hoshino T.2; Asada T.2; Blügel S.; Zeller R.; Dederichs P.H.
1Graduate School of Electronic Science and Technology, Shizuoka University, Japan
2Faculty of Engineering, Shizuoka University, Japan
Full Potential KKR-calculations for Metals and Semiconductors
Phys. Rev. B 60, 5202 (1999)
23.20.0

Brener E.
Pattern formation in three-dimensional dendritic growth
Physica A 263 (1999) 338-344
23.15.0

Brener E.; Iordanskii S.V.1; Marchenko V.I.2
1L.D. Landau Institute for Theoretical Physics, Chernogolovka, Russia
2P.L. Kapitza Institute for Physical Problems, Moscow, Russia
Elastic effects on the kinetics of a phase transition
Physical Review Letters, Vol. 82, No. 7 (1999) 1506-1509
23.15.0

Brener E.; Marchenko V.I.1
1P.L. Kapitza Institute for Physical Problems, Moscow, Russia
Nonlinear theory of dislocations in smectic crystals: An exact solution
Physical Review E, Vol. 59, No. 5 (1999) 4752-4753
23.15.0

Brener E.; Marchenko V.I.1
1P.L. Kapitza Institute for Physical Problems, Moscow, Russia
Surface instabilities in cracks
Physical Review Letters, Vol. 81, No. 23 (1998) 5141-5144
23.15.0

Brener E.; Müller-Krumbhaar H.
Comment on "Electrically induced morphological instabilities in free dendrite growth"
Physical Review Letters 83, 1698 (1999)
23.15.0

Brener E.; Temkin D.E1
1Institute of Physics of Metals, I.P. Bardin Central Scientific Research Institute of Ferrous Metallurgy, Moscow, Russia
Theory of diffusional growth in cellular precipitation
Acta Mater., Vol. 47, No. 14, 3759-3765 (1999)
23.15.0

Drchal V.1,2; Kudrnovský J.1,2; Bruno P.3; Dederichs P.H.; Weinberger P.2
1Institute of Physics, Academy of Science of the Czech Republic, Praha
2Center for Computational Material Science, Technical University Vienna, Austria
3MPI für Mikrostrukturphysik, Halle/Saale
The combined effect of temperature and disorder on interlayer exchange coupling in magnetic multilayers
Phil. Mag. B78, 571 (1998)
23.20.0

Drchal V.1; Kudrnovský J.1; Bruno P.2; Turek I.3; Dederichs P.H.; Weinberger P.4
1Institute of Physics, Academy of Science of the Czech Republic, Praha
2MPI für Mikrostrukturphysik, Halle
3Institute of Physics, Academy of Sciences of the Czech Republic, Brno and Institute for Technical for Technical Electrochemistry, Technical University, Vienna, Austria
4Center for Computational Material Science, Technical University Vienna, Austria
Temperature dependence of the interlayer exchange coupling in magnetic multilayers: An ab-initio approach
Phys. Rev. B 60, 9588 (1999)
23.20.0

Feng X.; Brener E.; Temkin D.E.; Saito Y.1; Müller-Krumbhaar H.
1Department of Physics, Keio University, Yokohama, Japan
Creep motion of a solidification front in a two-dimensional binary alloy
Physical Review E 59, 512 (1999)
23.15.0

Gaukel C.; Kluge M.; Schober H.
Diffusion Mechanisms in Under-Cooled Binary Liquids of Zr67Cz33
J. Non-Cryst. Solids 250-252, 664 (1999)
23.15.0

Gaukel C.; Kluge M.; Schober H.
Diffusion and relaxations in liquid and amorphous metals
Philosophical Magazine B 79, 1907 (1999)
23.15.0

Hauck J.; Henkel D.; Klein M.1; Mika K.
1Institut für Biotechnologie, FZ Jülich
Structure maps of close-packed layered compounds and DNA
J. Solid State Chem., 145 (1999) 150
23.15.0

Hauck J.; Mika K.
Structure maps for close-packed alloys by the Ising model
Z. Kristallogr., 214 (1999) 443
23.15.0

Hergert W.1; Stepanyuk V.S.1; Zeller R.; Dederichs P.H.
1Martin-Luther-Universität Halle Wittenberg
Unusual magnetic behavior in imperfect magnetic 4d and 5d clusters on the
Ag(001) surface
J. Magn. Magn. Mat. 198-199, 233 (1999)
23.20.0

Hoshino T.1; Papanikolaou N.; Zeller R.; Dederichs P.H.; Asato M.1; Asada T.1; Stefanou N.2
1Faculty of Engineering, Shizuoka University, Japan
2University of Athens, Athens, Greece
First-Principles Calculations for Vacancy Formation Energies in Cu and Al; Non-Local Effect beyond the LSDA and Lattice Distortion
Comp. Mater. Science 14, 56 (1999)
23.20.0

Müller-Krumbhaar H.; Saito Y.1
1Department of Physics, Keio University, Yokohama, Japan
Strain effect on Eden Model
J. Phys. Soc. Japan, 67, 3661 (1998)
23.15.0

Nonas B.; Wildberger K.; Zeller R.; Dederichs P.H.; Wille L.T.1; Dreysse H.2
1Florida Atlantic University, Boca Raton, USA
2Institute de Physique et Chimie des Materiaux de Strasbourg, France
Direct Exchange and Interaction of 3d Impurities on the (001) Surface of Iron
J. Magn. Magn. Mat. 198-199, 548 (1999)
23.20.0

Oligschleger C.1; Gaukel C.; Schober H.
1Theoretische u. Physikalische Chemie, Universität Bonn
Relaxations in Glasses
J. Non-Cryst. Solids 250-252, 660 (1999)
23.15.0

Oligschleger C.1; Schober H.
1Theoretische u. Physikalische Chemie, Universität Bonn
Molecular Dynamics Simulations of Glasses
J. Non-Cryst. Solids 250-252, 651 (1999).
23.15.0

Parshin D.A.1; Schober H.
1State Technical University, St. Petersburg, Russia
Distribution of fractal dimensions at the Anderson transition
Phys. Rev. Lett. 29 4590 (1999)
23.15.0

Peyla P.1; Vallat A.1; Misbah C.2; Müller-Krumbhaar H:
1Laboratoire de Physique et de Modelisation des Milicux Condenses, Universite J. Fourier, Grenoble, France
2Laboratoire de Spectrometrie, Universite J. Fourier, Grenoble, France
On elastic interaction between surface defect in thin layers
Phys. Rev. Lett. 82, 787 (1999)
23.15.0

Rzehak R.; Kienle D.; Kawakatsu T1; Zimmermann W.2
1Department of Computational Science and Engineering, Nagoya University, Japan
2Universität des Saarlandes, Saarbrücken
Partial Draining of a Tethered Polymer in Flow
Europhys. Lett. 46, 821 (1999)
23.15.0

Schober H.
Oligschleger C.; Schober H.
Collective jumps in a soft sphere glass
Phys. Rev. B59, 811 (1999)
23.15.0

Settels A.; Korhonen T.1; Papanikolaou N.; Zeller R.; Dederichs P.H.
1Laboratory of Physics, Helsinki University of Technology, Finnland
Ab-intio Study of Acceptor-Donor Complexes in Silicon and Germanium
Phys. Rev. B 83, 4369 (1999)
23.20.0

Smirnova E.A.1; Abrikosov I.A.2; Johansson B.2; Vekilov Yu.Kh.3; Baranov A.N.4; Stepanyuk V.S.5; Hergert W.5; Dederichs P.H.
1Department of Theoretical Physics, Moscow Steel and Alloys Institute, Moscow, Russia
2Condensed Matter Theory Group, Department of Physics, Uppsala University, Sweden
3Department of Theoretical Physics, Moscow State University, Moscow, Russia
4Department of Solid State Physics, Moscow State University, Moscow, Russia
5Fachbereich Physik, Martin-Luther-Universität, Halle/Saale
Calculated magnetic properties of an Fe1-xNix monolayer on Cu(001)
Phys. Rev. B 59, 14417 (1999)
23.20.0

Steinbrecher J.; Müller-Krumbhaar H.; Brener E.; Misbah C.1; Peyla, P.2
1Laboratoire de Spectrometrie, Universite J. Fourier, Grenoble, France
2Laboratoire de Physique et de Modelisation des Milicux Condenses, Universite J. Fourier, Grenoble, France
Fractal growth of epitaxial surface clusters with elastic interaction
Physical Review E 59, 5600 (1999)
23.15.0

Stepanyuk V.S.1,2; Hergert W.1; Rennert P.1; Wildberger K.; Zeller R.; Dederichs P.H.
1Martin Luther Universität Halle-Wittenberg
2MPI für Mikrostrukturphysik, Halle
Imperfect Magnetic Nanostructures on a Ag(001) Surface
Phys. Rev. B 59, 1681 (1999)
23.20.0

Wildberger K.; Korhonen T.; Zeller R.; Dederichs P.H.; Rampe A.1; Güntherodt G.1
1Physikalisches Institut, Technische Hochschule Aachen
Interface Reflectivity of Magnetic Layers in Cu: Effects of Adlayers
J. Magn. Magn. Mat. 198-199, 570 (1999)
23.20.0

Other publications

Gaukel C.; Kluge M.; Schober H.
Diffusion Mechanisms in Under-Cooled Binary Liquids,
Slow Dynamics in Complex Systems (M. Tokuyama and I. Oppenheim eds.)
AIP Conference Proceedings 469, 398 (1999)
23.15.0

Mantl S.1; Kappius L.1; Antons A.1; Löken M.1; Klinkhammer F.1; Dolle M.1; Zhao Q.T.1; Mesters S.1; Buchal Ch.1; Bay H.L.1; Kabius B.1; Trinkaus H.; Heinig H.2
1Institut für Schicht- und Ionentechnik, FZ Jülich
2Institut für Ionenstrahlphysi und Materialforschung, Forschungszentrum Rossendorf
Growth, Patterning and Microelectronic Applications of Epitaxial Cobaltdisilicide
MRS Proceedings 507 (1998)
23.42.0

Schober H.
Molecular dynamics in amorphous solids and liquids
Physics of Glasses (P. Jund and R. Jullien eds.) p.191, AIP Conference Proceedings 489, 1999
23.15.0

Invited talks

Brener E.
Instabilities in cracks
University Grenoble, Frankreich, 01.04.1999
23.15.0

Brener E.
Instabilities in cracks
Universität Montpellier, Frankreich, 20.09.1999
23.15.0

Brener E.
Pattern formation in diffusional growth
Universität Kiel, 29.10.1999
23.15.0

Dederichs P.H.
Ab-initio Study of Magnetic Adatoms and Small Clusters on Surfaces
Int. Conference on Clusters and Nanostructure Interfaces, Richmond, VA, USA, 27.10.1999
23.20.0

Dederichs P.H.
Conceptional Improvementrs of the KKR Method for Electronic Structure Calculations
Seminar, Oak Ridge National Laboratory, USA, 19.03.1999
23.20.0

Dederichs P.H.
Elektronische und magnetische Eigenschaften von Adsorbatatomen auf Oberflächen
Kolloquium, Hahn Meitner Institut, Berlin, 01.02.1999
23.20.0

Dederichs P.H.
Forces and Lattice Relaxations in Dilute Alloys
APS-March Meeting, Atlanta, USA, 22.03.1999
23.20.0

Dederichs P.H.
Komplexe Bandstruktur und Tunneln in Ferromagnet/Isolator/Ferromagnet Schichten
Universität Halle, 04.11.1999
23.20.0

Dederichs P.H.
Magnetic Adatoms and Small Clusters on Surfaces
Kolloquium Physics Department, Moscow State University, Moskau, 19.01.1999
23.20.0

Dederichs P.H.
Magnetic Adatoms and Small Clusters on Surfaces
Symposium on Multilayers and Nanostructures, Univ. Bielefeld, 17.04.1999
23.20.0

Dederichs P.H.
Magnetismus von Adatomen und kleinen Clustern auf Oberflächen
Physikalisches Kolloquium, Univ. Gesamthochschule Duisburg, 26.04.1999
23.20.0

Dederichs P.H.
Proposal for a RT-Network "Computational Magnetoelectronics"
TMR-Workshop "5th Framework", Orsay, Paris, 30.04.1999
23.20.0

Müller-Krumbhaar H.
Morphology diagram of diffusional growth
Seminar, DLR Porz, 27.10.1999
23.15.0

Müller-Krumbhaar H.
Strukturbildung an bewegten Phasengrenzflächen
Mathematisches Kolloquium, Universität Freiburg, 16.02.1999
23.15.0

Müller-Krumbhaar H.
Strukturbildung bei diffusionsbedingtem Wachstum
Physik-Workshop, Universität Kiel, Sehlendorf, 21.09.1999
23.15.0

Müller-Krumbhaar H.
Wie wächst ein Keim?
Kolloquium, Institut für Physik, Universität Göttingen, 25.10.99
23.15.0

Müller-Krumbhaar H.
Wie wächst ein Keim?
Kolloquium, Physikalische Chemie, TU Hannover, 17.03.1999
23.15.0

Schober H.
Dynamik in Gläsern
Institut für Physikalische Chemie, Universität Hannover, 1.2.1999
23.30.0

Schober H.
Molecular dynamics in amorphous solids and liquids
CNRS Summer School "Physics of Glasses: Structure and Dynamics", Cargese, Korsika, Frankreich17./18. 5. 1999
23.30.0

Schroeder K.
Surface Diffusion and Models of the Kinetics Epitaxial Growth
Intern. Symposium on Structure and Dynamics of Heterogeneous Systems, Univ. Duisburg, 25.02.-26.02.1999
23.42.0

Trinkaus H.
Evolution of Gas-Filled Nano-Cracks in Ceramics,
Comp. Mat. Sci., Lawrence Livermore Nat. Lab. Livermore, CA, USA, 21.07.1999
23.15.0/23.42.0/23.80.5

Trinkaus H.
Evolution of Gas-Filled Nano-Cracks in Ceramics,
Comp. Mat. Sci., Sandia Nat. Lab. Livermore, California, USA, 20.07.1999
23.15.0/23.42.0/23.80.5

Trinkaus H.
Evolution of Gas-Filled Nano-Cracks in Ceramics,
Mech.& Aerospace Dep., UC Los Angeles, USA, 30.06.1999
23.15.0/23.42.0/23.80.5

Trinkaus H.
Microstructural Evolution in Metals under Cascade Damage Conditions,
Dep. Mech. & Envirnm. Eng., UC Santa Barbara, USA, 06.07.1999
23.80.5

Trinkaus H.
Progress in Modeling the Microstructural Evolution in Metals under Cascade Damage Conditions,
Int. Conf. Fusion Reactor Mat. (ICFRM 9), Colorado Springs, USA, 10.-15.10.1999
23.80.5

Trinkaus H.
The Role of Cascade-Induced Glissile Interstitial Loops on the Plasticity of Metals,
Gordon Research Conf. on "Material Processes Far from Equilibrium", Plymouth, NH, USA, 12.07.1999
23.80.5

Zeller R.
Parallel Computing with the KKR Method
Annual Meeting of the TMR-Network: "Ab-initio Calculations of Magnetic Properties of Surfaces, Interfaces and Multilayers", Aussois, Frankreich, 28.03.1999
23.20.0

Other talks

Gutheim F.; Steinbrecher J.; Brener E.; Müller-Krumbhaar H.
Fraktales Wachstum epitaktischer Adsorbatcluster mit elastischer Wechselwirkung
DPG Frühjahrstagung, Münster, 22.03.- 26.03.1999
23.15.0

Kluge M.
Diffusion in Cu33 Zr67
Kolloquium "Unterkühlte Metallschmelzen: Phasenselektion und Glasbildung", DFG, Bad Honnef, 24.02.-26.02.1999
23.30.0

Müller-Krumbhaar H.
Strukturbildung bei Benetzung
DFG-Seminar, Bad Honnef, 18.10.1999
23.15.0

Schober H.
Diffusion and relaxations in liquid and amorphous CuZr
Seventh International Workshop on Disordered Systems, Molveno, Trento, Italien, 02.03.1999
23.30.0

Settels A.
Defektkomplexe in Si und Ge: Elektronenstruktur, Gitterrelaxationen und Elektrische Feldgradienten
Arbeitstreffen "Forschung mit nuklearen Sonden und Ionenstrahlen", Berlin, 06.10.-08.10.1999
23.20.0

Settels A.
Different Methods for Lattice Relaxations within the KKR-Formalism
TMR-Midterm Review, Aussois, Frankreich, 27.03.-01.04.1999
23.20.0

Settels A.
Vergleich verschiedener Verfahren zur Berücksichtigung von Gitterverschiebungen
DPG-Frühjahrstagung, Münster, 22.03.-26.03.1999
23.20.0

Spettmann R.1; Schroeder K.; Blügel S.; Entel P.1
1Theor. Tieftemperaturphysik, Gerhard Mercator Universität, GH Duisburg
Elektronische Struktur von Si(111): Sn (sqrt (3) x (sqrt(3))
DPG Frühjahrstagung Münster, 22.03.1999
23.42.0

Posters

Antons A.; Berger R.; Blügel S.; Schroeder K.
Ab-intio Untersuchungen der Adatom Diffusion auf Si(111) (3x3)
DPG-Frühjahrstagung, Münster, 22.03.1999
23.42.0

Antons A.; Berger R.; Blügel S.; Schroeder K.
Ab-intio Untersuchungen der Adatom Diffusion auf Si(111) (3x3)
European Research Conference on Dynamical Process at Surfaces, Lenggries, 19.-23.09.1999
23.42.0

Berger R.; Blügel S.; Antons A.; Kromen Wi.; Schroeder K.
A Parallelized ab intio Molecular Dynamics Code for the Investigation of Atomistic Growth Processes
NIC-Workshop "Molecular Dynamics on parallel Computers", FZ Jülich, 08.02.-10.02.1999
23.42.0

Kluge M.
Diffusion in unterkühlten Schmelzen und Gläsern aus Cu33 Zr67
DPG-Frühjahrstagung, Münster, 22.03.-26.03.1999
23.30.0

Kluge M.
Diffusion mechanisms in liquid and amorphous Cu33 Zr67
Summerschool "Physics of Glasses: Structure and Dynamics", Universität Montpellier, 10.05.-22.05.1999
23.30.0

Kluge M.
Diffusion mechanisms in under-cooled binary liquids of Cu33 Zr67
NIC-Workshop "Molecular Dynamics on Parallel Computers", FZ Jülich, 08.02.-10.02.1999
23.30.0

Spatschek R.; Brener E.; Müller-Krumbhaar H.
Oberflächeninstabilitäten von Rissen
DPG-Frühjahrstagung, Münster, 22.03.-26.03.1999
23.15.0

Patents applied for

Mantl S.; Zhao Q.T.; Kappius L.; Antons A.:
Verfahren zur Herstellung von Nanostrukturen in dünnen Filmen
PCT: PCT/DE99/03683 (18.11.99) (EP,US,CA,JP,KR)
PT 1.1626
29.87.0

Lecture courses

Dederichs P.H.
Computeranwendungen in der Festkörperphysik
Seminar RWTH Aachen, SS 1999
23.20.0

Dederichs P.H.
Magnetismus und Magnetoelektronik
RWTH Aachen, SS 1999
23.20.0

Dederichs P.H.
Spinabhängiges Tunneln
30. Ferienkurs des IFF: "Magnetische Schichtsysteme", FZ Jülich, 09.03.1999
23.20.0

Müller-Krumbhaar H.
Computeranwendungen in der Festkörperphysik
Seminar RWTH Aachen, SS 1999
23.15.0

Müller-Krumbhaar H.
Praktisches Rechnen für Naturwissenschaftler
RWTH Aachen, WS 98/99
23.15.0

Schroeder K.
Atomarer Magnetismus und Austauschwechselwirkung
30. IFF-Ferienkurs "Magnetische Schichtsysteme in Forschung und Anwendung", FZ Jülich, 01.03.1999
23.42.0

Schroeder K.
Computeranwendungen in der Festkörperphysik
Seminar RWTH Aachen, SS1999
23.42.0

Internal seminars

Hauck J.; Mika K.
Die Muster des W. Ostwald und die Adsorbatstrukturen
10. Wolfgang-Ostwald-Kolloquium der Kolloid-Gesellschaft: Adsorption an Nanopartikeln, FZ Jülich, 02.12.1999
23.15.0

Kluge M.
Theorien zum Glasübergang
Seminar "Aspekte des Glasübergangs", IFF, FZ Jülich, 27.04.1999
23.30.0

Schober H.
Computersimulation
Seminar zum Glasübergang, IFF, FZ Jülich, 15.06.1999
23.30.0

Zeller R.
Bandmagnetismus
30. Ferienkurs des IFF: "Magnetische Schichtsysteme", FZ Jülich, 02.03.1999
23.20.0

Institute for Scattering Methods

General Overview

Modern solid state physics goes far beyond a phenomenological description and bases the understanding of solid state properties and phenomena on atomistic theories. To obtain information about the atomic structure of solids, probes with sub-nanometer spatial resolution are needed. To study the excitation spectra, an appropriate energy resolution is necessary in addition. All these requirements can be met by scattering methods. In this sense, scattering methods provide the basis of our present understanding of the structure, excitations and phase transitions of condensed matter on a microscopic level.

At the Institute for Scattering Methods (ISM), synchrotron x-ray scattering and neutron scattering are employed for the investigation of condensed matter on an atomistic microscopic level. The emphasis lies on exploiting fully the complementarity of the two probes. Besides the application of scattering methods to solid state problems, major activities are concentrated on the methodology. This includes the further development of experimental techniques by improving instrument components and data treatment algorithms, the development of new experimental methods and the corresponding instruments and the development, construction and operation of scattering instruments at large-scale facilities. At present, ISM operates five instruments at the research reactor DIDO of the Research Center Jülich and two instruments at the Hamburger Synchrotronstrahlungslabor HASYLAB. In addition, we participate in the operation of a sector at the Advanced Photon Source APS in Argonne, USA. These instruments are open for the use by external groups from universities, research centers and industry. The instrument responsibles from ISM provide scientific and technical support during the experiment and the data processing. ISM is open for all research areas in condensed matter science, where scattering methods can be applied. At present, the research activities are concentrated in three fields: solid state magnetism, structural disorder and electrocatalytic processes. For the purpose of this research, ISM is also engaged in sample preparation (e.g. by molecular beam epitaxy) and characterisation (e.g. AC and DC susceptibility and magnetisation measurements).

Instrumentation for neutron and synchrotron x-ray scattering

- *SV 30 (Th. Zeiske, Th. Reif, G. Kluck / E. Küssel, B. Schmitz)*
  A new instrument for neutron polarisation analysis in the thermal energy range is under construction. This instrument will replace the old SV 4 triple axis spectrometer at the DIDO reactor. The instrument will employ ^{3}He filters for the production and analysis of polarised neutrons and will work at energies up to 110 meV. For inelastic measurements, a triple axis spectrometer module is foreseen, for diffraction measurements a neutron image plate detector will be developed. The design of the primary spectrometer, which comprises filter, monochromator and biological shielding, is completed. All essential parts are ordered or are built in the workshop of the Forschungszentrum. The design of the secondary spectrometer is in progress.
- *Polarised ^{3}He (R. Mueller, Ch. Horriar-Esser)*
  ^{3}He is a very effective neutron absorber (^{3}He +n $\rightarrow$ ^{4}He* $\rightarrow$ T+p). However, the absorption cross section is strongly dependent on the neutron spin direction (6000 barns for antiparallel n and ^{3}He spins, 5 barns for parallel spins). Therefore, ^{3}He can be used to build very efficient filter cells for neutron polarisation allowing polarisation analysis over a wide energy and angular range. We will produce polarised ^{3}He gas by optical pumping at low pressure and subsequent compression to several bar. The apparatus for polarising ^{3}He nuclei is well under way. A major breakthrough has been achieved in collaboration with a laser company by replacing the delicate LNA laser used elsewhere for optical pumping by a new 10 W fibre laser. Assembly of the optical pumping station will be finished in 1999 and the design of the compressor unit is well under way. We plan to use the ^{3}He filter cells for the new SV 30 spectrometer, but possibly also at other instruments. We want to emphasise that ^{3}He filters are an unique possibility to perform polarisation analysis experiments at pulsed sources such as the planed European Spallation Source (ESS).

- *Reflectometer HADAS (U. Rücker, B. Alefeld, W. Bergs)*
  To determine the magnitude and direction of magnetisation in thin film samples and multilayers, a neutron reflectometer with polarisation analysis is required. The reflectometer HADAS is currently being equipped with polarisation analysis. The supermirrors used to produce and analyse the polarised neutron beam have been delivered and tested. They are being assembled into benders. A concept for the instrument control (electronics hardware and software) has been established and will be installed next year.
- *Focusing small angle scattering instrument KWS 3 (B. Alefeld, L. Dohmen)*
  This new instrument, which will work as a small angle camera and a reflectometer, follows a completely new concept by focusing an entrance pinhole onto the detector. The focusing elements are a toroidal mirror and several concentric so-called replica mirrors. We expect an improvement in resolution compared to a standard pinhole camera by a factor of 10. The design and construction of all major mechanical components such as velocity selector, mirror and sample chamber are completed. A new neutron guide section has been installed. The toroidal mirror has been delivered and a process to produce the replica mirrors from a NiCu-alloy has been established.
- *Instrument for diffuse neutron scattering DNS (W. Schweika, A. Broch)*
  This compact time-of-flight instrument optimised for diffuse neutron scattering has been equipped with supermirror benders to allow polarisation analysis experiments. Taking full advantage of neutron focusing, this instrument reaches higher countrates as compared to the so far world leading instrument D 7 at the high flux reactor of the ILL in Grenoble. Additional detectors are being equipped with supermirror benders in order to enlarge the solid angle, for which polarisation analysis is available.
- *Developments for the ESS target station (H. Conrad)*
  Due to the high power deposition in the target of the planed European Spallation Source (ESS), shock waves represent a serious design problem. The newly developed laser interferrometric method for the measurement of theses shock waves could be validated. The comparison of the experiments at the AGS proton accelerator in Brookhaven and numerical simulations show a quantitative agreement only for the first shock pulse, i. e. up to a time of about 60 μs after the proton pulse. The numerical calculations suggest a strong dependence on the proton beam profile. In a larger international collaboration, an experiment has been set up on the proton accelerator COSY in Jülich with the aim to optimise the ESS target and moderator geometry. One of the aims of this so-called JESSICA experiment is to validate Monte Carlo codes for the simulation of the spallation process and the neutron transport. It is planned that the JESSICA experiment becomes operational during the next year.
- *Undulator station at APS (D. Hupfeld, P. Hiller)*
  In collaboration with American partners we are building the instrumentation for a sector (bending magnet plus insertion device line) at the Advanced Photon Source (APS) in Argonne, USA. The undulator line has just become operational and delivers photons in the energy range 4 - 20 keV into an experimental hutch equipped with a diffractometer for magnetic x-ray diffraction. FZ Jülich is currently building a high energy side station for the energy range 30 - 120 keV. The experimental enclosures have been erected, the monochromator unit is under construction and the diffractometer has been ordered. A major breakthrough was the development of water-cooled silicon monochromator crystals that can stand the high load of about 100 W/mm^2.
- *Wiggler station W 1 at HASYLAB (W. Caliebe)*
  A new cryomagnet with x-ray transparent windows designed for fields up to 5 T in the temperature range 1.5 up to 300 K has been designed. It has been tested in a modified setup of the diffractometer, which allows horizontal scattering geometry. The operating system of the beamline has been upgraded to a modern unix standard.
- *The JUSIFA instrument at HASYLAB for anomalous small angle x-ray scattering (ASAXS) (G. Goerigk, H.-G. Haubold)*
  The beam stability could be drastically improved by a new beam position regulation. For measurements on magnetic materials, a polarisation monitor is now available.

All these developments have only been possible with massive technical support by the central technical divisions at the Forschungszentrum Jülich, HASYLAB and APS. We especially want to acknowledge the support by ZAT, ZEL, BD and the construction, mechanical workshop and electronics group at the IFF.

Research Areas

The large number of activities related to instrumental developments described in the section above is characteristic for a young institute. However, the instrumentation is only a means to an end. The research areas, which are being pursuit in our institute, are:

- *Structural characterisation of thin film and multilayer devices for magnetoelectronics (W. Babik, E. Kentzinger, U. Rücker, Y.-G. Wang, W. Caliebe, G. Goerigk)*
  Within the framework of the HGF strategy project "magnetoelectronics", we collaborate with groups within the IFF, IGV and ISI. By means of x-ray and neutron reflectivity and diffuse scattering measurements, we characterise the interface morphology of technologically relevant multilayers, such as Fe/Cr/Fe, Co/Cu, Al_2O_3/Ni_3Al. Scattering methods are the only technique to access statistical parameters of buried interfaces. We have developed a program package for the analysis of reflectivity and diffuse scattering data and established the measurement procedure employing contrast variation with anomalous scattering at synchrotron based instruments. These techniques have been applied to the above systems and we could identify changes in the interface morphology depending on the preparation process in Fe/Cr/Fe-multilayers. The hope is to correlate these structural parameters with transport properties, such as the magnetoresistance, in order to improve the multilayer production and obtain a better understanding of the magnetoresistance phenomena.
- *Magnetism of δ-Mn (E. Kentzinger, S. Nerger, U. Rücker, W. Caliebe, G. Goerigk, J. Voigt)*
  We were able to stabilise the bct δ-Mn phase in the form of a thin epitaxial layer on top of an Fe thin film. The magnetism of this phase, which is thermodynamically stable only at very high temperatures, has recently attracted a lot of attention and several magnetic structures were predicted. We did an intensive characterisation of this multilayer system and could, by means of neutron diffraction, exclude the proposed antiferromagnetic structures. At present, we vary the Mn distance by evaporating Mn on a FeCo-alloy. We intend to study the magnetic order of δ-Mn as a function of the lattice parameters.
- *Magnetism of rare-earth multilayers (J. Voigt, U. Rücker, E. Kentzinger, S. Nerger, W. Caliebe, G. Goerigk)*
  To investigate proximity effects and the effects of restricted dimensionality, we have started a research program on multilayers consisting of two magnetic rare-earth elements. While multilayers of magnetic rare-earth elements separated by non-magnetic intermediate layers have been studied extensively in the past, little is known about multilayers consisting of two magnetic rare-earth elements. The first system we chose are Tb/Er-multilayers. These systems are being produced by MBE and the growth conditions are optimised by LEED, Auger-analysis and x-ray reflectometry. The magnetic order has been investigated with neutron diffraction, where we found magnetic order with finite correlation lengths. Resonant exchange scattering of synchrotron radiation will be employed to study the magnetic order element-specific.
- *Spin, charge, and orbital ordering in manganites (K. Istomin, W. Caliebe, Th. Zeiske)*
  Neutron scattering, high energy x-ray diffraction and resonant x-ray diffraction can be used to study the interplay between spin, charge and orbital ordering in the colossal magnetoresistance compounds. Currently, we are optimising the growth conditions for single crystals of $LaMnO_3$ with different dopings. Orbital and charge ordering in layered manganites has been studied in collaboration.
- *Magnetic x-ray scattering (D. Hupfeld, J. Voigt, J. Strempfer, W. Caliebe)*
  Resonant, as well as non-resonant magnetic scattering of synchrotron x-rays has been performed on Sm and Gd compounds, as well as metallic Cr and Tb. By combining high energy x-ray data with neutron diffraction, spin and orbital contributions could be separated in antiferromagnetic Cr. In SmBi, magnetic resonant scattering could be observed and the magnetic structure could be determined. With polarisation analysis, the mechanism of resonance exchange scattering in Tb has been investigated.
- *Fourth order exchange interactions (U. Köbler, R. Mueller, B. Olefs)*
  Fourth order exchange interactions have been shown to be present in many materials. They influence the magnetic phase transitions, the magnetic structure and the low temperature properties. Deviations from the Bloch $T^{3/2}$ law could be identified in many materials. Indications of weak first order phase transitions with changes of the critical exponent β for the sublattice magnetisation have been found in several materials.

- *Structural disorder: CuAu alloys (W. Schweika)*
  By means of surface sensitive x-ray scattering from a 1,0,0 surface of a CuAu alloy, an oscillating concentration profile has been found. Bulk disordered Cu_3Au alloys have been studied with diffuse anomalous x-ray scattering. The effects due to chemical short range order and displacements related to size and charge transfer could be separated.
- *Electrochemical process (H.-G. Haubold, Th. Vad, P. Hiller, H. Jungbluth)*
  Size distributions, oxidation states and surface coverage of platin catalyst particles on carbon supports were studied in situ by anomalous small angle scattering (ASAXS) and x-ray absorption spectroscopy (XANES) at the JUSIFA beamline. These processes are important for fuel cells and electrochemical sensor applications. For the direct methanol fuel cells, the best known membrane for use as a solid proton conducting electrolyte is Naphion. A small angle x-ray scattering study of this membrane gives new inside into the nanostructure.

Examples for the work accomplished at the Institute for scattering methods during the year 1999 are given by the progress reports on the following pages.

Thomas Brückel

Personnel 1999/2000 and areas of activity

Scientific Staff

Dr. B. Alefeld	Development of neutron scattering methods; instrument responsible for the lattice parameter instrument LAP; construction and development of the small angle scattering machine KWS III	23.891
Prof. Dr. Th. Brückel	Institute director; neutron and synchrotron x-ray scattering; magnetism	23.891
Dr. H. Conrad	European Spallation Source project ESS: target and moderators	23.891
Dr. G. Goerigk -HASYLAB, Hamburg-	Material research with anomalous x-ray small angle scattering; instrument responsible for Jülich's user-dedicated small-angle scattering facility JUSIFA	23.891
Dr. H.-G. Haubold	Anomalous small angle x-ray scattering ASAXS and x-ray absorption spectroscopy XAS from highly dispersive systems; in-situ studies of electro-chemical processes	23.891
Dr. U. Köbler	Magnetisation and neutron diffraction studies of materials with fourth-order exchange interactions	23.891
Dr. R. Mueller	Development of the ^{3}He filter for neutron polarisation analysis	23.891
Dr. W. Schweika	Diffuse neutron scattering for the investigation of short-range order in alloys, oxides, perovskites and quasi-crystals; instrument responsible for the diffuse neutron scattering instrument DNS	23.891

Technical Staff

W. Bergs	Reflectometer HADAS	23.891
A. Broch	Diffuse neutron scattering instrument DNS	23.891
L. Dohmen	Project engineer for the small angle scattering instrument KWS III	23.891
Dipl.-Ing. P. Hiller	Project engineer for μCAT-collaboration at the Advanced Photon Source APS; x-ray small angle scattering	23.891
Ms. C. Horriar-Esser	Ultra low-temperature magnetometry and ^{3}He filter project	23.891
H. Jungbluth	Software development for x-ray small angle scattering	23.891
Dipl.-Ing. G. Kluck -until 31.07.1999-	Project engineer for the new polarised thermal neutron scattering instrument	23.891
Ms. B. Köppchen	Secretary	23.891
Dipl.-Ing. E. Küssel -since 02.11.1999-	Project engineer for the new polarised thermal neutron scattering instrument	23.891
B. Olefs	Magnetometry, electronics and PC responsible	23.891
B. Schmitz	Triple axis spectrometer SV 4 and cryotechniques	23.891
F. Werges -until 30.06.1999-	Cryotechniques and molecular beam epitaxy	23.891

Scientists

Dr. W. Caliebe -HASYLAB, Hamburg, until 31.10.1999-	Magnetic x-ray scattering and spectroscopy; instrument responsible of the Wiggler beamline W1	23.891
Dr. D. Hupfeld -HASYLAB, Hamburg, since 1.7. APS, Argonne, USA-	Magnetic x-ray scattering; instrument responsible at the μ-CAT sector of the APS	23.891
Dr. Th. Reif -until 31.08.1999-	Second instrument responsible for SV 4; magnetic x-ray and neutron scattering; polarisation analysis	23.891
Dr. U. Rücker	Instrument responsible for the neutron reflectometer HADAS; preparation and characterisation of magnetic thin film systems	23.891

Dr. A. Schirmer -until 28.02.1999-	KWS III	23.891
Dr. O. Seeck -HASYLAB, Hamburg, since 01.12.1999-	X-ray scattering from ultrathin liquid films in confined geometries; instrument responsible of the Wiggler beamline W1	23.891
Dr. Th. Vad	Further development of the instrument control and data treatment programs for Jülich's user-dedicated small-angle scattering facility (JUSIFA); ASAXS measurements	23.891
Dr. Th. Zeiske	Instrument responsible of the triple axis spectrometer SV 4; Design of the new polarised neutron spectrometer	23.891

Thesis Students

Dipl.-Phys. W. Babik -since 01.07.1999-	(TH Aachen) Interface morphology of GMR and TMR layer structures	23.891
cand. phys. R. Goldstein until 31.08.1999-	(Univ. Hannover) Spin lattice relaxation with β-NMR	23.891
M.Sc. K. Istomin -since 01.07.1999-	(TH Aachen) Interplay of charge, orbital and magnetic ordering in manganites	23.891
cand. phys. S. Nerger -since 01.06.1999-	(TH Aachen) Structure and magnetic coupling in FeCo/Mn/FeCo layer systems	23.891
cand. phys. J. Voigt -since 15.04.1999-	(TH Aachen) Elementspecific magnetization density distribution in rare-earth superlattices	23.891

Guests

Dipl.-Phys. C. Byloos	(Università Ferrara, Italy) Shock waves in the ESS spallation target	23.891
Dr. E. Kentzinger	(Université Louis Pasteur, Straßbourg, France) Neutron and synchrotron x-ray scattering from magnetic thin film materials	23.891
Prof. V. Plakhty -since 03.11.1999-	(Petersburg Nuclear Physics Institute, Russia) Neutron and synchrotron x-ray study of the spin chirality in holmium	23.891
Dr. Y.-G. Wang -since 01.05.1999-	(Southeast University, Nanjing, China) Interface and magnetic characterization of magnetic multilayers using scattering methods	23.891

Trainees

J. Rademacher -until 30.09.1999-
J. Thelen -since 24.08.1999-

Interfacial and magnetic characterisation of Fe/Cr/Fe trilayers

Yin-gang Wang, E. Kentzinger, U. Rücker, W. Caliebe, G. Goerigk, W. Babik, and Th. Brückel
Institute of Scattering Methods
D.E. Bürgler, and P. Grünberg
Institute of Electronic Properties

We measured x-ray scattering spectra at grazing incidence of two Fe(5 nm)/Cr(2.5 nm)/Fe(5 nm) trilayers prepared at different temperatures using synchrotron radiation. Reflectivity and small angle diffuse scattering clearly demonstrate the structural difference between the two trilayer samples. The trilayer grown at room temperature has smoother interfaces or lower interdiffusion, while the trilayer grown at higher temperature has rougher interfaces or higher interdiffusion. From MOKE measurements, a difference of the strength of magnetic coupling between the Fe layers was found.

F&E-Nr: 23.891, 23.420

Metallic multilayers with giant magnetoresistance (GMR) effect are the subject of an active research field. GMR is governed by several physical parameters. Interface roughness is one of the most important parameters [1]. Fe/Cr/Fe(001) trilayers and Fe/Cr(001) multilayers were the first systems in which such exciting properties as magnetic interlayer exchange coupling, giant magnetoresistance, oscillatory exchange coupling, and short-period oscillatory exchange coupling were found. The interface roughness of this system has been quantitatively studied by scanning tunneling microscopy (STM) [2] and conversion electron Mössbauer spectroscopy (CEMS) [3]. STM can only give information about the surface accessible during the preparation process instead of the buried interface, and CEMS needs to introduce an additional probe layer at the interface to be investigated. On the other hand, scattering methods are very well suited to provide quantitative and statistical information on the interface morphology [4]. In this work, we performed small angle x-ray reflectivity and diffuse scattering at gracing incidence from which the interface roughness was extracted.

The Fe(5 nm)/Cr(2.5 nm)/Fe(5 nm) sandwiches were deposited at "mixed high temperatures (MT)" or at room temperature (RT) in UHV by thermal evaporation onto a GaAs/Fe(1 nm)/Ag(150 nm) substrate-buffer system. The Fe seed layer and the Ag buffer layer were grown at 100°C. For one sample (RT), all the sandwich and the top Au layer were grown at room temperature. For the other sample (MT), the first Fe layer was grown at 170°C for first 2 nm and at 300°C for the remaining 3 nm. The Cr and the second Fe layer were prepared at 250°C and the top layer was prepared at room temperature.

To investigate the interface morphologies, we performed small angle x-ray reflectivity and diffuse scattering of synchrotron radiation using the W1 beamline of HASYLAB at DESY in Hamburg. Fe is close to Cr in the periodic table of the elements. Therefore the energy E of the x-ray beam was chosen close to the absorption edge of Cr (5989 eV) in order to increase the contrast between the form factors of Fe and Cr. Fig. 1 shows the specular reflectivity and diffuse scattering measured on the RT sample. The sharp peaks at $\alpha_F = \alpha_I$ in the diffuse scans show that the specular reflectivity is the superposition of a "true specular" component and a "diffuse background". The oscillations in

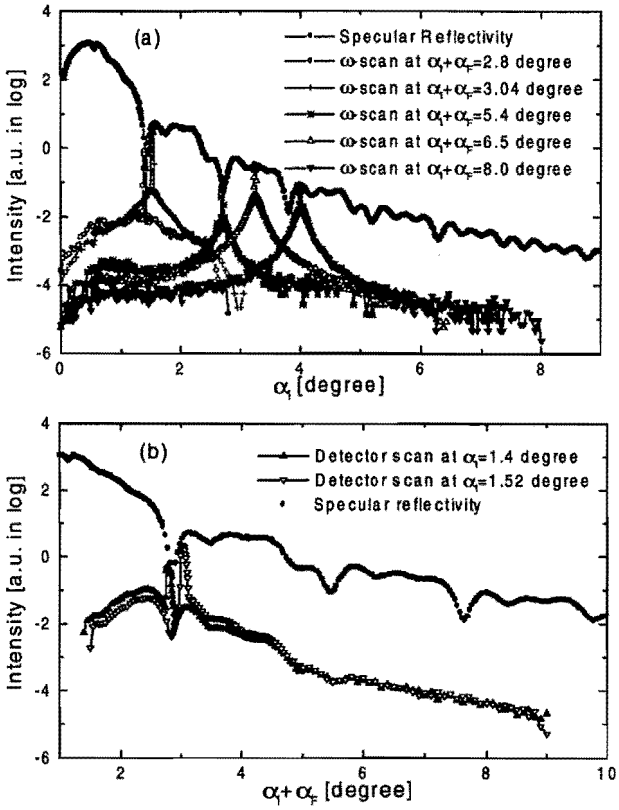

FIG.1. Specular reflectivity and diffuse scattering measured on the beamline W1 on the RT sample. (a) specular reflectivity together with ω-scans. Here ω has the same meaning as α_I; (b) specular reflectivity together with detector scans.

the detector scans (Fig. 1b) can be explained in terms of partially correlated roughness. Fig. 2 shows the true specular reflectivity together with the fits. For the RT sample there are still pronounced oscillations at high Q_z on the true specular reflectivity, while the oscillations die out for the MT sample. This may result from the sharper interface in the RT sample. From the refinement plotted in Fig.2, we can determine the root-mean-square roughness. As shown in Table I, the roughness we obtained is larger than that determined from

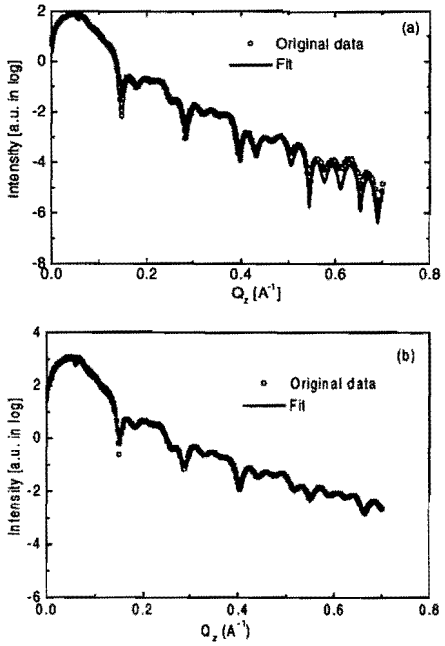

FIG.2. True specular reflectivity obtained by substracting the diffuse background from the specular reflectivity. This diffuse background is measured by scanning α_I and α_F with $\alpha_F = \alpha_I + 0.1°$. The solid line is a fit. (a) MT sample; (b) RT sample.

STM investigation [2]. This may be caused by the fact that, from the reflectivity alone, we cannot separate interdiffusion from real roughness. More information can be obtained from a simultaneous evaluation of all the specular, longitudinal and transverse diffuse intensities, which is still in progress. We want to point out that only such a simultaneous refinement allows one to evaluate the high Q_z data, where the specular reflectivity is comparable in intensity to the diffuse scattering. However, we can state that the MT sample has higher interdiffusion or roughness than the RT sample.

Table I: The root-mean-square roughness of given layer's top interface (in Angstrom).

	MT Sample		RT Sample	
	Our results	Ref. [2]	Our results	Ref. [2]
Ag	1.9±0.2		1.9±0.2	
Fe(1^{st})	2.8±0.1	1.9	2.6±0.2	2.1
Cr	4.5±0.2	1.9	2.3±0.2	1.8
Fe(2^{nd})	3.9±0.1		3.5±0.1	
Au	3.5±0.1		2.0±0.1	

To determine the difference in the magnetic properties caused by the interface features, we measured the room temperature hysteresis by MOKE. Fig. 3 shows the MOKE hystersis. It can be found that the evidence of 90° or near 90° coupling is present in both samples while the magnetic coupling between the Fe layers in the MT sample is stronger than that in the RT sample. This result is identical to that reported in [2].

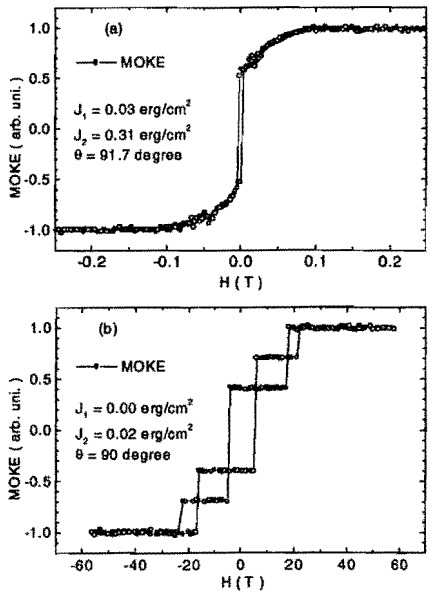

FIG.3. Longitudinal MOKE hysteresis measured with the external field H applied along the [100] easy axis of magnetization. The coupling parameters are calculated as described in [5]. Here θ is the angle between the magnetization vectors of .two Fe layers, and J_1 and J_2 represent bilinear coupling and 90° coupling, respectively. (a) MT sample; (b) RT sample.

In conclusion, we measured x-ray scattering spectra of two Fe(5 nm)/Cr(2.5 nm)/Fe(5 nm) trilayers prepared at different temperatures using synchrotron radiation. Anomalous scattering was essential to obtain a contrast between the Fe and Cr layers. We find that the sample prepared at "mixed higher temperatures" has a less well defined interface as the sample prepared at room temperature. The interface roughness determined by us is systematically higher than the surface roughness during the preparation process determined with a STM. We find that the interface morphology is clearly correlated to the interlayer coupling. More information on the interface morphology, such as height-height correlation functions will be obtained from a simultaneous refinement of specular and diffuse scattering spectra.

Acknowledgement
One of the authors, Y.G.W. thanks Dr. Shi-shen Yan for valuable discussion of MOKE results.

1. S. S. P. Parkin, in Ultrathin Magnetic Structures II, edited by B. Heinrich and J.A.C. Bland (Spring-Verlag, Berlin, 1994).
2. C.M. Schmidt, D.E. Bürgler, D.M. Schaller, F. Meisinger, and H.J. Güntherodt, Phys. Rev. B 60, 4158 (1999).
3. F. Klinkhammer, Ch. Sauer, E. Yu. Tsymbal, S. Handschuh, Q. Leng, and W. Zinn, J. Magn. Magn. Mater. 161, 49 (1996).
4. J. Stettner, L. Schwalowsky, O.H. Seeck, M. Tolan, W. Press, C. Schwarz, and H.V. Känel, Phys. Rev. B 53, 1398 (1996).
5. Shi-shen Yan, R. Schreiber, F. Voges, C. Osthöver, and P. Grünberg, Phys. Rev. B 59, R11641 (1999).

Proximity and Restricted Dimensionality: Magnetic Correlations in Er/Tb Multilayers

J. Voigt, S. Nerger, E. Kentzinger, U. Rücker, W. Caliebe, G. Goerigk, W. Schmidt* and Th. Brückel
Institute of scattering methods
**Intitute of neutron scattering*

We report on the growth and the magnetic properties of Er/Tb superlattices. The optimum growth conditions were determined by means of in situ LEED and Auger spectroscopy and ex situ grazing incidence x-ray diffraction. Magnetic correlations were studied with neutron diffraction. For multilayers, in which the layer thickness is comparable or less than the periodicity of the bulk antiferromagnetic structures, only magnetic short range order could be observed. We found indications that antiferromagnetic correlations in Er induce antiferromagnetic correlations in the Tb layers, despite their ferromagnetic ordering tendency.

F&E-Nr.: 23.891

The magnetism of bulk rare earth is fairly well understood [1], while rare earth superlattices are a field of active research. In superlattices of magnetic rare earth separated by a nonmagnetic layer (e.g. Er/Y/Er) the effects of clamping, epitaxial strain and interlayer coupling have been investigated in detail [2]. However, little is known about the magnetic properties of superlattices with alternating layers of magnetic rare earth elements. Er/Tb superlattices consist an example of such a system. Er orders antiferromagnetically in a CAM structure below 86 K. At 52 K and 18 K it undergoes phase transitions to a cycloidal and conical structure, respectively. Tb exhibits a helical structure between T_N= 230 K and T_C= 220 K and is basal plane ferromagnetic below T_C. In superlattices with layer thicknesses less than a magnetic period (e.g. less than 18 atomic layers for Tb) one can expect effects due to restricted dimensionality, but also effects due to the proximity of the other rare earth, which favours a different magnetic structure. The aim of the present study was to investigate these effects. Since it is obvious that the interface morphology plays an important role for such thin layers, a careful characterization of the buried interfaces was performed by means of grazing incidence diffraction.
Growing these superlattices is difficult because of the high tendency of the rare earth to intermix. A buffer layer of Nb of thickness 150nm was grown on an Al_2O_3 (1 1 0) substrate. Epitaxial growth of the hcp rare earth was achieved through a Y seed layer with a nearly perfect 3:4 lattice mismatch between the (1 1 0) surface of bcc Nb and the (0 0 1) surface of Y [3]. Various growth conditions have been tried for the following Er/Tb superlattice and these samples were characterized by in situ LEED and Auger spectroscopy as well as ex situ x-ray scattering on the CEMO and JUSIFA beamlines at HASYLAB, Hamburg. Synchrotron measurements are indispensible not only because of the larger dynamical range but mainly because of the possibility to achieve a contrast variation by means of anomalous scattering.

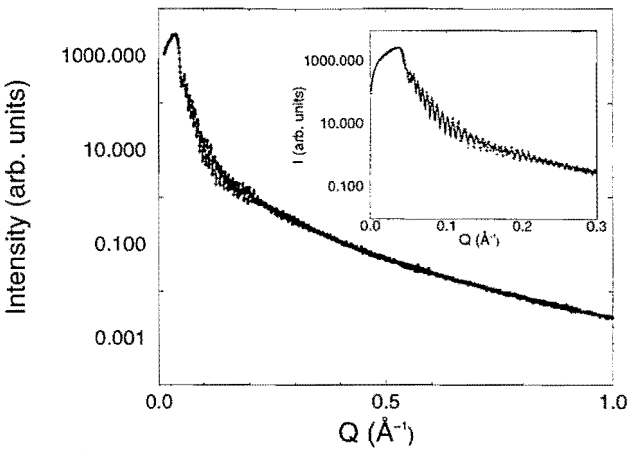

FIG. 1. X-ray reflectivity measurements of a $Tb_{5nm}/Er_{4nm}/Tb_{6nm}$ trilayer. The data show the true specular reflectivity, corrected for deadtime and diffuse scattering. The solid line in the inset is a fit assuming a nearly complete ErTbY alloy

In one attempt a trilayer $Tb_{5nm}/Er_{4nm}/Tb_{6nm}$ was grown at a temperature of 350 ° C with subsequent annealing at 570 ° C for 10 min to achieve a better crystallinity. A reflectivity measurement from this sample is shown in figure 1 , assuming a nearly complete ErTbY alloy. The data were corrected for dead time and diffuse scattering. One can see that interdiffusion occurs at these elevated temperatures.The reflectivity measurements were essential to improve the growth conditions. Optimized multilayers were produced at much lower temperatures in the order of 300 ° C.
After having optimized the growth conditions we have investigated the magnetic properties of superlattices with 80 periods by means of neutron diffraction. The thickness of a single layer of Tb and Er was 28 Å and 59 Å, respectively. The measurements were performed at the IN12 instrument of the ILL in Grenoble. Using a LHe-cryostat we investigated the temperature dependence of the magnetic moment in a temperature range from 5 K to 250 K.

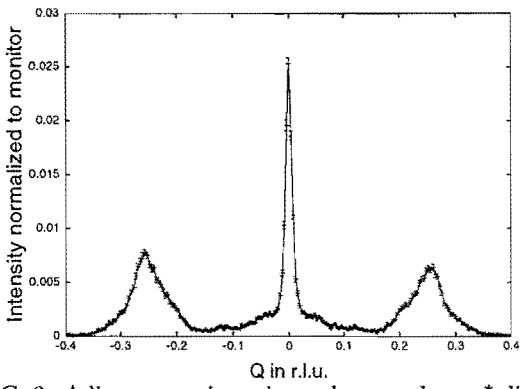

FIG. 2. A linear scan in reciprocal space along c* direction through the structural (1 0 0) Bragg reflection

Figure 2 shows as an example a scan along the c* axis. One sees clearly the magnetic satellites (1 0 $\pm\tau$) around (1 0 0) with $\tau \approx 0.26$. These satellites disappear on heating at T $\approx$ 80K as shown in figure 3. They are due to a helical structure of the basal plane components of the magnetic moments.

The width of the magnetic satellite reflections is clearly larger than the resolution given by the width of the nuclear peak in figure 2. Only short range order develops with a correlation length in the order of one Er/Tb bilayer thickness(see table I).

Additional short range ordered ferromagnetic correlations are present as can be seen from the broad peak underneath the nuclear Bragg reflection in figure 2. Their intensity also varies linear with temperature with a change of slope around 80 K (see figure 3).

From the Q-dependence we deduce that the ferromagnetic component lies in the basal plane between 200 K and 80 K and develops an additional c -axis component below 80 K. The ferromagnetic correlation length corresponds to roughly one Tb layer thickness (see table I).

	FWHM long [r.l.u.]	ξ [Å]	FWHM trans [r.l.u.]
(0 0 2) fm	0.149(1)	37.7(3)	0.0096(2)
(1 0 0) fm	0.121(4)	46(2)	0.0101(1)
(0 0 2$\pm\tau$)	0.0692(8)	81(1)	0.0181(8)
(1 0 $\pm\tau$)	0.061(1)	92(1.5)	0.0154(2)

TABLE I. Observed full width at half maximum (FWHM) at various positions in reciprocal space at T=15 K and correlation length ξ. The values in parenthesis represent estimated standard deviations and do not take systematic errors into acount.

The most surprising finding of our experiment is that despite the long ranged RKKY interaction only short range magnetic order develops. This might be due to the competing anisotropies in the two rare earth metals in combination with the interface structure. The fact that the antiferromagntic correlations extend over a Tb/Er bilayer indicates that proximity effects force the Tb layers to develop a helix component below 80 K in contrast to bulk Tb. This assumption will be tested by means of elementspecific x-ray resonance exchange scattering.

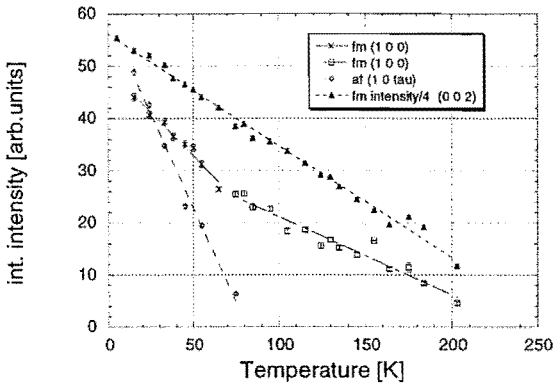

FIG. 3. Temperature dependence of the integrated intensity of the antiferromagnetic and ferromagnetic correlations in the Er/Tb multilayer

[1] Jensen J. and Mackintosh A.R.,*Rare Earth Magnetism*, Clarendon Press, Oxford, 1991

[2] Rhyne J. J. and Erwin R.W., ch. 1 in: K.H.J. Buschow (Ed.) *Handbook of magnetic materials*, Vol. 8, 1995

[3] Majkrzak C.F. et al. , Adv.Phys.**40** (1991), 99

[4] Koehler W.C. , ch. 3 in: R.J. Elliot *Magnetic properties of rare earth metals*, Plenum Press, New York, London , 1972

[5] Voigt J. , Diplomarbeit, RWTH Aachen, 2000

Form-Factor Measurements on Chromium with High-Energy Synchrotron Radiation and Neutrons

J. Strempfer[1*], Th. Brückel[2], W.A. Caliebe[2], A. Vernes[3], H. Ebert[3], Th. Zeiske[2] and J. R. Schneider[1]

[1] Hamburger Synchrotronstrahlungslabor HASYLAB at Deutsches Elektronen-Synchrotron DESY

[2] Institut für Streumethoden, Forschungszentrum Jülich

[3] Institut für Physikalische Chemie, Universität München

Results of high-energy magnetic x–ray diffraction and magnetic neutron diffraction on pure antiferromagnetic chromium are presented. The main purpose of these studies was to investigate the form-factor dependence of chromium to draw conclusions about the contributions of spin and orbital angular momentum. A spin-orbit separation has been performed by comparing x-ray to neutron data. The small orbital contribution to the magnetisation density turns out to be negligible, in agreement to relativistic band-structure calculations. In addition, the temperature dependence of the magnetic intensities measured with both, x-rays and neutrons, is presented.

F&E-Nr.: 23.89.1

The method of high-energy x-ray diffraction combines some advantages of both, neutron and conventional x-ray diffraction, such as bulk sensitivity and high momentum-space resolution [1]. This has been used in the study of antiferromagnetic chromium, where results of both, high-energy x-ray diffraction and neutron diffraction, are taken into account [2]. For magnetic diffraction with high-energy photons, the scattering cross section takes the following simple form [3]:

$$\frac{d\sigma}{d\Omega} = r_0^2 \left(\frac{\lambda_C}{d}\right)^2 |S_\perp|^2, \qquad (1)$$

where r_0 is the classical electron radius, λ_C the Compton wavelength, d the lattice spacing and $S_\perp$ the Fourier transform of the spin component perpendicular to the diffraction plane. For neutron diffraction, the diffracted intensity is proportional to the combination $\vec{L}(\vec{Q}) + 2\vec{S}(\vec{Q})$ of both spin ($\vec{S}(\vec{Q})$) and orbital ($\vec{L}(\vec{Q})$) momentum. Thus, by combining the results of high-energy x-ray and neutron diffraction, orbital and spin contributions can be separated.

Chromium is an itinerant antiferromagnet exhibiting an incommensurate spin-density wave (SDW) in the antiferromagnetic phase, depicted in Fig. 1. The phase transition from the paramagnetic to the antiferromagnetic state takes place at T_N=311 K [4]. This SDW gives rise to magnetic satellite peaks at positions corresponding to the magnetic propagation vector $\vec{q}_m$ of the SDW. Above the spin-flip transition at T_{SF}=123 K, the SDW is transversally polarised, whereas below T_{SF}, the polarisation rotates to become parallel to the modulation wave vector which leads to a longitudinally polarised SDW [5]. The magnetic satellite reflections are found near extinct charge reflections of the fundamental

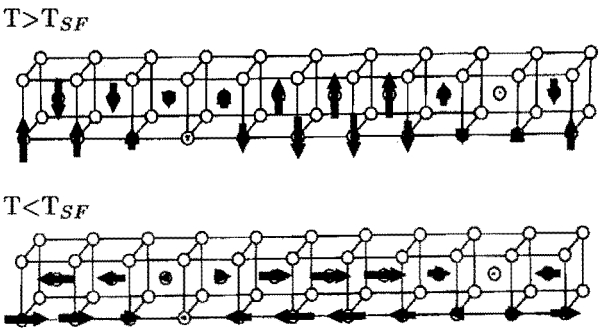

FIG. 1. The SDW of antiferrmagnetic chromium.

bcc-structure. The measurement of magnetic reflections of chromium with x-rays is difficult since the magnetic moment is very low. The amplitude of the magnetic moment amounts to $\mu = 0.62\mu_B$ [6]. With neutrons, the measurement of the satellites around the 1 0 0 and 1 1 1 position is possible without difficulties. Nevertheless, because of the very small magnetic form factor at higher momentum transfer, satellites at these positions are difficult to observe.

The experiments were conducted at the high-energy undulator beamline PETRA II, at the high-field wiggler beamline BW5 at HASYLAB, Hamburg and at the UNIDAS instrument in the DIDO reactor in Jülich. The x-ray experiments were performed at a photon-energy of 100keV and the neutron experiment at a wavelength of 1.551Å.

Fig. 2 shows the T-variation of the magnetic satellite intensities. For the x-ray data, the magnetic signal vanishes below the spin-flip transition temperature $T_{SF} = 123$ K, due to the form of the magnetic cross section (1). The difference between neutron and x-ray data is attributed to domain effects. The comparison of the intensities of the 1-δ 0 0 and the 1 0-δ satellite gives a

*Present address: Northern Illinois University, DeKalb

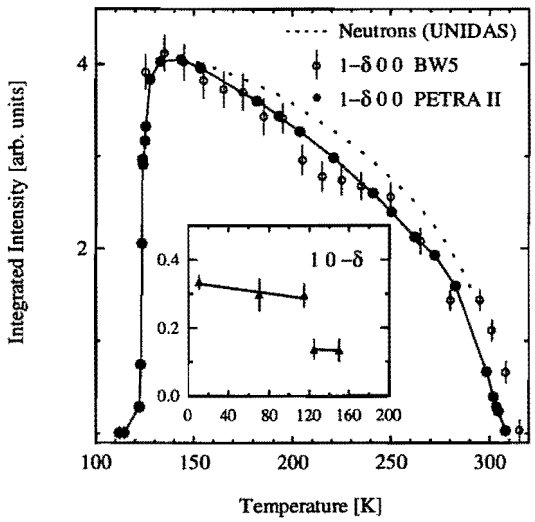

FIG. 2. Intensity of the magnetic 1-δ 0 0 satellite as a function of temperature. The inset shows the intensity of the 1 0 -δ satellite below and above the spin flip transition. Full circles show results from the PETRA undulator beamline, open circles an additional measurement with poorer statistic taken on the BW5 wiggler beamline. The solid lines are guides to the eye. The dotted line represents neutron diffraction data.

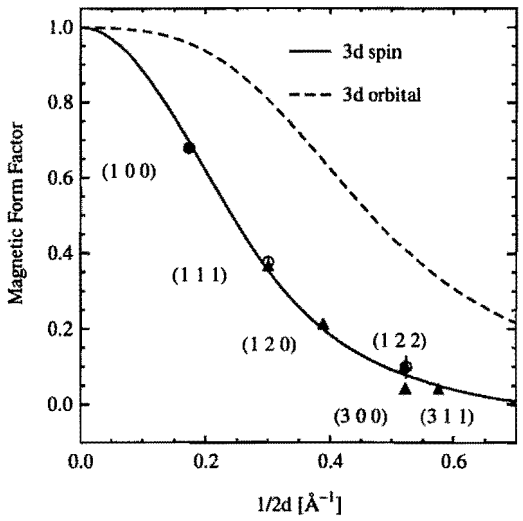

FIG. 3. Comparison of high energy synchrotron (open circles) with neutron diffraction data [7] (full triangles) and the calculated curves for the pure spin form-factor and the pure orbital form-factor.

very unequal domain population. The population of the $\langle 0\,0\,1\rangle$ domains is found to be 8% of that of the $\langle 1\,0\,0\rangle$ domain. A similar domain anisotropy has also been found by Hill et al. [9] and was attributed to stress induced by polishing, i.e. to near-surface effects. Here, we find that preferential domain population extends throughout the whole sample volume.

At the synchrotron, we were able to measure five different magnetic satellites: 1–δ 0 0, 1+δ 0 0, 1–δ 1 1, 1+δ 1 1 and 1+δ 2 2, with peak intensities from 60 counts/s to 0.1 counts/s. Our neutron diffraction results for the ratio between the satellite intensities indicate that the spin density wave varies continuously from cell to cell. In Fig. 3, the mean values of the respective two satellites are compared to neutron diffraction results [7]. Within the error bars, neutron and high-energy x-ray data show the same behaviour. The theoretical spin and orbital magnetic form factors, derived by band structure calculations, are plotted in Fig. 3, too. We deduce an orbital contribution of -4(8) %, in reasonable agreement with the value of -0.004 μ_B from the band structure calculation. It is interesting to note that the calculated orbital moment for antiferromagnetic chromium is about an order of magnitude smaller than that found for the pure ferromagnetic transition metals Fe, Co and Ni [8].

From the comparison of the temperature dependence of the magnetic intensity below and above the spin flip temperature we can assume an unequal domain occupation in the bulk of the sample for the SDW with equal propagation direction in the transverse polarised state. This could explain the difference in behaviour of the temperature dependence of the neutron and the x-ray measurement.

For the first time, we could perform a spin-orbit separation by combining high-energy x-ray and neutron diffraction. We could show that the orbital angular contribution is negligable for antiferromagnetic chromium, in agreement with relativistic band structure calculations.

References

[1] T. Brückel et al., Acta Cryst. A **49**, 679 (1993). M. Lippert, T. Brückel, T. Köhler, and J. Schneider, Europhysics Letters **27**, 537 (1994). J. Strempfer et al., Acta Cryst. A **52**, 438 (1996).

[2] J. Strempfer et al., Europ. Phys. J. B **accepted** (1999).

[3] J. Strempfer et al., Europhys. Lett. **40**, 569 (1997).

[4] Fawcett, E., Rev. of Mod. Phys. **60**, 209 (1988).

[5] Hastings, J.M., Bull. Am. Phys. Soc. **5**, 455 (1960).

[6] Arrot, A., Werner, S.A. & Kendrick, H., Physical Review **153**, 624 (1967).

[7] Moon, R.M., Koehler, W.C. & Trego, A.L., J. of Appl. Phys. **37**, 1036 (1966).

[8] P. S. H. Ebert and B. L. Györffy, J. Phys. F: Met. Phys. **18**, L135 (1988).

[9] Hill, J.P., Helgesen, G. & Gibbs, D., Phys Rev. B **51**, 10336 (1995).

Displacement patterns in disordered Cu_3Au

W. Schweika
Inst. Scattering Methods, IFF

G.E. Ice, J.L. Robertson, C.J. Sparks, and J. Bai
Metals and Ceramics Div., Oak Ridge National Laboratories

Diffuse x-ray scattering from a disordered Cu_3Au single crystal has been studied utilizing contrast variation by anomalous scattering. The data has been analyzed in view of separating (i) individual atomic pair-displacements and (ii) to distinguish atomic size differences from those due to charge transfer. A particularly interesting aspect of the latter approach is that higher order correlations related to charge transfer such as Fermi-surface effects may also be revealed in the pattern of displacement scattering.
F&E-Nr.: 23.55.0

The diffuse scattering from disordered systems like binary alloys contains the information on atomic pair-correlations that can be used to establish an effective Hamiltonian describing the configurational statistics and the coherent phase stabilty of an alloy. Most of the experiments have exploited only the chemical short-range ordering so far. Important further contributions to the configurational energy may stem from static displacements. The information about displacements can be inferred from the diffuse scattering as well, and lattice symmetry properties immediately separate both type of correlations. However, even for a binary system a variation of the scattering contrast between the alloying elements is required to distinguish the displacements between the three different types of atomic pairs, or alternatively, between "size" and "charge" as possible origins of displacements. In principle, for x-rays this can be achieved just by the atomic form factor dependence on the scattering vector, whereas in practice an additional contrast variation by using both x-rays and neutrons or by utilizing the anomalous x-ray scattering near absorption edges is advantageous if not necessary. A few studies with anomalous x-ray scattering have been performed and the analyses rely on the differences of weak diffuse intensities demanding an absolute calibration of each. In this work we achieved an considerably improved reliability of the results by analyzing the asymptotic behaviour near the Bragg peaks of the static displacements and of the phonon scattering. The disordered Cu_3Au alloy is a much studied model system both experimentally and theoretically, which serves here for a better general understanding of displacements in alloys. Furthermore, this alloy shows a splitting of short-range order peaks which has been related to Fermi-surface nesting effects as is typical for those nearly frustrated fcc alloys that form long-period ordered structures. Here we discuss also possible influences on the displacement patterns.

The diffuse x-ray scattering measurements were performed at beam-line X-14 at the National Synchrotron Light Source, Brookhaven National Laboratory. The sample was a Cu_3Au single crystal with a surface cut of (421) and a composition of $25.3\,at\%$ Au. During the experiment the sample was kept in an evacuated furnace under a Be-dome at a temperature of 723 K. Three different x-ray energies were chosen, 11909 eV (near Au L-edge at 11919 eV), 10500 eV and 8959 eV (near Cu-K edge at 8979 eV), to achieve a favorable scattering contrast by anomalous scattering. In addition to calculated anomalous scattering factors, absorption measurements (EXAFS) were made near the Au L-edge and Cu K-edge for a precise determination of changes in the real part f'(E) using the Kramers-Kronig relation.

Figure 1 displays the x-ray diffuse intensities in electron units as measured in the [h00] direction showing that the particular choice of the x-ray energies yielded a significant scattering contrast.

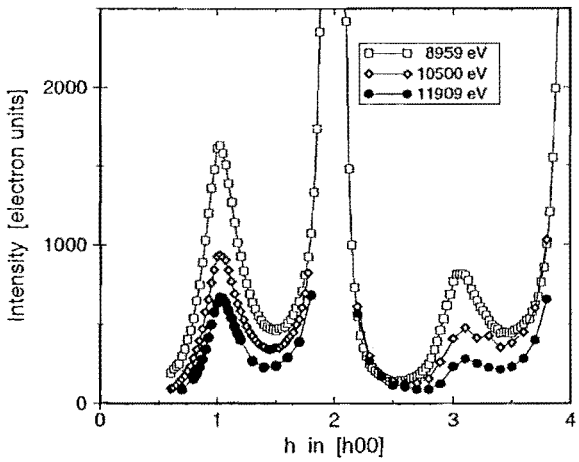

FIG. 1. Variation of the diffuse x-ray intensities by anomalous scattering near the Cu-K edge and Au-L edge.

Note that the resolution is sufficient so that the high intensities seen near the fundamental Bragg peaks (200) and (400) are still free from Bragg scattering and have

their origin in the local disorder. Near the zone boundaries at (100) and (300), there are short-range order peaks. A closer look reveals that the short-range order peaks are strongly asymmetric, which is indicative of strong displacements in this alloy. The asymptotic scattering near the Bragg-peaks has been calculated from known macroscopic properties, elastic constants and lattice parameter changes, see Fig. 2.

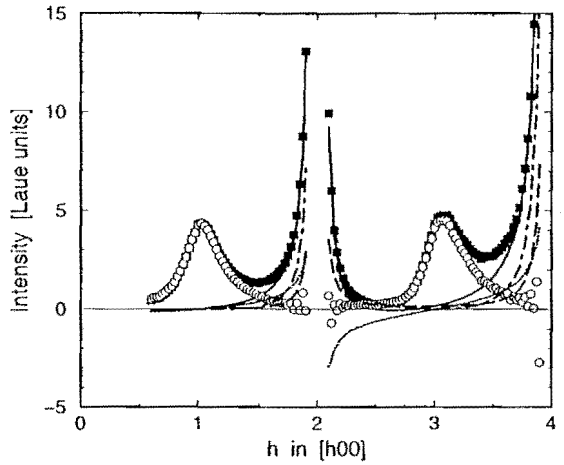

FIG. 2. X-ray diffuse intensities in the [h00] direction (*solid squares*) normalized to Laue units. The calculated intensities near the Bragg-peak are due to phonon scattering (*dashed line*) and static displacement scattering to first ((*dotted line*) and second order (*dashed-dotted line*), and have been subtracted from the measured intensities, (*open circles*).

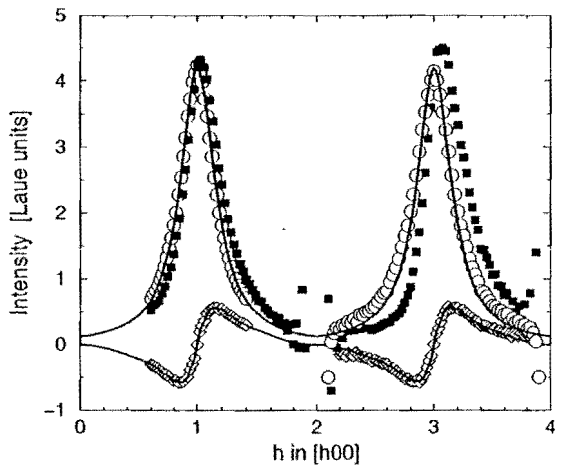

FIG. 3. Separation of the diffuse intensities (*solid squares*) into a (symmetric) short-range order term (*open circles*) and (anti-symmetric) displacement term (*open squares*). The reproducibility of the periodic patterns of the displacement term is best shown after removal of the h-dependence. Note that the same exponential decay determines the short-range order and displacement terms (*solid lines*, cosine- and sine-Fourier transforms).

After reproducing the observed asymptotic behaviour, we removed the contribution due to the local displacements as calculated in linear response of the lattice to nearest neighbor forces. Then the remaining intensity differences are separated with respect to their symmetry properties. The short-range order intensity has the usual translational symmetry properties of the lattice and is nicely described by a Lorentzian. Contrary the displacement scattering is anti-symmetric with respect to the translational invariance. These intensities follow the sine-Fourier transform of exponentially decaying displacements with a correlation length that is *identical* with the one for the short-range order, see Fig. 3. This is consistent with a model including only size effects (due to nearest neighbor forces) and the convolution of the displacement fields with the short-range order and, it also explains the typical spatial oscillations that have been found in the displacement parameters for many alloys.

The diffuse scattering near the zone boundary in [110] direction reveals a peak splitting in the short-range order intensity. This fine structure is already wellknown and has been attributed to Fermi surface effects. Different to the observation in the [100] direction, a calculation of the displacement scattering taking into account nearest neighbor forces and the convolution with the observed short-range order does not fully account for the fine structure in the anti-symmetric part of the scattering, see Fig. 4. These residual intensities can be attributed to displacements that arise directly from Friedel oscillations.

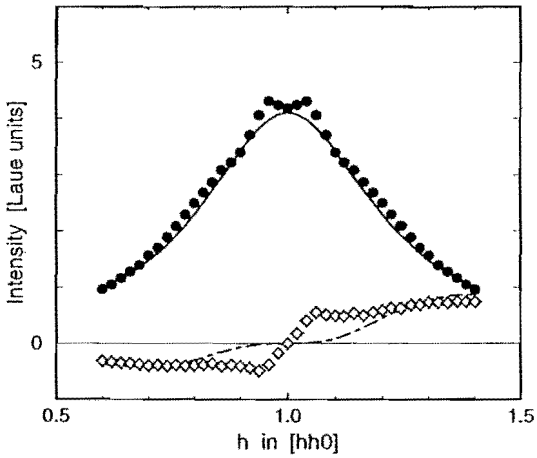

FIG. 4. The peak-splitting observed in the short-range order scattering has its counterpart in the (anti-symmetric) displacement scattering and can be related to Fermi surface effects.

Finally, from the variation of the intensities by anomalous x-ray scattering we are able to determine the absolute local displacements of each pair of species. In the present work precise results have been obtained, *e. g.* for the displacements between nearest neighbors pairs Au-Au, Au-Cu, and Cu-Cu, 0.165(15) Å, 0.014(2) Å, and −0.024(2) Å respectively.

Nano Structure of Nafion: A SAXS Study

H.-G. Haubold, Th. Vad, H. Jungbluth,P. Hiller
Institute Scattering Methods

Small angle scattering with synchrotron radiation is used to study the nano structure of NAFION polymer membranes. In the present work we focus on in situ measurement conditions, which are relevant for their use in direct methanol fuel cells.

F&E-Nr: 23.89.1

NAFION™ is the best-known ionomer membrane for use as a solid, proton conducting electrolyte in electrochemical technology. In low temperature Direct Methanol Fuel Cells (DMFC), it combines the roles of a solid polymer electrolyte [1] and a separator between the methanol-water mixture on one side of the membrane and air on the opposite side.

Nafion has a copolymer molecular architecture. The molecule is characterized by a hydrophobic poly-tetrafluoroethylene backbone chain and regularly spaced shorter perfluorovinyl ether side chains, each terminated by a strongly hydrophilic sulfonate ionic group. Schematically, its nano structure is illustrated in Fig.1.

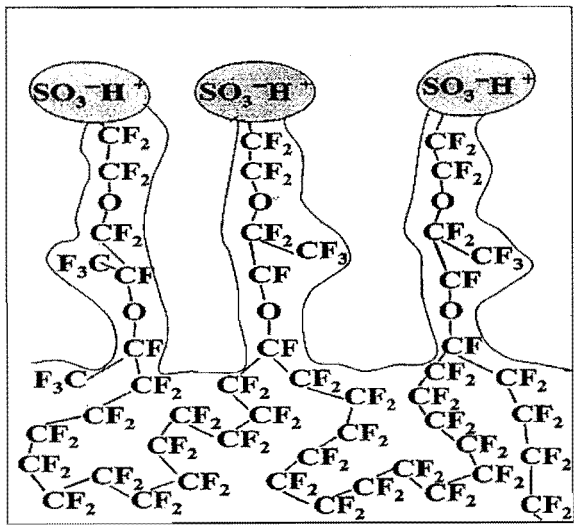

FIG.1. Basic structure unit of NAFION with hydro-phobic backbone chains and hydrophilic sulfonic side groups

The mechanical strength of Nafion membranes arises from the interaction of the perfluorinated backbone chains. For its use as a protonic conductor, the porous membrane contains about 20 wt.% water forming hydration shells around the fixed covalently bonded anionic sulfonic acid groups. The conductivity is assigned to the diffusion of hydrated protons (H_3O^+) as protonic charge carriers. For their passage through the membrane, a percolated sponge-like microstructure supplies the transport channels.

Numerous neutron and X-ray small angle studies have been performed to study the nano structure and the 10-20% swelling behavior of Nafion membranes after water uptake, which is necessary for its proton conductivity. Several structure models have been proposed for the interpretation of the scattering patterns. The details of these models are still under discussion.

We used small angle X-ray scattering with synchrotron radiation to study the nano structure of Nafion 117™ membranes and performed in situ experiments under the working conditions of membranes in Direct Methanol Fuel Cells: In pure water, a water-methanol mixture and in pure methanol.

The Nafion was available as a 175 µm thick membrane. The molecular weight of the copolymer was 250 000 with 8 wt.% sulfonic acid groups. After cleaning in hot H_2O_2, the membrane was mounted inside a flow cell and in situ small angle scattering measurements were carried out at room temperature in water, a 9 molar water-methanol mixture (mol ratio 1:4) and in pure methanol. The experiments were performed at our JUSIFA beamline [2] with synchrotron radiation from the DORIS synchrotron source (HASYLAB). The small angle scattering intensity for 11.5 keV X-rays was recorded with a 2-dimensional position sensitive detector. The radial averaged scattering cross sections are given in fig.2.

A common feature is a Porod Q^{-4} scattering law at the smallest scattering vectors Q, the appearance of a relative maximum at $Q=0.15Å^{-1}$ ("ionomer peak") and a shoulder in between

To retrieve structural information from the scattering data, we apply a structure model with hydrophobic backbone material inside of platelet like regions, which are surrounded by

hydrophilic ion and water group rich layers. Central for the understanding of this model is that phase separation is assumed to occur in the polymer. The quite different properties of polymer backbone and ionic groups in the copolymer molecule cause the polymer to organize itself so that the fluorocarbon chains interact together in a particle like structure and the ionic groups associate with one another in a surrounding hydrophilic shell.

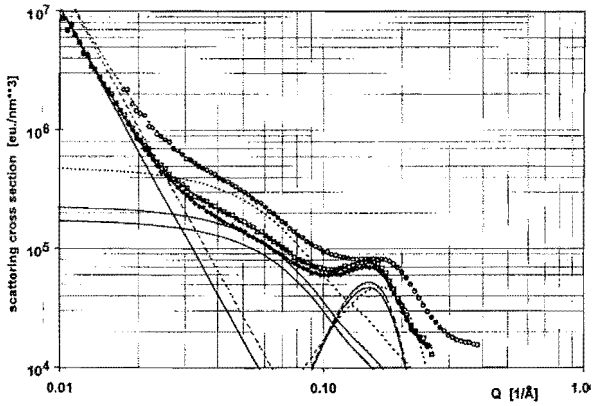

FIG.2: Small angle scattering from NAFION after equilibration in water (lowest curves), 9molar methanol (middle curves) and in pure methanol (upper curves).

We assume a random distribution of these regions inside the volume of the membrane. For simplicity, we describe the scattering cross section of these regions as the scattering from homogeneous and equally sized particles (discs of rotation).

We attribute the appearance of the ionomer peak at positions $Q = 2\pi/d$ to the constructive interference between ion rich regions which are separated by a distance d: For plate like particles, the two surface layers on the opposite flat sides of the particles can be regarded as two planes, which are separated by a nearly constant distance d, the order of the plate thickness. We apply a Gauss function for the fit of this intra particle interference peak. Towards the smallest scattering vectors, we attribute the Q^{-4} intensity upturn to the Porod scattering from the coarse pore structure within the membrane. Their characteristic length is above the 100 nm range and was not accessible in our measurements.

A fit of the model parameters to the measured scattering cross sections allows a separation into the scattering contributions from the porosity, the particle shape and the intra particle correlation from the hydrophilic surface layers. The results from a fit with platelet like particles after equilibration of the membrane in water, the methanol-water mixture and pure methanol are given in Fig.2. The particle scattering is found to arise from rather flat particles with a thickness of about 8Å and a larger diameter of 39Å. A slight trend towards more flat particles is observed for the sample which was flooded in pure methanol. The correlation peak remains nearly unaffected at $Q=0.15$ Å^{-1}, which corresponds to a correlation length of 42Å. Compared to the 8Å particle thickness, this indicates an ion shell thickness of about 17Å with a slight trend towards smaller values for the methanol flooded sample.

The scattering cross section is lowest for the water equilibrated membrane and increases with increasing methanol content. For scattering vectors not directly related to the intra particle correlation peak, the Q dependence, i.e. the shape of the scattering curves remains unchanged. This implies, that the nano structure of the membrane in form of its particle shape is not influenced by the methanol flooding. The observed overall intensity shift results from a change in the scattering contrast between particles and surrounding matrix atoms: Inside the particles, the Nafion molecules contribute an electron density of approximately 0.55 e/Å^3, the surrounding water in the water equilibrated sample a density of 0.33 e/Å^3. The scattering contrast from this difference increases, when the electron density of water becomes lowered with the addition of methanol with its smaller electron density of 0.26 e/Å^3.

The intensity shift indicates that pure methanol replaces the water and dehydrates the ionic shell. This is expected from the observation, that the protonic conductivity is lost in pure methanol.

In summery, we have shown that simple structure models with anisotropic structure units can be applied to describe the nanostructure of ionomers like NAFION .

References

[1] Ph. Colomban, Ann. Chim. Sci. Mat. **24**, 1-18 (1999)

[2] H.-G. Haubold et al., Sci. Instr. **60**, 1943-1946 (1989)

Publications in refereed journals

Benedetti A.1; Bertoldo L.1; Canton P.1; Goerigk G.; Pinna F.2; Rielio P.1; Polizzi S.1
1Università, Dipartimento di Chimica Fisica, Venezia, Italy
2Università, Dipartimento di Chimica, Venezia, Italy
ASAXS study of Au, Pd and Pd-Au catalysts supported on active carbon
Catalysis Today 49, 485 - 489, 1999
23.89.1

Brückel Th.; Strempfer J.1; Hupfeld D.; Schneider J. R.2; Mattenberger K.3
1APS at ANL, Ames, USA
2DESY, HASYLAB, Hamburg
3ETH, Laboratorium für Festkörperphysik, Zürich, Switzerland
Synchrotron Radiation Diffraction Studies of Antiferromagnetic Materials
Surface Investigation: X-ray, Synchrotron and Neutron Techniques, 8-9, 112 - 117, 1998
23.89.1

Ehlers G.1; Ritter C.2; Krutjakow A.1; Miekeley W.1; Stüßer N.1; Zeiske Th.; Maletta H.1
1HMI, Berlin
2ILL, Grenoble, France
Anomalous transition from antiferromagnetic to ferromagnetic order in Tb1-xYxNiAl
Physical Review B 59 13 8821 - 8827, 1999
23.89.1

Gawronski M.; Park J. T.1; Magee A. S.1; Conrad H.
1Alpha-Beta Technology, Worcester, USA
Microfibrillar Structure of PGG-Glucan in Aqueous Solution as Triple-Helix Aggregates by Small Angle X-Ray Scattering
Biopolymers, Vol. 50, 569 - 578, 1999
23.30.0

Hagdorn K.1; Hohlwein D.1,2; Ihringer J.1; Knorr K.1; Prandl W.1; Ritter H.1; Schmid H.1; Zeiske Th.
1Universität, Institut für Kristallographie, Tübingen
2HMI, Berlin
Canted antiferromagnetism and magnetoelastic coupling in metallic Ho0.1Ca0.9MnO3
Eur. Phys. J. B 11, 243 - 254, 1999
23.89.1

Haubold H.-G.; Hiller P.; Jungbluth H.; Vad Th.
Characterization of Electrocatalysts by In Situ SAXS and XAS Investigations
Jpn. J. Appl. Phys. 38, Suppl. 38-1, 36 - 39, 1999
23.89.1

Köbler U.; Hoser A.1; Graf H. A.1; Fernandez-Diaz M.-T.2; Fischer K.; Brückel Th.
1HMI, Berlin
2ILL, Grenoble, France
Investigations of the sublattice magnetizations Msub(T) in antiferromagnets with fourth-order exchange interactions: EuxSr1-xTe
Eur. Phys. J. B 8, 217 - 224, 1999
23.15.0

Köbler U.; Hoser A.1; Kawakami M.2; Chatterji T.3; Rebizant J.4
1HMI, Berlin
2University, Dep. of Physics, Kagoshima, Japan
3ILL, Grenoble, France
4Joint Research Center, Institut for Transuranium Elements, Karlsruhe
An unified view of the spin dynamics in two- and three-dimensional magnetic systems
Journal of Magnetism and Magnetic Materials 205, 343 - 356, 1999
23.15.0

Köbler U.; Hupfeld D.; Schnelle W.1; Mattenberger K.2; Brückel Th.
1MPI für Festkörperforschung, Stuttgart
2ETH, Laboratorium für Festkörperphysik, Zürich, Switzerland
Fourth-order exchange interactions in GdxEu1-xS
Journal of Magnetism and Magnetic Materials 205, 90 - 104, 1999
23.15.0

Lembke U.1; Hoell A.1; Kranold R.1; Müller R.2; Schüppel W.2; Goerigk G.; Gilles R.3; Wiedenmann A.3
1Universität, Fachbereich Physik, Rostock
2Institut für Physikalische Hochtechnologie, Jena
3HMI, Berlin
Formation of magnetic nanocrystals in a glass ceramic studied by small-angle scattering
Journal of Applied Physics 85 4, 2279 - 2286, 1999
23.89.1

Malis O.1; Ludwig Jr. K. F.1; Schweika W.; Ice G. E.2; Sparks C. J.2
1University, Department of Physics, Boston, USA
2ORNL, Oak Ridge, USA
Temperature dependence of the diffuse-scattering fine structure in equiatomic CuAu
Physical Review B 59 17 11105 - 11108, 1999
23.89.1

Mueller R.; Köbler U.; Fischer K.
On the T2 Bloch law in magnets with fourth-order exchange interaction
Eur. Phys. J. B 8, 207 - 216, 1999
23.15.0

Petrenko O. A.1; McPaul D.1; Ritter C.2; Zeiske Th.; Yethiraj M.3
1University of Warwick, Department of Physics, Coventry, UK
2ILL, Grenoble, France
3ORNL, Solid State Division, Oak Ridge, USA
Magnetic frustration and order in gadolinium gallium garnet
Physica B 266, 41 - 48, 1999
23.89.1

Schiffmann K. I.1; Fryda M.1; Goerigk G.; Lauer R.2; Hinze P.2; Bulack A.3
1Fraunhofer Institut für Schicht- und Oberflächentechnik, Braunschweig
2Physikalisch-Technische Bundesanstalt, Braunschweig
3Institut für Oberflächentechnik und plasmatechnische Werkstoffentwicklung, Braunschweig
Sizes and distances of metal clusters in Au-, Pt-, W- and Fe-containing diamond-like carbon hard coating: a comparative study by small angle X-ray scattering, wide angle X-ray diffraction, transmission electron microscopy and scanning tunnelling microscopy
Thin Solid Films 347, 60 - 71, 1999
23.89.1

Schmid H.1; Ihringer J.1; Knorr K.1; Prandl W.1; Ritter H.1; Zeiske Th.
1Universität, Institut für Kristallographie, Tübingen
Magnetization and magnetic phases in metallic and semiconducting HoxCa1-xMnO3
J. Mag. Soc. Japan 23, 525 - 527, 1999
23.89.1

Schukow H.1; Breitinger D. K.2; Zeiske Th.; Kubanek F.3; Mohr J.2; Schwab R. G.1
1Universität, Lehrstuhl für Mineralogie, Erlangen
2Universität, Lehrstuhl für Anorganische Chemie I, Erlangen
3HMI, Berlin
Localization of Hydrogen and Content of Oxonium Cations in Alunite via Neutron Diffraction
Z. Anorg. Allg. Chem., 625, 1047 - 1050, 1999
23.89.1

Seeck O.; Hupfeld D.; Krull H.1; Doerr A. K.1; Schlomka J.-P.1; Tolan M.1; Press W.1
1Universität, Institut für Experimentelle und Angewandte Physik, Kiel
Surface phase transition close to a bulk tricritical point: An x-ray study of ND4Cl
Physical Review B 59 5 3474 - 3479, 1999
23.89.1

Strempfer J.1; Brückel Th.; McIntyre G. J.2; Tasset F.2; Zeiske Th.; Burger K.3; Prandl W.3
1APS at ANL, Ames, USA
2ILL, Grenoble, France
3Universität, Institut für Kristallographie, Tübingen,
A reinvestigation of the field-induced magnetic form factor of chromium
Physica B 267 - 268, 56 - 59, 1999
23.89.1

Stunault A.1; de Bergevin F.2; Wermeille D.1; Vettier C.1; Brückel Th.; Bernhoeft N.1; McIntyre G. J.3; Henry J. Y.4
1ESRF, Grenoble, France
2CNRS, Laboratoire de Cristallographie, Grenoble, France
3ILL, Grenoble, France
4Centre d'Etudes Nucléaires, DRFMC/SPSMS/MDN, Grenoble, France
K-edge resonant x-ray magnetic scattering from RbMnF3
Physical Review B 60 14 10170 - 10179, 1999
23.89.1

Westermann S.; Kreitschmann M.; Pyckhout-Hintzen W.; Richter D.; Straube E.1; Farage B.2; Goerigk G.
1Universität Halle-Wittenberg, Fachbereich Physik, Halle
2ILL, Grenoble, France
Matric Chain Deformation in Reinforced Networks: a SANS Approach
Macromolecules 32 18, 5793 - 5802, 1999
23.89.1

Other publications

Brückel Th.
Elastische Streuung an Vielteilchensystemen
Neutronenpraktikum 1999, Vorlesungen, Forschungszentrum Jülich, 4-1 - 4-19
23.89.1

Brückel Th.
Magnetische Streuung und Polarisationsanalyse
Neutronenpraktikum 1999, Vorlesungen, Forschungszentrum Jülich, 5-1 - 5-20
23.89.1

Brückel Th.; Kentzinger E.
Streumethoden zur Untersuchung von Dünnschichtsystemen
Vorlesungsmanuskripte des 30. IFF-Ferienkurses "Magnetische Schichtsysteme in Forschung und Anwendung" vom 1. bis 12.3.1999 (1999), Schriften des Forschungszentrums Jülich, Reihe Materie und Material/Matter and Materials Band 2, B3.1 - B3.48
23.89.1

Brückel Th.; Kentzinger E.
Streuung unter streifendem Einfall
Neutronenpraktikum 1999, Vorlesungen, Forschungszentrum Jülich, 7-1 - 7-17
23.89.1

Conrad H.
Neutronenquellen - Von Radium-Beryllium zur Spallationsneutronenquelle -
Neutronenpraktikum 1999, Vorlesungen, Forschungszentrum Jülich, 2-1 - 2-16
23.89.1

Hill J. P.1; Kao C.-C.2; von Zimmermann M.1; Hämäläinen K.3; Huotari S.3; Berman L. E.2; Caliebe W.; Hirota K.4; Matsubara M.5; Kotani A.5; Peng J. L.6; Greene R. L.6; Tsukada I.7; Masuda T.7; Uchinokura K.7
1Brookhaven National Laboratory, Department of Physics, Upton, USA
2Brookhaven National Laboratory, National Synchrotron Light Source, Upton, USA
3University, Department of Physics, Helsinki, Finland
4Department of Physics, U. Tohoku, Sendai, Japan
5University, Institute for Solid State Physics, Tokyo, Japan
6University of Maryland, Center for Superconductivity Research, Department of Physics and Astronomy, USA
7Department of Applied Physics, U. Tokyo, Tokyo, Japan
Resonant Inelastic X-ray Scattering from Strongly Correlated Copper Oxides
Proceedings of the Second International Conference on Synchrotron Radiation in Materials Science (Kobe, 1998)
23.20.0

Hupfeld D.; Caliebe W.; Reif Th.; Hulliger F.1
1ETH, Laboratorium für Festkörperphysik, Zürich, Switzerland
Determination of the magnetic structure of SmBi with resonance exchange scattering
HASYLAB Jahresbericht, 943 - 944, 1998
23.89.1

Schweika W.
Schichtpräparation mit Sputterverfahren
Vorlesungsmanuskripte des 30. IFF-Ferienkurses "Magnetische Schichtsysteme in Forschung und Anwendung" vom 1. bis 12.3.1999 (1999), Schriften des Forschungszentrums Jülich, Reihe Materie und Material/Matter and Materials Band 2, A5.1 - A5.21
23.89.1

Invited talks

Alefeld B.
Focusing Neutron Reflectometer
Schloß Ringberg, "New Concepts in Neutron Reflectometry", 04. - 06.10.1999
23.89.1

Alefeld B.
GaAs, a new Crystal for Neutron-Backscattering
Vienna, Austria, PECNO TMR-Mid-Term Review Meeting, 04. - 06.03.1999
23.42.0

Alefeld B.
Space technology from x-ray telescopes for focusing neutron small angle scattering and neutron reflectometry
Budapest, Hungary, ECNS '99 Conference, 01. - 04.09.1999
23.89.1

Brückel Th.
Investigation of Spinstructures with Synchrotron Radiation
Bad Honnef, Physikzentrum, 211. WE-Heraeus-Seminar, 04. - 06.01.1999
23.89.1

Brückel Th.
Komplementarität von Neutronen- und Synchrotron-Röntgenstreuung in der Festkörperforschung
Dresden, Technische Universität, Fakultät Mathematik und Naturwissenschaften, Physikalisches Kolloquium, 12.01.1999
23.89.1

Brückel Th.
Komplementäre Anwendung von Neutronen- und Synchrotronröntgenstreuung bei Untersuchungen des Festkörpermagnetismus
Aachen, RWTH, Physikalisches Kolloquium, 26.04.1999
23.89.1

Brückel Th.
Magnetic Scattering: Synchrotron X-rays versus Neutrons
Berlin, HMI, Workshop on "Magnetism with Synchrotron Radiation and Neutrons, 22.11.1999
23.89.1

Caliebe W.
Scattering Methods to Study Magnetism in EuO
Brookhaven, USA, NSLS, Seminar, 11.01.1999
23.20.0, 23.89.1

Conrad H.
Die Europäische Spallationsquelle ESS - eine Neutronenquelle für das 21. Jahrhundert
Potsdam, Deutsche Neutronenstreutagung, 26.05.1999
23.60.0

Conrad H.
Experimental and computational studies of pressure waves in the ASTE mercury target
Oak Ridge, USA, International Workshop on Mercury Target Development for Pulsed Spallation Neutron Sources, 08. - 12.11.1999
23.60.0

Conrad H.
Moderator Development for ESS
Oak Ridge, USA, International Workshop on Mercury Target Development for Pulsed Spallation Neutron Sources, 10.11.1999
23.60.0

Conrad H.
Pressure waves in the ASTE mercury target
Ancona, Italy, 6th General ESS Meeting, 23.09.1999
23.60.0

Conrad H.
Stress and Pressure Waves in Solid and Liquid Metal Targets Induced by High Power Pulsed Electron and Proton Beams
Santa Fe, USA, 3rd International Conference on Spallation Materials Technology, 03.05.1999
23.60.0

Conrad H.; Ullmaier H.
Overview of the ESS Target Research and Development
Oak Ridge, USA, International Workshop on Mercury Target Development for Pulsed Spallation Neutron Sources, 08.11.1999
23.60.0

Goerigk G.
Materialforschung mit Anomaler Dispersion
Geesthacht, GKSS, Informationsveranstaltung zur Synchrotronstrahlung mit Ausblick auf TESLA, 08.09.1999
23.89.1

Goerigk G.
Materialuntersuchungen mit anomaler Röntgen-Kleinwinkelstreuung
Karlsruhe, Universität, Polymer-Institut, 18.11.1999
23.89.1

Köbler U.
Die Austauschwechselwirkungen 4. Ordnung in reinen Spinsystemen
Dresden, Technische Universität, 07.12.1999
23.15.0

Köbler U.
Die Bedeutung der Austauschwechselwirkungen 4. Ordnung in Materialien mit reinem Spinmagnetismus
Aachen, RWTH, 18.06.1999
23.15.0

Köbler U.
Kritisches magnetisches Verhalten für halb- und ganzzahlige Spinquantenzahl
Dresden, Technische Universität, 06.12.1999
23.15.0

Schweika W.
Diffuse Scattering of Cu3Au: Displacements and Fermi-Surface Effects
Davos, Switzerland, International Alloy Conference-2, 10.08.1999
23.89.1, 23.55.0

Schweika W.
Diffuse scattering of Cu3Au and Fe-Al alloys - x-rays and neutron studies
Saclay, France, LLB, Seminar, 15.04.1999
23.89.1

Other talks

Goerigk G.
Kleinwinkelstreuung bei JUSIFA
Hamburg, HASYLAB, Diskussionstreffen zur Röntgen-Kleinwinkelstreuung, 07.06.1999
23.89.1

Goerigk G.; Williamson D. L.1
1Colorado School of Mines, Department of Physics, USA
Nanostructural Characterization of Amorphous SiGe:H Alloys by Anomalous Small-Angle X-Ray Scattering Studies
Brookhaven, USA, NSLS, SAS99, XIth International Conference on Small-Angle Scattering, 17. - 20.05.1999
23.89.1

Haubold H.-G.; Vad Th.; Hiller P.; Jungbluth H.
ASAXS in situ studies of adsorbates on carbon supported electrocatalysts
Brookhaven, USA, National Synchrotron Light Source Laboratory, SAS99, XIth International Conference on Small-Angle Scattering, 20.05.1999
23.89.1

Schweika W.
Feinstruktur der diffusen Streuung in CuAu Legierungen und Fermiflächeneffekte
Münster, DPG-Tagung, 22.03.1999
23.55.0, 23.89.1

Schweika W.
Oberflächeninduzierte Ordnungsphänomene in Legierungen des Cu3 Au-Typs - eine Monte Carlo Studie
Münster, DPG-Tagung, 22.03.1999
23.15.0

Posters

Alefeld B.; Dohmen L.; Heidemann A.1
1ILL, Grenoble, France
GaAs as a Backscattering Crystal
Villigen, Switzerland, PSI, NOP99-Conference, 25. - 27.11.1999
23.89.1

Alefeld B.; Dohmen L.; Richter D.; Brückel Th.
X-Ray Space Technology for Focusing Small Angle Neutron Scattering and Neutron Reflectometry
Villigen, Switzerland, PSI, NOP99-Conference, 25. - 27.11.1999
23.89.1

Attenkofer K.1; Caliebe W.; Chatterji T.2; Richter R.1
1University, Würzburg
2ILL, Grenoble, France
Magnetism Probed with Synchrotron Radiation Methods
Hamburg, HASYLAB, Users' Meeting, 29.01.1999
23.20.0, 23.89.1

Goerigk G.; Williamson D. L.1
1Colorado School of Mines, Department of Physics, USA
Nanostructural Characterization of a-SiGe:H Alloys by Anomalous Small-Angle X-Ray Scattering
Hamburg, HASYLAB, Users' Meeting, 29.01.1999
23.89.1

Hupfeld D.; Schweika W.; Strempfer J.1; Caliebe W.; Mattenberger K.2; McIntyre G.3; Brückel Th.
1APS at ANL, Ames, USA
2ETH, Laboratorium für Festkörperphysik, Zürich, Switzerland
3ILL, Grenoble, France
Element-specific magnetic order and competing interactions in GdxEu1-xS
Plymouth, USA, Gordon research conference on x-ray physics, 25. - 30.07.1999
23.89.1

Kentzinger E.; Rücker U.; Caliebe W.; Goerigk G.; Werges F.; Nerger S.; Voigt J.; Schmidt W.; Alefeld B.; Fermon C.1; Brückel Th.
1DRECAM/SPEC, CEA Saclay, Gif sur Yvette, France
Structural and magnetic characterization of Fe/(-Mn thin films
Budapest, Hungary, ECNS '99 Conference, 01.09.1999
23.89.1

Köbler U.
Modifizierte Bloch Exponenten für halbzahlige und ganzzahlige Spinquantenzahlen
Potsdam, Deutsche Neutronenstreutagung 1999, 25.05.1999
23.15.0

Rücker U.
Charakterisierung von dünnen (-Mn-Schichten mit Streumethoden
Münster, DPG-Tagung, 23.03.1999
23.89.1

Rücker U.; Alefeld B.; Bergs W.; Kentzinger E.; Brückel Th.
The new polarized neutron reflectometer in Jülich
Villigen, Switzerland, NOP99-Conference, 25. - 27.11.1999
23.89.1

Rücker U.; Bergs W.; Alefeld B.; Kentzinger E.; Brückel Th.
The new polarized neutron reflectometer in Jülich
Budapest, Hungary, ECNS '99 Conference, 01.09.1999
23.89.1

Schweika W.
Einfluß des Magnetismus auf die chemische Ordnung und Nahordnung in Fe Al Legierungen
Potsdam, Deutsche Neutronenstreutagung N99, 25.05.1999
23.55.0

Schweika W.
Strukturfaktoren von polyalkylmethacrylaten als Beispiel für Seitenkettenpolymere
Potsdam, Deutsche Neutronenstreutagung N99, 26.05.1999
23.30.0, 23.89.1

Patents granted

Althaus M.; Küssel E.; Sonnenberg K.:
Verfahren und Vorrichtung zur Gewinnung rißfreier Kristalle
EP: 0760024 (07.07.99) (CH,DE, FR,GB,NL)
PT 1.1209
23.42.0

Lecture courses

Brückel, Th.
Beugungsmethoden zur Untersuchung von Dünnschichtsystemen
WS 98/99, RWTH Aachen und IFF-Ferienkurs, V2
1.2 FKF

Brückel, Th., Capellmann, H., Schweika, W., Zeiske, Th.
WS 98/99, Seminar: Aktuelle Aspekte des Festkörpermagnetismus
TÜ 2

Brückel, Th., Eberhardt, W.
WS 99/00, IFF-Ferienschule: Von neV bis fsec: Dynamik der kondensierten Materie
V 40 / Ü 10

Brückel, Th., Schweika, W., Zeiske, Th.
WS 99/00, Ferienschule (Praktikum) über Neutronenstreuung
TV 10 / TÜ 30

Schweika, W.
Schichtpräparation mit Sputterverfahren
WS 98/99, RWTH Aachen und IFF-Ferienkurs, V1
1.2 FKF

Internal reports

Brückel Th.
Elastische Streuung an Vielteilchensystemen
Institut für Festkörperforschung, Neutronenpraktikum 1999, 29.09.1999
23.89.1

Brückel Th.
Komplementarität von Neutronen- und Synchrotron-Röntgenstreuung in der Festkörperforschung
Auditorium der Zentralbibliothek, IFF-Kolloquium, 15.01.1999
23.89.1

Brückel Th.
Magnetische Streuung und Polarisationsanalyse
Institut für Festkörperforschung, Neutronenpraktikum 1999, 29.09.1999
23.89.1

Brückel Th.
Streumethoden zur Untersuchung von Dünnschichtsystemen-Teil I und Teil II
Auditorium der Zentralbibliothek, IFF-Ferienschule "Magnetische Schichtsysteme", 05.03.1999
23.89.1

Brückel Th.
Streuung unter streifendem Einfall
Institut für Festkörperforschung, Neutronenpraktikum 1999, 30.09.1999
23.89.1

Conrad H.
Neutronenquellen - Von Radium-Beryllium zur Spallationsneutronenquelle -
Institut für Festkörperforschung, Neutronenpraktikum 1999, 29.09.1999
23.89.1

Haubold H.-G.
In situ Untersuchungen von Oberflächenreaktionen auf Elektrokatalysatoren
Institut für Festkörperforschung, Seminar, 25.01.1999
23.89.1

Hupfeld D.
Untersuchung magnetischer Ordnungsphänomene in GdxEu1-xS mit resonanter Röntgenbeugung
IFF-Hörsaal, Informationstagung aus Anlaß der 14. Sitzung des Wissenschaftlichen Beirats des IFF, 22.04.1999
23.89.1

Plakhty V.
Spin Chirality and Polarised Neutrons
Institut für Festkörperforschung, 10.11.1999

23.89.1

Schweika W.
Schichtpräparation mit Sputterverfahren
Auditorium der Zentralbibliothek, IFF-Ferienschule
"Magnetische Schichtsysteme", 01.03.1999
23.89.1

Institute for Neutron Scattering

General Overview

In 1999 the Jülich research reactor FRJ-2 operated only for 62 days. The main part of the year was needed to exchange the pumps in the primary circuit of the reactor cooling system. Nevertheless, at the FRJ-2 altogether 134 experiments were performed 77 of them with external participation. Experiments were carried out with the support of the institute for neutron scattering (INS), the institute for scattering techniques and external collaborating research groups. In 1999 the third neutron laboratory course took place. Among the 35 accepted participants the course was well received and a next laboratory course is planned for the fall 2000. It is noteworthy to remark that by now the neutron laboratory courses are also part of the advanced practical course in material science in the frame of the physical chemistry curriculum at the university of Münster.

Neutron Instrumentation (FE 23.89.1)
The most important accomplishment in 1999 was the first demonstration of time of flight neutron spin echo TOF-NSE using the IN15 instrument at the ILL as a frame. This work was undertaken in collaboration with the HMI and the ILL and achieved the full explotation of a wide neutron pulse (wavelengths 6-18Å) allowing now for a dynamical range of nearly 4 orders of magnitude in Fourier time. Establishing the feasibility of TOF-NSE is a major step in the instrumentation development for future MW-Spallation Neutron Sources like the ESS. At that point I like to thank the experts of the ZEL for their indispensable help in establishing the necessary ramping of the magnetic fields in the different spin turn devices.

The new thermal time of flight instrument SV29 was commissioned, though problems with the fast background chopper in front of the beam hole still remained. On the backscattering spectrometer the first new perfect crystal analyzers were completed which improved the resolution function of the instrument from a Lorentzian to a Gaussian shape. Finally, the basic design for the backscattering spectrometer at the FRM-II was completed. As a technically very appealing new feature studies on a high speed velocity drive with air cushions and linear motor propulsion was started with a goal to arrive at a prototype in summer 2000.

Polymers, membranes and complex fluids (FE 23.30.0)
The main research activities within the INS are focussed in the field of polymer physics and complex fluids, a research program which demands a close cooperation between polymer and organic synthesis on the one hand and physics investigations on the resulting materials on the other hand.

- **Polymer synthesis**
  Apart of routine synthesis of homo- and diblockcopolymers, the synthesis of partially deuterium labelled branched polymers like H-polymers for SANS studies in connection with a BRITE EURAM project was one of the major activities. This synthesis encountered more difficulties than anticipated in particular because of tiny amounts of impurities in the deuterated butadiene. On the basis of sophisticated, purification techniques it became possible to prepare well defined H-polymers with labels at different positions. According to conventional analytical procedures like GPC, membrane osmosis and light scattering these materials were up to specifications. At present the H-polymers are studied with temperature gradient interaction chromatography (TGIC), a technique providing a much higher resolution than conventional GPC. First results seem to indicate that the H-polymers still contain higher or a lower branched structures which were invisible by conventional analytical techniques

  In order to study partial dynamic structure factors, partially labeled 1-4 and 1-2 polybutadienes were synthesized starting from the corresponding modified butadiene monomers. As a step stone to further well defined branched structures the synthesis of an organo lithium initiator bearing a protected OH group was undertaken. This initiator can be used for the preparation of OH terminated linear and branched telechilic and heterotelechilic polymers. Finally, I like to mention a patent application together with the biotechnology department on organic catalysts which are fixed at polymer backbones.

- **Polymer dynamics**
  The core activity of the institute focuses on dynamical properties of soft condensed matter systems including polymers and complex fluids. In this context, dynamical features from soft vibrations through secondary relaxations and the glass process up to large scale motions are investigated.

  On the high frequency side, combining X-ray and neutron Brillouin scattering, a fast coherent quasielastic component inside the Brillouin line was identified and correlated to strain relaxation in polymer melts. **(report Buchenau).** In the regime of the classical relaxation processes a thorough investigation of polymer blends was

undertaken. On the system PI/PVE previous studies by local probes displayed heterogeneous dynamic behavior of the two components, though the blend is perfectly miscible. Covering a Q-range of nearly two orders of magnitude by quasielastic neutron scattering it could be shown that this apparent local heterogeneities relate to a purely dynamic chain specific cross over from homogeneous entropy driven modes to chain specific local relaxation (**report Hoffmann**). In the merging regime of the α- and β-relaxations in polyvinylacetat a quasielastic neutron scattering study on the Q dependent relaxation behavior was performed. Other than for polymers studied so far, only a weak Q dependence of the characteristic relaxation rate was found. Rubbery electrolytes were studied both with dielectric spectroscopy and quasielastic neutron scattering. Thereby, the interplay between the polymer and ionic motion was investigated. It was found that the glass dynamics is significantly reduced upon addition of ions.

A series of neutron spin echo experiments on polyethylene melts with different molecular weights was performed, in order to study the reptation dynamics as a function of molecular weight. While the experiments confirm the model of De Gennes for high molecular weights, it was found that with decreasing chain length a significant increase of the main parameter of the De Gennes theory, namely tube diameters d occurs. Furthermore, for chains shorter than about 7 entanglement lengths the experimental data cannot be described in terms of the reptation model and a crossover to another dynamic regime occurs. These findings are in agreement with the packing model of entanglement formation which predicts a transition from entangled to nonentangled dynamics at a critical chain length of about 7 entanglement lengths. Experiments on diblockcopolymers with hydrogen labels at the chain connection point followed up recent investigations on the overall dynamics of such molecules. The NSE experiments revealed fast interface motions which are driven by the surface tension and display all characteristics of ripplon excitations. **(report Monkenbusch)**

- **Structure formation in polymer solutions and complex fluids**

Last year we reported the discovery of strong amphiphilicity boosting effects which occur upon addition of small amounts of amphiphilic diblockcopolymers into microemulsions. Performing careful two-dimensional contrast matching experiments, it became possible to identify the position and state of these polymers within the microemulsion system. The polymers are placed within the interface and stay there as single chains exhibiting mushroom like conformations **(report Endo).** In this way the elasticity properties of the surfactant layers are significantly altered, such as to change the phase boundery for the microemulsion phase to lower surfactant concentrations. Aside of structural properties also the dynamics of bicontinuos microemulsions containing polymers was systematically evaluated. At high momentum transfers the theoretically predicted relationship between characteristic relaxation time and momentum transfer ($\Omega \approx Q^3$) was observed. The presence of the polymer introduces qualitative changes into the microemulsion dynamics. The aggregation behavior of PEP/PEO amphiphilic diblocks was studied in water as a function of molecular weight. Upon reduction of chain length a transition from spherical to cylindrical micelles was observed. Finally the interplay of paraffin crystallization and random copolymers containing crystallizable parts in oil was investigated. The crystallization of C_{24} in decane is changed massively in the presence of the statistical copolymer PEB12. Instead of macroscopic wax crystals PEP12 induces two-dimensional large platelets. Using contrast variation the wax and the polymers were made visible separately. In both cases two-dimensional structures are observed, the thickness of the wax platelets agrees with that of a monomolecular layer of C_{24}.

- **Phase transitions in polymer melts**

The SANS studies on three component mixtures of two homopolymers and the corresponding diblockcopolymer were continued on the system PB/PS. Similarly, as for the system PEE/PDMS at small diblock concentrations a cross over from a 3d-Ising to the isotropical Liftshitz critical behavior was found. The critical range as well as the Ginsburg number are significantly smaller than in PEE/PDMS. Furthermore, close to the Liftshitz critical point a phase behavior similar to that of bicontinuos microemulsions was found.

- **Branched polymers and rubbers**

The ongoing research on rubbers now focuses on networks filled with commercial activated silica fillers. It became possible, to produce such networks with a good dispersion of the filler. By SANS the growth and the deformation dependence of the fractal filler clusters could be studied as a function of volume fraction and strain. Phase matched diblockcopolymers with cylindrical morphology of the microdomains were synthesized and allow now an observation of the overstrain of the matrix for anisotropic structures. First experiments have been performed. Rheological experiments on the universality of the exponents for the relaxation time spectrum in the flow and glass region of homopolymer melts were performed as a function of packing length. In particular, experiments on PVCH, the polymer with the largest packing length which can be synthesized anionically, was carried out. These investigations critically inspect whether the standard determination of the plateau modulus on monodisperse homopolymers from the peak height in the imaginary part of the complex modulus agree with that from the Kramers-Kronig relation.

Further research activities (F&E-Nr.: 23.15.0)

➢ **Our activities on tunneling system focussed on three central problems:**

- Rotational tunneling as a probe for the glassy state. These experiments were performed on toluene, a material where the rotational potential is completely intermolecular. In contrast to polymeric glasses, where the intramolecular rotational barrier dominates, the rotational potential within the toluene glass is much higher as in the crystalline material.
- Rotational tunneling in systems with methyl bridges - $A\ell(CH_3)_3$: Dimers connect via two methyl groups and form tetraeders which are linked through a corner. The reduced electron density on each bond of the joint methyl group leads to a stretching of the corresponding bond and a reduction of the rotational potential. The new five fold coordination increases the steric hindrance of rotation **(report Prager).**
- The polar glass ammonium hexachloroplatinate $(NH_4)_2$ Pt Cl_6: If these materials are partially deuterated NH_3D dipoles are created. The long range interaction couples statistically distributed NH_3D defects. Close to the phase transition in $(ND_4)_2$ Pt Cl_6 the coupling could be seen via the inhomogeneous line width of the tunneling line.

➢ **Biological macromolecules**

- The self correlation function of the hydrogen atoms in DNA was studied over a large frequences range. A power law relation of the dynamic susceptibility with frequency was found. The corresponding exponent β depends on the water content.
- Structural investigations of DNA containing ligands are not in agreement with the presently favored intercalation model (ligands go in between every second base pair).

Dieter Richter

Personnel 1999/2000 and areas of activity

Scientific Staff

Dr. J. Allgaier	Polymer synthesis	23.300
Prof. Dr. U. Buchenau	Dynamics of glassforming materials	23.300
Dr. H. Grimm	Molecular crystals, oriented macromolecules Responsable: Backscattering spectrometer BSS1	23.300
Dr. M. Monkenbusch	Dynamics of polymers and complex liquids Responsable: Spinecho Spectrometer NSE	23.300
Dr. M. Prager	Rotational tunneling Responsable: Thermal time of flight spectrometer SV29	23.150
Dr. W. Pyckhout-Hintzen	Polymer networks; branched polymers	23.300
Prof. Dr. D. Richter Institute Director	Structure and dynamics of polymers, glass transition, complex liquids	23.300
Dr. D. Schwahn	Phase transitions in polymer systems Responsable: Small angle neutron scattering KSW1 and double crystal diffractometer DKDin binary polymer melts and blockcopolymers	23.300
Dr. R. Stockmeyer	Dynamics of adsorbed molecules, diffusion in porous media Responsable: Cold time of flight spectrometer SV5	23.150
Dr. L. Willner	Polymer synthesis, polymer micelles	23.300
Dr. habil. R. Zorn	Rubbery electrolytes, glasstransition	23.300

Technical Staff

U. Bünten	Technician at SV29	23.891
Ms. M. Hintzen	Technician in the polymer characterization laboratory	23.300
Dipl.-Ing. M. Heiderich	Engineer responsable for the KWS1 and DKD instruments	23.891
M. Jungen	Technician at SV5	23.891
Dipl.-Ing. T. Kozielewski	Engineer backscattering spectrometer FRM-II	23.891
Ms. U. Sausen-Malka	Electronics laboratory	23.891
Dipl.-Phys. M. Ohl	Second Instrument responsable D23, IN22 at the ILL	23.891
Dipl.-Ing. R. Schätzler	Engineer responsable for the NSE and BSS1 spectrometer, head of technical service group	23.891
K. Schönknecht	Technician at BSS1 and NSE	23.891
K. Sellinghoff	Technician in the polymer characterization laboratory (until December 1999)	23.300
Dipl.-Ing. D. Triefenbach	Chemical Engineer in polymer laboratories (until December 1999)	23.300
Dipl.-Ing. G. Vehres	Electronics engineer, head of electronics laboratory	23.891
Ms M.-L. Schüsseler	Secretary	
Ms S. Oubenkhir	Secretary	

Scientists

Dr. M. Heinrich	Polymer processing, influence of branched polymers	23.300
Dr. St. Kahle	Dielectric spectroscopy, relaxations in complex polymer systems	23.300
Dr. O. Kirstein	Project scientist for backscattering instrument at FRM-II	23.891
Dr. M. Kreitschmann	Influence of polymer architecture on the aggregation properties of PI-PS blockcopolymers	23.300
Dr. W. Leube	Micellarisation and gelation of partially crystallizable polymers	23.300
Dr. S. Perny	Synthesis of branched model polymers and analysis of the structural quality	23.300
Dr. W. Schmidt	Instrument responsable IN12 at the ILL	23.891
Dr. J. Stellbrink	Star polymers and living polymerization	23.300
Dr. A. Wischnewski	Instrument development pulsed spin echo, topological constraints in polymer melts	23.891

Thesis Students

Dipl.-Chem. B. Abbas	(Univ. Münster) Critical concentration fluctuation; in blockcopolymer melts	23.300
Dipl.-Phys. A. Botti	(Univ. Münster) The role of amphiphilic polymers in the emulsifaction properties of microemulsions	23.300
M.Sc. H. Endo	(Univ. Münster) The role of amphiphilic polymers in the emulsification properties of microemulsions	23.300
M.Sc. M. Goad	(Univ. Münster) Dynamic modulus and entanglement formation in polymer melts of polymer blends	23.300
Dipl. Phys. S. Hoffmann	(Univ. Münster) Dynamics of polymer blends	23.300
Dipl.-Ing. H. Kaya	(Univ. Münster) Micellarisation of amphiphilic polymers	23.300
Dipl. Ing. M. Mihailescu	(Univ. Münster) Dynamic of microemulsions - influence of amphiphilic polymers	23.300
Dipl.-Chem. A. Poppe	(Univ. Münster) Micellarisation and exchange kinetics of PEO-PEP diblockcopolymers in selective solvents (until 09.02.99)	23.300

Guests

Dr. Ms. A. Arbe	(Univ. of San Sebastian) primary and secondary relaxation in polymer glasses	23.300
Dr. S. Borberly	(Research Institute for Solid State Physics and Optics, Budapest)	23.300
Prof. Dr. J. Colmenero	(Univ. of San Sebastian) $\alpha-\beta$ relaxation in polymers	23.300
Dr. L. J. Fetters	(Exxon, Annandale) experiments of living polymerization with neutron spin echo spectroscopy	23.300
Dipl.-Phys. M. Heuberger	(Weizmann Institute of Science) Investigation of PEP/PEP-PEO mixtures by small angle neutron scattering and neutron reflectivity	23.300
Dr. S. Koizumi	(JAERI Tokai) Heterogeneity in polymer glasses	23.300
Ms.Sc. K. Marton	(Univ. of Miskolc, Ungarn) Aggregation behaviour of partially crystalline polymers (until 31.08.99)	
Dr. Ms. H. Montes	(ESPCI, Paris) Concentration fluctuations and dynamic in diblock copolymers, neutron scattering approach	23.300
Prof. E. Straube	(Univ. Halle) The influence of topological at the microscopic in polymer networks	23.300

Trainees

A. Christ

R. Stollenwerk

Mixed Membranes of Surfactants and Amphiphilic Block Copolymers: Localization of the Block Copolymer

H. Endo, J. Allgaier, D. Richter, M. Monkenbusch, B. Jakobs[1], T. Sottmann[1], R.Strey[1]
Institute for Neutronscattering,
[1] *University Köln*

The effect of amphiphilic block copolymers on the structure and phase behavior of ternary amphiphilic systems (water, oil and non-ionic surfactant) has been investigated. Small amounts of PEP-PEO block copolymer lead to a dramatic increase in the volumes of oil and water, which can be solubilized in a bicontinuous microemulsion. High-precision neutron small angle scattering (SANS) experiments with a sophisticated contrast variation technique allow for the separation of polymer scattering contributions to the SANS intensity. The results prove that the polymer is distributed uniformly on the surfactant membrane.

F&E-Nr: 23.30.0

The effect of an amphiphilic block copolymer, with hydrophilic and hydrophobic blocks of comparable size, on the structure and phase behavior of ternary amphiphilic system of water, oil and surfactant has been investigated. For an illustration see Fig. 1. The addition of polymer in small amounts is found to lead to a dramatic decrease in the surfactant concentration, which is needed to solubilize oil and water [1].

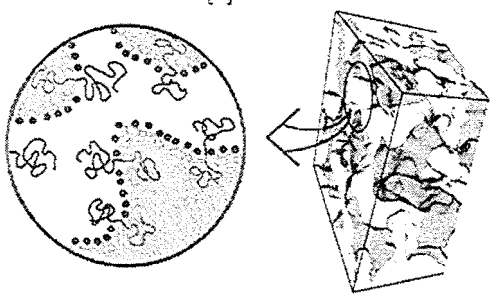

FIG. 1. Bicontinuous microemulsion with polymer.

We consider microemulsions consisting of water, *n*-decance, and the nonionic surfactant $C_{10}E_4$ (*n*-decyltetraoxyethylene) with equal volume fractions of oil and water. To these ternary microemulsions we added amphiphilic block copolymers polyethylenepropylene-*co*-polyethyleneoxide (PEPx-PEOy, where x and y denote the molecular weights of each block in kg/mol). The polymers were synthesized by living anionic polymerization and with a narrow molecular weight distribution [2]. The polymers mimic the structure of the C_iE_j surfactant and the PEP10-PEO10 corresponds roughly to $C_{715}E_{230}$.

For nonionic microemulsions temperature induces phase inversion by changing the spontaneous curvature of the surfactant film [3]. The lower-phase o/w microemulsion ($\underline{2}$) inverts to a w/o microemulsion ($\bar{2}$) with increasing temperature. Optimal solubilization of water and oil occurs at intermediate temperatures. There the microemulsion coexists with water- and oil-excess phases while at sufficiently high volume fractions of amphiphile ϕ a one-phase region is found. The optimal point, where the three-phase body and the one-phase region meet, is located at the lower ϕ the more efficient the surfactant. Addition of an amphiphilic PEPx-PEOy polymer increases the efficiency of the mixture dramatically. The one phase region is shifted toward lower concentrations of amphiphile and the effect becomes stronger with increasing volume fraction, δ_V, of polymer in the mixture of both amphiphiles. The phase inversion temperature of the microemulsion shifts at most marginally [1].

Small angle neutron scattering (SANS) experiments were performed on samples in the bicontinuous phase close to the optimal point ($\phi = 0.05$), which contain $\delta_V = 0.1$ of the amphiphilic PEP5-PEO15 block copolymer. With neutrons as probe, contrast variation techniques based on H/D-replacement can be used to modify the visibility of different components in the system, and have been applied to bicontinuous microemulsions [4]. In bulk contrast, with deuterated water and protonated oil, the scattering is dominated by the three-dimensional structure of the water network (see Fig. 1); any film or polymer contributions are only marginal. In principle, the location and structure of the polymer in the bicontinuous microemulsion can be examined in a system where all components except the polymer have exactly the same scattering length densities ρ_i. Using water, oil and surfactant consisting mainly of the deuterated species and protonated polymer this might be achieved. However, since the polymer scattering is about 5 orders of magnitude lower than the bulk contrast and 2 orders of magnitude lower than film-contrast scattering the required perfect match of the scattering length densities of water, oil *and* surfactant imposed by the 2-dimensional contrast tuning problem is practically unfeasable. However a careful analysis of data obtained close to the matching point yields (among others) the required polymer scattering functions. The scattering intensity, $I(Q)$, after background subtraction is given by

$$I(Q) = \sum_{i,j=\{o,f,p\}} (\rho_i - \rho_w)(\rho_j - \rho_w) S_{i,j}(Q) \qquad (1)$$

where $S_{i,j} = \int \langle c_i(\vec{r_i}) c_j(\vec{r_j}) \rangle \exp[i\vec{Q} \cdot (\vec{r_i} - \vec{r_j})] d^3\vec{r}$. Here, $c_i(\vec{r})$ describes the spatial distribution of component i, with $i = w, o, f, p$ for water, oil, film (or surfactant) and polymer, respectively, and ρ_i is the scattering length density. ρ_w is the scattering length density of the water region, arbitrarily chosen as the component of the system that is considered as background. In the experiment performed on the high intensity SANS instrument D22 at the ILL in Grenoble, contrast variation around the 2-dimensional matching point was achieved by a stepwise increment of ρ_o (adding tiny amounts of protonated decane) and ρ_f, which produced 15 different samples. Their scattering data were then used to extract the 6 partial scattering function $S_{o,o}, S_{f,f}, S_{o,f}, S_{o,p}, S_{f,p}$ and $S_{p,p}$ by inserting the measured intensities $I_m(Q)$ and the contrasts $(\rho_i^m - \rho_w)$ into Eq. (1) and solving the overdetermined set of equations ($m = 1 \cdots 15$). We improved the reliability of the results by adding pure bulk- and film-contrast data with very large weight as well as the relation $S_{o,f} = -(1/2)S_{f,f}$ suggested in Ref. [5] to this set of equations. Investigation of the sensitivity of the $S_{i,j}$ on the exact location of the matching point revealed that only $S_{o,p}$ is so sensitive that no reliable form can be inferred. Figure 2a shows the result for the polymer, $S_{p,p}$, and film, $S_{f,f}$, scattering functions. The comparison of the scattering curves indicates that the polymer scattering is dominated by the form of $S_{f,f}$ for small $Q < 0.02\text{Å}^{-1}$ and by polymer-coil scattering for higher Q-values. This demonstrates clearly that the polymer "decorates" the surfactant film. Due to the dilution of scattering length density, however, the corresponding intensity is about two orders of magnitude lower than the pure film-contrast scattering. The polymer-coil scattering intensity, on the other hand, is about one order of magnitude lower than the intensity to be expected from the same number of free, non-interacting coils. Obviously the mutual interaction imposed on the polymers by confinement onto the two-dimensional interface region leads to an increased importance of the second virial coefficient that reduces the forward scattering of the polymer coils accordingly. Any polymer-polymer aggregation (micellization) would immediately lead to orders of magnitude higher values for $S_{p,p}$ [2] and can be safely excluded. The film-polymer scattering, shown in Fig. 2b, exhibits a minimum at $Q \simeq 0.03\text{Å}^{-1}$, which is mainly due to the interference of maxima in the polymer density at a distance $\beta\mathcal{R}_{PEP}$ and $\beta\mathcal{R}_{PEO}$ from the interface, respectively, where $\mathcal{R}$ is the average end-to-end distance of a polymer coil, and $\beta = 4\ln 2/(3\sqrt{6}) = 0.38$ for ideal chains [6]. The solid line is a fit of the Fourier transform of the monomer density projected on the film-surface normal, as expected theoretically for ideal chains in the mushroom regime [6], including a Q^{-2} factor to account for the angular averaging (valid only for $Q > 0.01\text{Å}^{-1}$). The fitted average end-to-end radius amounts to 155 Å, which compares quite well with the end-to-end distance $\mathcal{R}_{PEO} = 140\text{Å}$ determined from homopolymer solutions [7]. The experimental results prove that the polymer is tethered to the interface, and that the "mushrooms" formed by the PEP-chain in the oil phase and by the PEO-chain in water lead to a clearly visible oscillation in $S_{f,p}$.

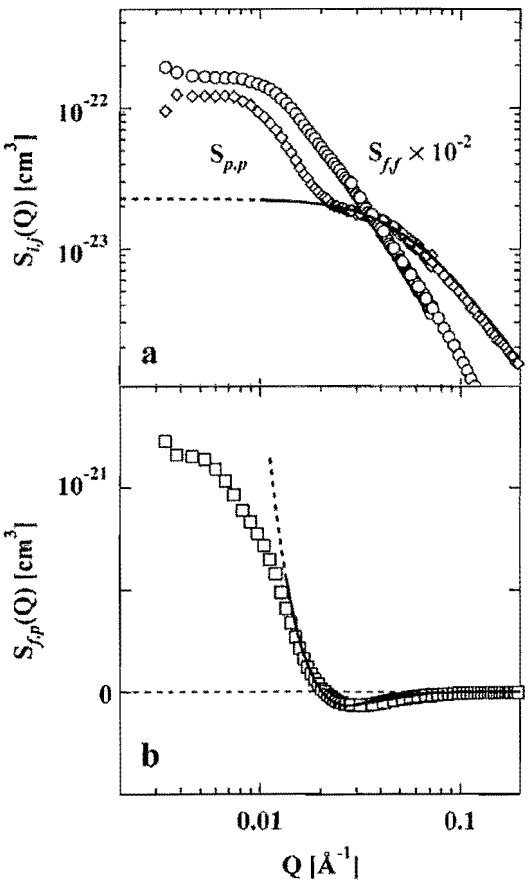

FIG. 2. Partial scattering function involving a polymer contribution. a.) comparison with the film (interface) scattering $S_{f,f}$ and polymer coils scattering (line). b.) polymer film interference term, see text.

[1] B. Jakobs *et al.*, Langmuir **15**, 6707 (1999).
[2] J. Allgaier, A. Poppe, L. Willner, and D. Richter, Macromolecules **30**, 1582 (1997); A. Poppe *et al.*, Macromolecules **30**, 7462 (1997).
[3] R. Strey, Curr. Opin. Coll. Interf. Sci. **1**, 402 (1996).
[4] L. Auvray, J.-P. Cotton, R. Ober, and C. Taupin, J. Phys. Chem. **88**, 4586 (1984).
[5] G. Gompper and M. Schick, Phys. Rev. B **41**, 9148 (1990).
[6] E. Eisenriegler, K. Kremer, and K. Binder, J. Chem. Phys. **77**, 6296 (1982).
[7] S. Kawaguchi *et al.*, Polymer **38**, 2885 (1995).

Local strain relaxation effects in branched polymers

M. Heinrich, W. Pyckhout-Hintzen, S. Perny, J. Allgaier, D. Richter, E. Straube[1]
Institut für Neutronenstreuung
[1] *Universität Halle, FB Physik, D-06099 Halle*

We have investigated the structure of partially labelled, stretched H-shaped polymers after different relaxation times. The SANS (Small Angle Neutron Scattering) technique permits the unique evaluation of the behaviour of the polymer molecules in a flow field. The selective labelling by deuterium allows measurements of disentanglement and alignment of the marked parts of the chains. Information obtained for H-polymers differing only in their labelling type gives access to the description of the relaxation process of the complete H-molecule.

F&E-Nr: 23.30.0

This study is part of a Brite-Euram project called "The Science and Technology of Long Chain Branching in Polyolefins and their Process Control", of which the main objective is the definition of new polymers with controlled processing and final properties, enabling thinner films to be used for many packaging applications.

From a technological point of view, monodisperse polymers are difficult to process. It has been shown that adding only small amounts of randomly branched polymers improves considerably their processing. The reason for the improved flow is unknown, but is thought to derive from the molecular behaviour of entangled branched polymers. For these, the tube model of constraints as for melts of homopolymers applies. Chains ends hereby play an important role as they alone can unravel by releasing the constraints of the surrounding tubes. The simplest topology of branched chains is the H-shaped structure. During the relaxation of the chains after a step strain, the arms of the H-polymer will relax faster than the cross-bar, the latter behaving more or less rubberlike.

SANS is a unique technique to examine the structure of entangled polymer melts. Experimentally, in the case of extensional flow, a deformed polymer melt is rapidly quenched to below its glass transition temperature to freeze the configuration instantaneously and the scattering pattern is taken. Quenched SANS experiments in extension of (weakly entangled) linear polystyrene failed to give strong evidence of the tube retraction mechanism [1], [2]. The highly entangled polyisoprene, on the other hand, gives a clear signature of the various retraction dynamics: preliminary experiments were able to identify the tube-diameter parameter of fluctutations from the anisotropy of the scattering [3], but the experiment lacked control in both rate and quenching time.

For our experiments, an improved strain rig compatible with SANS experimental configurations has been designed and built in Juelich (Fig. 1). It allows a perfect control of temperature in the range -100 to +200 degrees C and at the same time, of stretching and quenching conditions, unlike in Ref. [3]. A loadcell in the static cylinder provides an on-line inspection of the transduced force and allows stress-strain curves to be recorded simultaneously.

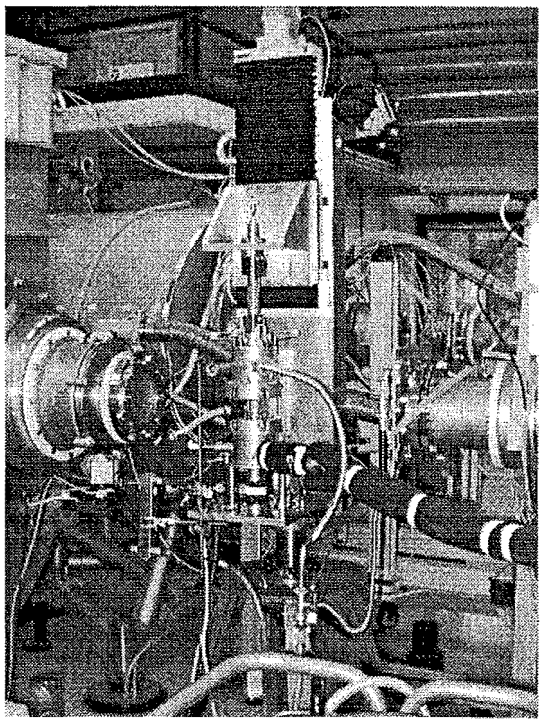

FIG. 1. Elongational strain rig with quench unit at the sample position at KWS1, Jülich.

The obtained structure factors in the directions parallel and perpendicular to the stretching as well as in the whole 2D-detector plane (e.g. Fig. 2 and Fig. 3), are interpreted in term of an extended Random Phase Approximation (RPA) theory [4]. Here, it is proposed that RPA corrections to the free chain and tube fluctuations can in a good approximation be taken as independent from each others. This assumption worked perfectly in the case of permanent networks made from triblock copolymers. Two different deuterium labelled (tips of the arms or cross-bar labelled) polyisoprene or polybutadiene samples, both adjusted to have the same number of entanglements per chain, covered in an exemplary way both

limits in the time domain or relaxation spectrum, i.e. both the slowest and the fastest segments were investigated with respect to strain, strain rate and temperature. In the light of a description within the tube model, the rapid retraction of deformed chain ends and the much slower reptation dynamics for the cross-bar part can be addressed separately. The experiments parallel measurements of the dynamic moduli in linear shear which clearly established a slowing down of the bridge terminal mode by several orders of magnitude compared to the attached chains. In view of the time scale on which relaxation after a step strain is predicted, the cross-bar labelled H-polymer closely resembles the behaviour of a deformed rubber network, disturbed only to a minor degree by the relaxation of the arms. The entanglement spacing in the early stages complies very well to rheological estimates. The arms of the H-polymers are modelled to be discretely built up from three sequences of different local strains, each characterized by a relaxation factor. The correction for the bridge is small. For the shortest relaxation times, the deformation is overall-affine with the external strain. The affinity of the bridge deformation up to long relaxation times of the order of those of the whole arm confirms the dynamical decoupling of the arm relaxation assumed in dynamical mechanical analysis. The agreement with the proposed model along both principal axes of strain is presented in Fig. 4. Here, the confinement parameter reduces as a function of relaxation time, i.e. the tube value increases. Although a more profound description in terms of the RPA of the deformation behavior as a function of strain, strain rate and time is lacking, the agreement is still appreciable.

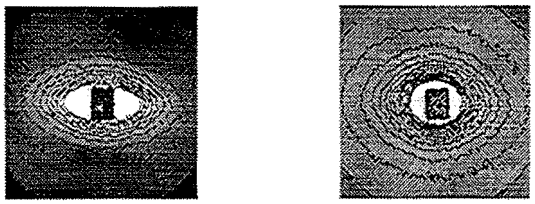

a b

FIG. 2. Bridge-labelled H-polymer strained by a factor 2 : (a) $\tau = 0s$ and (b) $\tau = 2.6s$ relaxation @RT

The lack of a proper modelling is felt clearly in the tip-labelled H-polymer. The deviation of the rubber-like theory from available scattering data shows itself by the appearance of unexplained butterfly-like patterns due to enhanced correlations along the direction of strain. Also the rise of intensity with increasing strain at constant strain rate is still beyond theoretical description. The data provide a challenge for theoreticians as well as rheologists. It is hoped that from a one-to-one comparison to non-linear elongational viscosity measurements, knowledge will evolve enabling the design of industrially important branched polymers with known relaxation time spectra, in order to ease their processing and moulding. The input of SANS into this is indispensable, since it identifies the mechanisms of relaxation directly.

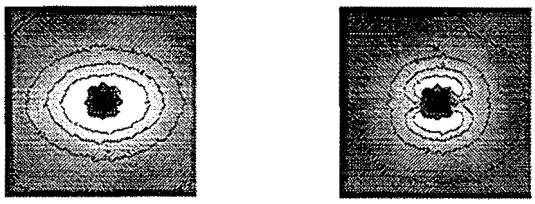

a b

FIG. 3. Tip-labelled H-polymer strained by a factor 2 : (a) $\tau = 0s$ and (b) $\tau = 0.105s$ relaxation @RT

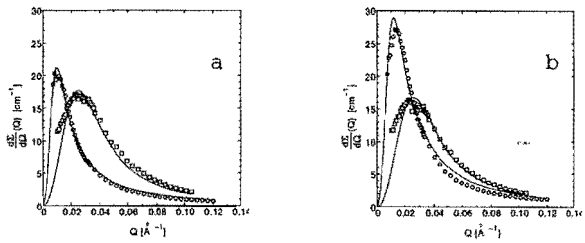

FIG. 4. Principal axes fits (lines) for the bridge-labelled H-polymer strained by a factor 2 : (a) $\tau = 0s$ and (b) $\tau = 2.6s$ relaxation @RT. Experimental points : circles for the direction parallel to the strain and squares for the direction perpendicular to the strain

[1] F. Boue, K. Osaki, R. C. Ball, J Polym Sci B-Polym Phys 1985, 23, 833.

[2] R. Muller, J. J. Pesce, C. Picot, Macromolecules 1993, 26, 4356.

[3] T. C. B. McLeish et al, Macromolecules 1999, 32, 6734.

[4] M. Heinrich, W. Pyckhout-Hintzen, S. Perny, J. Allgaier, D. Richter, E. Straube, in preparation

Dynamic miscibility of a binary polymer blend: A quasielastic neutron scattering study on the crossover from heterogeneous to homogeneous dynamic behaviour

S. Hoffmann[1,2], L. Willner[1], D. Richter[1], A. Arbe[3], J. Colmenero[3], and B. Farago[2]
[1] *Institut für Festkörperforschung, Forschungszentrum Jülich, 52425 Jülich, Germany*
[2] *Institut Laue-Langevin, B.P.156, 38042 Grenoble Cedex 9, France*
[3] *Departamento de Física de Materiales y Centro Mixto CSIC-UPV/EHU, Universidad del País Vasco, Apertado 1072, 20080 San Sebastian, Spain*

Quasielastic neutron scattering was applied in order to study the individual component dynamics in a blend of polyvinylethylene and polyisoprene. A wide range of different length scales was examined covering a large dynamic region from local segmental relaxations to mesoscopic chain motions. Within this range, a crossover from heterogeneous to homogeneous behaviour was revealed in the component dynamics when passing from local to mesoscopic length scales. By means of the experimental results, a comprehensive picture of the principles governing the molecular dynamics in a polymer blend can be drawn. It is shown that the observed heterogeneity of the local component dynamics can be understood as a purely dynamic phenomenon which is determined by the specific (intrinsic) properties of the two polymers.

F&E-Nr. 23.30.0

While theoretical concepts to understand the thermodynamics and the structure of polymer blends are well developed, the full range of dynamic behaviour in such systems is only at the beginning of being clarified. The question of dynamic miscibility, has recently been addressed by different spectroscopic approaches [1]-[9]. These works reveal that, on the local scale which is probed by these techniques, the two components dynamically behave very different compared to each other, although the blend is intimately mixed. This finding was commonly interpreted as a result of local inhomogeneities which were estimated to have a typical size of few nanometers from two-dimendional NMR studies [2].

In our investigations, we applied quasielastic neutron scattering in order to study the individual component dynamics in a blend of two miscible polymers, polyvinylethylene (PVE) and polyisoprene (PI). A wide range of wavevector transfer Q became accessible in combining two high resolution techniques, neutron backscattering (BS) for high and neutron spin echo spectroscopy (NSE) for low Q values. For a first time in the case of polymer blends, such a wide dynamic range reaching from entropy driven chain relaxations to local segmental dynamics has systematically been covered by neutron scattering. The sensitivity to each of the components in the blend was achieved by selective proton/deuteron labeling of the polymers.

The structural relaxations of a polymer chain on mesoscopic length scales can be well approximated by the Rouse model [10]. On intermediate length scales between the end-to-end distance R_E of the chain and the length l of a statistical segment, the polymer structure shows a fractal nature which translates via the Rouse model into a dynamic scaling law for the structure factor of the chain. The corresponding scaling variable is $x_R = \sqrt{Wl^4Q^4t}$ where W is a fundamental relaxation rate.

This universal behaviour breaks down in passing to smaller length scales, where the detailed chemical stucture of the polymer increasingly influences the polymer dynamics. Up to now, there is no general theoretical concept for this situation. Experimentally, the corresponding short-range diffusive motion of the chain segments has been identified with the α-process which is observed in relaxation spectroscopy methods. In analogy to these techniques, the incoherent dynamic structure factor $S_{inc}(Q,\omega)$ ($\hbar\omega$: energy transfer) may be described by the Fourier transform of a stretched exponential in the time domain which is known as the Kohlrausch-William-Watts (KWW) function [11] where the stretching exponent β generally agrees with dielectric spectroscopy results (here: $\beta_{PVE} = 0.43$ and $\beta_{PI} = 0.40$).

Both polymers have been synthesized by anionic polymerization in a protonated and a deuterated version of identical size and with a very low polydispersitivity of 1.02. The molecular weight of the protonated polymers amounted to roughly 80 000. All blends had an overall composition of 50 vol% PVE and 50 vol% PI.

By NSE spectroscopy, the dynamic single-chain form factor of each component was measured. The experiments were performed at the NSE spectrometer IN11 of the Institut Laue-Langevin (ILL) in Grenoble, France ($Q = 0.05 \cdots 0.20$ Å^{-1}, $T = 330, 368, 418$ K). All spectra scale very well with the Rouse variable x_R and can be described by the Rouse theory for times which are small against the entanglement time τ_e. By fitting the Rouse function to the experimental data, the quantity Wl^4 was obtained as the only free fit parameter and the avarage relaxation time of the self correlation function was calculated from $\langle\tau_{inc}^R\rangle = 18\pi/(Wl^4Q^4)$ (see also [12]).

The high Q range was measured at the neutron backscattering spectrometer BSS of the IFF/FZ Jülich ($Q = 0.3 \cdots 1.9$ Å^{-1}, $T = 270 \cdots 340$ K). The spectra

were analyzed by fitting a Fourier transformed KWW function folded with the instrumental resolution function. Multiple scattering corrections were performed by a Monte Carlo simulation of the scattering process. The average relaxation times were calculated from the KWW fit parameters by $\langle\tau\rangle = \tau_{\mathrm{KWW}}\Gamma(1/\beta)/\beta$.

In order to compare NSE and BS results, the different temperature ranges were merged by applying the appropriate shift factors to the NSE relaxation times. These shift factors were measured on the high resolution NSE spectrometer IN15 at the ILL. In case of pure and blended PI the shift factors agreed with corresponding results from dielectric normal mode spectroscopy.

The experimental results are condensed in the Figure 1 for an exemplary temperature of 330 K. It represents the main result of this investigation and displays the mean relaxation times for the individual polymer chains over the whole Q range for both, the polymer blend (open symbols) and the two pure homopolymers (filled symbols).

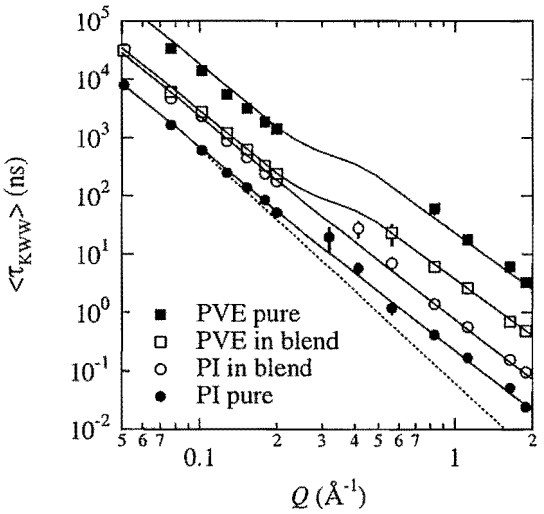

FIG. 1. Average relaxation times for the polymers in the four different materials investigated.

The dynamics of both homopolymers is compatible with the Rouse model at small Q values (dotted line of slope -4 in the figure). In moving to higher Q values, the average relaxation time of PI decreases slightly less than the extrapolated Rouse behaviour. In contrast to PI, the motional time scale of PVE is significantly retarded in comparison to the Rouse-like Q^{-4} behaviour. The shape of the dynamic crossover is therefore specific for each polymer and related to its intrinsic dynamic properties.

In the blend, the Rouse dynamics of both components is nearly identical. These dynamics appear as practically homogeneous on mesoscopic length scales. In passing towards larger Q values, the mean relaxation times show exactly the same crossover as for the respective homopolymers.

From this observation, the apparent dynamic heterogeneities which were found by applying local spectroscopic probes can be explained in a new comprehensive way. They appear mainly as a result of the difference in the individual crossover behaviour from Rouse-like to segmental chain dynamics of the two components in the blend. Due to the different dynamic crossovers of PVE and PI, the individual local dynamics in the blend is separated by one order of magnitude while the Rouse dynamics in the same system is essentially homogeneous. As the crossover is located around $Q \approx 0.2$ Å, one can associate a characteristic spacial crossover length of $2\pi/Q \approx 3$ nm. This value is very close to the NMR result cited above, but the mechanism which controles the component dynamics in a polymer blend is quite different to the supposed nanoheterogeneities which were invoked to explain the NMR results.

Summarizing, we can classify the local dynamic heterogeneities in a polymer blend as a purely dynamical phenomenon which is a consequence of the different intrinsic dynamic crossover behaviour of the two components.

[1] G. Katana, E. W. Fischer, T. Hack, V. Abetz, and F. Kremer, Macromolecules **28**, 2714 (1995).

[2] K. Schmidt-Rohr, J. Clauss, and H. W. Spiess, Macromolecules **25**, 3273 (1992).

[3] G.-C. Chung, J. A. Kornfield, and S. D. Smith, Macromolecules **27**, 5729 (1994).

[4] G. Fytas, G. Meier, and D. Richter, Journal of Chemical Physics **105**, 1208 (1996).

[5] S. K. Kumar, R. H. Colby, S. H. Anastiasadis, and G. Fytas, Journal of Chemical Physics **105**, 3777 (1996).

[6] F. Alvarez, A. Alegra, and J. Colmenero, Macromolecules **30**, 597 (1997).

[7] S. Adams and D. B. Adolf, Macromolecules **32**, 3136 (1999).

[8] I. Cendoya, A. Alegra, J. M. Alberdi, J. Colmenero, H. Grimm, D. Richter, and B. Frick, Macromolecules **32**, 4065 (1999).

[9] A. Arbe, A. Alegra, J. Colmenero, S. Hoffmann, L. Willner, and D. Richter, Macromolecules **32**, 7572 (1999).

[10] M. Doi and S. F. Edwards, *The Theory of Polymer Dynamics* (Clarendon, Oxford, 1986).

[11] A. Arbe, J. Colmenero, M. Monkenbusch, and D. Richter, Physical Review Letters **81**, 590 (1998).

[12] B. Ewen and D. Richter, *Advances in Polymer Science* (Springer-Verlag, Berlin Heidelberg, 1997), Vol. 134.

Ripplon Excitations of Domain Walls in Symmetric Diblock Copolymer Melts – a Neutron Spin Echo Study

H. Montes[1], D. Richter, M. Monkenbusch, L. Willner
L.J. Fetters[2], S. Rathgeber[3], B. Farago[4]
Institute for Neutronscattering,
[1] *ESPCI, Paris, France,*
[2] *Exxon Research, Annandale, USA,* [3] *NIST, Gaithersburg, USA,* [4] *ILL, Grenoble, France*

The interface dynamics in a lamellar A-B diblock copolymer was observed by neutron spin echo (NSE) spectroscopy. This observation was made feasible by judicious labeling around the junction point between the two blocks. The interfacial walls undulate in form of overdamped capillary waves (ripplons). Driven by the A-B surface tension these relaxation are faster than the polymer chain dynamics. The evaluated surface tension and local viscosities are well within theoretical predictions.

F&E-Nr: 23.30.0

The morphology of diblock copolymer melts is controlled by composition and incompatibility χN expressed in terms of the Flory Huggins monomer-monomer interaction parameter χ and the number of monomers per chain N [1]. For a symmetric system an order disorder transition (ODT) to a lamellar phase is expected at $\chi(T)N \simeq 10$. In the strong seggregation regime ($\chi(T)N >> 10$) well separated layers with a mutual interface tension γ are formed. For $\chi N \simeq 10$ the Random Phase Approximation (RPA) [1] predicts only sinusodial density modulations for two interpenetrating components. However X-ray and neutron small scattering (SAXS and SANS) experiments observe higher order peaks indicating sharper than sinusodial density profiles. This picture is supported by electron microscopic investigation by Hashimoto [2].

For the strong seggregation limit Helfand and Wassermann [3] used a self consistent field theory that permits quantitative calculations of free energies, composition profiles and chain conformations. In the narrow interface approximation (NIA) this theory yields:

$$\gamma = n_{mon} k_B T \sqrt{\frac{\chi(b_A^4 + b_B^4 + b_A^2 b_B^2)}{9(b_A^2 + b_B^2)}} \qquad (1)$$

for the surface tension and interfacial width $d = 2\sqrt{(b_A^2 + b_B^2)/(12\chi)}$ where b_i are the Kuhn segment lengths of the A and B polymers and n_{mon} the monomer number density. The validity of these expressions for large χN was confirmed experimentally by Hashimoto [4].

Using a A-B contact region labeled poly(ethylene-propylene)-polyethylethylene (PEP-PEE) diblock in the molten state close to the ODT, the first observation of A-B interface undulations in a block copolymer would be achieved. The h-labeling on 5% of the PEP chain at the junction end to PEE and otherwise completely deuterated chains made the interface dynamics accessible to the investigation by NSE spectroscopy. The total molecular weight was $M_w = 68000$ g/mol leading to a transition temperature $T_{ODT} = 433$ K. The ordered and labeled lamellar structure is sketched in fig. 1.

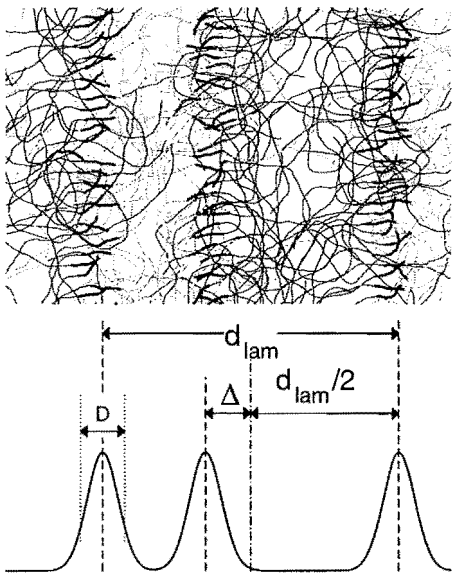

FIG. 1. Schematic diagram of a lamellar structure in a diblock copolymer and density profiles of the labels at the interface.

The SANS intensity from a structure as displayed in fig. 1 contains two contributions:

$$\frac{d\Sigma}{d\Omega}(Q) \propto P_{pol}(Q) + P_{interface}(Q)G(Q) \qquad (2)$$

where P_{pol} denotes the scattering from the individual labeled coil segments embedded in the interface region and $P_{interface}$ is the scattering due to the average contrast density modulation at the interfaces which is multiplied by the structure factor $G(Q)$ accounting for interference effects of adjacent interface regions. Analysis of the SANS intensities shows that their salient low Q features may be described by a model translating the

density modulation depicted in fig . 1 into an expression for $P_{interface}(Q)G(Q)$. The polymer scattering $P_{pol}(Q)$ is described by a Debye function, i.e. the scattering of a Gaussian coil, with a gyration radius corresponding to the size of the labeled section. It turns out that for the Q-range where NSE experiments could be performed the polymer scattering P_{pol} dominates the intensity $d\Sigma/d\Omega \propto S(Q)$, only the lowest measured Q-value contains some contribution from the second term in Eqn. 2.

Therefore the dynamics as measured by NSE consists mainly of contributions from single (incoherently added) labeled coils. These coils exhibit normal polymeric Rouse relaxations of a chain which is anchored at the interface. The usual center of mass diffusion observed for small polymer coils is therfore to be replaced by the motions imposed on the coil by the interface undulations. Since the label is small the latter contribution dominates in the intermediate Q-regime.

Assuming capillary waves damped by equal viscosity η on boths sides of the interface the relaxations have a linear dispersion [5] $\tau^{-1} = q\gamma/(4\eta)$ where q, the mode wavevector is not to be confused with the Q set in a scattering experiment. The undulation mode amplitudes follow from equipartition:

$$< |u^2(q)| >= \frac{k_B T}{q^2 \gamma} \tag{3}$$

Summing the modes with weights according to Eqn. 3 yields the time correlation of the displacements:

$$f(t) = \frac{1}{2} < |u(t) - u(0)|^2 > \quad = \quad \frac{k_B T}{4\pi\gamma}\left[\ln(\xi/) + \mathrm{Ei}(1, t/\tau[2\pi/\xi]) - \mathrm{Ei}(1, t/\tau[2\pi/l])\right] \tag{4}$$

The introduction $q_{min} = 2\pi/\xi$ and $q_{max} = 2\pi/l$ due to finite domain size ξ and molecular dimension l renders the required integrations convergent. Applying the Gaussian approximation and angular averaging the yields:

$$S(Q,t)_{pol} \propto S^0_{Rouse}(Q,t)\left[\frac{1}{2}\frac{\sqrt{\pi}\mathrm{erf}(Q\sqrt{f(t)})}{Q\sqrt{f(t)}}\right] \tag{5}$$

Fig. 2 shows a comparison of the NSE data obtained in Juelich and at the ILL with the expectation of a simple Rouse model and with the fit of Eqn. 5. The resulting values for $\gamma = 0.0023$ N/m at 433 K and 0.0024 N/m at 473 K agrees reasonably well with the NIA theoretical values of $\gamma = 0.0015$ N/m and 0.0014 N/m by Helfand. Since both the relative intensities (i.e. undulation amplitude) and the timescale determined by the dispersion coefficient influence the scattering also the effective viscosity could be determined as $\eta = 0.74 \times 10^{-3}$ Ns/m^2 compared to the effective viscosity felt by a monomeric unit according to the Rouse model $\eta_{Rouse} = 2.7 \times 10^{-3}$ Ns/m^2.

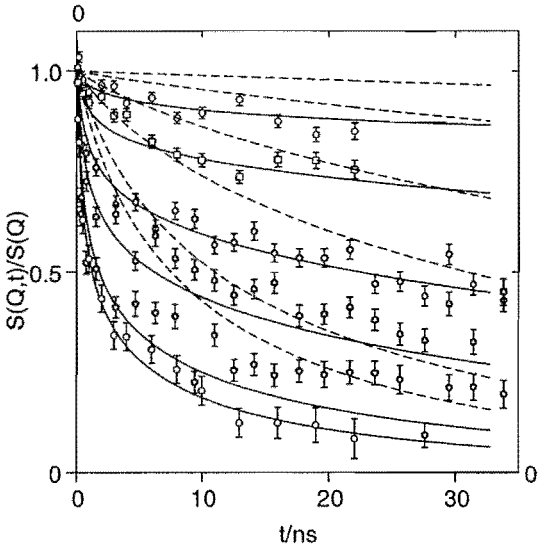

FIG. 2. NSE spectra at 433K obtained at the Jülich NSE spectrometer and at the ILL instrument IN15 (Grenoble) for momentum transfer values The dashed lines represent the Rouse dynamics of a hPEP block in a mixed homogeneous system. The solid lines correspond to the fit with the ripplon structure factor.

Summarizing, by combination of careful chemical synthesis with NSE-experiments on the limit of what can be achieved today concerning signal to noise it became possible to detect dynamic surface undulations of domain interfaces in diblock copolymer systems close to the ODT. The experimental scattering functions and the derived surface tension agree well with predictions for systems in the strong segregation limit indicating that even close to the ODT more order than inferred by the RPA theory is present. In recent NSE experiments on the collective dynamics of the same diblock copolymer in dA-hB labeling we observed fast relaxations in contradiction to the slowing down predicted by the RPA theory [6]. These fast fluctuations most likely also relate to the surface undulations (ripplons) of the interface.

[1] L. Leibler, Macromolecules **13**, 1602 (1980)

[2] T. Hashimoto, Ta. Koga, Ts. Koga, N. Sakamoto, J. Chem. Phys. **110**, 11076 (1999)

[3] E. Helfand, Z.R. Wassermann, Macromolecules **9**, 879 (1976); E. Helfand, Z.R. Wassermann in *Developments in block copolymers I*, Ed. I. Goodman, Appied Science, New York (1982)

[4] T. Hashimoto, M. Shibayama, H. Kawai, Macromolecules **13**, 1237 (1980)

[5] M. Papoular, J. Phys. Rad. **29**, 81 (1961)

[6] H. Montes, M. Monkenbusch, L. Willner, S. Rathgeber, L. Fetters, D. Richter, J. Chem. Phys **110**, 10188 (1999)

Rotational potentials of bridging and terminal methyl groups in trimethylaluminum-dimers

M. Prager, H. Grimm, S.F. Parker[1], S. McGrady[2]
Institut für Festkörperforschung, Forschungzzentrum Jülich D-52425 Jülich, Germany
[1] *ISIS facility, RAL, Chilton, Didcot, Oxon OX11 0QX, UK*
[2] *Kings College, London, UK*

Trimethylaluminum is a model electron deficiency compound. Dimerization via bridging methyl groups involves a new weak $C-Al$ bond. Neutron spectroscopy is used to determine internal and external modes. Librations of methyl groups are assigned on the basis of the isotope effect. Including rotational tunnelling rotational potentials are derived. The bridging CH_3 group shows the strongest potential: The splitting of the σ-bond to one Al into two equivalent bonds to the two Al (fivefold coordination) leads to steric hindrance which overcompensates the weakening by the elongated $Al-C$ bond.

F&E-Nr: 23.15.0

Group III trimethyl compounds form an interesting class of organometallic materials. Due to thermal instability the molecules can be used for doping semiconductors homogeneously with Al, Ga and In by thermal decomposition at a hot surface. Furthermore aluminum alkyls are used as Ziegler-Natta catalyst in polymerization of olefins. In both, the gas phase [1] and the crystalline state, e.g. [2–4], trimethyl aluminum (TMA) forms *dimers* with about tetrahedrally coordinated Al and fivefold coordinated C atoms of the two bridging methyl groups. In the solid state 3 inequivalent types of methyl groups exist (Fig. 1). Since the bridging C atom shares its charge with 5 bonds the $Al-C2$ bonds are weakened and its lengths increased by 10%.

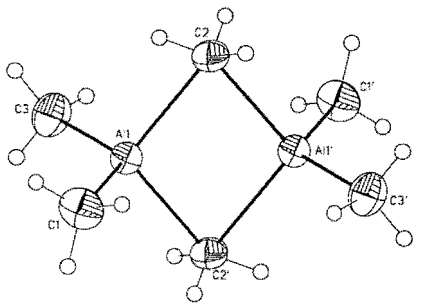

FIG. 1. Dimers form the structural unit of solid TMA. Carbons 1 and 3 are called terminal, 2 bridging.

So far dynamics of methyl groups was studied by the NMR-T_1 technique. Not distinghuishing between inequivalent methyl groups an average activation energy $E_a \sim 3.5$kJ/mol was obtained [5]. Such weak potentials allow the observation of Librations and rotational tunnelling by neutron spectroscopy.

Incoherent inelastic neutron scattering data in the energy range $0.001 \leq \Delta E[meV] \leq 500$ covers excitations from tunnelling to internal modes and allows to extract detailed information on all different methyl groups.

As samples both protonated and deuterated materials were studied. The protonated substance from Heraeus was used without further treatment. The highly reactive material was filled under argon into a 0.5mm thick stainless steel cell. The deuterated material was prepared at King's college.

Methyl rotational tunnelling of $Al(CH_3)_3$ was investigated by high resolution neutron spectroscopy using the backscattering spectrometer at the FRJ2 reactor in the offset configuration which gives acces to energy transfers $-32 < \hbar\omega[\mu eV] < 3$) at an energy resolution of $\delta E \sim 1.5\mu eV$. The spectrum (Fig. 2) shows two tunnel peaks of equal intensity. A comparison of inelastic and incoherent elastic intensities, based on the scattering function of the tunnelling methyl group [6,7], it can be shown that each line corresponds to $\frac{1}{3}$ of the CH_3 groups while the third one - known to be present from the crystal structure - is hidden in the elastic line. In agreement with this analysis no further tunnelling line was observed up to the free rotor energy. Transition energies are shown in Tab. I.

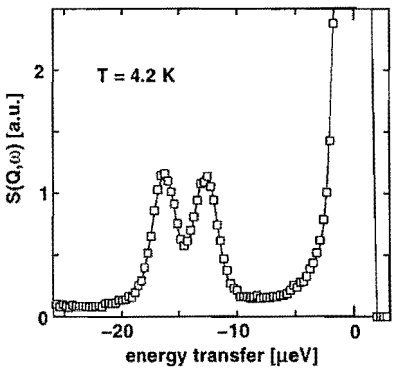

FIG. 2. TMA, T=4.5K, Instrument: BSS1 at FZ Jülich. Momentum Transfer $Q = 1.73\text{Å}$. Solid line: fit.

Lattice and internal modes werde measured in the energy regime 2-500meV for hydrogenated and deuterated species using the TOSCA spectrometer at the ISIS facility, Rutherford-Appleton Laboratory, UK (Fig. 3). Identification of low lying rotary modes was done on the basis of isotopic shifts. Three librational bands are observed around 6.4, 14.0 and 17.5meV (Tab. I). All bands show multiplett structures.

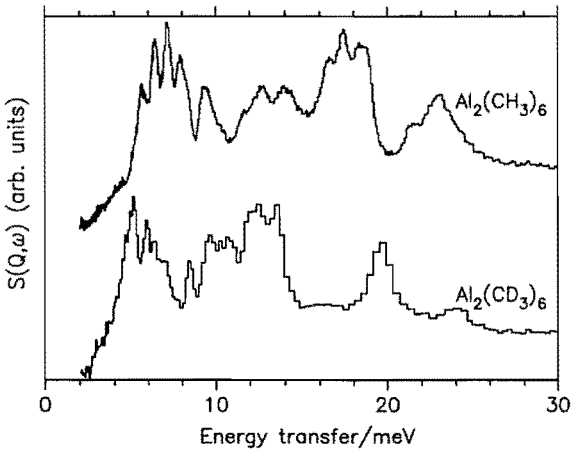

FIG. 3. Section of neutron scattering spectra of TMA at $T \sim 13K$ and energies <30meV. Instrument: TOSCA at the ISIS facility, RAL, UK.

In the single particle picture of molecular rotation [6] the librational and tunnelling modes of the onedimensional threefold rotor are solutions of the Mathieu equation with methyl rotational potentials written as

$$V(\varphi) = \sum_{n=1}^{2} \frac{V_{3n}}{2}(1 - cos(3n\varphi)) \qquad (1)$$

To parametrize the potentials of the 3 inequivalent CH_3 groups up to second order two excitations of each must be known. We combine low librational bands with large tunnel splittings. This is not completely free of arbitraryness in potentials of different shapes. This way the terminal $t - CH_3$ groups show weak potentials with strong sixfold contribution while the bridging $b - CH_3$ is strongly hindered (Tab. I). The appearance of a significant sixfold term for terminal methyl groups is the consequence of additional symmetry of the environment: their axes of rotation lie in almost a mirror plane of the dimer. In case of the bridging methyl groups a sixfold term is expected too. Lacking the knowledge of the tunnel splitting, however, only the simplest form of a pure 3-fold potential was extracted. - To check consistency with the deuterated spectrum librational energies of CD_3 were calculated for the same potentials just rescaled by the smaller rotational constant. We had to reduce the sixfold term by 30%, however, to get agreement (column 5 of Tab. I). Activation energies of the rotational potentials 1 are shown in the last column of Tab. I. Its average is very close to the value extracted from the NMR-T_1 experiment [5].

methyl group	$\hbar\omega_t$ $[\mu eV]$	E_{01} $[meV]$	V_3 $[meV]$	V_6 $[meV]$	E_a $[kJ/mol]$
C_bH_3	–	17.5	62	–	5.0
C_tH_3	11.9	14	21	13	1.6
C_tH_3	15.2	6.4	39	-21	3.8
C_bD_3	–	12.7	62		
C_tD_3	–	10.4	21	9	
C_tD_3	–	5.2	39	-14	

TABLE I. Observed transition energies and derived rotational potentials and activation energies. b=bridging, t=terminal

In **conclusion** three inequivalent methyl rotors are observed in TMA by neutron tunnelling spectroscopy in agreement with the measured crystal structure. Fourier coefficients of rotational potentials are derived up to second order for every CH_3 group. Terminal methyl groups show weak potentials with large 6-fold contributions due to the presence of a mirror plane. Despite an increased bond length bridging methyl groups are strongly hindered: The topology requires a breaking of the - weak - $C - Al$ bonds at rotation.

Both, the dimer geometry and the methyl librational energies of this unusual molecule, are badly reproduced by ab-initio methods [8]. Future studies will focuse on improving this description. - Furthermore with increasing weight/size of the metal ion the dimeric character is reduced up to lost. This tendency offers a possibility to study the influence of dimerization in a systematic way continuing with $Ga(CH_3)_3$.

[1] A. Almenningen, S. Halvorsen, A. Haaland, Acta Chem. Scand. **25**,1937(1971)
[2] R.G. Vranka, E.L. Amma, J. Am. Chem. Soc. **89**,3121(1967)
[3] P.H. Lewis, R.E. Rundle, J. Chem. Phys. **21**,986(1953)
[4] R.M. Ibberson, S. McGrady, M. Prager, to be published
[5] S. Albert, J.A. Ripmeester, J. Chem. Phys. **70**,722(1979)
[6] W. Press, *Single Particle Rotations in Molecular Crystals*, Springer Tracts in Modern Physics, Vol. 81, Springer, Berlin 1981
[7] M. Prager, A. Heidemann, Chem. Rev. **97**,2933(1997)
[8] D. Berthomieu, Y. Bacquet, L. Pedocchi, A. Coursot, J. Phys. Chem. **A102**,7821(1998)

Brillouin scattering in polybutadiene: comparison of neutron and X-rays

A. P. Sokolov[1], U. Buchenau[2], D. Richter[2], C. Masciovecchio[3], F. Sette[3], A. Mermet[3], D. Fioretto[4], G. Ruocco[5], L. Willner[2], B. Frick[6]

[1]*Department of Polymer Science, University of Akron, Akron, OH44325 - 3909, USA*
[2]*Institut für Festkörperforschung, Forschungszentrum Jülich Postfach 1913, D-52425 Jülich, Federal Republic of Germany*
[3]*European Synchrotron Radiation Facility, B. P. 220 F-38043 Grenoble Cedex, France*
[4]*Dipartimento di Fisica and INFM, Universita di Perugia, I-06100 Perugia, Italy*
[5]*Dipartimento di Fisica and INFM, Universita di L'Aquila, I-67100 L'Aquila, Italy*
[6]*Institute Laue-Langevin, BP 156, F-38042 Grenoble Cedex 9, France*

We report a comparison of high resolution inelastic X-ray Brillouin scattering to coherent inelastic neutron scattering for amorphous deuterated polybutadiene, done for a temperature in the glass phase and another one in the melt. The X-ray scattering proves to be by far the more powerful technique for such a polymer, though its resolution is limited. The neutron scattering allows to extend these measurements to a much better resolution, showing an additional quasielastic signal in the melt.

F&E-Nr.: 23.30.0

Significant information on the nature of the atomic motion in glass formers can be obtained from an analysis of S(Q,E), accessible by neutron and x-ray scattering. However, each technique has its characteristic limitations. Inelastic neutron scattering spectroscopy has a kinematic limitation at small Q which is related to the velocity of neutrons: if the latter is lower than the longitudinal sound velocity, then one cannot reach Brillouin conditions. The recent developement of high-resolution inelastic x-ray scattering allows to measure the Brillouin spectra of glasses without any kinematic limitation. But the x-ray technique still has only a resolution of about 1.5 meV, which does not allow to analyse S(Q,E) below this frequency. Nevertheless, the data obtained so far clearly demonstrate the presence of a strong sound-like contribution to S(Q,E) at energies of several meV, around and above the so-called boson peak [2].

The present work reports combined x-ray and neutron measurements on deuterated 1,4-polybutadiene (PB) in the liquid and in the glassy state [1]. This combination enabled the measurement of the dynamic structure factor for both Brillouin scattering at low momentum transfer Q and Umklapp scattering at higher momentum transfer Q. Our neutron experiment corroborated once again that the Brillouin scattering is significantly weaker than the Umklapp scattering. Here, we focus on the comparison of the two techniques in the Brillouin range.

PB, a well-known glass forming polymer, was chosen due to its relatively low sound velocity, important for the kinematic limitation of INS. Inelastic X-ray scattering was measured using the ID-16 high resolution spectrometer at the ESRF in Grenoble. The neutron scattering measurements were done on the cold neutron time of flight spectrometer IN5 at the ILL Grenoble. The neutron scattering spectra were treated in the usual way, with normalization to vanadium, empty container subtraction and multiple-scattering corrections. The latter were done assuming isotropic multiple scattering and a multiple scattering probability of 15 % after the first scattering process (the sample was a hollow cylinder with a transmission of 90 %). The neutron spectrometer IN5 at 2 $\AA$ has roughly the same resolution as the ID-16 and a kinematic limitation to a sound velocity v_l=2 km/s. Also, data of a previous IN6 measurement [3] have been used.

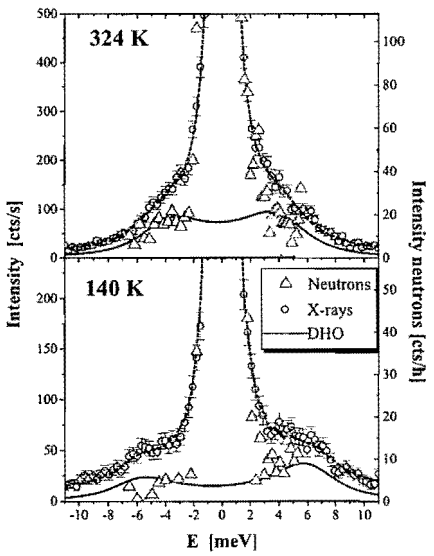

FIG. 1. X-ray and neutron spectra at Q=0.4 $\AA^{-1}$.

Fig. 1 compares typical IXS spectra of PB with 2 $\AA$ neutron spectra at two temperatures: 324 K, deep in the liquid state, and 140 K, deep in the glassy state (T_g=180 K). The x-ray data could be fitted in terms of a damped harmonic oscillator (DHO) model with a sound-like dispersion up to Q=0.4 $\AA^{-1}$ with the sound velocity v_l=1.92 km/s at 324 K and v_l=2.64 km/s at 140K. These results

are similar to findings in other glass forming systems [2] and are presented in more detail elsewhere [4].

For the quantitative comparison of neutron and x-ray data, we assumed that the coherent structure factor S(Q) in the Q-range 0.3-1.5 $\AA^{-1}$ is the same (in fact, the first sharp diffraction peak at 1.5 $\AA^{-1}$ looks quite similar in both techniques). The comparison showed good agreement between the two S(Q), assuming about 37 % of the neutron scattering to be incoherent, corresponding to 96 % deuteration of the sample. Using the same factor in the inelastic range, one obtains the neutron data points in Fig. 1. They agree within statistical error with the x-ray fit in terms of the DHO model (the neutrons in that case do not suffer from such broad resolution tails as the X-rays). So, using that normalization, the two measurements show a very satisfactory quantitative agreement with each other. This comparison normalization agrees within 10 % with the usual neutron normalization, using sample and vanadium weights and the theoretical expressions for the Brillouin scattering.

The comparison shows several disadvantages of the neutrons in the Brillouin region: (i) the Brillouin spectra are measured in a limited energy range (smaller than 6 meV) due to the kinematic limitation; (ii) very poor statistics (cts/h instead of cts/s for x-rays); (iii) strong multiple scattering contribution at small Q (it is nearly half of the signal); (iv) presence of an incoherent contribution even in a deuterated sample.

However, the neutron spectroscopy has also significant advantages: (i) the results can be presented in absolute values due to a well established procedure of the normalization to vanadium. The normalization enables a quantitative comparison of different measurements and with different model predictions; (ii) combining the measurements performed at different wavelengths one can reconstruct S(Q,E) with very high energy resolution, in our case down to 0.1 meV (Fig. 2).

Fig. 2 shows neutron spectra at 324 K in the interval Q=0.3-0.5 $\AA^{-1}$ using neutrons of different wavelengths, after subtraction of the multiple scattering. For all three wavelengths together, the spectrum consists of a central quasielastic line with a broad inelastic shoulder in the range from 2-4 meV, demonstrating the existence of an unexpectedly strong inelastic signal below the Brillouin line at 0.4 $\AA^{-1}$. This quasielastic contribution could be due to the presence of a relatively fast secondary relaxation process in the viscoelastic liquid, evidenced also in previous neutron spin echo [5] and Brillouin light scattering [4] data. The presence of extra intensity in S(Q,E) at low energies has also been seen in a simulation of model glasses [6].

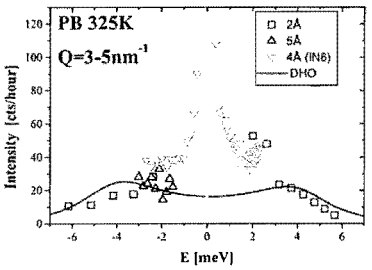

FIG. 2. Combined neutron spectra at Q=0.4 $\AA^{-1}$ and 324 K. The line shows the DHO fit.

In conclusion, the combined analysis of the neutron and x-ray data demonstrates that a combination of neutron spectra measured with different wavelengths gives the possibility to reconstruct the Brillouin spectra with high resolution. The latter is crucial for different model predictions, because it opens the range of S(Q,E) to energies below the Brillouin resonance.

In fact, our measurement shows that the present concept of a damped harmonic oscillator for the Brillouin scattering [2], based on the x-ray evidence alone, is incomplete. There is a quasielastic coherent signal at small momentum transfer, which can at present only be measured by neutrons. The signal demonstrates the existence of fast picosecond strain fluctuations on a nanometer scale. This result is of central importance for a theoretical understanding of disordered matter and should be studied further.

[1] A. P. Sokolov et al, Phys. Rev. E **60**, R2464 (1999)

[2] C. Masciovecchio, G. Monaco, G. Ruocco, F. Sette, A. Cunsolo, M. Krisch, A. Mermet, M. Soltwisch and R. Verbeni, Phys. Rev. Lett. **80**, 544 (1998) and further references therein.

[3] U. Buchenau, A. Wischnewski, D. Richter, and B. Frick, Phys. Rev. Lett. **77**, 4035 (1996)

[4] D. Fioretto et al, Phys. Rev. E **59**, 4470 (1999)

[5] A. Arbe, D. Richter, J. Colmenero and B. Farago, Phys. Rev. E **54**, 3853 (1996)

[6] P. Benassi, V. Mazzacurati and M. Sampoli, Phil. Mag. **79**, 2037 (1999)

Publications in refereed journals

Allgaier J.; Martin K.1; Räder H.J.1; Müllen K.1
1Max-Planck-Institut für Polymerforschung, Mainz
Many-Arm Star Polymers Syntheszied Using Chlorosilane Linking Agents: Their Structural Quality Concerning Arm Number and Polydispersity
Macromolecules, 32, 3190-3194, 1999
23.30.0

Arbe A.1; Alegria A.1; Colmenero J.1; Hoffmann S.; Willner L.; Richter D.
1Universidad del Pais Vasco, San Sebastian, Spanien
Segmental Dynamics in Polyvinylethylene/Polyisoprene Miscible Blends Revisited. A Neutron Scattering and Broad Band Dielectric Spectroscopy Investigation
Macromolecules, 32, 7572, 1999
23.30.0

Arbe A.1; Colmenero J.1; Gómez D.1; Richter D.; Farago B.2
1Universidad del Pais Vasco, San Sebastian, Spanien
2Institut Laue-Langevin, Grenoble
Reply to "Comment on 'Merging of the ? and ? relaxations in polybutadiene: A neutron spin echo and dielectric study' "
Phys.Rev.E., 60, 1103, 1999
23.30.0

Arbe A.1; Colmenero J.1; Monkenbusch M.; Richter D.
1Universidad del País Vasco, San Sebasitan, Spanien
Arbe et al. Reply:
Phys.Rev.Lett., 82, 1336, 1999
23.30.0

Buchenau U.; Wischnewski A.; Monkenbusch M.; Schmidt W.
Intensity sharing between Brillouin and Umklapp scattering in glasses
Philosophical Magazine B. Vol. 79, 2021-2026, 1999
23.30.0

Buzza D.M.1; Hamley I.W.2; Fzea A.H.3; Moniruzzaman M.3; Allgaier J.; Young R.N.3; Olmsted P.D.1; McLeish T.C.B.1
1Department of Physics and Astronomy and Polymer IRC, University of Leeds
2School of Chemistry, University of Leeds
3Department of Chemistry, University of Sheffield
Anomalous Difference in the Order-Disorder Transition Temperature Comparing a Symmetric Diblock Copolymer AB with Its Hetero-Four-Arm Star Analog A2B2
Macromolecules, Vol. 32, 7483-7495, 1999
23.30.0

Cendoya I.1; Alegría A.1; Alberdi J.M.1; Colmenero J.1; Grimm H.; Richter D.; Frick B.2
1Universidad del Pais Vasco, San Sebastian, Spain
2Institut Laue-Langevin, Grenoble
Effect of Blending on the PVME Dynamics - A Comparative Study by Means of Dielectric, NMR and QENS Spectroscopies
Macromolecules Vol. 32, 4065-4078, 1999
23.30.0

Colmenero J.1; Arbe A.1; Alegria A.1; Monkenbusch M.; Richter D.
1Universidad del Pais Vasco, San Sebastian, Spain
On the origin of the non-exponential behaviour of the (-relaxation in glass-forming polymers: incoherent neutron scattering and dielectric relaxation results
Journal of Phys.:Condens. Matter, A363-A370, 1999
23.30.0

Dreja M.1; Pyckhout-Hintzen W.; Mays H.2; Tieke B.1
1Institut für Physikalische Chemie, Universität Köln
2Department of Physical Chemistry, University Uppsala, USA
Cationic geminic surfactants with oligo (oxyethylene) spacer groups and their use in the polymerization of styrene in ternary microemulsion
Langmuir, 15(2), 391-399, 1999
23.30.0

Eilhard J.; Zirkel A.1; Tschöp W.2; Hahn O.2; Kremer K.2; Schärpf O.3; Richter D.; Buchenau U.
1Technische Universität München
2Max-Planck-Institut für Polymerforschung, Mainz
3Institut Laue-Langevin, Grenoble
Spatial correlations in polycarbonates: Neutron scattering and simulation
Journal of Chemical Physics Vol.10, 1819-1830, 1999
23.30.0

Engberg D.1; Wischnewski A.; Buchenau U.; Börjesson L.2; Dianoux A.J.3; Sokolov A.P.4; Torell L.M.1
1Chalmers University of Technology, Department of Experimental Physics, Sweden
2Chalmers University of Technology, Department of Applied Physics, Sweden
3Institut Laue-Langevin, Grenoble
4University of Akron, Department of Polymer Science, USA
Origin of the boson peak in a network glass B2O3
Phys.Rev.B 59, 6, 1999
23.30.0

Fioretto D.1; Buchenau U.; Comez L.1; Sokolov A.2; Masciovecchio C.3; Mermet A3; Ruocco G.4; Sette F.3; Willner L.; Frick B.5; Richter, D.; Verdini L.1
1Dipartimento di Fisica and INFM, Universita di Perugia, Italy
2Department of Polymer Science, University of Akron, USA
3European Synchrotron Radiation Facility, Grenoble
4Dipartimento di Fisica and INFM, Universita di L'Aquila, Italy
5Institut Laue-Langevin, Grenoble
High-frequency dynamics of glass-forming polybutadiene
Physical Review E, Vol.59, 4470-4475, 1999
23.30.0

Gapinski J.1; Steffen W.1; Patkowski A.1; Sokolov A.P.2; Buchenau U.; Russina M.3, Mezei F.3; Schober H.4
1Max-Planck-Institut für Polymerforschung, Mainz
2Department of Polymer Science, University of Akron, USA
3Hahn-Meitner-Institut, Berlin
4Institut Laue-Langevin, Grenoble
Spectrum of fast dynamics in glass forming liquids: Does the "knee" exist?
Journal of Chemical Physics, Vol.110, 2312-2315, 1999
23.30.0

Gliß C.1; Randel O.2; Casalta H.2; Sackmann E.3; Zorn R.; Bayerl T.1
1Institut für Experimentelle Physik, Universität Würzburg
2Institute Laue-Langevin, Grenoble
3Institut für Biophysik, Technische Universität München
Anisotropic Motion of Cholesterol in Oriented DPPC Bilayers Studied by Quasielastic Neutron Scattering: The Liquid-Ordered Phase
Biophys. J. 77 331-340, 1999
23.15.0

Gorski N.1; Kalus J.1; Meier G.2; Schwahn D.
1Universität Bayreuth
2Max-Planck-Institut Mainz
The Temperature Dependence of the Chemical Potential of Tretradecyldimethylaminoxid Micelles in D2O - A SANS Study
Langmuir 12, 3476-3482, 1999
23.30.0

Gorski N.1; Kalus J.1; Schwahn D.
1Universität Bayreuth
The Pressure Dependence of the Chemical Potential of Tetradecyldimethylaminoxid Micelles in D2O - A SANS Study
Langmuir 15, 8080-8085, 1999
23.30.0

Hasegawa H.1; Sakamot N.1; Takeno H.1; Jinnai H.1; Hashimoto T.1; Schwahn D.; Frielinghaus H.2; Janßen S.3; Imai S.1; Mortensen K.2
1University of Kyoto, Japan

2Risø National Laboratory, Roskilde, Denmark
3Paul-Scherrer-Institut in Villigen, Schweiz
SANS Studies on Phase Behavior of Block Copolymers
Journ.Phys.Chem.Solids, 60, 1307-1312, 1999
23.30.0

Jakobs B.1; Sottmann T.1; Strey R.1; Allgaier J.; Willner L.; Richter D.
1Institut für Physikalische Chemie, Köln
Amphiphilic Block Copolymers as Efficiency Boosters for Microemulsions
Langmuir, The ACS Journal of Surfaces and Colloids
Vol.15, 6707-6711, 1999
23.30.0

Johnson M.R.1; Prager M.; Grimm H.; Neumann M.A.1; Kearley G.J.1; Wilson C.C.2
1Institut Laue-Langevin, Grenoble
2ISIS, Rutherford Appleton Laboratory, United Kingdom
Methyl group dynamics in paracetamol and acetanilide: probing the static properties of intermolecular hydrogen bonds formed by peptide groups
Chemical Physics 244, 49-66, 1999
23.15.0

Kahle S.; Schröter K.1; Hempel E.1; Donth E.1
1Fachbereich Physik, Universität Halle
Calorimetic indications of a cooperativity onset in the crossover region of dynamic glass transition for benzoin isobutylether
Journal of Chemical Physics, Vol.111, 6462, 1999

Kirstein O.; Grimm H.; Prager M., Richter D.
Design and Optimization of a Backscattering Spectrometer Using a Phase Space Transformation and Super Mirror Guides
Journal of Neutron Research, Vol. 8/2, 119-132, 1999
23.30.0

McLeish T.C.B.1; Allgaier J.; Bick D.K.1; Bishko G.1; Biswas P.1; Blackwell R.1; Blottière B.1; Clarke N.1; Gibbs B.1; Groves J.1; Hakiki A.2; Heenan R.K.3; Johnson J.M.4; Kant R.1; Read D.J.1; Young R.N.3
1University of Leeds
2Department of Physics, University of Sheffield
3Rutherford Appleton Laboratory
4Department of Physics, University of Sheffield
Dynamics of Entangled H-Polymers: Theory, Rheology and Neutron Scattering
Macromolecules, 32, 6734-6758, 1999
23.30.0

Monkenbusch M.
Correction scheme for divergent beams in zero-field spin-echo spectrometers
Nuclear Instruments and Methods in Physics Research, Vol.437, p455-458, 1999
23.89.1

Montes H.1; Monkenbusch M.; Willner L.; Rathgeber S.2; Fetters L.3; Richter D.
1ESPCI, Physico-Chimie Structurale et Macromoleculaire, France
2National Institute of Standards and Technology, USA
3EXXON, Research and Engineering Company, USA
Neutron spin echo investigation of the concentration fluctuation dynamics in melts of diblock copolymers
Journal of Chemical Physics, Vol.110, 10188, 1999
23.30.0

Nakano M.1; Matsuoka H.1; Yamaoka H.1; Poppe A.; Richter D.
1Kyoto University, Japan
Sphere to Rod Transition of Micelles Formed by Amphiphilic Diblock Copolymers of Vinyl Ethers in Aqueous Solution
Macromolecules, Vol.32, 697-703 1999
23.30.0

Ozaki Y.1; Prager M.; Asmussen B.2
1Nagoya Institute of Technology, Nagoya, Japan
2Institut f. Experimentelle und Angewandte Physik, Universität Kiel
Calculation of rotational states of methane molecules in a square lattice
Journal of Physics and Chemistry of Solids 60, 1523-1526, 1999
23.15.0

Prager M.; Schiebel P.1; Johnson M.2; Grimm H.; Hagdorn H.1; Ihringer J1; Prandl W.1; Lalowicz Z.3
1Institut für Kristallographie, Universität Tübingen
2Institut Laue-Langevin, Grenoble
3H Niewodniczanski Institute of Nuclear Physics, Krakow, Poland
The isotope effect and phase transitions in ammonium hexachloropalladate studied by neutron tunnelling spectroscopy
Journal Physics Condensed Matter, 5483-5495, 1999
23.30.0

Prager M.; Schiebel P.1; Johnson M.2; Grimm H.; Hagdorn H.1; Prandl W.1; Lalowicz Z.3
1Institut f. Kristallographie, Universität Tübingen
2Institut Laue-Langevin, Grenoble
3Institut of Nuclear Physics, Jagellonian University Krakow
Isotope effect and phase transitions in ammoniumhexachloropalladate studied by neutron tunnelling spectroscopy
Journal of Physics: Condensed Matter 11, 5341, 1999
23.15.0

Rathgeber S.1; Willner L.; Richter D.; Brulet A.2; Farago B.3; Appel M.4; Fleischer G.4
1National Institute of Standards and Technology, USA
2Laboratoire Léon Brillouin, France
3Institute Laue-Langevin, Grenoble
4Institut f. Experimentalphysik, Universität Leipzig
Polymer dynamics in bimodal polyethylene melts: A study with neutron spin echo spectroscopy and pulsed filed gradient nuclear magnetic resonance
Journal of Chemical Physics, Vol.110, 10171, 1999
23.30.0

Richter D.; Monkenbusch M.; Allgaier J.; Arbe A.1; Colmenero J.1; Farago B.2; Cheol Bae Y.3; Faus R.3
1Universidad del Pais Vasco, San Sebastian, Spanien
2Institut Laue-Langevin, Grenoble
3University of Massachusetts-Lowell, USA
From Rouse dynamics to local relaxation: A neutron spin echo study on polyisobutylene melts
Journal of Chemical Physics, Vol. 111, 6107, 1999
23.30.0

Richter D.; Monkenbusch M.; Arbe A.1; Colmenero J.1; Farago B.2; Faust R.3
1Universidad del Pais Vasco, San Sebastian
2Instiut Laue-Langevin, Grenoble
3University of Massachusetts, USA
Space time observation of the (-process in polymers by quasielastic neutron scattering
J. Phys.: Condens. Matter11, A297-A306, 1999
23.30.0

Rush J.J.1; Udovic T.J.1; Berk N.F.1; Richter D.; Magerl A.2
1National Institute of Standards and Technology, Gaithersburg, USA
2Institut Laue-Langevin, Grenoble
Excited-State Vibrational Tunnel Splitting of Hydrogen Trapped by Nitrogen in Niobium
Eur.Phys.Lett., 48, 187, 1999
23.30.0

Schleger P.1; Farago B.1; Lartigue C.1; Kollmar A.; Richter D.
1Institut Laue-Langevin, Grenoble

Clear evidence of reptation in polyethylene from neutron spin-echo spectroscopy
Phys.Rev.Lett. 81, 124, 1998
23.30.0

Schwahn D.; Mortensen K.1; Frielinghaus H.1; Almdal K.1
1Risø National Laboratory, Roskilde, Denmark
Crossover from 3d-Ising to Isotope Lifshitz Critical Behavior in a Mixture of a Homopolymer Blend and Diblock Copolymer
Phys. Rev. Lett., 82, 505, 1999
23.30.0

Seto H.1; Kato T.2; Monkenbusch M.; Takeda T.1; Kawabata Y.1; Nagao M.3; Okuhara D.1; Imai M.4; Komura S.5
1Hiroshima University, Japan
2Metropolitan University, Japan
3University of Tokyo, Japan
4Ochanomizu University, Japan
Collective motions of a network of wormlike micelles
Journal of Physics and Chemistry of Solids 60, 1371-1373, 1999
23.30.0

Sokolov A.P.1; Buchenau U.; Richter D.; Masciovecchio C.2; Sette F.2; Mermet A.2; Fioretto D.3; Ruocco G.4; Willner L.2; Frick B.5
1Department of Polymer Science, University of Akron, USA
2European Synchrotron Radiation Facility, Grenoble
3Dipartimento di Fisica and INFM, Universita di Perugia, Italy
4Dipartimento di Fisica and INFM, Universita di L'Aquila, Italy
5Institut Laue-Langevin, Grenoble
Brillouin and Umklapp scattering in polybutadiene: Comparison of neutron and x-ray scattering
Physical Review E, Vol. 60, 2464-2467, 1999
23.30.0

Sokolov A.P.1; Grimm H.; Kahn R.2
1Department of Polymer Science, University of Akron, USA
2Laboratoire Léon Brillouin, Saclay, France
Glassy dynamics in DNA: Ruled by water of hydration?
Journal of Chemical Physics, 110, 7053, 1999
23.30.0

Stellbrink J.; Willner L.; Richter D.; Lindner P.1; Fetters L.J.2; Huang J.S.2
1Institut Laue-Langevin, Grenoble
2Exxon Research and Engineering Company, Annandale, USA
Self-Assembling Behavior of Butadienyllithium Headgroups in Benzene via SANS Measurements
Macromolecules, Vol.32, 5321-5329, 1999
23.30.0

Takeda T.1; Seto H.1; Kawabata Y.1; Okuhara D.1; Krist T.2; Zeyen C.M.E.3, Anderson I.S.3; Hoghoj P.3; Nagao M.4; Yoshizawa H.4; Komura S.5; Ebisawa T.6; Tasaki S.6; Monkenbusch M.
1Hiroshima University, Japan
2Hahn-Meitner-Institut, Berlin
3Institut Laue-Langevin, Grenoble
4University of Tokyo, Tokai, Japan
5Ochanomizu University, Ootsuka, Japan
6Kyoto University, Japan
Improvement of neutron spin echo spectrometer at C2-2 of JRR3M
Journal of Physics and Chemistry of Solids 60, 1599-1601, 1999
23.89.1

Westermann S.; Kreitschmann M.; Pyckhout-Hintzen W.; Richter D.; Straube E.1; Farago B.2; Goerigk G.
1Martin-Luther-Universität, Fachbereich Physik, Halle
2Institut Laue-Langevin, Grenoble
Matrix Chain Deformation in Reinforced Networks: A SANS approach
Macromolecules 32, 5793-5802, 1999
23.30.0

Zorn R.
Applicability of distribution functions for the Havriliak-Negami spectral function
J.Polym.Sci.Bpolym.Phys. 37, 1043-1044, 1999
23.15.0

Other publications

Carlsson P.1; Zorn R.; Andersson D.1; Farago B.2; Richter D.; Torell L.M.1; Börjesson L.3; Jacobbson P.1
1Department of Experimental Physics, Chalmers University of Technology, Göteborg
2Institut Laue-Langevin, Grenoble
3Department of Applied Physics, Chalmers University of Technology, Göteborg
The segmental dynamics of a Polymer Electrolyte Investigated by Neutron Spin Echo Technique
AIP Conf. Proc. CP469; 607-614 1999
23.15.0

Fetters L.J.1; Wheeler L.M.1; Xenidou M.1; Richter D.
1Exxon Research and Engineering Co., Annandale, USA
Modification Potential for ShellvisTM Star Polymers
Company report; CR.17BU.99
23.30.0

Leube W.; Marton K.; Schwahn D.; Richter D.; Fetters L.J.1; Wright P.; Symon C2; Vanhaeren G.3
1Exxon Research and Engineering Co., Annandale, USA
2Esso Center, Machelen, Belgium
Aggregation Behavior of Nucleating and Growth Arresting Fuel Additives
Company report; CR.5BU.99, 1999
23.30.0

Leube W.;Monkenbusch M.; Schneiders D.; Richter D.; Dounis P.2; Lovegrove R.2; Fetters L.J.3; Symon C.3
1Exxon Chemical Ltd., Milton Hill, Abbingdon, England
2Exxon Research and Engineering Co. Annandale, USA
Wax-Crystal Modification in Fuel Oil by Self-Aggregation Partially Crystallizable Hydrocarbon Blockcopolymers
Exxon Company, CR.1A.99, 1999
23.30.0

Prager M.; Schiebel P.1; Johnson M.2
1Institut für Kristallographie, Universität Tübingen
2Institut Laue-Langevin, Grenoble
Deuteration induced Phase Transition in an Ammonium Perovskite
DIM-Newsletter 12, 10, 1999
23.15.0

Richter D.
Poylmer Dynamics by Neutron Spin Echo Spectroscopy
"Scattering in Polymeric and Colloidal Systems"
Ed by Wyn Brown and Kell Mortenson, Gordon and Breach, London, 1999
23.30.0

Richter D.; Monkenbusch M.; Farago B.1; Schleger P.1; Montes H.2
1Institut Laue-Langevin, Grenoble
2ESPCI, Laboratoire PCSM, France
Large scale motions in dense polymer systems
AIP Conference Proceedings, Vol.469, 587-598, 1999
23.30.0

Rosov N.1; Rathgeber S.1; Monkenbusch M.
1NIST Center for Neutron Research, Gaithersburg, USA
Neutron Spin Echo Spectroscopy at the NIST Center for Neutron Research
American Chemical Society Books Department, Symposium Series No. 739, Chapter 7
ISBN: 0-84112-3644-5
23.30.0

Schleger P.1; Ehlers G.2; Kollmar A.; Alefeld B.; Barthelomy J.F.1; Casalta H.1; Farago B.1; Giraud P.1; Hayes C.1; Lartigue C.3; Mezei F.2; Richter D.
1Institut Laue-Langevin, Grenoble
2Hahn-Meitner Institut, Berlin
3Laboratoire de Spectrométrie, France
The sub-neV resolution NSE spectrometer IN15 at the Institut Laue-Langevin
Elsevier Preprint 09.09.1998
23.30.0

Seto H.1; Kato T.2; Monkenbusch M.; Takeda T.1; Komura S.3
1Hiroshima University, Japan
2Metropolitan University, Japan
3Ochanomizu University, Japan
A Neutron Spin Echo Study of Network of Wormlike Micelles
8th Tohwa University International Symposium edited by Michio Tokuyama and Irwin Oppenheim
The American Institute of Physics 1-56396-811, 1999
23.30.0

Invited talks

Kahle S.
Suszeptibilitätsuntersuchungen in der Crossover Region des dynamischen Glasübergangs von Benzoin isobutylether - eine Kooperativitätsanalyse
Soft Condensed Matter Seminar des SFB in Halle am 14.01.99
23.15.0

Kahle S.
Vergleich zwischen inkohärenter Neutronenstreuung und dielektrischer Spektroskopie am Polyvinylacetat
Glasübergangstreffen in Rostock am 13.12.99
23.30.0

Monkenbusch M.; Richter D.; Montes H.1
1ESPCI, Physic-Chimie Structurale et Macromoleculaire, Paris, France
Neutron Spin Echo Spectroscopy on large scale motions in dense polymer systems - recent advances
3rd International Symposium (IUPAC) in Saint-Petersburg vom 07.06.-10.06.99
23.30.0

Monkenbusch M.; Schneiders D.; Richter D.; Willner L.; Leube W.; Fetters L.J.1; Huang J.S.1; Lin M.1
1EXXON, Research and Engineering Company, Annandale, USA
Aggregation Behaviour of PE-PEP Copolymers and Winterization of Diesel Fuels
2nd European Conference on Neutron Scattering in Budapest vom 01.09.-04.09.99
23.30.0

Montes H.1; Monkenbusch M.; Willner L.; Rathgeber S.2; Fetters L.J.3; Richter D.
1ESPCI, Physic-Chimie Structurale et Macromoleculaire, Paris, France
2EXXON, Research and Engineering Company, Annandale, USA
Neutronenspinechospektroskopie: Dynamik von Einzelketten und Konzentrationsfluktuationen in BlockKopolymeren
Deutsche Neutronenstreutagung in Potsdam vom 25.05.-27.05.99
23.30.0

Prager M.
Phase space transformation at the FRM-2 backscattering spectrometer
Neutron Optics '99 in Villigen am 28.11.99
23.89.1

Prager M.
Molecular excitations, intermolecular interactions and ab-initio calculations
Janik-Friends-Meeting, Zakopane am 15.07.99
23.15.0

Prager M.
A concerted study of methyl-bridged compounds: trimethylaluminum
QAMTS'99 in Krakau am 29.09.99
23.15.0

Prager M.
Das Rückstreuspektrometer mit Phasenraumtransformation für den FRM-2
Technische Universität München am 23.07.99
23.89.1

Prager M.
Deuterierung-induzierte Phasenübergänge in Ammonium-Hexachloropalladate
Seminar am Institut für Kristallographie, Universtiät Tübingen am 07.06.99
23.15.0

Prager M.
Verbindungen mit Methylbrücken: Methylgruppenrotation in Trimethylaluminium
Deutsche Neutronenstreutagung in Potsdam am 27.05.99
23.15.0

Pyckhout-Hintzen W.
Kettendeformation in ungefüllten und gefüllten Netzwerken mittels SANS
DPG in Münster am 23.03.99
23.30.0

Pyckhout-Hintzen W.
Kettendeformation in ungefüllten und gefüllten Netzwerken mittels SANS
Institutsseminar Universität Regensburg am 14.01.99
23.30.0

Pyckhout-Hintzen W.; Westermann S.; Botti A.; Richter D.; Straube E.1
1Martin-Luther-Universität, Fachbereich Physik, Halle
Chain deformation in unfilled and filled polymer networks: a SANS approach
15th ACS Meeting, Rubber Division in Chicago vom 13.04 - 16.04.99
23.30.0

Pyckhout-Hintzen W.; Westermann S.; Botti A.; Richter D.; Straube E.1
1Martin-Luther-Universität, Fachbereich Physik, Halle
Chain deformation in unfilled and filled polymer networks: a SANS approach
IPNS Meeting in Argonne am 16.04.99
23.30.0

Richter D.
Dynamik von Polymeren
Kolloquiumsvortrag, Institut für Physikalische Chemie in Göttingen am 03.05.99
23.30.0

Richter D.
Forschung mit Neutronen in Deutschland - eine Strategie für die nächsten 15 Jahre
Deutsche Neutronenstreutagung in Potsdam, 25.05. - 27.05.99
23.30.0

Richter D.
Neutron Scattering in Chemistry - Chances and Perspectives
IUPAC - Konferenz in Berlin am 18.08.99

23.30.0

Richter D.
Neutron Scattering in Polymer Physics
2nd European Conference on Neutron Scattering in Budapest (ECNS'99); 01.09. - 04.09.99
23.30.0

Richter D.
Neutron Scattering in Polymer Physics
2nd Spanish Symposium on Neutron Scattering in Oviedo, Spanien, 02.06. - 04.06.99
23.30.0

Richter D.
Neutron Scattering on Soft Condensed Matter
ETH in Zürich, 23.06.99
23.30.0

Richter D.
Neutronen in der Polymerphysik
Chemisches Kolloquium in Köln am 29.11.99
23.30.0

Richter D.
Neutronenspinechountersuchung zur Dynamik von Polyisobutylen
Glasübergangstreffen an der Universität Rostock am 13.12.99
23.15.0

Richter D.
Neutronenstreuung in der Polymerphysik
Physikkolloquium der ETH Zürich am 08.12.99
23.15.0

Richter D.
Neutronenstreuung in der Polymerphysik
Physikkolloquium in Essen, 12.05.99
23.30.0

Richter D.
Random copolymers as wax crystal modifiers
Vortrag bei Exxon, USA, vom 13.03. - 19.03.99
23.30.0

Richter D.
Struktur und Dynamik von Polymeren
Kolloquiumsvortrag, Fa. Bayer in Leverkusen am 03.02.99
23.30.0

Richter D.
What is New in Neutron Scattering - Reflections on the ECNS'99 Budapest Conference
6th ESS General Meeting in Ancona am 21.09.99
23.15.0

Schwahn D.
Effect of Thermal Composition Fluctuations in a Critical Polymer Blend Mixed with a Diblock Copolymer
ORNL-Neutron Scattering Group of the Solid State Division in Oak Ridge, USA am 12.03.99
23.30.0

Schwahn D.
Phase Behavior of Binary Polymer Blends in Pressure Fields and with small Additions of a third Component-Studies with Small Angle Neutron Scattering
European Conference on Polymer Blends in Mainz am 17.05.99
23.30.0

Schwahn D.
Phase Behavior of a Ternary Symmetric Homopolymer/ Homopolymer/ Diblock Copolymer Blend studied with Small Angle Neutron Scattering
Brooklyn, Department of Polymer Engineering am 14.06.99
23.30.0

Schwahn D.
Phase Behavior of a Ternary Symmetric Homopolymer/ Homopolymer/ Diblock Copolymer Blend studied with Small Angle Neutron Scattering, NIST, Department of Polymer Engineering am 07.06.99
23.30.0

Schwahn D.
Phase Behavior of a Ternary Symmetric Homopolymer/ Homopolymer/ Diblock Copolymer Blend studied with Small Angle Neutron Scattering, The University of Akron, Department of Polymer Engineering am 04.06.99
23.30.0

Zorn R.
Experiments on glass forming liquids in confined media by neutron time-of-flight and backscattering studies
DyProSo (Dynamical Properties of Solids) XXVII, Tours, Frankreich am 14.09.99
23.15.0

Zorn R.
Neutronenstreuexperimente zur mikroskopischen Dynamik in ungeordneten Polymersystemen
Seminar des Sonderforschungsbereichs 294, Universität Leipzig am 27.01.99
23.15.0

Other talks

Abbas B.
Thermische Fluktuationen der Zusammensetzung in einer binären Polymermischung und dem entsprechenden Diblockcopolymers als Funktion der Temperatur und des Druckes
Deutsche Neutronenstreutagung in Potsdam; 25.05. - 27.05.99
23.30.0

Abbas B.
Thermische Fluktuationen der Zusammensetzung in einer binären Polymermischung und dem entsprechenden Diblockcopolymers als Funktion der Temperatur und des Druckes
Frühjahrstagung der DPG in Leipzig; 01.03. - 03.03.99
23.30.0

Beiner M.1; Kahle S.; Meissner M.2; Hempel E.1; Donth E.1
1Fachbereich Physik, Universität Halle
2HMI in Berlin
Zusammenhang von Tieftemperatur-Wärmekapazität und Kooperativität des Glasübergangs
DPG-Frühjahrstagung in Leipzig vom 01.03.99-03.03.99
23.30.0

Endo H.; Allgaier J.; Monkenbusch M.; Richter D.; Jakobs B.1; Sottmann T.1; Strey R.1
1Institut für Physikalische Chemie, Köln
PEP-PEO block copolymers as efficiency booster for microemulsions: a SANS investigation of the role of the block copolymer
73. ACS Colloid and Surface Science Symposium, MIT, Cambridge, Massachusetts, USA, 13.07.99 - 16.07.99
23.30.0

Endo H.; Allgaier J.; Monkenbusch M.; Richter D.; Jakobs B.1; Sottmann T.1; Strey R.1
1Institut für Physikalische Chemie, Köln
PEP-PEO block copolymers as efficiency booster for microemulsions: a SANS investigation of the role of the block copolymer
Conference of the European Colloid and Interface Society, Dublin, Irland, 12.09.99 - 17.09.99
23.30.0

Heinrich M.; Pyckhout-Hintzen W.; Richter D.; Straube E.1

1Martin-Luther-Universität, Fachbereich Physik, Halle
A SANS study of quenched H-polymer melts under strain
Frontiers in SAXS/SANS workshop in Grenoble, France; 12.02.99 - 13.02.99
23.30.0

Heinrich M.; Pyckhout-Hintzen W.; Richter D.; Straube E.1
1Martin-Luther-Universität, Fachbereich Physik, Halle
A SANS study of quenched H-polymers under strain
DPG-Frühjahrstagung in Leipzig vom 01.03. - 03.03.99
23.30.0

Heinrich M.; Pyckhout-Hintzen W.; Richter D.; Straube E.1
1Martin-Luther-Universität, Fachbereich Physik, Halle
Frühjahrstagung der Deutschen Physikalischen Gesellschaft in Leipzig; 01.03.99 - 03.03.99
23.30.0

Hempel E.1; Kahle S.; Donth E.1
1Fachbereich Physik, Universität Halle
Charakteristische Länge und Kooperativität des dynamischen Glasübergangs in einem breiten Fragilitätsbereich
Frühjahrstagung in Leipzig vom 01.03.99-03.03.99
23.30.0

Kahle S.; Schröter E.1; Hempel E.1; Donth E.1
1Fachbereich Physik, Universität Halle
Temperaturabhängigkeit der Kooperativität in der Crossover Region des dynamischen Glasübergangs von Benzoin isobutylether
DPG Frühjahrstagung in Leipzig vom 01.03.-03.03.99
23.15.0

Kirstein O.; Grimm H.; Prager M.; Kozielewski T.
Designstudien zum Rückstreuspektrometer für den FRM-2
Verbundtreffen in Potsdam am 26.05.99
23.89.1

Kirstein O.; Prager M.;Johnson M.R.; Combet J.
Ammonia group rotation in Zn(NH3)4I2
QAMS '99, Krakow, Polen 26.09. - 30.09.99
23.15.0

Prager M.
Schiebel P.1; Prager M.; Ritter H.2; Ihringer J.1; Prandl W.1
1Institut für Kristallographie, Universität Tübingen
2Institut Laue-Langevin, Grenoble
Phase transition in partially deuterated (NX4PdCl6(X= H1-yDy) studied by inelastic neutron scattering and diffraction methods
Verbundtreffen in Potsdam am 26.05.99
23.15.0

Prager M.
The thermal time-of-flight spectrometer SV29 at FZ-Jülich: focusing in space and time
Neutron Optics '99 in Villigen am 28.11.99
23.89.1

Prager M.; Grimm H.; Parker S.F.1; McGrady S.2
1Rutherford-Appleton Laboratories, Chilton, United Kingdom
2Kings College, London
Rotational potentials of bridging and terminal methyl groups in trimethylaluminum-dimers
2nd European Conference on Neutron Scattering in Budapest (ECNS'99) am 03.09.99
23.15.0

Pyckhout-Hinten W.; Westermann S.; Botti A.; Urban V.1; Richter D.; Straube E.2
1ESRF in Grenoble
2Martin-Luther-Universität, Fachbereich Physik, Halle
Studies of reinforcement by SANS
Gordon Research Conference on elastomers, networks and gels in New Hamp vom 18.07. - 23.07.99
23.30.0

Schätzler R.
Instrumentierung am FRJ-II in Jülich
Deutsche Neutronenstreutagung 1999, Potsdam, 25.-27.05.1999
23.89.1

Willner L.; Poppe A.; Allgaier J.; Monkenbusch M.; Richter D
Micellarization of Amphiphilic PEP-PEO Block Copolymers
Gordon Research Conference on Polymers in Oxford; 04.07. - 08.07.99
23.30.0

Willner L.; Poppe A.; Allgaier J.; Stellbrink J.; Lindner P.1; Richter D.
1Institut Laue-Langevin, Grenoble
Aggregation Behavior of Amphiphilic PEP-PEO Block Copolymers
Polymer & Materials Research Symposium in Bayreuth; 11.04 - 13.04.99
23.30.0

Zorn, R.
Absence of ageing effect in the vibrational density of states of glass-forming polybutadiene
Sonderforschungsbereich 262, Workshop Aging Phenomena in Glassy Systems, Mainz, 03.12.99
23.15.0

Posters

Abbas B.; Schwahn D.; Willner L.
Composition Fluctuations in a PB-PS Diblock Copolymer and PB-PS Copolymer with a good Solvent
2nd European Conference on Neutron Scattering, Budapest am 03.09.99
23.30.0

Borbely S.; Heiderich M.; Schwahn D.; Seidl E.1
1Atominstitut Wien, Österreich
Resolution of the USANS Diffractometer at the FRJ-2 Research Reactor in Jülich
2nd European Conference on Neutron Scattering, Budapest am 01.9.99
23.30.0

Crossover from 3d-Ising to Isotropic Lifshitz Critical Behavior
APS Centennial Meeting in Atlanta, USA am 26.03.99
23.30.0

Jakobs B.1, Sottmann T.1; Strey R.1; Allgaier J.; Willner L.; Richter D.
1Institut f. Physikalische Chemie, Universität Köln
Amphiphilic block copolymers: Efficiency boosters for microemulsions
23.15.0

Kirstein O.
The use of a phase space transformation chopper system for a neutron backscattering spectrometer
Institut Laue-Langevin, Grenoble, France 04.03 - 05.03.99
23.89.1

Kirstein O.; Kozielewski T.; Prager M.; Richter D.
The backscattering spectrometer for the FRM-II reactor in Munich
ECNS'99 in Budapest, Ungarn 01.09. - 04.09.99
23.89.1

Koizumi, S.; Annaka M.1; Borbely S.; Schwahn D.
1Chiba University, Japan
Fractal Structure of a Polymer Gel observed by Small-angle Neutron Scattering over a Q-range from 10-5 to 0.1 Å-1
2nd European Conference on Neutron Scattering, Budapest am 03.09.99
23.30.0

Prager M.
The layout of the backscattering spectrometer for the FRM-2
National Institute of Standards and Technology, Washington am 16.04.99
23.89.1

Prager M.; Kirstein O.; Kozielewski T.; Richter D.
The backscattering spectrometer for the FRM-II reactor in Munich
NOP 99, Villigen, Schweiz 25.11. - 27.11.99
23.89.1

Schwahn D.
Möglichkeiten der Neutronenkleinwinkelstreuung gezeigt am Beispiel der Synthese von TiO2 Kolloiden in einem mizellaren Kern
Kolloquium zum DFG-Schwerpunktprogramm "Prinzipien der Biomineralisation" in Bonn am 20.10.99
23.30.0

Schwahn D.
Phasenverhalten einer binären Polymermischung nach Zugabe des entsprechenden Diblockcopolymers - Experimente mit der Neutronenstreuung
Frühjahrstagung des Fachverbandes Polymerphysik der DPG in Leipzig am 03.03.99
23.30.0

Schwahn D.
Phasenverhalten einer binären Polymermischung nach Zugabe des entsprechenden Diblockcopolymers-Experimente mit der Neutronenstreuung
Deutsche Neutronenstreutagung 1999 in Potsdam am 26.05.99
23.30.0

Schwahn D.; Mortensen K.1; Frielinghaus H.1; Almdal K.1
1Risø National Laboratory, Roskilde, Denmark
3d-Ising and Lifshitz Critical Behavior in a Mixture of a Polymer Blend and a Diblock Copolymer
2nd European Conference on Neutron Scattering, Budapest am 03.09.99
23.30.0

Wischnewski A.
Reptation in polyethylene-melts with different molecular weights
2nd European Conference on Neutron Scattering (ECNS'99) in Budapest, Ungarn, 03.09.99
23.30.0

Patents granted

Allgaier J.; Richter D.; Willner L.; Strey R.; Jakobs B.; Sottmann T.:
Verfahren zur Effiziensteigerung von Tensiden bei simultaner Unterdrückung lamellarer Mesophasen sowie Tenside, welchen ein Additiv beigefügt ist
PCT: PCT/DE99/02748 (26.08.99) (EP,US,JP)
PT 1.1605 G
23.15.0

Dohmen L.; Alefeld B.:
Geschwindigkeitsselektor zur Monochromatisierung eines Neutronenstrahls
DE: 19904562.3 (04.02.99)
PT 1.1656
23.89.1

Sonnenberg K.; Küssel E.; Bünger Th.; Flade T.; Weinert B.; Fa. Freiberger:
Vorrichtung zur Herstelung von Einkristallen
DE: 19912484.1 (19.03.99)
PT 1.1680 G
23.42.0

Sonnenberg K.; Küssel E.; Bünger Th.; Flade T.; Weinert B.; Fa. Freiberger:
Verfahren und Vorrichtung zur Herstellung von Einrkristallen
DE: 19912486.8 (19.03.99)
PT 1.1681 G
23.42.0

Patents applied for

Allgaier J.; Richter D.; Willner L.; Strey R.; Jakobs B.; Sottmann T.:
Verfahren zur Effiziensteigerung von Tensiden bei simultaner Unterdrückung lamellarer Mesophasen sowie Tenside, welchen ein Additiv beigefügt ist
PCT: PCT/DE99/02748 (26.08.99) (EP,US,JP)
PT 1.1605 G
23.15.0

Dohmen L.; Alefeld B.:
Geschwindigkeitsselektor zur Monochromatisierung eines Neutronenstrahls
DE: 19904562.3 (04.02.99)
PT 1.1656
23.89.1

Sonnenberg K.; Küssel E.; Bünger Th.; Flade T.; Weinert B.; Fa. Freiberger:
Vorrichtung zur Herstelung von Einkristallen
DE: 19912484.1 (19.03.99)
PT 1.1680 G
23.42.0

Sonnenberg K.; Küssel E.; Bünger Th.; Flade T.; Weinert B.; Fa. Freiberger:
Verfahren und Vorrichtung zur Herstellung von Einrkristallen
DE: 19912486.8 (19.03.99)
PT 1.1681 G
23.42.0

Lecture courses

Grimm H.
Kristallspektrometer: das Dreiachsen- und das Rückstreuspektrometer
SS 99, Neutronenphysikalisches Praktikum, Sept. '99
23.30.0

Monkenbusch M.
Flugzeitspektrometer
SS 99, Neutronenphysikalisches Praktikum, Sept. '99
23.30.0

Monkenbusch M.
Flugzeitspektrometer und Neutronenspinechospektrometer, NSE
SS 99, Neutronenphysikalisches Praktikum, Sept. '99
23.89.1

Prager M.
Translations- und Rotationsdynamik
SS 99, Neutronenphysikalischs Praktikum, Sept. '99
23.30.0

Richter D.
Atomkerne als Festkörpersonden
WS 98, 30. IFF Ferienkurs: Magnetische Schichtsysteme, 04.03.99
23.30.0

Richter D.
Dynamik Weicher Materie
SS 99, Neutronenphysikalisches Praktikum, Sept. '99

23.30.0

Richter D.
Korrelationsfunktionen
SS 99, Neutronenphysikalisches Praktikum, Sept. '99
23.30.0

Richter D.
Struktur und Dynamik fester Ionenleiter
SS 99, Forschungspraktikum in Münster
23.30.0

Richter D.
Über die Bedeutung der Forschung mit Neutronen
SS 99, Neutronenphysikalisches Praktikum, Sept. '99
23.89.1

Richter D.
Polymerdynamik
SS 99, DPG-Sommerschule Soft Condensed Matter am 27.09.99 in Bad Honnef
23.30.0

Schwahn D.
Kleinwinkelstreuung und Reflexion mit Neutronen
SS 99, Neutronenphysikalisches Praktikum, Sept. '99
23.30.0

Schwahn D.
Weiche Materie - Struktur
SS 99, Neutronenphysikalisches Praktikum, Sept. '99
23.30.0

Institute of Electroceramic Materials

General Overview

Research Areas

The research areas of the institute comprise (1) technologies for the integration of electroceramic materials into microelectronics and microsystems, (2) dielectric and ferroelectric properties of oxide ceramics, and (3) the defect structure in the vicinity of internal and external interfaces in oxides. These areas are complementary to the research areas of the Institute for Electronic Materials 2 (IWE 2) at the Aachen Technical University (RWTH). Project groups often comprise staff members and students from both institutes.

Integration Technologies

In 1999, the major event in the area of the *integration technologies* has been the completion of the clean room and the installation of the equipment. An official opening celebration has been on September, 23th, 1999. The deposition of oxide thin films is performed by means of MOCVD (MOCVD = Metal Organic Chemical Vapor Deposition) systems. In cooperation with AIXTRON AG, a multiwafer planetary reactor has been installed for the development and optimization of (Ba,Sr)TiO_3 films. In a first step, systematic parameter studies have been performed. Equipment for the electrical characterization of MOCVD processed BST films has been built and tested as part of an ESPRIT project (HECTOR 300). Our horizontal research MOCVD reactor has been tested by the deposition of $SrTiO_3$, $BaTiO_3$, and $PbTiO_3$ thin films and it is now employed for new model systems, such as the (Ba,Pb)TiO_3 solid solution which allows the materials tuning in a broad range of tetragonal ferroelectric distortions. Thin films made by CSD (Chemical Solution Deposition) at the IWE 2 in Aachen were prepared to provide high-precision compositional standards for the XRF analysis of the MOCVD films for both, the multiwafer planetory reactor and the horizontal reactor. In addition, alternative vaporizer systems have been tested. For the patterning of the ceramic films and electrode / ceramic film stacks, Reactive Ion Beam Etching (RIBE) and Reactive Ion Etching (RIE) techniques will be employed. In contrast to the situation in the standard Si and compound semiconductor technologies, dry etching processes of oxide ceramics have hardly been investigated as yet and, hence, represent a research area in which basic studies and industrially funded applied research can be linked in a beneficial manner. The RIBE system has been installed in the clean room is currently tested for a variety of reactive gases. The integration processes are complemented by metallization methods based on electron beam and sputter techniques. Within this area, our studies aim at a better understanding of the processes and material parameters which govern the adhesion, the mechanical stress, and the microstructure.

Dielectric and ferroelectric properties

The second research area focuses on the *dielectric and ferroelectric properties* of oxide thin films and bulk materials, which are being investigated in Jülich as well as in Aachen. The material systems are based on compositions used for practical devices and model systems, e.g. $SrTiO_3$, $BaTiO_3$, $SrBi_2Ta_2O_9$, Pb(Zr,Ti)O_3 and $(Ba_{1-x}Pb_x)TiO_3$. One of the research topics is the microscopic understanding of ferroelectric hysteresis including new approaches for the separation of *reversible* and *irreversible* contributions to polarisation based on the analysis of frequency-dependent small and large signals. These studies are linked to the *aging* (imprint) phenomenon, i.e. the polarisation-dependent shift of the hysteresis curve with time and to the ferroelectric *fatigue* process, i. e. the reduction of the remanent polarisation by cycling. Both aging and fatigue processes play an important role in the operation of the novel non-volatile memories (Ferroelectric Random Access Memories, FeRAM). Impedance spectroscopy in the lower GHz regime is employed to determine the relaxation of the ferroelectric *domain wall* motion and to separate this contribution from the contribution of the crystal lattice. By varying the microstructure of the ceramics and by comparison between bulk ceramics and thin films, the model of Arlt will be extended with respect to the impact on 2D constraints imposed by mechanical stress due to the presence of substrates. For *dielectric* ceramics, impedance spectroscopy is used to elucidate the interrelation of *extrinsic* losses and lattice defects. This activity includes the development and characterization of new microwave ceramics and is embedded into a cooperation with the Institute for Microstructural Research (Urban) and Norbert Klein's group within the framework of a BMBF-Leitprojekt. In the case of ferroelectric materials, existing theories are further developed and extended towards a more quantitative description of the dielectric, piezoelectric, and elastic properties. Numerical *finite-element-methods* are used to describe the mutually coupled mechanical, thermal, and electrical properties of ceramic components such as multilayer capacitors and actuators.

Lattice disorder in the vicinity of internal interfaces

Our third research area comprises the *lattice disorder in the vicinity of internal interfaces* (grain boundaries) and external interfaces (surfaces and electrode interfaces) and their impact on electronic and ionic (oxygen ions and protons) charge transport. In the case of acceptor and donor doped titanate ceramics, the studies are focused on the formation of space charge depletion layers at grain boundaries as well as the related potential barriers and the transport of charge carriers along and across the grain boundary barrier. A hot-pressing technology has been developed to decorate the grain boundary area with additional dopants and to study the influence of these artifical grain boundary states. In some material systems, such as titanate-zirconate solid solutions, it is necessary to determine the equilibrium constants of the defect reactions and the diffusion constants of the system in order to create the basis for the research on interfaces. In this respect, the comparison of bulk ceramics and thin films of the same composition is of vital interest. In thin film systems, the significant influence of the electrode metals, the unexpectedly high stability under conditions of dc-voltage-induced resistance degradation, as well as the tolerance of the lattice concerning the incorporation of non-stoichiometries represent current research topics. Research on electronically conducting perovskites can be divided into studies on *semiconducting* and on *metallically conducting* oxides. In semiconducting, donor-doped $SrTiO_3$, the emphasis is placed on the interrelationship between point defects and extended defects involved in oxidation and reduction processes using single crystals and ceramics. The metallically conducting manganates and cobaltates are investigated with respect to their magnetoresistive and ferromagnetic properties. By comparing epitaxial and polycrystalline thin films, the influence of the grain boundaries on charge transport and magnetic properties is studied. Artificial grain boundaries have been built and charge transport, including tunneling, across the barriers is investigated.

"Scaling effects in integrated electroceramic materials"- The HGF-proposal "PICCOLO"

The proposed HGF-Strategie-Fund Project "Piccolo" is embedded in the information technology program PGI (Physikalische Grundlagen der Informationstechnologie) of the Research Center Jülich. Beyond the Institut für Elektrokeramische Materialien (1), the (2) Institut für Mikrostrukturforschung IMF headed by K. Urban, (3) the Theorie III, headed by H. Müller-Krumbhaar, and (4) the Ion Technology (IT) group at the Institut für Schicht- und Ionentechnik headed by S. Mantl are involved. Several external international and international universities and research centers participate in "Piccolo", too. The main focus of the proposal "Piccolo" is a fundamental as well as applied research on scaling effects of electroceramic materials. Today, typically polycrystalline films exhibit grain sizes much smaller than the feature sizes of the microelectronic devices. However, along with the sustaining trend towards further miniaturization, the decreasing feature sizes in microelectronic technology will approach the typical crystallite sizes of the perovskite-type oxide structures. Specific scaling effects are anticipated along this route, due to the long-range nature of the ferroelectric interaction of the oxides involved. The project aims at an (1) elucidation of the physical origin of these scaling effects, (2) an exploitation and extension of the limits to which the ferroelectric properties and high permittivities of the oxides involved can be used, and (3) the development of technological design rules for the integration of the perovskite-type oxides on a decreasing scale. It will combine production-type process and research-type methods. The spectrum of designated results of the project comprises (semiquantitative) models for the superparaelectric limit of FE oxides, the dead layer at interfaces, the phase stability and segregation processes of perovskite films during annealing, the nucleation and growth of films by MOCVD, recipes for the deposition of single grain capacitors and ultrathin FE films as well as for reactive ion etching and a ferroelectric field-effect transistor (FE-FET) as a demonstrator. In summary the proposal "Piccolo" is an initiative to pursue resea5rch on the basic properties of electroceramic materials under scaling and the relevance of these effects for the integration of perovskite-type ferroelectric (FE) oxides into microelectronics.

Rainer Waser

Institute of Electroceramic Materials

Head: Prof. Dr.-Ing. Rainer Waser
Secretariat: Maria Garcia
Tel. (02461) 61 5811; Fax: (02461) 61 8209
e-mail: r. waser@fz-juelich.de/m.garcia@fz-juelich.de

Personnel 1999/2000 and areas of activity

SCIENTISTS:

Dr. R.R. Arons	Structure of magnetoresistive and ferroelectric oxides; charge transport in proton conductors	23.42.0
Dr. H.G. Bohn	Mechanical and dielectric relaxation in solids. Impedance spectroscopy. Defect chemistry. Electrochemical characterization of ceramic conductors	23.42.0
Dr. P. Ehrhart	MOCVD methods for electroceramical thin films; X-ray diffraction and optical spectroscopy	23.42.0
Dr. S. Hoffmann	High-permittivity electroceramic thin films: MOCVD, dielectric properties, charge transport, defect chemistry	23.42.0
Dr. H.H. Kohlstedt	Reactive ion beam etching of ceramic and metallic materials, superconducting and magnetic multilayers	23.42.0
Dr. W. Krasser	Optical excitation-processes in electroceramic materials;light-annealing processes	23.42.0
Dr. P. Meuffels	Processing of electroceramic materials; defect chemistry of electroceramic materials	23.42.0
Dr. R. Otterstedt	Development of microwave ceramics; dielectric characterization; extrinsic losses in microwave ceramics	23.42.0
Dr. Ch. Pithan	Processing of hot pressed nanocrystalline and grain boundary decorated bulk electroceramics	23.42.0
Prof. T. Schober	High temperature proton conduction, thermogravimetry, impedance spectroscopy, transmission electron microscopy	23.90.0
Dr. H. Schroeder	Technology and properties of (metal) electrodes for electroceramic thin films; mechanical properties and electromigration in thin films and interconnects	23.42.0
Dr. K. Szot	Study of surface layer of perovskite materials of ABO_3 structure	23.42.0
Prof. R. Waser	Electronic ceramics and integration of ceramic thin films	23.42.0

TECHNICAL ENGINEERS:

H. Bierfeld	Ceramic technology and sputtering techniques	23.42.0
U. Dedek	Electrical characterization of electronic ceramics; design of measuring setups	23.42.0
DI J. Friedrich	Thermogravimetric analysis; Transmission electron microscopy	23.42.0
DI H. Haselier	Metallization and thin film technology as well as clean-room technology	23.42.0
B. Hermanns	MOCVD, RIBE, sputtering of magnetic materials	23.42.0
DI H. John	Clean-room technology, microlithography and optical laboratory; LRP	23.42.0
R. Speen	Relaxation spectroscopy and electrochemical characterization	23.42.0

Ph.D. STUDENTS

O. Baldus (TH Aachen)	Laser annealing of CSD, MOCVD electroceramic thin films	23.42.0
F. Fitsilis (TH Aachen)	Thin film capacitors for future DRAM applications using the MOCVD technique	23.42.0
R. Ganster (TH Aachen)	Heterostructures of Titanate thin films, MOCVD growth and numerical simulations	23.42.0
St. Regnery (TH Aachen)	MOCVD planetary reactor processes	23.42.0
J. Rickes (TH Aachen)	Reconfigurable multimedia processors based on ferroelectric RAM (FeRAM)	23.42.0

S. Ritter (TH Aachen)	MOCVD growth of ultrathin ferroelectric thin films and electrical characterization	23.42.0
S. Schmitz, (TH Aachen)	Influence of the contact metal on leakage current and dielectric permittivity of electroceramic thin film capacitors	23.42.0
R. Schmitz (Uni Köln)	Magnetic tunnel junctions, fabrication and experiments	23.42.0
St. Schneider (TH Aachen)	Reactive ion etching (RIE) and reactive ion beam etching (RIBE) of ceramic thin films.	23.42.0
P. Schäfer (TH Aachen)	Evaluation of novel MOCVD systems for the deposition of ferroelectric thin films	23.42.0

GRADUANTS:

N. Giannas (TH Aachen)	Preparation of structured $SrTiO_3$ thin films and characterization of the dielectric properties at microwave frequencies	23.42.0
J. Hövelmann (TH Aachen)	Computer control system for a laser annealing device	23.42.0
L. Kretschmar (TH Aachen)	Design of a pulse generator in the kilovolt regime using ahigh voltage cable to investigate the switching kinetics of ferroelectric thick films in the nanosecond regime	
Ch. Ohly (TH Aachen)	Investigations of the high-temperature conductivity of doped titanate thin films	23.42.0
C. Reinartz (TH Aachen)	Characterization of electrodes for electroceramic thin films	23.42.0
S. Stein (Uni Köln)	Double barrier tunnel junctions with ferromagnets/superconductors	23.42.0

GUEST SCIENTISTS:

Dr. St. Hwang Univ. of California (USA)	Polarization switching models in polycrystalline ceramics	23.42.0
Dr. W. Ma Southeast Univ., Nanjing (China)	Growth, microstructure and electrical property of ferro- electric thin films of perovskite-type oxides by MOCVD	23.42.0
Dr. N. Pertsev A..F. Ioffe Institute St. Petersburg (Russia)	Theoretical calculations on the effects of strain and stress on the dielectric response of ferroelectric thin films grown on the sole substrates	23.42.0

Deposition of electroceramic thin films by MOCVD

P. Schäfer[1], P. Ehrhart[1], F.Fitsilis[1], W. Ma[1], S.Regnery [1,2]

[1] *Institute of Electroceramic Materials*
[2] *AIXTRON AG, Aachen*

We report on the installation of two MOCVD reactors for the deposition of electroceramic thin films. The first system is a research type reactor which is based on an AIX-200 reactor and the second one is based on an AIX-2600G3 planetary reactor which can handle five 6-inch wafers simultaneously. First results are reported for thin films within the solid solution system $SrTiO_3$ – $(Ba,Sr)TiO_3$ – $BaTiO_3$. The binary border systems have been investigated with the research tool and $(Ba,Sr)TiO_3$ deposition parameters for the larger production tool are investigated in cooperation with AIXTRON.

F&E-Nr: 23.42.0

Chemical Vapor Deposition (CVD) techniques have been widely used for the deposition of thin films in many fields of modern technology and are standard processes in the CMOS technology for the deposition of insulators and interlayer dielectrics like SiO_2 and SiN_x and BPSG glasses. For the processing of many metals special precursors in the form of organo-metallic compounds had to be developed in order to obtain a sufficient volatility and a special subgroup of CVD techniques, MOCVD (Metal Organic CVD), has therefore evolved. A large impetus for the development of deposition techniques for perovskite type metal oxides came along with the interest in High–T_c superconductors. The perovskite oxides of interest in electroceramic films, i.e. high epsilon materials like $(Ba,Sr)TiO_3$ (BST) for advanced DRAM concepts [1,2] as well as ferroelectric materials like $Pb(Zr,Ti)O_3$ (PZT) and $SrBi_2Ta_2O_9$ (SBT) for ferroelectric memories[3,4,5] have largely benefited from this development. MOCVD techniques are considered as the primer deposition techniques in this field due to their high deposition rates, and amenability to large wafer-size scaling. Moreover, the need for a high degree of film thickness conformality over the complex device topographies common to ULSI-scale circuits makes MOCVD one of the most appealing synthesis methods.
Remarkable progress has been achieved in the metal-organic chemical vapor deposition of thin oxide films [3,4]. Nevertheless, there is not yet a reliable production tool on the market, and many details of the involved reactions are not under control. We started our investigations with the installation of two reactors in our cleanroom facilities: The first system is a research type reactor which is based on a AIX-200 reactor (fig.1) which is used for fundamental studies of the MOCVD process and for the test of new components, especially new injection systems, and for the deposition of new material combinations. The second reactor is based on an AIX-2600G3 planetary reactor which can handle five 6-inch wafers simultaneously and is used at present for the evaluation of a MOCVD process which is reliable enough for large scale production of BST. In spite of the differences between these reactors there are basic similarities in the design as horizontal gas flow, gas foil rotation of the substrate, and low pressure operation, which should allow a direct know how transfer between the two systems. In addition we use liquid precursor delivery systems for both reactors i.e., solutions of $Ba(thd)_2$, $Sr(thd)_2$ and $Ti(O\text{-}iPr)_2(thd)_2$.

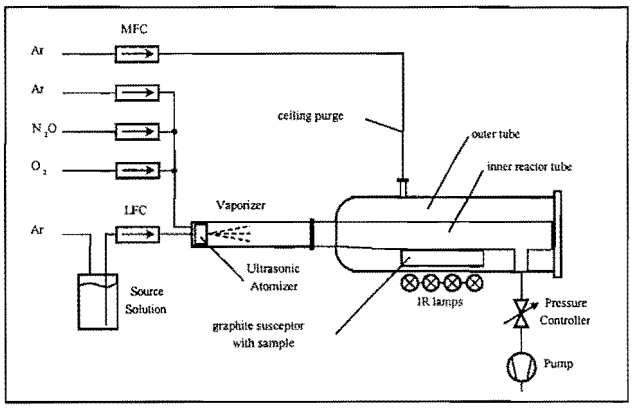

FIG.1. Schematic diagram of the MOCVD research reactor

The film thickness was varied between 10 and 100 nm. The composition and microstructure of the films were routinely investigated by X-ray diffraction (XRD), X-ray fluorescence (XRF) analysis, using different calibration standards prepared by chemical solution deposition, and Rutherford backscattering techniques (RBS).
With the research reactor good films of $SrTiO_3$ and $BaTiO_3$ have been obtained on 1″ x 1″ substrates of Si, SiO_2 or Pt. In the following we will show some examples for the film growth within the multidimensional space of the process parameters.

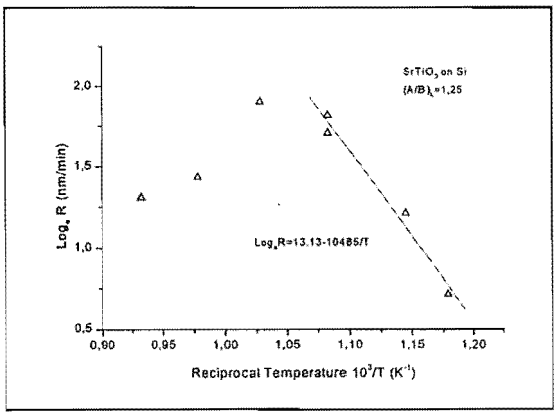

FIG.2. Arrhenius plot for the growth kinetics of $SrTiO_3$

Fig.2: shows the deposition rate as a function of growth temperature for the $SrTiO_3$ thin films grown by MOCVD from a source with a molar ration of the precursors of $(Sr/Ti)_L$=1.25. The growth rate increases with increasing substrate temperature up to around 700 °C. As indicated by the Arrhenius line, the thin film deposition process was dominated by a surface-reaction-limited mechanism up to 700 °C. The 'effective' activation energy for the thin film growth was calculated to be about 87 kJ/mol. or 0.9 eV/atom. Further increase of the growth temperature above 700 °C leads to a decrease of growth rate, which may be attributed to the transition to the to mass transfer limited regime and/or a depletion of the precursors in the vicinity of the reactor inlet zone.

Fig. 3 shows, for films grown at 700°C, the evolution of the microstructure as a function of the film stoichiometry. The x-ray diffraction patterns show that the film composition has a considerable effect on the film structure and crystallinity. The $SrTiO_3$ thin films grown at 700 °C with different film composition $(Sr/Ti)_F$. The $(Sr/Ti)_F$=0.61 thin film is amorphous, while the $(Sr/Ti)_F$=0.7 and $(Sr/Ti)_F$=0.83 thin films display strong reflections from the pure $SrTiO_3$ phase.

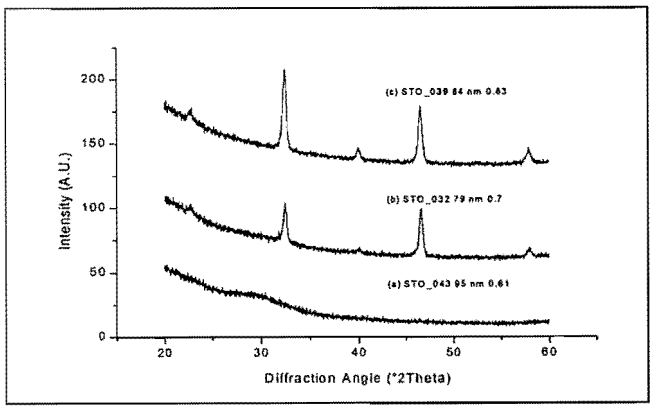

FIG.3. X-ray diffraction pattern for $SrTiO_3$ films deposited at 700°C. The films were grown from different precursor concentrations and have different stoichiometry.

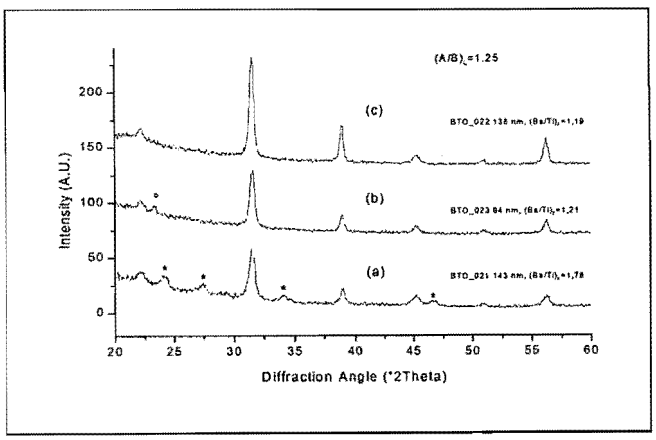

FIG.4. X-ray diffraction pattern for $BaTiO_3$ films deposited at 635°C. The films were grown from different precursor concentrations and have different stoichiometry.

$BaTiO_3$ films behave in many respects very similar there is, however, a strong tendency for the formation of carbonate phases as demonstrated by the lowest curve in figure 4.

BST is one of the prime candidates as a high-k-dielectric in future DRAM memory cells, however, this material will only be implemented into ULSI-devices if suitable production processes are avalable. Most of the advanced reactors intended for mass production presently use showerhead designs and we investigate as a comparison the performance of a planetary multi-wafer reactor. As a direct consequence of the reactor design we obtain efficiencies for the precursor incorporation (i.e., 40% for Ti and 20-30% for Ba, Sr) which are much higher than those of ≈10% reported for showerhead reactors (fig.5) and therefore promise a big advantage in the cost of ownership.

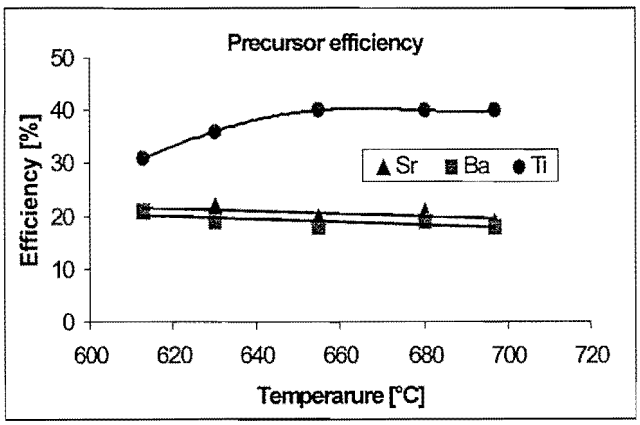

FIG.5. Efficiency of the precursor deposition at different deposition temperatures within the planetary reactor.

In addition we obtain a high uniformity of the films over 6 inch wafers, i.e.: a few percent deviation in thickness and off-stoichiometry. However, further optimization of the processes are necessary for a optimal stoichiometry control as well as process reproducibility and stability for an application as a production tool.

1. S.R. Summerfelt, in *Thin Film Ferroelectric Materials and Devices* (Ramash R. ed., Kluwer Acad. Publ., Boston, 1997) p.1-42
2. A.I. Kingon, S.K. Streiffer, C. Basceri, S.R. Summerfelt, *MRS Bulletin,* **21**,7, 46 (1996)
3. C.M. Foster, in *Thin Film Ferroelectric Materials and Devices* (Ramash R. ed., Kluwer Acad. Publ., Boston, 1997) p.167-197
4. B.W. Wessels, *Annu.Rev.Mater.Sci.,* **25**, 525 (1995)
5. J.F. Scott, F.M.Ross, C.A. Paz de Araujo, M.C. Scott, and M.Huffman, *MRS Bulletin,* **21**,7, 33 (1996)

Anomalous behaviour of thermally reduced $SrTiO_3$.

K.Szot[1] , W.Speier[2], R.Carius[3], U.Zastrow[3] and R.Waser[1]

[1] Institut für Festkörperforschung (IFF), Forschungszentrum Jülich, 52425 Jülich, Deutschland
[2] Institut für Chemie und Dynamik der Geosphäre (ICG), Forschungszentrum Jülich ,52425 Jülich, Deutschland
[3] Institut für Schicht- und Ionentechnik (ISI), Forschungszentrum Jülich, 52425 Jülich, Deutschland

Anomalous behaviour in the electrical conductivity and optical absorption is observed for thermally reduced single crystals of (100)$SrTiO_3$ after prolonged annealing. Secondary ion mass spectrometry of tracer diffusion (re-oxidation with ^{18}O) confirm that this behaviour is related to a decrease of the density of vacancy defects in time, indicative of an annihilation of defects by some type of "self-oxidation" either by local redistribution of oxygen or induced structural changes.

F&E-Nr.23.420

The defect structure of the perovskite of ABO_3-type is traditionally described in terms of point defect chemistry [1]. The concentration of oxygen vacancies and non-stoichiometry in the AO-sublattice are determined in a routine manner by measurement of the so-called equilibrium electrical conductivity in dependence of the partial pressure of oxygen and temperature. The use of point defect chemistry however relies on the assumption of an ideal solution of the defects in an otherwise homogeneous material. But according to recent studies, structural imperfections of perovskite crystals in the so-called skin region with an unusually high density of dislocations [2] and the formation of non-perovskite phases on the surfaces and in the near-surface region at elevated temperatures [3] may affect the macroscopic properties. This raises the question to what extent the electrical characteristics at elevated temperatures of the perovskite are influenced by these factors.

Single-crystalline $SrTiO_3$ has been chosen to serve as model substance for the perovskite of ABO_3-type. Figure 1a represents the characteristic behaviour of the electrical conductivity on thermal reduction at elevated temperatures. On a sudden change of oxygen partial pressure the resistivity reaches a plateau after relatively short time which is taken as a measure of the equilibrium concentration of defects (based on the assumption of a constant mobility of charge carriers) [4]. The observed behaviour is typical for samples which have been exposed previously to various reducing or oxidising conditions at elevated temperatures (ill-defined thermal history). In contrast, measurements of the electrical conductivity of virgin crystals (as received) show a completely different behaviour. As can be taken from figure 1b, the resistivity decreases as expected for a sudden exposure to reducing conditions, but shows an increase for prolonged annealing. This behaviour implies that the crystal does not reach immediately an equilibrium and that several counteracting processes are involved. Electrical measurements may be influenced by segregation phenomena such as electrochemical segregation or formation of space charge, especially near the metal/sample interface.

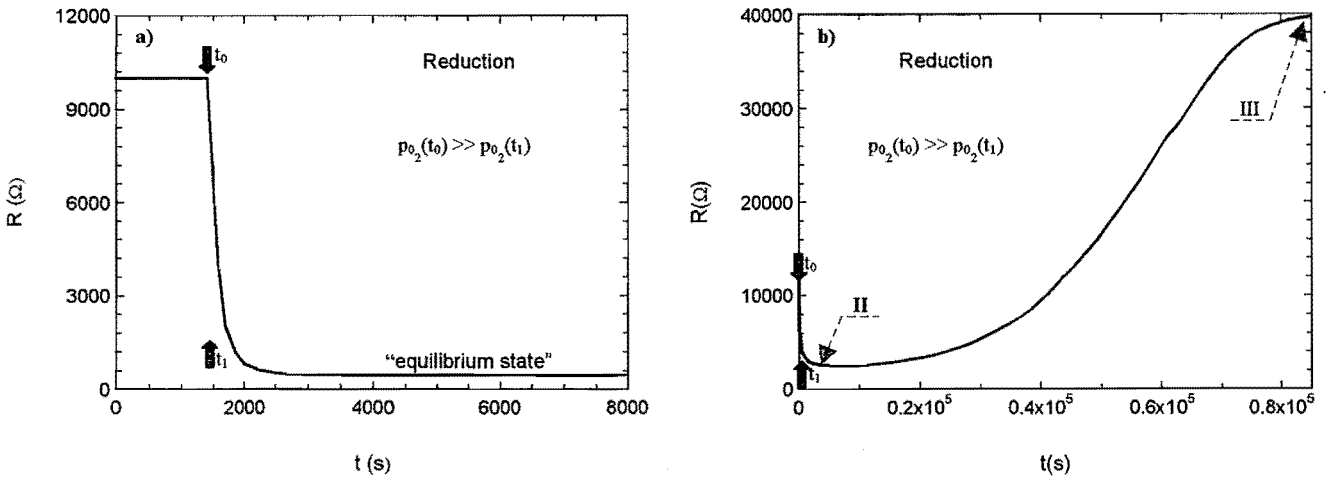

FIG.1. *Behaviour of electrical resistivity of $SrTiO_3$ at elevated temperatures as a result of a change in partial pressure of oxygen: a) crystals with ill-defined thermal history (adapted from [4]), b) virgin single crystals*

However, the same general trends in the apparent concentration of defects are confirmed by optical measurements (without external field and electrodes). As can be taken from figure 2, the sub-gap absorption rises at first as a consequence of exposure to reducing conditions (point II in fig 1b), but decreases again after extensive annealing (compare with point III in fig 1b).

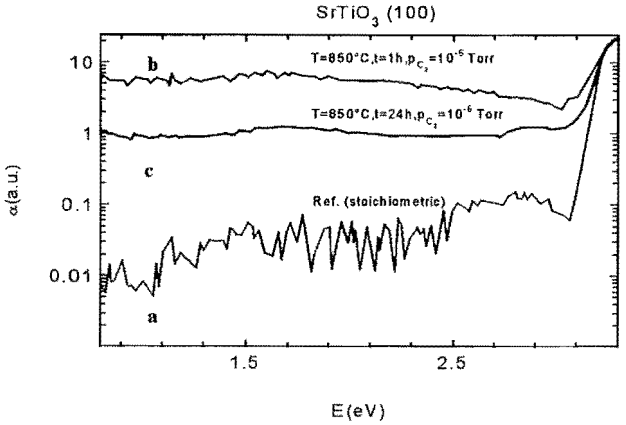

FIG. 2. *Optical absorption spectra for a: as-received single crystals, b: samples reduced in HV for short time corresponding to point II in fig 1b and c: for extensive annealing in HV corresponding to point III in fig. 1b.*

Whereas the absorption spectra shown in fig. 2 gives evidence for a decreasing number of defects for long reduction times the concomitant decrease of the carrier concentration has been confirmed by IR reflection measurements. More detailed analysis of the optical absorption allowed to determine that the largest contribution of the sub-gap absorption stems form the outer portions of the crystals (skin region). Further information about the nature of the processes involved can be obtained by tracer diffusion (^{18}O) and analysis of the depth profiles by secondary ion mass spectrometry. Considering the amount of ^{18}O incorporated into the crystals by re-oxidation experiments, the depth profiles given in figure 3 reveal that the density of available defects is substantially lowered for $SrTiO_3$ after extensive annealing, both near the surface as well as in deeper portions of the sample. This is in contrast with the standard picture which assumes that the amount of oxygen vacancies generated as a consequence of the reduction process should continue to rise or should remain constant after finally reaching its equilibrium density. The deep penetration of the ^{18}O-tracer (tails of the depth profiles) is particular noteworthy as it is related to fast diffusion paths along extended defects, well known for other perovskite such as $CaTiO_3$ or $KNbO_3$.

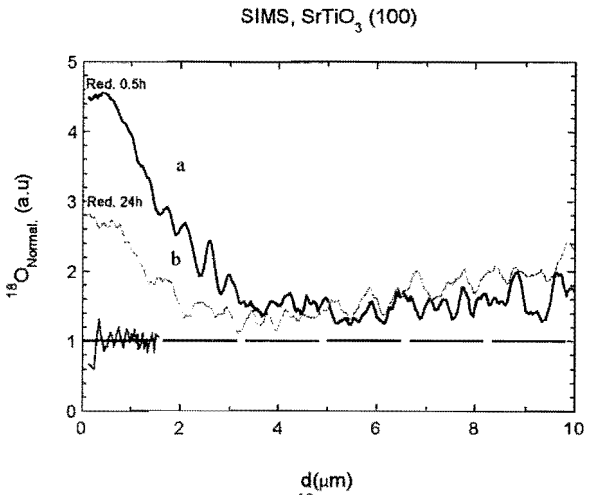

FIG. 3. *Depth profile for ^{18}O for samples re-oxidized in ^{18}O-atmosphere after short (a) and prolonged (b) reduction, with reference to the natural background level of ^{18}O obtained for as-received crystals without heat-treatment.*

These extended defects may play the key role in understanding the observed anomalous behaviour of reduced crystals. The above-mentioned high density of such defects in the skin region of $SrTiO_3$ and their role as fast diffusion paths allow the easy generation of oxygen vacancies in deeper regions of the crystals. In the first stage, oxygen vacancies form along these extended defects beside those formed directly at the surface/atmosphere interface. However, the additional redistribution of SrO-complexes and subsequent formation of non-perovskite phases such as TiO_{2-x} and SrO-rich Ruddlesden-Popper phases give rise to a heterogeneous layer structure in the near-surface region (ranging from a few nm to several tens of nm) which may establish a barrier of further oxygen transport in time. The apparent decrease in the density of oxygen vacancies for prolonged annealing within the crystal must then be related to a type of "self-oxidation", either due to a local redistribution of oxygen or, more likely, the annihilation of vacancies by a shearing mechanism well known for the binary transition metal oxides such as TiO_{2-x}. Further studies on the microscopic scale combining modern surface and micro-analytical tools will be necessary to provide a detailed description of the complex processes involved.

1 R.Waser and D.M.Smyth in "Ferroelectric Thin Films: Synthesis and Basic Properties", p. 584, Gordon and Breach, USA (1994)

2 R. Wang, Y. Zhu, and S.M. Shapiro, Physical Review Letters **80**, 2370 (1998)

3 K. Szot and W. Speier, Phys. Rev. B. **60**, 5909 (1999); K.Szot, W.Speier, J.Herion, and Ch.Freiburg, Applied Physics A **64**, 55 (1997)

4 P.Pasierb, S.Komornicki, M.Rekas, J.Phys Chem. Solids **60** 1835 (1999)

Tunnelmagnetoresistive elements for memory applications

R. Schmitz [1], P. Rottländer[2], S. Stein[1] and H. Kohlstedt[1]

[1] *Institute for Elektroceramic Materials*
[2] *Institute for Electronic Properties*

Abstract – Ultraviolet assisted oxidation has been applied to oxidize the barriers in ferromagnetic tunnel junctions. It is shown, that this method produces junctions of good quality with an area resistance in the order of 0.1 to 100 kΩμm². This results in resistance ranges attractive for large scale integration applications, i.e. the non-volatile magnetic random access memory application. The fabrication procedure using magnetron sputtering, ion beam etching and lithography will be explained in detail.

F&E-Nr: 23.42.0

Magnetic tunnel junctions (MTJ) show a large magnetoresistive effect. These devices consist of ferromagnetic top and bottom metal electrodes separated by an insulating layer. If a magnetic field is applied to the multilayer and turns the relative orientation of the magnetization from parallel to antiparallel, a change in the magnetoresistance ($\Delta R/R > 20$ %) is observed. The insulator (tunnel barrier) is formed by depositing a 1.0 nm to 1.5 nm thin aluminum film on the ferromagnetic bottom layer and a subsequent oxidation procedure. Magneto Random Access Memory is one of the main potential applications of MTJs [1,2]. In contrast to the GMR-effect the TMR effect shows higher values of resistance changes and is thus more favorable for applications.

We present a different method for fabricating tunnel junctions by oxidizing with the assistance of an ultraviolet lamp. The tunnel barrier is made of a thin sputtered aluminum film which is usually oxidized by an oxygen plasma. This results in a very high area resistance (R·A). Especially in memory applications, where the highly integrated elements are in the sub-μm region this is undesirable. On the other hand the R·A-product is too small when using thermal oxidation. In our case we followed the idea by Fritsch et al. [3] who described the in situ oxidation with ultraviolet light illumination. This method seems to be easy on the junction and we receive the appropiate low area resistances of 0.1...100 kΩμm².

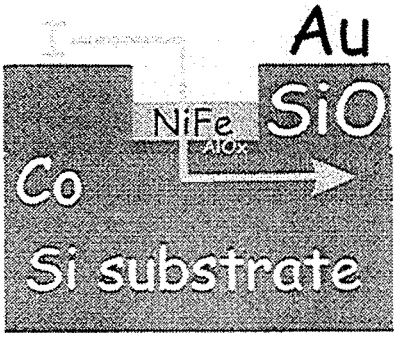

Fig. 1 *Schematic cross section of a magnetic tunnel junction.*

The samples are prepared by sputtering on thermally oxidized Si wafers. The ferromagnetic bottom electrode consists of a 19 nm Co thin film, which is dc-magnetron sputtered. The Al thin film (about 1.3 nm) for the barrier is rf sputtered and then oxidized, assisted by a low-pressure-mercury-lamp (4 W). It emits wavelengths of 185 nm (ozone generating) and 254 nm in the ultraviolet range. The generation of ozone is probably not the dominating effect but the process proposed by Cabrera and Mott [4] based on the photo electric effect: During thermal oxidation of aluminum, electrons tunnel through the forming oxide layer and surface charges are formed. A resulting field pulls positive aluminum ions through the barrier. The oxide growth stops as soon as the electric field across the barrier is too small for moving the Al ions. UV light excites further electrons in the metal which pass through the barrier and are trapped at the surface. Increasing the surface charges by the UV-light, and thus the electric field yields to a larger limiting thickness.

The oxygen pressure in the chamber is varied between 1 and 100 mbar. Oxidation time is usually within a few minutes up to one hour. The top electrode is a sputtered permalloy ($Ni_{81}Fe_{19}$) layer (18 nm) followed by a gold wiring layer.

The structure is patterned by optical lithography and ion beam etching (IBE). End point detection is provided by a secondary ion mass spectroscopy (SIMS). A self-aligned process is used to define the junction. The same photomask is used for etching through the top electrode and depositing the SiO insulator with "lift-off" technology.

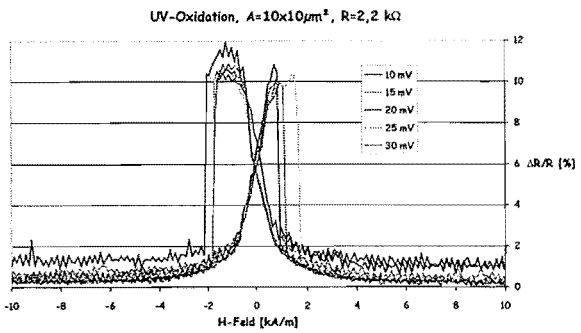

Fig. 2 *Magnetoresistance plot at room temperature*

Processing 3"-wafers with the same oxidation time of one hour, but different oxygen pressures between 1 and 100 mbar show, that the highest TMR-effect is produced at 10

mbar. It is also seen that all of the MTJs across the wafer show tunneling I-V-curves as well as $\Delta R/R > 10\%$.

[1] BMBF-Leitprojekt "Magnetoelektronik" together with Siemens Erlangen (ZT MF 1), 13N7380/4
[2] HGF-Strategiefond "Magnetoelektronik" together with ISI and IGV
[3] L. Fritsch et al. Physica C, 296 (3-4):319, 1998
[4] N. Cabrera and N.F. Mott, Rep. Prog. Phys. 12:163, 1949

Ba-zirconate: an important high temperature proton conductor

T. Schober , H.G. Bohn

[1] *Institute for Electroceramic Materials*

Abstract – High temperature proton conduction in ceramics is a potentially very useful property which may be used in fuel cells and sensors. In this department perovskitic proton conductors are investigated. Typical representatives are $Ba_3Ca_{1.18}Nb_{1.82}O_{9-x}$ and Y-doped Ba and Sr zirconates.

F&E-Nr: 23.90.0

Perovskite-type cerates and zirconates of the form ABO_3 (A=Ba, Sr; B=Ce, Zr) are known to dissolve significant amounts of water when doped with trivalent elements such as Y or Yb. Because the protons are mobile these systems become good proton conductors at elevated temperatures (high temperature proton conductors, HTPCs). It has been reported that cerates are better HTPCs than zirconates, and the best proton conducting system known up to now was $BaCeO_3$:5%Y. The disadvantage of this system (and in general all cerates) is that it becomes chemically instable in CO_2-containing atmospheres as it readily forms carbonates. This prohibits applications as electrolytes in SOFCs or hydrogen sensors. Thus research activities (in particular in this institute) have concentrated in recent years on a new family of HTPCs, namely complex perovskites of the form $A_3B'_{1+x}B''_{2-x}O_{9-\delta}$ and here in particular on $Ba_3Ca_{1.18}Nb_{1.82}O_{9-\delta}$ (BCN18). This material is now well understood in many details and turned out to be a HTPC with electrical conductivity (in the grain interior) rather close to that of Ba-cerate . However, drawbacks of this system are unfavorable grain boundary properties such as high impedance, blocking of proton transport, and formation of cavities at the grain boundaries in reducing environments.

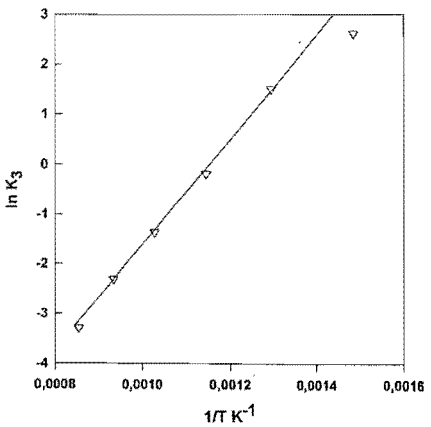

Fig. 1.Equilibrium constant of water uptake reaction vs 1/T

Concentrating on another promising system ceramic samples of $BaZr_{0.9}Y_{0.1}O_3$ were prepared using the mixed-oxide route. Surprisingly, proton uptake up to 8% (the theoretical limit being 10%) was observed by *in situ* thermogravimetry. Fig.1 shows the equilibrium constant of the water uptake reaction vs 1/T.Good linearity is observed. From the data we extract a dissolution energy of (-0.77±0.03) eV and an entropy of $(-0.9\pm0.1)\times10^{-3}$ eV/K.
Of prime importance in considering the quality of such a HTPC are the transport numbers in oxidizing and reducing atmospheres which were extensively investigated in this work. As an example, we show in Fig. 2 the proton transport number measurement at 400 °C for BZY10 in reducing atmosphere. Nernst's law is almost perfectly obeyed here.

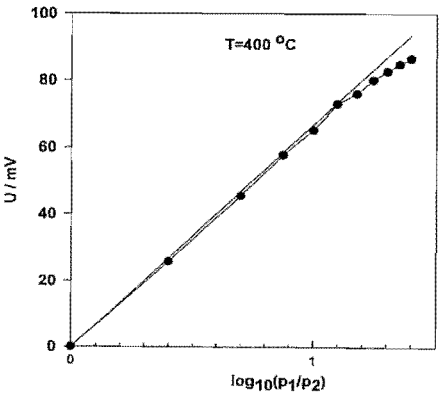

Fig. 2. Nernst voltages of a hydrogen concentration cell from which a proton transport number of roughly unity is deduced for reducing conditions.(BZY10).

BZY10 was also investigated as an electrolyte for a fuel cell operation.As shown in Fig. 3, EMFs were observed which were roughly 20% below the theoretically expected values. This result demonstrates that rather large losses are produced by electronic (hole) conduction which makes this composition rather unattractive for a commercial application as a fuel cell electrolyte.

Proton induced amorphization of BCN18

In different experiments the interaction of HTPCs with weak acids or aquous media at room temperature was investigated.Again the prototypical compound BCN18 was used. Exposure of plates of BCN18 to such weak acids or even to water produced an amorphous surface layer which may extend several µm into the solid. An analysis of various experimental techniques resulted in the following mechanism for the amorphization: protons enter into the BCN18 structure and take part in ion exchange processes with the A-site cations. Ba and Ca migrate along internal

planar defects to the surface and go into solution. The remaining structure of water-rich Nb oxide, presumably $HNbO_3$, collapses in an amorphous structure since thermal activation for crystallization is missing. Fig. 4 shows the increase in the amorphous background observable in powder X-ray diffraction when BCN18 is exposed to aqueous environments (details in caption).

The above mechanism provides a novel pathway for the introduction of protons into such oxides. Finally, it is very probable that many perovskites show such detrimental effects from the interaction with environmental water.

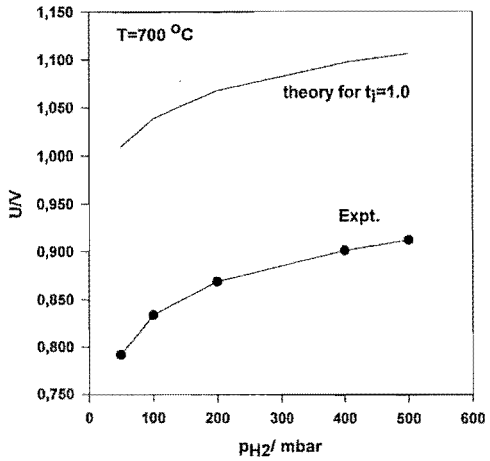

Fig. 3.Open cell voltage of a fuel cell using BZY10 as an electrolyte. Anode hydrogen pressure between 50 and 500 mbar, cathode: moist air. Theoretical voltage for an ionic transport number of unity is also shown.

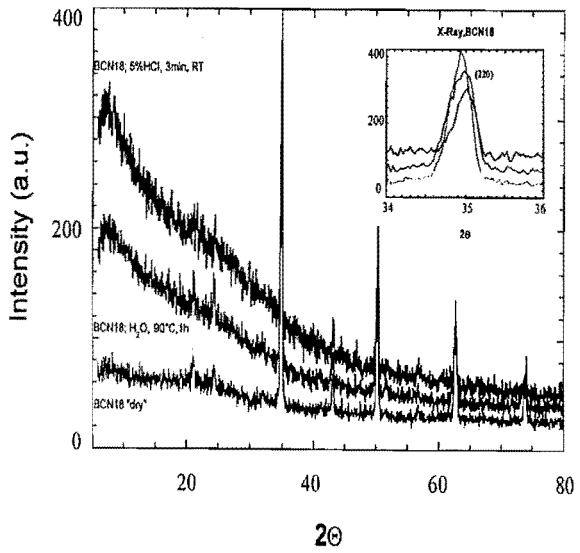

Fig. 4.Change in powder diffraction pattern of BCN18 when exposed to 5% HCl for 3 min at room temperature (uppermost curve), after exposure to hot water for 1 h (center). Dry reference curve:below. A drastic increase of the amorphous background is observed.

1. T.Schober, H.G. Bohn, Solid State Ionics, (in press)
2. H. G. Bohn, T. Schober, J. Amer. Ceramic Soc.(in press)
3. H.G. Bohn, T. Schober, T. Mono, W. Schilling, "The high temperature proton conductor Ba_3 $Ca_{1.18}$ $Nb_{1.82}$ O_{9-x} .I Electrical conductivity", Solid State Ionics ,117 (1999) 219
4. T. Schober, H. G. Bohn, T. Mono, W. Schilling, "The high temperature proton conductor Ba_3 $Ca_{1.18}$ $Nb_{1.82}$ O_{9-x} II:electrochemical cell measurements and TEM", Solid State Ionics 118 (1999) 173
5. T. Schober, J. Friedrich, "Thermogravimetry of the high temperature proton conductors $BaCa_{0.3}Nb_{0.6}$ $Nd_{0.1}O_{3-x}$, $SrCa_{(1+x)/3}Nb_{(2-x)/3}O_{(3-x/2)}$ and $Sr(Zr_{0.8}Ce_{0.2})_{0.8}In_{0.2}O_{(3-x)}$ ",Solid State Ionics 125 (1999) 319
6. T. Schober, J. Friedrich, "Laboratory Application and Demonstration of Automotive Oxygen Sensors", J.Chem. Education 76 (1999)1697-1700
7. T. Schober, J. Friedrich, "Proton Conductor $Ba_3Ca_{1.18}Nb_{1.82}O_{9-\delta}$ (BCN18): Effect of Reducing Environments", J. Am. Ceram. Soc. 82 (1999) 3125-28
8. T. Schober, K. Szot, M. Barton, B. Kessler, U. Breuer, H.J. Penkalla, W. Speier ,"Cation loss of $BaCa_{0.393}Nb_{0.606}O_{2.91}$ in aqueous media: amorphization at room temperature",J. Solid State Chemistry, (in press:Dec.1999 issue)

Publications in refereed journals

Bohn H.G.; Schober T.; Mono T.; Schilling W.
The high temperature proton conductor Ba3Ca1.18Nb1.82O9-x. I. Electrical conductivity
Solid State Ionics 117 (1999) 219
23.90.0

Ehrhart P.
Nordlung K.1; Partyka P.1; Zong Y.1; Robinson I.K.1; Averback R.S.1; Ehrhart P.
Glancing incidence diffuse X-ray scattering studies of implantation damage in Si
Nucl. Instr. Meth. In Phys. Res. B147 (1999) 399-409
23.55.0

Ehrhart P.; Zillgen H.
Vacancies and interstitial atoms in e-irradiated germanium
J. Appl. Phys. 85 (1999) 3503-3511
23.55.0

Grossmann M.1; Slowak R.1; Hoffmann S.; John H.; Waser R.
1IWE RWTH Aachen, Germany
A novel integrated thin film capacitor realized by a multilayer ceramic-electrode sandwich structure
J. Europ. Ceram. Soc. 19 (1999) 1413-1415
23.42.0

Hartner W.1; Schindler G.1; Weinreich V.1; Ahlstedt M.1; Schroeder H.; Waser R.; Dehm C.1; Mazuré C.1
1Siemens AG, München, Germany
Influence of dry etching using argon on structural and electrical properties of crystalline and non-crystalline SrBi2Ta2O9 thin films
Proc. of Int. Symposium on Integrated Ferroelectrics (ISIF) 1999, Colorado Springs (USA), 2/99, to be published in Integrated Ferroelectrics
23.42.0

Hoffmann S.; Grossmann M.1; Schroeder H.; Liedtke R.1; Schumacher M.2; Dietz G.W.3; Schneller Th.4; Gerhardt, R.1; Waser R.
1IWE RWTH Aachen, Germany
2 Aixtron AG, Aachen, Germany
3 Siemens AG, München, Germany
4 aixacct, Aachen, Germany
Charge transport, dc field effects, and long-term reliability of electroceramic thin films
COST 514 Ferroelectric Ceramic Thin Films, Final Report 1999, S. Hoffmann, Th. Schneller, R. Waser (eds.), Shaker Verlag, Aachen 1999, ISBN 3-8265-4960-0
23.42.0

Hoffmann S.; Waser R.
Control of the Morphology of CSD-prepared (Ba,Sr)TiO3 thin films
J. Europ. Ceram. Soc. 19 (1999) 1339-1343
23.42.0

Huck H.; Ehrhart P.; Schilling W.
High temperature optical absorption spectroscopy at pure and Y-doped BaCeO3
J. European Ceramic Soc. 19 (1999) 939-944
23.90.0

Pertsev N.A.1, Zembilgotov A.G.1; Hoffmann S.; Waser R.; Tagantsev A.K.2
1 St. Petersburg
2 EPFL, Lausanne, Switzerland
Ferroelectric thin films grown on tesnile substrates: Renormalization of the Curie-Weiss law and apparent absence of ferroelectricity
J. Appl. Phys. 85 (1999) 1698-1701
23.42.0

Schober T.; Bohn H.G.; Mono T.; Schilling W.
The high temperature proton conductor Ba3Ca1.18Nb1.82O9-x. II. Electrochemical cell measurements and TEM
Solid State Ionics 118 (1999) 173
23.90.0

Schober T.; Friedrich J.
Laboratory application and demonstration of automotive oxygen sensors
J. Chem. Education 76 (1999) 1697-1700
23.90.0

Schober T.; Friedrich J.
Proton conductor Ba3Ca1.18Nb1.82O9-((BCN19): Effect of reducing environments
J. Am. Ceram. Soc. 82 (1999) 3125-28
23.90.0

Schober T.; Friedrich J.
Thermogravimetry of the high temperature proton conductors BaCa0.3Nb0.6Nd0.1O3-xSrCa(1+x)/3O(3-x)/2 and Sr(Zr0.8Ce0.2)0.8In0.2O((3-x)
Solid State Ionics 125 (1999) 319
23.90.0

Schroeder H.
Stress and electromigration-induced voiding and its correlation to macroscopic stress changes
Materials Research Scoeity (MRS) Symposium Proceedings 516 (1998) 237
23.42.0

Shur, V.Ya.; Blankova E.B.; Subbotin A.L.; Borisova E.A., Poelegov D.V.; Hoffmann S.; Bolten D.; Gerhardt R.; Waser R.
Influence of crystallization kinetics on texture of sol-gel PZT and BST thin films
J. Europ. Ceram. Soc. 19 (1999) 1391-1395
23.42.0

Szot K.; Czyrska-Filemonowicz A.1; Wasilkowska A.1; Quadakkers W.J.2
1 Univ. of Mining and Metallurgy, Faculty of Metallurgy and Materials Science, Krakow, Poland
2 Institut for Materials in Energy Systems, FZJ
Microscopy (AFM, TEM, SEM) studies of oxide scale formation on FeCrAl based ODS alloys
Solid State Ionics 117 (1999) 13

Szot K.; Speier W.1
1Institut für Chemie und Dynamik der Geosphäre, FZJ
Surfaces of reduced and oxidized SrTiO3 from atomic force microscopy
Phys. Rev. B60 (1999) 5909
23.42.0

Szot K.; Waser R.; Meyer R.1
1 Institut für Werkstoffe der Elektrotechnik, RWTH Aachen
Restructuring the surface region of donor doped SrTiO3 single crystals under oxidizing conditions
Ferroelectrics 224 (1999) 323
23.42.0

Waser R.
Modeling of Electroceramics - Applications and Prospects
J. European Ceramic Society 19 (1999) 655
23.42.0

Waser R.; Bolten D.1; Hoffmann M.1; Hasenkox U.1; Lohse O.1
1 Institut für Werkstoffe der Elektrotechnik, RWTH Aachen
Chemical solution deposition (CSD) and characterization of the solid solution series Ba(1-x)Pbx(Ti,Mn)O3
Ferroelectrics 225 (1999) 117
23.42.0

Waser R.; Bolten D.1; Lohse O.1; Grossmann M.1
1 Institut für Werkstoffe der Elektrotechnik, RWTH Aachen
Reversible and irreversible domain wall contributions to the polarization in ferroelectric thin films
Ferroelectrics 221 (1999) 251
23.42.0

Waser R.; Grossmann M.1; Lohse O.1; Bolten D.1; Hartner W.2; Schindler G.2; Nagel N.2; Dehm C.2
1 Institut für Werkstoffe der Elektrotechnik, RWTH Aachen
2 Infineon AG, München
Origin of imprint in ferroelectric CSD SrBi2Ta2O9 thin films
Mat. Res. Soc. Symp. Proc. 541 (1999 269
23.42.0

Waser R.; Hagenbeck R.1
1 Institut für Werkstoffe der Elektrotechnik, RWTH Aachen
Detailed temperature dependence of the space charge layer width at grain boundaries in acceptor-doped SrTiO3-ceramics
J. Europ. Ceram. Soc. 19 (1999) 683
23.42.0

Waser R.; Hasenkox U.1
1 Institut für Werkstoffe der Elektrotechnik, RWTH Aachen
Microstructure and properties of highly oriented PZT thin films on epitaxial ceramic electrodes prepared by CSD
Ferroelectrics 225 (1999) 107
23.42.0

Waser R.; Hasenkox U.1; Mitze C.1; Arons R.R.; Pommer J.1; Güntherodt G.
1 Institut für Werkstoffe der Elektrotechnik, RWTH Aachen
2 RWTH Aachen
J. Electroceramics 3 (1999) 255
23.42.0

Waser R.; Prume K.1; Leuerer T.1
1 Institut für Werkstoffe der Elektrotechnik, RWTH Aachen
3-dimensional FEM simulations of resonances in the impedance characteristics of ceramic multilayer capacitors
Ferroelectrics 224 (1999) 185
23.42.0

Invited talks

Ehrhart P.
Deposition of electroceramic thin films by MOCVD
16th Umbrella Symposium, Aachen, 08.-12.11.1999
23.42.0

Hartner W.1; Schindler G.1; Weinreich V.1; Ahlstedt M.1; Schroeder H.; Waser R.; Dehm C.1; Mazuré C.1
1Siemens AG, München, Germany
Influence of dry etching using argon on structural and electrical properties of crystalline and non-crystalline SrBi2Ta2O9 thin films
11th Int. Symp. On Integrated Ferroelectrics (ISIF), 1999, Colorado Springs (USA), 07.-10.03.1999
23.42.0

Hoffmann S.
Leakage current and resistance degradation of doped (Ba,Sr)TiO3 thin films
School of Conduction and Breakdown, Chateaux d'Oex, 28.02.-02.03.1999
23.42.0

Hoffmann S.; Grossmann M.1; Waser R.
1 IWE, RWTH Aachen, Germany
Leakage current and resistance degradation behavior of doped (Ba1-xSrx)TiO3 thin films for DRAM applications
11th Int. Symp. Integrated Ferroelectrics, Colorado Springs, Colorado, USA, 07.03.-10.03.1999
23.42.0

Hoffmann S.; Waser R.
High permittivity dielectrics: from bulk ceramics to thin films
41th Electronic Materials Conference (EMC), Santa Barbara, California, 30.06.-02.07.1999
23.42.0

Schober T.; Bohn H.G.
Electrochemical characterization and impedance of the high temperature proton conductor BaZr0.9Y0.1O2.95
6th Euroconference on Solid State Ionics, Cetraro, Italien, 16.09.1999
23.90.0

Schober T.; Friedrich J.
The proton conductor Ba3Ca1.18Nb1.82O9-((BCN18): Effect of reducing enviroments
12th Int. Conf. Solid State Ionics, Halkidiki, Griechenland, 10.06.1999
23.90.0

Schober T.; Szot K.; Barton M.; Kessler B.; Breuer U.1; Penkalla H.J.1; Speier W.1
1 Zentralinstitut für Chemische Analysen, FZJ
Cation loss of the proton conductor BaCa0.393Nb0.606O2.91 in aqueous media: amorphization at room temperature
6th Euroconference on Solid State Ionics, Cetraro, Italien, 18.09.1999
23.90.0

Schroeder H.
On the interpretation of leakage current: Models for thin films
School on Conduction & Breakdown, Chateaux d'Oex (Schweis), 28.02.-02.03.1999
23.42.0

Waser R.
"Elektrokeramische Dünnschichten in der Mikroelektronik - Chancen und Perspektiven"
Universität Augsburg, 21.05.1999
23.42.0

Waser R.
Defect chemistry and charge transport in perovskite-type thin films
School on Conductivity and breakdown, Cheateau d'Oex, Schweiz, 28.02.-02.03.1999
23.42.0

Waser R.
Frequency dependence of the coercive voltage of ferroelectric thin films
MRS Fall Meeting, Boston, 28.11.-03.12.1999
23.42.0

Waser R.
Modeling of Electroceramics - Applications and Prospects
Hebrew University, Jerusalem, Israel 10.01.1999
23.42.0

Waser R.
Modeling of Oxide Materials for Memory Applications
41st Electronic Materials Conference, Santa Barbara, 30.06.-02.07.1999
23.42.0

Waser R.
Neue keramische Materialien in der Informationstechnik von morgen
9. Tag für Wissenschaft und Wirtschaft, IHK Köln, 19.08.1999
23.42.0

Waser R.
Preparation and Fatigue Behaviour of PZT Thin Films with P- and N-Type Conducting Oxide Electrodes
11th Int. Symp. on Integrated Ferroelectrics, Colorado Springs, 06.-10.03.1999
23.42.0

Waser R.
Transport Properties of Ferroelectric Thin Films
9th European Meeting on Ferroelectricity (EMF-9), Praha, 12.-16.07.1999
23.42.0

Posters

Allen C.W.1; Schroeder H.; Hiller J.M.1
1Madison Area Techn. Coll., Madison
In situ study of dislocation behaviour in columnar of Al thin films on Si-substrate during thermal cycling
MRS Fall Meeting 1999, Boston, Symp. V "Thin Films - Stresses and Mechanical Properties VIII, 30.11.1999-12-19
23.42.0

Emtsev V.V.1; Ehrhart P.; Poloskin D.S.1; Dedek U.
1 IOFFE Institut, St. Petersburg, Russia
Electron irradiation of heavily doped silicon: group-III impurty ion pairs
20th Int. Conf. Defects in Semiconductors, ICDS-20, Berkeley, CA, 26.07.-30.07.1999-12-19
23.55.0

Schroeder H.; Allen C.W.1; Hiller J.M.2
1 ANL, Argonne, USA
2 Madison Area Techn. Coll., Madison, USA
In situ study of dislocation behaviour in columnar of Al thin films on Si-substrate during thermal cycling
MRS Fall Meeting 1999, Boston Symposium V "Thin Films - Stresses and Mechancial Properties VIII", 30.11.99
23.42.0

Patents granted

Speier W.; Szot K.:
ABO_3 Perowskit mit Stufe
DE: 19808778 (01.06.99)
PT 1.1563
23.42.0

Patents applied for

Baldus O.; Waser R.; Krasser W.:
Lasersystem mit steuerbarer Pulsdauer
DE: 199 (.12.99)
PT 1.1754
23.42.0

Baldus O.; Waser R., Krasser W.:
Verfahren zur Herstellung einer kristallisierten keramischen Schicht durch Laser-Annealing
DE 199 (.12.99)
PT 1.1755
23.42.0

Grossmann M. 1; Hoffmann S.; Slowak R.1; Waser, R.
1 Institut für Werkstoffe der Elektrotechnik
Keramischer Mehrlagen-Dünnschichtkondensator
PT 1.1560
Deutsche Patentanmeldung 198 06 002.5
23.42.0

Hoffmann S.; Waser R.; Slowak R.1; Liedtke R.1
1 Institut für Werkstoffe der Elektrotechnik, RWTH Aachen
Dünnschichtkondensator
Deutsche Patentanmeldung 199 42 341.5

Kohlstedt H.H.
Speicherkondensator
Deutsche Patentanmeldung 199 32 844.7
23.42.0

Kohlstedt, H.H.; Rottländer P.
Verfahren zur Herstellung eines magnetischen Tunnelkontaktes sowie magnetischer Tunnelkontakt
DE 199 38 215.8
23.42.0

Rickes J.; Tiedke S.1
1 Institut für Werkstoffe der Elektrotechnik, RWTH Aachen
Ein-/Ausleseverfahren zur Speicherung/Ausgabe eines Signalmusters unter Verwendung eines dynamischen Halbleiterspeichers
Deutsche Patentanmeldung 199 40 923.4
23.42.0

Speier W.; Szot K.:
ABO_3-Perowski mit Stufe
PCT: PCT/DE99/00587 (25.02.99) (EP,US,JP)
PT 1.1563
23.32.0

Szot K., Speier W.1
1 Institut für Chemische Analysen
Teleskopartiger Mikromanipulator mit Piezomaterialien
Deutsche Patentanmeldung 199 16 277.8-15

Waser R.; Baldus O.; Hoffmann S.; Schuster A.:
Verfahren zur Herstellung einer oder mehrer kristallisierter keramischer Dünnschichten sowie Bauelement mit einer solchen Schicht
PCT: PCT/DE 99/00478 (15.02.99) (EP,US,JP,KR)
PT 1.1557
23.42.0

Lecture courses

Ehrhart P.
Präparation dünner Schichten: Molekularstrahlepitaxie
30. IFF-Ferienkurs "Magnetische Schichtsysteme in Forschung und Anwendung", 01.03.1999
23.42.0

Ehrhart P.; Lüth H.1; Mantl S.1
1 Institut für Schicht- und Ionentechnik
Physik moderner Halbleiterbauelemente
RWTH Vorlesung SS 99
23.42.0

Schober T.
Untersuchung von Materialien mit Elektronen- und Röntgenstrahlen
RWTH Aachen, WS 1999/2000
23.42.0

Schroeder H.
Neue Materialien und Bauelemente für die Informationstechnik I
RWTH Aachen, WS 1999/2000
23.42.0

Schroeder H.
Theoretische Metallkunde I
RWTH Aachen, WS 1999/2000
23.42.0

Schroeder H.
Theoretische Metallkunde I
RWTH Aachen, WS 98/99
23.42.0

Waser R.
Vorlesung Werkstoffe der Elektrotechnik
Sensoren und Sensormeßtechnik I+II
RWTH Aachen

Waser, R.; Ehrhart P., Hoffmann S.; Kohlstedt H.H.; Schroeder, H.

Neue Materialien und Bauelemente für die Informationstechnik
I
RWTH Aachen, WS 1999/2000
23.42.0

Internal reports

Schroeder H.
Leckstromeigenschaften elektrokeramischer Dünnschichten
Seminar des Instituts für Werkstoffe der Elektrotechnik der
RWTH Aachen, 27.10.1999
23.42.0

Waser R.
Chancen und Perspektiven elektrokeramischer Materialien in
der Informations- und Sensortechnik
IFF-Kolloquium, 05.02.1999

Institute for Microstructure Research

General Overview

The Institut für Mikrostrukturforschung (Institute for Microstructure Research) is working in a number of scientific fields. These were selected with an emphasis on modern-materials aspects, on the importance of an atomistic and microstructural understanding for materials performance and, if possible, on the possibility of an evolution of research into technical devices. The goal is an interdisciplinary research group working on a spectrum of scientific problems sufficiently wide to allow a flexible and rapid reaction to new scientific developments. In some of these fields the competence should span the whole range from materials preparation via basic physics investigations to technical devices. In others access to interesting materials and device problems is provided by qualified collaborations inside and outside the Jülich research centre. Besides this general-physics and technology part of the institute there is a second part of special competence. This is the structure research by means of modern transmission electron microscopy and scanning tunnelling microscopy. This work is carried out within the Centre for High-Resolution Electron Microscopy. It is operated by the institute and serves a wider community of users.

Research Fields

The research fields can be characterised as follows:

(1) Ceramic Superconductors: Here the emphasis is (a) on thin-film and heterostructures production, Josephson effects, and their application in magnetometer systems and spectroscopic techniques.

(2) Semiconductors: Here the emphasis is on III-V compounds. In collaboration with various research groups we are studying, mainly by transmission electron microscopy, the growth of thin films and heterostructures and problems related to the production and application of low-temperature GaAs. Another topic is the study of electronic states in compound semiconductors by scanning tunnelling microscopy employing a technique pioneered in our group. It permits, via the detection of the far-reaching Debye screening cloud at the surface, an investigation of charged doping or impurity atoms in the bulk of the samples.

(3) Metallic Alloys: These are at present quasicrystalline alloys and related normalcrystalline approximants. We are growing large single-quasicrystals for our own research but also for users world-wide, in particular for the participants in the DFG priority program on quasicrystals. Our own work on quasicrystals and approximants concentrates on phase-diagrams, plasticity and surface physics.

(4) Electroceramics: In the field of electroceramic materials we take advantage of our long-standing experience with respect to perovscitic materials both in preparation and in microstructure research by means of transmission electron microscopy. In collaboration with the Institut für Electrokeramische Materialien (Prof. Waser) we dedicate a large research capacity to the investigation of the structural aspects of the production and properties of electroceramic thin films.

(5) High-Resolution Electron Microscopy: Although in the beginning primarily considered as a tool for high-quality materials investigations the theoretical, methodical and technical aspects of atomic-resolution transmission electron microscopy have in recent years become one of the central fields of interest of our group. We have developed special competence in the theory of high-resolution electron microscopy. Advanced application packages for the exit wave-function reconstruction are installed and serviced by us world-wide. Since 1991 and 1997 we have in collaboration with EMBL Heidelberg and Technical University of Darmstadt developed the word's first aberration-corrected transmission electron microscope with record resolution, 1.3 Å at 200 kV. These developments are continued (see below).

Equipment

The institute has at its disposal sputtering deposition machines, some of them with three-target facilities which were developed and built in the institute for the high-quality deposition of ceramic superconductor thin films and heterostructures. For device production local clean room, structuring and packaging facilities are available.

The institute operates together with the Institut für Streumethoden (Prof. Brückel) the laboratory for crystal-growth which was part of the former Institut für Materialentwicklung (Prof. Wenzl). This permits to maintain part of the outstanding expertise in the field of crystal growth for the benefit of the whole Department.

The institute operates the Jülich Centre for High-Resolution Electron Microscopy with two 400 kV JEOL machines of the type 4000 EX/FX, a JEOL 2000 EX, a PHILIPS CM20 FEG, the spherical-aberration corrected PHILIPS CM200 FEG and a JEOL 840A scanning microscope.

The priority in scanning tunnelling microscopy is on high-temperature investigations a field only rarely served by other competing groups. We have at our disposal two microscopes with in-situ cleaving facilities and ex-situ heating up to 750 °C. These instruments were designed and built inside the institute. An in-situ heating STM (Omicron) was installed and successfully tested end of 1999.

For the work on alloy plasticity a ZWICK mechanical testing system has been installed in 1998. The collaboration with the Max-Planck-Institut für Mikrostrukturphysik at Halle in this field is continued.

Special results and developments

The institute was very successful in recent years in application of high-temperature superconductivity to communication systems. In particular the dielectric, and more recently the multipole dielectric filters designed in the institute received considerable attention world-wide. In 1998, as partner of BOSCH, we won the competition for a project "High-Temperature Superconductivity for the Communication Technology of the Future" which became one of the five priority programs of the German Federal Minister of Science and Technology. We also succeeded in obtaining funding for a project with the same title by the HGF-Strategiefonds. During the year 1999, in the course of a reorganisation of the Institut für Schicht- und Ionentechnik (ISI), Dr. Norbert Klein, who was responsible for our high-frequency superconductivity research, became head of the superconductivity group in ISI. In fact the very technology-oriented research of our group fits well into the mission of ISI. The free capacity, both with respect to personnel and funds, obtained in our institute by the shift of the whole high-frequency research group to ISI offers an excellent opportunity for development of new research competence.

Due to our unique position in this field we choose to direct our resources towards the development of Hilbert-transform spectroscopy. This technique provides an excellent and novel tool for spectroscopy in the frequency range of 10^{10} to 10^{13} Hertz. It is broad band and orders of magnitude faster than Fourier spectroscopy. Here we have an excellent collaboration with the Institute for Radioelectronics in Moscow. We succeeded in acquiring a BMBF-project for the development of a fast gas-spectrometer and a project with DESY, Hamburg. The latter is a consequence of our successful test of Hilbert-transform spectroscopy for the determination of the shape of electron bunches in the beam of the TESLA test facility in Hamburg. The goals are: Improving the sensitivity of the technique by development of even better Josephson junctions and constructing facilities for fast molecule spectroscopy in our own group.

Our dc-SQUIDs on the basis of ramp-type junction geometry continue their success both in performance and in their acceptance on the market. As a supplier of TRISTAN Company (USA, formerly Conductus) we deliver a larger number of SQUIDs and magnetometers per month. The new developments arising from the market demands are still meeting our scientific interests. Our dc-SQUIDs are also employed in a number of projects carried out together with ISI. Outstanding is the success of an investigation on stress-corroded steel rods in the concrete of highway-bridges in which cracks could be detected. This technique is under consideration for routine inspection of bridges on German highways.

The strategy for further developments in superconductivity will be to use our expertise in front technology in this field to develop applications which can also be used for our own research. Hilbert-transform spectroscopy has already been mentioned. SQUID-microscopy is another field. This project has been intensively followed in 1999 in a collaboration with ZEL (Prof. Halling) with the aim to built a SQUID-microscope prototype within this year 2000.

The successful project of the spherical-aberration corrected transmission electron microscope described above has triggered a priority program of the DFG. In the framework of this new program 3.8 Mio DM were granted in 1998 to our institute for the development, in collaboration with CEOS Company, Heidelberg, and ZEISS-LEO, Oberkochen, of the world's first Subangström-Instrument. Besides ultra-high resolution the 200 kV machine will contain a monochromator and an in-column energy filter of the Krahl-type. This will maintain the institute's position as a pioneer in advanced instrument development.

The institute is partner of PHILIPS Electron Optics with respect to theory and application of exit-wave function reconstruction in high-resolution electron microscopy. In this field our institute is respected as an international key institute. Recent developments, in particular in computer-controlled alignment, will be subject of further industry collaboration.

The quasicrystal group has currently three DFG funded projects. During 1999 we were lucky to find good scientists for the positions offered by DFG. This also concerns a young engineer, Carsten Thomas, who will be able to run a part of our crystal-growth facilities after the retirements expected for 2001. Great efforts went into a new PhD program with the Russian Academy of Sciences and other GUS state universities and universities in China. In the framework of this special program designed by the institute and the partners abroad the PhD students are working two years in Jülich on a grant supervised by the Jülich Doktorandenausschuß, but they will pass their examina in their home university.

We are happy that Mr. Werner Pieper joined our group in 1999 as an engineer. He will take over Jörg Hanssen's position after his retirement in early 2000. Mr. Hanssen was the technical father of our Electron Microscopy Centre from its very beginning in 1987 and he has rendered invaluable services to our group.

It is always difficult to select a few of the outstanding results and bring them to special attention here. This year the following results are mentioned:

- In a $\Sigma 3\{111\}$ twin boundary in $BaTiO_3$ an expansion of the Ti-Ti spacing across the boundary and a contraction of the nearest BaO-BaO spacing was measured for the first time using quantitative phase-retrieval electron microscopy. This technique was pioneered in our group (Phys. Rev. Lett. 82, 5052, 1999).
- A new pronounced effect of the dopant Te atoms on the roughness, morphology and optical mirror properties of GaAs cleavage surfaces was detected by means of STM (Appl. Phys. Lett. 76, 300, 2000).
- By means of STM and Monte Carlo simulations strong many body effects were demonstrated in Zn-dopant atom clustering in GaAs. These result in an effective attractive interaction in addition to the screened Coulomb repulsion between charged dopants (Phys. Rev. Lett. 83, 757, 1999).

Knut Urban

Institute for Microstructure Research

Personnel 1999 / 2000 and areas of activity

Scientific Staff

Dr. Y. Divin	Hilbert-spectroscopy	(23.42.0)
Dr. Ph. Ebert	Scanning tunnelling microscopy of semiconductors and quasicrystals	(23.55.0)
Dr. M. Faley	High-Tc-Superconductor SQUIDs	(23.42.0)
Dr. M. Feuerbacher	Plasticity of quasicrystals	(23.55.0)
Dr. B. Grushko	Crystal growth, phase diagrams of alloys	(23.55.0)
Dr. C.L. Jia	Characterization of superconductors, diamond and electroceramic films by high resolution electron microsopy	(23.42.0)
Dr. M. Luysberg	Transmission electron microscopy of semiconductor heterostructures, low temperature GaAs and microcrystalline silicon	(23.42.0)
Dr. U. Poppe	Superconductivity, tunneling spectroscopy, High-Tc superconductor thin films and multilayers	(23.42.0)
Dr. H. Soltner	High-Tc thin films and heterostructures, Josephson junctions and SQUIDs, SQUID-Microscopy	(23.42.0)
Dr. A. Thust	Reconstruction techniques in high-resolution electron microscopy, Cs-corrected Transmission Electron Microscopy for imaging of interfaces in semiconductors, electron microscopy of superconducting materials	(23.42.0, 23.55.0)
Prof. Dr. K. Urban	Head of Institute	(23.42.0, 23.55.0)

Technical Staff

M. Beyss	Crystal growth, Materials preparation and characterization	(23.55.0)
DI W. Evers	Physical experimental technique, low temperature technique, thin film production	(23.55.0, 23.42.0)
A. Fattah	Crystal growth, Materials preparation and characterization	(23.55.0)
K. Fischer	Crystal growth, Materials preparation and characterization	(23.55.0)
R. Fischer	Metallography, materials preparation and characterization	(23.55.0)
DI K.-H. Graf	Electronics, electronic data processing, scanning tunnelling microscopy	(23.55.0, 23.42.0)
J. Hanssen	Technical supervisor, Center of High Resolution Electron Microscopy	(23.55.0, 32.42.0)
D. Meertens	Metallography, semiconductor preparation, scanning- and transmission electron microscopy	(23.55.0, 23.42.0)
W. Pieper	Technical supervisor, Center of High Resolution Electron Microscopy	(23.55.0, 32.42.0)
I. Rische-Radloff	Secretary	
C. Thomas	Crystal growth, Materials preparation and characterization	(23.55.0)
G. Waßenhoven	Photolaboratory, photography technique	(23.55.0, 23.42.0)
E. Würtz	Metallography, semiconductor preparation, scanning- and transmission electron microscopy	(23.55.0, 23.42.0)

Post-doc

Dr. M. Lentzen	Reconstruction techniques in high-resolution electron microscopy, Cs-corrected transmission electron Microscopy for imaging of interfaces in Semiconductors and of superconducting materials	(23.42.0)

Doctor students

V. Chirotov	Broadband Hilbert-Transform Spectroscopy with high-Tc Josephson junctions	(23.42.0)
B. Jahnen	Interdiffusion in antimonid-based heterostructures	(23.42.0)
Ch. Lei	Investigation of lattice defects in electroceramic thin films by high resolution electron microscopy	(23.42.0)
R. Rosenfeld	Phase reconstruction techniques in high-resolution electron microscopy, electron microscopy of electroceramic Materials	(23.42.0)
P. Schall	Plasticity of quasicrystals and related intermetallic phases	(23.55.0)
F. Kluge	Scanning tunnelling microscopy of quasicrystals	(23.42.0)
M. Winter	Microwave frequency standards	(23.42.0)
M. Yurechko	Formation of intermetallic phases in ternary alloys of aluminium with transition metals	(23.55.0)

Diploma students

B. Jungbluth	Simulation and experiments for optimization of a high permeability magnetic conductor for the application in a squid-microscope	(23.42.0)
M. Heggen	Investigation of plastic behaviour of icosahedral Zn-Mg-Re quasicrystals	(23.55.0)
R. Ott	Production of structured dielectric layer systems and investigation of their dielectric properties in dependence of morphology and granularity.	(23.42.0)
P. Quadbeck	Scanning tunnelling microscopy of Si and Te-doped GaAs	(23.42.0)
C. Scholten	Influence of the microstructure of microcrystalline silicon solar cells on their optoelectronic properties	(23.42.0)

Guests

Dr. T. Cai	STM of semiconductors	(23.42.0)
Dr. J. Chen	Cs-corrected Transmission Electron Microscopy	(23.42.0)
Dr. M. Vijayalakshmi	Irradiation-induced phase transformations in quasicrystals	(23.55.0)
Dr. J. Wu	Electronmicroscopy and production of perovscitic quasicrystals	(23.42.0)

Limitations to epitaxial growth of low-temperature grown GaAs

M. Luysberg

Institut für Mikrostrukturforschung

Even at low growth temperatures molecular beam epitaxy is successfully applied to deposit perfect epitaxial GaAs layers onto GaAs substrates. However, the single-crystalline growth extends only up to a certain epitaxial thickness, where a change in growth mode to a columnar, polycrystalline growth is observed. We investigate the influence of different growth parameters, i.e. temperature, As/Ga flux ratio and Be-doping level, on the breakdown of epitaxial growth. The breakdown of single-crystalline growth is governed by the formation of pyramidal defects consisting of microtwins, stacking faults and dislocations, which mark the onset of the polycrystalline growth. The nucleation of the defects is found to be clearly correlated with hillocks on the growing surface. Furthermore, an anisotropy of the shape of the hillocks and of the type of defects is observed when comparing the (011) and (0-11) orientation.

F&E-Nr: 2342 8000

The unique properties of GaAs grown by MBE at low temperatures (LT-GaAs) make this material suitable for device applications like terahertz photodetectors. The ultrashort carrier lifetimes and the high resistivity in annealed samples can be attributed to the incorporation of excess As during growth. The formation of a high density of up to 10^{20} cm^{-3} As antisite defects induces a dilation of the GaAs lattice, which leads to a mismatch of up to 0.16% between the LT-GaAs layer and the GaAs substrate [1]. Despite the low growth temperatures the as-grown LT-GaAs layers are free of structural defects such as dislocations or precipitates. However, the perfect single crystalline growth extends only up to a certain thickness, where a change in growth mode is observed. The mechanisms of the breakdown of single crystallinity are investigated for Be-doped and undoped LT-GaAs samples grown by MBE in a temperature range of 150°C to 200°C using beam equivalent pessure (BEP) ratios of 11 to 40.

The breakdown of single crystalline growth is governed by the formation of "pyramidal" defects consisting of a high density of microtwins, stacking faults and dislocations [2]. The epitaxial thickness D_{epi} to which the layers can be grown single-crystalline is summarized in Figure 1. D_{epi} is defined as the distance from the substrate/epilayer interface where the epitaxial (single-crystalline) volume fraction is 50%. D_{epi} increases with increasing growth temperature and decreasing As/Ga flux ratio as measured by the BEP ratio. In particular at low growth temperatures (155°C) the epitaxial thickness varies within a factor of 2, which may be indicative of local inhomogeneities and/or different impurity levels. In case of high Be doping levels of 10^{20} cm^{-3}, a considerably smaller epitaxial thickness is observed (Fig. 1). Again, a larger thickness is found for smaller BEP ratio values. The lowering of the growth temperature and/or the increase of the BEP ratio results in higher As_{Ga} concentrations incorporated during growth [3]. The increase of the non-stoichiometry may contribute to the instability of the perfect single crystalline growth.

The formation of defects leading to the breakdown of single-crystalline growth is illustrated in the bright field TEM images of a LT-GaAs sample grown at 200°C and a BEP ratio of 20 (Fig. 2). The sample is shown in two

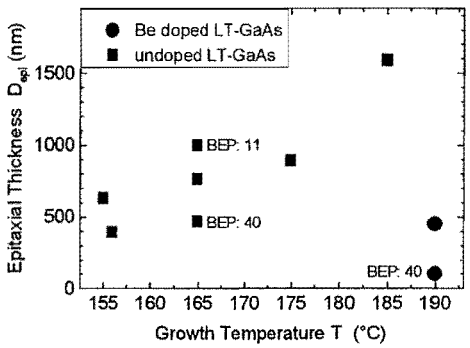

Figure 1: Epitaxial thickness plotted versus the growth temperature. All samples were grown at a BEP ratio of 20 unless indicated differently.

different {110} orientations. AlAs marker layers were introduced to monitor the morphology of the growth front. A defect-free, epitaxial layer extends from the GaAs substrate (marked by arrows) up to a thickness of about 1.3 µm. The AlAs marker layers reveal an anisotropic morphology of the growing surface, i.e. hillocks elongated along the [0-11] direction. In the (011) orientation the AlAs layers are perfectly flat and perpendicular to the [100] growth direction (Fig. 2a). In contrast, the (0-11) projection reveals increasing surface roughness with increasing thickness (Fig. 2b), which is seen more clearly in the (002) dark field image showing the AlAs marker layers as bright lines (Fig. 3). High resolution images reveal that the onset of defect formation occurs as soon as the faces of the hillocks approach a {111} facet [4].

Besides the surface morphology, the defect structure is also observed to be anisotropic. In both {110} projections planar defects like twins and stacking faults as well as dislocations are observed. However, the density of primary twins is much higher in the (011) orientation, where the planar defects lie on As terminated {111} planes. By contrast the (0-11) orientation reveals predominantly dense dislocation networks [4].

The results of the structural investigation clearly demonstrate the influence of surface roughening on the breakdown of epitaxy. Similar results were reported on the transition from epitaxial to amorphous growth of Si and GaAs [5]. In the case of low-temperature epitaxy thermally

activated processes with high activation energies are suppressed. Therefore, relaxation mechanisms, like the formation of misfit dislocations, are not the dominant processes. The same argument applies to stress induced surface diffusion, which has been evoked to explain surface roughening. However, it has to be pointed out that the formation of surface undulations and of the defects is not induced by global strain. This can be concluded from the fact, that some of the Be doped samples, which have a nearly vanishing lattice mismatch with respect to the substrate, show even smaller epitaxial thickness than it's undoped counterparts with a mismatch of about 0.16% (see Fig. 1). Therefore, kinetic roughening, i.e. statistical fluctuations during growth, has to be considered as dominant mechanism of the buildup of surface undulations. Recently, this model has been successfully applied to simulate the roughness measured by AFM of LT-GaAs samples [6]. The anisotropy was explained by anisotropic surface diffusion. On the other hand the role of excess As incorporation may have to be considered as well. The formation of As_{Ga} defects accounting for the non-stoichiometry imposes locally a dilation of the bonds. Therefore, the formation energy of As_{Ga} defects may be considerably lower on top of the hillocks, where the bonds are stretched. Although there is no evidence of inhomogeneous As_{Ga} incorporation on a macroscopic scale [2], microscopically the incorporation can be favored on top of the hillocks, which can gradually increase the buildup of surface undulations.

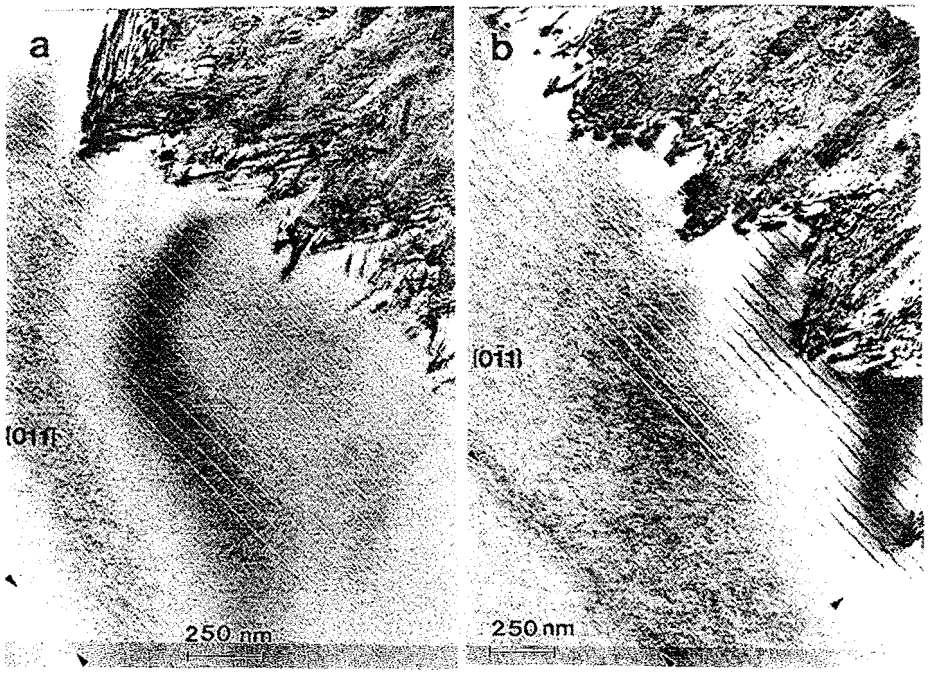

Figure 2: Bright field electron micrographs obtained with (004) two beam conditions (s>0). The cross sections in the (011) orientation (a) and (0-11) orientation (b) reveal the transition from epitaxial to polycrystalline growth. AlAs marker layers appear as bright lines. The substrate/epilayer interface is marked by arrows.

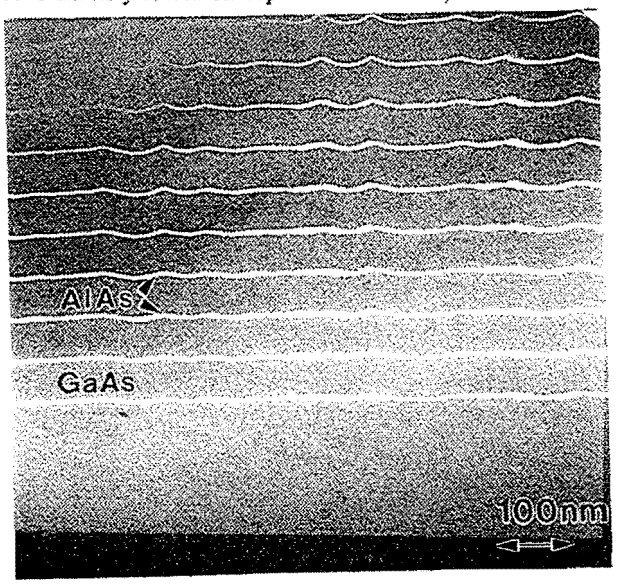

Figure 3: Dark field electron micrograph obtained with a (002) reflection. AlAs layers appear bright.

Acknowledgments:

MBE growth was performed in the NSF supported Integrated Materials Laboratory of UC Berkeley. The collavoration and fruitful dicussion with P.Specht and E.R. Weber are greatfully acknowledged.

References

[1] Liliental-Weber Z, Ager J, Look D, Lin X W, Liu X, Nishio J, Nichols K, Schaff W, Swider W, Wang W, Washburn J, Weber E R , and Whitaker J 1994, in: *Proc. of the 8th Conf. on Semiinsulating III-V Materials*, ed. M Godlewski (World Scientific) p. 305.

[2] Liliental-Weber Z, Mat. Res. Soc. Symp. Proc. 1992 **241** 101.

[3] Luysberg M, Sohn H, Prasad A, Specht P, Liliental-Weber Z, Weber E R , Gebauer J, and Krause-Rehberg R 1998, J. Appl. Phys. **83** 561.

[4] M. Luysberg, P. Specht, E. R. Weber *Proceedings of the XIth Conference on Microscopy of Semiconducting Materials*, 22-25 March 1999, Oxford, accepted for publication

[5] Eaglesham D J 1995, J. Appl. Phys. 77 3597

[6] Apostolopoulos G, Herfort J, Däweritz L, Ploog, K H, and Luysberg, M, submitted to Phys. Rev. B

The importance of many-body effects in the clustering of charged Zn dopant atoms in GaAs

Ph. Ebert[1], Tianjiao Zhang[2,3], F. Kluge[1], M. Simon[1], Zhenyu Zhang[3,2], and K. Urban[1]

[1] *Institut für Mikrostrukturforschung*
[2] *Department of Physics, University of Tennessee, Knoxville, TN 37996, U.S.A.*
[3] *Solid State Division, Oak Ridge National Laboratory, Oak Ridge, TN 37831, U.S.A.*

The spatial distribution of negatively charged Zn dopant atoms in GaAs has been investigated by cross-sectional scanning tunneling microscopy. The dopant atoms exhibit a clear clustering, suggesting the existence of an effective attractive interaction in addition to the screened Coulomb repulsion between two dopants. By analyzing the data through Monte Carlo simulations, we extracted the intrinsic screening length at different dopant densities and attributed the effective attraction to strong many-body effects in the dopant-dopant repulsion.

F&E numbers: 23.420, 23.550

The ability to incorporate reproducibly dopant atoms with precisely controlled concentrations and spatial distributions is essential in various technological applications of semiconductor materials. As the effort for device miniaturization continues to intensify, how to achieve this goal is becoming increasingly difficult. Dopant incorporation in submicrometer- and nanometer-scale systems is ultimately governed by the intrinsic interactions between the dopant atoms. The generally accepted view is that the charge of a dopant atom is screened by the charge carriers in a given semiconductor, resulting in a repulsive screened Coulomb interaction between the dopants [1]. Such a repulsion in turn will lead to a rather homogeneous distribution of the dopant atoms in the semiconductor.

Using cross-sectional scanning tunneling microscopy (XSTM) and Monte Carlo simulations we demonstrated that negatively charged Zn dopant atoms in GaAs are inhomogeneously distributed and form clusters of dopant atoms [2]. At the first sight, the clustering behavior seems to suggest the existence of an effective attractive interaction in addition to the screened Coulomb repulsion between two dopants. Our quantitative analysis of the dopant distributions by Monte Carlo simulations leads to the conclusion that the effective attraction actually results from strong many-body effects in the otherwise repulsive dopant-dopant interactions. Furthermore, we illustrate a methodology to determine quantitatively the intrinsic screening length of point charges in semiconductors based on a statistical analysis of the positions of dopant atoms in XSTM images.

We investigated Zn-doped GaAs crystals with different carrier concentrations (n) ranging between 2.5×10^{18} and 2.5×10^{20} cm^{-3}. The Zn dopant atoms were introduced into the crystals during growth ($n<10^{20}$ cm^{-3}) or by diffusion at $\approx$1180 K ($n>10^{20}$ cm^{-3}). Samples cut from the different crystals were cleaved in ultrahigh vacuum and the isolated dopant atoms exposed on the (110) cleavage surfaces were imaged with atomic resolution by XSTM.

Figure 1a shows a typical STM image of such a cleavage surface. The dopant atoms appear as bright bright contrast features arising from the imaging of the local screening potential around the isolated charged dopants [3]. One of the most distinctive features in the STM images is the long-range contrast change (on the scale of about 5 to 10 nm) superposed on the localized features of the dopant atoms. The long-range contrast is the signature of variations of the local band bending, namely, the position of the valence band edge changes locally relative to the Fermi level [3]. In order to unravel the origin of this effect, we calculated the local concentrations of dopant atoms (Fig. 1b). Figure 1b demonstrates that the concentration of the dopant atoms varies by nearly one order of magnitude on the scale of about 10 nm and all the bright areas in Fig. 1b correspond to the bright areas in Fig. 1a. Thus local fluctuations of the dopant concentration on the scale of about 10 nm cause fluctuations of the Fermi level on the same scale imaged as long-range contrast in Fig. 1a. Figure 1 also demonstrates that the dopant atoms tend to cluster. Because we have observed the clustering of dopants in all the samples investigated the observed effect is not simply due to sample preparation, but rather an intrinsic nature of the dopants. To our knowledge this is the first direct observation of clustering of dopant atoms on such a length scale.

As mentioned earlier, all the dopant atoms are negatively charged, and should therefore mutually interact

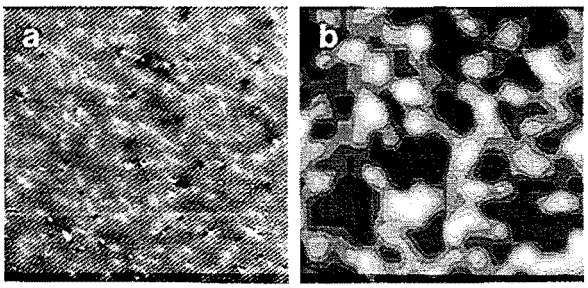

Fig. 1 (a) STM image of a 70×70 nm^2 area of the (110) cleavage surface of 2.5×10^{20} Zn cm^{-3} doped GaAs. A long range contrast variation is superposed onto the atomic-scale corrugation of the atomic rows along the [1$\bar{1}$0] direction. The bright contrast features are dopant atoms. (b) Local concentration of the dopant atoms. A high concentration is shown as white contrast. The images show a clustering of the dopant atoms.

with the repulsive screened Coulomb potential

$$V(r) = \frac{e}{4\pi\varepsilon_0\varepsilon_r} \cdot \frac{1}{r} \cdot e^{-\frac{r}{R_S}} \quad . \tag{1}$$

with R_S being the screening length

$$R_S = \sqrt{\frac{2\pi^2\varepsilon_0\varepsilon_r\hbar^3}{e^2\,(m_e)^{3/2}\cdot(2\pi\,kT)^{1/2}\cdot F_{-1/2}(\eta)}} \quad . \tag{2}$$

$F_k(\eta)$ are the Fermi-Dirac integrals with the reduced Fermi energy $\eta = E_F/kT$. Therefore we proceed by first studying the effects of the short-range repulsion on the dopant distribution. The existence of the short-range repulsion is clearly indicated by the fact that although clustering occurs the probability of finding a very close pair of dopant atoms is negligible. In order to quantify the repulsive interaction we deduced from the XSTM images the pair correlation function c(r), which is related to the mean force potential, $W(r)$, through [4]

$$W(r) = -kT \cdot \ln[c(r)] \quad . \tag{3}$$

It should be noted that only if the extension of the interaction is smaller than the average separation of the dopants, correlation effects can be neglected and the mean force potential equals the interaction energy.

The data values $-\ln[c(r)]$ as a function of the distance r show in all cases a repulsive interaction, whose extension increases from 2 to 5 nm if the carrier concentration decreases. This reflects the carrier concentration dependence of the screening (Eq. 2). If we assume the low dopant density limit, we can fit the data shown with a Yukawa potential and determine the screening length as a function of the carrier concentration (filled squares in Fig. 2). As expected, the screening length increases with decreasing carrier concentration. However, the data does not agree quantitatively with the theoretical values for the screening length (solid line in Fig. 2) determined according to Eq. (2).

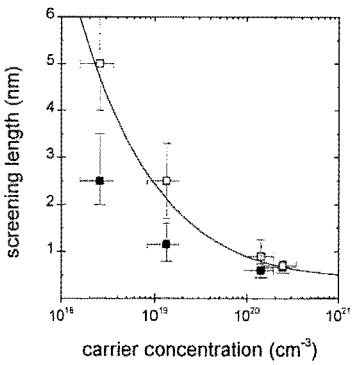

Fig. 2 Screening lengths R_S determined from the pair correlation function as a function of the carrier concentration (filled squares). The solid line represents the theoretical screening length calculated according to Eq. (2). The open squares show the screening length corrected for many-body interactions.

The effective attraction between the dopants and the discrepancy in the screening lengths described above, both strongly suggest the importance of many-body effects in the otherwise repulsive interaction between the dopants. For a collection of mutually repelling particles, many-body effects can result in oscillatory features in the pair correlation function, with the minima indicating effective attractive interactions [4,5]. Furthermore, if the repulsion is a screened one, such as here, many-body effects can also result in a shorter apparent screening length than the true one. To demonstrate that this is indeed the case for the present system, we have performed Monte-Carlo simulations of the experiment and analyzed the spatial distribution as we did for the XSTM images. We determined the (output) screening length from the simulated pair correlation function for different (input) screening lengths of the Yukawa potential. At the experimental dopant concentrations the output screening lengths are considerably smaller than the input screening lengths due to many-body effects, i.e. interactions between more than two dopants. Using these simulations we determined the intrinsic screening length in GaAs crystals as a function of the carrier concentration by comparing the measured screening length with the output screening length of the simulation. The corresponding input screening length is the intrinsic one (empty squares in Fig. 2), which agrees very well with the theoretical calculations according to Eq. (2). We note that Fig. 2 shows the first quantitative microscopic measurement of the screening length in semiconductors.

The importance of many-body effects is further corroborated by the simulated pair correlation function, which shows beyond the short-range repulsive core, a clear attractive part [2] leading to the observed clustering of dopant atoms.

In conclusion, we have used cross-sectional scanning tunneling microscopy to demonstrate that negatively charged Zn dopant atoms in GaAs are inhomogeneously distributed and form clusters of dopant atoms. The clustering behavior suggests the existence of a possible attractive interaction in addition to the screened Coulomb repulsion between the dopants. Our quantitative analysis of the dopant distributions by Monte Carlo simulations leads to the conclusion that the effective attraction actually results from strong many-body effects in the otherwise repulsive dopant-dopant interactions. Many-body effects are also shown to be important in extracting the intrinsic screening length of the Yukawa potential as a function of the carrier concentration in the system. Our study reveals a basic physical origin limiting the homogeneity of dopant atoms achievable in semiconductors.

[1] R. B. Dingle, Philos. Mag. **46**, 861 (1955).

[2] Ph. Ebert, T. Zhang, F. Kluge, M. Simon, Z. Zhang, and K. Urban, Phys. Rev. Lett. **83**, 757-760 (1999).

[3] Ph. Ebert, Surf. Sci. Reports **33**, 121-304 (1999).

[4] T.L. Hill, *Statistical Mechanics* (McGraw-Hill, New York, 1956).

[5] T. T. Tsong, Phys. Rev. Lett. **31**, 1207 (1973).

Constitution of Al-Pd alloys with Mn and Co

B. Grushko and M. Yurechko

Institut für Mikrostructurforschung

A part of the Al-Pd-Mn phase diagram in the vicinity of the icosahedral phase was refined. The Al-rich part of the Al-Pd-Co phase diagram was investigated for the first time. The phase usually designated Al_3Pd is formed at lower Al than according to the formula and exhibits two different structural variants depending on composition. It extends to the ternary compositions up to about 5 at.% Mn or 18 at.% Co. Three ternary Al-Pd-Co phases were observed.

F&E-Nr:

The interest in the Al-(Ni,Pd)-(Mn,Fe,Co) phase diagrams is due to the discovery of quasicrystals in these alloy systems. The phase equilibrium in Al-Pd-Mn was earlier studied [1] but the compositional ranges of phases were only determined very approximately. More precise knowledge of the composition of the icosahedral phase (I-APM) is necessary because its single quasicrystals are regularly produced in the crystal growth group of IFF for the internal and external use. Also the orthorhombic phase based on Al_3Pd (also called ξ' *approximant*) becomes attractive due to its suggested structural similarity to quasicrystals. There is also some information on Al-Pd-Fe [2] but not on Al-Pd-Co.

In the reported research the region of the Al-Pd-Mn phase diagram close to I-APM was refined. Partial isothermal sections at 710, 850, 870 and 880°C were published [3]. The composition and precipitation behavior of the I-APM single quasicrystals was studied in more detail [4]. The Al-rich part of Al-Pd-Co was investigated for the first time at 790-1050°C. Some preliminary results are included in [5]. Investigation of the ternary alloy systems required reinvestigation of Al-Pd close to Al_3Pd.

"Al_3Pd" in Al-Pd and Al-Pd-Mn. The orthorhombic phase usually designated Al_3Pd was observed in two variants in a compositional range which at 710°C was between 71.5 and 72.5 at.% Al. The lattice parameters a=2.35 and b=1.65 nm were the same in both variants while the lattice parameter c=1.23 nm was observed at the higher Al limit and c=4.59 (i.e. in about 22/6 times more) at the lower Al limit (see Fig.1). The structures are designated ε_6 and ε_{22} accordingly. A further revision of the Al-Pd phase diagram is required. The ε_{22}-phase extends to the ternary compositions up to about 5 at.% Mn. The miscibility of Mn in ε_6 is not clear. In samples containing about 4 at.% Mn this phase (so-called ξ') seems to be metastable. The ε_{22}-phase can dissolve significantly more Co (see below).

Al-Pd-Mn I-phase. Our refinement of Al-Pd-Mn [3] revealed that between 710°C and the highest melting point (about 890°C) the overall composition of I-APM ranges in 5.8-10.5 at.% Mn and 69.5-71.5 at.% Al. It shifts to lower Mn at lower temperatures. This is argued in [4] that I-APM (stable or metastable) forms in the whole range between about $Al_{78}Mn_{22}$ and $Al_{70}Pd_{25}Mn_5$. Accordingly, the basic composition of I-APM should be *binary*. Pd is not necessary for the formation of the I-phase but necessary for its stability. Pd can replace Mn in I-APM, a decrease of the Al concentration with the increase of Pd could also be achieved by replacement of Al by Pd or by formation of vacancies.

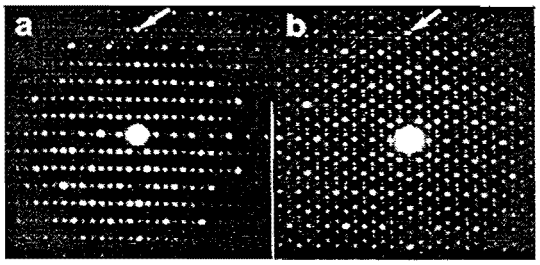

Fig.1. The [010] electron diffraction patterns of ε_6 (a) and ε_{22} (b). The arrows show the 6-th and 22-th reflections of the corresponding interplanar distances.

Precipitation in single I-APM quasicrystals. The typical composition of the studied single quasicrystals was found to be around $Al_{70.5}Pd_{21.0}Mn_{8.5}$, which corresponds to the high-Mn limit of the I-APM region at 710°C (Fig.2).

The samples annealed at 600°C for more than 2000 h contained numerous precipitates whose composition was typical of the H-phase (the ternary extension of high-temperature $Al_{11}Mn_4$). The samples did not contain pores after this heat treatment in contrast to as-grown I-APM which always contained faceted pores of about 10 to 50 μm in diameter. Formation of the precipitates starts

around the pores in the as-grown material and occur via intermediate stages. Precipitates were first observed after annealing for 3 h at 600°C and were similar after 15 and 150 h except that with longer annealing the affected areas were larger. Annealing at 800°C results in the dissolution of precipitates. Formation of precipitates indicates the super-saturated state of our standard single I-APM quasicrystals and may result in specific diffraction effects close to the Bragg reflections. Some effects were indeed observed in I-APM and related to a phason disorder typical of quasicrystals [6]. In contrast to the intended phason disorder, formation of diffuse scattering due to pre-precipitation phenomena in quasicrystals does not follow from their specific quasiperiodicity [4].

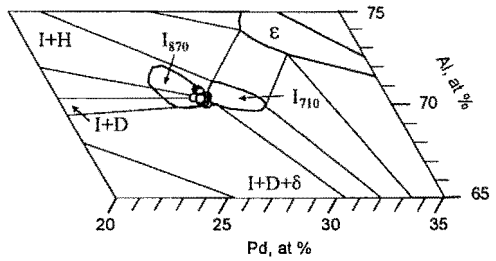

Fig.2 Partial 710°C isothermal section of the Al-Pd-Mn system and the I-APM range at 870°C [4]. The "standard" compositions of single-crystal I-APM are marked by the open circles.

Al-Pd-Co. The study was based on the Al-Co phase diagram in [7]. At 1050°C the isostructural AlCo and AlPd phases form the continuous range of solid solutions β. Al_5Co_2 exhibited extensions to the ternary composition up to about 3.0 at.% Pd and the Z-phase up to 3.4 at.% Pd. Ternary phases were also revealed at this temperature. One was identified with the orthorhombic W-phase [8] (a=2.36, b=0.82 and c=2.07 nm) exhibiting a strong resemblance to the decagonal phase formed in the same rapidly solidified alloys. Another, new phase designated V exhibited diffraction pattern very similar to that of monoclinic $Al_{70}Rh_{30}$ [9]. It was indexed suggesting a primitive monoclinic unit cell with a=1.0068 nm, b=0.3755 nm, c=0.6512 nm and β=102.38°.

At 790°C an additional phase was found in ternary alloys containing 73-75 at.% Al. Single-phase samples were obtained at 5.0, 8.0, 10.0 and 13.8 at.% Co and they exhibited powder XRD patterns very similar to that associated with orthorhombic ε_{22}. This ternary extension of ε_{22} can contain up to 18 at.% Co. At the high-Co limit it was found in equilibrium (see Fig.3) with Al_5Co_2(Pd), Al_9Co_2(Pd) and Y'-phase (not clear yet monoclinic or orthorhombic, see [10] for detail) and a new ternary phase designated U. Electron diffraction revealed that the U-phase has a periodic structure. At 790°C the U-phase was found in the range between $Al_{68.8}Pd_{18.6}Co_{12.6}$ and $Al_{69.8}Pd_{13.8}Co_{16.4}$.

In agreement with the literature data our study did not reveal any stable decagonal phase (D-phase) in Al-Pd-Co while the stable D-phase is formed in a wide compositional range in Al-Ni-Co [11]. At the compositions corresponding in Al-Ni-Co to the high-Co D-phase the W-phase is formed in Al-Pd-Co. This phase belongs to the so-called *pseudodecagonal* structures which were also observed in Al-Ni-Co [12]. Results of the investigation of several pseudodecagonal structures in Al-Ni-Co [12] are in favor of their metastability. On the other hand, the Al-Pd-Co W-phase seems to be thermodynamically stable.

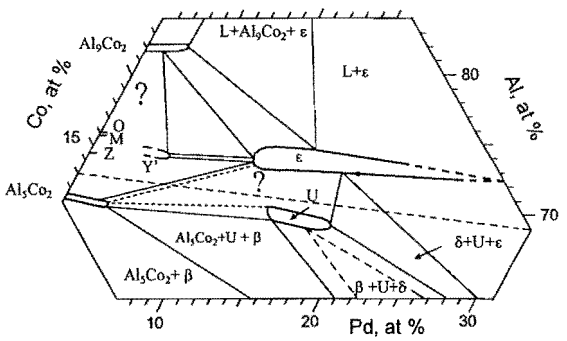

Fig.3. Partial Al-Pd-Co phase diagram at 790°C. M and O are monoclinic and orthorhombic $Al_{13}Co_4$ accordingly, δ is Al_3Pd_2, L is the liquid. The regions marked by ? are not investigated in detail. The broken line across the diagram indicates the compositions corresponding to the Al-Ni-Co D-phase.

References

[1] T. Gödecke and R. Lück, Z. Metallkd. 86 (1995) 2.
[2] F. Edler, Ph.D. Thesis. ETH Zürich, 1997.
[3] B. Grushko, M. Yurechko and N. Tamura, J. Alloys Comp. 290 (1999) 164.
[4] B. Grushko, Mater. Sci. Eng. A. Submitted.
[5] M. Yurechko and B. Grushko, Mater. Sci. Eng. A. Submitted.
[6] M. de Boissieu et al. Phys. Rev. Lett. B75 (1995) 89.
[7] B. Grushko et al., J. Alloys Comp. 233 (1996) 279.
[8] K. Yubuta, W. Sun and K. Hiraga, Phil. Mag., A75 (1997) 273.
[9] B. Grushko and M. Yurechko, Z. Metallkd. 214 (1999) 313.
[10] X.L. Ma, U. Köster and B. Grushko, Z. Metallkd. 213 (1997) 75.
[11] B. Grushko and D. Holland-Moritz, J Alloys Comp. 262-263 (1997) 350.
[12] B. Grushko, D. Holland-Moritz, R. Wittmann and G. Wilde, J Alloys Comp. 280 (1998) 215.

Publications in refereed journals

Braun St.1; Meyer D.C.1; Paufler P.1; Grushko B.
1 Institut für Kristallographie und Festkörperphysik, Fachrichtung Physik, Technische Universität Dresden, D-01062 Dresden
Short-range order in a thin film of decagonal Al-Co-Ni quasicrystal: calculated from a structure model and measured with EXAFS
23.55.0

Chao K.-J.1; Zhang Zhenyu2; Ebert Ph. and Shih C.K.1
1Dept. of Physics, University of Texas, Austin
2Solid State Division, Oak Ridge National Laboratory, Oak Ridge
Substrate effects on the formation of flat Ag films on (110) surfaces of III-V compound semiconductors.
Phys. Rev. B 60, 4988-4991 (1999).
23.55.0

Divin Y.Y.; Poppe U., Urban K., Volkov O.Y.1, Shirotov V.V.1, Pavlovskii V.V.1, Schueser P.2, Hanke K.2, Geitz M.2, Tonutti M.3
1 Institute of Radioengineering & Electronics of RAS, Moscow, 103907, Russia
2 DESY, Hamburg, D-22603, Germany
3 III Physikalisches Institut A, RWTH-Aachen, Aachen, D-52056, Germany
Hilbert-Transform Spectroscopy with High-Tc Josephson Junctions: First Spectrometers and First Applications.
IEEE Trans. Applied Supercond., Vol. 9, No. 2, 3346-3349 (1999)
23.42.0

Ebert Ph.
Nano-scale properties of defects in compound semiconductor surfaces
Surface Science Reports, Vol. 33, Nos. 4-8, 121-304 (1999)
23.55.0

Ebert Ph.1; Chao K.-J.1; Niu Q.1 and Shih C. K.1
1Dept. of Physics, University of Texas, Austin
Dislocations, phason defects, and domain walls in a one-dimensional quasiperiodic superstructure of a metallic thin film. Phys. Rev. Lett. 83, 3222-3225 (1999).
23.55.0

Ebert Ph.; , Zhang Tianjiao1,2; Kluge F.; Simon M.; Zhang Zhenyu 2,1 and Urban K.
1 Department of Physics, University of Tennessee, Knoxville, TN 37996
2 Solid State Division, Oak Ridge National Laboratory, Oak Ridge, TN 37831-6032
The importance of many-body effects in the clusterin of charged Zn dopant atoms in GaAs
Physical Review Letters 83, 757-760 (1999)
23.55.0

Ebert Ph.; Kluge F. and Urban K.
Evidence for a two-step evolution of the surface structure during heat treatment of cleaved icosahedral Al-Pd-Mn single-quasicrystals. Surf. Sci. 433-435, 312-316 (1999).
23.55.0

Ebert Ph.; Kluge F.; Grushko B.; Urban K.
Evolution of the composition and structure of cleaved and heat-treated icosahedral Al-Pd-Mn quasicrystal surfaces
Physical Review B, Vol. 60, No. 2 874-880 (1999)
23.55.0

Faley M.I.; Poppe U.; Urban K.; Zimmermann E.; Glaas W.; Halling H.; Bick M.; Paulson D.N.1; Starr T.1; Fagaly R.L.1
1 TRISTAN Technologies Inc., San Diego/USA
Operation of HTS dc-SQUID Sensors in High Magnetic Fields,
IEEE Transactions on Appl. Supercond., Vol. 9, No. 2, 3386-3391 (1999).
23.42.0

Franz V.1; Feuerbacher M.; Wollgarten M.. and Urban K.
1 Institut für Physikalische Chemie, Universität Mainz, D-55099 Mainz
Electron diffraction analysis of plastically deformed icosahedral Al-Pd-Mn single quasicrystals
Philosophical Magazine Letters, Vol. 79, No. 6, 333-342 (1999)
23.55.0

Grushko B. and Yurechko M.
Aluminium-rhodium phases at compositions close to Al5Rh2
Z. Kristallogr. 214, 313-315 (1999)
23.55.0

Grushko B.; Yurechko M. and Tamura N.
A contribution to the Al-Pd-Mn phase diagram
Journal of Alloys and Compounds 290, 164-171 (1999)
23.55.0

Haiml M.1; Siegner U.1; Morier-Genoud F.1; Keller U.1; Luysberg M.; Lutz R.C.2; Specht P.2; Weber E.R.2
1 Institute of Quantum Electronics, ETH Zürich/CH
2 University of California, Berkeley/USA
Optical nonlinearity in low-temperature grown GaAs: microscopic limitations and optimization strategies
Appl. Phys. Lett. 74, 3134 (1999)
23.42.0

Haiml M.1; Siegner U.1; Morier-Genoud F.1; Keller U.1; Luysberg M.; Specht P.2; Weber E.R.2
1 Institute of Quantum Electronics, ETH Zürich/CH
2 University of California, Berkeley/USA
Femtosecond response times and high optical nonlinarity in Beryllium doped low-temperature grown GaAs
Appl. Phys. Lett. 74, 1269 (1999)
23.42.0

Holland-Moritz D1.; Lu I.R1.; Wilde G2.; Schroers J.2 and Grushko B.
1 DLR; Institut für Raumsimulation, Köln
2 Dept. of Materials Science and Engineering, University of Wisconsin/Madison, USA
Melting entropy of Al-based quasicrystals.
J. Non-Cryst. Solids. 250-252, 829-832 (1999).
23.55.0

Houben L.; Lundszien D.; Luysberg M.; Carius R.; Fölsch J.; Carius R.; Wagner H.
Structural properties of microcrystalline silicon germanium
Philosophical Magazine Letters, Vol. 79, No. 2, 71-78 (1999)
23.42.0

Hradil K.1; Weidner E.2; Neder R.B.2; Frey F.2 and Grushko B.
1 Institut fuer Mineralogie, Universität Würzburg
2 Institut für Kristallographie und angewandte Mineralogie, LMU, Muenchen
Superordering in Ni-rich and Ni-poor decagonal Al-Co-Ni phases
Philosophical Magazine A, Vol. 79, No. 8, 1963-1976 (1999)
23.55.0

Jia C.L. and Urban K.
The atomic structure of the dislocation cores in a small-angle grain boundary in BaTiO3 thin films
Philosophical Magazine Letters, Vol. 79, No. 11, 859-867 (1999).
23.42.0

Jia C.L.; Hojczyk R.; Faley M.; Poppe U. and Urban K.
Interfaces in YBa2Cu3O7/BaTbO3 and PrBa2Cu3O7/BaTbO3 heterostructure thin films
Philosophical Magazine A, Vol. 79, No. 4, 873-891 (1999)
23.42.0

Jia C.L.; Rosenfeld R.; Thust A. and Urban K.
Atomic Structure of a (-3, (111(twin-boundary junction in a BaTiO3 thin film
Philosophical Magazine Letters, Vol. 79, No. 3, 99-106 (1999)
23.42.0

Jia C.L.; Thust A.
Investigation of Atomic Displacements at a (3 (111(Twin Boundary in BaTiO3 by Means of Phase Retrieval Electron Microscopy
Physical Review Letters, Vol. 82, No. 25, 5052-5055 (1999)
23.42.0

Klein H.; Feuerbacher M.; Schall P. and Urban K.
Novel Type of Dislocation in an Al-Pd-Mn Quasicrystal Approximant
Physical Review Letters, Vol. 82, No. 17, 3468-3471 (1999).
23.55.0

Lei C.H.; Jia C.L.; Siegert M.; Schubert J.; Buchal Ch.; Urban K.
Microstructure and orientation relations of BaTiO3/MgO/YSZ multilayers deposited on Si(001) substrates by laser ablation
Journal of Crystal Growth 204, 137-144 (1999).
23.42.0

Lopera W.1; Baca E.1; Gomez E.1; Prieto P.1; Poppe U.; Evers W.
1 Universidad del Valle, Cali/Kolumbien
Properties of Bi-2212/Bi-22Y2 Step-Stack Josephson Junctions
IEEE Transactions on Appl. Supercond. , Vol. 9, 4288 (1999)
23.42.0

Messerschmidt U.1; Bartsch M.1; Feuerbacher M.; Geyer B.1 and Urban K.
1 Max-Planck-Institut für Mikrostrukturphysik, Weinberg 2, 06120 Halle/Saale,
Germany
Friction mechanism of dislocation motion inicosahedral Al-Pd-Mn quasicrystals
Philosophical Magazine A, Vol. 79, No. 9, 2123-2135 (1999)
23.55.0

Poppe U.; Hojczyk R.; Jia C.L.; Faley M.I.; Evers W.; Bobba F.1; Urban K., Horstmann C.; Dittmann R.; Breuer U.; Holzbrecher H.
1 Universität Salerno / I
BaTbO3 as a new Material for Insulation and Junction Barriers in High-Tc Devices
IEEE Transactions on Appl. Supercond. , Vol. 9, 3452 (1999)
23.42.0

Quadbeck P.; Ebert Ph.; Urban K.; Gebauer J.1 and Krause-Rehberg R.1
1 FB Physik, Martin-Luther-Universität Halle, Halle
Effect of dopant atoms on the roughness of III-V seminconductor cleavage surfaces
Applied Physics Letters, Vol. 76, No. 3, 300 (1999)
23.55.0

Rodmar M.1; Grushko B.; Tamura N.; Urban K.; Rapp Ö.1
1Fasta Tillstandets Pysik, Kungliga Tekniska Högskolan, SE 10044 Stockholm/S
Isotropic magnetoresistance of icosahedral Al-Pd-Mn
Physical Review B, Vol. 60, No. 10, 7208-7212 (1999)
23.55.0

Schall P.; Feuerbacher M.; Wollgarten M. and Urban K.
Dislocation density evolution upon plastic deformation of Al-Pd-Mn single quasicrystals
Phil. Mag. Lett. 79, 785 (1999)
23.55.0

Siemens B.; Domke C.; Ebert Ph. and Urban K.
Point defects, dopant atoms, an compensation effects in CdSe and CdS cleavage surfaces
Thin Solid Films Vol. 343-344, 537-540 (1999).
23.55.0

Siemens B.; Domke C.; Ebert Ph. and Urban K.
Steps on CdSe (1120) and (1010) cleavage surfaces: Evidence for crack propagation in competing cleavage planes.
Physical Review B, Vol. 56, No. 4, 3000-3007 (1999)
23.55.0

Siemens B.; Domke C.; Heinrich M.; Ebert Ph. and Urban K.
Imaging individual dopant atoms on cleavage surfaces of wurtzite-structure compound semiconductors
Physical Review B, Vol. 59, No. 4, 2995-2999 (1999)
23.55.0

Zhang Y.; He D.F.; Wolters N.; Otto R.; Barthels K.; Zeng X.H.; Yi H.R.; Krause H.-J.; Braginski A.I.; Faley M.I.
Radio frequency bias current scheme for dc superconducting quantum interference device
IEEE Transactions on Appl. Supercond., Vol. 9, No. 2, 3813-3816 (1999).
23.42.0

Other publications

Dekorsy T.1; Hey R.1; Luysberg M.; Segschneider G.1
1 Institut für Halbleitertechnik II, RWTH Aachen
Ultraschnell durch Nanocluster - Grundlagen für die Terabit Optoelektronik
RWTH Themen - Berichte aus der RWTH Aachen 1/99, 44 (1999)
23.42.0

Haiml M.1; Siegner U.1; Morier-Genoud F.1; Keller U.1; Luysberg M.; Specht P.2; Weber E.R.2
1 Institute of Quantum Electronics, ETH Zürich
2 University of California, Berkeley/USA
Annealing of low-temperature grown semiconductors: Material optimization for ultrafast all-optical gating
Int. Conf. On Lasers and Electrooptics, Baltimore, CLEO'99 Technical Digest, OSA, Washington DC, (1999) p.197
23.42.0

Houben L.; Luysberg M.; Carius R.; Hapke P.; Finger F.; Wagner H.
Limitations to homoepitaxial silicon growth in plasma-enhanced
chemical vapour deposition at low temperature
Proceedings of the XIth Conference on Microscopy of Semiconducting Materials, 22-25 March 1999, Oxford, Microscopy of Semiconducting Materials 1999, Inst. Phys. Conf. Ser. 164, 211 (1999)
23.42.0

Luysberg M.; Specht P.1; Thul K.; Liliental-Weber Z.1; Weber E.R.1
1 University of California, Berkeley/USA
Change of electrical and structural properties of non-stoichiometric GaAs through Be doping
IEEE conference on semiconducting and insulating materials SIMC X, Berkeley, CA 1998, eds. Z. Liliental-Weber, C. Miner, (1999), p. 87
23.42.0

Luysberg M.; Specht P.1; Weber E.R.1
1 University of California, Berkeley/USA
Limitations to epitaxial growth of low-temperature grown GaAs
Proc of the 2nd Symposium on non-stoichiometric III-V compounds, Erlangen (1999) in: Physik mikrostrukturierter Halbleiter Vol 10 ed.: T. Marek, S. Malzer, and P. Kiesel, Verlag: Lehrstuhl für Mikrocharakterisierung, Universität Erlangen 1999 p.97
23.42.0

Luysberg M.; Specht P.1; Weber E.R.1
1 University of California, Berkeley/USA

Mechanisms of the formation of structural defects during low temperature growth of GaAs
Proceedings of the XIth Conference on Microscopy of Semiconducting Materials, 22-25 March 1999, Oxford, Microscopy of Semiconducting Materials 1999, Inst. Phys. Conf. Ser. 164, 279 (1999)
23.42.0

Specht P.1; Lutz R.C.1; Zhao R.1; Weber E.R.1; Liu W.K.2; Bacher K.2; Towner F.J.2; Stewart T.R.2; Luysberg M.
1 University of California, Berkeley/USA
2 Quantum Epitaxial Designs Inc., Bethlehem/USA
Improvemente of MBE-grown LT-GaAs through p-doping with Be and C
J. Vac. Sci. Technol. B 17 1200 (1999)

Urban K.
Die Physik - die Leitwissenschaft des Jahrhunderts
Leitartikel (ganzseitig) in Natur & Wissenschaft der Frankfurter Allgemeinen Zeitung zum Millenium (29.12.99), gleichzeitig Abschluß der Serie Physik im Wandel (April bis Dezember 1999) in der FAZ (Herausgegeber und Koordinator: K. Urban)
23.42.0

Urban K.
Die multidisziplinäre Welt der Information.
Artikel in dem Buch: Unsere Welten der Information (Herausgeber: D. Ganten, K. Urban et al. ; Gesellschaft Deutscher Naturforscher und Ärzte, S. Hirzel-Verlag, 1999)
23.42.0

Urban K.; Feuerbacher M.; Wollgarten M.; Bartsch M.1 und Messerschmidt U.1
1 Max-Planck-Institut für Mikrostrukturphysik, Weinberg 2, 06120 Halle/Saale,
Germany
Eingeladener Buchbeitrag: Kapitel 11: Mechanical Properties of Quasicrystals
in: Physical Properties of Quasicrystals, Z.M. Stadnik (Ed.) Solid-State Sciences, Springer-Verlag (1999) pp. 361-401
23.55.0

Invited talks

Ebert Ph.
Defects on semiconductors surfaces.
Seminar at the Physics Department, Prof. Dr. F. Himpsel, University of Wisconsin, Madison, Wisconsin, U.S.A., October 29, 1999
23.55.0

Lentzen M.; Thust A.; Chen J.H.; Urban K.
Auf dem Weg zur Sub-Angström-Mikroskopie: Materialwissenschaftliche Anwendung aberrationskorrigierter Elektronenmikroskopie
WE-Heraeus-Ferienkurs über "Moderne Fernfeld- und Nahfeld-Mirkoskopien, 20.09.-01.10.1999, Chemnitz
23.42.0

Lentzen M.; Thust A.; Chen J.H.; Urban K.
Contrast transfer of a Cs-corrected microscope
International Workshop on "Prospects and Future Needs of High-Resolution Electron Microscopy, Schloß Ringberg, 21.-24.07.1999
23.42.0

Luysberg M.
Influence of Defects in non-stoichiometric GaAs on the electrical and optical properties
Paul-Drude-Institut Berlin, Januar 1999
Eigenschaften von p-dotiertem Low-Temperature GaAs
Universität Karlsruhe, Januar 1999
23.42.0

Luysberg M.
Wachstum von GaAs bei niedrigen Temperaturen:Konsequenzen fuer die strukturellen und elektrischen Eigenschaften
Universität Bremen, März 1999
23.42.0

Thust A.
From the image to the wave function: The technique of focal-series reconstruction in HRTEM
Internal Seminar 15 07.1999, Wright-Pattern Air Force Base, Dayton, Ohio/USA
23.42.0

Thust A.
Materialuntersuchung mittels der Fokusvariationsmethode: Neue Einblicke nahe 1 Angström Auflösung
29. Tagung der Deutschen Gesellschaft für Elektronenmikroskopie, 5-10.09.1999, Dortmund
23.42.0

Thust A.
Rekonstruktion der Austrittswellenfunktion in der hochauflösenden Elektronenmikroskopie
WE-Heraeus Ferienkurs für Physik mit dem Titel "Moderne Fernfeld- und Nahfeld-Mikroskopien, 20.09-01.10.1999, Chemnitz
23.42.0

Thust A.
The Use of the Focal-Series Reconstruction Technique in HRTEM for Solving Materials Problems
MRS Fall Meeting, 29.11.-03.12.1999, Boston/USA
23.42.0

Other talks

Baier F.1; Müller M.A.1; Grushko B and Schaefer H.-E.1
1 ITAP, Universität Stuttgart
Atomic defects in quasicrystals: an approach with positron annihilation spectroscopy and time differential dilatometry.
ICQ-7 Stuttgart 1999
23.55.0

Bartsch M.; Geyer B.; Häussler D.; Feuerbacher M.; Urban K.; Messerschmidt U.
1 Max-Planck-Institut für Mikrostrukturphysik, Weinberg 2, 06120 Halle/Saale,
Germany
Plastic properties of icosahedral Al-Pd-Mn single quasicrystals
ICQ7 Stuttgart 1999, in press
23.42.0
3.55.0

Blüher R.1; Frank W.2 and Grushko B.
Diffusion of 103Pd and 195Au in icosahedral Al70.2Pd21.3Mn8.5 under proton irradiation.
1 ITAP, Unversität Stuttgart
2 Max-Planck-Institut für Metallforschung, Stuttgart
ICQ-7 Stuttgart 1999
23.55.0

Damson B.1; Weller M.1; Feuerbacher M.; Grushko B. and Urban K.
1 Max-Planck-Institut für Metallforschung, Seestraße 92, 70174 Stuttgart,
Germany
Mechanical spectroscopy of d-AlNiCo and i-AlPdMn
ICQ7 Stuttgart 1999, in press
23.55.0

Divin Y.
First Applications of Hilbert-Transform Spectroscopy
Beirat IFF, April 22, 1999, Forschungszentrum Jülich
23.42.0

Divin Y.
Far-Infrared Hilbert-Transform Spectroscopy
PGI Tag "Supraleitung", 11.11.99, Forschungszentrum Jülich.
23.42.0

Divin Y.; Poppe U.; Jia C.L.; Seo J.W.1; Glyantsev V.1
1 IBM Rüschlikon/CH
2 Conductus Inc., Sunny Vail/USA
Epitaxial (101) YBa2Cu3O7 thin-films on (103) NdGaO3 substrates
EUCAS'99, September 14-17, 1999, Barcelona, Spain.
23.42.0

Döblinger M.1.; Wittmann R.1.; Gerthsen D.1 and Grushko B.
1 Laboratorium für Elektronenmikroskopie, Universität Karlsruhe
Structural relationship and mutual transformation of approximants of the decagonal Al-Co-Ni phase.
ICQ-7 Stuttgart 1999
23.55.0

Ebert Ph.; , Zhang Tianjiao2,3; Kluge F.; Simon M.; Zhang Zhenyu3,2; Urban K.
2 Department of Physics, University of Tennessee, Knoxville, TN 37996
3 Solid State Division, Oak Ridge National Laboratory, Oak Ridge, TN 37831-6032
The importance of many-body effects in the clustering of charged Zn dopant atoms in GaAs
American Vacuum Society 46th International Symposium, Seattle, Washington, October 25-29, 1999.
23.55.0

Ebert Ph.; Chao K.-J.2; Niu Q.2 and Shih C. K.2
2 Dept. of Physics, University of Texas, Austin
Dislocations, phason defects, and domain walls in a one-dimensional quasiperiodic superstructure of a metallic thin film.
American Vacuum Society 46th International Symposium, Seattle, Washington, October 25-29, 1999.
23.55.0

Ebert Ph.; Kluge F.; Grushko B.; Urban K.
Investigation of cleavage surfaces of decagonal Al-Ni-Co quasicrystals
ICQ7 Stuttgart 1999
23.55.0

Ebert Ph.; Zhang Tianjiao2,1; Kluge F.; Simon M.; Zhang Zhenyu1,2; Urban K.
1 Oak Ridge National Laboratory, Oak Ridge
2 Dept. of Physics, University of Texas, Austin
The importance of many-body effects in the clustering of charged Zn dopant atoms in GaAs
Materials Research Society Fall Meeting, Boston, Massachusetts, November 29 - December 3, 1999.
23.55.0

Faley M.; Soltner H.; Poppe U.; Urban K.; Paulson D.N.1; Starr T.N.1 and Fagaly R. L.1
1 TRISTAN Technologies Inc., San Diego/USA
HTS dc-SQUID with gradiometric multilayer flux transformer
Submitted to EUCAS'99, 1999, Barcelona, in press
23.42.0

Faley M.; Soltner H.; Poppe U.; Urban K.; Paulson D.N.1; Starr T.N.1; Fagaly R.L.1
1 TRISTAN Technologies Inc., San Diego/USA
HTS dC-SQUID with gradiometric multilayer flux transformer
Submitted to EUCAS'99, Sept. 14-17, 1999, Barcelona, Spain
23.42.0

Faley M.I.; Poppe U.; Urban K.; Paulson D.N.1; Starr T.1 and Fagaly R. L.1
1 TRISTAN Technologies Inc., San Diego/USA
HTS dc-SQUID with gradiometric multilayer flux Transformer, to be pubished in the Proceedings of EUCAS'99, September 14-17, 1999, Barcelona, Spain.
23.42.0

Faley M.I.; Poppe U.; Urban K.; Zimmermann E.; Glaas W.; Halling H.; Bick M.; Krause H.-J.; Paulson D.N.1; Starr T.1; Fagaly R.L.1
1 TRISTAN Technologies Inc., San Diego/USA
Hochtemperatursupraleiter DC-SQUID Sensoren für den Betrieb in magnetischen Feldern,
DPG-Frühjahrstagung, Münster, 23.3.99
23.42.0

Feuerbacher M.; Klein H.; Schall P.; Bartsch M.1; Messerschmidt U.1 and Urban K.
1 Max-Planck-Institut für Mikrostrukturphysik, Weinberg 2, 06120 Halle/Saale,
Germany
Plasticity of Quasicrystals
Mat. Res. Soc. Symp. Proc. Vol. 553, 307-318 (1999)
23.55.0

Grushko B.
Composition and precipitation behavior of icosahedral Al-Pd-Mn quasicrystals.
ICQ-7 Stuttgart 1999
23.55.0

Gwodzsch J.1; Grushko B.; Surowiec M.1,
1 Institute of Physics and Chemistry of Metals, University of Silesia, Katowice, Poland
Mosaic structure of single quasicrystals.
ICQ-7 Stuttgart 1999
23.55.0

Heggen M.; Schall P.; Feuerbacher M.; Klein H.; Fisher I.R.1; Canfield P.C.1 and Urban K.
1 Ames Laboratory and Department of Physics and Astronomy, Iowa State
University, Ames, IA 50011, USA
Plastic behaviour of icosahedral Zn-Mg-Dy single-quasicrystal
ICQ7 Stuttgart 1999, in press
23.55.0

Jiang S.-C.1; Yu H.1; Ebert Ph.; Wang X.-D.1; Diener R.1; Niu Q.1; Shih C. K. 1
1 Dept. of Physics, University of Texas, Austin
Chaotic-like wavefunction beating in thin silver films with a quasiperiodic superstructure
American Vacuum Society 46th International Symposium, Seattle, Washington, October 25-29, 1999.
23.55.0

Klein H.; Feuerbacher M.; Schall P. and Urban K.
Plastic Deformation of Approximants: Dislocations vs. Phason Lines
Mat. Res. Soc. Symp. Proc. Vol. 553, 325-330 (1999)
23.55.0

Klein H.; Feuerbacher M.; Urban K.
locations in Al-Pd-Mn approximants: an HREM study
ICQ7 Stuttgart 1999, in press
23.55.0

Kluge F.; Ebert Ph.; Grushko B.; Urban K.
Änderungen der chemischen Zusammensetzung und der Struktur von gespaltenen ikosaedrischen Al-Pd-Mn-Quasikristalloberflächen nach Heizbehandlung.
Frühjahrstagung des Arbeitskreises Festkörperphysik bei der DPG, Münster, Germany, 22.-26 .3.1999.
23.55.0

Kluge F.; Grushko B.; Ebert Ph. and Urban K.
Structure and composition changes of cleaved Al-Pd-Mn quasicrystal surfaces induced by heat treatments investigated by AES, SEM and STM
ICQ7 Stuttgart 1999

23.55.0

Lentzen M.; Urban K.
Reconstruktion des projizierten Kristallpotentials mittels einer Maximum-Likelihood-Optimierung
29. Tagung der Deutschen Gesellschaft für Elektronenmikroskopie, 05.-10.09.1999, Dortmund
23.42.0

Luysberg M.; Houben L.; Specht P.1 and Weber E.R.1
1 University of California, Berkeley/USA
Mechanisms of the formation of structural defects during low temperature growth of GaAs
XIth Conference on Microcopy of Semiconducting Materials, Oxford, 21.-25.3.1999
23.42.0

Luysberg M.; Specht P.1; Weber E.R.1
1 University of California, Berkeley/USA
Limitations to epitaxial growth of low-temperature grown GaAs
2nd Symposium on non-stoichiometric III-V compounds, Erlangen, 4.-6. 10.1999
23.42.0

Luysberg M.; Specht P.1; Weber E.R.1
1 University of California, Berkeley/USA
Mechanisms of the formation of structural defects during low temperature growth of GaAs
Xth Conference on Microscopy of Semiconducting Materials, Oxford 1999
23.42.0

Messerschmidt U.1; Bartsch M.1; Geyer B.1; Häussler D.1; Feuerbacher M. and Urban K.
1 Max-Planck-Institut für Mikrostrukturphysik, Weinberg 2, 06120 Halle/Saale,
Germany
Microprocesses of the plastic deformation of icosahedral Al-Pd-Mn single quasicrystals
ICQ7 Stuttgart 1999, in press
23.55.0

Messerschmidt U.1; Geyer B.1; Bartsch M.1; Feuerbacher M.; Urban K.
1 Max-Planck-Institut für Mikrostrukturphysik, Weinberg 2, 06120 Halle/Saale,
Germany
The Activation Parameters and the Mechanisms of Plastic Deformation of Al-Pd-Mn Single Quasicrystals
Mat. Res. Soc. Symp. Proc. Vol. 553, 319-324 (1999)
23.55.0

Rotenberg E.1, Theis W.2, Barman S.R.3, Paggel J.J.4, Horn K.5, Ebert Ph. Urban K.
1 Advanced Light Source, Lawrence Berkely Lab, Berkeley CA
2 FB Physik, Freie Universität Berlin, Berlin
3 IUC-DAEF. Indore, Indien
4 FB Physik, Philipps-Universität Marburg
5 Fritz-Haber-Institut der MPG, Berlin
Band-like valence states in i-AlPdMn Quasicrystals?
American Physical Society Centennial Meeting, Atlanta, Georgia, March 20-26, 1999.
23.55.0

Rotenberg E.1, Theis W.2, Barman S.R.3, Paggel J.J.4, Horn K.5, Ebert Ph., and Urban K.6
1 Advanced Light Source, Lawrence Berkely Lab, Berkeley CA
2 FB Physik, Freie Universität Berlin, Berlin
3 IUC-DAEF. Indore, Indien
4 FB Physik, Philipps-Universität Marburg
5 Fritz-Haber-Institut der MPG, Berlin
Elektronische Struktur von i-AlPdMn-Quasikristallen.
Frühjahrstagung des Arbeitskreises Festkörperphysik bei der DPG, Münster, Germany, 22.-26.3.1999.
23.55.0

Rotenberg E.1; Theis W2.; Barman S.R3.; Paggel J.J4.; Horn K.5; Ebert Ph.6 and Urban K.6
1 Advanced Light Source, Lawrence Berkely Lab, Berkeley CA
2FB Physik, Freie Universität Berlin, Berlin
3 IUC-DAEF. Indore, Indien
4 FB Physik, Philipps-Universität Marburg
5 Fritz-Haber-Institut der MPG, Berlin
6 Institut für Festkörperforschung, Forschungszentrum Jülich
Photoemission study of dispersive states in i-Al-Pd-Mn.
7th International Conference on Quasicrystals (ICQ7), Stuttgart, Germany, Sept. 20-24, 1999.
23.55.0

Rotenberg E.1; Theis W2.; Barman S.R3.; Paggel J.J4.; Horn K.5; Ebert Ph.; Urban K.
1 Advanced Light Source, Lawrence Berkely Lab, Berkeley CA
2 FB Physik, Freie Universität Berlin, Berlin
3 IUC-DAEF. Indore, Indien
4 FB Physik, Philipps-Universität Marburg
5 Fritz-Haber-Institut der MPG, Berlin
Photoemission study of dispersive states in i-AlPdMn
ICQ7 Stuttgart 1999, in press
23.55.0

Schall P.; Feuerbacher M.; Messerschmidt U.1 and Urban K.
1 Max-Planck-Institut für Mikrostrukturphysik, Weinberg 2, 06120 Halle/Saale,
Germany
Dislocation structure and density in deformed Al-Pd-Mn single quasicrystals
ICQ7 Stuttgart 1999, in press
23.55.0

Urban K.
A new way towards higher resolution: Spherical aberration correction
Int. Symp. On Advanced Materials and Electron Microscopic Techniques for the Third Millenium, Hokkaido University 1998, Journal of Microscopy, in press (1999)
23.42.0

Urban K.
Plasticity of quasicrystals and related intermetallic phases
Int. Conf. on Rapidly Quenched and Metastable Metals, Bangalore, 1999, in press
23.42.0

Urban K.
Spherical aberration corrected transmission electron microscopy
Congress of Latin American Electron Microscopy Societies, Porlamar, Venezuela, 1999, in press.
23.42.0

Urban K.
Spherical aberration corrected transmission electron microscopy
Congress of the Int. Mat. Res. Soc. Beijing 1999
23.42.0

Yu H.1; Jiang S.-C.1; Ebert Ph.; Wang X.-D.1; Shih C. K.1
1 Dept. of Physics, University of Texas, Austin
Enhanced interlayer mass transport and dynamics of film smoothening on a symmetry-broken Ag(111) surface
American Vacuum Society 46th International Symposium, Seattle, Washington, October 25-29, 1999.
23.55.0

Yurechko M.; Grushko B.
Investigation of Al-Pd-Co alloy system.
Frühjahrstagung des Arbeitskreises Festkörperphysik bei der DPG, Münster, Germany, 22-26.3.1999
23.55.0

Yurechko M.; Grushko B.
Study of Al-Pd-Co alloy system.
ICQ7 Stuttgart 1999, in press

23.55.0

Patents granted

Divin Y.Y.; Seo J.W.; Poppe U.:
Schichterfolge mit wenigstens einer epitaktischen nicht c-Achsen orientierten Schicht aus einer mit Hochtemperatursupraleitern kristallographisch vergleichbaren Struktur
DE: 19648234 (08.07.99)
PT 1.1333a
23.42.0

Ghosh I.; Klein N.; Poppe U.:
Abstimmbarer Hochraumresonator
DE: 19841078 (12.10.99)
PT 1.1617
23.42.0

Hojczyk R.; Jia C.L.; Poppe U.:
Schichtenfolge mit einem hochtemperatursupraleitenden Material und deren Verwendung
DE: 19634645 (24.06.99)
PT 1.1386
23.42.0

Klein N.; Dähne U.; Tellmann N.:
Verfahren zur Qualitätsbestimmung eines einzelnen supraleitenden Filmes und Vorrichtung zur Durchführung dieses Verfahrens
EP: 0580836 (13.01.99) (DE, FR, GB, NL)
PT 1.1117
23.42.0

Poppe U.; Schubert J.; Evers W.;
Verfahren zur Herstellung dünner Schichten aus oxydischem Hochtemperatur-Supraleiter
JP: 2868526 (25.12.98)
PT 1.889
23.42.0

Patents applied for

Gosh I.; Klein N.; Poppe U.
Abstimmbarer Hohlraumresonator,
PT 1.1617
23.42.0

Schornstein S.; Klein N.; Ghosh I.:
Mehrpol–Bandpaßfilter mit elliptischer Filtercharakteristik
PCT: PCT/DE99/01447 (12.05.99) (EP,US,CA,RU,JP)
PT 1.1596
23.42.0

Zimmermann E.; Faley M.; Poppe U.
Magnetflußsensor mit schleifenförmigem Magnetfeldleiter sowie dessen Herstellung
PT 1.1674
23.42.0

Lecture courses

Urban K.; Luysberg M.; Ebert Ph.; Klein N.
Experimentalphysikseminar "Die Physik und Technik der Nanostrukturen"
WS 98/99
23.42.0
23.55.0

Urban K.; Luysberg M.; Ebert Ph.; Thust A.; Klein N.
Experimentalphysikseminar "Physik der Nanostrukturen"
SS 1999
23.42.0
23.55

Institute Electronic Properties

General Overview

Research Areas

The research program of the IFF institute 'Electronic Properties' is devoted towards the investigation of the electronic structure of atoms, molecules, clusters, and solids. The ultimate goal is the development of an understanding and thus a base for the control of the properties of (new) materials. The electronic structure constitutes the microscopic origin for all materials properties. The electronic interactions determine whether a solid is metallic, insulating, or semiconducting, whether it is transparent or exhibits a distinctive color, whether it is a magnet or a superconductor. Even the elastic properties and the thermal conductivity and heat capacity are determined by the electronic structure.
The electronic structure of simple solids consisting of a regular lattice formed by one or two atomic constituents, like pure metals or semiconductors such as GaAs, is quite well understood. Thin film systems introduce a modification of the intrinsic materials properties due to the interaction at the surface and the interfaces. In structures where at least one of the dimensions is in the nanometer range, the interface or surface properties in conjunction with quantum size effects result in large modifications of the original materials properties. This has led to the concept of 'atomic engineering of materials', whereby the materials properties are controlled by a variation of the atomic constituents at the microscopic atomic level. These concepts establish the central and interconnecting aspect of our research program, where we use both experimental as well as theoretical tools for our explorations. In our research we are not only interested in the ground state properties but also in the dynamic short time response to an external stimulus, as for example a short light pulse.
A large part of our research program is devoted towards the development of a microscopic understanding of classes of materials with a direct connection to a technological application. Such materials where the microscopic control and the variation of the atomic constituents have a dominating influence for the technological application include semiconductor layer systems and heterostructures as well as thin film magnetic systems for sensors and storage media.
Oriented towards these technological applications the research efforts of the institute are organized in the following areas:

(A) **Magnetism of thin Films and Nanostructures; from basic Research to Magnetoelectronics**

(B) **Clusters as new Materials**

Additionally in our institute there is an effort to develop new

(C) **Methods and Instrumentation** for our research. Hereby plays the application of synchrotron radiation a central role. This includes the design and construction of beamlines and instruments for research with synchrotron radiation. In the following these programs are described in more detail. At the end of each section some current research highlights are listed which either are included as short reports or have appeared in print recently.

A.1. Magnetism of thin films and nanostructures

Thin film systems and nanostructures such as magnetic quantum wires or dots exhibit distinctively different magnetic properties than their bulk counterparts. Obviously there is a close connection between the control of the magnetic properties of these novel nanostructured systems and the understanding derived from basic research on an microscopic atomic level. This has recently led to significant advances in technological applications of thin film systems as magnetic sensors and storage media. Additionally, this development is in line with the demand put forward by the increase in miniaturization in information technology.
Our long range goal is to develop a microscopic understanding of the magnetic phenomena. Magnetism is an electronically derived collective phenomenon influenced by the structure, composition and dimensionality of the system. As experimental techniques we are using spin and angle resolved photoemission, circular dichroism, and other synchrotron radiation related techniques in combination with (relativistic) band structure calculations. With spin- and angle resolved photoemission we determine the bandstructure $E(\sigma,k)$ of the occupied electronic states. These data can be directly compared with bandstructure calculations based on the density functional theory. Element specific magnetic information about multilayer and multicomponent systems is obtained making use of the circular

dichroism at core level absorption edges. In addition these studies yield element specific information about the collective ordering phenomena as a function of temperature
As outlined above, electronic structure theory is an integral part of our research program and central to the development of a microscopic understanding of magnetic materials. The existence of a magnetically ordered phase is determined by a delicate balance between the exchange interaction and the kinetic energy of the electrons. The symmetry of the magnetic order (ferromagnetic or anti ferromagnetic) is also determined by the electronic structure and the geometry of the system. Spin-orbit interactions, which in general contribute only a small amount to the total energy of the system, influence macroscopic parameters such as the magnetic anisotropy, the coercivity, and the magneto optical properties. The existence of a preferred orientation also leads to the breaking of symmetries and a lifting of the degeneracies of electronic states. At the present level most calculations do not yet incorporate these effects and efforts are undertaken to include some of these, for example non-collinear spin structures, into the calculations in order to get a more realistic treatment.

Scientific highlights of 1999

- Non collinear magnetism in fcc-Co/Fe/Co (100)
- Three dimensional spin-structure on a two-dimensional lattice
- Massively parallelized FLAPW program for large-scale applications

A.2. Magnetoelectronics; a new field of information technology

Magnetoelectronics is one of the key areas of information technology with a large potential for future expansion. In general the term magneto electronics has been coined to describe electronic devices where, in analogy to the microelectronics, the spin dependent charge transport is used for data storage and processing as well as for sensor applications. In the past year we were successful in obtaining approval and funding for this project within the framework of the HGF-Strategiefonds.
The roots of magneto electronics can be found in the discovery of antiferromagnetic coupling in thin magnetic films separated by a non-magnetic metallic spacer and the "giant magneto resistive" properties of these multilayers by P. Grünberg (FZ Jülich) and A. Fert (Paris) in the late 1980's. Even though it was not part of a technology roadmap or forecast, this unexpected quantum mechanical effect in the area of nanostructured devices has made its way from basic research to commercial devices in the amazingly short time span of less than 8 years. New types of magnetic field sensors were developed which are incorporated into the latest generation of readout heads for magnetic discs. This has resulted in an unexpected strong increase in storage density, since these new heads have a much higher sensitivity. New rotary sensors are being developed which are of interest in robotics and for multiple applications in automobiles. Further applications of the GMR sensors may be in non-destructive testing of structural materials, such as reinforced concrete, or of high speed train wheels, with high spatial resolution. Additionally prototypes for novel non-volatile magnetic random access memory devices (MRAM) are being developed, based upon the resistance change in magnetic tunnel junctions (TMR) upon reversal of the magnetization of one of the layers.
GMR sensors with applications as readout heads in hard discs or video recorders and as sensors in car-electronics guarantee a high volume and large revenues. The MRAM development on the basis of the TMR effect offers the possibility to build all solid state memory devices, which are non-volatile and directly compatible with integrated CMOS technology. The worldwide market for (semiconductor) memory devices presently (1998) amounts to 38 Billion $ and is projected to increase to more than 100 Billion $ in the year 2002.

Short description of the research objectives in the HGF-Program Magnetoelectronics
The main goal of the HGF-program is to carry out a series of focused basic research projects in order to improve and expand the knowledge and materials basis for GMR sensors and TMR MRAM devices which are currently being developed jointly with industry within the framework of the "BMBF Leitprojekt Magnetoelektronik". The HGF-program is organized as a joint effort bridging institute boundaries whereby scientists from the IFF, the IGV and the ISI participate in this research.
These novel magnetoelectronics devices are functional nanostructures consisting of ultrathin metal or metaloxide films, which have a thickness of only a few nanometers. Accordingly, quantization phenomena modify the electronic states and thus influence the magnetic properties. The alternating exchange coupling in magnetic thin films separated by a non-magnetic metallic spacer, which was at the origin of the development of GMR sensors, is indeed caused by the energetics of quantized conduction band states of the metallic spacer layer. Therefore it is obvious that the morphology of the layers and interfaces and their electronic properties determine the device characteristics. With respect to layout development questions arise concerning the transition into the superparamagnetic behavior with increasing miniaturization. Furthermore cross talk and the general influence of the lateral shape of the memory cells need to be investigated.
Until recently, the development of actual GMR sensors was largely empirical by trying out a large number of material combinations and process conditions. The development of TMR elements on the other hand is even less

advanced. For both kinds of devices even the basic limitations for the optimum achievable performance, which are subject to the proper choice of materials and the modification of the interfaces, have not yet been established.
In the case of GMR sensors, for example, the relationship between the resistivity of the layers and the interface roughness has not yet been quantified. The development of artificial antiferromagnetic structures, such as FeMn multilayers is just at the beginning. Furthermore the influence of an antiferromagnetic insulating substrate, such as NiO, on the characteristics of the sensor is largely unexplored. Currently NiO has been used to pin the magnetization of one of the sensor layers and was found to also increase the GMR effect.
Concerning TMR junctions for the MRAM development, for the influence of the height of the tunneling barrier and even in general the variation of the spin dependent tunneling current upon magnetization reversal are not explained on a quantitative scale. Another largely unexplored, but nevertheless very important area, concerns the magnetization dynamics of thin film systems for MRAM cells. Furthermore, so far all TMR developments have used Al_2O_3 as the oxide barrier, mostly due to historical reasons. Different oxides might lead to an improvement of the TMR characteristics.

Scientific highlights of 1999 (IFF only)

- Layered magnetic structures; Interlayer exchange coupling and giant magnetoresistance (review article by P. Grünberg)
- Observation of the inverse GMR effect in Fe/Cr/Au/Fe layer systems
- Giant magnetoresistance: influence of the interface roughness

B. Clusters as new materials

Clusters are aggregates of a well defined, selectable number n of atoms. In our studies this number n varies between 3 and about 100 atoms, whereby we can select each size individually. In these experiments we can study the transition from the single atom to the solid. Of special interest is that this transition is not smooth and continuous, but rather leaves ample room for 'surprises'. The 'materials properties' of individual clusters are quite unique and may in general not be extrapolated from the properties of the corresponding infinite solid. The most famous example is C_{60}, the soccer ball shaped cluster, which can be condensed into a solid consisting only of carbon atoms. Thin films of C_{60} become superconducting at temperatures above 30 K when 'doped' with alkali atoms, and exhibit in general distinctly different properties than graphite or diamond, the other forms of solid carbon. A special highlight in this context a few years ago was our determination of the electron phonon coupling parameters from high resolution photoemission spectra of C_{60}^-. Thus we could show that the mechanism of the superconductivity of the alkali doped fullerenes, which are second in terms of their transition temperatures only to the high Tc materials, may be explained by BCS-theory. This is only one example how cluster research can lead to the discovery and development of new materials.
Our cluster research program exhibits quite some anologies to the corresponding research programs in solid state physics (magnetism, electronic properties) and surface physics (chemisorption, catalysis). This is in accordance with the main goals formulated above for our research program to develop an understanding for the properties of new materials on the microscopic atomic level.

B.1. Electron spectroscopy of mass-selected clusters in a molecular beam

Clusters of a monoatomic size are quite difficult to produce and separate in large quantities. Accordingly the investigation of the electronic properties of these individual mass selected clusters requires methods far beyond the capabilities of conventional electron spectroscopies.
Laser excited photoemission from anionic mass selected clusters has turned out to be a method which can be appplied to this task on a large variety of clusters in a mass selected molecular beam experiment. The clusters are produced by condensation of a plasma generated by a focussed laser beam or an electric discharge in a high pressure He atmosphere. Following adiabatic expansion and the formation of a molecular beam the cluster anions are accelerated by a pulsed electric field. According to their mass difference the anions thus arrive at different times in the ionization region of the magnetic bottle electron spectrometer. Adjusting the timing sequence of the laser used to excite the photoelectrons (detachment) electron spectroscopy on clusters of an unique mass can be performed. The electron energy distribution spectra reveal the electronic structure of the individual clusters. Under favorable conditions vibrational substructures may be resolved which reveal characteristic vibrational modes of the cluster and thus give additional information about the geometry of the atomic positions in the cluster. For the interpretation of these spectra and the identification of unique cluster structures a comparison with high level calculations and a collaboration with theory plays an important role. Using femtosecond pump-probe techniques the mechanisms of energy transfer and relaxations processes are also studied. These particular experiments will be described later under the heading of fs 2 photon photoemission.

Scientific highlights of 1999

- Photoelectron spectroscopy of benzene adsorbed metal cluster anions

B.2. Deposition of mass selected clusters on surfaces

For technological applications the individual properties of the clusters have to be conserved. This can be achieved by depositing mass selected cluster onto a suitable substrate. For this purpose we are developing a high intensity source capable of delivering a sufficient amount of mass selected clusters onto a substrate within a few minutes to prevent contamination. Cluster ions are produced in a specially designed high intensity laser vaporization source. The cluster-ions present in the molecular beam following the adiabatic expansion are accelerated and deposited onto a substrate after mass selection by a sector magnet. The substrate can be prepared and characterized in a conventional XPS/UPS system before and after the deposition. Both systems are connected vía an UHV sample transfer system. The substrates can also be transferred to additional facilities including STM characterization in-house as well as spectroscopy with synchrotron radiation.
Typical areas of applications for deposited mass selected clusters may be in catalysis or nanoelectronics. In catalysis it is well known that small particles may exhibit special properties, increasing the reactivity or more important the selectivity of the process. It can be expected that these properties may be enhanced by mass selecting the catalyst particles. In electronic applications (nanoelectronics) the concept of a 'single electron transistor' may be realized using deposited clusters. This is due to the fact that the clusters have discrete quantized electronic states, whereby the 'Fermi level' of a small cluster may change by an energy on the order of 1 eV, when a single electron is added to it or removed from it.

Our major research interests are:

- Characterization of the properties of the deposited clusters --- including the atomic geometry and electronic structure in comparison with the 'free' cluster in a molecular beam, diffusion and agglomeration phenomena, and generally the interaction with the support material
- Catalytic properties of mass selected deposited clusters
- Electronic properties of nanocontacts on semiconducting substrates
- Magnetism of nanostructures

Scientific highlights of 1999

- Cluster deposition experiment at the IFF/IEE first results

B.3. Cluster materials

Semiconductor nanaostructures and cluster materials can also be prepared by (electro-)chemical methods. Electrochemical etching for example transforms crystalline Si into porous Si, which exhibits electroluminescence. In the long term this might lead to electro-optical devices based upon Si, a technology which for crystalline Si is inhibited by the indirect bandgap. Demonstration models of electroluminescent displays have been fabricated. We have studied the electronic structure of porous Si by soft X-ray emission spectroscopy earlier and found that the remaining material is crystalline in character and that the shift of the luminescence wavelength is consistent with the opening of the gap due to quantum confinement. Furthermore, II-VI cluster materials can also be produced by chemical methods. Here we collaborate with the group of Prof. H, Weller, University of Hamburg, and characterize the materials produced by this group with respect to their electronic structure.
In this area we also had a collaboration with partners from industry (AEG, Daimler-Benz), where we successfully demonstrated that the photoconductivity of organic photoconductor systems used in photocopiers and laser printers can be improved by more than an order of magnitude by doping with small quantities of C_{60}. This effect was explained by a very efficient charge separation due to the high electron affinity of C_{60}.

Scientific highlights of 1999

- Electronic structure of $(C_{59}N)_2$ studied locally at the N-site by soft X-ray emission

C. Methods and instrumentation

Both aspects, the design and realization of new instruments as well as the development of novel methods for spectroscopy, are part of our research efforts. The powerful infrastructure provided by a large research center is especially helpful when designing new and complex instruments. Our interests in this area are centered around the application of synchrotron radiation. On the hardware side this includes the design and construction of synchrotron

radiation beamlines or specific spectrometers and detectors. Additionally new methods for spectroscopy are also being explored, especially under the aspects of resonance excitation conditions with synchrotron radiation and two-color pump-probe photoemission spectroscopy with fs time-resolution.
At the future FEL-sources the synchrotron beam properties will match the performance of laboratory laser sources with respect to coherence, pulse power, and timestructure (pulse-lengths) in the fs range. This will extend the capabilities we currently have at visible and UV photon energies into the VUV and (soft) X-ray range and open up the possibilities for a whole set of new and exciting experiments.

C.1. Synchrotron radiation beamlines; spectroscopy and scattering

We have finished the installation of an undulator beamline for the photon energy range from 10 eV to 300 eV the DELTA storage ring. This beamline will be largely devoted to bandstructure investigations and high resolution core level spectroscopy of magnetic thin film systems for magnetoelectronics, solid state systems and cluster materials. We have built a plane grating type monochromator, since this type of instrument is, for the selected photon energy range, best suited to match the performance of the existing undulator source at DELTA. This beamline has recently been commissioned and shown excellent performance.
Additionally we are designing an undulator based beamline with a spherical grating monochromator at the BESSY II storage ring for the photon energy range from 50 eV to 1.5 keV to be installed at a pair of undulators offering adjustable polarization of the light, which is extremely useful for element specific investigations of magnetic systems including the determination of magnetic moments by using the sum rules developed for CMXD.We will also employ resonant inelastic X-ray scattering at this new BESSY beamline, a method which we have developed over the past years extensively. In the past year we have built up a new experimental station to conduct scattering experiments with coherent soft X-ray photons. This work was featured as the cover story in Synchrotron Radiation News. Even if the reconstructions of the interference patterns observed have not been unambiguously demonstrated, we nevertheless feel that this might become a very interesting field of research in the future for the study of dynamical processes (m-sec) in magnetic systems, semiconductors and polymers with an exceptional sensitivity tunable to the length scale of a few to tenths of nanometers.

Scientific highlights of 1999

- Development of RIXS as a method to determine the bandstructure of solids (review article by S. Eisebitt and W. Eberhardt)
- Installation and first experiments on the soft X-ray beamline at DELTA.
- Orientation and self assembly of hydrophobic fluoro-alcyl-silanes

C.2. Fs two color pump probe photoelectron spectroscopy

Time resolved pump probe photoemission spectroscopy is a new and very exciting field of physics. These experiments directly reveal the electron scattering and relaxation processes following the creation of an optical excited state in real-time. The shortest observed timescales of a few fs are due to electron electron scattering, whereas electron phonon scattering involves slightly larger timescales in the sub-ps regime. These processes also serve to populate electronic conduction band states not necessarily accessible by direct optical excitation. Recording the photoelectrons in an angle resolved mode allows the observation of the scattered excited electrons at specific points of the bandstructure. Since the excited electrons are observed directly, this technique does not require the presence or existence of recombination centers, which are exploited in ultrafast luminescence studies.
In the past we have largely studied charge transfer and excited electronic states involving C_{60} either as a film on a metal substrate or as an acceptor in a photoconductor system. Since we were able to improve the time resolution of our laser system recently, we also can study electronic relaxation processes at metal surfaces directly now. In the future, we will follow up on our earlier work on the timescales of the magneto optical recording process and continue with investigations of the magnetization dynamics of thin film systems with fs-spin-resolved photoemission.
Fs spectroscopy of clusters in a molecular beam is another very interesting scientific topic. Here energy relaxation processes may be followed in real time for systems where the total energy remains localized spatially to a few atoms and correspondingly only a few degrees of freedom. Thus these processes evolve quite different than in solid state systems, where the total energy is spread rapidly over an extended volume of the sample involving more and more atoms. The energy can only be removed from the cluster by the emission of an electron or photon or by evaporation of an atom. This may occur finally after the system was evolving over a timescale up to the msec range. On the other hand very fast fs electronic relaxation processes may be observed also including the dissociation. Thus one is able to follow the development of the electronic structure as the fragments separate. This enables us to gain data about short lived transition states, which govern the pathways in chemical reactions. Accordingly these states are essential in developing a deeper understanding of chemical reactions. For the development of this field of fs-chemistry, A. Zewail was awarded the 1999 Nobel Prize in chemistry.

Scientific highlights of 1999

- Ultrafast hot-electron dynamics observed in Pt_3^- using time resolved photoelectron spectroscopy (Phys. Rev. Lett. (in press))
- Electron dynamics at a Ag/C_{60} metal semiconductor interface
- Lifetimes of image potential states on Pt(111)

C.3. Theory and experiments concerning STM image interpretation

The theory activities of the institute are largely concentrated in two areas. One of them is the theory of magnetism in thin films including electron transport phenomena in magnetoelectronics as introduced above and the second topic concerns the theoretical modeling of STM images. This latter activity starts with the calculation of the electronic structure of the surface under investigation and the calculation of the tunneling current into a tip represented by an atomic s-, p-, or d-wavefunction which is supposed to resemble the tip atom mostly responsible for the tunneling process. In the future a more accurate inclusion of the electronic structure of the tip is planned. However, even on the basis of this simple Tersoff-Hamannn model (s-wavefunction) effects like the corrugation reversal of metallic substrates and the contributions to the STM image from atoms buried below the surface of metals could be observed, helping in the interpretation and correct assignment of some experimental puzzles. Previously these effects had only been reported for semiconductor surfaces, where electron screening is much less effective.
In the future we also plan to conduct experiments along these lines of the image development of the STM using our newly purchased variable temperature STM. Together with the theoretical activities we want to furnish compelling experimental evidence that even for metallic systems the STM images are substantially determined by the details of the electronic structure of the surface.

Scientific highlights of 1999

- STM images of transition metal structures buried below noble metal surfaces
  Phys. Rev. Lett. **83**, 4808 (1999)

I hope that I could give a satisfactory overview of our research program and the common thread linking all these activities. Foremost in importance however are the people engaged in these activities and therefore I would like to conclude with a few general remarks about the changes among the members of the institute.
Dr. Barbara Kessler has received her 'Habilitation' from the University of Cologne and almost immediately was appointed as professor at the 'Fachhochschule Koblenz' in Remagen. She is the third member of the institute within the last two years who was appointed to a professorship. She certainly leaves a large gap in the research program concerning cluster materials and organic photoconductors, but we hope to continue a collaboration with her.
After many years of very productive and well received scientific work in the IFF, Dr. C. Sauer has left us to retire from active service. We wish him very well for the future. Dr. Sauer has been mostly known for his work on CEMS on magnetic systems and our recent nuclear scattering experiments at the ESRF were stimulated by discussions with him.
Dr. Daniel Bürgler, formerly from the University of Basel and Dr. Hermann Dürr, formerly from Daresbury Laboratory have joined our institute to strengthen the efforts in the area of magnetoelectronics.
K. Bickmann has joined the technical staff of the institute. He is working on the design of beamline components and experiments using synchrotron radiation.
Prof. M. Olmstead from the University of Seattle has received an A.von Humboldt award and is spending several months with us working on the growth and dynamics of semiconductor nanostructures.
Dr. K. Maiti and Dr. S.S. Yan have each won a stipend from the A. von Humboldt foundation. Dr. Maiti works with us on the determination of the electronic structure of metal-oxide interfaces and Dr. Yan investigates magnetic thin film systems for magnetoelectronics.
Apart from these the following guests have spent extended periods time collaborating with us during the past year: Dr. R. Abt, Prof. T. Asada, Dr. R. Gareev, Prof. K. Hirai, Prof. B. Kuanr.
J. Morenzin and P. Rottländer have graduated and received a PhD during the last year and M. Buchmeier and M. Freiwald have finished their Diploma thesis in the institute.

I would like to close this report by thanking all members of the institute for their efforts during the past year which have again resulted in many scientific accomplishments.

Wolfgang Eberhardt

Institute "Electronic Properties"

December 1999

Director: Prof. Dr. W. Eberhardt
Tel.: 4428, Fax: 2620

Secretary: J. Gollnick
Tel.: 5814, Fax: 2620

Groups	Research Areas
Dr. C. Carbone Dr. K. Maiti A. Dallmeyer (PhD-student) M. Malagoli (PhD-student)	Thin film magnetism Spin-polarized photoemission and CMXD with synchrotron radiation
Dr. L. Baumgarten Dr. H. Dürr S. Link (PhD-student) C. Zilkens (PhD-student)	F-sec laser photoemission and high resolution photoemission from solids Photoelectron microscopy
Dr. S. Cramm D. Schondelmaier (Diploma-student)	Beamlines at DELTA and BESSY II Characterization of functionalized surfaces
Dr. S. Eisebitt A. Karl (PhD-student) R. Scherer (PhD-student) G. Kann (PhD-student) I. Wirth (PhD-student) M. Freiwald (Diploma-student) M. Lörgen (Diploma-student) A. Zimina (Diploma-student)	Soft x-ray emission spectroscopy STM microscopy and spectroscopy
Dr. S. Blügel Dr. G. Bihlmayer Dr. S. Clarke Dr. X. Nie P. Kurz (PhD-student) F. Förster (Diploma-student) D. Wortmann (Diploma-student)	Electronic structure theory of solids and multilayers STM-theory
Dr. P.S. Bechthold Dr. M. Neeb R. Klingeler (PhD-student) G. Lüttgens (PhD-student) N. Pontius (PhD-student) C. Friedrich (Diploma-student)	Electronic structure, geometry and materials properties of clusters F-sec dynamics of clusters
Dr. J. Morenzin	Development of a magnetic security system
J. Lauer H. Pfeifer	Electronic-Laboratory
K. Bickmann B. Küpper	Vacuum-Laboratory

Research Group "Magnetic Multilayers"

Prof. Dr. P. Grünberg Dr. D. Bürgler Dr. R. Gareev Prof. B. Kuanr Dr. S.-S. Yan P. Rottländer (PhD-student) D. Olligs (PhD-student) J. Wingbermühle (PhD-student) M. Buchmeier (PhD-student) M. Breidbach (Diploma-student) F.-J. Köhne R. Schreiber	Magnetic multilayers for sensors and memory applications

Non-collinear magnetism in fcc-Co/Fe/Co(100)

A. Dallmeyer[1], M.C. Malagoli[1], K. Maiti[1], J. Wingbermühle[1], C. Carbone[1], W. Eberhardt[1], D.L. Nagy[2], L. Deak[2], L. Bottyan[2], R. Rüffer[3] and O. Leupold[3]

[1]*Institute for Electronic Properties*

[2]*KFKI Research Institute for Particle and Nuclear Physics, P.O.B. 49, H-1525 Budapest*

[3]*European Synchrotron Radiation Facility, BP 220, F-38043 Grenoble Cedex*

Layer-resolved measurements by nuclear magnetic resonance spectroscopy with synchrotron radiation on a 7 atomic layer fcc-Fe film reveal a non-collinear magnetic structure where the orientation of the moments changes layer by layer.

F&E-Nr.: 23200

A fundamental question in solid state physics is the relation between atomic geometry and magnetism. Being at the borderline between antiferromagnetically and ferromagnetically ordered transition metals, Fe is an exemplary case for the influence of structural effects on the magnetic properties. Fe is a simple ferromagnet in its normal bcc-structure, it becomes non-magnetic under pressure and in amorphous phases, and it is theoretically expected to order antiferromagnetically in the fcc-structure for a range of lattice parameters which also includes the ground state. By examining with nuclear magnetic resonance spectroscopy ultrathin films epitaxially stabilized in the fcc-phase, we discovered a new kind of magnetic ordering in Fe. Fcc-Fe(100) films sandwiched between Co(100) layers exhibit a non-collinear magnetic structure, where the orientation of the Fe moments coherently rotates monolayer by monolayer.

Fcc-Fe films have been extensively investigated in the past years by several different methods. Their magnetic properties are known to depend very critically on the film thickness and lattice volume. This is regarded as a manifestation of the magneto-volume instabilities already predicted for fcc-Fe and for fcc-Invar alloys by Weiss in 1963 [1]. In addition, the magnetic behaviour of the outmost layers of the films is expected to be profoundly distinct from the one in the film interior as a consequence of the modified symmetry and bonding at the interfaces. However, a detailed microscopic picture of the magnetic structure of fcc-Fe films has not yet been achieved, also because the magnetization of the individual atomic layers is hardly accessible to the experimental investigation.

We have used nuclear resonance scattering with synchrotron radiation at the ESRF in Grenoble to examine the magnetic structure of fcc-Fe films. By combining selective nuclear excitation with linearly-polarized radiation this method offers site sensitivity and is able to determine the hyperfine-field magnitude and orientation in films with monolayer resolution. Grazing-incidence radiation (of $\approx$14.4 keV photon energy) was scanned across fcc-Fe films grown in a wedge geometry and sandwiched between two fcc-Co films. An ^{57}Fe film wedge of 1-10 monolayer (ML) thickness (Fig. 1a) was investigated to obtain layer-integrated information on the magnetism as a function of the film thickness.

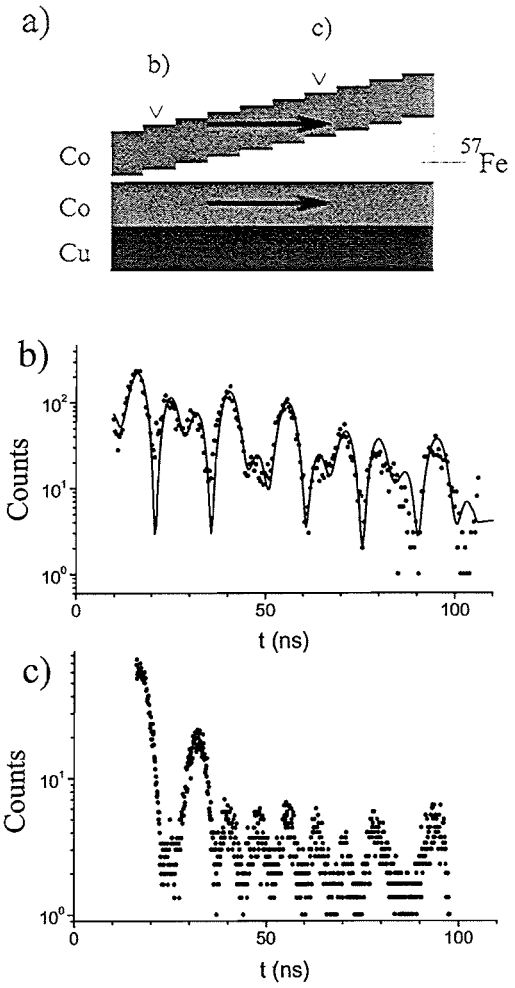

FIG. 1. a) Scheme of a 1-10 ML fcc-Fe wedge consisting entirely of ^{57}Fe, sandwiched between two Co(100) films. Time spectra of nuclear forward scattered radiation have been measured scanning the synchrotron beam along the wedge.
b) Time dependence of nuclear forward scattered radiation from a 2 ML fcc-Fe film. c) Time dependence of nuclear forward scattered radiation from a 7 ML fcc-Fe film.

A second type of sample consisted of a 7 ML Fe film, where an ^{57}Fe monolayer was inserted at different positions (Fig. 2a) in an ^{56}Fe film.

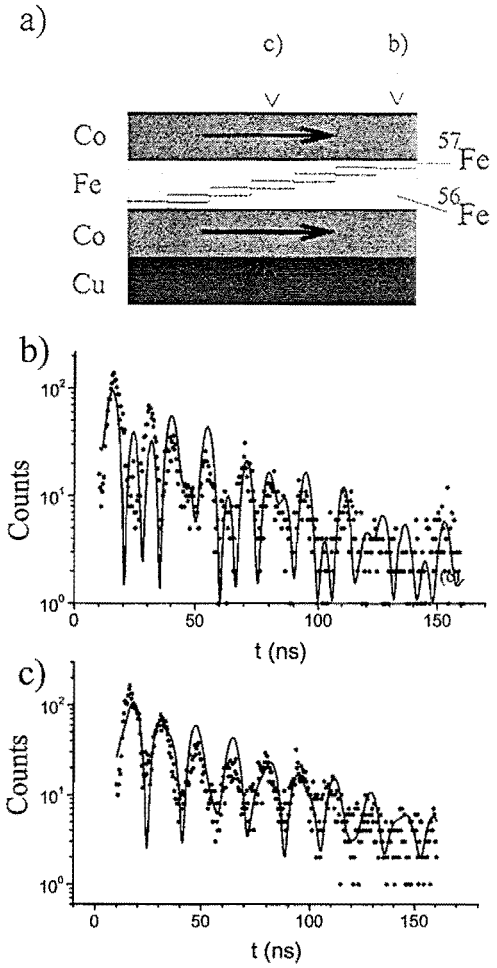

FIG. 2. a) Scheme of a sample with a uniform fcc-Fe film thickness of 7 ML. A single ^{57}Fe monolayer is inserted at various positions within an ^{56}Fe film. Layer-resolved spectra have been measured by scanning the radiation on the sample. b) Time dependence of nuclear forward scattered radiation from the ^{57}Fe layer at the interface. c) Time dependence of nuclear forward scattered radiation from the ^{57}Fe layer in the center of the Fe film.

Scanning the radiation beam across this sample provided layer-resolved information on the hyperfine-field vector distribution within the film. The linearly-polarized synchrotron radiation selectively excites groups of ^{57}Fe nuclear transitions that depend on the relative orientation of the x-ray polarization and the hyperfine-field vector. The time resolved spectra of the scattered radiation display a quantum beat pattern, arising from the interference between the different nuclear excitation channels, that reflects the hyperfine-field orientation and magnitude [2]. Time spectra of nuclear forward scattered radiation from films entirely consisting of ^{57}Fe are shown in Fig. 1b, c for two selected film thicknesses. The 2 ML beat pattern closely corresponds to the one expected for the hyperfine-field vector in the film plane and aligned to the Co film magnetization. The 7 ML spectrum instead does not fit any simple pattern,
suggesting either spin-canting or a non-uniform distribution of the hyperfine-field in this Fe film. The analysis of the 7 ML film magnetic structure is made possible by the layer-resolved spectra (Fig. 2b, c) from a sample with a ^{57}Fe monolayer located at different distances from the interfaces (Fig. 2a). The spectrum of the central atomic layer (Fig. 2c) displays a beat-pattern with a more uniform frequency than the one of the interface (Fig. 2b). These two different patterns are readily explained by a rotation of the hyperfine-field vector. Spectral evaluation shows that the hyperfine-field vector at the interface lies parallel to the Co film magnetization, whereas it points along a nearly perpendicular direction in the inner atomic layers. A schematic picture of a simple magnetic structure consistent with the above results and with complete series of layer-resolved time spectra is shown in Fig. 3.

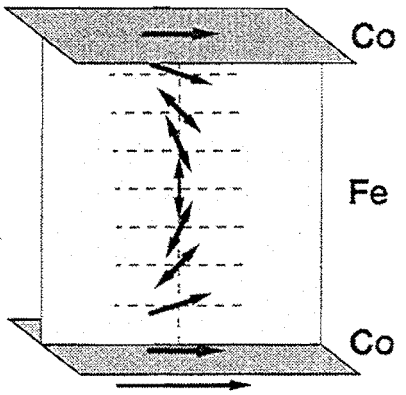

FIG. 3. Schematic picture of a magnetic structure consistent with the results from layer-resolved nuclear resonance scattering measurements.

While either ferromagnetic or antiferromagnetic configurations were commonly assumed to represent the magnetic ground state of fcc-Fe films, depending on their thickness and atomic volume, nuclear resonance scattering gives clear evidence for a non-collinear spin structure in Fe films of 7 ML thickness. The occurrence of such a non-collinear spin state was not previously observed nor theoretically predicted for fcc-Fe films, and it appears to be a unique case among ultrathin (<10 atomic layers) layers of itinerant-electron systems.

[1] R.J. Weiss, Proc. Phys. Soc., London, 82, 281 (1963).
[2] G.V. Smirnov, Hyp. Int., 97/98, 551 (1996).

Three-dimensional Spin-structure on a Two-dimensional Lattice

Ph. Kurz[1], K. Hirai[2], and S. Blügel[1]
[1] *Institute "Electronic Properties"*
[2] *Department of Physics, Nara Medical University, Kashihara, Nara 634-8521, Japan*

Based on vector spin-density first-principles total-energy calculations of the magnetic and electronic structure of Cr and Mn transition-metal monolayers on the triangular lattice of a (111) oriented Cu surface, we propose for Mn a three-dimensional non-collinear spin structure on a two-dimensional triangular lattice as minimum energy magnetic state. This new spin-structure is a multiple spin-density wave of three columnar spin states and comes about due to magnetic interactions beyond the nearest neighbors and due to higher order spin interactions (i.e. four-spin). The magnetic ground state of Cr is the coplanar non-collinear periodic Néel structure.

F&E-Nr: 23420

The effect of frustration on the magnetic properties has been intensively investigated in the last decade. High current interest is driven by the investigation of exchange bias systems. In magnetic systems the term *frustration* refers to the inability to satisfy the competing exchange interactions to neighboring atoms. Frustration is known to be responsible for a number of diverse phenomena such as spin-glass behavior, non-collinear and incommensurate magnetic order, and unusual critical properties. One of the most evident examples of frustration is the so-called geometric frustration of an antiferromagnet on a triangular lattice. In fact, triangular antiferromagnets can be crystallized i.e. in form of stacked antiferromagnets. Typical compounds are $RbNiCl_3$, VCl_2, or $CuCrO_2$ and they are *localized* spin systems. The magnetic properties of these triangular antiferromagnets are described in terms of the classical (and recently also in terms of the quantum) Heisenberg model:

$$H = -\sum_{i,j} J_{ij} \mathbf{S}_i \mathbf{S}_j \,, \qquad (1)$$

where J_{ij} describes the exchange interaction between spins at lattice site i and j. $\mathbf{S}$ is the classical spin-vector related to the magnetic moment vector $\mathbf{m}$, $\mathbf{m} = g\mathbf{S}$. Localized spin systems are well described by restricting the antiferromagnetic ($J_{ij} < 0$) interaction to the nearest-neighbors (n.n), $J_{ij} \approx J_1$. In this case the minimum energy configuration is a two-dimensional non-collinear 120^0 structure with three atoms per surface unit-cell, which consists of coplanar spins forming $\pm 2\pi/3$ angles between nearest neighbors, which leads to a $\sqrt{3} \times \sqrt{3}$ periodic Néel state.

Until now there is no investigation of *itinerant* antiferromagnets on a triangular lattice. Itinerant antiferromagnetism in three dimensions is observed for transition metals and compounds synthesized with V, Cr, Mn, The electrons that are responsible for the magnetic order of these metals do participate in the formation of the Fermi-surface. Thus electrons responsible for the formation of the magnetic state hopp across the lattice and it is by no means clear in how far the magnetic interaction on a triangular lattice can be described just by the short-ranged n.n. interaction and in how far the Heisenberg model can be applied at all. A triangular lattice is easily provided by (111) oriented (noble metal) substrates on which transition-metal monolayers are grown or by a pseudo-hexagonal growth as for example of c(8 × 2)Mn on Cu(100).

The aim of this work is to investigate the ground-state spin structure of Cr and Mn monolayers on Cu(111) beyond the (n.n.) Heisenberg model by performing *ab initio* calculations based on the density functional theory. Due to the limited space available we focus here on the discussion of unsupported (free standing) monolayers (UML) of Cr and Mn taken at the Cu lattice constant. The UML represents a model system for monolayers (ML) on a noble metal substrate, because the hybridization with the noble metal is rather small.

The calculations are carried out with the full-potential linearized augmented plane-wave (FLAPW) method in film geometry as implemented in the program FLEUR. The method has been extended to treat non-collinear magnetism as well as incommensurable spin-spiral structures with local spin-quantization axes around the atoms and the full continuous vector magnetization-density without any shape approximation in the region between the atoms and in the vacuum.

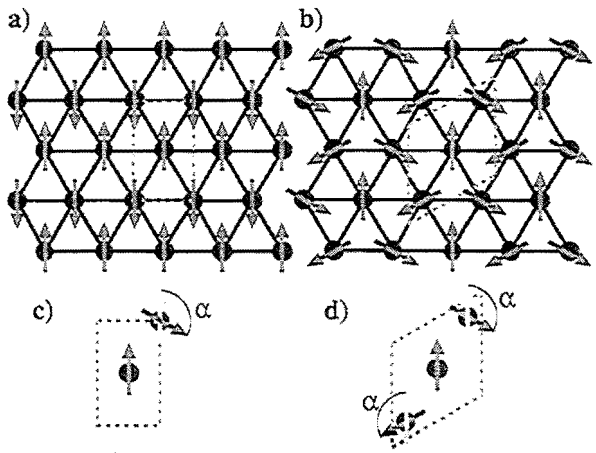

FIG. 1. a) The row-wise or columnar antiferromagnetic structure. b) The non-collinear 120° configuration. The ferromagnetic structure can be transformed by a continuous rotation into structure a) as indicated in c) and into structure b) as indicated in d).

Compared are the total energies and magnetic moments along continous rotation paths described by the angle α of the local moments connecting the ferromagnetic, the row-wise or columnar antiferromagnetic and the periodic Néel state in the corresponding 2 atom and 3 atom unit cells as indicated in Fig. 1.

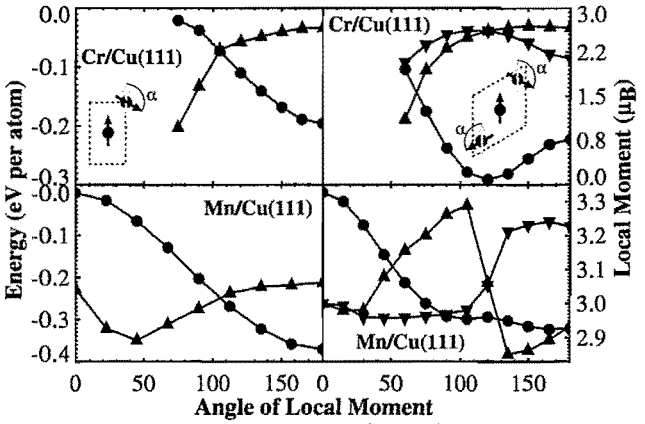

FIG. 2. Calculated total energy (circles) and magnetic moments (triangles) as function of the rotation angle α of the local moment for the UML of Cr (upper panels) and Mn (lower panels) with the Cu(111) geometry. The left panels show rotations that transform the ferromagnetic structure into the row-wise antiferromagnetic structure. The right panels show the rotations according to Fig. 1d. The scales of the left and right panels are equal, they differ, however, between Cr and Mn. Generally, the moments of the center atom (up-triangles) and the outer atoms (down-triangles) differ in the unit cell with three atoms.

The results of the calculations are presented in Fig. 2. Consider first Cr: Starting from the row-wise antiferromagnetic solution (Fig. 2 upper left panel) and rotating towards the ferromagnetic structure the magnetic moment decreases rapidly and finally disappears at $\alpha \approx 60°$. Thus, a ferromagnetic solution of the Cr(111) UML in the lattice constant of Cu does not exist. Although the moment changes drastically, the energy shows a cosine-like behavior in the region where a magnetic solution exists, as the n.n. Heisenberg model predicts for an antiferromagnet. The total energy along the rotation path in the unit cell Fig. 1d (Fig. 2 upper right panel) reveals a pronounced minimum at 120°. This minimum and shape of the energy curve matches very well the expectation from the Heisenberg model. It is clearly visible that the 120° configuration is the lowest energy configuration among all configurations studied here. Thus, it is the magnetic ground state of the Cr UML predicted by the present investigation.

Now turning to Mn and comparing the results in the two-atom unit-cell (Fig. 2 lower left panel) with those of Cr (Fig. 2 upper left panel) we find the behavior of Mn and Cr is very similar, i.e. the energy curve is cosine-like and Mn prefers to be antiferromagnetic. However, in contrast to Cr the ferromagnetic state exists and the magnetic moments change only within a narrow range, 2.9 μ_B - 3.05 μ_B, with the rotation. The calculations reveal, however, 2 surprises: (i) The total energy of the Mn system with 3 atoms per unit cell does not exhibit a minimum at 120°, as commonly expected by the n.n. Heisenberg model, but a local maximum or saddle point. (ii) The lowest energy configuration among all magnetic structures investigated so far, is the row-wise antiferromagnetic configuration.

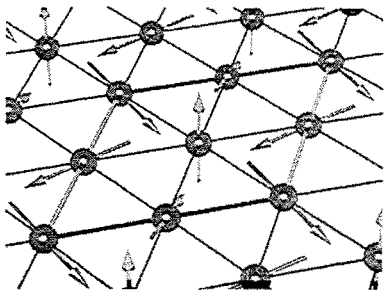

FIG. 3. An image of the 3Q-structure structure.

Consequences: In the Heisenberg model including the exchange interactions between the nearest, next-nearest, and next-next nearest neighbors, J_1, J_2, J_3, respectively, the energy as function of the relative angle α is given as $E(\alpha) = -(J_1 + J_3)(4\cos\alpha + 2\cos 2\alpha) - 6J_2$. This energy dependence is not in agreement with the functional form of the results (i). Instead a term $\sim \cos 3\alpha$ is missing to explain the results, which is indicative of a higher order spin interaction due to the itinerant nature of the electrons. The lowest order correction to the Heisenberg model is due to four-spin interactions

$$H_{4-spin} = -\sum_{ijkl} K_{ijkl}\big[(\mathbf{S}_i\mathbf{S}_j)(\mathbf{S}_k\mathbf{S}_l) + (\mathbf{S}_j\mathbf{S}_k)(\mathbf{S}_l\mathbf{S}_i) - (\mathbf{S}_i\mathbf{S}_k)(\mathbf{S}_j\mathbf{S}_l)\big]. \quad (2)$$

Within the n.n. approximation ($K_{ijkl} = K_1$), $E_{4-spin} = -K_1(4 + 8\cos 3\alpha)$, a functional form in agreement with result (i).

The columnar magnetic structure corresponds to a spin-density wave state with a single **Q**-vector, which coincides with the $\overline{M}$-point of the two-dimensional Brillouin-zone (BZ), $\mathbf{Q} = (\pi, \pi/\sqrt{3})$. In the BZ there are three equivalent $\overline{M}$-points with three different **Q**-vectors. Within the Heisenberg model the energy of the three spin-density waves and any linear combination of these spin-density waves are degenerate. The four-spin interaction lifts this degeneracy and multiple spin-density waves may become lower in energy. For Mn we predict the existence of a new magnetic ground state, a so-called 3**Q**-structure, 15 meV/atom lower in energy than the single **Q**-structure, which is a three-dimensional non-collinear spin-structure (see Fig. 3) with four atoms per surface unit-cell, and is formed as linear combination of the columnar magnetic structures with **Q**-vectors of the three inequivalent $\overline{M}$-points.

Massively-parallelized FLAPW-program for large-scale applications

G. Bihlmayer and S. Blügel
Institute 'Electronic Properties'

We report on the development of a parallelized *ab-initio* bandstructure code FLEUR, suitable for large scale applications on massively parallel computer systems as well as smaller applications on workstation clusters. Our program is a realization of the full-potential linearized augmented planewave (FLAPW) method that was parallelized on the $\vec{k}$-point as well as on the eigenvector level. The parallelization was implemented with the message passing interface (MPI) and our tests were made on a Cray-T3E.

F&E-Nr: 23200

Since nowadays more and more massively parallel computer systems succeed the former vector-supercomputers, it is – for numerically intensive applications – of great importance to perform satisfactorily on these parallel machines. Unfortunately, the very complex structure of a FLAPW-program [1] does not lend itself so directly to parallelization as other applications do. The fact, that there is no single, well defined part of the program that consumes almost all computer-time, calls for flexible parallelization strategies.

When metallic systems of moderate size are calculated, the eigenvalue problem has to be solved for a number of $\vec{k}$-points, $N_{\vec{k}}$, that equals or even surpasses the number of processors, N_{pe}, available for the application. Since most of the computing-time is proportional to $N_{\vec{k}}$, to distribute this problems in a way, that each processor takes care of one or several $\vec{k}$-points is an appropriate parallelization strategy. But as the size of the system gets larger, the Brillouin-zone shrinks and $N_{\vec{k}}$ falls below N_{pe}. On the other hand, the matrices involved in the eigenvalue problem get bigger and the memory requirements quickly surpass the resources available on a single processor. Evidently, the need to distribute the eigenvalue problem over several processors is growing if we want to migrate from the traditional supercomputers to massively parallel systems, even if we loose some time due to the communication needed for a parallel eigensystem-solver. But also for smaller systems $\vec{k}$-point parallelization may not be satisfactory: insulators and semiconductors can be calculated with very few $\vec{k}$-points and, if the eigenvalue problem is only of moderate size, a large portion of the cpu-time may be spent in unparallelized parts of the program, most prominently the construction of the charge density from the eigenvectors. Here a strategy that distributes the charge density construction for different eigenvalues over the processors is the most natural way of parallelization.

To fulfill adequately the needs of all different kinds of calculations we introduced parallelization on two levels: $\vec{k}$-point parallelization and a combined eigenvector and eigenvalue parallelization. Depending on the actual values of $N_{\vec{k}}$ and N_{pe} as well as on the memory-resources on the individual processors, the program and the user are free to decide how many processors should work on a single $\vec{k}$-point, $N_{\mathrm{pe}}^{\mathrm{ev}}$.

We choose a calculation of a 9-layer film of Cu(110) in a p(4×2) unit cell as reference system for our tests (this system was also chosen in performance tests of the unparallelized WIEN-code [2]). In an calculation with only one $\vec{k}$-point we found that the 92.6 % of the cpu-time was spent in the $\vec{k}$-dependent part of the code, whereas the rest was used mainly for the potential construction (5.7 %). From this we expect that the $\vec{k}$-point parallelization will be a very efficient strategy.

In the parallelized version of the program the setup and the potential construction is done on a single processor to avoid write-conflicts with a minimum of additional programming work. All necessary variables are then broadcasted to the other processors and the potential can be read from file. The eigenvalue problem can now easily be distributed over the processors and the results (eigenvalues and -vectors) are written to a global direct access-file, if a common file system is available for all processors. Otherwise, each node may write his results to a private file and send the eigenvalues back to the node that did the setup and is now in charge of the determination of the Fermi-level. With this result the occupancy of the eigenvalues can be calculated and this 'weights' are sent back to all processors.

Given its 'private' eigenvectors and the weights, all nodes can now calculate a partial charge density and also other, partial quantities that are normally determined in this step, e.g. each node calculates the forces on the atoms, orbital moments etc. for those $\vec{k}$-points it calculated in the last step. Up to this point the communication between the nodes was almost negligible, but now the charge densities from all nodes are sent back to and summed up by the first node. Here, the mixing step and all necessary output is done that finishes a step of the self-consistency cycle.

Since there is no additional computational effort and a moderate amount of communication between the nodes, the performance is almost ideal. In our case a more than 92%-parallel program can be expected from the unparallelized calculation. But due to memory limitations (512 MB in our case) we cannot test this assumption, therefore we present in Fig.1 data of a smaller problem, a nine-layer calculation of p(1×1) Fe(100). This tests were done

for a 196 $\vec{k}$-point calculation as it occurs typically in the connection with calculations of the magnetic anisotropy calculations where often even a denser sampling of the Brillouin-zone is necessary.

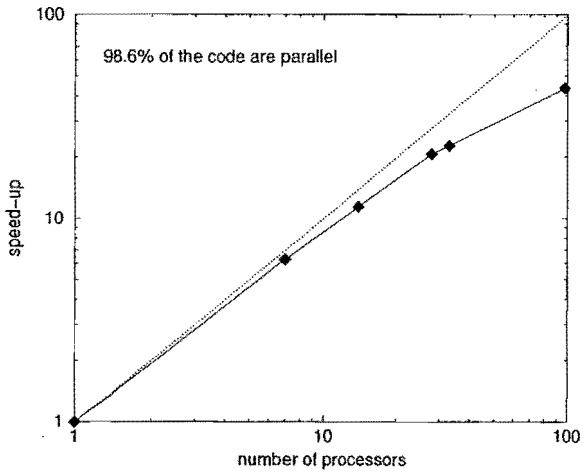

FIG. 1. Speed-up from the parallelization of the $\vec{k}$-points for a 9-layer film of Fe(100) with 196 $\vec{k}$-points.

Since $\vec{k}$-point parallelization alone does not suffice to calculate big systems on parallel machines (with normally much less memory per node than the classical vector-supercomputers), we have to split the eigenvalue problem in such a way, that the use of memory on each node is reduced.

For our purposes we found it most useful to adopt a parallel QR-algorithm for the solution of the generalized (symmetric or hermitian) eigenvalue problem that uses the matrices in a column-wise distributed fashion, i.e. a column i of the Hamilton- and overlap-matrix can be found on the processor with the number $mod(i, N_{\mathrm{pe}}^{\mathrm{ev}})$. Since our matrices are symmetric or hermitian we calculate only one part of every column, the other part is sent from the other nodes to complete the column. Compared to the unparallelized code, where symmetric-packed matrices are used, this gives us no big improvement on the use of memory if $N_{\mathrm{pe}}^{\mathrm{ev}} = 2$, but when four processors work on one $\vec{k}$-point we use only half of the memory per node for the matrices (and they normally use most of the memory in this step). Since the communication is moderate and no additional computational effort arises for the matrix setup, the scaling of this part with the number of processors is almost linear.

The parallel QR-algorithm reduces the generalized eigenvalue problem via a Cholesky-factorization to a normal one and uses a Householder transform to get a tridiagonal matrix. From this matrix the lowest eigenvalues are determined and the eigenvectors of the n-th of these eigenvalues are calculated on processor $mod(n, N_{\mathrm{pe}}^{\mathrm{ev}})$ by inverse iteration and back-transformation. Finally, each processor holds approximately the same number of eigenvalue/eigenvector pairs that can be dumped on a global or private file.

For the determination of the charge density there is no principal difference whether each node calculates a partial charge density from a subset of $\vec{k}$-points or from a subset of eigenvalues of a selected $\vec{k}$-point. Therefore, it is rather easy to implement a parallelized charge-density generator once the complete eigenvectors are available on the nodes. In this context it might also be worth mentioning that a reduction of the number of eigenvectors (and other quantities that are proportional to this number) further reduces the memory requirements of the code.

Now we can finally test the efficiency of the parallelization on the above mentioned example of the Cu(110) surface (Fig. 2). The memory requirements for the calculation with two processors was extrapolated and a similar value was also found for an unparallelized calculation on a computer with more memory available.

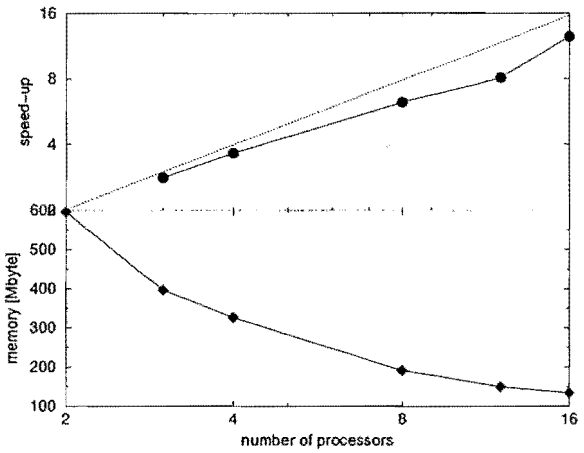

FIG. 2. Speed-up and memory requirements due to eigenvector parallelization tested on a 9-layer film of p(4 × 2) Cu(110) with a single $\vec{k}$-point.

For a program that covers a large range of possible applications and is run on a variety of platforms ranging from workstations to supercomputers it is difficult to find a strategy that optimizes the performance in all situations. With our implementation we sought to combine a maximum of transparency in the source-code with an acceptable performance for massively parallel calculations. So far, the use of the parallel version of our program has enabled calculations of systems with unprecedented complexity, e.g. of decorated step-edges and complex non-collinear structures.

[1] E. Wimmer, H. Krakauer, M. Weinert and A. J. Freeman, Phys. Rev. B **24**, 864 (1981).

[2] M. Petersen, F. Wagner, L. Hufnagel and M. Scheffler, Computer Physics Comm., in print (1999)

Inverse GMR-Effect in Fe/Cr/Au/Co-Systems

M. Buchmeier and P. Grünberg and R. Schreiber
Institute "Electronic Properties"

The inverse GMR-effect, which so far has only been found in few systems, is important for testing theories of spindependent electron scattering. We have found an inverse GMR-effect in MBE-grown Fe/Cr/Au/Co-samples. The magnetic layers are decoupled, and antiparallel alignment is achieved by the different coercivities of the Fe and Co layers of about 5 mT and 25 mT respectively. The GMR ratio is about an order of magnitude smaller than the anisotropic magnetoresistance in the same sample and the GMR in comparable Fe/Cr/Fe-systems. Although the resistivity decrease with magnetization reversal of the iron-layer is clearly due to inverse GMR, the exact size of the effect cannot be determined because of geometry dependent domain processes which are not yet understood.

F&E-Nr: 23420

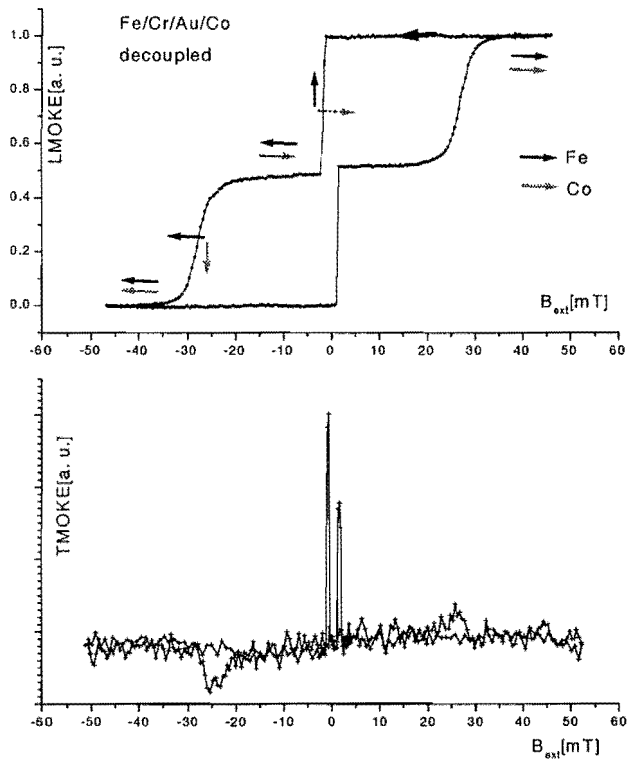

FIG. 1. Longitudinal and transversal hysteresis loops of Fe/Cr/Au/Co.

Giantmagnetoresistance (GMR) is caused by spin dependent scattering of electrons. Normally the resistivity is larger when the magnetizations of the layers are antiparallel. This occurs whenever the sign of spin dependent scattering is the same for both magnetic layers, e. g. majority electrons are more strongly scattered than minority electrons in both layers. However when the sign of spin dependent scattering is different, that is majority electrons are more strongly scattered in one layer and minority electrons in the other, the GMR-effect has a different sign. In this case called inverse GMR-effect the resistivity becomes smaller for antiparallel magnetizations. The inverse GMR-effect has only been found in few systems [1] [2], and was always small compared to normal GMR. Yet from simple calculations the GMR-effect of A/B/C/D-structures where A and D are ferromagnetic layers and B/C the interlayer should to first approximation equal the geometric average of the GMR of A/B/A and D/C/D. That is why for the Fe/Cr/Au/Co-system one would expect a big inverse GMR comparable in magnitude to the normal GMR of Fe/Cr/Fe and Co/Au/Co as the spin scattering asymmetry Fe/Cr is supposed to be opposite to that of Co/Au.

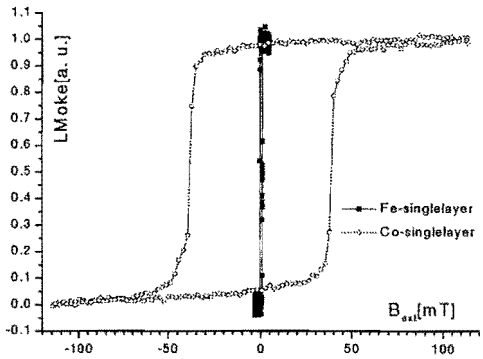

FIG. 2. Hysteresis loops of a single Fe and Co layer.

All samples where prepared by the MBE-technique at pressures of about 10^{-10}mbar and on GaAs(001)-substrates. After cleaning, the substrate was annealed in situ for 1h at 610 °C to obtain an oxygen-free surface. Then we deposited a 500 Å Au-bufferlayer on a 10 Å Fe-seedlayer. After annealing the buffer for 1h at 300 °C the GMR-system was prepared at room temperature with rates of 0.1 Å/s with the exception of the Co-layer which was grown at 320 °C. The layers were prepared

with the following thickness:
Au(500Å/Fe(50Å)/Cr(15Å)/Au(15-35Å)/Co(30Å).

The epitaxial relationship between the layers was Au(001)||Fe(001)||Cr(001)||Au(001) ||Co($11\bar{2}0$), Au[100]||Fe[110]||Cr[110]||Au[100] ||Co[0001]. This orientation of the Co-layer on Au(001) is favourable because it gives the least lattice mismatch and was found in Ref [3]. We did not establish this growth of the Co layer in detail but the monolayer thickness measured by RHEED-oscillations was in agreement with Co($11\bar{2}0$). The Co($11\bar{2}0$)-layer can grow in two twined crystallographic domains which has been found [4] to yield a four-fold symmetry with easy axes parallel to that of the Fe as was also the case for our samples. MOKE measurements of the in plane magnetization components parallel, "LMOKE", and perpendicular, "TMOKE", to an external field applied in easy-axis direction are shown in figure 1. They reveal decoupled layers in accordance with the hysteresis-loops of the single Fe- and Co-layers in figure 2. The somewhat larger coercivity of about 40 mT of the single Co-layer compared to 25 mT in the multilayer can be explained by the different quality. The samples were structured to obtain conductive strips of 0.5 mm width and 5 mm length by mounting a mask on top of the substrate before deposition. Magnetoresistance was measured by four-point technique using a high-precision DC-comparator-bridge. The curves in figure 3 clearly show an inverse GMR-effect of about 0.05 ‰ together with an anisotropic magnetoresistance (AMR) of about 0.5 ‰. Anyhow the GMR in the geometry $B_{ext} \perp I$ is only half as big as for $B_{ext} \parallel I$. This could be explained assuming out-of-plane magnetization components, non-perfect antiparallel alignment, or a geometry dependent magnetization reversal. Indeed the magnetization reversal curves for structured samples in figure 4 reveal a difference between B_{ext} applied perpendicular and parallel to the strips.

One reason for the rather small measured GMR-ratio is the shunting-effect which arises from the parallel current through the buffer layer with a much smaller resistance than the magnetic layer. The shunting effect cannot be easily calculated but a rough estimation gives a decrease of magnetoresistance by a factor 20. On the other hand comparable Fe/Cr/Fe samples show that our inverse GMR effect is still one order of magnitude smaller than normal GMR. This can be due to the additional Cr/Au interface in the interlayer.

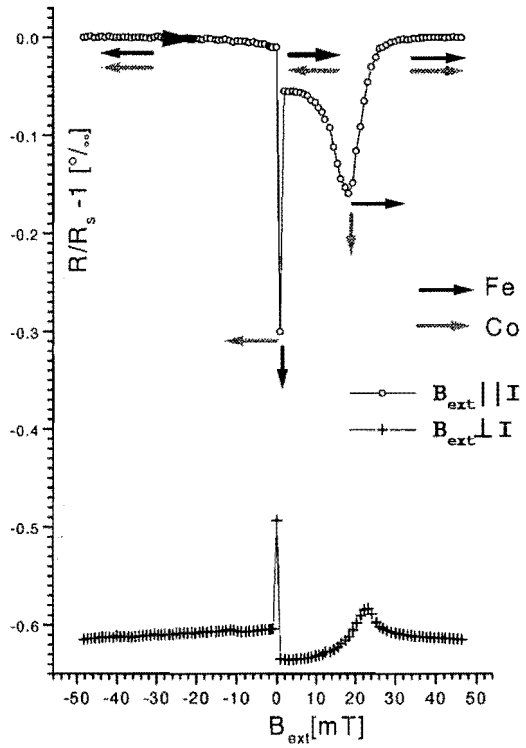

FIG. 3. Magnetoresistance for $I \perp B_{ext}$ and $I \parallel B_{ext}$

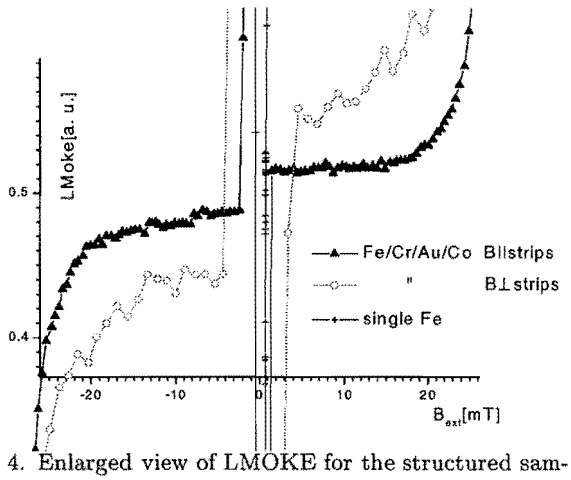

FIG. 4. Enlarged view of LMOKE for the structured samples and a single Fe-layer

[1] J. M. George *et al.*, Physics Review Letters **72**, 408 (1994).
[2] P. A. Schroeder *et al.*, Journal of Magnetism and Magnetic Materials **177**, 1464 (1998).
[3] S. Oikawa *et al.*, Journal of Magnetism and Magnetic Materials **156**, 73 (1996).
[4] K. Theis-Bröhl *et al.*, Physical Review B **53**, 11613 (1996).

Giant Magnetoresistance: Influence of Interface Roughness

D. Olligs, D. E. Bürgler, and P. Grünberg
Institute "Electronic Properties"

Epitaxial Fe/Cr/Fe trilayers have been grown on GaAs(001) substrates. In order to improve the growth, the substrate was covered with a Au(001) buffer layer. This enabled monitoring the roughness of the surface during growth by observing reflection high-energy electron diffraction (RHEED) oscillations. By this means, it was possible to change the roughness of the interfaces between the Fe and Cr layers while other properties of the trilayers were left nearly unchanged. Showing almost identical magnetic behavior, the magnetoresistance of trilayers with different interface roughness were significantly different, with the rougher samples having larger giant magnetoresistance ratios.

F&E-Nr.: 23.42.0

Since its discovery in 1988 [1], Giant Magnetoresistance (GMR) has attracted great interest due to a wide range of applications. GMR occurs in layered structures and granular systems consisting of ferromagnetic and non-ferromagnetic materials. Briefly described, normal GMR is a decrease in electrical resistivity with increasing magnetic order, *i.e.* alignment of the magnetizations of the ferromagnetic layers (or granules) which can be induced by an external magnetic field. In the commonly accepted picture, spin-dependent electron mobility and spin-dependent electron scattering account for this effect yielding a highly conductive spin channel in the case of ferromagnetic alignment. Spin-dependent scattering has previously been shown to occur at the interfaces of the ferromagnetic and non-ferromagnetic layers [2]. In this work, we will demonstrate that increasing the interface roughness of Fe/Cr/Fe(001) trilayers enlarges the GMR ratio, *i.e.* the ratio $(R_{AP} - R_P)/R_P$ where R_{AP} and R_P) are the resistivity for antiferromagnetically and ferromagnetically aligned Fe layers, respectively.

In order to achieve good reproducibility, it is mandatory to have well-defined samples. This requirement can be best fulfilled by using epitaxially grown layers prepared by molecular beam epitaxy (MBE) deposition onto monocrystalline substrates. The layer structure of our samples is shown in Fig. 1. We used (001)-oriented GaAs covered with a 1 nm-thick Fe seed layer and a 50 nm-thick Au layer which was annealed at 300° C for 1 h. With the substrate held at room temperature, Fe and Cr were deposited at a rate of 0.1 Å/s. At the same time, the intensity of the (00) reflection high-energy electron diffraction (RHEED) spot was observed, which is indicative of the density of (monoatomic) steps on the surface. As the intensity oscillates with a period corresponding to an increase of one monolayer in thickness, it was possible to tailor surfaces with high and low step densities by stopping the deposition process of the bottom Fe layer [Fig. 2(a)] and the Cr layer [Fig. 2(b)] at minimum or maximum RHEED intensity. In the following we will call these samples *rough* and *flat*, respectively. Of course, this is only a qualitative measure of the interface roughness, but nevertheless a clear distinction of the samples. The difference in surface roughnesses persisted as different interface roughnesses of the complete trilayer, which was confirmed by x-ray reflectivity measurements [3]: The rms-roughness of the rough samples was 0.5 Å larger than that of the flat samples. We prepared several samples with flat and rough interfaces, the individual thicknesses of the bottom Fe layer, t_{Fe}, being 14.0 and 14.5 monolayers (≈ 20 Å), respectively, 9 monolayers (≈ 13 Å) for the Cr layers, and 40 Å for the top Fe layers (see Fig. 1).

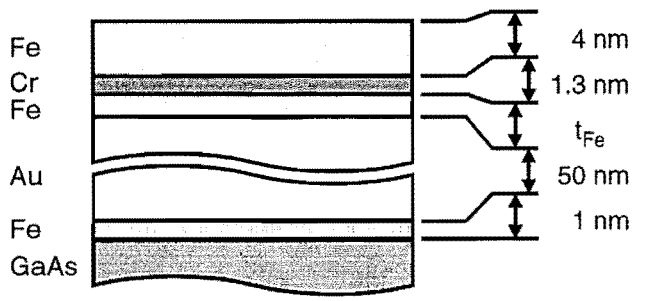

FIG. 1. Schematic structure of the sample. The thickness of the bottom Fe layer is $t_{Fe} = 14.0$ ML and $t_{Fe} = 14.5$ ML for "flat" and "rough" samples, respectively. Note, that the Au buffer layer is much thicker than the Fe/Cr/Fe trilayer.

Examination of the magnetic behaviour was performed using the magnetooptical Kerr-effect (MOKE). In all samples, the magnetizations of the two Fe layers were coupled antiferromagnetically and could be aligned parallel in an external magnetic field. The transition to parallel alignment occurred via an intermediate state of nearly 90° canted orientation of the magnetizations at intermediate fields of approximately 50–120 mT.

Subsequently, the samples were lithographically patterned to enable four-probe resistivity measurements. Since the underlying Au buffer layer is much thicker than the Fe/Cr/Fe trilayer, the in-plane conductivity of the samples is dominated by the buffer which results in a strong decrease of the magnetoresistance ratio (shunting effect). In order to be able to measure magnetoresistance accurately, a DC current comparator bridge was

used and the samples were held at constant temperature in a cryostat [4]. Resistance measurements presented here were performed at 300° C. Normalized magnetoresistance curves obtained from samples with rough and flat interfaces with the external magnetic field applied

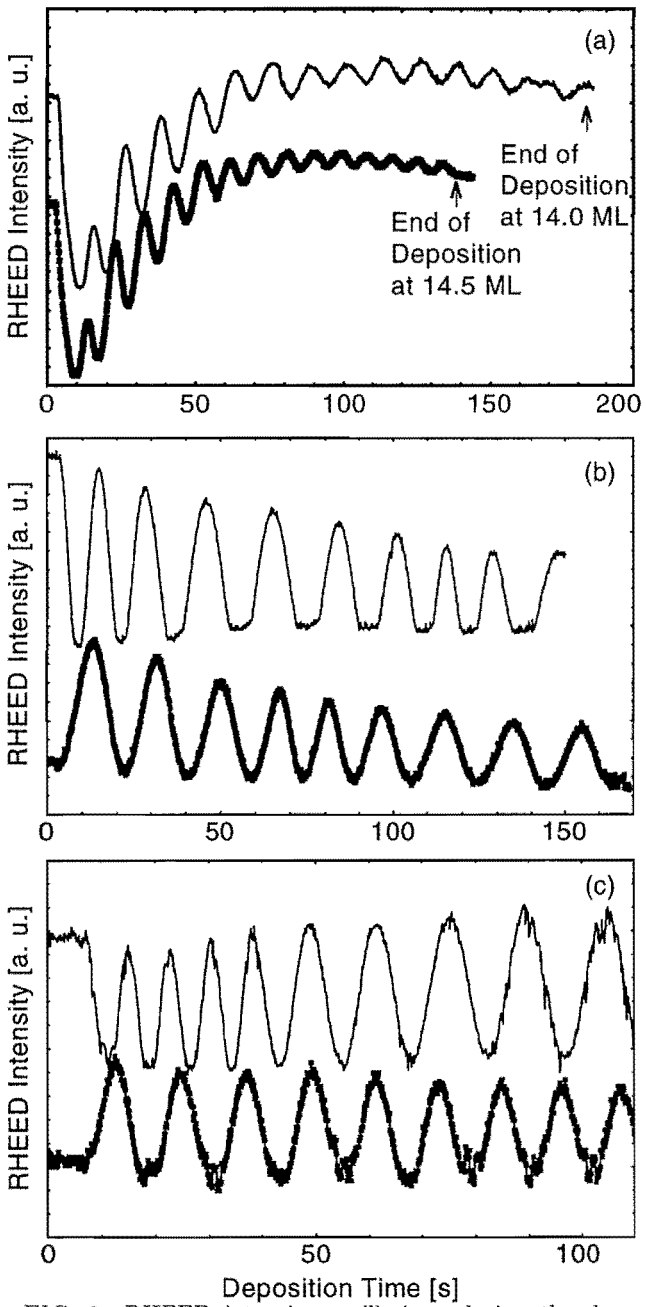

FIG. 2. RHEED intensity oscillations during the deposition of Fe/Cr/Fe(001) trilayers: (a) bottom Fe layer on (001)-oriented Au buffer layer, (b) Cr layer, and (c) top Fe layer. Curves are vertically displaced for clarity. The respective upper curves correspond to the sample with flatter interfaces obtained by ending the deposition at maximum RHEED intensity. Note that no phase slips occur at the beginning of the deposition of the subsequent layers.

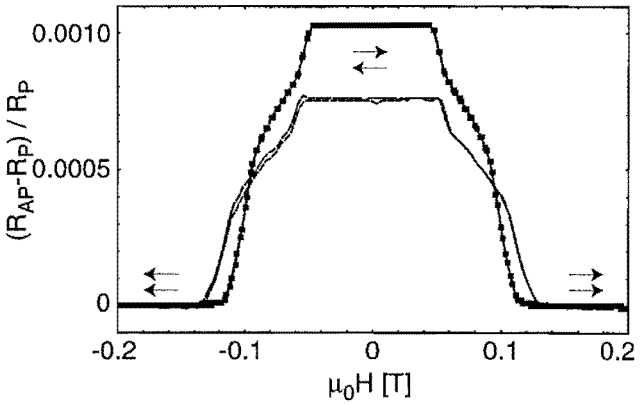

FIG. 3. Normalized GMR curves of samples with rough (thick line) and flat (thin line) Fe/Cr interfaces. The rougher interfaces result in a larger resistivity change from antiparallel to parallel orientation of the magnetizations.

in the magnetically easy Fe (100) direction are shown in Fig. 3. The sample with rougher interfaces revealed a significantly higher GMR ratio $(R_{AP} - R_P)/R_P$ and needed a slightly lower external field to achieve magnetic saturation. With the well-defined magnetic configurations at zero field (antiparallel alignment) and at saturation (parallel alignment) being the same for both samples, the differences in the GMR ratio must be due to the structural difference and therefore due to the difference in roughness. The dependence of the GMR ratio on the Fe layer thickness ($t_{Fe} = 14.0$ ML *versus* $t_{Fe} = 14.5$ ML) is too weak to account for the observed effect. In the case of the measurements presented in Fig. 3, the change in roughness caused by going from RHEED maximum to minimum leads to a 36% increase of the GMR ratio.

With these experiments we have demonstrated the importance of spin-dependent scattering at the ferromagnetic/non-ferromagnetic interfaces. Moreover we were able to show that increasing the interface roughness in Fe/Cr/Fe trilayers leads to higher GMR ratios. This result is in agreement with the qualitative statement by Schad *et al.* [5] based on annealing-induced roughness variations in Fe/Cr(001) multilayers. Further studies including STM characterization of roughness are required to determine the optimum degree and type of roughness to achieve maximal GMR ratios.

[1] G. Binasch, P. Grünberg, F. Saurenbach, and W. Zinn, Phys. Rev. B **39**, 4828 (1989); M.N. Baibich, J.M. Broto, A. Fert, F. Nguyen Van Dau, F. Petroff, P. Etienne, G. Creuzet, A. Friederich, and J. Chazelas, Phys. Rev. Lett. **61**, 2472 (1988).

[2] S. S. P. Parkin, Phys. Rev. Lett. **71**, 1641 (1993).

[3] Cooperation with E. Kentzinger, U. Rücker: Institut für Streumethoden, IFF, Forschungszentrum Jülich.

[4] D. Olligs, PhD thesis, Universität Köln (1999).

[5] R. Schad, P. Beliën, G. Verbanck, V. V. Moshalkov, Y. Bruynseraede, H. E. Fischer, S. Lefebvre, and M. Bessiere, Phys. Rev. B **59**, 1242 (1999).

Photoelectron Spectroscopy of Benzene-Adsorbed Metal-Cluster-Anions

G. Lüttgens, C. Friedrich, N. Pontius, P.S. Bechthold, M. Neeb
Institute "Electronic Properties"

Photoelectron detachment spectra of mass-selected organometal-clusters $M_n(C_6H_6)^-$ (M=Pt, Pd, Pb) have been measured using photon energies of a Nd:Yag laser. The photoelectron spectra of the benzene-adsorbed clusters show distinct differences to the corresponding spectra of the unreacted clusters. Vibrational fine structure on the lowest photoelectron peak of $Pt_2(C_6H_6)^-$ provides spectroscopic information about the intermetallic bond of the cluster-adsorbate-systems. The mass resolution of the cluster beam apparatus used is currently under improvement.

F+E-Nr. 23200

Studies of molecules adsorbed on clusters are of great interest since these systems can serve as models for chemical catalysts. In spite of this potential technological importance, information about the electronic structure of organometallic clusters is quite rare [1] since most of them cannot be produced by chemical synthesis.

In our group platinum-benzene, palladium-benzene and lead-benzene clusters have been produced in a laser vaporization source combined with an adsorbate gas valve. The cluster anions produced in the source are accelerated and mass-separated in a time-of-flight mass spectrometer and subsequently photodetached by a Nd:YAG laser (photon energies: 1.16 eV, 2.33 eV, 3.49 eV).

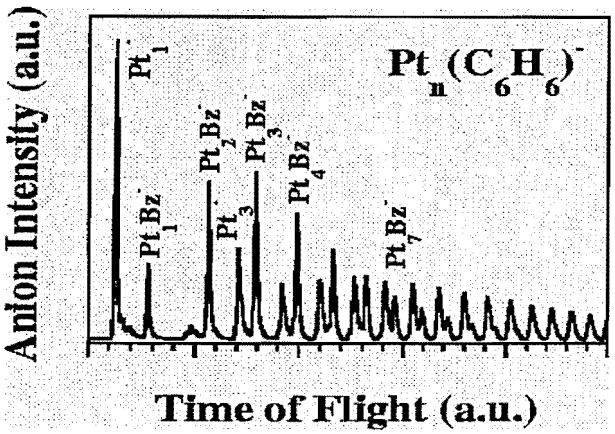

FIG. 1.: (a) Mass spectrum of $Pt_n(C_6H_6)^-$

A typical $Pt_2(C_6H_6)^-$ mass spectrum is presented in Fig. 1. The $Pt_n(C_6H_6)^-$ peaks appear between the peaks of the pure Pt-clusters. Higher adsorbed Pt-clusters could be produced by increasing the opening time of the adsorbate valve.

The photoelectron spectra of the benzene-adsorbed Pt-clusters clearly differ from the corresponding spectra of the pure Pt-clusters (see fig. 2). The peak at the lowest binding energy of the reacted Pt-dimer (X in fig. 2d) can be attributed to the transition from the ground state of the anion to the ground state of the neutral cluster. It is well separated from the peaks at higher binding energies. This indicates a closed shell system. The peak exhibits a vibrational fine structure when recorded at a photon energy of 2.33 eV (Fig.3). The vibrational energy is about 21meV which is slightly lower than the vibrational energy of unreacted Pt_2 (27meV).

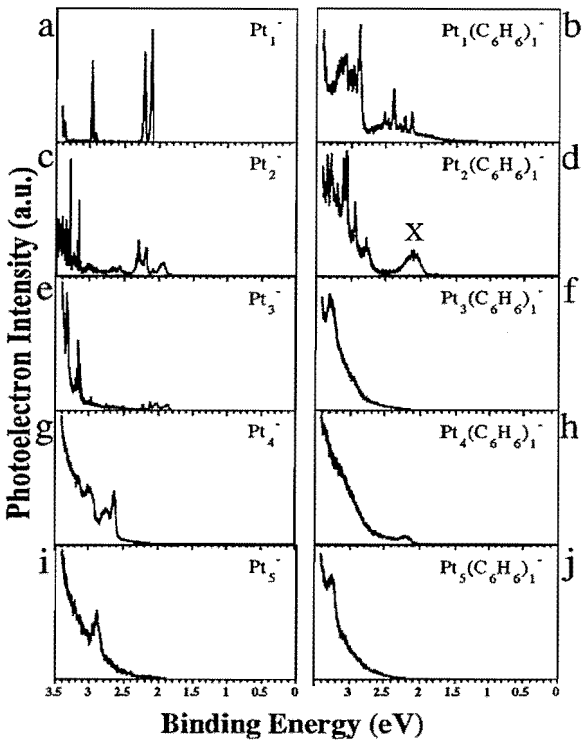

FIG. 2.: Photoelectron spectra of reacted and unreacted Pt_n^-

A detailed harmonic Franck-Condon analysis carried out using a recently adopted and modified computer program [2] gives the molecular parameters listed in Table I. The fit reveals a relative shift of the Pt-Pt equilibrium distance in $Pt_2(C_6H_6)$ between the neutral cluster and the anion by 11 pm. This together with the decrease

	$Pt_2(C_6H_6)$	$Pt_2(C_6H_6)^-$	Pt_2[Ref. 3]	Pt_2[Ref. 3]
electronic state	X	X	X $5d^{18}6s\sigma_g^2$	X $5d^{18}6s(\sigma_g^2\sigma_u^1)$
ω_e/meV	24.21	18.97	26.7	22.1
$\Delta r_e/pm$	11.0	11.0	7.4	7.4
electron affinity/eV	2.01		1.898	

TABLE I.: Spectroscopic data of the ground state of $Pt_2(C_6H_6)$

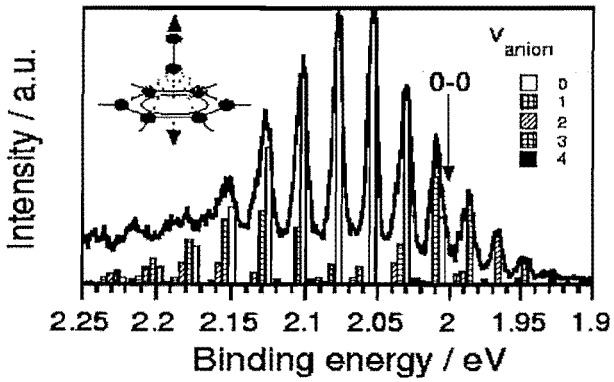

FIG. 3.: Franck-Condon profile of $Pt_2(C_6H_6)^-$

of the vibrational constant upon photodetachment and the extended Franck-Condon-profile leads to the conclusion that the $6s\sigma_u$-LUMO (lowest unoccupied molecular orbit) of $Pt_2(C_6H_6)$ is antibonding.

Although the relative bond length is distinctly altered upon photodetachment, the force constant of the metal-metal bond in $Pt_2(C_6H_6)$ is just 7% smaller than the one of bare Pt_2. This suggests that the intermetallic σ-bond ($5d\sigma$, $6s\sigma$) is scarcely affected by the bonding to benzene. As the frontier orbitals of benzene belong to π_u and π_g symmetry, the bonding between the metal dimer and benzene is most likely mediated by the d(π, σ)-or bitals of Pt_2. This d-orbital participation in the platinum-benzene bond is indicated by the intense photoelectron signal above 2.5 eV in Fig. 2d.

Numerous overlapping and sharp peaks are observed within this region which are strongly enhanced with respect to the photoelectron spectrum of free Pt_2^- shown in Fig. 2c. These enhanced peaks are attributed to transitions from the hybridized d-states which are particularly suitable to interact with the frontier orbitals of benzene. From both the strong interaction of the d-orbitals and the observed metal-metal stretch vibration we conclude that the platinum dimer is most probably bound perpendicular to the benzene ring (C_{6v}).

With respect to symmetry adapted orbitals in C_{6v} (Fig. 3), the twofold degenerate e_{1g} orbital (HOMO, highest occupied molecular orbital) of benzene is able to hybridize with the $d\pi_{u,g}$ orbitals of Pt_2, forming a $d\pi$-$p\pi$ bond. The degenerate e_{2u} orbital of benzene, on the other hand, is allowed to interact with the $d\sigma_{u,g}$ or-

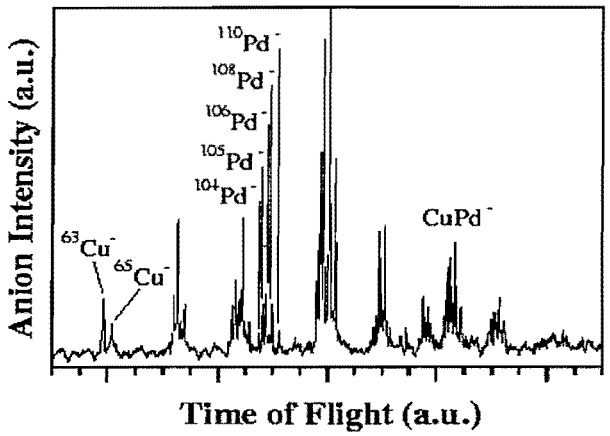

FIG. 4.: Mass spectrum of CuPd. The isotopic splitting of Cu, Pd and CuPd is resolved. The remaining peaks are due to contamination.

bitals of Pt_2 which results in a $d\sigma_{u,g}$-$p\pi^*$ back-donation from the metal into the LUMO of benzene. An orientation of the dimer parallel to the plane of benzene (C_{2v}) is not probable as this would not result in a vibrational frequency almost to that of free Pt_2.

Further studies of reacted clusters require an improved mass resolution of our time-of-flight mass spectrometer to separate heavy clusters with light molecules adsorbed. Lately a mass resolution ($m/\Delta m$)$\approx$ 400 has been reached using a perpendicularly accellerating Wiley-McLaren ion optics [5]. A resolution more than ten times better than before has been achieved. The mass spectrum of copper-palladium in Fig. 4 demonstrates the improved resolution. The isotopic splitting of the mass peaks is resolved. The improved mass spectrometer will allow us to study a great variety of organometallic clusters and other adsorbed clusters (e.g. $M_m(CO)_n$, $M_m(H_2O)_n$, Si_mH_n).

We gratefully acknowledge B. Küpper, J. Lauer and H. Pfeifer for technical support and K. Wingerath for his computational support.

[1] K. Judai, M. Hirano, H. Kawamata, S. Yabushita, A. Katajima, K. Kaya, Chem. Phys. Lett. **270**, No. 1-2 (1997), 23-30

[2] U. Telle, H. Telle, Comput. Phys. Commun., **28** (1982), 1, fitting routine: VA05AD, Harwell Subroutine Library, Combination: K. Wingerath, IFF

[3] J. Ho, K. M. Ervin, M. L. Polak, M. K. Gilles, W. C. Lineberger, J. Chem. Phys. **99**, 11 (1993), 8542-8551

[4] W. A. de Heer and P. Milani, Rev. Sci. Instrum. **62**, 670 (1991)

[5] G. Lüttgens, C. Friedrich, R. Klingeler, P. S. Bechthold, M. Neeb and W. Eberhardt, submitted

Cluster Deposition Experiment at the IFF/IEE
First Results: Mass Spectra of Metal-Doped Carbon and Fullerene Clusters

R. Klingeler, P.S. Bechthold, M. Neeb, and W. Eberhardt
Institute "Electronic Properties"

We present mass spectra of metal-doped carbon cluster cations $M_xC_n^+$ (M=Ca, Sc, Y, La, Ce, Gd; x=1, 2) produced in a 100 Hz laser evaporation source which is designed to deposit mass selected gas phase cluster ions onto a substrate under UHV conditions. The clusters are mass selected by a magnetic field deflector and are detected by a secondary electron amplifier behind the exit slit. The mass spectra of MC_n^+ reveal the onset of endohedrally doped fullerenes from which the smallest possible cage size can be deduced. $Y_2C_n^+$ and $La_2C_n^+$ show a distinct transition from odd-even to even-odd alternation at n = 69 and n = 71, respectively, which can be explained by a substantial change in the doped fullerene structure.

F&E-Nr: 23200

Short time after having clarified the fullerene structure of small carbon clusters, Smalley et *al.* found evidence for the existence of carbon cages with a single lanthanum atom trapped inside (endohedrally doped) [1]. In laser fragmentation experiments LaC_{60}^+ shrank by successive C_2 losses, and it was "difficult to fragment past LaC_{44}^+ and impossible to go past LaC_{36}^+ without bursting the cluster" [1]. This observation was the dawn of an extensive research activity on endohedrally doped carbon cages, since they were expected to exhibit useful properties controlled by the attributes of the encapsulated atom. However, basic properties are still not understood, e.g. the vanishing density of states at the Fermi level in bulk La@C_{82} [2], which is expected to be a metal.

So far, only a few M@C_n compounds are available in bulk quantities for conventional investigation techniques, among those are only clusters with 60 or more carbon atoms. However, one should consider that there is a multitude of endohedrally doped fullerenes covering a far wider range of masses.

In 1999 we set up a new experimental apparatus in our laboratory devoted to the deposition of mass selected cluster ions onto a substrate surface under UHV conditions. The clusters will be available for investigations using STM (scanning tunneling microscopy) and XPS (X-ray photoelectron spectroscopy). The whole machine consists of a three stage setup containing a laser evaporation source, a magnetic field mass analyzer, and a deposition chamber providing soft landing conditions (E_{kin}/atom < 1eV).

Fig. 1. shows mass spectra of metal doped carbon cluster cations as produced in the laser evaporation source using metal-carbon mixed sample rods. The spectra are taken by scanning the magnetic flux density of the magnetic ion deflector. Clusters between 30 amu and about 1700 amu are shown in the spectra. The spectra can be divided into two domains. On the left hand side the spectra always start with the metal monomer, followed by the subsequent addition of carbon atoms. No intensity of pure carbon clusters is observed below the metal monomer. This leads to the assumption of a metal induced carbon cluster condensation. The high mass domain to the right of each spectrum corresponds to cage structures.

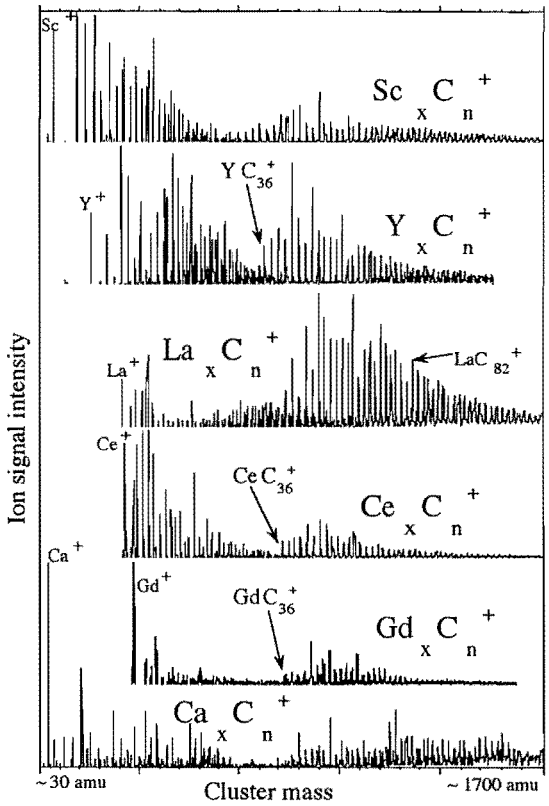

Fig. 1. Mass spectra of metal-doped carbon cluster cations as produced from a metal-doped carbon rod in a laser evaporation source. Metal-carbon compounds cover a wide range of cluster masses.

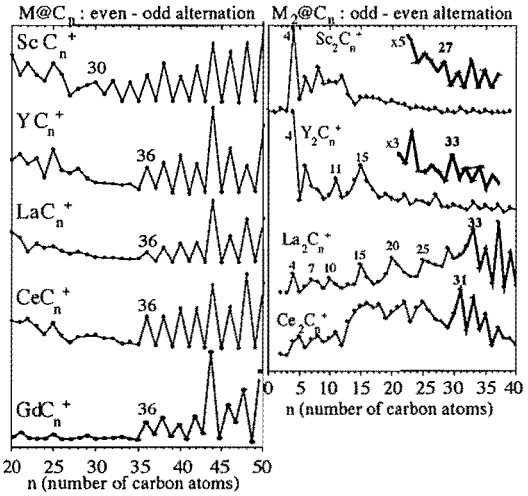

Fig. 2. Intensities of singly doped (left panel) and twofold doped (right panel) carbon cluster cations as a function of n. The intensity oszillation is characteristic for cage structures. From the onset the smallest possible endohedrally doped cage size can be deduced.

The intensities of singly doped carbon clusters MC_n^+ reveal the onset of a distinct even-odd alternation at a certain cluster size, which we consider to be the onset of endohedrally doped carbon cages. Thus, the smallest possible cage size for $M@C_n^+$ (n=30 for Sc, and n=36 for Y, La, Ce, and Gd) can be deduced directly from the spectra (Fig. 2).

In contrast, the intensities of twofold doped carbon cluster cations $M_2C_n^+$ reveal the onset of an odd-even alternation as a function of n at n=27 for Sc, n=33 for Y and La, and n=31 for Ce. As cages with an odd number of carbon atoms appear to be more stable than their even numbered neighbours, we suspect one metal atom to occupy the defect site of the carbon cage, while the other one is encapsulated within the cage (see Fig. 4 center sketch) as proposed by the results of ion mobility measurements [3]. Again, the smallest possible endohedrally doped cage size for these networked cages can be deduced from the mass spectra. It turns out that the smallest observed endohedrally doped networked cage size falls below the smallest observed endohedrally doped pure carbon cage size, namely by two atoms for the group III B transition metals and by four atoms for the 4f transition metal cerium. In order to replace the missing carbon atom, the networked metal cation needs to form three bonds with the neighbouring carbon atoms. The missing electron might be taken from the carbon π-system, thus lowering the electron density at the inside of the carbon sphere. This, in turn, creates additional space for the metal atom inside the cage in comparison to pure doped cages. More detailled information about the charge transfer processes in

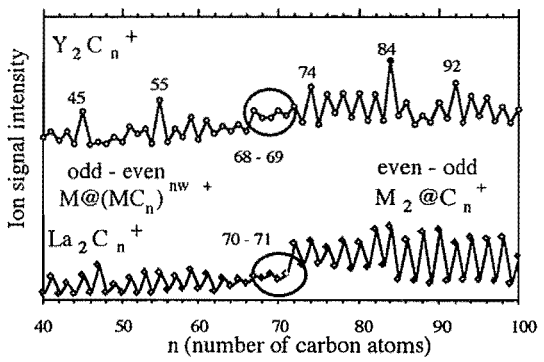

Fig. 3. Intensities of $Y_2C_n^+$ and $La_2C_n^+$ as a function of n. The transition from alternation odd-even to even-odd at n = 69 and 71, respectively, indicates a structural transition from endohedrally doped networked cages to biendohedrally doped cages.

these compounds should be taken from XPS studies and high level density functional calculations.

The intensities of twofold doped $Y_2C_n^+$ and $La_2C_n^+$ clusters show another interesting feature at higher masses, namely a sharp transition from an alternation odd-even to even-odd as a function of n at n=69 and n=71, respectively (see Fig. 3). Carbon cages containing more than 69 and 71 atoms, respectively, provide enough space to encapsulate two metal atoms inside ($M_2@C_n^+$), whereas smaller cages prefer endohedrally doped networked structures with one metal atom as part of the carbon network ($M@(MC_n)^{nw+}$, see Fig. 4); thus, a structural transition as a function of n takes place.

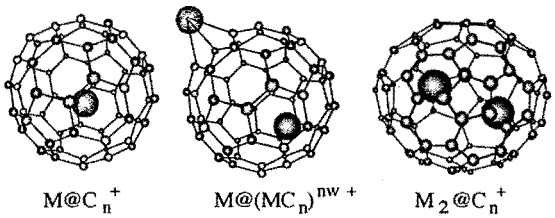

Fig. 4. Proposed structures for metal-doped carbon cages.

Future projects will focus on the size-selected deposition of doped fullerenes, metal clusters (open d-shell), and magnetic clusters (Fe, Co, Ni, Rh, $Gd@C_n$). Available experimental methods will be STM and synchrotron radiation based methods like photoemission (XPS/UPS), Auger, and absorption spectroscopy (NEXAFS). Very recently, we performed a first XPS experiment on deposited $Ce@C_{44}$ on copper revealing a metal to cage charge transfer induced Ce $3d_{3/2,5/2}$ core level shift of 2.8 eV.

[1] Y. Chai et al., J. Phys. Chem. **95**, 7564 (1991)
[2] B. Kessler et al., Phys. Rev. Lett. **79**, 2289 (1997)
[3] K. B. Shelimov and M. F. Jarrold, J. Am. Chem. Soc. **118**, 1139 (1996)

Electronic Structure of $(C_{59}N)_2$Studied Locally at the Nitrogen Site by Soft X-ray Emission

A. Karl[1], S. Eisebitt[1], R. Scherer[1], M. Freiwald [1], and W. Eberhardt[1]
A. Weidinger [2] and A. Hirsch[3]
[1] *Institute "Electronic Properties"*
[2] *Hahn-Meitner-Institut, Glienicker Str.100, D-14109 Berlin, Germany*
[3] *Institut für organische Chemie, Universität Erlangen, Henkestr.42, D-91054 Erlangen, Germany*

On cage doping in C_{60} was studied by investigating $(C_{59}N)_2$, where a C atom in each C_{60} ball is substituted by N. Using atom selective soft x-ray spectroscopy, we can detect the "extra electron" locally at the N site. The results are in good agreement with electronic structure calculations.

F&E-Nr. 23200

The possibility to dope fullerene structures in order to alter the electronic structure of these materials has stimulated a large number of experimental and theoretical studies over the last years. Historically, the first experimental results were obtained by adding one atom or ion either outside (intercalation) or inside the fullerene cage (endohedral fullerenes). In both cases, the fullerene cage is unaltered. For the substitution of one C atom by N in the fullerene cage of C_{60} an electronic behaviour resembling that of a donator-doped semiconductor was predicted.[1] The extra electron introduced into the occupied states by the N atom is difficult to detect by any non element-specific spectroscopy (such as photo electron spectroscopy) simply because there are more C than N atoms in each $(C_{59}N)_2$molecule. Consequently, the overall appearance of *e.g.* PES spectra for $(C_{59}N)_2$[1] and C_{60} is very similar and conclusions have to be drawn from small differences.[3]

Soft x-ray emission (SXE) is an atom selective spectroscopy, which allows to observe these small changes in the electronic structure locally at the N-atom. After excitation of the N 1s core electron into a specific unoccupied state of the heterofullerene by x-ray absorption using monochromatized synchrotron radiation, the fluorescent decay by transitions of valence electrons to the core vacancy is monitored. The emission transition probability reflects the *local partial* density of states at the N site. As a transition to a localized core orbital is involved, only electrons having overlap with the core orbital will contribute to the spectra. SXE was performed at the undulator beamline BW3 of the Hamburger Synchrotronstrahlungslabor, HASYLAB at DESY, Hamburg, by using a grazing incidence Rowland spectrometer, with a resolution set to 1.0 eV(C) and 1.5 eV(N).[2]

In Figure 1 we present the absorption spectra of C_{60} (I) and $(C_{59}N)_2$ (II) measured near the C 1s absorption edge. As expected, the spectra are virtually identical, as the C-p-DOS of the fullerenes is probed. Additionally, the absorption spectrum (SXA) measured at the N 1s edge in $(C_{59}N)_2$ (III) is shown. For a direct comparison the spectrum has been shifted to lower energies by 115.5 eV, which is the difference of the N1s and the C1s core level binding energies in $(C_{59}N)_2$. The strongest peak C coincides exactly with the t_{2u} derived state in C_{60} and $(C_{59}N)_2$ and can thus be interpreted as due to the transition of the N core electron in an empty state of the fullerene cage.

We now turn our attention to the occupied states as studied by SXE. In Fig. 2(a) we compare the C 1s SXE spectra of C_{60} and $(C_{59}N)_2$, excited at a photon energy of 284.5 eV, *i.e.* the core electron is promoted into the t_{1u} state. The overall shape of the $(C_{59}N)_2$ spectrum is very similar to the C_{60} spectrum, if one takes the different experimental resolution into account. This similarity is to be expected, as the spectra average over all C atoms on the fullerene. It is therefore useful to investigate the differences in the occupied electronic states of $(C_{59}N)_2$ and C_{60} by looking atom-selectively at the N site. This is shown in Fig. 2b, where the N 1s SXE of $(C_{59}N)_2$ is compared to the C 1s spectrum. Both spectra are shown on a relative binding energy scale corresponding to the respective core level binding energies in $(C_{59}N)_2$. Clear differences can be seen between the N 1s and C 1s SXE spectra, which approximate the N-p-DOS and C-p-DOS

[1] In a solid film as prepared by evaporation, $C_{59}N$ is found to be dimerized to $(C_{59}N)_2$.[2]

[2] The C_{60} spectra were recorded at the beamline 7.0.1 of the ALS, Berkeley, with a similar experimental setup.[4]

of $(C_{59}N)_2$, respectively. Here, we only want to turn our attention to region I, as indicated in Fig. 2. In region I, *i.e.* above the C_{60} HOMO, some extra intensity can be seen in the N-p-DOS of $(C_{59}N)_2$ as compared to the C-p-DOS of $(C_{59}N)_2$ and C_{60}, resulting in a high energy cutoff that is located at lower electron binding energy in the $(C_{59}N)_2$ spectrum as compared to the C_{60} data. The intensity at the valence band maximum stems from the "extra" electron of the N-atom. It remains mainly at the N-site and forms a new HOMO which is higher in energy than the HOMO in C_{60}. These measurements are in excellent agreement with theoretical calculations by W.Andreoni [1], which are included in the figure as vertical bars at the bottom of the graph. The dashed lines represent the LUMO, while the solid lines show the occupied states. The occupied state at about -0.2 eV in the calculation corresponds to the extra intensity in region I in the $(C_{59}N)_2$ spectrum. Due to the atom selectivity of SXE, this result is direct experimental proof for the conclusion drawn in Ref. [4], that the HOMO in $(C_{59}N)_2$ is mainly localized at the N atom. The fact that the additional valence electron in N (as compared to C) is localized at the N site illustrates the limits of the doping picture for $(C_{59}N)_2$: in a typical shallow doping situation in a semiconductor, the doping electron would be delocalized in the conduction band at room temperature.

We have started to prepare other doped fullerene structures such as N@C_{60} and K doped single wall carbon nanotubes in order to compare the effects of the doping on the electronic structure in these different systems.

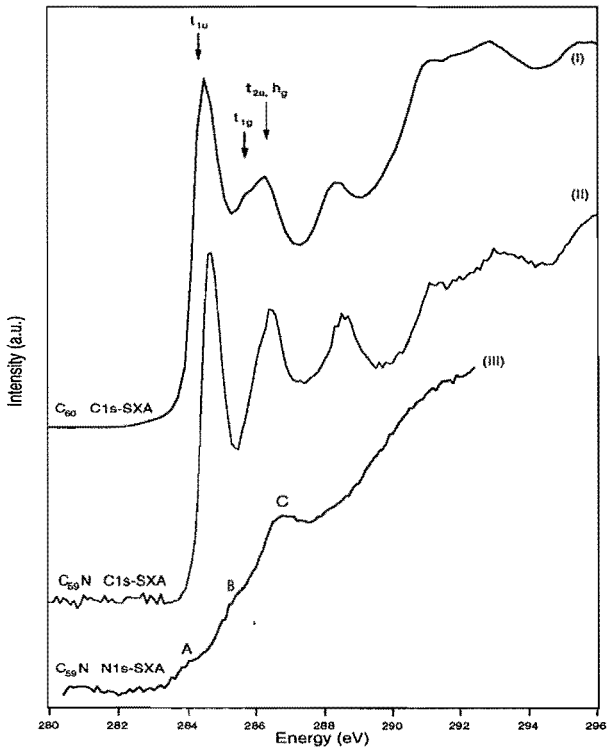

FIG. 1. SXA of C_{60}(a) and $(C_{59}N)_2$(b) around the C1s edge, (c) SXA of $(C_{59}N)_2$around the N1s edge

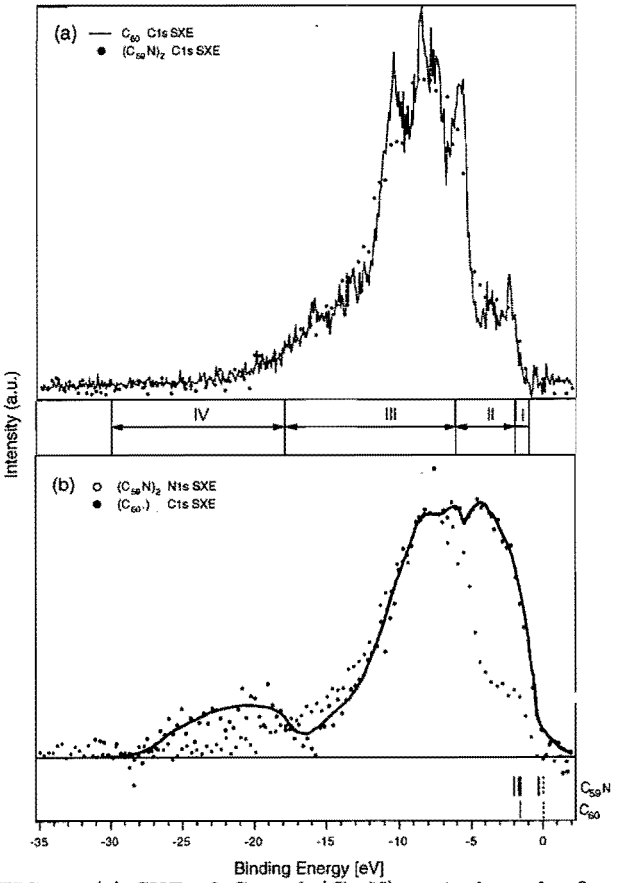

FIG. 2. (a) SXE of $C_{60}$and $(C_{59}N)_2$excited at the first peak of the C1s SXA; (b) Comparison of the SXE of $(C_{59}N)_2$excited at the C1s edge (open symbols) and the N1s edge (solid symbols, with line to guide the eye). The regions of interest I-IV are defined in between (a) and (b)

[1] W. Andreoni, F. Gygi, and M. Parinello, Chem. Phys. Lett.**190**, 159 (1992)

[2] B. Nuber, A. Hirsch, Chem. Commun. **1**, 1421 (1996)

[3] S. Eisebitt, et al., Appl. Phys. A **67**, 89 (1998)

[4] T. Pichler et al., Phys. Rev. Lett. **78**, 2289 (1997)

Installation and First Experiments on the Soft X-Ray Beamline at the Synchrotron DELTA in Dortmund

S.Cramm, B.Küpper, H.Feilbach, H.Sachsenhausen*, J.Lauer, H.Pfeifer, C.Zilkens

*Institute "Electronic Properties", *Dept. ZAT*

Abstract

The installation and commissioning of our beamline, dedicated to the synchrotron radiation research on the electronic structure of thin films, surfaces and nanostuctures, has been completed.
The mechanical and vacuum specifications were shown to be met. During a synchrotron run in March 1999 we carried out first test experiments in order to study the performance of the monochromator and the optical elements as well as the characteristics of the undulator, serving as the source of the soft X-Rays. An excellent resolving power E/ΔE of ≈ 10 000 was demonstrated at the Argon L_{23}-edge (241eV) and at the Neon $2s^{-1}$ 3p excitation threshold (45eV), respectively. The variability of the fixfocus constant c_{ff} and the source size of the electron beam in the storage ring can be further optimized.

F&E-Nr.:23891

The beamline[1] consists of a plane grating monochromator without entrance slit, 2 exchangeable gratings, a first mirror for horizontally collimating the beam and a refocusing mirror for the concentration of the monochromatized radiation onto the sample (see fig.2). The photon energy is selected by variation of both the grating and the premirror angle. Typical experiments are photoemission (XPS / UPS and spin resolved), absorption spectroscopy and soft X-Ray fluorescence spectroscopy.

The main parameters of the beamline are:

Photon energy range	8eV-400eV
(Wavelength	155nm-3nm)
Vertical acceptance	1mrad
Horizontal acceptance	2mrad
Grating line density	1200l/mm and 300l/mm
Fixfocus constant c_{ff}	1.4 – 10.0

The Free Electron Laser FELICITA I, lasing in the visible range when the electron storage ring DELTA is operated at an energy of 0.5 GeV, serves for our beamline as an Undulator in the soft X-Ray regime, operating DELTA at 1.5 GEV.

The parameters of the Undulator are as follows:

Magnetic field	zero to 0.13T
Deflection parameter k	zero to 3.12
Period length	250mm
Number of periods	16
Source size (design goal)	40μm

Stored current, design goal 500mA

A typical output spectrum of the beamline, demonstrating the variation of the undulator flux with the photon energy, is shown in fig.1:

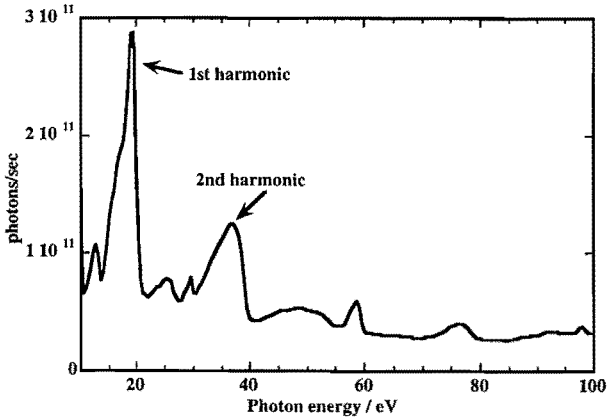

Fig.1: Flux at K_{Und}=2.0, slit=0.2mm and I_{DELTA}=5mA, storage ring electrons at 1.3GeV

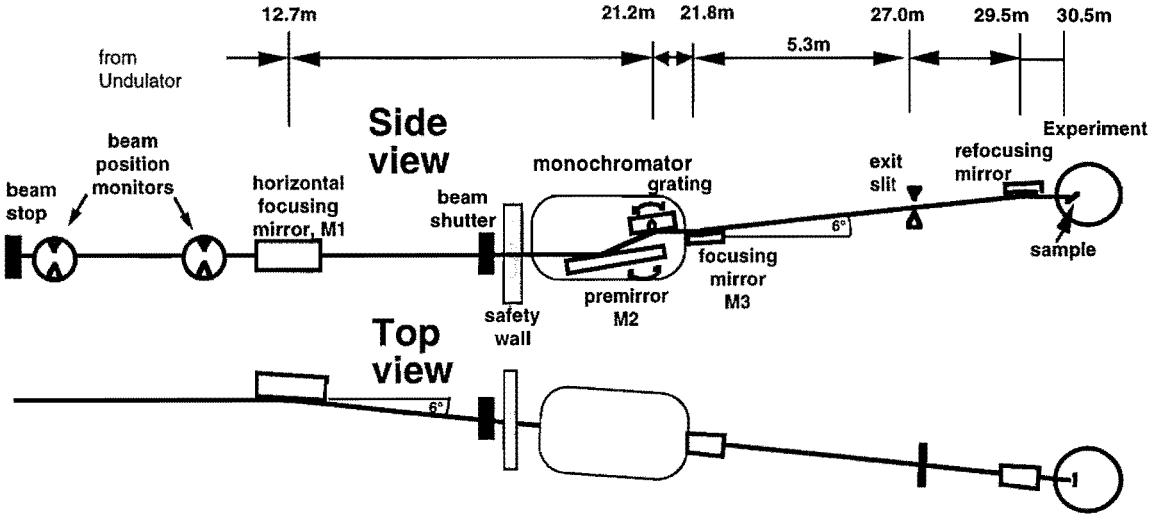

Fig.2: schematic layout of the optical elements of the IFF-beamline at DELTA

In order to study the resolving power of the beamline, we performed absorption spectra of various gases. Fig.3 shows an absorption spectrum of Argon at the $L_{2,3}$-edge.

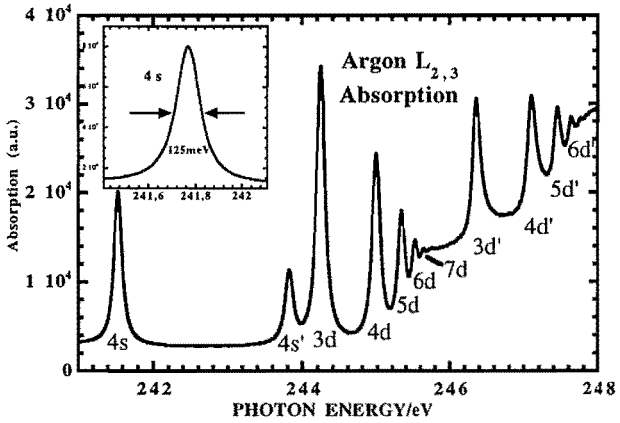

Fig.3: Ion yield spectra of Ar at the L_{23}-edge. Slit=8μm

All known features of the 2p – 4s and 2p –nd excitations are seen. As shown in the inset, the total width of the 2p – 4s peak is 125 meV, due to the largest extent to the natural linewidth (121meV) and only to a minor part to limited resolution of the monochromator (≈ 25meV). We deduce a resolving power of ≈ 10 000 at the Ar L_{23} edge.

On Neon gas we have recorded the 2s-1np absorption threshold. As can be seen in fig.4, excitation peaks up to n=17 are observable compared to 15 peaks previously reported[2]. In the upper inset it is shown that the total width of the n=3 slope is as low as 7meV.

As the electron beam in the storage ring serves as an entrance slit, the resolution of the monochromator is depending on the source size. To further improve the resolution at a given source size, the virtual magnification. of the source distance by the factor c_{ff} can be varied by

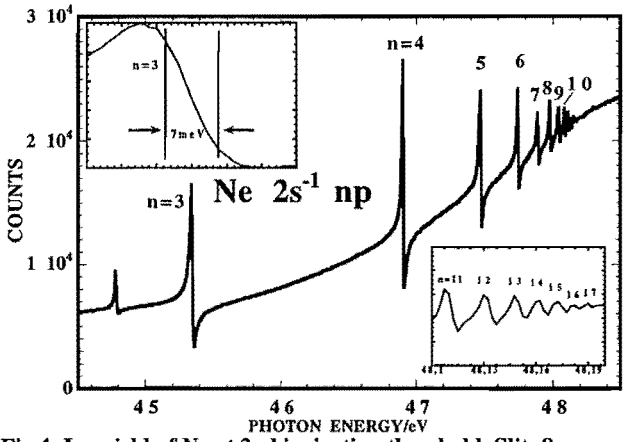

Fig.4: Ion yield of Ne at 2nd ionization threshold. Slit=8μm

choosing the incidence angles of the premirror and the grating. Each photon energy can be achieved both with a) more grazing incidence angles (large c_{ff} - better resolution) or b) steeper angles (small c_{ff} - better suppression of higher orders) [3]. It should be noted that during the measurements shown here only a standard value c_{ff}=2.5 was achievable. Hence the moderate demagnifacation of the source in combination with a larger than expected vertical source size turned out to be the limiting factor for the resolution. In the future we will be able to realize a value of cff=10. Furthermore the electron beam size in DELTA can be optimized. Therefore we are expecting an even better resolving power in the future.

The thermal stability of the optical elements under full heat load could not yet be tested since during our beamtime only storage ring currents of up to 50 mA were achieved.

[1] IFF-Jahresbericht 1993/95, Forschungszentrum Jülich

[2] BESSY-Jahresbericht 1995, p.130

[3] R.Reininger and V.Saile, Nucl. Instr.and Meth. **A288** (1990) 343

Orientation and Self-Assembly of hydrophobic fluoro-alcyl-silanes

D.Schondelmaier, J.Morenzin, S.Cramm and W.Eberhardt

Institute 'Electronic Properties'

Water repelling coatings combined with structured surfaces are the major key for the recently discussed ‚self cleaning mechanism'[1]. In the search of highly hydrophobic substances fluoro-alcyl-silanes prove to be an interesting representative of this kind. Optimisation of the applications of such molecular coatings requires a deep understanding of the structure and a detailed characterisation of the layers.
With synchrotron radiation (XANES, X-ray Absorption Near Edge Spectroscopy) we were able to show a high degree of orientation of tridecafluoro-octyl-triethoxy-silane molecules on different substrates. The analysis of the structure of the layers shows a strong bond of a single layer of molecules to the substrates. Further layers can weakly bind to the monolayer.
.

F&E-Nr.: 23.20.0

If a structured surface, containing holes and pins vertical to the surface is additional highly hydrophobic, drops of water can show contact angles close to 180°[2,3]. With such extreme contact angles the drops of water are nearly shaped spherical and show a different habit of floating. The drop of water is able to 'roll' on the surface. While 'rolling' it can bond and drag dirt. Surfaces like this are called selfcleaning surfaces. The important part of this effect is the high hydrophobic character of the surface in contact with the drop of water. The production of hydrophobic structured surfaces accordingly is of high industrial interest.

We have investigated the orientation and thickness of hydrophobic and selfassembling tridecafluoro-octyl-triethoxy-silane layers with polarisation dependent XANES (X-Ray Absorption Near Edge Spectroscopy)[4] at the BESSY synchrotron in Berlin and XPS (X-ray Photoelectron Spectroscopy) in our institute.

Tridecafluoro-octyl-triethoxy-silan (Fig.1) contains Silicon-ethoxide as a functional group ($Si(OCH_2CH_3)_3$). The end group reacts with water to form silicon hydroxide as reactive group at the end of the molecule. It is

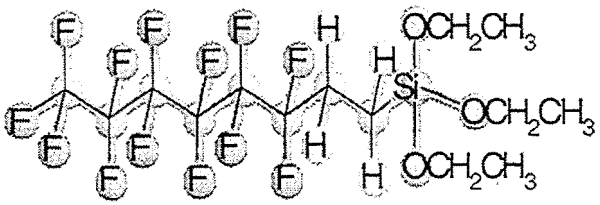

Fig. 1: 3,3,3,4,4,5,5,6,6,7,7,8,8,8 – tridecafluoro-octyl-triethoxy-silane, left: hydrophobic fluoro-alcyl right: reactive Silicon-ethoxide

responsible for the chemically bond with the substrate. The Fluoroalcylgroup is the hydrophobic part of the molecule.

According to the characteristic molecular structure, we expect a self-assembled, chemically bound mono-layer on the substrate. The hydrophobic ends of the fouro-alcyl group should orientates themselves away from the substrate. A chemical reaction between neighbouring molecules is likely

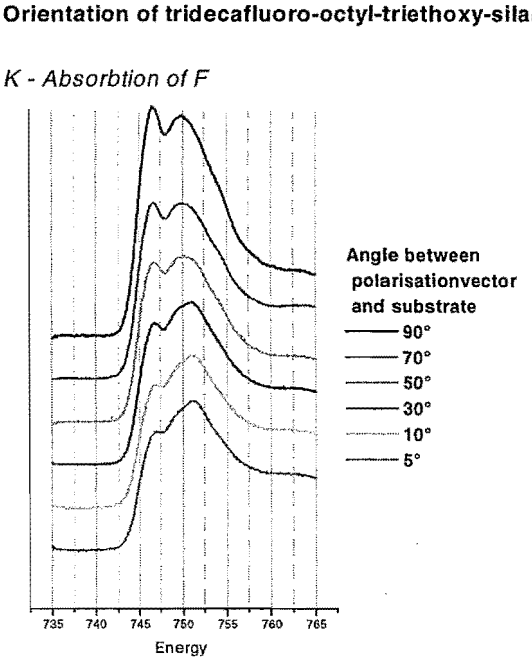

Fig. 2: polarisation dependent XANES

For the experiments planar substrates (e.g. Al, Si or ITO) were dip-coated from a solution. By this process several layers of molecules are grown on the substrate. The upper ones can easily be removed by washing (e.g. water, propanol, acetone).
The orientation of the Tridecafluoroctyltriethoxysilan molecules in the remaining layer has been determined by varying the orientation of the surface with respect to the polarisation of the synchrotron radiation. Fig.2 shows the K absorption spectrum of fluorine at different angles. The angular dependence of the relative peak intensities can be assigned to the orientation of the molecular axis. The strong dependence on the polarisation is well noticeable and shows the high amount of oriented molecules in the layer. An exact analysis of the data shows that the molecular axis is predominantly oriented perpendicular to the substrate surface.

Additional XPS measurements were made to determine the thickness of the layers. Therefore samples were prepared with and without different rinsing methods: 15 minutes ultrasonically in water, rubbing in water, 15 minutes ultrasonically in propanol and at last 15 minutes ultrasonically in aceton. The photoelectron emission intensity of fluorine 1s was compared (Fig. 3). The result of this study shows a strong bond between the lowest molecular layer and the substrate. Even rubbing or washing by aceton or propanol can't detach the lowest layer easily. Further layers are weakly bound to the lowest layer. These upper layers can be removed by rinsing in water. The coverage of the lowest layer can be estimated by comparison of the XPS intensity of a 6 Å layer of CaF_2. By heating the sample for several hours the upper layers are bond stronger but can also be removed up to the former described monolayer by washing.

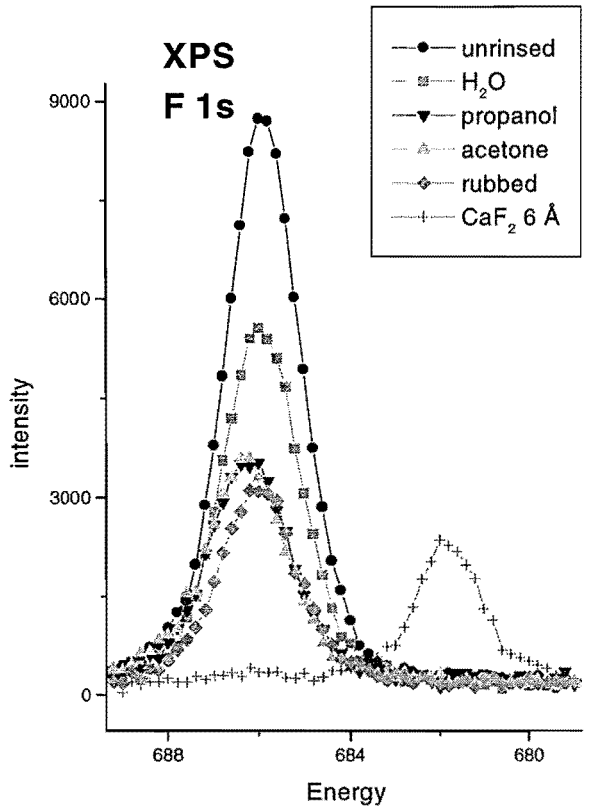

Fig. 3: Comperision of film thickness by the XPS F 1s intensity

In conclusion the coverage depends on the substrate and the way of deposition while the lowest layer always seems to be highly oriented.

In addition studies concerning the influence of the length of the flouro-alcyl group and furthermore the influence of ultraviolet light on the molecules are planned.

[1] W. Barthlott and C. Neinhuis, *Planta,* **202** (1997) 1
[2] J. Bico, C. Marzolin and D. Quéré, *Europhys. Lett.* ,**47** (1999) 220
[3] T. Onda, S. Shibuichi, N. Satho and K. Tsujii, *Langmuir,* **12** (1996) 2125
[4] J. Stöhr and R. Jaeger, *Phys. Rev. B,* **26** (1982) 41111

Electron dynamics at a Ag/C_{60} metal semiconductor interface

S. Link, A. Scholl, R. Jacquemin and W. Eberhardt
Institute "Electronic Properties"

The dynamics of excited electrons in C_{60} for various film thicknesses down to approximately one monolayer have been investigated. Using time resolved two photon photoemission this gives a direct probe both for the electronic structure of the normally unoccupied states and the population and depopulation of these states.

F&E-Nr. 23200

Ever since laser systems provide ultrashort pulses in the fs-time regime, the spectroscopy of relaxation dynamics of excited electrons in solids became a wide field of interest. However, in technical applications scattering processes at interfaces play an important role [1]. New relaxation mechanisms can be expected, since the electronic structure at the interface is affected by metal-semiconductor interactions [2].

Here we report on the changes of the relaxation times of optically excited states in C_{60} in dependence of the C_{60}-layer thickness and thus demonstrate the influence of the metal substrate on the electronic decay mechanisms. As substrate we chose a Ag(100) single crystal. Working with C_{60}/Ag(100), we can expect variations in the lifetimes by decreasing the C_{60} thickness, since the electronic structure of thin C_{60}-films is affected by the metal substrate [3].

A Ti:sapphire system is used as our light source which produces a train of ultrashort pulses of 170 fs pulseduration and a photon energy of 1.5 eV. Higher harmonics of the 1.5 eV output were used for the photoemission experiments. The experiments were performed in a UHV-system with a base pressure of 5×10^{-10} mbar. C_{60}-powder was evaporated from a tungsten crucible onto a sputtered and annealed Ag(100)-single crystal and the evaporation rate was controlled using a quartz monitor.

Figure 1 shows the occupied and unoccupied energy levels of a 20 nm thick C_{60} film. The valence band was determined using a photon energy of 8.82 eV. One can clearly see the two highest lying occupied states HOMO-1 and HOMO (Highest Occupied Molecular Orbital) with binding energies of 2.18 and 3.4 eV with respect to the Fermi level, respectively. In order to excite electrons in C_{60}, we use a photon energy of 3 eV where it is well known that C_{60} shows strong absorption within this energy region. To probe the excited electron distribution caused by the 3 eV pump photons, we used the fourth harmonic (6 eV). Having both beams in spatial and temporal overlap on the sample, two features next to the vacuum cutoff in the EDC can be observed. The peak at 2.3 eV (close to E_F) above the HOMO is attributed to free electrons in the LUMO and the second peak at 3 eV is attributed to electrons occupying the next higher lying band LUMO+1.

The EDC at the right in figure 1 is taken with a photon energy of 4.5 eV.It shows the next higher lying unoccupied energy bands LUMO+1 and LUMO+2 due to subsequent absorption of two photons by the same electron.

In order to follow the excited population in real time, we will now focus on the temporal evolution in the spectra taken with 3 and 6 eV. If the 6 eV probe pulse is delayed with respect to the pump pulse, another peak at 1.9 eV can be resolved which is attributed to the singlet exciton. It can easily be shown that these states relax with different time scales which is in agreement with recent observations. Here it should only be mentioned that the LUMO+1 decays with a relaxation time of about 300 ±35 fs while the deeper lying states like the LUMO (about 130± 30 ps) and the singlet exciton (1± 0.1 ns) decay on longer time scales. A detailed description of the relaxation dynamics for thick films is given elsewhere [4].

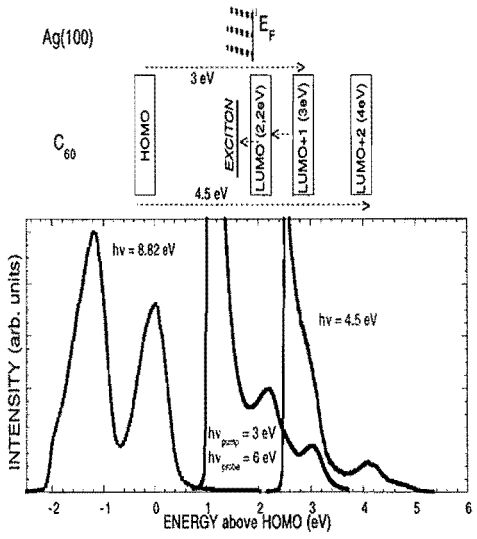

FIG. 1. Occupied and unoccupied orbitals of C_{60}, taken with various photon energies.

Changing the thickness of the C_{60}-layer down to 6 nm, no significant changes in the lifetimes are visible. A further reduction of the layers' thickness results in an appreciable amount of one photon photoemission from the Ag substrate with the 6 eV probe pulse because of the

large mean free path of electrons due to the relatively small photon energy. Taking this into consideration the laser intensity had to be reduced to avoid space charge effects. Additionally, the C_{60}-signal became weaker due to the decreasing number of C_{60} molecules contributing to the absorption of photons.

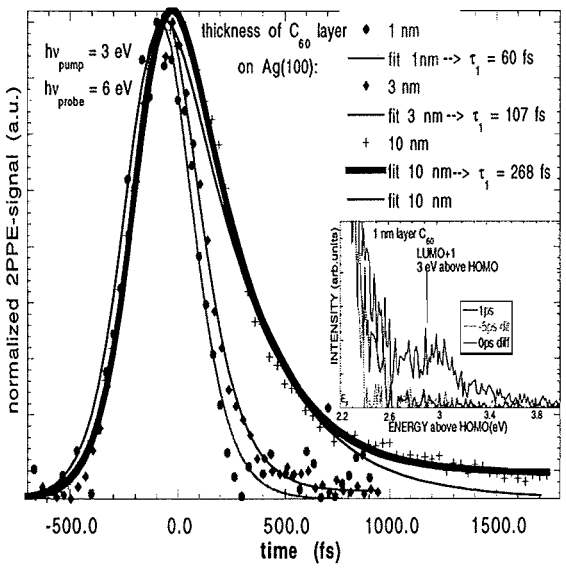

FIG. 2. Temporal electronic evolution of the LUMO+1 for C_{60} layers of 1nm, 3 nm and 10 nm. The plotted lines are the fits to the data. The inset shows that the LUMO+1 is still visible for a layer of 1 nm. The EDC's in the inset are taken for temporal delays of -5 ps, 0 ps and +1 ps.

The inset of figure 2 shows difference spectra at distinct time delays for a 1nm thick C_{60} film, taken with photon energies of 3 eV and 6 eV. Because of the large background due to one photon photoemission from the substrate and the small 2PPE-signal, it is difficult to make exact statements of the situation in the vicinity (of about 0.1 - 0.2 eV) above E_F corresponding to an energy of 2.3 to 2.4 eV above the HOMO. At higher kinetic energies, the LUMO+1 and its temporal evolution is still clearly observable, since the background in this region remains very small.

Figure 2 shows the time dependent 2PPE signal for the energy position of the LUMO+1 for 10, 3 and 1 nm thick C_{60} layers. The experimental intensity curves are fitted with the solution of the rate equation $\frac{dN(t)}{dt} = -\frac{1}{\tau} \times N(t) + Af(t)$ (thin solid lines), f(t) denotes the laser pulse.

For the curve representing the 10 nm C_{60} layer the fit based upon a single exponential decay doesn' t match the data. Another fit for the 10 nm layer where we assume that two states with different decay times describe the evolution of the signal is in good agreement with our data (thick solid line). The two independent relaxation times suggest that two states contribute to the 2PPE signal. The fast decay with a relaxation time of τ_1=270 fs is attributed to the decay of free electrons in the LUMO+1 while we attribute the slow decay with a relaxation time τ_2 in the pico second regime to the high energy tail of electrons in the LUMO, which also gives a contribution to our 2PPE-signal. The loss of the high energy tail can be explained by cooling of the distribution due to electron-phonon scattering. Reducing the C_{60} layer to below 6 nm and fitting the data with the two different theoretical channels described above, two effects can be observed. Apart from a decrease of τ_1 down to decay times of 60 fs for a 1 nm thick layer it is conspicious that the contribution from the second decay attributed to the LUMO first weakens and finally disappears entirely by reducing the thickness of the film.

We attribute the decrease of the lifetime τ_1 to scattering of the excited electrons into states of the Ag substrate. Scattering processes of excited electrons from bulk to surface states [5] or diffusion from excited electrons at the surface into the bulk [6] have been earlier reported in the literature. This effect is not limited to the C_{60} layer immediately in contact with the substrate. Rather, electron hopping is responsible for a reduction of the lifetimes several layers deep into the C_{60} film.

Considering C_{60}, the bandwidth of the unoccupied bands is on the order of 0.5 eV and accordingly the hopping time of an electron from one C_{60} to the neighboring C_{60} is on the order of 1-2 fs. For the measured lifetimes of about 130 ps for the LUMO we conclude that for thick C_{60} films electron hopping plays a minor role. Reducing the film thickness, the contribution concerning electron hopping increases so that the lifetime of the observed signal decreases.

Therefore we conclude, that electron scattering into the substrate is responsible for the accelerated relaxation.

In summary lifetimes of excited electrons in C_{60} in contact with a metallic substrate have been measured. It is shown that in layers thinner than 6 nm lifetimes begin to shorten rapidly due to influences of the substrate.

[1] R. Haight, Surface Science Reports 21, 275 (1995)
[2] R. Klaesges, C. Carbone, C.Pampuch, O.Rader, T. Kachel and W. Eberhardt, Phys. Rev. B 56, 10801 (1997)
[3] G.K. Wertheim and D.N.E. Buchanan, Phys. Rev. B 50, 11070 (1994)
[4] R. Jacquemin, S. Kraus and W. Eberhardt, Solid State Comm. 105, 449, (1998)
[5] M. Baeumler and R. Haight, Phys. Rev. Lett. 67, 1153 (1991)
[6] A. Rettenberger, P. Leiderer, M. Probst and R. Haight, Phys. Rev. B 56, 12092 (1997)

Lifetimes of image potential states on Pt(111)

S. Link, H.A. Dürr and W. Eberhardt
Institute "Electronic Properties"

The binding energies and femtosecond relaxation dynamics of image potential states were studied on the clean Pt(111) surface. We found lifetimes of 23 ± 10 fs and 54 ± 10 fs for the n=1 and n=2 states, respectively. The results are in contrast to the (111) surfaces of Cu and Ag.

F&E-Nr. 23200

The reduced dimensionality at solid surfaces gives rise to novel electronic states that are unknown in the bulk. These surface states provide model systems for understanding the interaction of electrons localized at a surface with bulk electrons. Since surface states can strongly modify the density of states at the surface they are known to influence chemisorption and adatom mobility [1].

Of particular interest are electrons bound to metallic surfaces by their own image charges. Such electrons are repeatedly reflected between the crystal and the image barrier. These image potential states (IPS) form a Rydberg series of discrete energy levels with binding energies $E_B \sim 1/(n+\Delta)^2$ converging towards the vacuum level. The quantum defect Δ is related to the phase shift for a reflection at the crystal surface. A major ingredient in the formation of IPSs is a high electron reflectivity at the crystal surface for energies just below the vacuum level. On (100) and (111) oriented face-centered cubic (fcc) surfaces this is provided by gaps in the bulk band structure.

With increasing n electrons in IPSs are localized further and further outside the metal surface. Due to the decreasing wavefunction overlap with adjacent bulk states they should have lifetimes that increase with n. This is indeed observed for fcc (100) surfaces where the vacuum level is positioned in the middle of a bulk band-gap ($k_{\|}$=0) [2]. However, the situation is reversed on the (111) surfaces of Cu and Ag where the vacuum level is close to the high energy gap edges [3] [4]. While the n=1 states are still located inside the band gap, the higher IPSs are degenerate with bulk bands. This implies that those electrons can easily decay into the crystal. Consequently the n=2 IPS lifetimes are strongly reduced and become comparable to that of the n=1 states.

The Pt(111) surface has a valence electron configuration and band gap position [5] similar to Cu(111) and Ag(111). The IPSs on these surfaces should therefore have very similar lifetimes. Surprisingly we find that this is not the case. We observe a significantly longer lifetime for the n=2 IPS than for the n=1 state.

Experiments were performed in a UHV chamber at a base pressure of $5 \cdot 10^{-10}$ mbar. Cycles of sputtering and annealing with subsequent heating in oxygen and flashing to 1000 K to remove any residual contamination were performed to get a clean and well ordered surface. A Ti:sapphire lasersystem was used as a light source which produces a train of ultrashort fs pulses. Pulses with photon energies of 5.84 eV (pulse duration 145 fs) first populate the IPSs while the population is probed with 60 fs pulses (2.92 eV) via photoemission.

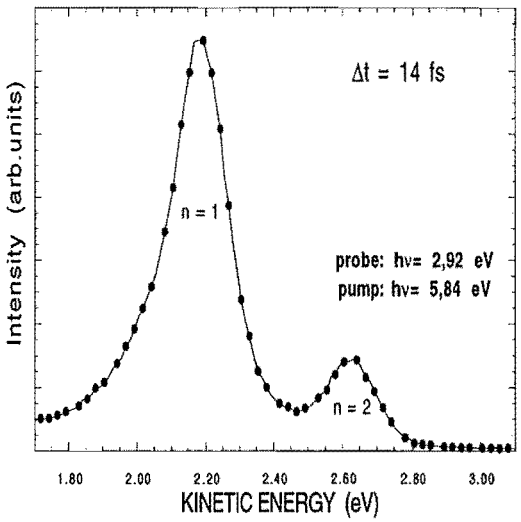

FIG. 1. Two photon photoemission (2PPE) spectrum of the first two image potential states of the Pt(111) surface. The photon energies are 5.84 eV and 2.92 eV for the pump and probe pulses, respectively.

Typical 2PPE spectra of the Pt(111) surface are displayed in Fig. 1. Here the probe pulse arrives 14 fs after the 5.84 eV pump pulse at the sample. The two peaks can be attributed to the n=1 and n=2 IPSs at kinetic energies of 2.22 and 2.67 eV, respectively. Using the measured workfunction of 5.93 eV this corresponds to binding energies of 0.70 and 0.25 eV, respectively (see Tab. 1). The observed different peak intensities are characteristic for the larger excitation cross-section for the n=1 state since it is localized closer to the surface then the n=2 IPS. All higher order IPS were found to be quenched similar to the Cu(111) and Ag(111) systems [3] [4]. This can be

attributed to a negligible reflectivity in this energy range leading to a rapid decay of the n >2 IPS electrons into bulk states.

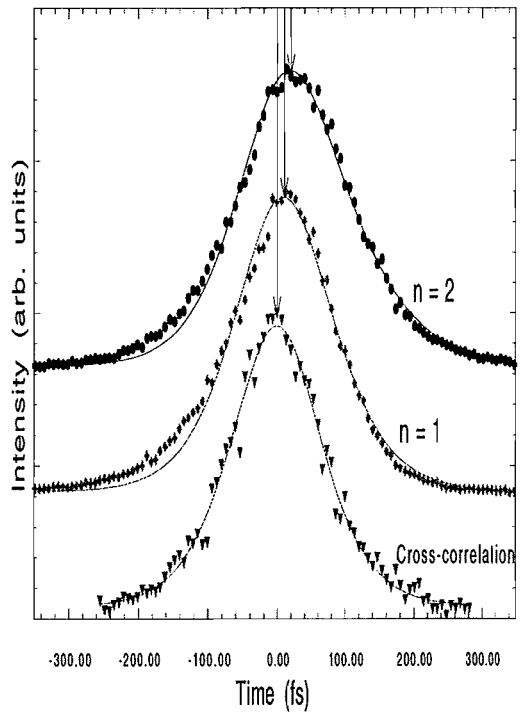

FIG. 2. Cross-correlation traces obtained for the n=1 (centered curve) and n=2 (upper trace) IPS. The cross-correlation curve at the bottom shows the instrumental function. Due to the finite lifetimes of the IPSs the cross-correlation curves broaden and they are shifted to positive delays. The lines are fits to the data.

To study the dynamics of the transient occupation the probe pulse (photon energy 2.92 eV) was delayed with respect to the pump pulse (5.84 eV). The lifetime measurements are shown in Fig. 2. The instrumental cross-correlation function (bottom curve in Fig. 2) was measured on an unprepared Pt(111) surface where the IPSs were completely quenched. The cross-correlation functions measured for the n=1 and n=2 IPS show clear lifetime broadening. From the fit to a simple rate equation model where the laser pulse envelope is involved we obtain 23±10 fs and 54±10 fs for the n=1 and n=2 IPS, respectively.

	Cu(111)		Ag(111)		Pt(111)	
	E_B (eV)	τ (fs)	E_B (eV)	τ (fs)	E_B (eV)	τ (fs)
n=1	0.82±0.05	18±5	0.77	<20	0.7	24±10
n=2	0.25±0.05	17±5	0.23	<20	0.25	54±10

Table 1. Binding energies E_B and lifetimes τ of IPSs on different fcc (111) surfaces.

The results are summarized in Tab. 1 for the (111) surfaces of Cu, Ag and Pt. In all three cases the position of the IPSs relative to the bulk band gap is very similar. This is indicated by the absence of IPSs with n >2. There are dramatic changes in the measured lifetimes especially of the n=2 IPS. While for Cu(111) and Ag(111) the n=2 IPS lifetime is comparable to that of the n=1 IPS, it is a factor of two larger for Pt(111). This demonstrates a strongly reduced coupling between the n=2 IPS and energetically adjacent bulk bands. The wavefunction of the Pt(111) n=2 IPS extends less into the bulk than on Cu and Ag, thus, leading to a weaker depopulation into bulk states. This should also affect the IPS binding energies through a change in the quantum defect Δ. Since the n=1 IPS is especially sensitive we can attribute the observed reduced binding energy on Pt(111) to such a mechanism.

[1] N. Memmel, E. Bertel, Phys. Rev. Lett. 75, 485 (1995)
[2] J.L. Shumay at al., Phys. Rev. B 58, 13974 (1998)
[3] M. Wolf, E. Knoesel, T. Hertel, Phys. Rev. B 54, R2595 (1996)
[4] R.W. Schoenlein, J.G. Fujimoto, G.L. Eesley, T.W. Capeheart, Phys. Rev. B 43, 4688 (1991)
[5] I. Kinoshita, T. Anazawa, Y. Matsumoto, Chem. Phys. Lett. 259, 445 (1996)

Publications in refereed journals

Adamcyk M.1; Nicoll C.1; Pinnington T.1; Tiedje T.1; Eisebitt S.; Karl A.; Scherer R.; Eberhardt W.
1University of British Columbia, Vancouver, Canada
Coherent soft x-ray scattering from InP islands on a semiconductor substrate
J. Vac. Sci. Technol. B 17, 1728 (1999)
23.20.0

Asada T.1;Bihlmayer G.; Handschuh S.; Heinze S.2; Kurz Ph.; Blügel S.
1Faculty of Engineering, Shizuoka University, Hamamatsu, Japan
2Zentrum für Mikrostrukturforschung, Universität Hamburg
First-principles theory of ultrathin magnetic films
J. Phys. Cond. Matter 48, 9347 (1999)

Asato M.1; Settels A.; Hoshino T.2; Asada T.2; Blügel S.; Zeller R.; Dederichs P.H.
1Graduate School of Electronic Science and Technology, Shizuoka University, Hamamatsu, Japan
2Department of Applied Physics, Shizuoka University, Hamamatsu, Japan
Full potential KKR-calculations for metals and semiconductors
Phys. Rev. B 60, 5202 (1999)
23.20.0

Bürgler D.E.; Meisinger F.1; Schmidt C.M.1; Schaller D.M.1; Güntherodt H.-J.1; Grünberg P.
1Institut für Physik, Universität Basel
In-plane momentum conservation in Fe/Cr/Au/Fe(001) layered structures
Phys. Rev. B 60, R3732 (1999)
23.42.0

Eisebitt S.; Lüning J.; Rubensson J.-E.; Eberhardt W.
Resonant inelastic soft X-ray scattering as a bandstructure probe: A primer
Phys. Stat. Sol. B 214, 803 (1999)
23.20.0

Eisebitt S.; Wirth I.; Kann G.; Eberhardt W.
Statistical analysis of the electronic structure of single wall carbon nanotubes in Buckypaper
Phys. Rev. B 1999 (accepted)

Heinze S.; Abt R.; Blügel S.; Gilarowski G.1; Niehus H.1
1Institut für Physik, Humboldt-Universität zu Berlin
Scanning tunneling microscopy images of transition-metal structures buried below noble-metal surfaces
Phys. Rev. Lett. 83, 4808, (1999)
23.20.0

Heinze S.; Nie X.; Blügel S.; Weinert M.1
1Department of Physics, Brookhaven National Laboratory, Upton, NY, USA
Electric-field-induced changes in scanning tunneling microscopy images of metal surfaces
Chem. Phys. Lett. 315, 167 (1999)
23.20.0

Link S., Scholl A., Jacquemin R.; Eberhardt W.
Electron dynamics at a Ag/C60 metal semiconductor interface
Solid State Comm. 1999 (accepted)

Lüning J.; Eisebitt S.; Rubensson J.-E.; Ellmers C.; Eberhardt W.
Electronic structure of silicon carbide polytypes studied by soft X-ray spectroscopy
Phys. Rev. B 59, 10 573 (1999)
23.20.0

Lüning J.; Rockenberger J.1; Eisebitt S.; Rubensson J.-E.; Karl A.; Kornowski A.1; Weller H.1; Eberhardt W.
Soft X-ray spectroscopy of single sized CdS nanocrystals: size confinement and electronic structure
1Institut für Physikalische Chemie, Universität Hamburg
Solid State Comm. 112, 5 (1999)
23.20.0

Maus M.; Ganteför G.; Eberhardt W.
The electronic structure and the bandgap of nano-sized Si particles: competition between
Quantum confinement and surface reconstrcution
Applied Physics A 1999 (accepted)

Morenzin J.; Schlebusch C.; Kessler B.; Eberhardt W.
Phthalocyanine/C60 composites as improved photosensitive materials
Phys. Chem. Chem. Phys. 1, 1765 (1999)
23.20.0

Piancastelli M.N.1; Kivimäki A.2; Kempgens B.3; Neeb M.; Maier K.3; Hergenhahn U.3; Rüdel A.3; Bradshaw A.M.3
1Department of Chemical Sciences and Technologies, University "Tor Vergata", Rome
2Department of Chemical Sciences, University of Oulu, Finland
3Fritz-Haber-Institut der Max-Planck-Gesellschaft, Berlin
Electron decay following the N 1s (r) (* excitation in N2 studied under resonant Raman conditions
J. of Electron Spectrosc. and Rel. Phenomena 98-99, 111 (1999)
23.20.0

Pontius N.; Bechthold P.S.; Neeb M.; Eberhardt W.
Femtosecond multi-photon photoemission of small transition metal cluster anions
J. of Electron Spectrosc. and Rel. Phenomena 1999 (accepted)

Pontius N.; Bechthold P.S.; Neeb M.; Eberhardt W.
Ultrafast hot-electron dynamics observed in Pt3- using time-resolved
photoelectron spectroscopy
Phys. Rev. Lett. 1999 (accepted)

Rader,O.1; Pampuch, C.1; Gudat, W.1; Dallmeyer, A.; Carbone, C.; Eberhardt, W.
Parallel, antiparallel and no magnetic coupling in submonolayer Mn/Fe(110)
1Bessy GmbH, Berlin
Europhysics Lett. 46, 231 (1999)
23.20.0

Rennie E.E.1; Köppe H.M.1; Kempgens B.1; Hergenhahn U.1; Kivimäki A.2; Maier K.1; Neeb M.;Rüdel A.1; Bradshaw A.M.1
1Fritz-Haber-Institut der Max-Planck-Gesellschaft, Berlin
2Department of Physical Science, University of Oulu, Finland
Vibrational and shake-up excitations in the C 1s photoionization of ethane and deuterated ethane
J. Phys. B: At. Mol. Opt. 32, 2691 (1999)
23.20.0

Schlebusch C.; Morenzin J.; Kessler B.; Eberhardt W.
Organic photoconductors with C60 for xerography
Carbon 37, 717 (1999)
23.20.0

Schmitz D.; Charton C.; Scholl A.; Carbone C.; Eberhardt W.
Magnetic moments of fcc Fe overlayers on Cu(100) and Co(100)
Phys. Rev. B 59, 1 (1999)
23.20.0

Yan S.-S.; Schreiber R.; Voges F.; Osthöver C.; Grünberg P.
Oscillatory interlayer coupling in Fe/Mn/Fe trilayers
Phys. Rev. B 59, R11 641 (1999)
23.42.0

Yoshihara A.1; Wang Z.J.2; Takanashi K.2; Grünberg P.; Motokawa M.2; Fujimori H.2

1Faculty of Science and Engineering, Ishinomaki Senshu University, Japan
2Institute of Materials Research, Tohoku University, Japan
Spin wave modes in fine layered structures of Fe and Au
J. Magn. Soc. Japan 23, 161 (1999)
23.42.0

Other publications

Eisebitt S.; Eberhardt W.
Band structure information and resonant inelastic soft X-ray scattering in broad band solids
J. Electron Spectrosc. on Rel. Phenomena 1999 (accepted)

Eisebitt S.; Wirth I.; Kann G.; Eberhardt W.
Statistical analysis of the electronic structure of single wall Carbon nanotubes in buckypaper
Electronic Properties of Novel Materials: Proceeding of the XIII International Workshop
p. 304, edited by H. Kuzmany et al., AIP Conference Proceedings 486, Melville, New York
Kirchberg, 1999
23.20.0

Grünberg P.
Layered magnetic structures: Interlayer exchange coupling and giant magnetoresistance (review)
Springer Series in Surface Sciences, Vol. 37, 49 (1999) on Magnetic Multilayers and Giant Magnetoresistance, ed. by U. Hartmann
23.42.0

Schlebusch C.; Morenzin J.; Kessler B.; Eberhardt W.
Charge transfer and relaxation dynamics of excited electronic states in organic photoreceptor materials with and without C60
Electronic Properties of Novel Materials: Proceeding of the XIII International Workshop
p. 487 , edited by H. Kuzmany et al., AIP Conference Proceedings 486, Melville, New York
Kirchberg, 1999
23.20.0

Turek I.1; Kudrnovsk J.1; Blügel S.
1Institute of Physics of Materials, AS CR, CZ-61662 Brno
2Institute of Physics, AS CR, CZ-18040 Praha
Surface magnetism of disordered alloys
Acta Physics Slovaca Vol. 48, 1 (1999)
23.20.0

Invited talks

Blügel S.
Von der Quantentheorie der Elektronen zu neuen Nanomaterialien
Kolloquiumsvortrag vor der Fakultät Physik, Martin Luther Universität, Halle/Saale
05.06.1999
3.20.0

Blügel S.
Von der Quantentheorie der Elektronen zu neuen Nanomaterialien
Kolloquiumsvortrag vor der Fakultät Physik, RWTH Aachen
13.12.1999
3.20.0

Blügel S.
Von der Quantentheorie der Elektronen zu neuen Nanomaterialien
Kolloquiumsvortrag vor der Fakultät Physik, Universität Bremen
15.06.1999
3.20.0

Blügel S.
Von der Quantentheorie der Elektronen zu neuen Nanomaterialien
Kolloquiumsvortrag vor der Fakultät Physik, Universität Düsseldorf
04.11.1999
3.20.0

Blügel S.
Von der Quantentheorie der Elektronen zu neuen Nanomaterialien
Seminar TU-Clausthal-Zellerfeld
03.05.1999
3.20.0

Bürgler D.E.
Control of magnetic interlayer coupling on the nanometer scale: Morphology and fermiology
UMBRELLA Symposium, TH Aachen
08.11.1999
3.42.0

Bürgler D.E.
Magnetische Zwischenschichtkopplung: Effekte der Grenzflächen und Fermioberflächen
RWTH Aachen
13.12.1999
3.42.0

Dürr H.
Soft X-ray magnetic spectroscopy
SR Satellite to the 18th IUCr General Assembly and Congress
Daresbury Lab., Warrington
03.08.1999
3.20.0

Eberhardt W.
Coherent soft x-ray scattering from random surfaces
Evaluation Session, MPT-Projekte im Rahmen der deutsch-kanadischen WTZ
Laser-Lab. Göttingen
27.01.1999
3.20.0

Eberhardt W.
F-Sek Dynamik von Festkörpern und Clustern
ETH Zürich
21.01.1999
3.20.0

Eberhardt W.
F-sek Dynamik von Festkörpern und Clustern
Festkörperphysik-Kolloquium, FU Berlin
12.11.1999
3.20.0

Eberhardt W.
Femtosecond electronic relaxation processes in clusters and solids
Ringberg Symposium " Ultrafast Surface Dynamics"
30.03.1999
3.20.0

Eberhardt W.
IBM Research Almaden
F-sec dynamics of magnetic thin films and photoconductor systems
19.02.1999
3.20.0

Eberhardt W.
MAX-lab Lund
Opportunities for experiments using thetTime structure and Coherence of the VUV
25.09.1999
3.20.0

Eberhardt W.
Opportunities for Experiments Using the Time Structure and Coherence of the VUV, FEL at DESY
21st International Free Electron Laser Conference and 6th FEL Application Workshop, Hamburg
27.08.1999
3.20.0

Eberhardt W.
Scattering experiments with coherent soft X-ray photons
VUV FEL User Workshop, Hamburg
12.03.1999
3.20.0

Eberhardt W.
Soft X-ray emission and scattering from solids
17.09.1999
tanford Univesity
23.20.0

Eberhardt W.
Soft X-ray emission and scattering from solids
Seminarvortrag im MPI Stuttgart
07.05.1999
3.20.0

Eisebitt S.
Resonant inelastic soft x-ray scattering: Investigating electronic structure
2nd International SLS Workshop on Synchrotron Radiation
Brunnen, CH
27.10.1999
3.20.0

Eisebitt S.
Soft x-ray emission on solids
SSG Lecture Series at the Advanced Light Source, Berkeley, USA
18.11.1999
3.20.0

Eisebitt S.
Weichröntgen-Emissions-Spektroskopie an nanostrukturierten Halbleitern
Universität Bonn
15.01.1999
3.20.0

Grünberg P.
Layered magnetic structures in research and application
Argonne National Labs, USA
29.03.1999
3.42.0

Grünberg P.
Magnetische Multilagen in Forschung und Anwendung
Physikalisches Kolloquium, Universität Düsseldorf
04.02.1999
3.42.0

Grünberg P.
Magnetische Multilagen in Forschung und Anwendung
Workshop on Multilayers and Nanostructures, Universität Bielefeld
09.06.1999
3.42.0

Grünberg P.
Magnetische Schichtstrukturen in Forschung und Anwendung
Fraunhofer Institut Duisburg
09.06.1999
3.42.0

Grünberg P.
Magnetische Schichtstrukturen in Forschung und Anwendung
IBM Mainz
26.04.1999
3.42.0

Grünberg P.
Magnetische Schichtstrukturen in Forschung und Anwendung
Stiftung Cäsar, Bonn
19.10.1999
3.42.0

Grünberg P.
Magnetische Schichtsysteme in Forschung und Anwendung
FZ Kolloquium
22.01.1999
3.42.0

Grünberg P.
Magnetoelectronics in research and application
UMBRELLA Symposium, TH Aachen
09.11.1999
3.42.0

Grünberg P.
Magnetoelektronik in Forschung und Anwendung
Max-von-Laue-Kolloquium, Berlin
25.12.1999
3.42.0

Grünberg P.
Magnetoelektronik in Forschung und Anwendung
Physikalisches Kolloquium, Gesamthochschule Essen
20.10.1999

Grünberg P.
Magnetoelektronik in Forschung und Anwendung
Physikalisches Kolloquium, Ruhr Universität Bochum
08.11.1999
3.42.0

Grünberg P.
Magnetoelektronik in Forschung und Anwendung
Physikalisches Kolloquium, Universität Mainz
26.10.1999
3.20.0

Grünberg P.
The GMR effect in research and application
225. WE-Heraeus Seminar, Bad Honnef
13.08.1999
3.20.0

Grünberg P.
The history of layered magnetic structures
American Physical Society,
Centennial Meeting, Atlanta, Georgia
22.03.1999
3.42.0

Grünberg P.
Zwischenschicht-Austauschkopplung in Forschung und Anwendung
15. Sitzung des Arbeitskreises "Magnetische Schichten für technische Anwendungen"
Institut für Mikrostrukturtechnologie und Optoelektronik, Wetzlar
18.06.1999
3.20.0

Heinze S.; Abt R.; Blügel S.
Interpretation von STM-Bildern von Übergangsmetallstrukturen auf der Basis der Elektronentheorie
Seminarvortrag am Institut für Oberflächenphysik und Atomstoßprozesse, Humboldt Universität Berlin
03.05.1999
3.20.0

Klingeler R.

Mass spectra of metal-doped carbon and fullerene clusters Mx@Cn<120 (M = Sc, Y, La, Ca, Ce; x = 1,2)
A. German-French Seminar, Nanotubes and Fullerenes - Recent Advances and Future Trends
IFW Dresden
25.09.1999
3.20.0

Kurz Ph.; Blügel S.
Nichtkolinearer Magnetismus in der FLAPW-Methode
Seminarvortrag am Zentrum füer Mikrostrukturforschung, Universität Hamburg
04.02.1999
3.20.0

Neeb M.
Photoelectron spectroscopy on mass-selected clusters using VUV-lasers
VUV FEL User Workshop, Hamburg
11.03.199
3.20.0

Wingbermühle J.
Schichtentwicklung und magnetische Charakterisierung
MALVE-Meeting
Forschungszentrum Karlsruhe, Institut für Materialforschung
23.02.1999
3.42.0

Other talks

Antons A.; Berger R.; Blügel S.; Schroeder, K.
Ab-initio Untersuchungen der Adatom Diffusion auf Si(111)
DPG-Frühjahrstagung, Münster
März 1999
23.20.0

Bihlmayer G.; Kurz Ph; Blügel S.
Mangan-Oberflächenlegierungen auf einer Cu(111) Oberfläche
DPG-Frühjahrstagung, Münster
März 1999
23.20.0

Blügel S.
Influence of magnetism for the alloy formation of ultrathin films
International Symposium on Structure and Dynamics of Heterogeneous Systems - SDHS'99
Gesamthochschule Duisburg
26.02.1999
3.20.0

Blügel S.
Theory of ultrathin magnetic films
Workshop on Interface anisotropy, spin and orbital magnetism, Riksgränsen, Schweden
05.05.1999
3.20.0

Blügel S.
Wachstum
Sondierungsgespräch: Halbleitergrenzflächen in nächsten Jahrhundert
DESY/HASYLAB Hamburg
04.10.99
3.20.0

Blügel S.; Nie X.; Weinert M.1
1Brookhaven National Laboratory, Upton, USA
Modifikation eines Ummagnetisierungsfeldes durch ein externes elektrisches Feld
DPG-Frühjahrstagung, Münster
März 1999
23.20.0

Bürgler D.E.; Grünberg P.
In-plane momentum Conservation in Fe/Cr/Au/Fe(001) layered Structures
44th Annual Conference on Magnetism and Magnetic Materials, San Jose, CA
16.11.99
3.42.0

Dallmeyer, A.
Electronic states and magnetism of 1-D monatomic wires
DPG-Frühjahrstagung in Münster 1999
22.03.1999
3.20.0

Eisebitt S.
Weichröntgenspektroskopie an nanostrukturierten Halbleitern
Sondierungsgespräch: Halbleitergrenzflächen in nächsten Jahrhundert
DESY/HASYLAB Hamburg
04.10.99
3.20.0

Heinze S.; Blügel S.
Theoretical analysis of STM and STS of thin magnetic films
211. Heraeus Seminar (Magnetic Nanostructures), Bad Honnef
04.01.1999
3.20.0

Heinze S.; Blügel S.
Theoretical analysis of STM of ultra-thin magnetic films
European Research Conference on Computational Physics for Nanotechnology,
Castelvecchio Pascoli, Italy
19.09.99
3.20.0

Heinze S.; Blügel S.; Weinert M.1
1Brookhaven National Laboratory, Upton, USA
Einfluss des elektrischen Feldes auf STM-Bilder von Metalloberflächen
DPG-Frühjahrstagung, Münster
März 1999
23.20.0

Heinze S.; Blügel S.; Wiesendanger R.1
1Universität Hamburg
What can be learn't by non-spinpolarized STM about surface magnetism of Cr and Mn on Fe(001)?
10th International Conference on M/STS and Related Techniques 1999 , Seoul, Korea
Juli 1999
23.20.0

Karl A.
Der unvollständige Ladungstransfer in endohedral dotiertem La@C82
DPG-Frühjahrstagung in Heidelberg 1999
17.03.1999
3.20.0

Klingeler R.
La20n (n=1-6): Photoelektronenspektroskopie und Dichtefunktionalrechnungen
DPG-Frühjahrstagung in Heidelberg 1999
18.03.1999
3.20.0

Klingeler R.; Bechthold P.S.; Neeb M.; Eberhardt W.
Mass spectra of metal-doped carbon and fullerene clusters Mx@Cn<120 (M = Sc, Y, La, Ca, Ce; x = 1,2)
Arbeitstreffen des SFB 341, Aachen
07.10.99
3.20.0

Kurz Ph.; Bihlmayer G.; Blügel S.
Non-collinear Magnetism of Monolayers on Ag(111) and Cu(111)
44th Annual Conference on Magnetism and Magnetic Materials, San Jose, CA
17.11.1999

Kurz Ph.; Bihlmayer G.; Blügel S.
Non-collinear magnetism of monolayers on Ag(111) and Cu(111)
International Workshop on Interface ansisotropy, spin and orbital moment
Riskgränsen, Schweden
05.05.1999
3.20.0

Kurz Ph.; Bihlmayer G.; Blügel S.
Non-collinear magnetism of monolayers on Ag(111) and Cu(111)
TMR-Workshop Interface Magnetism, Aussois, Frankreich
28.03.1999
3.20.0

Kurz Ph.;Bihlmayer G.; Blügel S.
Nichtkollinearer Magnetismus von magnetischen Monolagen auf Ag(111) und Cu(111)
DPG-Frühjahrstagung, Münster
März 1999
23.20.0

Lüttgens G.
Photoelektronenspektroskopie an kleinen massenselektierten Germanium-
Oxidclusteranionen
DPG-Frühjahrstagung in Heidelberg 1999
16.03.1999
3.20.0

Neeb M.
Photoelectron spectra of metal cluster anions reacted with Benzene
Clustertreffen, Sassnitz, Rügen
28.09.99
3.20.0

Neeb M.
Zeitaufgelöste 2-Photonen-Photoelektronenspektroskopie an massenselektierten Metallclusteranionen
DFG-Antragskolloquium, Schwerpunktprogramm "Femtosekunden-Spektroskopie elementarer Anregungen in Atomen, Molekülen und Clustern, Bad Honnef
15.11.1999

Nie X.; Blügel S.
Investigation of chemical Trends of the Magnetocrystalline Anisotropy for Magnetic Monolayers
44th Annual Conference on Magnetism and Magnetic Materials, San Jose, CA
17.11.1999

Pontius N.
Mehrphotonen-Photoemission aus kleinen Übergangsmetallclustern mit Femtosekundenlaserpulsen
DPG-Frühjahrstagung in Heidelberg 1999
16.03.1999
3.20.0

Rottländer P.; Kohlstedt H.; Girgis E.; de Gronckel H.; Schelten, J.; Grünberg P.
Ferromagnetische Tunnelkontakte mit UV-unterstützter Oxidation der Barriere
DPG-Frühjahrstagung in Münster 1999
24.03.1999
3.20.0

Rottländer P.; Kohlstedt H.; Grünberg P.
Barrier Formation by Ultraviolet light assisted Oxidation for Magnetic Tunnel Junctions
44th Annual Conference on Magnetism and Magnetic Materials, San Jose, CA
17.11.99
3.42.0

Schroeder K.; Blügel S.
Diffusion und Einbau von Ge- und Si-Adatomen auf As-terminiertem Si(111): ein Vergleich
DPG-Frühjahrstagung, Münster
März 1999
23.20.0

Spettmann R.1; Schroeder K.; Blügel S.; Entel P.1
1Universität Duisburg
Elektronische Struktur von Si(111): Sn-
DPG-Frühjahrstagung, Münster
März 1999
23.20.0

Wortmann D.
Theorie der Rastertunnelmikroskopie von metallischen Oberflächenlegierungen
Seminar des Zentrums für Mikrostrukturforschung, Universität Hamburg
19.10.1999
3.20.0

Posters

Antons A.; Berger R.; Blügel S.; Schroeder K.
Ab initio investigation of ad-atom diffusion at surfaces
European Research Conference on Dynamical Processses at Surfaces, Lenggries
19. - 23.09.1999
23.20.0

Asada T.1; Blügel S.; Bihlmayer G.; Abt R.
1Faculty of Engineering, Shizuoka University, Hamamatsu, Japan
First Principles Investigation of the Stability of 3d Monolayer/Fe(001) against Bilayer Formation
44th Annual Conference on Magnetism and Magnetic Materials, San Jose, CA
16.11.1999
3.20.0

Dallmeyer A.
Electronic structure of epitaxial fcc-Mn films
DPG-Frühjahrstagung in Münster
März 1999
23.20.0

Eisebitt S.; Wirth I.; Kann G.; Eberhardt W.
Electronic structure of single wall carbon nanotubes in buckypaper
XIII International Winterschool on Electronic Properties of novel Materials - Science and Technology of Molecular Nanostructures, Kirchberg, Tirol
März 1999
23.20.0

Heinze S.; Asada T.1; Blügel S.
1Faculty of Engineering, Shizuoka University, Hamamatsu, Japan
Ab initio Calculations of STM and STS on Magnetic thin Films: Mn and Cr on Fe(001)
44th Annual Conference on Magnetism and Magnetic Materials, San Jose, CA
18.11.1999
3.20.0

Karl A.; Eisebitt S.; Freiwald M.; Scherer R.; Eberhardt W.
Soft X-ray emission and resonant inelastic soft X-ray scattering on InP

HASYLAB Annual Users Meeting 1999, Hamburg
29.01.1999
3.20.0

Karl A.; Eisebitt S.; Scherer R.; Eberhardt W.; Weidinger A.1; Hirsch A.2
1Hahn-Meitner-Institut, Berlin
2Universität Erlangen
Electronic structure of (C59N)2 studied locally at the Nitrogen site by soft x-ray emission and resonant inelastic scattering
18th International Conference on X-ray and Inner-shell Processes, Chicago, IL
23. - 27.08.1999
23.20.0

Klingeler R.
Mass spectra of metal-doped carbon and fullerene clusters Mx@Cn<120 (M = Sc, Y, La,
Ca, Ce; x = 1,2)
Clustertreffen, Sassnitz, Rügen
26.09. - 01.10.99
23.20.0

Kohlstedt H.; de Gronckel H.; Schmitz R.
Oxidation Methods and Analytical Studies of the Structure of Magnetic Tunnel Junctions
44th Annual Conference on Magnetism and Magnetic Materials, San Jose, CA
15.11.99
3.42.0

Kromen W.; Berger R.; Antons A.; Schroeder K.; Blügel S.
EStCoMMP, a parallelized (ab initio) molecular dynamics code for the investigation of atomistic growth processes
European Research Conference on Dynamical Processses at Surfaces, Lenggries
19. - 23.09.1999
23.20.0

Lüttgens G.; Ponitius N.; Friedrich C.; Bechthold P.S.; Neeb M.; Eberhardt W.
Photoelectron spectra of benzene-adsorbed metal cluster anions
Gordon Conference on Photoions, Photoionization and Photodetachment, Plymouth State College, New Hampshire, USA
18.07.1999
3.20.0

Lüttgens G.; Pontius N.; Friedrich C.; Bechthold P.S.; Neeb M.; Eberhardt W.
Photoelectron spectroscopy of Benzene-adsorbed metal cluster anions
Clustertreffen, Sassnitz, Rügen
26.09. - 01.10.99
23.20.0

Morenzin J.; Schlebsuch C.; Kessler B.; Eberhardt W.
Charge Transfer and relaxation dynamics of excited electronic states in organic photoreceptor materials with and without C60
XIII International Winterschool on Electronic Properties of novel Materials - Science and Technology of Molecular Nanostructures, Kirchberg, Tirol
März 1999
23.20.0

Nie X.; Heinze S.; Weinert M.1; Blügel S.
1Brookhaven National Laboratory, Upton, USA
Magnetic surfaces under static external electric fields
211. WE-Heraeus Seminar (Magnetic Nanostructures), Physikzentrum Bad Honnef
04. - 06.01.1999
23.20.0

Pontius N.; Bechthold P.S.; Neeb M.; Eberhardt W.
Time-resolved photoelectron spectra of Pt3- using femtosecond laser pulses
Gordon Conference on Photoions, Photoionization and Photodetachment, Plymouth State College, New Hampshire, USA
18.07.1999
3.20.0

Pontius N.; Bechthold P.S.; Neeb M.; Eberhardt W.
Ultrafast hot-electron dynamics observed in Pt3- using time-resolved photoelectron spectroscopy
Clustertreffen, Sassnitz, Rügen
26.09. - 01.10.99
23.20.0

Rottländer P.; Kohlstedt H.; Girgis E.; de Gronckel H.; Schelten J.; Grünberg P.
TMR structures with barriers produced by UV oxidation
DPG-Frühjahrstagung in Münster
23.03.1999
3.42.0

Wirth I.; Kann G.; Eisebitt S.; Eberhardt W.
Elektronische Struktur von Kohlenstoffnanoröhren in "Buckypaper"
DPG-Frühjahrstagung in Münster
24.03.1999
3.20.0

Wortmann D.
Scanning tunneling microscopy of magnetic surface alloys
5th Workshop Full-Potential LAPW calculations with the WIEN97 code, Wien
09.04.1999
3.20.0

Yan S.-S.; Schreiber R.; Grünberg P.
Noncollinear Coupling in Fe/Mn/Fe Trilayers and ist Dependence on Growth Conditions
44th Annual Conference on Magnetism and Magnetic Materials, San Jose, CA
17.11.1999-09-01
3.42.0

Patents granted

Blügel S.; Nie X.:
Elektrisches Feld für Ummagnetisierung eines dünnes Films
DE: 19841034 (06.08.99)
PT 1.1610
23.20.0

Patens applied for

Blügel S.; Nie X.:
Elektrisches Feld für Ummagnetisierung eines dünnen Films
PCT: PCT/DE99/02840 (08.09.99) (EP,US,JP)
PT 1.1610
23.20.0

Eberhardt W.; Morenzin J.:
Markierungseinrichtung
PCT: PCT/EP 99/08433 (03.11.99) (EP,US,JP)
PT 1.1633
23.42.0

Lecture courses

Baumgarten L.
Winkelaufgelöste Photoemission zur Bandstrukturbestimmung in Festkörpern
IFF-Ferienschule 1999
05.03.1999
3.20.0

Bechthold P.S.
Cluster und Clustermaterie
SS 1999

Blügel S.
Theorie der magnetischen Anisotropie
IFF-Ferienschule 1999
03.03.1999
3.20.0

Carbone C.
Photoemission from magnetic films
IFF-Ferienschule 1999
05.03.1999
3.20.0

Eberhardt W.; Grünberg P.; Bürgler D.
Oberseminar: "Magnetische Schichtsysteme in Forschung und Anwendung"
WS 99/00

Eisebitt S.
Zirkulardichroismus in der Rumpfabsorption
IFF-Ferienschule 1999
09.03.1999

Grünberg P.
Zwischenschichtaustauschkopplung: Phänomenologische Beschreibung, Materialabhängigkeit
IFF Ferienschule 1999
03.03.1999
3.42.0

Internal reports

Blügel S.
Theorie der magnetischen Anisotropie und Magnetostriktion
In: Magnetische Schichtstrukturen in Forschung und Anwendung, Jülich: 30. Ferienkurs des Instituts für Festkörperforschung 1999
23.20.0

Pontius N.; Bechthold P.S.; Neeb M.; Eberhardt W.
Infinity - Der Pumplaser der Wahl für nachverstärkende fs-Systeme
Laserline, Coherent (Deutschland) GmbH, 01/1999
23.20.0

Wirth I.
Jül-3619
Rastertunnelmikroskopie und Rastertunnelspektroskopie an einwandigen Kohlenstoff-Nanoröhren
23.20.0

Special Group „Materials under heavy irradiation loads“

General Overview

Research on Fusion Materials

The main part of the activities of the group is still concerned with radiation damage effects in candidate structural fusion materials. This work is a contribution of the IFF to the Nuclear Fusion Project in Jülich which is financed to 25 and 45%, respectively, by EURATOM. The research topics are part of the European Fusion Programme. In addition to these activities, the group is increasingly involved in materials investigations for the targets of the planned European high-power spallation neutron source ESS.

Scientific goal of the work are investigations of irradiation-induced changes of properties of technical- and model-materials. Because an intensive source of fusion neutrons is still missing, their action is simulated by light ion bombardment at a cyclotron. For the spallation case there is the additional possibility to investigate "spent" targets of operating medium power sources (ISIS, LANSCE) in the Hot Cells of FZJ.
The emphasis of the efforts is an improvement of the basic understanding of processes underlying radiation damage effects. A close interaction with theoreticians is therefore mandatory and the close long-standing and fruitful collaboration with H. Trinkaus (Institut Theorie II) will be continued.

In the field of **metallic structural fusion materials** the work concentrated on the combined influence of atomic displacements, hydrogen and helium on the mechanical properties and the hydrogen permeation of martensitic steels, particularly their low activation versions. These investigations will be extended to steel-ceramics composites in order to test the effectiveness of ceramic layers as diffusion-barriers for hydrogen isotopes.
The influence of (n, α)-produced helium in beryllium (a favourite **plasma-facing candidate material**) on its tensile properties has been studied for a wide range of temperatures and He-concentrations (see following article). Transmission-electron-microscopy (TEM) is under way to uncover the reasons for the observed severe embrittlement.
During the work on irradiation-induced dimensional changes in **ceramics**, unusual morphologies of **helium bubbles** have been found. Systematic experiments and TEM investigations together with the development of a theoretical model led to a detailed understanding of the development of such bubble structures.
Concluding electron irradiations confirmed the suspicion that the alledged **Radiation Induced Electrical Degradation (RIED) effect** is an artefact. It could be clearly shown that the drastic increases in conductivity of Al_2O_3 found by some authors were due to unsuitable techniques of measuring high insulation resistances.

Research on Spallation Target and Moderator Materials

The emphasis of this research is on the most highly loaded components of the European Spallation Source (ESS), i.e. target and moderators. The integrity of these parts will be decisive for the duration of uninterrupted operation periods of the entire facility. The extraordinary loads on the mercury target are on the container proper and its secondary enclosure, in particular the respective proton beam windows. These loads have mainly two causes. First, the stress waves, which are due to the shock-like energy deposition into the target and its multiple shells. Stress waves within the container walls are generated by the direct heating of the beam window as well as by the pressure waves due to the pulsed heating of the mercury. The second concern is radiation damage and foreign atom production (mainly hydrogen and helium) induced by the high energetic protons and neutrons.

Experiments on the stress wave problem have been performed at the Alternating Gradient Synchrotron (AGS) at Brookhaven with the mercury target of the international ASTE (AGS Spallation Target Experiment) collaboration. A recently developed laser interferometric technique for measuring pressure waves in liquid metal targets provided reproducible results.

The comparison of experiments with results from numerical calculations (employing finite elements) of the expected stress and pressure waves within the ASTE target subject to high power proton pulses is satisfactory only for the time interval between power input and arrival of the pressure wave front at the target container wall. For a quantitative description of the pressure wave at later times a more sophisticated modeling of the pressure sensor is needed and being developed.

Numerical calculations show that the time dependence of the pressure wave within a mercury target for a given total energy deposition strongly depends of the proton beam profile. This way may offer a means of mitigating the impact of pressure waves on the target structure.

Radiation damage and foreign atom production are investigated with proton accelerators. Life time estimates of components are made by analyzing long term irradiated targets and proton beam windows of already operating medium power spallation sources (LANSCE, Los Alamos and ISIS, Rutherford Appleton Lab). The stress wave problem is studied with experiments on pulsed high power proton accelerators.

The **mechanical tests and micro-structural investigations** of samples cut from components of existing spallation sources are nearly finished. The results show a remarkable strengthening and embrittlement with all three investigated materials classes (austenitic and martensitic steels as well as nickel-based alloys). The residual ductility observed with specimens subject to the highest available dose of 10 dpa (corresponding to about 2 months of operation of ESS) is, however, sufficient for being employed as structural materials of ESS targets.

Spallation nuclides have been identified applying capillary electrophoresis combined with ICP mass spectroscopy to separate the rare earth elements. All 14 lanthanides from an 800 MeV irradiated tantalum target from ISIS have been analyzed. The results were in good agreement with theoretically predicted distributions as well as with data from HPLC-ICP mass spectroscopy.

Cold moderators have gained increasing importance in the past. Quality and quantity of neutrons produced with a pulsed source can be particularly improved, if cold moderators can deliver and sustain short pulses over a broad energy range. The ideal slowing down medium for that purpose is methane because of its high proton density and many low lying rotational vibration modes. Unfortunately, in the radiation field of a target, highly active radicals are formed in methane, in particular CH_3^- and H^+. In liquid methane (100-K-moderator) this gives rise to the formation of higher alkane homologues, which are eventually clogging the piping. In its solid state (20-K-moderator), in addition to radiolysis, crystal defects like interstitials are generated. The stored energy together with recombination of radicals can lead to spontaneous energy release (Wigner effect), which in turn may destroy the moderator vessels.

Within the present R&D phase several paths for developing radiation resistant or at least better manageable cold moderators are being followed. One way is the production of small methane pebbles (2 to 3 mm diameter), which as a bed are cooled by flowing liquid hydrogen. A second possibility is the inclusion of methane in porous substances (e.g. zeolites) or clathrates (e.g. from water ice), both again as small pebbles. Radiation damage and Wigner effect will thus be restricted to small particles. A timely and regular exchange of the pebble beds would prevent the destruction of the vessel and sustain the neutronic quality of the moderator. A third way would be the utilization of different hydrocarbons (with many freely rotating methyl groups), which do not exhibit the unfavorable radiolysis behavior of methane.

Irradiation behavior of moderator media are being performed at reactors (CARE in England and IBR-2 in Russia). The neutronic properties (intensities and pulse shapes) of the different variants will be studied in a to scale mock-up of the ESS target-moderator-reflector module. This test facility is under construction at the cooler synchrotron (COSY) of the Institut für Kernphysik of Forschungszentrum Jülich. The experiments will be performed under the auspices of the international collaboration JESSICA (Jülich Experimental Spallation target Set-up In COSY Area).

H. Ullmaier and H. Conrad

Collaboration

Internal (Forschungszentrum Jülich)
IKP, ZAT, ZEL, ZFK-HZ

External (international)
BNL (Upton, USA) , JINR (Dubna, Russland),KEK (Tsukuba, Japan), Kurchatov Inst. (Moskau, Russland), JAERI (Tokai, Japan), LANL (Los Alamos, USA), ORNL (Oak Ridge, USA), PSI (Villigen, CH), RAL (Chilton, UK), RISO (Roskilde, DK), Universita di Ancona (Ancona, IT)

Personnel 1999/2000 and areas of activities

Scientific Staff

Dr. J. Chen	Mechanical tests and TEM on irradiated spallation materials	23.60.0
Dr. H. Conrad (Institute for Scattering Methods)	European Spallation Source: Target and Moderators	23.60.0
Dr. P. Jung	Radiation damage and hydrogen effects in metals and ceramics, thermal desorption spectroscopy	23.80.5
Dr. W. Kesternich	Radiation effects in metals and insulators, TEM	23.80.5
Dr. G. Küppers (ZCH)	Chemical analysis of spallation products	62.50.0
Dr. H. Tietze-Jaensch	Co-ordinator of international ESS-experiment "JESSICA" Instruments for pulsed neutron sources	23.60.0
Prof. H. Ullmaier (Head of Project "European spallation Source ESS" at FZJ)	Mechanical properties of irradiated metals,	23.60.0 23.80.5

Technical Staff

J. Deutz (until end of 99)	Preparation of ceramic TEM specimens	23.80.5
A. Fournier	Secretary, Project Assistant ESS	23.80.5 23.60.0
H. Klein	Instrumentation and data processing, TEM, irradiation experiments	23.80.5 23.60.0
W. Schmitz	SEM, irradiation experiments, specimen preparation	23.80.5

Guests

J. Abasolo-Hernandez	(IPN Mexico) Radiation-induced segregation in metals and ceramics	23.80.5
C. Byloos (Institute for Scattering Methods)	Shock waves in ESS target	23.60.0
F. Carsughi	(Univ. of Ancona, Italy) Investigations of spent spallation target components	23.60.0
A. Garcia-Borquez	(IPN Mexico) Radiation-induced segregation in metals and ceramics	23.80.5
C. Liu	(NPCI, Chengdu, China) Hydrogen embrittlement of ferritic/ martensitic steels	23.80.5
A. Ryazanov	(Kurchatov Inst., Moskau) Theory of radiation damage in metals	23.60.0
E. Shabalin	(JINR, Dubna) Radiation damage in solid methane and ice	23.60.0

The Influence of Helium on Mechanical Properties and Microstructure of Beryllium

W. Kesternich
Special Group "Materials under heavy irradiation loads"

Beryllium is a promising candidate material for plasma-facing components in future fusion reactors for several reasons. A disadvantage is the high helium production rate by (n, α) processes in this low-Z material. We have investigated He-induced changes of the mechanical properties of Be in a fusion-relevant range of He concentrations and temperatures. Severe hardening and losses in ductility have been found, connected with changes in fracture modes. TEM investigations of the microstructure are under way to uncover the underlying mechanisms.

F&E-Nr.: 23.80.5

The poisoning of a fusion plasma by impurities sputtered off the first wall decreases with decreasing atomic number Z of the plasma facing materials. Therefore, beryllium (Z=4) is one of the favourite plasma facing material. On the other hand, the production of helium by (n, α)-processes strongly increases with decreasing Z and experience from other materials shows that even small concentrations of He can lead to severe embrittlement. A knowledge of He-effects in Be is therefore of great importance.
We have investigated the influence of helium on the tensile properties and the microstructure of Be for a wide range of temperatures (RT-600°C) and He-concentrations (30-800 appm). The highest investigated He-concentration of 800 appm corresponds to the production in a typical fusion reactor after approximately 6 months full power operation. The (n, α)-production of He was simulated by homogeneous α-particle implantation at a cyclotron.
Fig. 1 shows the yield stress, the ultimate tensile strength and the total strain to failure as a function of the He-concentration for specimens irradiated and tested at 600 °C. Helium causes a strong hardening (increase of yield stress by a factor of 3 at 800 appm) with a simultaneous reduction in ductility (from an initial strain to failure of 70% to 10%).

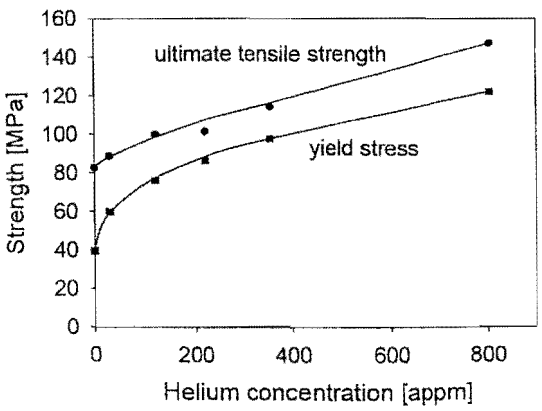

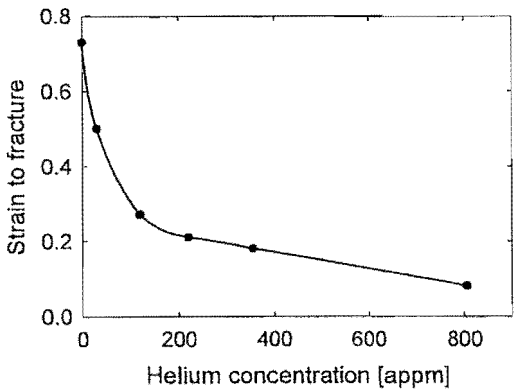

Fig.1: Ultimate tensile strength and yield stress(upper diagram) and strain to fracture(lower diagram) as a function of the helium concentration of beryllium, implanted and tested at 600°C.

At lower temperatures the effect is even more pronounced, e.g. at room temperature the ductility drops from an initial value of 9% to 0.4% at only 220 appm He. Annealing of RT-implanted specimens at 900 °C (corresponding to 0,75 of the melting temperature) strongly reduces the effect of helium on hardening and embrittlement.
For a given He-concentration, the strain to failure shows a maximum at an implantation/test temperature of 300 °C for the non-implanted specimen which shifts to 250 °C after He-implantation. The strength of the material decreases monotonically with increasing temperature in all cases.
If the implantation temperature was higher than the test temperature, He-induced strengthening and embrittlement are less pronounced, the influence being the smaller the large the difference between implantation and test temperature becomes.
The case test temperature higher than implantation temperature has no practical importance and was not investigated.
Transmission electron microscopy (TEM) observation of the development of the fine-scale microstructure (dislocation loops, small bubbles, etc.) is under way. Scanning electron microscopy (SEM)) showing larger features on fracture surfaces has been completed and revealed ductile, cleavage and intergranular failures and mixtures of these basic fracture modes.

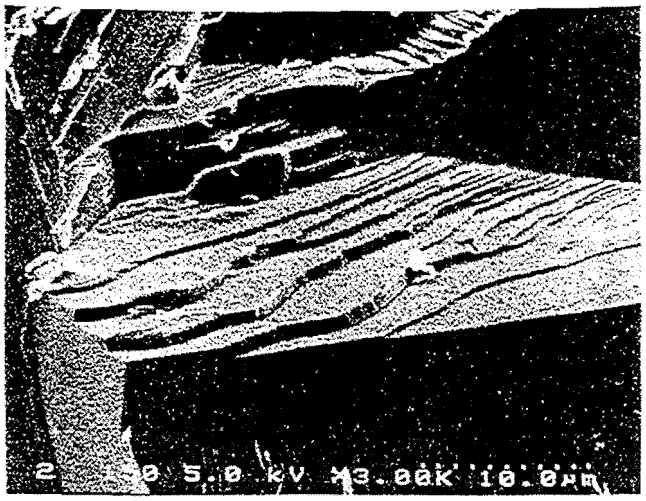

Fig.2: Scanning electron micrograph showing cleavage fracture of a specimen implanted to 220 appm He and tested at 100°C.

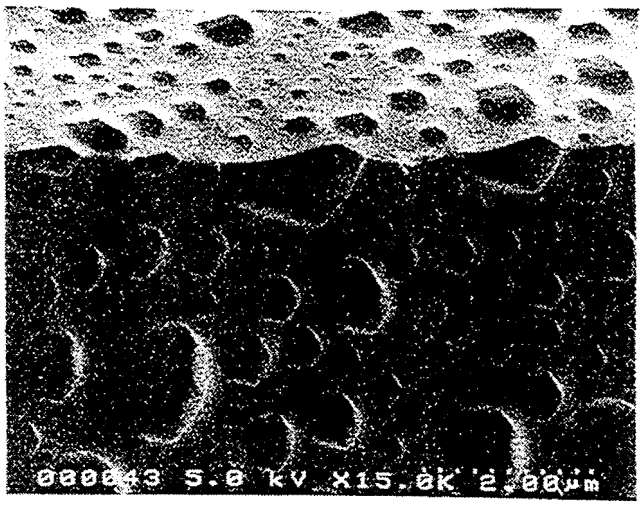

Fig.3: Scanning electron micrograph showing intergranular failure induced by large He bubbles in the grain boundaries. The specimens were implanted at 100°C to 220 appm He and then tempered at 900 °C.

Fig. 2 shows the example of a transgranular cleavage fracture with a dense sequence of cleavage steps. An analysis of the side surfaces of the tested specimens shows glide processes within the grains and in grain boundaries for a wide range of experimental conditions. The influence of the glide systems on the formation of microcracks and fracture initiation has been studied.

At high temperatures large bubbles in the matrix and the grain boundaries appear. Fig. 3 shows facetted bubbles in two grain boundaries and at their intersecting line. The influence of the bubble distribution on the fracture behaviour has been investigated.

Radiation - Induced Changes of Mechanical Properties of Target Structural Materials

J. Chen, F. Carsughi and H. Ullmaier
"Special Group under heavy irradiation loads"

Specimen obtained from spent components of operating medium-power spallation sources are a valuable source of information for lifetime predictions of target structural materials in high-power sources such as ESS. In the Hot Cells of the FZJ we are investigating 3 types of candidate materials (austenitic and martensitic steels, Ni-based alloy) obtained from LANSCE (Los Alamos) and ISIS (Rutherford-Appleton Lab.). As an example of the results, the article gives tensile data for AISI 304 L and DIN 1.4926 steel, showing severe embrittlement effects.

F&E-Nr: 23.60.0

The lifetime of the ESS target structure (proton beam window, return hull, Hg-container) will be determined by radiation damage (atomic displacement ("dpa"). H- and He-production) due to high energy protons and neutrons [1]. Because of the different radiation conditions, data from fission and fusion materials research cannot be directly transferred to the spallation case. At present, the only supply of information are specimens obtained from spent target components of already operating medium-power sources such as ISIS (UK) and LANSCE (USA). The ESS-target group was able to collect all available high dose components of these sources in the Hot Cells of the FZ-Jülich and specimen preparation and first mechanical test were started in 1997. The results obtained up to now [2-4] can be summarized as follows:

The irradiation causes a hardening/strengthening connected with a decrease in ductility (the so-called low-temperature embrittlement) in all 3 investigated types of materials: an austenitic stainless steel (AISI 304 L), see Fig. 1a)), a martensitic/ferritic steel (DIN 1.4926 (see Fig. 1b)) and a high-strength Ni-based alloy (Inconel 718). The fracture mode is, however, different: whereas the fracture remains transgranular for 1.4926, it changes from ductile transgranular in the initial material (see Fig. 2a) to brittle intergranular in 304 L (see Fig. 2b) and Inconel 718. At present detailed transmission-electron-microscope (TEM) investigations are under way to correlate the mechanical behaviour with the irradiation-induced changes of the microstructure.

The maximum doses available up to now are limited to about 10 dpa which corresponds to a full power operation time of about 2 months for ESS conditions. The observed ductilities at this dose level are small (>1%) but acceptable, especially if the fracture toughnesses of >50 $MPam^{½}$ measured in similar specimens is taken into account.

Higher dose levels are expected from the international irradiation programme STIP in the SINQ target. First specimens should arrive middle of 2000 in Jülich for mechanical tests in the hot cells.

Complementary information, especially on the basic radiation damage mechanisms is obtained by simulation irradiations with light ions from the Jülich Kompakt-Zyklotron (see also FE 23.80.5). A preliminary analysis of the data suggests that the observed changes of properties are mainly due to displacement effects whereas the simultaneously produced helium plays only a minor role for concentrations below several 0.1 at %.

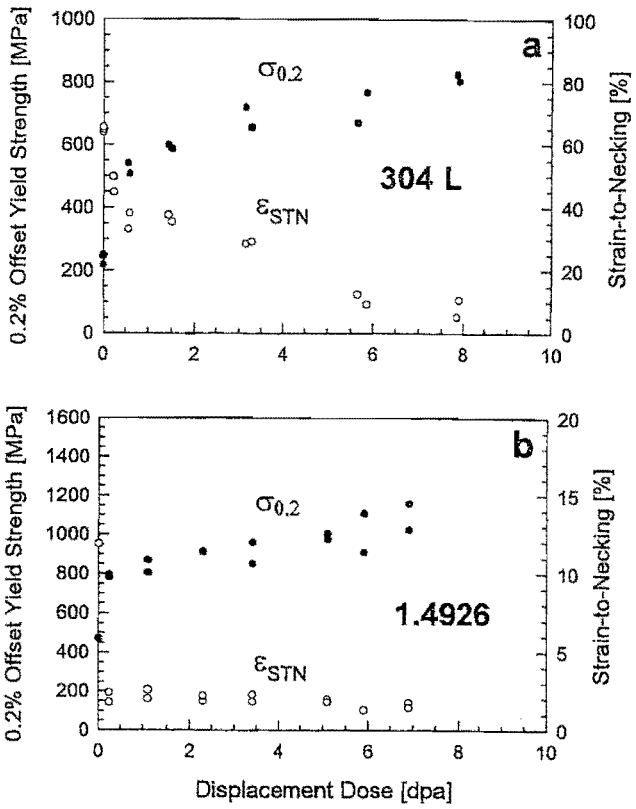

Fig.1: Yield strength and strain to necking measured at 20°C vs. Displacement dose after 800 MeV proton irradiation for (a) austenitic steel AISI 304 L and (b) martensitic steel DIN 1.4926.

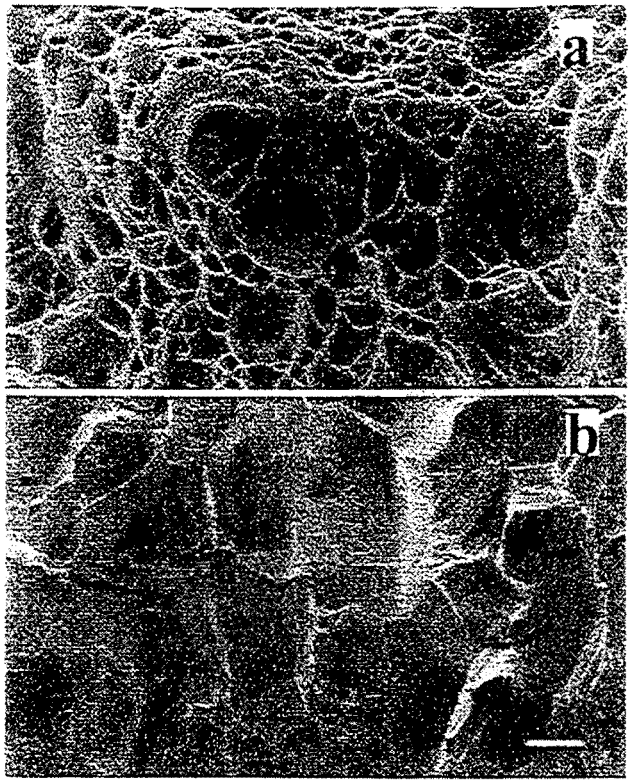

Fig. 2: Scanning electron micrographs of fracture surfaces of 304 L steel after tensile testing for (a) unirradiated reference material and (b) specimen after irradiation to 8 dpa. The change in fracture mode from ductile-transgranular to brittle-intergranular is obvious.

[1] H. Ullmaier and F. Carsughi, Nucl. Instr. Methods B101 (1995) 406

[2] F. Carsughi, H. Derz, P. Ferguson, G. Pott, W.F. Sommer and H. Ullmaier, J. Nucl. Mater. 264 (1999) 78

[3] Y. Dai, G. Bauer, F. Carsughi, H. Ullmaier, S.A. Malloy and W.F. Sommer, J. Nucl. Mater. 265 (1999) 203

[4] J. Chen, Y. Dai, F. Carsughi, W.F. Sommer, G.S. Bauer and H. Ullmaier, J. Nucl. Mater. 275 (1989) 115

FEM calculations of the pressure waves in the ASTE mercury spallation target

Carla Byloos

Time dependent finite elements calculations of the pressure waves in a liquid mercury spallation target have been performed. Comparison with experiment show that a very detailed modeling of the pressure sensor is necessary in order to obtain a quantitative agreement over the entire time interval of the measurement. It had been found that adequate proton beam profiles can mitigate the pressure impact on the target container.

The ESS (European Spallation Source) project is now in the final Research & Development phase demanding precise and reliable answers. The geometry of the target system, even the simplified form of the international ASTE (Alternating gradient synchroton Spallation Target Experiment) collaboration target, is too complicated to permit a pure analytical approach of the stress and pressure waves problem. In these cases one uses the calculation capacity of computers to divide the system in a (usually great) number of little pieces in which the equilibrium equations can be simply solved, in other words, the finite elements method (FEM) and in our case the finite element program ABAQUS.

The ASTE target is constituted of a cylindrical, 2.5 mm thick steel hull with a hemispherical beam window and at the opposite side with a thick flange. Figure 1 shows the FEM model of a quarter of the ASTE target. Inside the hull is liquid mercury.

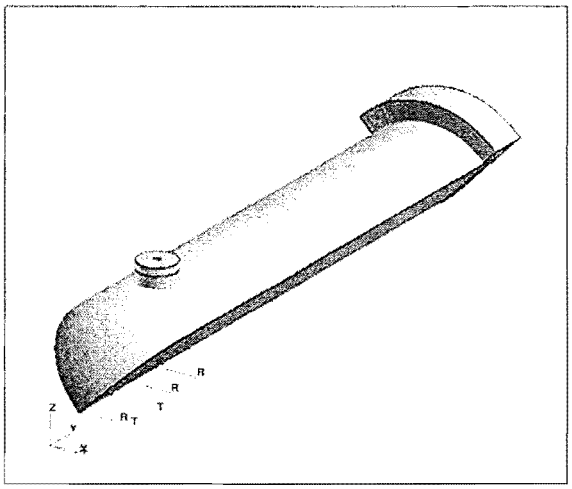

Fig. 1: The FEM model of a quarter of the ASTE mercury target

The aim of the Jülich part of the ASTE experiment campaigns was (and is) to measure the magnitude of the pressure waves in the liquid mercury induced by the temperature rise due to the beam energy deposition and of the stress waves propagating in the steel hull in turn due to the direct rapid beam energy deposition. For this scope flanges of ca. 5 cm diameter along the circumference of the cylindrical hull at 15 cm from the apex of the cylindrical window permitting access into the container, were equipped with a mechanical pressure sensor. The sensor is a thin (0.3 - 0.4 mm) circular steel membrane (joined to a proper flange) whose displacements from the equilibrium position are measured with laser interferometry and converted into pressure values with the help of a static calibration of the sensor.

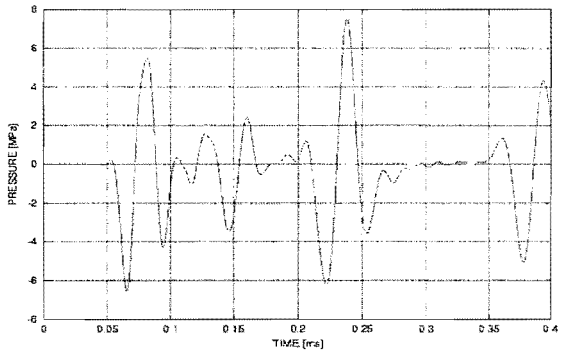

Fig. 2: Calculated time-dependent pressure in mercury at the location of the pressure sensor for a single pulse with a deposited energy of 10 kJ and a proton beam radius of 2 cm.

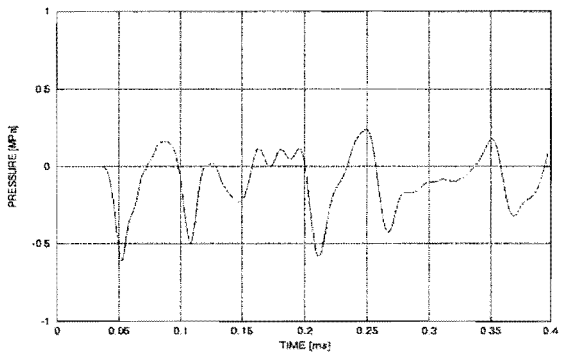

Fig. 3: Calculated time-dependent pressure in mercury at the location of the pressure sensor for a single pulse with a deposited energy of 10 kJ and a proton beam radius of 4 cm.

The pressure sensor was modeled and meshed and FEM static calculations were performed to confirm the experimental calibration and this is in fact the case. Its eigenfrequencies were calculated to recognize them if accidentally measured.

In a first step a simplified geometry was modeled for the FEM calculations on the ASTE target and the flanges for the pressure sensors were not taken into account. For different radii of the circular beam cross section and also for different deposited energies, the pressure values for times up to 400 μs after the proton pulse were determined at points in the mercury corresponding to the experimental ones. One can see in fig. 2 and Fig. 3 that the pressure is zero for the time the pressure wave front needs to travel at the velocity

(for mercury ca. 1400 m/s) from the zone in which it is originated (corresponding to the beam profile contour) to the sampling zone.

The agreement between calculations and experiment (not shown) is good only for the first 100 μs in which the value and the shape of the first peak in compression (negative values in figs. 2 and 3) resembles the measured one. The bigger the beam radius the smoother and smaller are the peaks where the mercury is under tensile stresses. Later the oscillations differ completely from experiment. This could have many causes, starting from the great simplicity of the geometry and the boundary conditions between the nodes in the two different materials till the fact that the experimental beam profile has a quite different shape from the one we used. Last but not least: the values of the pressure are taken in the mercury and do not take into account the dynamical behavior of the sensor interfering with the pressure waves.

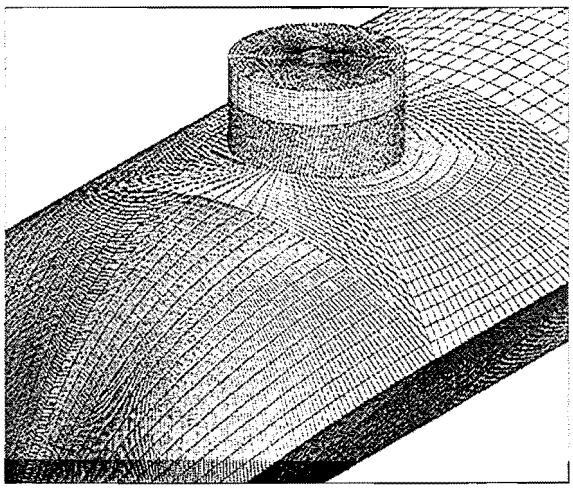

Fig. 4: Detail of the mesh used for modeling the pressure sensor location of one quarter of the ASTE target

For this reason a new, less simplified geometry was modeled and meshed. The very small time interval of the beam pulse would require, to have accurate answers, a very large number of elements (so a very fine mesh 0.1× 0.1 mm in the mercury and 0.3×0.3 mm in the steel). This would mean, considering the target dimensions, to have millions of elements - a long, hard task also for fast computers. Nevertheless, one can have enough accurate results even with coarse meshes, providing fines ones in the zones of interest and using the symmetry property of the system geometry to model only parts of it. In this case a quarter of the ASTE target including the sensor flange and the pressure sensor and the rear flange is modeled. In Fig. 4 a detail of the mesh for the measurement flange and the upper part of the sensor is shown. For a complete view see Fig. 1, where a quarter of the model target is shown (assuming that 4 instead 2 measurements sites exist). Even in this approximate form the number of the elements is ca. 300000. The calculations are in progress.

Publications in refereed journals

Carsughi F.; Derz H.; Ferguson P.1; Pott G.; Sommer W.F.2; Ullmaier H.
1LANSCE, USA
2LANL, USA
Investigations on Inconel 718 Irradiated with 800 MeV Protons
J. Nucl. Mater. 264 (1999) 78
23.60.0

Chen J.; Dai Y.1; Carsughi F.; Sommer W.F.2; Bauer G.S1; Ullmaier H.
1Paul-Scherrer-Institut, Schweiz
2LANL, USA
Mechanical Properties of 304L Stainless Steel Irradiated with 800 MeV Protons
J. Nucl. Mater. 275 (1999) 115
23.60.0

Chen J.; Jung P.; Trinkaus H.
Evolution of helium platelets and associated dislocation loops in (-SiC
Phys. Rev. Lett. 82 (1999) 2709
23.80.5

Dai Y.1; Bauer G.1; Carsughi F.; Ullmaier H.; Maloy S.A.2; Sommer W.F.2
1Paul-Scherrer-Institut, Schweiz
2LANL, USA
Microstructure in Martensitic Steel DIN 1.4926 after 800 MeV Proton Irradiation
J. Nucl. Mater. 265 (1999) 203
23.60.0

Jung P.
Creep and electrical resitivity of metallic glass Ni78B14Si8 under proton irradiation
J. Appl. Phys. 86 (1999) 4876
23.80.5

Kesternich W.
Search for radiation-induced electrical degradation in ion irradiated saphire and polycrystalline Al2O3
J. Appl. Phys. 85 (1999) 748
23.80.5

Kesternich W.; Garcia-Borquez A.;Crecelius G.
Reversal from Depletion to Enrichment of Solute Elements in Radiation-Induced Segregation at Grain Boundaries
Materials Science Forum 294-296 (1999) 149
23.80.5

Other publications

Carsughi F.; Fournier A.; Ullmaier H. (Eds.)
Proceedings of the 6th ESS General Meeting, Ancona, Italy, Sept. 20-23 (1999)
ESS-Report 99-99, 5 Volumes (Nov. 1999), ISSN 1433-559X
23.60.0

Chen J.; Jung P.
Effect of helium on radiation damage in a SiC/C Composite
Proc. 9th Cimtec-World Forum on News Materials, Symp. VII (Vincenzini, P. ed.) Techna Srl, 1999, p. 523
23.80.5

Deister P.1; Rauh H.1;Ullmaier H.:
1TU Darmstadt
Hydrogen Concentrations Around Cracks in Target Materials for Spallation Neutron Sources
ESS Report 98-79 T, Nov. 1998
23.60.0

Invited talks

Jung P.
Helium in Nuclear Material
Vortrag am National Institute of Metals, 18.2.1999, Tsukuba, Japan
23.80.5

Ullmaier H.
Das Target einer Spallations-Neutronenquelle
Kolloquium des Instituts für Kernphysik des Forschungszentrums Jülich, 26.01.1999, Jülich
23.60.0

Ullmaier H.
Materials Research and Development for the European Spallation Neutron Source
3rd International Workshop on Spallation Materials Technology, 29.04.1999, Santa Fe, New Mexico
23.60.0

Other talks

Chen J.
Mechanical Properties and Microstructure of LANSCE-irradiated 304L
Third International Workshop on Spallation Materials Technology, Apr. 29-May 4, 1999, Santa Fe, New Mexico
23.60.0

Chen J.; Carsughi F.; Derz H.; Dai Y.1; Sommer W.T.2; Broome T.3; Pott G.; Bauer G.1; Ullmaier H.
1Paul-Scherrer-Institut, Schweiz
2LANL, USA
3Rutherford Appleton Lab., Großbrittannien
Mechanical Properties and Microstructure of 800 MeV p-irradiated 304L and Tantalum
6th ESS General Meeting and Connected Workshops, Sep. 20-23, 1999, Portonovo/Ancona, Italy
23.60.0

Jung P.
Effects of irradiation and helium implatation on microstructure and physical and mechanical properties
Monitoring of Underlying Technology in the European Fusion Programme, 5.5.1999
23.80.5

Jung P.; Schliefer F.; Liu C.
Diffusion and permeation of hydrogen in low activation martensitic stainless steel - effect of irradiation
9th Int. Conf. on Fusion Reactor Materials, 12.10.1999, Colorado Springs
23.80.5

Ullmaier H.
Status des Projekts Europäische Spallationsquelle ESS
Sitzung des Komitees für die Forschung mit Neutronen, 19.02.1999, Jülich
23.60.0

Ullmaier H.
The European Spallation Neutron Source ESS
4th Internat. Workshop on Advanced Cold Moderators (AcoM IV), 25.02.1999, Jülich
23.60.0

Ullmaier H.
The Project European Spallation Neutron Source
Besuch der Parlamentarier der Nordatlantischen Versammlung, 02.03.1999, Jülich
23.60.0

Posters

Jung P.; Klein H.; Chen J.

A comparison of defects included in helium implanted (- and (-
SiC
9th Int. Conf. on Fusion Reactor Materials, 12.10.1999,
Colorado Springs, USA
23.80.5

The number at the end of each contribution characterize the associated R&D program:

23.06.0	Special and guest program in solid state research
23.15.0	Cooperative phenomena in condensed matter
23.20.0	Electronic structure of solids, surfaces and layered systems
23.30.0	Polymers, membranes and complex fluids
23.42.0	Solid State Reserarch for information technology
23.55.0	Research on novel and advanced materials
23.60.0	Material problems in target components
23.80.5	Materials under high doses of radiation
23.89.1	Applications of synchrotron and neutron radiation
23.90.0	Basic reserarch on materials for fuel cells

Publications

Publications in refereed journals

IFF-99-11-001
Adamcyk M.1; Nicoll C.1; Pinnington T.1; Tiedje T.1; Eisebitt S.; Karl A.; Scherer R.; Eberhardt W.
1University of British Columbia, Vancouver, Canada
Coherent soft x-ray scattering from InP islands on a semiconductor substrate
J. Vac. Sci. Technol. B 17, 1728 (1999)
23.20.0

IFF-99-11-002
Allgaier J.; Martin K.1; Räder H.J.1; Müllen K.1
1Max-Planck-Institut für Polymerforschung, Mainz
Many-Arm Star Polymers Syntheszied Using Chlorosilane Linking Agents: Their Structural Quality Concerning Arm Number and Polydispersity
Macromolecules, 32, 3190-3194, 1999
23.30.0

IFF-99-11-003
Ambaye, H., Kehr, K.
Toy Model for Molecular Motors
Physica A, 267 (1999) 111-123

IFF-99-11-004
Antal, T.1; Racz, Z. 1; Rakos, A.1; Schütz, G.M.:
1 Eötvös Univ. Budapest, Hungary
Transport in the XX-chain at zero temperature: Emergence of flat magnetization profiles
Phys. Rev. E59 (1999) 4912-4918

IFF-99-11-005
Arbe A.1; Alegria A.1; Colmenero J.1; Hoffmann S.; Willner L.; Richter D.
1Universidad del Pais Vasco, San Sebastian, Spanien
Segmental Dynamics in Polyvinylethylene/Polyisoprene Miscible Blends Revisited. A Neutron Scattering and Broad Band Dielectric Spectroscopy Investigation
Macromolecules, 32, 7572, 1999
23.30.0

IFF-99-11-006
Arbe A.1; Colmenero J.1; Gómez D.1; Richter D.; Farago B.2
1Universidad del Pais Vasco, San Sebastian, Spanien
2Institut Laue-Langevin, Grenoble
Reply to "Comment on 'Merging of the α and β relaxations in polybutadiene: A neutron spin echo and dielectric study' "
Phys.Rev.E., 60, 1103, 1999
23.30.0

IFF-99-11-007
Arbe A.1; Colmenero J.1; Monkenbusch M.; Richter D.
1Universidad del País Vasco, San Sebasitan, Spanien
Arbe et al. Reply:
Phys.Rev.Lett., 82, 1336, 1999
23.30.0

IFF-99-11-008
Asada T.1; Bihlmayer G.; Handschuh S.; Heinze S.2; Kurz Ph.; Blügel S.
1Faculty of Engineering, Shizuoka University, Hamamatsu, Japan
2Zentrum für Mikrostrukturforschung, Universität Hamburg
First-principles theory of ultrathin magnetic films
J. Phys. Cond. Matter 48, 9347 (1999)

IFF-99-11-009
Asato M.1; Settels A.; Hoshino T.2; Asada T.2; Blügel S.; Zeller R.; Dederichs P.H.
1Graduate School of Electronic Science and Technology, Shizuoka University, Hamamatsu, Japan
2Department of Applied Physics, Shizuoka University, Hamamatsu, Japan
Full potential KKR-calculations for metals and semiconductors
Phys. Rev. B 60, 5202 (1999)
23.20.0

IFF-99-11-010
Asato M.1; Settels A.; Hoshino T.2; Asada T.2; Blügel S.; Zeller R.; Dederichs P.H.
1Graduate School of Electronic Science and Technology, Shizuoka University, Japan
2Faculty of Engineering, Shizuoka University, Japan
Full Potential KKR-calculations for Metals and Semiconductors
Phys. Rev. B 60, 5202 (1999)
23.20.0

IFF-99-11-011
Ballone P.; Marchi M.1
1CECAM, ENS Lyon and DBCM, CEA Saclay, France
Density Functional Study of a New Family of Anticaner Drugs: Paclitaxel, Taxotere, Epothilone, and Discodermolide
J. Phys. Chem. A, 103, 3097-3102, 1999
23.20.0

IFF-99-11-012
Ballone P.; Montanari B.; Jones R.; Hahn O.1
1MPI für Polymerforschung, Mainz
Polycarbonate Simulations with a Density Functional Based Force Field
J. Phys. Chem. A, 103, 5387-5398, 1999
23.20.0

IFF-99-11-013
Benedetti A.1; Bertoldo L.1; Canton P.1; Goerigk G.; Pinna F.2; Riello P.1; Polizzi S.1
1Università, Dipartimento di Chimica Fisica, Venezia, Italy
2Università, Dipartimento di Chimica, Venezia, Italy
ASAXS study of Au, Pd and Pd-Au catalysts supported on active carbon
Catalysis Today 49, 485 - 489, 1999
23.89.1

IFF-99-11-014
Bohn H.G.; Schober T.; Mono T.; Schilling W.
The high temperature proton conductor Ba3Ca1.18Nb1.82O9-x. I. Electrical conductivity
Solid State Ionics 117 (1999) 219
23.90.0

IFF-99-11-015
Braun St.1; Meyer D.C.1; Pauller P.1; Grushko B.
1 Institut für Kristallographie und Festkörperphysik, Fachrichtung Physik, Technische Universität Dresden, D-01062 Dresden
Short-range order in a thin film of decagonal Al-Co-Ni quasicrystal: calculated from a structure model and measured with EXAFS
23.55.0

IFF-99-11-016
Brener E.
Pattern formation in three-dimensional dendritic growth
Physica A 263 (1999) 338-344
23.15.0

IFF-99-11-017
Brener E.; Iordanskii S.V.1; Marchenko V.I.2
1L.D. Landau Institute for Theoretical Physics, Chernogolovka, Russia
2P.L. Kapitza Institute for Physical Problems, Moscow, Russia
Elastic effects on the kinetics of a phase transition
Physical Review Letters, Vol. 82, No. 7 (1999) 1506-1509
23.15.0

IFF-99-11-018
Brener E.; Marchenko V.I.1
1P.L. Kapitza Institute for Physical Problems, Moscow, Russia
Nonlinear theory of dislocations in smectic crystals: An exact solution

Physical Review E, Vol. 59, No. 5 (1999) 4752-4753
23.15.0

IFF-99-11-019
Brener E.; Marchenko V.I.1
1P.L. Kapitza Institute for Physical Problems, Moscow, Russia
Surface instabilities in cracks
Physical Review Letters, Vol. 81, No. 23 (1998) 5141-5144
23.15.0

IFF-99-11-020
Brener E.; Müller-Krumbhaar H.
Comment on "Electrically induced morphological instabilities in free dendrite growth"
Physical Review Letters 83, 1698 (1999)
23.15.0

IFF-99-11-021
Brener E.; Temkin D.E1
1Institute of Physics of Metals, I.P. Bardin Central Scientific Research Institute of Ferrous Metallurgy, Moscow, Russia
Theory of diffusional growth in cellular precipitation
Acta Mater., Vol. 47, No. 14, 3759-3765 (1999)
23.15.0

IFF-99-11-022
Bringer A.; Eisenriegler E.; Schlesener, F.1; Hanke A.1
1FB Physik, Universität Wuppertal
Polymer Depletion Interaction between a Particle and a Wall
Eur. Phys. J. B11, 101-119, 1999
23.30.0

IFF-99-11-023
Brückel Th.; Strempfer J.1; Hupfeld D.; Schneider J. R.2; Mattenberger K.3
1APS at ANL, Ames, USA
2DESY, HASYLAB, Hamburg
3ETH, Laboratorium für Festkörperphysik, Zürich, Switzerland
Synchrotron Radiation Diffraction Studies of Antiferromagnetic Materials
Surface Investigation: X-ray, Synchrotron and Neutron Techniques, 8-9, 112 - 117, 1998
23.89.1

IFF-99-11-024
Buchenau U.; Wischnewski A.; Monkenbusch M.; Schmidt W.
Intensity sharing between Brillouin and Umklapp scattering in glasses
Philosophical Magazine B. Vol. 79, 2021-2026, 1999
23.30.0

IFF-99-11-025
Buzza D.M.1; Hamley I.W.2; Fzea A.H.3; Moniruzzaman M.3; Allgaier J.; Young R.N.3; Olmsted P.D.1; McLeish T.C.B.1
1Department of Physics and Astronomy and Polymer IRC, University of Leeds
2School of Chemistry, University of Leeds
3Department of Chemistry, University of Sheffield
Anomalous Difference in the Order-Disorder Transition Temperature Comparing a Symmetric Diblock Copolymer AB with Its Hetero-Four-Arm Star Analog A2B2
Macromolecules, Vol. 32, 7483-7495, 1999
23.30.0

IFF-99-11-026
Bürgler D.E.; Meisinger F.1; Schmidt C.M.1; Schaller D.M.1; Güntherodt H.-J.1; Grünberg P.
1Institut für Physik, Universität Basel
In-plane momentum conservation in Fe/Cr/Au/Fe(001) layered structures
Phys. Rev. B 60, R3732 (1999)
23.42.0

IFF-99-11-027
Carsughi F.; Derz H.; Ferguson P.1; Pott G.; Sommer W.F.2; Ullmaier H.
1LANSCE, USA
2LANL, USA
Investigations on Inconel 718 Irradiated with 800 MeV Protons
J. Nucl. Mater. 264 (1999) 78
23.60.0

IFF-99-11-028
Cendoya I.1; Alegría A.1; Alberdi J.M.1; Colmenero J.1; Grimm H.; Richter D.; Frick B.2
1Universidad del Pais Vasco, San Sebastian, Spain
2Institut Laue-Langevin, Grenoble
Effect of Blending on the PVME Dynamics - A Comparative Study by Means of Dielectric, NMR and QENS Spectroscopies
Macromolecules Vol. 32, 4065-4078, 1999
23.30.0

IFF-99-11-029
Chao K.-J.1; Zhang Zhenyu2; Ebert Ph. and Shih C.K.1
1Dept. of Physics, University of Texas, Austin
2Solid State Division, Oak Ridge National Laboratory, Oak Ridge
Substrate effects on the formation of flat Ag films on (110) surfaces of III-V compound semiconductors.
Phys. Rev. B 60, 4988-4991 (1999).
23.55.0

IFF-99-11-030
Chen J.; Dai Y.1; Carsughi F.; Sommer W.F.2; Bauer G.S1; Ullmaier H.
1Paul-Scherrer-Institut, Schweiz
2LANL, USA
Mechanical Properties of 304L Stainless Steel Irradiated with 800 MeV Protons
J. Nucl. Mater. 275 (1999) 115
23.60.0

IFF-99-11-031
Chen J.; Jung P.; Trinkaus H.
Evolution of helium platelets and associated dislocation loops in αSiC
Phys. Rev. Lett. 82 (1999) 2709
23.80.5

IFF-99-11-032
Colmenero J.1; Arbe A.1; Alegria A.1; Monkenbusch M.; Richter D.
1Universidad del Pais Vasco, San Sebastian, Spain
On the origin of the non-exponential behaviour of the (-relaxation in glass-forming polymers: incoherent neutron scattering and dielectric relaxation results
Journal of Phys.:Condens. Matter, A363-A370, 1999
23.30.0

IFF-99-11-033
Dai Y.1; Bauer G.1; Carsughi F.; Ullmaier H.; Maloy S.A.2; Sommer W.F.2
1Paul-Scherrer-Institut, Schweiz
2LANL, USA
Microstructure in Martensitic Steel DIN 1.4926 after 800 MeV Proton Irradiation
J. Nucl. Mater. 265 (1999) 203
23.60.0

IFF-99-11-034
Divin Y.Y.; Poppe U., Urban K., Volkov O.Y.1, Shirotov V.V.1, Pavlovskii V.V.1, Schueser P.2, Hanke K.2, Geitz M.2, Tonutti M.3
1 Institute of Radioengineering & Electronics of RAS, Moscow, 103907, Russia
2 DESY, Hamburg, D-22603, Germany
3 III Physikalisches Institut A, RWTH-Aachen, Aachen, D-52056, Germany
Hilbert-Transform Spectroscopy with High-Tc Josephson Junctions: First Spectrometers and First Applications.
IEEE Trans. Applied Supercond., Vol. 9, No. 2, 3346-3349 (1999)
23.42.0

IFF-99-11-035
Drchal V.1,2; Kudrnovský J.1,2; Bruno P.3; Dederichs P.H.; Weinberger P.2
1Institute of Physics, Academy of Science of the Czech Republic, Praha
2Center for Computational Material Science, Technical University Vienna, Austria
3MPI für Mikrostrukturphysik, Halle/Saale
The combined effect of temperature and disorder on interlayer exchange coupling in magnetic multilayers
Phil. Mag. B78, 571 (1998)
23.20.0

IFF-99-11-036
Drchal V.1; Kudrnovský J.1; Bruno P.2; Turek I.3; Dederichs P.H.; Weinberger P.4
1Institute of Physics, Academy of Science of the Czech Republic, Praha
2MPI für Mikrostrukturphysik, Halle
3Institute of Physics, Academy of Sciences of the Czech Republic, Brno and Institute for Technical for Technical Electrochemistry, Technical University, Vienna, Austria
4Center for Computational Material Science, Technical University Vienna, Austria
Temperature dependence of the interlayer exchange coupling in magnetic multilayers: An ab-initio approach
Phys. Rev. B 60, 9588 (1999)
23.20.0

IFF-99-11-037
Dreja M.1; Pyckhout-Hintzen W.; Mays H.2; Tieke B.1
1Institut für Physikalische Chemie, Universität Köln
2Department of Physical Chemistry, University Uppsala, USA
Cationic geminic surfactants with oligo (oxyethylene) spacer groups and their use in the polymerization of styrene in ternary microemulsion
Langmuir, 15(2), 391-399, 1999
23.30.0

IFF-99-11-038
Dumas, P.1; Hein, M.2; Otto, A.2; Persson, B.; Rudolf, P.3; Raval, R.4; Williams, G.P.5
1LURE and LASIR, Orsay, France
2Universität Düsseldorf
3LISE, Namur, Belgium
4University of Liverpool
5NSLS, BNL, Upton, USA
Vibrational Spectroscopy in the far- to mid-Infrared Range Using Synchrotron Radiation
Surface Science, 433-435, 797-805, 1999
23.20.0

IFF-99-11-039
Ebert Ph.
Nano-scale properties of defects in compound semiconductor surfaces
Surface Science Reports, Vol. 33, Nos. 4-8, 121-304 (1999)
23.55.0

IFF-99-11-040
Ebert Ph.1; Chao K.-J.1; Niu Q.1 and Shih C. K.1
1Dept. of Physics, University of Texas, Austin
Dislocations, phason defects, and domain walls in a one-dimensional quasiperiodic superstructure of a metallic thin film. Phys. Rev. Lett. 83, 3222-3225 (1999).
23.55.0

IFF-99-11-041
Ebert Ph.; , Zhang Tianjiao1,2; Kluge F.; Simon M.; Zhang Zhenyu 2,1 and Urban K.
1 Department of Physics, University of Tennessee, Knoxville, TN 37996
2 Solid State Division, Oak Ridge National Laboratory, Oak Ridge, TN 37831-6032
The importance of many-body effects in the clusterin of charged Zn dopant atoms in GaAs
Physical Review Letters 83, 757-760 (1999)
23.55.0

IFF-99-11-042
Ebert Ph.; Kluge F. and Urban K.
Evidence for a two-step evolution of the surface structure during heat treatment of cleaved icosahedral Al-Pd-Mn single-quasicrystals. Surf. Sci. 433-435, 312-316 (1999).
23.55.0

IFF-99-11-043
Ebert Ph.; Kluge F.; Grushko B.; Urban K.
Evolution of the composition and structure of cleaved and heat-treated icosahedral Al-Pd-Mn quasicrystal surfaces
Physical Review B, Vol. 60, No. 2 874-880 (1999)
23.55.0

IFF-99-11-044
Ehlers G.1; Ritter C.2; Krutjakow A.1; Miekeley W.1; Stüßer N.1; Zeiske Th.; Maletta H.1
1HMI, Berlin
2ILL, Grenoble, France
Anomalous transition from antiferromagnetic to ferromagnetic order in Tb1-xYxNiAl
Physical Review B 59 13 8821 - 8827, 1999
23.89.1

IFF-99-11-045
Ehrhart P.
Nordlung K.1; Partyka P.1; Zong Y.1; Robinson I.K.1; Averback R.S.1; Ehrhart P.
Glancing incidence diffuse X-ray scattering studies of implantation damage in Si
Nucl. Instr. Meth. In Phys. Res. B147 (1999) 399-409
23.55.0

IFF-99-11-046
Ehrhart P.; Zillgen H.
Vacancies and interstitial atoms in e-irradiated germanium
J. Appl. Phys. 85 (1999) 3503-3511
23.55.0

IFF-99-11-047
Eilhard J.; Zirkel A.1; Tschöp W.2; Hahn O.2; Kremer K.2; Schärpf O.3; Richter D.; Buchenau U.
1Technische Universität München
2Max-Planck-Institut für Polymerforschung, Mainz
3Institut Laue-Langevin, Grenoble
Spatial correlations in polycarbonates: Neutron scattering and simulation
Journal of Chemical Physics Vol.10, 1819-1830, 1999
23.30.0

IFF-99-11-048
Eisebitt S.; Lüning J.; Rubensson J.-E.; Eberhardt W.
Resonant inelastic soft X-ray scattering as a bandstructure probe: A primer
Phys. Stat. Sol. B 214, 803 (1999)
23.20.0

IFF-99-11-049
Eisebitt S.; Wirth I.; Kann G.; Eberhardt W.
Statistical analysis of the electronic structure of single wall carbon nanotubes in Buckypaper
Phys. Rev. B 1999 (accepted)

IFF-99-11-050
Engberg D.1; Wischnewski A.; Buchenau U.; Börjesson L.2; Dianoux A.J.3; Sokolov A.P.4; Torell L.M.1
1Chalmers University of Technology, Department of Experimental Physics, Sweden
2Chalmers University of Technology, Department of Applied Physics, Sweden
3Institut Laue-Langevin, Grenoble
4University of Akron, Department of Polymer Science, USA
Origin of the boson peak in a network glass B2O3
Phys.Rev.B 59, 6, 1999
23.30.0

IFF-99-11-051
Faley M.I.; Poppe U.; Urban K.; Zimmermann E.; Glaas W.; Halling H.; Bick M.; Paulson D.N.1; Starr T.1; Fagaly R.L.1
1 TRISTAN Technologies Inc., San Diego/USA
Operation of HTS dc-SQUID Sensors in High Magnetic Fields,
IEEE Transactions on Appl. Supercond., Vol. 9, No. 2, 3386-3391 (1999).
23.42.0

IFF-99-11-052
Feng X.; Brener E.; Temkin D.E.; Saito Y.1; Müller-Krumbhaar H.
1Department of Physics, Keio University, Yokohama, Japan
Creep motion of a solidification front in a two-dimensional binary alloy
Physical Review E 59, 512 (1999)
23.15.0

IFF-99-11-053
Fioretto D.1; Buchenau U.; Comez L.1; Sokolov A.2; Masciovecchio C.3; Mermet A3; Ruocco G.4; Sette F.3; Willner L.; Frick B.5; Richter, D.; Verdini L.1
1Dipartimento di Fisica and INFM, Universita di Perugia, Italy
2Department of Polymer Science, University of Akron, USA
3European Synchrotron Radiation Facility, Grenoble
4Dipartimento di Fisica and INFM, Universita di L'Aquila, Italy
5Institut Laue-Langevin, Grenoble
High-frequency dynamics of glass-forming polybutadiene
Physical Review E, Vol.59, 4470-4475, 1999
23.30.0

IFF-99-11-054
Franz V.1; Feuerbacher M.; Wollgarten M.. and Urban K.
1 Institut für Physikalische Chemie, Universität Mainz, D-55099 Mainz
Electron diffraction analysis of plastically deformed icosahedral Al-Pd-Mn single quasicrystals
Philosophical Magazine Letters, Vol. 79, No. 6, 333-342 (1999)
23.55.0

IFF-99-11-055
Gapinski J.1; Steffen W.1; Patkowski A.1; Sokolov A.P.2; Buchenau U.; Russina M.3, Mezei F.3; Schober H.4
1Max-Planck-Institut für Polymerforschung, Mainz
2Department of Polymer Science, University of Akron, USA
3Hahn-Meitner-Institut, Berlin
4Institut Laue-Langevin, Grenoble
Spectrum of fast dynamics in glass forming liquids: Does the "knee" exist?
Journal of Chemical Physics, Vol.110, 2312-2315, 1999
23.30.0

IFF-99-11-056
Gaukel C.; Kluge M.; Schober H.
Diffusion Mechanisms in Under-Cooled Binary Liquids of Zr67Cz33
J. Non-Cryst. Solids 250-252, 664 (1999)
23.15.0

IFF-99-11-057
Gaukel C.; Kluge M.; Schober H.
Diffusion and relaxations in liquid and amorphous metals
Philosophical Magazine B 79, 1907 (1999)
23.15.0

IFF-99-11-058
Gawronski M.; Park J. T.1; Magee A. S.1; Conrad H.
1Alpha-Beta Technology, Worcester, USA
Microfibrillar Structure of PGG-Glucan in Aqueous Solution as Triple-Helix Aggregates by Small Angle X-Ray Scattering
Biopolymers, Vol. 50, 569 - 578, 1999
23.30.0

IFF-99-11-059
Gliß C.1; Randel O.2; Casalta H.2; Sackmann E.3; Zorn R.; Bayerl T.1
1Institut für Experimentelle Physik, Universität Würzburg
2Institute Laue-Langevin, Grenoble
3Institut für Biophysik, Technische Universität München
Anisotropic Motion of Cholesterol in Oriented DPPC Bilayers Studied by Quasielastic Neutron Scattering: The Liquid-Ordered Phase
Biophys. J. 77 331-340, 1999
23.15.0

IFF-99-11-060
Gorski N.1; Kalus J.1; Meier G.2; Schwahn D.
1Universität Bayreuth
2Max-Planck-Institut Mainz
The Temperature Dependence of the Chemical Potential of Tretradecyldimethylaminoxid Micelles in D2O - A SANS Study
Langmuir 12, 3476-3482, 1999
23.30.0

IFF-99-11-061
Gorski N.1; Kalus J.1; Schwahn D.
1Universität Bayreuth
The Pressure Dependence of the Chemical Potential of Tetradecyldimethylaminoxid Micelles in D2O - A SANS Study
Langmuir 15, 8080-8085, 1999
23.30.0

IFF-99-11-062
Grossmann M.1; Slowak R.1; Hoffmann S.; John H.; Waser R.
1IWE RWTH Aachen, Germany
A novel integrated thin film capacitor realized by a multilayer ceramic-electrode sandwich structure
J. Europ. Ceram. Soc. 19 (1999) 1413-1415
23.42.0

IFF-99-11-063
Grushko B. and Yurechko M.
Aluminium-rhodium phases at compositions close to Al5Rh2
Z. Kristallogr. 214, 313-315 (1999)
23.55.0

IFF-99-11-064
Grushko B.; Yurechko M. and Tamura N.
A contribution to the Al-Pd-Mn phase diagram
Journal of Alloys and Compounds 290, 164-171 (1999)
23.55.0

IFF-99-11-065
Hagdorn K.1; Hohlwein D.1,2; Ihringer J.1; Knorr K.1; Prandl W.1; Ritter H.1; Schmid H.1; Zeiske Th.
1Universität, Institut für Kristallographie, Tübingen
2HMI, Berlin
Canted antiferromagnetism and magnetoelastic coupling in metallic Ho0.1Ca0.9MnO3
Eur. Phys. J. B 11, 243 - 254, 1999
23.89.1

IFF-99-11-066
Haiml M.1; Siegner U.1; Morier-Genoud F.1; Keller U.1; Luysberg M.; Lutz R.C.2; Specht P.2; Weber E.R.2
1 Institute of Quantum Electronics, ETH Zürich/CH
2 University of California, Berkeley/USA
Optical nonlinearity in low-temperature grown GaAs: microscopic limitations and optimization strategies
Appl. Phys. Lett. 74, 3134 (1999)
23.42.0

IFF-99-11-067
Haiml M.1; Siegner U.1; Morier-Genoud F.1; Keller U.1; Luysberg M.; Specht P.2; Weber E.R.2
1 Institute of Quantum Electronics, ETH Zürich/CH
2 University of California, Berkeley/USA
Femtosecond response times and high optical nonlinarity in Beryllium doped low-temperature grown GaAs
Appl. Phys. Lett. 74, 1269 (1999)
23.42.0

IFF-99-11-068
Hanke A.1; Eisenriegler E.; Dietrich S.1
1FB Physik, Universität Wuppertal
Polymer Depletion Effects near Mesoscopic Particles
Phys. Rev. E, 59, 6853-6878, 1999
23.30.0

IFF-99-11-069
Hartner W.1; Schindler G.1; Weinreich V.1; Ahlstedt M.1; Schroeder H.; Waser R.; Dehm C.1; Mazuré C.1
1Siemens AG, München, Germany
Influence of dry etching using argon on structural and electrical properties of crystalline and non-crystalline SrBi2Ta2O9 thin films
Proc. of Int. Symposium on Integrated Ferroelectrics (ISIF) 1999, Colorado Springs (USA), 2/99, to be published in Integrated Ferroelectrics
23.42.0

IFF-99-11-070
Hasegawa H.1; Sakamot N.1; Takeno H.1; Jinnai H.1; Hashimoto T.1; Schwahn D.; Frielinghaus H.2; Janßen S.3; Imai S.1; Mortensen K.2
1University of Kyoto, Japan
2Risø National Laboratory, Roskilde, Denmark
3Paul-Scherrer-Institut in Villigen, Schweiz
SANS Studies on Phase Behavior of Block Copolymers
Journ.Phys.Chem.Solids, 60, 1307-1312, 1999
23.30.0

IFF-99-11-071
Haubold H.-G.; Hiller P.; Jungbluth H.; Vad Th.
Characterization of Electrocatalysts by In Situ SAXS and XAS Investigations
Jpn. J. Appl. Phys. 38, Suppl. 38-1, 36 - 39, 1999
23.89.1

IFF-99-11-072
Hauck J.; Henkel D.; Klein M.1; Mika K.
1Institut für Biotechnologie, FZ Jülich
Structure maps of close-packed layered compounds and DNA
J. Solid State Chem., 145 (1999) 150
23.15.0

IFF-99-11-073
Hauck J.; Mika K.
Structure maps for close-packed alloys by the Ising model
Z. Kristallogr., 214 (1999) 443
23.15.0

IFF-99-11-074
Heinze S.; Abt R.; Blügel S.; Gilarowski G.1; Niehus H.1
1Institut für Physik, Humboldt-Universität zu Berlin
Scanning tunneling microscopy images of transition-metal structures buried below noble-metal surfaces
Phys. Rev. Lett. 83, 4808, (1999)
23.20.0

IFF-99-11-075
Heinze S.; Nie X.; Blügel S.; Weinert M.1
1Department of Physics, Brookhaven National Laboratory, Upton, NY, USA
Electric-field-induced changes in scanning tunneling microscopy images of metal surfaces
Chem. Phys. Lett. 315, 167 (1999)
23.20.0

IFF-99-11-076
Helbing, D.1,2, Mukamel, D.2, Schütz, G.M.:
1 Univ. Stuttgart
2 Weizmann Institute, Rehovot, Israel
Global phase diagram of a one-dimensional driven lattice gas
Phys. Rev. Lett. 82 (1999) 10-13

IFF-99-11-077
Hergert W.1; Stepanyuk V.S.1; Zeller R.; Dederichs P.H.
1Martin-Luther-Universität Halle Wittenberg
Unusual magnetic behavior in imperfect magnetic 4d and 5d clusters on the
Ag(001) surface
J. Magn. Magn. Mat. 198-199, 233 (1999)
23.20.0

IFF-99-11-078
Hoffmann S.; Grossmann M.1; Schroeder H.; Liedtke R.1; Schumacher M.2; Dietz G.W.3; Schneller Th.4; Gerhardt, R.1; Waser R.
1IWE RWTH Aachen, Germany
2 Aixtron AG, Aachen, Germany
3 Siemens AG, München, Germany
4 aixacct, Aachen, Germany
Charge transport, dc field effects, and long-term reliability of electroceramic thin films
COST 514 Ferroelectric Ceramic Thin Films, Final Report 1999, S. Hoffmann, Th. Schneller, R. Waser (eds.), Shaker Verlag, Aachen 1999, ISBN 3-8265-4960-0
23.42.0

IFF-99-11-079
Hoffmann S.; Waser R.
Control of the Morphology of CSD-prepared (Ba,Sr)TiO3 thin films
J. Europ. Ceram. Soc. 19 (1999) 1339-1343
23.42.0

IFF-99-11-080
Holland-Moritz D1.; Lu I.R1.; Wilde G2.; Schroers J.2 and Grushko B.
1 DLR; Institut für Raumsimulation, Köln
2 Dept. of Materials Science and Engineering, University of Wisconsin/Madison, USA
Melting entropy of Al-based quasicrystals.
J. Non-Cryst. Solids. 250-252, 829-832 (1999).
23.55.0

IFF-99-11-081
Hoshino T.1; Papanikolaou N.; Zeller R.; Dederichs P.H.; Asato M.1; Asada T.1; Stefanou N.2
1Faculty of Engineering, Shizuoka University, Japan
2University of Athens, Athens, Greece
First-Principles Calculations for Vacancy Formation Energies in Cu and Al; Non-Local Effect beyond the LSDA and Lattice Distortion
Comp. Mater. Science 14, 56 (1999)
23.20.0

IFF-99-11-082
Houben L.; Lundszien D.; Luysberg M.; Carius R.; Fölsch J.; Carius R.; Wagner H.
Structural properties of microcrystalline silicon germanium
Philosophical Magazine Letters, Vol. 79, No. 2, 71-78 (1999)
23.42.0

IFF-99-11-083
Hradil K.1; Weidner E.2; Neder R.B.2; Frey F.2 and Grushko B.
1 Institut fuer Mineralogie, Universität Würzburg
2 Institut für Kristallographie und angewandte Mineralogie, LMU, Muenchen
Superordering in Ni-rich and Ni-poor decagonal Al-Co-Ni phases
Philosophical Magazine A, Vol. 79, No. 8, 1963-1976 (1999)
23.55.0

IFF-99-11-084
Huck H.; Ehrhart P.; Schilling W.
High temperature optical absorption spectroscopy at pure and Y-doped BaCeO3
J. European Ceramic Soc. 19 (1999) 939-944
23.90.0

IFF-99-11-085

Jakobs B.1; Sottmann T.1; Strey R.1; Allgaier J.; Willner L.; Richter D.
1Institut für Physikalische Chemie, Köln
Amphiphilic Block Copolymers as Efficiency Boosters for Microemulsions
Langmuir, The ACS Journal of Surfaces and Colloids
Vol.15, 6707-6711, 1999
23.30.0

IFF-99-11-086
Jia C.L. and Urban K.
The atomic structure of the dislocation cores in a small-angle grain boundary in BaTiO3 thin films
Philosophical Magazine Letters, Vol. 79, No. 11, 859-867 (1999).
23.42.0

IFF-99-11-087
Jia C.L.; Hojczyk R.; Faley M.; Poppe U. and Urban K.
Interfaces in YBa2Cu3O7/BaTbO3 and PrBa2Cu3O7/BaTbO3 heterostructure thin films
Philosophical Magazine A, Vol. 79, No. 4, 873-891 (1999)
23.42.0

IFF-99-11-088
Jia C.L.; Rosenfeld R.; Thust A. and Urban K.
Atomic Structure of a (-3, (111(twin-boundary junction in a BaTiO3 thin film
Philosophical Magazine Letters, Vol. 79, No. 3, 99-106 (1999)
23.42.0

IFF-99-11-089
Jia C.L.; Thust A.
Investigation of Atomic Displacements at a (3 (111(Twin Boundary in BaTiO3 by Means of Phase Retrieval Electron Microscopy
Physical Review Letters, Vol. 82, No. 25, 5052-5055 (1999)
23.42.0

IFF-99-11-090
Johnson M.R.1; Prager M.; Grimm H.; Neumann M.A.1; Kearley G.J.1; Wilson C.C.2
1Institut Laue-Langevin, Grenoble
2ISIS, Rutherford Appleton Laboratory, United Kingdom
Methyl group dynamics in paracetamol and acetanilide: probing the static properties of intermolecular hydrogen bonds formed by peptide groups
Chemical Physics 244, 49-66, 1999
23.15.0

IFF-99-11-091
Jones R.
Cluster Geometries from Density Functional Calculations - Prospects and Limitations
Euro. Phys. J. D, 9, 1-4, 1999
23.20.0

IFF-99-11-092
Jones R.
Density Functional Study of Carbon Clusters C2n (2(n (16): I. Structure and Bonding in the Neutral Clusters
J. Chem. Phys., 101, 5189-5200, 1999
23.20.0

IFF-99-11-093
Jung P.
Creep and electrical resitivity of metallic glass Ni78B14Si8 under proton irradiation
J. Appl. Phys. 86 (1999) 4876
23.80.5

IFF-99-11-094
Kahle S.; Schröter K.1; Hempel E.1; Donth E.1
1Fachbereich Physik, Universität Halle
Calorimetic indications of a cooperativity onset in the crossover region of dynamic glass transition for benzoin isobutylether
Journal of Chemical Physics, Vol.111, 6462, 1999

IFF-99-11-095
Kesternich W.
Search for radiation-induced electrical degradation in ion irradiated saphire and polycrystalline Al2O3
J. Appl. Phys. 85 (1999) 748
23.80.5

IFF-99-11-096
Kesternich W.; Garcia-Borquez A.;Crecelius G.
Reversal from Depletion to Enrichment of Solute Elements in Radiation-Induced Segregation at Grain Boundaries
Materials Science Forum 294-296 (1999) 149
23.80.5

IFF-99-11-097
Kirstein O.; Grimm H.; Prager M., Richter D.
Design and Optimization of a Backscattering Spectrometer Using a Phase Space Transformation and Super Mirror Guides
Journal of Neutron Research, Vol. 8/2, 119-132, 1999
23.30.0

IFF-99-11-098
Klein H.; Feuerbacher M.; Schall P. and Urban K.
Novel Type of Dislocation in an Al-Pd-Mn Quasicrystal Approximant
Physical Review Letters, Vol. 82, No. 17, 3468-3471 (1999).
23.55.0

IFF-99-11-099
Koza, Z.1
Univ. Wroclaw, Poland
General technique of calculating the drift velocity and diffusion coefficient in arbitrary periodic systems
J. Phys. A: Math. Gen. 32 (1999) 7637-7651

IFF-99-11-100
Köbler U.; Hoser A.1; Graf H. A.1; Fernandez-Diaz M.-T.2; Fischer K.; Brückel Th.
1HMI, Berlin
2ILL, Grenoble, France
Investigations of the sublattice magnetizations Msub(T) in antiferromagnets with fourth-order exchange interactions: EuxSr1-xTe
Eur. Phys. J. B 8, 217 - 224, 1999
23.15.0

IFF-99-11-101
Köbler U.; Hoser A.1; Kawakami M.2; Chatterji T.3; Rebizant J.4
1HMI, Berlin
2University, Dep. of Physics, Kagoshima, Japan
3ILL, Grenoble, France
4Joint Research Center, Institut for Transuranium Elements, Karlsruhe
An unified view of the spin dynamics in two- and three-dimensional magnetic systems
Journal of Magnetism and Magnetic Materials 205, 343 - 356, 1999
23.15.0

IFF-99-11-102
Köbler U.; Hupfeld D.; Schnelle W.1; Mattenberger K.2; Brückel Th.
1MPI für Festkörperforschung, Stuttgart
2ETH, Laboratorium für Festkörperphysik, Zürich, Switzerland
Fourth-order exchange interactions in GdxEu1-xS
Journal of Magnetism and Magnetic Materials 205, 90 - 104, 1999
23.15.0

IFF-99-11-103
Lei C.H.; Jia C.L.; Siegert M.; Schubert J.; Buchal Ch.; Urban K.

Microstructure and orientation relations of BaTiO3/MgO/YSZ multilayers deposited on Si(001) substrates by laser ablation
Journal of Crystal Growth 204, 137-144 (1999).
23.42.0

IFF-99-11-104
Lembke U.1; Hoell A.1; Kranold R.1; Müller R.2; Schüppel W.2; Goerigk G.; Gilles R.3; Wiedenmann A.3
1Universität, Fachbereich Physik, Rostock
2Institut für Physikalische Hochtechnologie, Jena
3HMI, Berlin
Formation of magnetic nanocrystals in a glass ceramic studied by small-angle scattering
Journal of Applied Physics 85 4, 2279 - 2286, 1999
23.89.1

IFF-99-11-105
Liebsch A.
Theory of Sum Frequency Generation from Metal Surfaces
Appl. Phys. B, 68, 301-304, 1999
23.20.0

IFF-99-11-106
Liebsch A.; Goncalves S.1; Kiwi M.2
1Universidad Federal, Porto Alegre
2Universidad Catolica, Santiago de Chile
Electronic vs Phononic Friction of Xenon on Silver
Phys. Rev. B, 60, 5034-5043, 1999
23.20.0

IFF-99-11-107
Link S.; Scholl A.; Jacquemin R.; Eberhardt W.
Electron dynamics at a Ag/C60 metal semiconductor interface
Solid State Comm. 1999 (accepted)

IFF-99-11-108
Lopera W.1; Baca E.1; Gomez E.1; Prieto P.1; Poppe U.; Evers W.
1 Universidad del Valle, Cali/Kolumbien
Properties of Bi-2212/Bi-22Y2 Step-Stack Josephson Junctions
IEEE Transactions on Appl. Supercond. , Vol. 9, 4288 (1999)
23.42.0

IFF-99-11-109
Lustfeld H.; Neufeld Z.1
1Eötvös University, Budapest
Chemical Dynamics vs Transport Dynamics in a Simple Model
J. Phys. A, 32, 3717-3731, 1999
23.15.0

IFF-99-11-110
Lüning J.; Eisebitt S.; Rubensson J.-E.; Ellmers C.; Eberhardt W.
Electronic structure of silicon carbide polytypes studied by soft X-ray spectroscopy
Phys. Rev. B 59, 10 573 (1999)
23.20.0

IFF-99-11-111
Lüning J.; Rockenberger J.1; Eisebitt S.; Rubensson J.-E.; Karl A.; Kornowski A.1; Weller H.1; Eberhardt W.
Soft X-ray spectroscopy of single sized CdS nanocrystals: size confinement and electronic structure
1Institut für Physikalische Chemie, Universität Hamburg
Solid State Comm. 112, 5 (1999)
23.20.0

IFF-99-11-112
Malis O.1; Ludwig Jr. K. F.1; Schweika W.; Ice G. E.2; Sparks C. J.2
1University, Department of Physics, Boston, USA
2ORNL, Oak Ridge, USA
Temperature dependence of the diffuse-scattering fine structure in equiatomic CuAu
Physical Review B 59 17 11105 - 11108, 1999
23.89.1

IFF-99-11-113
Maus M.; Ganteför G.; Eberhardt W.
The electronic structure and the bandgap of nano-sized Si particles: competition between
Quantum confinement and surface reconstrcution
Applied Physics A 1999 (accepted)

IFF-99-11-114
McLeish T.C.B.1; Allgaier J.; Bick D.K.1; Bishko G.1; Biswas P.1; Blackwell R.1; Blottière B.1; Clarke N.1; Gibbs B.1; Groves J.1; Hakiki A.2; Heenan R.K.3; Johnson J.M.4; Kant R.1; Read D.J.1; Young R.N.3
1University of Leeds
2Department of Physics, University of Sheffield
3Rutherford Appleton Laboratory
4Department of Physics, University of Sheffield
Dynamics of Entangled H-Polymers: Theory, Rheology and Neutron Scattering
Macromolecules, 32, 6734-6758, 1999
23.30.0

IFF-99-11-115
Messerschmidt U.1; Bartsch M.1; Feuerbacher M.; Geyer B.1 and Urban K.
1 Max-Planck-Institut für Mikrostrukturphysik, Weinberg 2, 06120 Halle/Saale,
Germany
Friction mechanism of dislocation motion inicosahedral Al-Pd-Mn quasicrystals
Philosophical Magazine A, Vol. 79, No. 9, 2123-2135 (1999)
23.55.0

IFF-99-11-116
Monkenbusch M.
Correction scheme for divergent beams in zero-field spin-echo spectrometers
Nuclear Instruments and Methods in Physics Research, Vol.437, p455-458, 1999
23.89.1

IFF-99-11-117
Montanari B.; Ballone P.; Jones R.
Density Functional Study of Polycarbonate. 2. Crystaline Analogs, Cyclic Oligomers, and Their Fragments
Macromolecules, 32, 3396-3404, 1999
23.20.0

IFF-99-11-118
Montes H.1; Monkenbusch M.; Willner L.; Rathgeber S.2; Fetters L.3; Richter D.
1ESPCI, Physico-Chimie Structurale et Macromoleculaire, France
2National Institute of Standards and Technology, USA
3EXXON, Research and Engineering Company, USA
Neutron spin echo investigation of the concentration fluctuation dynamics in melts of diblock copolymers
Journal of Chemical Physics, Vol.110, 10188, 1999
23.30.0

IFF-99-11-119
Morenzin J.; Schlebusch C.; Kessler B.; Eberhardt W.
Phthalocyanine/C60 composites as improved photosensitive materials
Phys. Chem. Chem. Phys. 1, 1765 (1999)
23.20.0

IFF-99-11-120
Mueller R.; Köbler U.; Fischer K.
On the T2 Bloch law in magnets with fourth-order exchange interaction
Eur. Phys. J. B 8, 207 - 216, 1999
23.15.0

IFF-99-11-121
Müller-Krumbhaar H.; Saito Y.1
1Department of Physics, Keio University, Yokohama, Japan

Strain effect on Eden Model
J. Phys. Soc. Japan, 67, 3661 (1998)
23.15.0

IFF-99-11-122
Nakano M.1; Matsuoka H.1; Yamaoka H.1; Poppe A.; Richter D.
1Kyoto University, Japan
Sphere to Rod Transition of Micelles Formed by Amphiphilic Diblock Copolymers of Vinyl Ethers in Aqueous Solution
Macromolecules, Vol.32, 697-703 1999
23.30.0

IFF-99-11-123
Nonas B.; Wildberger K.; Zeller R.; Dederichs P.H.; Wille L.T.1; Dreysse H.2
1Florida Atlantic University, Boca Raton, USA
2Institute de Physique et Chimie des Materiaux de Strasbourg, France
Direct Exchange and Interaction of 3d Impurities on the (001) Surface of Iron
J. Magn. Magn. Mat. 198-199, 548 (1999)
23.20.0

IFF-99-11-124
Oligschleger C.1; Gaukel C.; Schober H.
1Theoretische u. Physikalische Chemie, Universität Bonn
Relaxations in Glasses
J. Non-Cryst. Solids 250-252, 660 (1999)
23.15.0

IFF-99-11-125
Oligschleger C.1; Schober H.
1Theoretische u. Physikalische Chemie, Universität Bonn
Molecular Dynamics Simulations of Glasses
J. Non-Cryst. Solids 250-252, 651 (1999).
23.15.0

IFF-99-11-126
Ortiz G.1; Harris M.2; Ballone P.
1Los Alamos National Laboratory, USA
2MPI für Festkörperforschung, Stuttgart
Zero Temperature Phases of the Electron Gas
Phys. Rev. Lett., 82, 5317-5320, 1999
23.20.0

IFF-99-11-127
Ozaki Y.1; Prager M.; Asmussen B.2
1Nagoya Institute of Technology, Nagoya, Japan
2Institut f. Experimentelle und Angewandte Physik, Universität Kiel
Calculation of rotational states of methane molecules in a square lattice
Journal of Physics and Chemistry of Solids 60, 1523-1526, 1999
23.15.0

IFF-99-11-128
Parshin D.A.1; Schober H.
1State Technical University, St. Petersburg, Russia
Distribution of fractal dimensions at the Anderson transition
Phys. Rev. Lett. 29 4590 (1999)
23.15.0

IFF-99-11-129
Persson B.
Brittle Fracture of Polymers
J. Chem. Phys., 110, 9713- 9724, 1999
23.20.0

IFF-99-11-130
Persson B.
Sliding Friction
Surface Science Reports, 33, 83-120, 1999
23.20.0

IFF-99-11-131
Persson, B; Tosatti, E.1; Fuhrmann, D.2; Witte, G.2; Wöll, Ch.2
1ICTP/SISSA, Trieste, Italy
2Ruhr Universität Bochum
Low-Frequency Adsorbate Vibrational Relaxation and Sliding Friction
Phys. Rev. B, 59, 11777-11791, 1999
23.20.0

IFF-99-11-132
Pertsev N.A.1, Zembilgotov A.G.1; Hoffmann S.; Waser R.; Tagantsev A.K.2
1 St. Petersburg
2 EPFL, Lausanne, Switzerland
Ferroelectric thin films grown on tesnile substrates: Renormalization of the Curie-Weiss law and apparent absence of ferroelectricity
J. Appl. Phys. 85 (1999) 1698-1701
23.42.0

IFF-99-11-133
Petrenko O. A.1; McPaul D.1; Ritter C.2; Zeiske Th.; Yethiraj M.3
1University of Warwick, Department of Physics, Coventry, UK
2ILL, Grenoble, France
3ORNL, Solid State Division, Oak Ridge, USA
Magnetic frustration and order in gadolinium gallium garnet
Physica B 266, 41 - 48, 1999
23.89.1

IFF-99-11-134
Peyla P.1; Vallat A.1; Misbah C.2; Müller-Krumbhaar H:
1Laboratoire de Physique et de Modelisation des Milicux Condenses, Universite J. Fourier, Grenoble, France
2Laboratoire de Spectrometrie, Universite J. Fourier, Grenoble, France
On elastic interaction between surface defect in thin layers
Phys. Rev. Lett. 82, 787 (1999)
23.15.0

IFF-99-11-135
Piancastelli M.N.1; Kivimäki A.2; Kempgens B.3; Neeb M.; Maier K.3; Hergenhahn U.3; Rüdel A.3; Bradshaw A.M.3
1Department of Chemical Sciences and Technologies, University "Tor Vergata", Rome
2Department of Chemical Sciences, University of Oulu, Finland
3Fritz-Haber-Institut der Max-Planck-Gesellschaft, Berlin
Electron decay following the N 1s (r) (* excitation in N2 studied under resonant Raman conditions
J. of Electron Spectrosc. and Rel. Phenomena 98-99, 111 (1999)
23.20.0

IFF-99-11-136
Pontius N.; Bechthold P.S.; Neeb M.; Eberhardt W.
Femtosecond multi-photon photoemission of small transition metal cluster anions
J. of Electron Spectrosc. and Rel. Phenomena 1999 (accepted)

IFF-99-11-137
Pontius N.; Bechthold P.S.; Neeb M.; Eberhardt W.
Ultrafast hot-electron dynamics observed in Pt3- using time-resolved
photoelectron spectroscopy
Phys. Rev. Lett. 1999 (accepted)

IFF-99-11-138
Popkov, V.; Schütz, G.M.
Steady-state selection in driven diffusive systems with open boundaries
Europhys. Lett. 48 (1999) 257-263

IFF-99-11-139

Poppe U.; Hojczyk R.; Jia C.L.; Faley M.I.; Evers W.; Bobba F.1; Urban K., Horstmann C.; Dittmann R.; Breuer U.; Holzbrecher H.
1 Universität Salerno / I
BaTbO3 as a new Material for Insulation and Junction Barriers in High-Tc Devices
IEEE Transactions on Appl. Supercond. , Vol. 9, 3452 (1999)
23.42.0

IFF-99-11-140
Prager M.; Schiebel P.1; Johnson M.2; Grimm H.; Hagdorn H.1; Ihringer J1; Prandl W.1; Lalowicz Z.3
1Institut für Kristallographie, Universität Tübingen
2Institut Laue-Langevin, Grenoble
3H Niewodniczanski Institute of Nuclear Physics, Krakow, Poland
The isotope effect and phase transitions in ammonium hexachloropalladate studied by neutron tunnelling spectroscopy
Journal Physics Condensed Matter, 5483-5495, 1999
23.30.0

IFF-99-11-141
Prager M.; Schiebel P.1; Johnson M.2; Grimm H.; Hagdorn H.1; Prandl W.1; Lalowicz Z.3
1Institut f. Kristallographie, Universität Tübingen
2Institut Laue-Langevin, Grenoble
3Institut of Nuclear Physics, Jagellonian University Krakow
Isotope effect and phase transitions in ammoniumhexachloropalladate studied by neutron tunnelling spectroscopy
Journal of Physics: Condensed Matter 11, 5341, 1999
23.15.0

IFF-99-11-142
Quadbeck P.; Ebert Ph.; Urban K.; Gebauer J.1 and Krause-Rehberg R.1
1 FB Physik, Martin-Luther-Universität Halle, Halle
Effect of dopant atoms on the roughness of III-V seminconductor cleavage surfaces
Applied Physics Letters, Vol. 76, No. 3, 300 (1999)
23.55.0

IFF-99-11-143
Rader,O.1; Pampuch, C.1; Gudat, W.1; Dallmeyer, A.; Carbone, C.; Eberhardt, W.
Parallel, antiparallel and no magnetic coupling in submonolayer Mn/Fe(110)
1Bessy GmbH, Berlin
Europhysics Lett. 46, 231 (1999)
23.20.0

IFF-99-11-144
Rathgeber S.1; Willner L.; Richter D.; Brulet A.2; Farago B.3; Appel M.4; Fleischer G.4
1National Institute of Standards and Technology, USA
2Laboratoire Léon Brillouin, France
3Institute Laue-Langevin, Grenoble
4Institut f. Experimentalphysik, Universität Leipzig
Polymer dynamics in bimodal polyethylene melts: A study with neutron spin echo spectroscopy and pulsed filed gradient nuclear magnetic resonance
Journal of Chemical Physics, Vol.110, 10171, 1999
23.30.0

IFF-99-11-145
Rennie E.E.1; Köppe H.M.1; Kempgens B.1; Hergenhahn U.1; Kivimäki A.2; Maier K.1; Neeb M.; Rüdel A.1; Bradshaw A.M.1
1Fritz-Haber-Institut der Max-Planck-Gesellschaft, Berlin
2Department of Physical Science, University of Oulu, Finland
Vibrational and shake-up excitations in the C 1s photoionization of ethane and deuterated ethane
J. Phys. B: At. Mol. Opt. 32, 2691 (1999)
23.20.0

IFF-99-11-146
Richter D.; Monkenbusch M.; Allgaier J.; Arbe A.1; Colmenero J.1; Farago B.2; Cheol Bae Y.3; Faus R.3
1Universidad del Pais Vasco, San Sebastian, Spanien
2Institut Laue-Langevin, Grenoble
3University of Massachusetts-Lowell, USA
From Rouse dynamics to local relaxation: A neutron spin echo study on polyisobutylene melts
Journal of Chemical Physics, Vol. 111, 6107, 1999
23.30.0

IFF-99-11-147
Richter D.; Monkenbusch M.; Arbe A.1; Colmenero J.1; Farago B.2; Faust R.3
1Universidad del Pais Vasco, San Sebastian
2Instiut Laue-Langevin, Grenoble
3University of Massachusetts, USA
Space time observation of the (-process in polymers by quasielastic neutron scattering
J. Phys.: Condens. Matter11, A297-A306, 1999
23.30.0

IFF-99-11-148
Rodmar M.1; Grushko B.; Tamura N.; Urban K.; Rapp Ö.1
1Fasta Tillstandets Pysik, Kungliga Tekniska Högskolan, SE 10044 Stockholm/S
Isotropic magnetoresistance of icosahedral Al-Pd-Mn
Physical Review B, Vol. 60, No. 10, 7208-7212 (1999)
23.55.0

IFF-99-11-149
Rush J.J.1; Udovic T.J.1; Berk N.F.1; Richter D.; Magerl A.2
1National Institute of Standards and Technology, Gaithersburg, USA
2Institut Laue-Langevin, Grenoble
Excited-State Vibrational Tunnel Splitting of Hydrogen Trapped by Nitrogen in Niobium
Eur.Phys.Lett., 48, 187, 1999
23.30.0

IFF-99-11-150
Rzehak R.; Kienle D.; Kawakatsu T1; Zimmermann W.2
1Department of Computational Science and Engineering, Nagoya University, Japan
2Universität des Saarlandes, Saarbrücken
Partial Draining of a Tethered Polymer in Flow
Europhys. Lett. 46, 821 (1999)
23.15.0

IFF-99-11-151
Schall P.; Feuerbacher M.; Wollgarten M. and Urban K.
Dislocation density evolution upon plastic deformation of Al-Pd-Mn single quasicrystals
Phil. Mag. Lett. 79, 785 (1999)
23.55.0

IFF-99-11-152
Schiffmann K. I.1; Fryda M.1; Goerigk G.; Lauer R.2; Hinze P.2; Bulack A.3
1Fraunhofer Institut für Schicht- und Oberflächentechnik, Braunschweig
2Physikalisch-Technische Bundesanstalt, Braunschweig
3Institut für Oberflächentechnik und plasmatechnische Werkstoffentwicklung, Braunschweig
Sizes and distances of metal clusters in Au-, Pt-, W- and Fe-containing diamond-like carbon hard coating: a comparative study by small angle X-ray scattering, wide angle X-ray diffraction, transmission electron microscopy and scanning tunnelling microscopy
Thin Solid Films 347, 60 - 71, 1999
23.89.1

IFF-99-11-153
Schlebusch C.; Morenzin J.; Kessler B.; Eberhardt W.
Organic photoconductors with C60 for xerography
Carbon 37, 717 (1999)
23.20.0

IFF-99-11-154
Schleger P.1; Farago B.1; Lartigue C.1; Kollmar A.; Richter D.
1Institut Laue-Langevin, Grenoble
Clear evidence of reptation in polyethylene from neutron spin-echo spectroscopy
Phys.Rev.Lett. 81, 124, 1998
23.30.0

IFF-99-11-155
Schmid H.1; Ihringer J.1; Knorr K.1; Prandl W.1; Ritter H.1; Zeiske Th.
1Universität, Institut für Kristallographie, Tübingen
Magnetization and magnetic phases in metallic and semiconducting HoxCa1-xMnO3
J. Mag. Soc. Japan 23, 525 - 527, 1999
23.89.1

IFF-99-11-156
Schmitz D.; Charton C.; Scholl A.; Carbone C.; Eberhardt W.
Magnetic moments of fcc Fe overlayers on Cu(100) and Co(100)
Phys. Rev. B 59, 1 (1999)
23.20.0

IFF-99-11-157
Schober H.
Oligschleger C.; Schober H.
Collective jumps in a soft sphere glass
Phys. Rev. B59, 811 (1999)
23.15.0

IFF-99-11-158
Schober T.; Bohn H.G.; Mono T.; Schilling W.
The high temperature proton conductor Ba3Ca1.18Nb1.82O9-x. II. Electrochemical cell measurements and TEM
Solid State Ionics 118 (1999) 173
23.90.0

IFF-99-11-159
Schober T.; Friedrich J.
Laboratory application and demonstration of automotive oxygen sensors
J. Chem. Education 76 (1999) 1697-1700
23.90.0

IFF-99-11-160
Schober T.; Friedrich J.
Proton conductor Ba3Ca1.18Nb1.82O9-((BCN19): Effect of reducing environments
J. Am. Ceram. Soc. 82 (1999) 3125-28
23.90.0

IFF-99-11-161
Schober T.; Friedrich J.
Thermogravimetry of the high temperature proton conductors BaCa0.3Nb0.6Nd0.1O3-xSrCa(1+x)/3O(3-x)/2 and Sr(Zr0.8Ce0.2)0.8In0.2O((3-x)
Solid State Ionics 125 (1999) 319
23.90.0

IFF-99-11-162
Schroeder H.
Stress and electromigration-induced voiding and its correlation to macroscopic stress changes
Materials Research Scoeity (MRS) Symposium Proceedings 516 (1998) 237
23.42.0

IFF-99-11-163
Schukow H.1; Breitinger D. K.2; Zeiske Th.; Kubanek F.3; Mohr J.2; Schwab R. G.1
1Universität, Lehrstuhl für Mineralogie, Erlangen
2Universität, Lehrstuhl für Anorganische Chemie I, Erlangen
3HMI, Berlin
Localization of Hydrogen and Content of Oxonium Cations in Alunite via Neutron Diffraction
Z. Anorg. Allg. Chem., 625, 1047 - 1050, 1999
23.89.1

IFF-99-11-164
Schwahn D.; Mortensen K.1; Frielinghaus H.1; Almdal K.1
1Risø National Laboratory, Roskilde, Denmark
Crossover from 3d-Ising to Isotope Lifshitz Critical Behavior in a Mixture of a Homopolymer Blend and Diblock Copolymer
Phys. Rev. Lett., 82, 505, 1999
23.30.0

IFF-99-11-165
Schütz, G.M.
Non-equilibrium relaxation law for entangled polymers
Europhys. Lett. 48 (1999)

IFF-99-11-166
Schütz, G.M.; Trimper, S.1
1 Martin-Luther-Univ. Halle, Germany
Relaxation and Aging in Quantum Spin Systems
Europhys. Lett. 47 (1999) 164-170

IFF-99-11-167
Seeck O.; Hupfeld D.; Krull H.1; Doerr A. K.1; Schlomka J.-P.1; Tolan M.1; Press W.1
1Universität, Institut für Experimentelle und Angewandte Physik, Kiel
Surface phase transition close to a bulk tricritical point: An x-ray study of ND4Cl
Physical Review B 59 5 3474 - 3479, 1999
23.89.1

IFF-99-11-168
Seto H.1; Kato T.2; Monkenbusch M.; Takeda T.1; Kawabata Y.1; Nagao M.3; Okuhara D.1; Imai M.4; Komura S.5
1Hiroshima University, Japan
2Metropolitan University, Japan
3University of Tokyo, Japan
4Ochanomizu University, Japan
Collective motions of a network of wormlike micelles
Journal of Physics and Chemistry of Solids 60, 1371-1373, 1999
23.30.0

IFF-99-11-169
Settels A.; Korhonen T.1; Papanikolaou N.; Zeller R.; Dederichs P.H.
1Laboratory of Physics, Helsinki University of Technology, Finnland
Ab-intio Study of Acceptor-Donor Complexes in Silicon and Germanium
Phys. Rev. B 83, 4369 (1999)
23.20.0

IFF-99-11-170
Shur, V.Ya.; Blankova E.B.; Subbotin A.L.; Borisova E.A., Poelegov D.V.; Hoffmann S.; Bolten D.; Gerhardt R.; Waser R.
Influence of crystallization kinetics on texture of sol-gel PZT and BST thin films
J. Europ. Ceram. Soc. 19 (1999) 1391-1395
23.42.0

IFF-99-11-171
Siemens B.; Domke C.; Ebert Ph. and Urban K.
Point defects, dopant atoms, an compensation effects in CdSe and CdS cleavage surfaces
Thin Solid Films Vol. 343-344, 537-540 (1999).
23.55.0

IFF-99-11-172
Siemens B.; Domke C.; Ebert Ph. and Urban K.
Steps on CdSe (1120) and (1010) cleavage surfaces: Evidence for crack propagation in competing cleavage planes.
Physical Review B, Vol. 56, No. 4, 3000-3007 (1999)
23.55.0

IFF-99-11-173
Siemens B.; Domke C.; Heinrich M.; Ebert Ph. and Urban K.

Imaging individual dopant atoms on cleavage surfaces of wurtzite-structure compound semiconductors
Physical Review B, Vol. 59, No. 4, 2995-2999 (1999)
23.55.0

IFF-99-11-174
Smirnova E.A.1; Abrikosov I.A.2; Johansson B.2; Vekilov Yu.Kh.3; Baranov A.N.4; Stepanyuk V.S.5; Hergert W.5; Dederichs P.H.
1Department of Theoretical Physics, Moscow Steel and Alloys Institute, Moscow, Russia
2Condensed Matter Theory Group, Department of Physics, Uppsala University, Sweden
3Department of Theoretical Physics, Moscow State University, Moscow, Russia
4Department of Solid State Physics, Moscow State University, Moscow, Russia
5Fachbereich Physik, Martin-Luther-Universität, Halle/Saale
Calculated magnetic properties of an Fe1-xNix monolayer on Cu(001)
Phys. Rev. B 59, 14417 (1999)
23.20.0

IFF-99-11-175
Sokolov A.P.1; Buchenau U.; Richter D.; Masciovecchio C.2; Sette F.2; Mermet A.2; Fioretto D.3; Ruocco G.4; Willner L.2; Frick B.5
1Department of Polymer Science, University of Akron, USA
2European Synchrotron Radiation Facility, Grenoble
3Dipartimento di Fisica and INFM, Universita di Perugia, Italy
4Dipartimento di Fisica and INFM, Universita di L'Aquila, Italy
5Institut Laue-Langevin, Grenoble
Brillouin and Umklapp scattering in polybutadiene: Comparison of neutron and x-ray scattering
Physical Review E, Vol. 60, 2464-2467, 1999
23.30.0

IFF-99-11-176
Sokolov A.P.1; Grimm H.; Kahn R.2
1Department of Polymer Science, University of Akron, USA
2Laboratoire Léon Brillouin, Saclay, France
Glassy dynamics in DNA: Ruled by water of hydration?
Journal of Chemical Physics, 110, 7053, 1999
23.30.0

IFF-99-11-177
Steinbrecher J.; Müller-Krumbhaar H.; Brener E.; Misbah C.1; Peyla, P.2
1Laboratoire de Spectrometrie, Universite J. Fourier, Grenoble, France
2Laboratoire de Physique et de Modelisation des Milicux Condenses, Universite J. Fourier, Grenoble, France
Fractal growth of epitaxial surface clusters with elastic interaction
Physical Review E 59, 5600 (1999)
23.15.0

IFF-99-11-178
Stellbrink J.; Willner L.; Richter D.; Lindner P.1; Fetters L.J.2; Huang J.S.2
1Institut Laue-Langevin, Grenoble
2Exxon Research and Engineering Company, Annandale, USA
Self-Assembling Behavior of Butadienyllithium Headgroups in Benzene via SANS Measurements
Macromolecules, Vol.32, 5321-5329, 1999
23.30.0

IFF-99-11-179
Stepanyuk V.S.1,2; Hergert W.1; Rennert P.1; Wildberger K.; Zeller R.; Dederichs P.H.
1Martin Luther Universität Halle-Wittenberg
2MPI für Mikrostrukturphysik, Halle
Imperfect Magnetic Nanostructures on a Ag(001) Surface
Phys. Rev. B 59, 1681 (1999)
23.20.0

IFF-99-11-180
Strempfer J.1; Brückel Th.; McIntyre G. J.2; Tasset F.2; Zeiske Th.; Burger K.3; Prandl W.3
1APS at ANL, Ames, USA
2ILL, Grenoble, France
3Universität, Institut für Kristallographie, Tübingen,
A reinvestigation of the field-induced magnetic form factor of chromium
Physica B 267 - 268, 56 - 59, 1999
23.89.1

IFF-99-11-181
Stunault A.1; de Bergevin F.2; Wermeille D.1; Vettier C.1; Brückel Th.; Bernhoeft N.1; McIntyre G. J.3; Henry J. Y.4
1ESRF, Grenoble, France
2CNRS, Laboratoire de Cristallographie, Grenoble, France
3ILL, Grenoble, France
4Centre d'Etudes Nucléaires, DRFMC/SPSMS/MDN, Grenoble, France
K-edge resonant x-ray magnetic scattering from RbMnF3
Physical Review B 60 14 10170 - 10179, 1999
23.89.1

IFF-99-11-182
Szot K.; Czyrska-Filemonowicz A.1; Wasilkowska A.1; Quadakkers W.J.2
1 Univ. of Mining and Metallurgy, Faculty of Metallurgy and Materials Science, Krakow, Poland
2 Institut for Materials in Energy Systems, FZJ
Microscopy (AFM, TEM, SEM) studies of oxide scale formation on FeCrAl based ODS alloys
Solid State Ionics 117 (1999) 13

IFF-99-11-183
Szot K.; Speier W.1
1Institut für Chemie und Dynamik der Geosphäre, FZJ
Surfaces of reduced and oxidized SrTiO3 from atomic force microscopy
Phys. Rev. B60 (1999) 5909
23.42.0

IFF-99-11-184
Szot K.; Waser R.; Meyer R.1
1 Institut für Werkstoffe der Elektrotechnik, RWTH Aachen
Restructuring the surface region of donor doped SrTiO3 single crystals under oxidizing conditions
Ferroelectrics 224 (1999) 323
23.42.0

IFF-99-11-185
Takeda T.1; Seto H.1; Kawabata Y.1; Okuhara D.1; Krist T.2; Zeyen C.M.E.3, Anderson I.S.3; Hoghoj P.3; Nagao M.4; Yoshizawa H.4; Komura S.5; Ebisawa T.6; Tasaki S.6; Monkenbusch M.
1Hiroshima University, Japan
2Hahn-Meitner-Institut, Berlin
3Institut Laue-Langevin, Grenoble
4University of Tokyo, Tokai, Japan
5Ochanomizu University, Ootsuka, Japan
6Kyoto University, Japan
Improvement of neutron spin echo spectrometer at C2-2 of JRR3M
Journal of Physics and Chemistry of Solids 60, 1599-1601, 1999
23.89.1

IFF-99-11-186
Volokitin, A.I.1; Persson, B.
1Samara University, Samara, Russia
Theory of Friction: Contribution from Fluctuating Electromagnetic Field
J. Phys. C, 11, 345-359, 1999
23.20.0

IFF-99-11-187
Waser R.
Modeling of Electroceramics - Applications and Prospects

Waser R.; Bolten D.1; Hoffmann M.1; Hasenkox U.1; Lohse O.1
1 Institut für Werkstoffe der Elektrotechnik, RWTH Aachen
Chemical solution deposition (CSD) and characterization of the solid solution series Ba(1-x)Pbx(Ti,Mn)O3
Ferroelectrics 225 (1999) 117
23.42.0

IFF-99-11-189
Waser R.; Bolten D.1; Lohse O.1; Grossmann M.1
1 Institut für Werkstoffe der Elektrotechnik, RWTH Aachen
Reversible and irreversible domain wall contributions to the polarization in ferroelectric thin films
Ferroelectrics 221 (1999) 251
23.42.0

IFF-99-11-190
Waser R.; Grossmann M.1; Lohse O.1; Bolten D.1; Hartner W.2; Schindler G.2; Nagel N.2; Dehm C.2
1 Institut für Werkstoffe der Elektrotechnik, RWTH Aachen
2 Infineon AG, München
Origin of imprint in ferroelectric CSD SrBi2Ta2O9 thin films
Mat. Res. Soc. Symp. Proc. 541 (1999 269
23.42.0

IFF-99-11-191
Waser R.; Hagenbeck R.1
1 Institut für Werkstoffe der Elektrotechnik, RWTH Aachen
Detailed temperature dependence of the space charge layer width at grain boundaries in acceptor-doped SrTiO3-ceramics
J. Europ. Ceram. Soc. 19 (1999) 683
23.42.0

IFF-99-11-192
Waser R.; Hasenkox U.1
1 Institut für Werkstoffe der Elektrotechnik, RWTH Aachen
Microstructure and properties of highly oriented PZT thin films on epitaxial ceramic electrodes prepared by CSD
Ferroelectrics 225 (1999) 107
23.42.0

IFF-99-11-193
Waser R.; Hasenkox U.1; Mitze C.1; Arons R.R.; Pommer J.1; Güntherodt G.
1 Institut für Werkstoffe der Elektrotechnik, RWTH Aachen
2 RWTH Aachen
J. Electroceramics 3 (1999) 255
23.42.0

IFF-99-11-194
Waser R.; Prume K.1; Leuerer T.1
1 Institut für Werkstoffe der Elektrotechnik, RWTH Aachen
3-dimensional FEM simulations of resonances in the impedance characteristics of ceramic multilayer capacitors
Ferroelectrics 224 (1999) 185
23.42.0

IFF-99-11-195
Westermann S.; Kreitschmann M.; Pyckhout-Hintzen W.; Richter D.; Straube E.1; Farage B.2; Goerigk G.
1Universität Halle-Wittenberg, Fachbereich Physik, Halle
2ILL, Grenoble, France
Matric Chain Deformation in Reinforced Networks: a SANS Approach
Macromolecules 32 18, 5793 - 5802, 1999
23.89.1

IFF-99-11-196
Westermann S.; Kreitschmann M.; Pyckhout-Hintzen W.; Richter D.; Straube E.1; Farago B.2; Goerigk G.
1Martin-Luther-Universität, Fachbereich Physik, Halle
2Institut Laue-Langevin, Grenoble
Matrix Chain Deformation in Reinforced Networks: A SANS approach
Macromolecules 32, 5793-5802, 1999
23.30.0

IFF-99-11-197
Wildberger K.; Korhonen T.; Zeller R.; Dederichs P.H.; Rampe A.1; Güntherodt G.1
1Physikalisches Institut, Technische Hochschule Aachen
Interface Reflectivity of Magnetic Layers in Cu: Effects of Adlayers
J. Magn. Magn. Mat. 198-199, 570 (1999)
23.20.0

IFF-99-11-198
Yan S.-S.; Schreiber R.; Voges F.; Osthöver C.; Grünberg P.
Oscillatory interlayer coupling in Fe/Mn/Fe trilayers
Phys. Rev. B 59, R11 641 (1999)
23.42.0

IFF-99-11-199
Yoshihara A.1; Wang Z.J.2; Takanashi K.2; Grünberg P.; Motokawa M.2; Fujimori H.2
1Faculty of Science and Engineering, Ishinomaki Senshu University, Japan
2Institute of Materials Research, Tohoku University, Japan
Spin wave modes in fine layered structures of Fe and Au
J. Magn. Soc. Japan 23, 161 (1999)
23.42.0

IFF-99-11-200
Zhang Y.; He D.F.; Wolters N.; Otto R.; Barthels K.; Zeng X.H.; Yi H.R.; Krause H.-J.; Braginski A.I.; Faley M.I.
Radio frequency bias current scheme for dc superconducting quantum interference device
IEEE Transactions on Appl. Supercond., Vol. 9, No. 2, 3813-3816 (1999).
23.42.0

IFF-99-11-201
Zorn R.
Applicability of distribution functions for the Havriliak-Negami spectral function
J.Polym.Sci.Bpolym.Phys. 37, 1043-1044, 1999
23.15.0

List of references

Abt R.	IFF-99-11-074
Allgaier J.	IFF-99-11-002 IFF-99-11-025 IFF-99-11-085 IFF-99-11-146
Allgaier J.	IFF-99-11-114
Ambaye, H.	IFF-99-11-003
Arons R.R.	IFF-99-11-193
Ballone P.	IFF-99-11-011
Ballone P.	IFF-99-11-012 IFF-99-11-117 IFF-99-11-126
Bechthold P.S.	IFF-99-11-136 IFF-99-11-137
Bihlmayer G.	IFF-99-11-008
Blügel S	IFF-99-11-075
Blügel S.	IFF-99-11-008 IFF-99-11-009 IFF-99-11-010 IFF-99-11-074
Bohn H.G.	IFF-99-11-014 IFF-99-11-158
Brener E.	IFF-99-11-016 IFF-99-11-017 IFF-99-11-018 IFF-99-11-019 IFF-99-11-020 IFF-99-11-021 IFF-99-11-052 IFF-99-11-177
Bringer A.	IFF-99-11-022
Brückel Th.	IFF-99-11-023 IFF-99-11-100 IFF-99-11-102 IFF-99-11-180 IFF-99-11-181
Buchenau U.	IFF-99-11-024 IFF-99-11-047 IFF-99-11-050 IFF-99-11-053 IFF-99-11-055 IFF-99-11-175
Bürgler D.E.	IFF-99-11-026
Carbone C.	IFF-99-11-143 IFF-99-11-156
Carsughi F.	IFF-99-11-027 IFF-99-11-030 IFF-99-11-033
Charton C.	IFF-99-11-156
Chen J.	IFF-99-11-030 IFF-99-11-031
Conrad H.	IFF-99-11-058
Crecelius G.	IFF-99-11-096
Dallmeyer A.	IFF-99-11-143
Dederichs P.H.	IFF-99-11-009 IFF-99-11-010 IFF-99-11-035 IFF-99-11-036 IFF-99-11-077 IFF-99-11-081 IFF-99-11-123 IFF-99-11-169 IFF-99-11-174 IFF-99-11-179 IFF-99-11-197
Derz H.	IFF-99-11-027
Divin Y.Y.	IFF-99-11-034
Domke C.	IFF-99-11-171 IFF-99-11-172 IFF-99-11-173
Eberhardt W.	IFF-99-11-001 IFF-99-11-048 IFF-99-11-049 IFF-99-11-107 IFF-99-11-110 IFF-99-11-111 IFF-99-11-113 IFF-99-11-119 IFF-99-11-136 IFF-99-11-137 IFF-99-11-143 IFF-99-11-153 IFF-99-11-156
Ebert Ph.	IFF-99-11-029 IFF-99-11-039 IFF-99-11-040 IFF-99-11-041 IFF-99-11-042 IFF-99-11-043 IFF-99-11-142 IFF-99-11-171 IFF-99-11-172 IFF-99-11-173

Jones R.	IFF-99-11-012	IFF-99-11-091	IFF-99-11-092
	IFF-99-11-117		
Jung P.	IFF-99-11-031	IFF-99-11-093	
Jungbluth H.	IFF-99-11-071		
Kahle S.	IFF-99-11-094		
Kann G.	IFF-99-11-049		
Karl A.	IFF-99-11-001	IFF-99-11-111	
Kehr, K.	IFF-99-11-003		
Kessler B.	IFF-99-11-119	IFF-99-11-153	
Kesternich W.	IFF-99-11-095	IFF-99-11-096	
Kienle D.	IFF-99-11-150		
Kirstein O.	IFF-99-11-097		
Klein H.	IFF-99-11-098		
Kluge F.	IFF-99-11-041	IFF-99-11-042	IFF-99-11-043
Kluge M.	IFF-99-11-056	IFF-99-11-057	
Kollmar A.	IFF-99-11-154		
Korhonen T.	IFF-99-11-197		
Koza, Z.	IFF-99-11-099		
Kreitschmann M.	IFF-99-11-195	IFF-99-11-196	
Kurz Ph.	IFF-99-11-008		
Köbler U.	IFF-99-11-100	IFF-99-11-101	IFF-99-11-102
	IFF-99-11-120		
Lei C.H.	IFF-99-11-103		
Liebsch A.	IFF-99-11-105	IFF-99-11-106	
Link S.	IFF-99-11-107		
Lustfeld H.	IFF-99-11-109		
Luysberg M.	IFF-99-11-066	IFF-99-11-067	IFF-99-11-082
Lüning J.	IFF-99-11-048	IFF-99-11-110	IFF-99-11-111
Maus M.	IFF-99-11-113		
Mika K.	IFF-99-11-072	IFF-99-11-073	
Monkenbusch M.	IFF-99-11-024	IFF-99-11-032	IFF-99-11-116
	IFF-99-11-118	IFF-99-11-146	IFF-99-11-147
	IFF-99-11-168	IFF-99-11-185	
Mono T.	IFF-99-11-014	IFF-99-11-158	
Montanari B.	IFF-99-11-012	IFF-99-11-117	
Morenzin J.	IFF-99-11-119	IFF-99-11-153	
Mueller R.	IFF-99-11-120		
Müller-Krumbhaar H.	IFF-99-11-020	IFF-99-11-052	IFF-99-11-121
	IFF-99-11-134	IFF-99-11-177	
Neeb M.	IFF-99-11-135	IFF-99-11-136	IFF-99-11-137
	IFF-99-11-145		
Nie X.	IFF-99-11-075		

Other publications

IFF-99-12-001
Ballone P.; Andreone W.1
1IBM Research Division, Zürich
Density Functional Theory and Car-Parrinello Molecular Dynamics for Metal Clusters
In Metal Clusters, Ed. W. Ekardt, pp. 71-144, Wiley, New York, 1999
23.20.0

IFF-99-12-002
Brückel Th.
Elastische Streuung an Vielteilchensystemen
Neutronenpraktikum 1999, Vorlesungen, Forschungszentrum Jülich, 4-1 - 4-19
23.89.1

IFF-99-12-003
Brückel Th.
Magnetische Streuung und Polarisationsanalyse
Neutronenpraktikum 1999, Vorlesungen, Forschungszentrum Jülich, 5-1 - 5-20
23.89.1

IFF-99-12-004
Brückel Th.; Kentzinger E.
Streumethoden zur Untersuchung von Dünnschichtsystemen
Vorlesungsmanuskripte des 30. IFF-Ferienkurses "Magnetische Schichtsysteme in Forschung und Anwendung" vom 1. bis 12.3.1999 (1999), Schriften des Forschungszentrums Jülich, Reihe Materie und Material/Matter and Materials Band 2, B3.1 - B3.48
23.89.1

IFF-99-12-005
Brückel Th.; Kentzinger E.
Streuung unter streifendem Einfall
Neutronenpraktikum 1999, Vorlesungen, Forschungszentrum Jülich, 7-1 - 7-17
23.89.1

IFF-99-12-006
Carlsson P.1; Zorn R.; Andersson D.1; Farago B.2; Richter D.; Torell L.M.1; Börjesson L.3; Jacobbson P.1
1Department of Experimental Physics, Chalmers University of Technology, Göteborg
2Institut Laue-Langevin, Grenoble
3Department of Applied Physics, Chalmers University of Technology, Göteborg
The segmental dynamics of a Polymer Electrolyte Investigated by Neutron Spin Echo Technique
AIP Conf. Proc. CP469; 607-614 1999
23.15.0

IFF-99-12-007
Carsughi F.; Fournier A.; Ullmaier H. (Eds.)
Proceedings of the 6th ESS General Meeting, Ancona, Italy, Sept. 20-23 (1999)
ESS-Report 99-99, 5 Volumes (Nov. 1999), ISSN 1433-559X
23.60.0

IFF-99-12-008
Chen J.; Jung P.
Effect of helium on radiation damage in a SiC/C Composite
Proc. 9th Cimtec-World Forum on News Materials, Symp. VII (Vincenzini, P. ed.) Techna Srl, 1999, p. 523
23.80.5

IFF-99-12-009
Conrad H.
Neutronenquellen - Von Radium-Beryllium zur Spallationsneutronenquelle -
Neutronenpraktikum 1999, Vorlesungen, Forschungszentrum Jülich, 2-1 - 2-16
23.89.1

IFF-99-12-010
Deister P.1; Rauh H.1;Ullmaier H.:
1TU Darmstadt
Hydrogen Concentrations Around Cracks in Target Materials for Spallation Neutron Sources
ESS Report 98-79 T, Nov. 1998
23.60.0

IFF-99-12-011
Dekorsy T.1; Hey R.1; Luysberg M.; Segschneider G.1
1 Institut für Halbleitertechnik II, RWTH Aachen
Ultraschnell durch Nanocluster - Grundlagen für die Terabit Optoelektronik
RWTH Themen - Berichte aus der RWTH Aachen 1/99, 44 (1999)
23.42.0

IFF-99-12-012
Eisebitt S.; Eberhardt W.
Band structure information and resonant inelastic soft X-ray scattering in broad band solids
J. Electron Spectrosc. on Rel. Phenomena 1999 (accepted)

IFF-99-12-013
Eisebitt S.; Wirth I.; Kann G.; Eberhardt W.
Statistical analysis of the electronic structure of single wall Carbon nanotubes in buckypaper
Electronic Properties of Novel Materials: Proceeding of the XIII International Workshop
p. 304, edited by H. Kuzmany et al., AIP Conference Proceedings 486, Melville, New York
Kirchberg, 1999
23.20.0

IFF-99-12-014
Fetters L.J.1; Wheeler L.M.1; Xenidou M.1; Richter D.
1Exxon Research and Engineering Co., Annandale, USA
Modification Potential for ShellvisTM Star Polymers
Company report; CR.17BU.99
23.30.0

IFF-99-12-015
Gaukel C.; Kluge M.; Schober H.
Diffusion Mechanisms in Under-Cooled Binary Liquids, Slow Dynamics in Complex Systems (M. Tokuyama and I. Oppenheim eds.)
AIP Conference Proceedings 469, 398 (1999)
23.15.0

IFF-99-12-016
Grünberg P.
Layered magnetic structures: Interlayer exchange coupling and giant magnetoresistance (review)
Springer Series in Surface Sciences, Vol. 37, 49 (1999) on Magnetic Multilayers and Giant Magnetoresistance, ed. by U. Hartmann
23.42.0

IFF-99-12-017
Haiml M.1; Siegner U.1; Morier-Genoud F.1; Keller U.1; Luysberg M.; Specht P.2; Weber E.R.2
1 Institute of Quantum Electronics, ETH Zürich
2 University of California, Berkeley/USA
Annealing of low-temperature grown semiconductors: Material optimization for ultrafast all-optical gating
Int. Conf. On Lasers and Electrooptics, Baltimore, CLEO'99 Technical Digest, OSA, Washington DC, (1999) p.197
23.42.0

IFF-99-12-018
Hill J. P.1; Kao C.-C.2; von Zimmermann M.1; Hämäläinen K.3; Huotari S.3; Berman L. E.2; Caliebe W.; Hirota K.4; Matsubara M.5; Kotani A.5; Peng J. L.6; Greene R. L.6; Tsukada I.7; Masuda T.7; Uchinokura K.7
1Brookhaven National Laboratory, Department of Physics, Upton, USA

2Brookhaven National Laboratory, National Synchrotron Light Source, Upton, USA
3University, Department of Physics, Helsinki, Finland
4Department of Physics, U. Tohoku, Sendai, Japan
5University, Institute for Solid State Physics, Tokyo, Japan
6University of Maryland, Center for Superconductivity Research, Department of Physics and Astronomy, USA
7Department of Applied Physics, U. Tokyo, Tokyo, Japan
Resonant Inelastic X-ray Scattering from Strongly Correlated Copper Oxides
Proceedings of the Second International Conference on Synchrotron Radiation in Materials Science (Kobe, 1998)
23.20.0

IFF-99-12-019
Houben L.; Luysberg M.; Carius R.; Hapke P.; Finger F.; Wagner H.
Limitations to homoepitaxial silicon growth in plasma-enhanced
chemical vapour deposition at low temperature
Proceedings of the XIth Conference on Microscopy of Semiconducting Materials, 22-25 March 1999, Oxford, Microscopy of Semiconducting Materials 1999, Inst. Phys. Conf. Ser. 164, 211 (1999)
23.42.0

IFF-99-12-020
Hupfeld D.; Caliebe W.; Reif Th.; Hulliger F.1
1ETH, Laboratorium für Festkörperphysik, Zürich, Switzerland
Determination of the magnetic structure of SmBi with resonance exchange scattering
HASYLAB Jahresbericht, 943 - 944, 1998
23.89.1

IFF-99-12-021
Leube W.; Marton K.; Schwahn D.; Richter D.; Fetters L.J.1; Wright P.; Symon C2; Vanhaeren G.3
1Exxon Research and Engineering Co., Annandale, USA
2Esso Center, Machelen, Belgium
Aggregation Behavior of Nucleating and Growth Arresting Fuel Additives
Company report; CR.5BU.99, 1999
23.30.0

IFF-99-12-022
Leube W.;Monkenbusch M.; Schneiders D.; Richter D.; Dounis P.2; Lovegrove R.2; Fetters L.J.3; Symon C.3
1Exxon Chemical Ltd., Milton Hill, Abbingdon, England
2Exxon Research and Engineering Co. Annandale, USA
Wax-Crystal Modification in Fuel Oil by Self-Aggregation Partially Crystallizable Hydrocarbon Blockcopolymers
Exxon Company, CR.1A.99, 1999
23.30.0

IFF-99-12-023
Luysberg M.; Specht P.1; Thul K.; Liliental-Weber Z.1; Weber E.R.1
1 University of California, Berkeley/USA
Change of electrical and structural properties of non-stoichiometric GaAs through Be doping
IEEE conference on semiconducting and insulating materials SIMC X, Berkeley, CA 1998, eds. Z. Liliental-Weber, C. Miner, (1999), p. 87
23.42.0

IFF-99-12-024
Luysberg M.; Specht P.1; Weber E.R.1
1 University of California, Berkeley/USA
Limitations to epitaxial growth of low-temperature grown GaAs
Proc of the 2nd Symposium on non-stoichiometric III-V compounds, Erlangen (1999) in: Physik mikrostrukturierter Halbleiter Vol 10 ed.: T. Marek, S. Malzer, and P. Kiesel, Verlag: Lehrstuhl für Mikrocharakterisierung, Universität Erlangen 1999 p.97
23.42.0

IFF-99-12-025
Luysberg M.; Specht P.1; Weber E.R.1
1 University of California, Berkeley/USA
Mechanisms of the formation of structural defects during low temperature growth of GaAs
Proceedings of the XIth Conference on Microscopy of Semiconducting Materials, 22-25 March 1999, Oxford, Microscopy of Semiconducting Materials 1999, Inst. Phys. Conf. Ser. 164, 279 (1999)
23.42.0

IFF-99-12-026
Mantl S.1; Kappius L.1; Antons A.1; Löken M.1; Klinkhammer F.1; Dolle M.1; Zhao Q.T.1; Mesters S.1; Buchal Ch.1; Bay H.L.1; Kabius B.1; Trinkaus H.; Heinig H.2
1Institut für Schicht- und Ionentechnik, FZ Jülich
2Institut für Ionenstrahlphysi und Materialforschung, Forschungszentrum Rossendorf
Growth, Patterning and Microelectronic Applications of Epitaxial Cobaltdisilicide
MRS Proceedings 507 (1998)
23.42.0

IFF-99-12-027
Prager M.; Schiebel P.1; Johnson M.2
1Institut für Kristallographie, Universität Tübingen
2Institut Laue-Langevin, Grenoble
Deuteration induced Phase Transition in an Ammonium Perovskite
DIM-Newsletter 12, 10, 1999
23.15.0

IFF-99-12-028
Richter D.
Poylmer Dynamics by Neutron Spin Echo Spectroscopy
"Scattering in Polymeric and Colloidal Systems"
Ed by Wyn Brown and Kell Mortenson, Gordon and Breach, London, 1999
23.30.0

IFF-99-12-029
Richter D.; Monkenbusch M.; Farago B.1; Schleger P.1; Montes H.2
1Institut Laue-Langevin, Grenoble
2ESPCI, Laboratoire PCSM, France
Large scale motions in dense polymer systems
AIP Conference Proceedings, Vol.469, 587-598, 1999
23.30.0

IFF-99-12-030
Rosov N.1; Rathgeber S.1; Monkenbusch M.
1NIST Center for Neutron Research, Gaithersburg, USA
Neutron Spin Echo Spectroscopy at the NIST Center for Neutron Research
American Chemical Society Books Department, Symposium Series No. 739, Chapter 7
ISBN: 0-84112-3644-5
23.30.0

IFF-99-12-031
Schlebusch C.; Morenzin J.; Kessler B.; Eberhardt W.
Charge transfer and relaxation dynamics of excited electronic states in organic photoreceptor materials with and without C60
Electronic Properties of Novel Materials: Proceeding of the XIII International Workshop
p. 487 , edited by H. Kuzmany et al., AIP Conference Proceedings 486, Melville, New York
Kirchberg, 1999
23.20.0

IFF-99-12-032
Schleger P.1; Ehlers G.2; Kollmar A.; Alefeld B.; Barthelomy J.F.1; Casalta H.1; Farago B.1; Giraud P.1; Hayes C.1; Lartigue C.3; Mezei F.2; Richter D.
1Institut Laue-Langevin, Grenoble
2Hahn-Meitner Institut, Berlin
3Laboratoire de Spectrométrie, France

The sub-neV resolution NSE spectrometer IN15 at the Institut Laue-Langevin
Elsevier Preprint 09.09.1998
23.30.0

IFF-99-12-033
Schober H.
Molecular dynamics in amorphous solids and liquids
Physics of Glasses (P. Jund and R. Jullien eds.) p.191, AIP Conference Proceedings 489, 1999
23.15.0

IFF-99-12-034
Schweika W.
Schichtpräparation mit Sputterverfahren
Vorlesungsmanuskripte des 30. IFF-Ferienkurses "Magnetische Schichtsysteme in Forschung und Anwendung" vom 1. bis 12.3.1999 (1999), Schriften des Forschungszentrums Jülich, Reihe Materie und Material/Matter and Materials Band 2, A5.1 - A5.21
23.89.1

IFF-99-12-035
Schütz, G.M.
Rezension von Non-equilibrium Statistical Mechanics in One Dimension
V. Privman (ed.) (Cambridge University Press, Cambridge, 1997), in Contemporary Physics 40 (1999),159

IFF-99-12-036
Schütz, G.M.
Stochastic many-body systems and quantum spin chains
Proc. of the II Brazilian Probability School, Barra do Sahy 1998, Resenhas 4, 17-43 (1999)

IFF-99-12-037
Seto H.1; Kato T.2; Monkenbusch M.; Takeda T.1; Komura S.3
1Hiroshima University, Japan
2Metropolitan University, Japan
3Ochanomizu University, Japan
A Neutron Spin Echo Study of Network of Wormlike Micelles
8th Tohwa University International Symposium edited by Michio Tokuyama and Irwin Oppenheim
The American Institute of Physics 1-56396-811, 1999
23.30.0

IFF-99-12-038
Specht P.1; Lutz R.C.1; Zhao R.1; Weber E.R.1; Liu W.K.2; Bacher K.2; Towner F.J.2; Stewart T.R.2; Luysberg M.
1 University of California, Berkeley/USA
2 Quantum Epitaxial Designs Inc., Bethlehem/USA
Improvemente of MBE-grown LT-GaAs through p-doping with Be and C
J. Vac. Sci. Technol. B 17 1200 (1999)

IFF-99-12-039
Turek I.1; Kudrnovsk J.1; Blügel S.
1Institute of Physics of Materials, AS CR, CZ-61662 Brno
2Institute of Physics, AS CR, CZ-18040 Praha
Surface magnetism of disordered alloys
Acta Physics Slovaca Vol. 48, 1 (1999)
23.20.0

IFF-99-12-040
Urban K.
Die Physik - die Leitwissenschaft des Jahrhunderts
Leitartikel (ganzseitig) in Natur & Wissenschaft der Frankfurter Allgemeinen Zeitung zum Millenium (29.12.99), gleichzeitig Abschluß der Serie Physik im Wandel (April bis Dezember 1999) in der FAZ (Herausgegeber und Koordinator: K. Urban)
23.42.0

IFF-99-12-041
Urban K.
Die multidisziplinäre Welt der Information.
Artikel in dem Buch: Unsere Welten der Information (Herausgeber: D. Ganten, K. Urban et al. ; Gesellschaft Deutscher Naturforscher und Ärzte, S. Hirzel-Verlag, 1999)
23.42.0

IFF-99-12-042
Urban K.; Feuerbacher M.; Wollgarten M.; Bartsch M.1 und Messerschmidt U.1
1 Max-Planck-Institut für Mikrostrukturphysik, Weinberg 2, 06120 Halle/Saale,
Germany
Eingeladener Buchbeitrag: Kapitel 11: Mechanical Properties of Quasicrystals
in: Physical Properties of Quasicrystals, Z.M. Stadnik (Ed.) Solid-State Sciences, Springer-Verlag (1999) pp. 361-401
23.55.0

IFF-99-12-043
Zeiske Th.
Magnetismus und magnetische Neutronenstreuung
Neutronenpraktikum 1999, Vorlesungen, Forschungszentrum Jülich, 17-1 - 17-17
23.89.1

List of references

Alefeld B.	IFF-99-12-032
Ballone P.	IFF-99-12-001
Blügel S.	IFF-99-12-039
Brückel Th.	IFF-99-12-002 IFF-99-12-003 IFF-99-12-004 IFF-99-12-005
Caliebe W.	IFF-99-12-018 IFF-99-12-020
Carsughi F.	IFF-99-12-007
Chen J.	IFF-99-12-008
Conrad H.	IFF-99-12-009
Eberhardt W.	IFF-99-12-012 IFF-99-12-031
Eberhardt W.	IFF-99-12-013
Eisebitt S.	IFF-99-12-012 IFF-99-12-013
Feuerbacher M.	IFF-99-12-042
Fournier A.	IFF-99-12-007
Gaukel C.	IFF-99-12-015
Grünberg P.	IFF-99-12-016
Hupfeld D.	IFF-99-12-020
Jung P.	IFF-99-12-008
Kann G.	IFF-99-12-013
Kentzinger E.	IFF-99-12-004 IFF-99-12-005
Kessler B.	IFF-99-12-031
Kluge M.	IFF-99-12-015
Kollmar A.	IFF-99-12-032
Leube W.	IFF-99-12-021 IFF-99-12-022
Luysberg M.	IFF-99-12-011 IFF-99-12-017 IFF-99-12-019 IFF-99-12-023 IFF-99-12-024 IFF-99-12-025 IFF-99-12-038
Marton K.	IFF-99-12-021
Monkenbusch M.	IFF-99-12-022 IFF-99-12-029 IFF-99-12-030 IFF-99-12-037
Morenzin J.	IFF-99-12-031
Prager M.	IFF-99-12-027
Reif Th.	IFF-99-12-020
Richter D.	IFF-99-12-006 IFF-99-12-014 IFF-99-12-022 IFF-99-12-021 IFF-99-12-028 IFF-99-12-029 IFF-99-12-032
Schlebusch C.	IFF-99-12-031
Schneiders D.	IFF-99-12-022
Schober H.	IFF-99-12-015 IFF-99-12-033
Schwahn D.	IFF-99-12-021
Schweika W.	IFF-99-12-034

Schütz, G.M.	IFF-99-12-035	IFF-99-12-036	
Trinkaus H.	IFF-99-12-026		
Ullmaier H.	IFF-99-12-007	IFF-99-12-010	
Urban K.	IFF-99-12-040	IFF-99-12-041	IFF-99-12-042
Wirth I.	IFF-99-12-013		
Wollgarten M.	IFF-99-12-042		
Zeiske Th.	IFF-99-12-043		
Zorn R.	IFF-99-12-006		

Invited talks

IFF-99-21-001
Alefeld B.
Focusing Neutron Reflectometer
Schloß Ringberg, "New Concepts in Neutron Reflectometry", 04. - 06.10.1999
23.89.1

IFF-99-21-002
Alefeld B.
GaAs, a new Crystal for Neutron-Backscattering
Vienna, Austria, PECNO TMR-Mid-Term Review Meeting, 04. - 06.03.1999
23.42.0

IFF-99-21-003
Alefeld B.
Space technology from x-ray telescopes for focusing neutron small angle scattering and neutron reflectometry
Budapest, Hungary, ECNS '99 Conference, 01. - 04.09.1999
23.89.1

IFF-99-21-004
Blügel S.
Von der Quantentheorie der Elektronen zu neuen Nanomaterialien
Kolloquiumsvortrag vor der Fakultät Physik, Martin Luther Universität, Halle/Saale
05.06.1999
3.20.0

IFF-99-21-005
Blügel S.
Von der Quantentheorie der Elektronen zu neuen Nanomaterialien
Kolloquiumsvortrag vor der Fakultät Physik, RWTH Aachen
13.12.1999
3.20.0

IFF-99-21-006
Blügel S.
Von der Quantentheorie der Elektronen zu neuen Nanomaterialien
Kolloquiumsvortrag vor der Fakultät Physik, Universität Bremen
15.06.1999
3.20.0

IFF-99-21-007
Blügel S.
Von der Quantentheorie der Elektronen zu neuen Nanomaterialien
Kolloquiumsvortrag vor der Fakultät Physik, Universität Düsseldorf
04.11.1999
3.20.0

IFF-99-21-008
Blügel S.
Von der Quantentheorie der Elektronen zu neuen Nanomaterialien
Seminar TU-Clausthal-Zellerfeld
03.05.1999
3.20.0

IFF-99-21-009
Brener E.
Instabilities in cracks
University Grenoble, Frankreich, 01.04.1999
23.15.0

IFF-99-21-010
Brener E.
Instabilities in cracks
Universität Montpellier, Frankreich, 20.09.1999
23.15.0

IFF-99-21-011
Brener E.
Pattern formation in diffusional growth
Universität Kiel, 29.10.1999
23.15.0

IFF-99-21-012
Brückel Th.
Investigation of Spinstructures with Synchrotron Radiation
Bad Honnef, Physikzentrum, 211. WE-Heraeus-Seminar, 04. - 06.01.1999
23.89.1

IFF-99-21-013
Brückel Th.
Komplementarität von Neutronen- und Synchrotron-Röntgenstreuung in der Festkörperforschung
Dresden, Technische Universität, Fakultät Mathematik und Naturwissenschaften, Physikalisches Kolloquium, 12.01.1999
23.89.1

IFF-99-21-014
Brückel Th.
Komplementäre Anwendung von Neutronen- und Synchrotronröntgenstreuung bei Untersuchungen des Festkörpermagnetismus
Aachen, RWTH, Physikalisches Kolloquium, 26.04.1999
23.89.1

IFF-99-21-015
Brückel Th.
Magnetic Scattering: Synchrotron X-rays versus Neutrons
Berlin, HMI, Workshop on "Magnetism with Synchrotron Radiation and Neutrons, 22.11.1999
23.89.1

IFF-99-21-016
Bürgler D.E.
Control of magnetic interlayer coupling on the nanometer scale: Morphology and fermiology
UMBRELLA Symposium, TH Aachen
08.11.1999
3.42.0

IFF-99-21-017
Bürgler D.E.
Magnetische Zwischenschichtkopplung: Effekte der Grenzflächen und Fermioberflächen
RWTH Aachen
13.12.1999
3.42.0

IFF-99-21-018
Caliebe W.
Scattering Methods to Study Magnetism in EuO
Brookhaven, USA, NSLS, Seminar, 11.01.1999
23.20.0, 23.89.1

IFF-99-21-019
Conrad H.
Die Europäische Spallationsquelle ESS - eine Neutronenquelle für das 21. Jahrhundert
Potsdam, Deutsche Neutronenstreutagung, 26.05.1999
23.60.0

IFF-99-21-020
Conrad H.
Experimental and computational studies of pressure waves in the ASTE mercury target
Oak Ridge, USA, International Workshop on Mercury Target Development for Pulsed Spallation Neutron Sources, 08. - 12.11.1999
23.60.0

IFF-99-21-021
Conrad H.

Moderator Development for ESS
Oak Ridge, USA, International Workshop on Mercury Target Development for Pulsed Spallation Neutron Sources, 10.11.1999
23.60.0

IFF-99-21-022
Conrad H.
Pressure waves in the ASTE mercury target
Ancona, Italy, 6th General ESS Meeting, 23.09.1999
23.60.0

IFF-99-21-023
Conrad H.
Stress and Pressure Waves in Solid and Liquid Metal Targets Induced by High Power Pulsed Electron and Proton Beams
Santa Fe, USA, 3rd International Conference on Spallation Materials Technology, 03.05.1999
23.60.0

IFF-99-21-024
Conrad H.; Ullmaier H.
Overview of the ESS Target Research and Development
Oak Ridge, USA, International Workshop on Mercury Target Development for Pulsed Spallation Neutron Sources, 08.11.1999
23.60.0

IFF-99-21-025
Dederichs P.H.
Ab-initio Study of Magnetic Adatoms and Small Clusters on Surfaces
Int. Conference on Clusters and Nanostructure Interfaces, Richmond, VA, USA, 27.10.1999
23.20.0

IFF-99-21-026
Dederichs P.H.
Conceptional Improvementrs of the KKR Method for Electronic Structure Calculations
Seminar, Oak Ridge National Laboratory, USA, 19.03.1999
23.20.0

IFF-99-21-027
Dederichs P.H.
Elektronische und magnetische Eigenschaften von Adsorbatatomen auf Oberflächen
Kolloquium, Hahn Meitner Institut, Berlin, 01.02.1999
23.20.0

IFF-99-21-028
Dederichs P.H.
Forces and Lattice Relaxations in Dilute Alloys
APS-March Meeting, Atlanta, USA, 22.03.1999
23.20.0

IFF-99-21-029
Dederichs P.H.
Komplexe Bandstruktur und Tunneln in Ferromagnet/Isolator/Ferromagnet Schichten
Universität Halle, 04.11.1999
23.20.0

IFF-99-21-030
Dederichs P.H.
Magnetic Adatoms and Small Clusters on Surfaces
Kolloquium Physics Department, Moscow State University, Moskau, 19.01.1999
23.20.0

IFF-99-21-031
Dederichs P.H.
Magnetic Adatoms and Small Clusters on Surfaces
Symposium on Multilayers and Nanostructures, Univ. Bielefeld, 17.04.1999
23.20.0

IFF-99-21-032
Dederichs P.H.
Magnetismus von Adatomen und kleinen Clustern auf Oberflächen
Physikalisches Kolloquium, Univ. Gesamthochschule Duisburg, 26.04.1999
23.20.0

IFF-99-21-033
Dederichs P.H.
Proposal for a RT-Network "Computational Magnetoelectronics"
TMR-Workshop "5th Framework", Orsay, Paris, 30.04.1999
23.20.0

IFF-99-21-034
Dürr H.
Soft X-ray magnetic spectroscopy
SR Satellite to the 18th IUCr General Assembly and Congress Daresbury Lab., Warrington
03.08.1999
3.20.0

IFF-99-21-035
Eberhardt W.
Coherent soft x-ray scattering from random surfaces
Evaluation Session, MPT-Projekte im Rahmen der deutsch-kanadischen WTZ
Laser-Lab. Göttingen
27.01.1999
3.20.0

IFF-99-21-036
Eberhardt W.
F-Sek Dynamik von Festkörpern und Clustern
ETH Zürich
21.01.1999
3.20.0

IFF-99-21-037
Eberhardt W.
F-sek Dynamik von Festkörpern und Clustern
Festkörperphysik-Kolloquium, FU Berlin
12.11.1999
3.20.0

IFF-99-21-038
Eberhardt W.
Femtosecond electronic relaxation processes in clusters and solids
Ringberg Symposium " Ultrafast Surface Dynamics"
30.03.1999
3.20.0

IFF-99-21-039
Eberhardt W.
IBM Research Almaden
F-sec dynamics of magnetic thin films and photoconductor systems
19.02.1999
3.20.0

IFF-99-21-040
Eberhardt W.
MAX-lab Lund
Opportunities for experiments using thetTime structure and Coherence of the VUV
25.09.1999
3.20.0

IFF-99-21-041
Eberhardt W.
Opportunities for Experiments Using the Time Structure and Coherence of the VUV, FEL at DESY
21st International Free Electron Laser Conference and 6th FEL Application Workshop, Hamburg
27.08.1999

3.20.0

IFF-99-21-042
Eberhardt W.
Scattering experiments with coherent soft X-ray photons
VUV FEL User Workshop, Hamburg
12.03.1999
3.20.0

IFF-99-21-043
Eberhardt W.
Soft X-ray emission and scattering from solids
17.09.1999
tanford Univesity
23.20.0

IFF-99-21-044
Eberhardt W.
Soft X-ray emission and scattering from solids
Seminarvortrag im MPI Stuttgart
07.05.1999
3.20.0

IFF-99-21-045
Ebert Ph.
Defects on semiconductors surfaces.
Seminar at the Physics Department, Prof. Dr. F. Himpsel, University of Wisconsin, Madison, Wisconsin, U.S.A., October 29, 1999
23.55.0

IFF-99-21-046
Ehrhart P.
Deposition of electroceramic thin films by MOCVD
16th Umbrella Symposium, Aachen, 08.-12.11.1999
23.42.0

IFF-99-21-047
Eisebitt S.
Resonant inelastic soft x-ray scattering: Investigating electronic structure
2nd International SLS Workshop on Synchrotron Radiation Brunnen, CH
27.10.1999
3.20.0

IFF-99-21-048
Eisebitt S.
Soft x-ray emission on solids
SSG Lecture Series at the Advanced Light Source, Berkeley, USA
18.11.1999
3.20.0

IFF-99-21-049
Eisebitt S.
Weichröntgen-Emissions-Spektroskopie an nanostrukturierten Halbleitern
Universität Bonn
15.01.1999
3.20.0

IFF-99-21-050
Eisenriegler E.
Colloids in polymer solution
Klausurtagung des SFB 513 "Nanostrukturen an Grenzflächen", 14.10.1999, Tschagguns, Austria
23.30.0

IFF-99-21-051
Eisenriegler E.
Polymers interacting with colloids
International Conference on Liquid Matter, 03-07.07.1999, Granada
23.30.0

IFF-99-21-052
Goerigk G.
Materialforschung mit Anomaler Dispersion
Geesthacht, GKSS, Informationsveranstaltung zur Synchrotronstrahlung mit Ausblick auf TESLA, 08.09.1999
23.89.1

IFF-99-21-053
Goerigk G.
Materialuntersuchungen mit anomaler Röntgen-Kleinwinkelstreuung
Karlsruhe, Universität, Polymer-Institut, 18.11.1999
23.89.1

IFF-99-21-054
Gompper, G.
Soft Matter: Amphiphile, Membranen, Mikroemulsionen
Institut für Computeranwendungen 1, Universität Stuttgart.,
13.12.1999

IFF-99-21-055
Gompper, G.
Statistische Physik von Membranen und Vesikeln: Schmelzen, Ondulationen, Topologie-Fluktuationen",
RWTH Aachen, 21.06.1999

IFF-99-21-056
Grünberg P.
Layered magnetic structures in research and application
Argonne National Labs, USA
29.03.1999
3.42.0

IFF-99-21-057
Grünberg P.
Magnetische Multilagen in Forschung und Anwendung
Physikalisches Kolloquium, Universität Düsseldorf
04.02.1999
3.42.0

IFF-99-21-058
Grünberg P.
Magnetische Multilagen in Forschung und Anwendung
Workshop on Multilayers and Nanostructures, Universität Bielefeld
09.06.1999
3.42.0

IFF-99-21-059
Grünberg P.
Magnetische Schichtstrukturen in Forschung und Anwendung
Fraunhofer Institut Duisburg
09.06.1999
3.42.0

IFF-99-21-060
Grünberg P.
Magnetische Schichtstrukturen in Forschung und Anwendung
IBM Mainz
26.04.1999
3.42.0

IFF-99-21-061
Grünberg P.
Magnetische Schichtstrukturen in Forschung und Anwendung
Stiftung Cäsar, Bonn
19.10.1999
3.42.0

IFF-99-21-062
Grünberg P.
Magnetische Schichtsysteme in Forschung und Anwendung
FZ Kolloquium
22.01.1999
3.42.0

IFF-99-21-063
Grünberg P.

Magnetoelectronics in research and application
UMBRELLA Symposium, TH Aachen
09.11.1999
3.42.0

IFF-99-21-064
Grünberg P.
Magnetoelektronik in Forschung und Anwendung
Max-von-Laue-Kolloquium, Berlin
25.12.1999
3.42.0

IFF-99-21-065
Grünberg P.
Magnetoelektronik in Forschung und Anwendung
Physikalisches Kolloquium, Gesamthochschule Essen
20.10.1999

IFF-99-21-066
Grünberg P.
Magnetoelektronik in Forschung und Anwendung
Physikalisches Kolloquium, Ruhr Universität Bochum
08.11.1999
3.42.0

IFF-99-21-067
Grünberg P.
Magnetoelektronik in Forschung und Anwendung
Physikalisches Kolloquium, Universität Mainz
26.10.1999
3.20.0

IFF-99-21-068
Grünberg P.
The GMR effect in research and application
225. WE-Heraeus Seminar, Bad Honnef
13.08.1999
3.20.0

IFF-99-21-069
Grünberg P.
The history of layered magnetic structures
American Physical Society,
Centennial Meeting, Atlanta, Georgia
22.03.1999
3.42.0

IFF-99-21-070
Grünberg P.
Zwischenschicht-Austauschkopplung in Forschung und Anwendung
15. Sitzung des Arbeitskreises "Magnetische Schichten für technische Anwendungen"
Institut für Mikrostrukturtechnologie und Optoelektronik, Wetzlar
18.06.1999
3.20.0

IFF-99-21-071
Harris J.
The Seven Pillars of Wisdom: How shall we construct the house?
Materials Modelling Laboratory Workshop, 03.09.1999, University of Oxford
23.20.0

IFF-99-21-072
Hartner W.1; Schindler G.1; Weinreich V.1; Ahlstedt M.1; Schroeder H.; Waser R.; Dehm C.1; Mazuré C.1
1Siemens AG, München, Germany
Influence of dry etching using argon on structural and electrical properties of crystalline and non-crystalline SrBi2Ta2O9 thin films
11th Int. Symp. On Integrated Ferroelectrics (ISIF), 1999, Colorado Springs (USA), 07.-10.03.1999
23.42.0

IFF-99-21-073
Heinze S.; Abt R.; Blügel S.
Interpretation von STM-Bildern von Übergangsmetallstrukturen auf der Basis der Elektronentheorie
Seminarvortrag am Institut für Oberflächenphysik und Atomstoßprozesse, Humboldt Universität Berlin
03.05.1999
3.20.0

IFF-99-21-074
Hoffmann S.
Leakage current and resistance degradation of doped (Ba,Sr)TiO3 thin films
School of Conduction and Breakdown, Chateaux d'Oex, 28.02.-02.03.1999
23.42.0

IFF-99-21-075
Hoffmann S.; Grossmann M.1; Waser R.
1 IWE, RWTH Aachen, Germany
Leakage current and resistance degradation behavior of doped (Ba1-xSrx)TiO3 thin films for DRAM applications
11th Int. Symp. Integrated Ferroelectrics, Colorado Springs, Colorado, USA, 07.03.-10.03.1999
23.42.0

IFF-99-21-076
Hoffmann S.; Waser R.
High permittivity dielectrics: from bulk ceramics to thin films
41th Electronic Materials Conference (EMC), Santa Barbara, California, 30.06.-02.07.1999
23.42.0

IFF-99-21-077
Jones R.
Dichtefunktional mit Molekulardynamik - Neue Anwendungen, neue Perspektiven
Graduierter Kolleg der Universität Regensburg, 22.07.1999
23.20.0

IFF-99-21-078
Jones R.
Structure, energies, and reactions in model polycarbonates
Tagung Arbeitsgruppe Parrinello, 19.01.1999, Schloss Ringberg
23.20.0

IFF-99-21-079
Jung P.
Helium in Nuclear Material
Vortrag am National Institute of Metals, 18.2.1999, Tsukuba, Japan
23.80.5

IFF-99-21-080
Kahle S.
Suszeptibilitätsuntersuchungen in der Crossover Region des dynamischen Glasübergangs von Benzoin isobutylether - eine Kooperativitätsanalyse
Soft Condensed Matter Seminar des SFB in Halle am 14.01.99
23.15.0

IFF-99-21-081
Kahle S.
Vergleich zwischen inkohärenter Neutronenstreuung und dielektrischer Spektroskopie am Polyvinylacetat
Glasübergangstreffen in Rostock am 13.12.99
23.30.0

IFF-99-21-082
Kehr, K.
Toy Model for Molecular Motors
Theoretische Physik, Ludwig-Maximilian-Universitaet, München
5. 3. 1999

IFF-99-21-083
Klingeler R.
Mass spectra of metal-doped carbon and fullerene clusters Mx@Cn<120 (M = Sc, Y, La, Ca, Ce; x = 1,2)
A. German-French Seminar, Nanotubes and Fullerenes - Recent Advances and Future Trends
IFW Dresden
25.09.1999
3.20.0

IFF-99-21-084
Kurz Ph.; Blügel S.
Nichtkolinearer Magnetismus in der FLAPW-Methode
Seminarvortrag am Zentrum füer Mikrostrukturforschung, Universität Hamburg
04.02.1999
3.20.0

IFF-99-21-085
Köbler U.
Die Austauschwechselwirkungen 4. Ordnung in reinen Spinsystemen
Dresden, Technische Universität, 07.12.1999
23.15.0

IFF-99-21-086
Köbler U.
Die Bedeutung der Austauschwechselwirkungen 4. Ordnung in Materialien mit reinem Spinmagnetismus
Aachen, RWTH, 18.06.1999
23.15.0

IFF-99-21-087
Köbler U.
Kritisches magnetisches Verhalten für halb- und ganzzahlige Spinquantenzahl
Dresden, Technische Universität, 06.12.1999
23.15.0

IFF-99-21-088
Lentzen M.; Thust A.; Chen J.H.; Urban K.
Auf dem Weg zur Sub-Angström-Mikroskopie: Materialwissenschaftliche Anwendung aberrationskorrigierter Elektronenmikroskopie
WE-Heraeus-Ferienkurs über "Moderne Fernfeld- und Nahfeld-Mirkoskopien, 20.09.-01.10.1999, Chemnitz
23.42.0

IFF-99-21-089
Lentzen M.; Thust A.; Chen J.H.; Urban K.
Contrast transfer of a Cs-corrected microscope
International Workshop on "Prospects and Future Needs of High-Resolution Electron Microscopy, Schloß Ringberg, 21.-24.07.1999
23.42.0

IFF-99-21-090
Liebsch A,
Linear and nonlinear time dependent response of metal surfaces
Workshop on Time Dependent Density Functional Theory, 15.04.1999, Institute of Theoretical Physics, Santa Barbara, USA
23.20.0

IFF-99-21-091
Liebsch A.
Electronic Excitations at Metals Surfaces
07.09.1999, Academy of Sciences, Prag
3.20.0

IFF-99-21-092
Liebsch A.
Elektronische Anregungen an Metalloberflächen: von der Reibung zur nichtlinearen Optik
04.05.1999, RWTH Aachen
3.20.0

IFF-99-21-093
Liebsch A.
Elektronische Anregungen an Metalloberflächen: von der Reibung zur nichtlinearen Optik
09.12.1999, Universität Würzburg
3.20.0

IFF-99-21-094
Liebsch A.
Elektronische Anregungen an Metalloberflächen: von der Reibung zur nichtlinearen Optik
19.05.1999, TU München
3.20.0

IFF-99-21-095
Liebsch A.; Liechtenstein A.1
1University of Nijmegen
Photoemission quasi-particle spectra of Sr2RuO4
Symposium on Surface Physics, 28.06-02.07.1999, Trest, Czech Repubic
23.20.0

IFF-99-21-096
Lustfeld H.
Reaktionsgleichungen in der Atmosphärenchemie und Groebner Basen
19.01.1999, Universität Passau
3.15.0

IFF-99-21-097
Luysberg M.
Influence of Defects in non-stoichiometric GaAs on the electrical and optical properties
Paul-Drude-Institut Berlin, Januar 1999
Eigenschaften von p-dotiertem Low-Temperature GaAs
Universität Karlsruhe, Januar 1999
23.42.0

IFF-99-21-098
Luysberg M.
Wachstum von GaAs bei niedrigen Temperaturen:Konsequenzen fuer die strukturellen und elektrischen Eigenschaften
Universität Bremen, März 1999
23.42.0

IFF-99-21-099
Monkenbusch M.; Richter D.; Montes H.1
1ESPCI, Physic-Chimie Structurale et Macromoleculaire, Paris, France
Neutron Spin Echo Spectroscopy on large scale motions in dense polymer systems - recent advances
3rd International Symposium (IUPAC) in Saint-Petersburg vom 07.06.-10.06.99
23.30.0

IFF-99-21-100
Monkenbusch M.; Schneiders D.; Richter D.; Willner L.; Leube W.; Fetters L.J.1; Huang J.S.1; Lin M.1
1EXXON, Research and Engineering Company, Annandale, USA
Aggregation Behaviour of PE-PEP Copolymers and Winterization of Diesel Fuels
2nd European Conference on Neutron Scattering in Budapest vom 01.09.-04.09.99
23.30.0

IFF-99-21-101
Montes H.1; Monkenbusch M.; Willner L.; Rathgeber S.2; Fetters L.J.3; Richter D.
1ESPCI, Physic-Chimie Structurale et Macromoleculaire, Paris, France
2EXXON, Research and Engineering Company, Annandale, USA

Neutronenspinechospektroskopie: Dynamik von Einzelketten und Konzentrationsfluktuationen in BlockKopolymeren
Deutsche Neutronenstreutagung in Potsdam vom 25.05.-27.05.99
23.30.0

IFF-99-21-102
Müller-Krumbhaar H.
Morphology diagram of diffusional growth
Seminar, DLR Porz, 27.10.1999
23.15.0

IFF-99-21-103
Müller-Krumbhaar H.
Strukturbildung an bewegten Phasengrenzflächen
Mathematisches Kolloquium, Universität Freiburg, 16.02.1999
23.15.0

IFF-99-21-104
Müller-Krumbhaar H.
Strukturbildung bei diffusionsbedingtem Wachstum
Physik-Workshop, Universität Kiel, Sehlendorf, 21.09.1999
23.15.0

IFF-99-21-105
Müller-Krumbhaar H.
Wie wächst ein Keim?
Kolloquium, Institut für Physik, Universität Göttingen, 25.10.99
23.15.0

IFF-99-21-106
Müller-Krumbhaar H.
Wie wächst ein Keim?
Kolloquium, Physikalische Chemie, TU Hannover, 17.03.1999
23.15.0

IFF-99-21-107
Neeb M.
Photoelectron spectroscopy on mass-selected clusters using VUV-lasers
VUV FEL User Workshop, Hamburg
11.03.199
3.20.0

IFF-99-21-108
Persson B.
Brittle Fracture
International Meeting on the Dynamics of Fracture, 25-27.10.1999, Austin, USA
23.20.0

IFF-99-21-109
Persson B.
Dynamical processes at surfaces
XIV International School Seminar "Spectroscopy of Molecules and Crystals", 7-12.06.1999, Odessa, Ukraine
23.20.0

IFF-99-21-110
Persson B.
Sliding Friction
Annual Meeting on Condensed Matter Physics of the Brazilian Physical Society, 11-15.05.1999, Sao Lourenco, Brazil
23.20.0

IFF-99-21-111
Persson B.
Sliding Friction
GAMM, 12-16.04.1999, Metz, France
23.20.0

IFF-99-21-112
Persson B.
Sliding Friction
Gordon Research Conference on "Dynamics at Surfaces", 08-13.08.1999, Andover, USA
23.20.0

IFF-99-21-113
Persson B.
Sliding Friction
international Meeting on Wetting, 15-18.06.1999, Trieste, Italy
23.20.0

IFF-99-21-114
Prager M
Molecular excitations, intermolecular interactions and ab-initio calculations
Janik-Friends-Meeting, Zakopane am 15.07.99
23.15.0

IFF-99-21-115
Prager M.
A concerted study of methyl-bridged compounds: trimethylaluminum
QAMTS'99 in Krakau am 29.09.99
23.15.0

IFF-99-21-116
Prager M.
Das Rückstreuspektrometer mit Phasenraumtransformation für den FRM-2
Technische Universität München am 23.07.99
23.89.1

IFF-99-21-117
Prager M.
Deuterierung-induzierte Phasenübergänge in Ammonium-Hexachloropalladate
Seminar am Institut für Kristallographie, Universtiät Tübingen am 07.06.99
23.15.0

IFF-99-21-118
Prager M.
Phase space transformation at the FRM-2 backscattering spectrometer
Neutron Optics '99 in Villigen am 28.11.99
23.89.1

IFF-99-21-119
Prager M.
Verbindungen mit Methylbrücken: Methylgruppenrotation in Trimethylaluminium
Deutsche Neutronenstreutagung in Potsdam am 27.05.99
23.15.0

IFF-99-21-120
Pyckhout-Hintzen W.
Kettendeformation in ungefüllten und gefüllten Netzwerken mittels SANS
DPG in Münster am 23.03.99
23.30.0

IFF-99-21-121
Pyckhout-Hintzen W.
Kettendeformation in ungefüllten und gefüllten Netzwerken mittels SANS
Institutsseminar Universität Regensburg am 14.01.99
23.30.0

IFF-99-21-122
Pyckhout-Hintzen W.; Westermann S.; Botti A.; Richter D.; Straube E.1
1Martin-Luther-Universität, Fachbereich Physik, Halle
Chain deformation in unfilled and filled polymer networks: a SANS approach
15th ACS Meeting, Rubber Division in Chicago vom 13.04 - 16.04.99
23.30.0

IFF-99-21-123
Pyckhout-Hintzen W.; Westermann S.; Botti A.; Richter D.; Straube E.1

1Martin-Luther-Universität, Fachbereich Physik, Halle
Chain deformation in unfilled and filled polymer networks: a SANS approach
IPNS Meeting in Argonne am 16.04.99
23.30.0

IFF-99-21-124
Richter D.
Dynamik von Polymeren
Kolloquiumsvortrag, Institut für Physikalische Chemie in Göttingen am 03.05.99
23.30.0

IFF-99-21-125
Richter D.
Forschung mit Neutronen in Deutschland - eine Strategie für die nächsten 15 Jahre
Deutsche Neutronenstreutagung in Potsdam, 25.05. - 27.05.99
23.30.0

IFF-99-21-126
Richter D.
Neutron Scattering in Chemistry - Chances and Perspectives
IUPAC - Konferenz in Berlin am 18.08.99
23.30.0

IFF-99-21-127
Richter D.
Neutron Scattering in Polymer Physics
2nd European Conference on Neutron Scattering in Budapest (ECNS'99); 01.09. - 04.09.99
23.30.0

IFF-99-21-128
Richter D.
Neutron Scattering in Polymer Physics
2nd Spanish Symposium on Neutron Scattering in Oviedo, Spanien, 02.06. - 04.06.99
23.30.0

IFF-99-21-129
Richter D.
Neutron Scattering on Soft Condensed Matter
ETH in Zürich, 23.06.99
23.30.0

IFF-99-21-130
Richter D.
Neutronen in der Polymerphysik
Chemisches Kolloquium in Köln am 29.11.99
23.30.0

IFF-99-21-131
Richter D.
Neutronenspinechountersuchung zur Dynamik von Polyisobutylen
Glasübergangstreffen an der Universität Rostock am 13.12.99
23.15.0

IFF-99-21-132
Richter D.
Neutronenstreuung in der Polymerphysik
Physikkolloquium der ETH Zürich am 08.12.99
23.15.0

IFF-99-21-133
Richter D.
Neutronenstreuung in der Polymerphysik
Physikkolloquium in Essen, 12.05.99
23.30.0

IFF-99-21-134
Richter D.
Random copolymers as wax crystal modifiers
Vortrag bei Exxon, USA, vom 13.03. - 19.03.99
23.30.0

IFF-99-21-135
Richter D.
Struktur und Dynamik von Polymeren
Kolloquiumsvortrag, Fa. Bayer in Leverkusen am 03.02.99
23.30.0

IFF-99-21-136
Richter D.
What is New in Neutron Scattering - Reflections on the ECNS'99 Budapest Conference
6th ESS General Meeting in Ancona am 21.09.99
23.15.0

IFF-99-21-137
Schober H.
Dynamik in Gläsern
Institut für Physikalische Chemie, Universität Hannover, 1.2.1999
23.30.0

IFF-99-21-138
Schober H.
Molecular dynamics in amorphous solids and liquids
CNRS Summer School "Physics of Glasses: Structure and Dynamics", Cargese, Korsika, Frankreich17./18. 5. 1999
23.30.0

IFF-99-21-139
Schober T.; Bohn H.G.
Electrochemical characterization and impedance of the high temperature proton conductor BaZr0.9Y0.1O2.95
6th Euroconference on Solid State Ionics, Cetraro, Italien, 16.09.1999
23.90.0

IFF-99-21-140
Schober T.; Friedrich J.
The proton conductor Ba3Ca1.18Nb1.82O9-((BCN18): Effect of reducing enviroments
12th Int. Conf. Solid State Ionics, Halkidiki, Griechenland, 10.06.1999
23.90.0

IFF-99-21-141
Schober T.; Szot K.; Barton M.; Kessler B.; Breuer U.1; Penkalla H.J.1; Speier W.1
1 Zentralinstitut für Chemische Analysen, FZJ
Cation loss of the proton conductor BaCa0.393Nb0.606O2.91 in aqueous media: amorphization at room temperature
6th Euroconference on Solid State Ionics, Cetraro, Italien, 18.09.1999
23.90.0

IFF-99-21-142
Schroeder H.
On the interpretation of leakage current: Models for thin films
School on Conduction & Breakdown, Chateaux d'Oex (Schweis), 28.02.-02.03.1999
23.42.0

IFF-99-21-143
Schroeder K.
Surface Diffusion and Models of the Kinetics Epitaxial Growth
Intern. Symposium on Structure and Dynamics of Heterogeneous Systems, Univ. Duisburg, 25.02.-26.02.1999
23.42.0

IFF-99-21-144
Schwahn D.
Effect of Thermal Composition Fluctuations in a Critical Polymer Blend Mixed with a Diblock Copolymer
ORNL-Neutron Scattering Group of the Solid State Division in Oak Ridge, USA am 12.03.99
23.30.0

IFF-99-21-145

Schwahn D.
Phase Behavior of Binary Polymer Blends in Pressure Fields and with small Additions of a third Component-Studies with Small Angle Neutron Scattering
European Conference on Polymer Blends in Mainz am 17.05.99
23.30.0

IFF-99-21-146
Schwahn D.
Phase Behavior of a Ternary Symmetric Homopolymer/ Homopolymer/ Diblock Copolymer Blend studied with Small Angle Neutron Scattering
Brooklyn, Department of Polymer Engineering am 14.06.99
23.30.0

IFF-99-21-147
Schwahn D.
Phase Behavior of a Ternary Symmetric Homopolymer/ Homopolymer/ Diblock Copolymer Blend studied with Small Angle Neutron Scattering, NIST, Department of Polymer Engineering am 07.06.99
23.30.0

IFF-99-21-148
Schwahn D.
Phase Behavior of a Ternary Symmetric Homopolymer/ Homopolymer/ Diblock Copolymer Blend studied with Small Angle Neutron Scattering, The University of Akron, Department of Polymer Engineering am 04.06.99
23.30.0

IFF-99-21-149
Schweika W.
Diffuse Scattering of Cu3Au: Displacements and Fermi-Surface Effects
Davos, Switzerland, International Alloy Conference-2, 10.08.1999
23.89.1, 23.55.0

IFF-99-21-150
Schweika W.
Diffuse scattering of Cu3Au and Fe-Al alloys - x-rays and neutron studies
Saclay, France, LLB, Seminar, 15.04.1999
23.89.1

IFF-99-21-151
Schütz, G.
Diffusion and Interaction of Shocker in the asymmetric exclusion process
Erwin-Schrödinger-Institut, Wien, 2. 3. 1999

IFF-99-21-152
Schütz, G.
Integrable Stochastic Processes for Biological and Chemical Systems
Universität Genf, 3. 5. 1999

IFF-99-21-153
Schütz, G.
Integrable Stochastic Processes for Biological and Chemical Systems
Universität Lausanne, 4. 5. 1999

IFF-99-21-154
Schütz, G.
Nonequilibrium Steady States of Quantum Spin Chains
Universidade Federal, Sao Carlos (Brasilien), 12. 8. 1999

IFF-99-21-155
Schütz, G.
Phasendiagramm von getriebenen diffusiven Systemen mit offenen Rändern
Universität Leipzig, 4. 7. 1999

IFF-99-21-156
Schütz, G.
Phasendiagramm von getriebenen diffusiven Systemen mit offenen Rändern
Universität Saarbrücken, 2. 2. 1999

IFF-99-21-157
Schütz, G.
Stationäre Nichtgleichgewichtszustände von integrablen Quantenspinketten
Freie Universität Berlin, 12. 7. 1999

IFF-99-21-158
Schütz, G.
Steady-State Selection in Driven Diffusive Systems with Open Boundaries
Erwin-Schrödinger-Institut, Wien, 25. 2. 1999

IFF-99-21-159
Schütz, G.
Relaxationsgesetz für gestreckte Polymere in Polymernetzwerken
DPG Frühjahrstagung, Münster, 26. 3. 1999

IFF-99-21-160
Thust A.
From the image to the wave function: The technique of focal-series reconstruction in HRTEM
Internal Seminar 15 07.1999, Wright-Pattern Air Force Base, Dayton, Ohio/USA
23.42.0

IFF-99-21-161
Thust A.
Materialuntersuchung mittels der Fokusvariationsmethode: Neue Einblicke nahe 1 Angström Auflösung
29. Tagung der Deutschen Gesellschaft für Elektronenmikroskopie, 5-10.09.1999, Dortmund
23.42.0

IFF-99-21-162
Thust A.
Rekonstruktion der Austrittswellenfunktion in der hochauflösenden Elektronenmikroskopie
WE-Heraeus Ferienkurs für Physik mit dem Titel "Moderne Fernfeld- und Nahfeld-Mikroskopien, 20.09-01.10.1999, Chemnitz
23.42.0

IFF-99-21-163
Thust A.
The Use of the Focal-Series Reconstruction Technique in HRTEM for Solving Materials Problems
MRS Fall Meeting, 29.11.-03.12.1999, Boston/USA
23.42.0

IFF-99-21-164
Trinkaus H.
Evolution of Gas-Filled Nano-Cracks in Ceramics,
Comp. Mat. Sci., Lawrence Livermore Nat. Lab. Livermore, CA, USA, 21.07.1999
23.15.0/23.42.0/23.80.5

IFF-99-21-165
Trinkaus H.
Evolution of Gas-Filled Nano-Cracks in Ceramics,
Comp. Mat. Sci., Sandia Nat. Lab. Livermore, California, USA, 20.07.1999
23.15.0/23.42.0/23.80.5

IFF-99-21-166
Trinkaus H.
Evolution of Gas-Filled Nano-Cracks in Ceramics,
Mech.& Aerospace Dep., UC Los Angeles, USA, 30.06.1999
23.15.0/23.42.0/23.80.5

IFF-99-21-167
Trinkaus H.

Microstructural Evolution in Metals under Cascade Damage Conditions,
Dep. Mech. & Envirnm. Eng., UC Santa Barbara, USA, 06.07.1999
23.80.5

IFF-99-21-168
Trinkaus H.
Progress in Modeling the Microstructural Evolution in Metals under Cascade Damage Conditions,
Int. Conf. Fusion Reactor Mat. (ICFRM 9), Colorado Springs, USA, 10.-15.10.1999
23.80.5

IFF-99-21-169
Trinkaus H.
The Role of Cascade-Induced Glissile Interstitial Loops on the Plasticity of Metals,
Gordon Research Conf. on "Material Processes Far from Equilibrium", Plymouth, NH, USA, 12.07.1999
23.80.5

IFF-99-21-170
Ullmaier H.
Das Target einer Spallations-Neutronenquelle
Kolloquium des Instituts für Kernphysik des Forschungszentrums Jülich, 26.01.1999, Jülich
23.60.0

IFF-99-21-171
Ullmaier H.
Materials Research and Development for the European Spallation Neutron Source
3rd International Workshop on Spallation Materials Technology, 29.04.1999, Santa Fe, New Mexico
23.60.0

IFF-99-21-172
Waser R.
"Elektrokeramische Dünnschichten in der Mikroelektronik - Chancen und Perspektiven"
Universität Augsburg, 21.05.1999
23.42.0

IFF-99-21-173
Waser R.
Defect chemistry and charge transport in perovskite-type thin films
School on Conductivity and breakdown, Cheateau d'Oex, Schweiz, 28.02.-02.03.1999
23.42.0

IFF-99-21-174
Waser R.
Frequency dependence of the coercive voltage of ferroelectric thin films
MRS Fall Meeting, Boston, 28.11.-03.12.1999
23.42.0

IFF-99-21-175
Waser R.
Modeling of Electroceramics - Applications and Prospects
Hebrew University, Jerusalem, Israel 10.01.1999
23.42.0

IFF-99-21-176
Waser R.
Modeling of Oxide Materials for Memory Applications
41st Electronic Materials Conference, Santa Barbara, 30.06.-02.07.1999
23.42.0

IFF-99-21-177
Waser R.
Neue keramische Materialien in der Informationstechnik von morgen
9. Tag für Wissenschaft und Wirtschaft, IHK Köln, 19.08.1999
23.42.0

IFF-99-21-178
Waser R.
Preparation and Fatigue Behaviour of PZT Thin Films with P- and N-Type Conducting Oxide Electrodes
11th Int. Symp. on Integrated Ferroelectrics, Colorado Springs, 06.-10.03.1999
23.42.0

IFF-99-21-179
Waser R.
Transport Properties of Ferroelectric Thin Films
9th European Meeting on Ferroelectricity (EMF-9), Praha, 12.-16.07.1999
23.42.0

IFF-99-21-180
Wingbermühle J.
Schichtentwicklung und magnetische Charakterisierung
MALVE-Meeting
Forschungszentrum Karlsruhe, Institut für Materialforschung
23.02.1999
3.42.0

IFF-99-21-181
Zeller R.
Parallel Computing with the KKR Method
Annual Meeting of the TMR-Network: "Ab-initio Calculations of Magnetic Properties of Surfaces, Interfaces and Multilayers", Aussois, Frankreich, 28.03.1999
23.20.0

IFF-99-21-182
Zorn R.
Experiments on glass forming liquids in confined media by neutron time-of-flight and backscattering studies
DyProSo (Dynamical Properties of Solids) XXVII, Tours, Frankreich am 14.09.99
23.15.0

IFF-99-21-183
Zorn R.
Neutronenstreuexperimente zur mikroskopischen Dynamik in ungeordneten Polymersystemen
Seminar des Sonderforschungsbereichs 294, Universität Leipzig am 27.01.99
23.15.0

List of references

Abt R.	IFF-99-21-073
Alefeld B.	IFF-99-21-001 IFF-99-21-002 IFF-99-21-003
Barton M.	IFF-99-21-141
Blügel S.	IFF-99-21-004 IFF-99-21-005 IFF-99-21-006 IFF-99-21-007 IFF-99-21-008 IFF-99-21-073 IFF-99-21-084
Bohn H.G.	IFF-99-21-139
Botti A.	IFF-99-21-122 IFF-99-21-123
Brener E.	IFF-99-21-009 IFF-99-21-010 IFF-99-21-011
Breuer U.	IFF-99-21-141
Brückel Th.	IFF-99-21-012 IFF-99-21-013 IFF-99-21-014 IFF-99-21-015
Bürgler D.E.	IFF-99-21-016 IFF-99-21-017
Caliebe W.	IFF-99-21-018
Chen J.H.	IFF-99-21-088 IFF-99-21-089
Conrad H.	IFF-99-21-019 IFF-99-21-020 IFF-99-21-021 IFF-99-21-022 IFF-99-21-023 IFF-99-21-024
Dederichs P.H.	IFF-99-21-025 IFF-99-21-026 IFF-99-21-027 IFF-99-21-028 IFF-99-21-029 IFF-99-21-030 IFF-99-21-031 IFF-99-21-032 IFF-99-21-033
Dürr H.	IFF-99-21-034
Eberhardt W.	IFF-99-21-035 IFF-99-21-036 IFF-99-21-037 IFF-99-21-038 IFF-99-21-039 IFF-99-21-040 IFF-99-21-041 IFF-99-21-042 IFF-99-21-043 IFF-99-21-044
Ebert Ph.	IFF-99-21-045
Ehrhart P.	IFF-99-21-046
Eisebitt S.	IFF-99-21-047 IFF-99-21-048 IFF-99-21-049
Eisenriegler E.	IFF-99-21-050 IFF-99-21-051
Friedrich J.	IFF-99-21-140
Goerigk G.	IFF-99-21-052 IFF-99-21-053
Gompper, G.	IFF-99-21-054 IFF-99-21-055
Grünberg P.	IFF-99-21-056 IFF-99-21-057 IFF-99-21-058 IFF-99-21-059 IFF-99-21-060 IFF-99-21-061 IFF-99-21-062 IFF-99-21-063 IFF-99-21-064 IFF-99-21-065 IFF-99-21-066 IFF-99-21-067 IFF-99-21-068 IFF-99-21-069 IFF-99-21-070
Harris J.	IFF-99-21-071
Heinze S.	IFF-99-21-073
Hoffmann S.	IFF-99-21-074 IFF-99-21-075 IFF-99-21-076
Jones R.	IFF-99-21-077 IFF-99-21-078
Jung P.	IFF-99-21-079
Kahle S.	IFF-99-21-080 IFF-99-21-081
Kehr, K.	IFF-99-21-082
Kessler B.	IFF-99-21-141

Klingeler R.	IFF-99-21-083		
Kurz Ph.	IFF-99-21-084		
Köbler U.	IFF-99-21-085	IFF-99-21-086	IFF-99-21-087
Lentzen M.	IFF-99-21-088	IFF-99-21-089	
Leube W.	IFF-99-21-100		
Liebsch A.	IFF-99-21-090	IFF-99-21-091	IFF-99-21-092
	IFF-99-21-093	IFF-99-21-094	IFF-99-21-095
Lustfeld H.	IFF-99-21-096		
Luysberg M.	IFF-99-21-097	IFF-99-21-098	
Monkenbusch M.	IFF-99-21-099	IFF-99-21-100	IFF-99-21-101
Müller-Krumbhaar H.	IFF-99-21-102	IFF-99-21-103	IFF-99-21-104
	IFF-99-21-105	IFF-99-21-106	
Neeb M.	IFF-99-21-107		
Penkalla H.J.	IFF-99-21-141		
Persson B.	IFF-99-21-108	IFF-99-21-109	IFF-99-21-110
	IFF-99-21-111	IFF-99-21-112	IFF-99-21-113
Prager M.	IFF-99-21-114	IFF-99-21-115	IFF-99-21-116
	IFF-99-21-117	IFF-99-21-118	IFF-99-21-119
Pyckhout-Hintzen W.	IFF-99-21-120	IFF-99-21-121	IFF-99-21-122
	IFF-99-21-123		
Richter D.	IFF-99-21-099	IFF-99-21-100	IFF-99-21-101
	IFF-99-21-122	IFF-99-21-123	IFF-99-21-124
	IFF-99-21-125	IFF-99-21-126	
	IFF-99-21-127	IFF-99-21-128	IFF-99-21-129
	IFF-99-21-130	IFF-99-21-131	IFF-99-21-132
	IFF-99-21-133	IFF-99-21-134	IFF-99-21-135
	IFF-99-21-136		
Schneiders D.	IFF-99-21-100		
Schober H.	IFF-99-21-137	IFF-99-21-138	
Schober T.	IFF-99-21-139	IFF-99-21-140	IFF-99-21-141
Schroeder H.	IFF-99-21-072	IFF-99-21-142	
Schroeder K.	IFF-99-21-143		
Schwahn D.	IFF-99-21-144	IFF-99-21-145	IFF-99-21-146
	IFF-99-21-147	IFF-99-21-148	
Schweika W.	IFF-99-21-149	IFF-99-21-150	
Schütz, G.	IFF-99-21-151	IFF-99-21-152	IFF-99-21-153
	IFF-99-21-154	IFF-99-21-155	IFF-99-21-156
	IFF-99-21-157	IFF-99-21-158	IFF-99-21-159
Speier W.	IFF-99-21-141		
Szot K.	IFF-99-21-141		
Thust A.	IFF-99-21-088	IFF-99-21-089	IFF-99-21-160
	IFF-99-21-161	IFF-99-21-162	IFF-99-21-163
Trinkaus H.	IFF-99-21-164	IFF-99-21-165	IFF-99-21-166
	IFF-99-21-167	IFF-99-21-168	IFF-99-21-169
Ullmaier H.	IFF-99-21-024	IFF-99-21-170	IFF-99-21-171
Urban K.	IFF-99-21-088	IFF-99-21-089	
Waser R.	IFF-99-21-072	IFF-99-21-075	IFF-99-21-076

	IFF-99-21-172	IFF-99-21-173	IFF-99-21-174
	IFF-99-21-175	IFF-99-21-176	IFF-99-21-177
	IFF-99-21-178	IFF-99-21-179	
Westermann S.	IFF-99-21-122	IFF-99-21-123	
Willner L.	IFF-99-21-100	IFF-99-21-101	
Wingbermühle J.	IFF-99-21-180		
Zeller R.	IFF-99-21-181		
Zorn R.	IFF-99-21-182	IFF-99-21-183	

Other talks

IFF-99-22-001
Abbas B.; Schwahn D.; Willner L.
Composition Fluctuations in a PB-PS Diblock Copolymer and PB-PS Copolymer with a good Solvent
2nd European Conference on Neutron Scattering, Budapest am 03.09.99
23.30.0

IFF-99-22-002
Antons A.; Berger R.; Blügel S.; Schroeder, K.
Ab-initio Untersuchungen der Adatom Diffusion auf Si(111)
DPG-Frühjahrstagung, Münster
März 1999
23.20.0

IFF-99-22-003
Baier F.1; Müller M.A.1; Grushko B and Schaefer H.-E.1
1 ITAP, Universität Stuttgart
Atomic defects in quasicrystals: an approach with positron annihilation spectroscopy and time differential dilatometry.
ICQ-7 Stuttgart 1999
23.55.0

IFF-99-22-004
Bartsch M.; Geyer B.; Häussler D.; Feuerbacher M.; Urban K.; Messerschmidt U.
1 Max-Planck-Institut für Mikrostrukturphysik, Weinberg 2, 06120 Halle/Saale,
Germany
Plastic properties of icosahedral Al-Pd-Mn single quasicrystals
ICQ7 Stuttgart 1999, in press
23.42.0
3.55.0

IFF-99-22-005
Bihlmayer G.; Kurz Ph; Blügel S.
Mangan-Oberflächenlegierungen auf einer Cu(111) Oberfläche
DPG-Frühjahrstagung, Münster
März 1999
23.20.0

IFF-99-22-006
Blügel S.
Influence of magnetism for the alloy formation of ultrathin films
International Symposium on Structure and Dynamics of Heterogeneous Systems - SDHS'99
Gesamthochschule Duisburg
26.02.1999
3.20.0

IFF-99-22-007
Blügel S.
Theory of ultrathin magnetic films
Workshop on Interface anisotropy, spin and orbital magnetism, Riksgränsen, Schweden
05.05.1999
3.20.0

IFF-99-22-008
Blügel S.
Wachstum
Sondierungsgespräch: Halbleitergrenzflächen in nächsten Jahrhundert
DESY/HASYLAB Hamburg
04.10.99
3.20.0

IFF-99-22-009
Blügel S.; Nie X.; Weinert M.1
1Brookhaven National Laboratory, Upton, USA
Modifikation eines Ummagnetisierungsfeldes durch ein externes elektrisches Feld
DPG-Frühjahrstagung, Münster
März 1999
23.20.0

IFF-99-22-010
Blüher R.1; Frank W.2 and Grushko B.
Diffusion of 103Pd and 195Au in icosahedral Al70.2Pd21.3Mn8.5 under proton irradiation.
1 ITAP, Unversität Stuttgart
2 Max-Planck-Institut für Metallforschung, Stuttgart
ICQ-7 Stuttgart 1999
23.55.0

IFF-99-22-011
Borbely S.; Heiderich M.; Schwahn D.; Seidl E.1
1Atominstitut Wien, Österreich
Resolution of the USANS Diffractometer at the FRJ-2 Research Reactor in Jülich
2nd European Conference on Neutron Scattering, Budapest am 01.9.99
23.30.0

IFF-99-22-012
Bürgler D.E.; Grünberg P.
In-plane momentum Conservation in Fe/Cr/Au/Fe(001) layered Structures
44th Annual Conference on Magnetism and Magnetic Materials, San Jose, CA
16.11.99
3.42.0

IFF-99-22-013
Chen J.
Mechanical Properties and Microstructure of LANSCE-irradiated 304L
Third International Workshop on Spallation Materials Technology, Apr. 29-May 4, 1999, Santa Fe, New Mexico
23.60.0

IFF-99-22-014
Chen J.; Carsughi F.; Derz H.; Dai Y.1; Sommer W.T.2; Broome T.3; Pott G.; Bauer G.1; Ullmaier H.
1Paul-Scherrer-Institut, Schweiz
2LANL, USA
3Rutherford Appleton Lab., Großbrittannien
Mechanical Properties and Microstructure of 800 MeV p-irradiated 304L and Tantalum
6th ESS General Meeting and Connected Workshops, Sep. 20-23, 1999, Portonovo/Ancona, Italy
23.60.0

IFF-99-22-015
Crossover from 3d-Ising to Isotropic Lifshitz Critical Behavior
APS Centennial Meeting in Atlanta, USA am 26.03.99
23.30.0

IFF-99-22-016
Dallmeyer, A.
Electronic states and magnetism of 1-D monatomic wires
DPG-Frühjahrstagung in Münster 1999
22.03.1999
3.20.0

IFF-99-22-017
Damson B.1; Weller M.1; Feuerbacher M.; Grushko B. and Urban K.
1 Max-Planck-Institut für Metallforschung, Seestraße 92, 70174 Stuttgart,
Germany
Mechanical spectroscopy of d-AlNiCo and i-AlPdMn
ICQ7 Stuttgart 1999, in press
23.55.0

IFF-99-22-018
Divin Y.
First Applications of Hilbert-Transform Spectroscopy
Beirat IFF, April 22, 1999, Forschungszentrum Jülich
23.42.0

IFF-99-22-019
Divin Y.
Far-Infrared Hilbert-Transform Spectroscopy
PGI Tag "Supraleitung", 11.11.99, Forschungszentrum Jülich.
23.42.0

IFF-99-22-020
Divin Y.; Poppe U.; Jia C.L.; Seo J.W.1; Glyantsev V.1
1 IBM Rüschlikon/CH
2 Conductus Inc., Sunny Vail/USA
Epitaxial (101) YBa2Cu3O7 thin-films on (103) NdGaO3 substrates
EUCAS'99, September 14-17, 1999, Barcelona, Spain.
23.42.0

IFF-99-22-021
Döblinger M.1.; Wittmann R.1.; Gerthsen D.1 and Grushko B.
1 Laboratorium für Elektronenmikroskopie, Universität Karlsruhe
Structural relationship and mutual transformation of approximants of the decagonal Al-Co-Ni phase.
ICQ-7 Stuttgart 1999
23.55.0

IFF-99-22-022
Ebert Ph.; Chao K.-J.2; Niu Q.2 and Shih C. K.2
2 Dept. of Physics, University of Texas, Austin
Dislocations, phason defects, and domain walls in a one-dimensional quasiperiodic superstructure of a metallic thin film.
American Vacuum Society 46th International Symposium, Seattle, Washington, October 25-29, 1999.
23.55.0

IFF-99-22-023
Ebert Ph.; Kluge F.; Grushko B.; Urban K.
Investigation of cleavage surfaces of decagonal Al-Ni-Co quasicrystals
ICQ7 Stuttgart 1999
23.55.0

IFF-99-22-024
Ebert Ph.; Zhang Tianjiao2,1; Kluge F.; Simon M.; Zhang Zhenyu1,2; Urban K.
1 Oak Ridge National Laboratory, Oak Ridge
2 Dept. of Physics, University of Texas, Austin
The importance of many-body effects in the clustering of charged Zn dopant atoms in GaAs
Materials Research Society Fall Meeting, Boston, Massachusetts, November 29 - December 3, 1999.
23.55.0

IFF-99-22-025
Ebert Ph.; Zhang Tianjiao2,3; Kluge F.; Simon M.; Zhang Zhenyu3,2; Urban K.
2 Department of Physics, University of Tennessee, Knoxville, TN 37996
3 Solid State Division, Oak Ridge National Laboratory, Oak Ridge, TN 37831-6032
The importance of many-body effects in the clustering of charged Zn dopant atoms in GaAs
American Vacuum Society 46th International Symposium, Seattle, Washington, October 25-29, 1999.
23.55.0

IFF-99-22-026
Eisebitt S.
Weichröntgenspektroskopie an nanostrukturierten Halbleitern
Sondierungsgespräch: Halbleitergrenzflächen in nächsten Jahrhundert
DESY/HASYLAB Hamburg
04.10.99
3.20.0

IFF-99-22-027
Faley M.; Soltner H.; Poppe U.; Urban K.; Paulson D.N.1; Starr T.N.1 and Fagaly R. L.1
1 TRISTAN Technologies Inc., San Diego/USA
HTS dc-SQUID with gradiometric multilayer flux transformer
Submitted to EUCAS'99, 1999, Barcelona, in press
23.42.0

IFF-99-22-028
Faley M.; Soltner H.; Poppe U.; Urban K.; Paulson D.N.1; Starr T.N.1; Fagaly R.L.1
1 TRISTAN Technologies Inc., San Diego/USA
HTS dC-SQUID with gradiometric multilayer flux transformer
Submitted to EUCAS'99, Sept. 14-17, 1999, Barcelona, Spain
23.42.0

IFF-99-22-029
Faley M.I.; Poppe U.; Urban K.; Paulson D.N.1; Starr T.1 and Fagaly R. L.1
1 TRISTAN Technologies Inc., San Diego/USA
HTS dc-SQUID with gradiometric multilayer flux Transformer, to be pubished in the Proceedings of EUCAS'99, September 14-17, 1999, Barcelona, Spain.
23.42.0

IFF-99-22-030
Faley M.I.; Poppe U.; Urban K.; Zimmermann E.; Glaas W.; Halling H.; Bick M.; Krause H.-J.; Paulson D.N.1; Starr T.1; Fagaly R.L.1
1 TRISTAN Technologies Inc., San Diego/USA
Hochtemperatursupraleiter DC-SQUID Sensoren für den Betrieb in magnetischen Feldern,
DPG-Frühjahrstagung, Münster, 23.3.99
23.42.0

IFF-99-22-031
Feuerbacher M.; Klein H.; Schall P.; Bartsch M.1; Messerschmidt U.1 and Urban K.
1 Max-Planck-Institut für Mikrostrukturphysik, Weinberg 2, 06120 Halle/Saale,
Germany
Plasticity of Quasicrystals
Mat. Res. Soc. Symp. Proc. Vol. 553, 307-318 (1999)
23.55.0

IFF-99-22-032
Goerigk G.
Kleinwinkelstreuung bei JUSIFA
Hamburg, HASYLAB, Diskussionstreffen zur Röntgen-Kleinwinkelstreuung, 07.06.1999
23.89.1

IFF-99-22-033
Goerigk G.; Williamson D. L.1
1Colorado School of Mines, Department of Physics, USA
Nanostructural Characterization of Amorphous SiGe:H Alloys by Anomalous Small-Angle X-Ray Scattering Studies
Brookhaven, USA, NSLS, SAS99, XIth International Conference on Small-Angle Scattering, 17. - 20.05.1999
23.89.1

IFF-99-22-034
Grushko B.
Composition and precipitation behavior of icosahedral Al-Pd-Mn quasicrystals.
ICQ-7 Stuttgart 1999
23.55.0

IFF-99-22-035
Gutheim F.; Steinbrecher J.; Brener E.; Müller-Krumbhaar H.
Fraktales Wachstum epitaktischer Adsorbatcluster mit elastischer Wechselwirkung
DPG Frühjahrstagung, Münster, 22.03.- 26.03.1999
23.15.0

IFF-99-22-036
Gwodzsch J.1; Grushko B.; Surowiec M.1,

1 Institute of Physics and Chemistry of Metals, University of Silesia, Katowice, Poland
Mosaic structure of single quasicrystals.
ICQ-7 Stuttgart 1999
23.55.0

IFF-99-22-037
Harris J.
Computational Methods in Materials Science
Seminar, 16.04.1999, National Research Council of Canada, Ottawa, Canada
23.20.0

IFF-99-22-038
Harris J.
Computational Methods in Materials Science: Advances and Limitations
Seminar, 08.07.1999, National Center of High-Speed Computing, Shinsu, Taiwan
23.20.0

IFF-99-22-039
Harris J.
Dichte-Funktional-Theorie: Aspekte zur Anwendung
Seminar, 15.12.1999, Ringvorlesung Rechenverfahren in der Quantenchemie, FB Chemie, TU Darmstadt
23.20.0

IFF-99-22-040
Haubold H.-G.; Vad Th.; Hiller P.; Jungbluth H.
ASAXS in situ studies of adsorbates on carbon supported electrocatalysts
Brookhaven, USA, National Synchrotron Light Source Laboratory, SAS99, XIth International Conference on Small-Angle Scattering, 20.05.1999
23.89.1

IFF-99-22-041
Heggen M.; Schall P.; Feuerbacher M.; Klein H.; Fisher I.R.1; Canfield P.C.1 and Urban K.
1 Ames Laboratory and Department of Physics and Astronomy, Iowa State
University, Ames, IA 50011, USA
Plastic behaviour of icosahedral Zn-Mg-Dy single-quasicrystal
ICQ7 Stuttgart 1999, in press
23.55.0

IFF-99-22-042
Heinze S.; Blügel S.
Theoretical analysis of STM and STS of thin magnetic films
211. Heraeus Seminar (Magnetic Nanostructures), Bad Honnef
04.01.1999
3.20.0

IFF-99-22-043
Heinze S.; Blügel S.
Theoretical analysis of STM of ultra-thin magnetic films
European Research Conference on Computational Physics for Nanotechnology,
Castelvecchio Pascoli, Italy
19.09.99
3.20.0

IFF-99-22-044
Heinze S.; Blügel S.; Weinert M.1
1Brookhaven National Laboratory, Upton, USA
Einfluss des elektrischen Feldes auf STM-Bilder von Metalloberflächen
DPG-Frühjahrstagung, Münster
März 1999
23.20.0

IFF-99-22-045
Heinze S.; Blügel S.; Wiesendanger R.1
1Universität Hamburg
What can be learn't by non-spinpolarized STM about surface magnetism of Cr and Mn on Fe(001)?
10th International Conference on M/STS and Related Techniques 1999 , Seoul, Korea
Juli 1999
23.20.0

IFF-99-22-046
Jakobs B.1, Sottmann T.1; Strey R.1; Allgaier J.; Willner L.; Richter D.
1Institut f. Physikalische Chemie, Universität Köln
Amphiphilic block copolymers: Efficiency boosters for microemulsions
23.15.0

IFF-99-22-047
Jiang S.-C.1; Yu H.1; Ebert Ph.; Wang X.-D.1; Diener R.1; Niu Q.1; Shih C. K. 1
1 Dept. of Physics, University of Texas, Austin
Chaotic-like wavefunction beating in thin silver films with a quasiperiodic superstructure
American Vacuum Society 46th International Symposium, Seattle, Washington, October 25-29, 1999.
23.55.0

IFF-99-22-048
Jones R.
Density functional studies of organic systems - Structure, vibration frequencies, and reactions in polycarbonates
Kolloquium, 19.05.1999, Dept. of Chemistry, Rutgers University, Piscataway, USA
23.20.0

IFF-99-22-049
Jones R.
Density functional studies of organic systems - Structure, vibration frequencies, and reactions in polycarbonates
Kolloquium, 20.05.1999, Dept. of Chemistry, Princeton University, Princeton, USA
23.20.0

IFF-99-22-050
Jones R.
Density functional studies of polycarbonate systems - Structure, vibration frequencies, and reactions
Kolloquium, 17.05.1999, Dept. of Chemistry, University of Pennsylvania, Philadelphia, USA
23.20.0

IFF-99-22-051
Jones R.
Density functional studies of polycarbonate systems - Structure, vibration frequencies, and reactions
Seminar, 26.05.1999, General Electric Research and Development Laboratories, Schenectady, USA
23.20.0

IFF-99-22-052
Jones R.
Geometrie und Spektroskopie von atomaren Clustern - Möglichkeiten und Grenzen von Dichtefunktionalrechnungen
Seminar, 02.07.1999, Physikalisches Institut, Universität Hamburg
23.20.0

IFF-99-22-053
Jones R.
Simulations of polycarbonate systems - Density functional studies of structure, vibration frequencies, and reactions
Kolloquium, 08.12.1999, Dept. of Polymer Science and Engineering, University of Massachusetts, Amherst, USA
23.20.0

IFF-99-22-054
Jones R.
Struktur und Spektroskopie von Kohlenstoffclustern - Möglichkeiten und Grenzen der Theorie

Seminar, 14.06.1999, I. Physikalisches Institut, Universität zu Köln
23.20.0

IFF-99-22-055
Jones R.
Thermal expansion of anisotropic materials - density functional study of high quartz systems
01.12.1999, Materials and Research Society Symposium, Boston, USA
3.20.0

IFF-99-22-056
Jung P.
Effects of irradiation and helium implatation on microstructure and physical and mechanical properties
Monitoring of Underlying Technology in the European Fusion Programme, 5.5.1999
23.80.5

IFF-99-22-057
Jung P.; Schliefer F.; Liu C.
Diffusion and permeation of hydrogen in low activation martensitic stainless steel - effect of irradiation
9th Int. Conf. on Fusion Reactor Materials, 12.10.1999, Colorado Springs
23.80.5

IFF-99-22-058
Karl A.
Der unvollständige Ladungstransfer in endohedral dotiertem La@C82
DPG-Frühjahrstagung in Heidelberg 1999
17.03.1999
3.20.0

IFF-99-22-059
Kehr, K.
Muon Spin Relaxation by Random Walks of Electrons
Workshop "Application of Low-Energy Muons", Paul-Scherrer Institute,
Villigen, Schweiz
17. 2. 1999

IFF-99-22-060
Kirstein O.
The use of a phase space transformation chopper system for a neutron backscattering spectrometer
Institut Laue-Langevin, Grenoble, France 04.03 - 05.03.99
23.89.1

IFF-99-22-061
Kirstein O.; Kozielewski T.; Prager M.; Richter D.
The backscattering spectrometer for the FRM-II reactor in Munich
ECNS'99 in Budapest, Ungarn 01.09. - 04.09.99
23.89.1

IFF-99-22-062
Klein H.; Feuerbacher M.; Schall P. and Urban K.
Plastic Deformation of Approximants: Dislocations vs. Phason Lines
Mat. Res. Soc. Symp. Proc. Vol. 553, 325-330 (1999)
23.55.0

IFF-99-22-063
Klein H.; Feuerbacher M.; Urban K.
locations in Al-Pd-Mn approximants: an HREM study
ICQ7 Stuttgart 1999, in press
23.55.0

IFF-99-22-064
Klingeler R.
La20n (n=1-6): Photoelektronenspektroskopie und Dichtefunktionalrechnungen
DPG-Frühjahrstagung in Heidelberg 1999
18.03.1999
3.20.0

IFF-99-22-065
Klingeler R.; Bechthold P.S.; Neeb M.; Eberhardt W.
Mass spectra of metal-doped carbon and fullerene clusters Mx@Cn<120 (M = Sc, Y, La, Ca, Ce; x = 1,2)
Arbeitstreffen des SFB 341, Aachen
07.10.99
3.20.0

IFF-99-22-066
Kluge F.; Ebert Ph.; Grushko B.; Urban K.
Änderungen der chemischen Zusammensetzung und der Struktur von gespaltenen ikosaedrischen Al-Pd-Mn-Quasikristalloberflächen nach Heizbehandlung.
Frühjahrstagung des Arbeitskreises Festkörperphysik bei der DPG, Münster, Germany, 22.-26 .3.1999.
23.55.0

IFF-99-22-067
Kluge F.; Grushko B.; Ebert Ph. and Urban K.
Structure and composition changes of cleaved Al-Pd-Mn quasicrystal surfaces induced by heat treatments investigated by AES, SEM and STM
ICQ7 Stuttgart 1999
23.55.0

IFF-99-22-068
Kluge M.
Diffusion in Cu33 Zr67
Kolloquium "Unterkühlte Metallschmelzen: Phasenselektion und Glasbildung", DFG, Bad Honnef, 24.02.-26.02.1999
23.30.0

IFF-99-22-069
Koizumi, S.; Annaka M.1; Borbely S.; Schwahn D.
1Chiba University, Japan
Fractal Structure of a Polymer Gel observed by Small-angle Neutron Scattering over a Q-range from 10-5 to 0.1 Å-1
2nd European Conference on Neutron Scattering, Budapest am 03.09.99
23.30.0

IFF-99-22-070
Kurz Ph.; Bihlmayer G.; Blügel S.
Non-collinear Magnetism of Monolayers on Ag(111) and Cu(111)
44th Annual Conference on Magnetism and Magnetic Materials, San Jose, CA
17.11.1999

IFF-99-22-071
Kurz Ph.; Bihlmayer G.; Blügel S.
Non-collinear magnetism of monolayers on Ag(111) and Cu(111)
International Workshop on Interface ansisotropy, spin and orbital moment
Riskgränsen, Schweden
05.05.1999
3.20.0

IFF-99-22-072
Kurz Ph.; Bihlmayer G.; Blügel S.
Non-collinear magnetism of monolayers on Ag(111) and Cu(111)
TMR-Workshop Interface Magnetism, Aussois, Frankreich
28.03.1999
3.20.0

IFF-99-22-073
Kurz Ph.;Bihlmayer G.; Blügel S.
Nichtkollinearer Magnetismus von magnetischen Monolagen auf Ag(111) und Cu(111)
DPG-Frühjahrstagung, Münster
März 1999
23.20.0

IFF-99-22-074
Lentzen M.; Urban K.
Reconstruktion des projizierten Kristallpotentials mittels einer Maximum-Likelihood-Optimierung
29. Tagung der Deutschen Gesellschaft für Elektronenmikroskopie, 05.-10.09.1999, Dortmund
23.42.0

IFF-99-22-075
Liebsch A.; Liechtenstein A.1
1University of Nijmegen
Photoemission quasi-particle spectra of Sr2RuO4
Workshop on Strong Correlations in Solids, 02-06.10.1999, Prag
23.20.0

IFF-99-22-076
Lustfeld H.
Dynamical flows and Poincaré maps of simple repellers
Seminar, 07.09.1999, Eötvös University, Budapest
23.15.0

IFF-99-22-077
Luysberg M.; Houben L.; Specht P.1 and Weber E.R.1
1 University of California, Berkeley/USA
Mechanisms of the formation of structural defects during low temperature growth of GaAs
XIth Conference on Microcopy of Semiconducting Materials, Oxford, 21.-25.3.1999
23.42.0

IFF-99-22-078
Luysberg M.; Specht P.1; Weber E.R.1
1 University of California, Berkeley/USA
Limitations to epitaxial growth of low-temperature grown GaAs
2nd Symposium on non-stoichiometric III-V compounds, Erlangen, 4.-6. 10.1999
23.42.0

IFF-99-22-079
Luysberg M.; Specht P.1; Weber E.R.1
1 University of California, Berkeley/USA
Mechanisms of the formation of structural defects during low temperature growth of GaAs
Xth Conference on Microscopy of Semiconducting Materials, Oxford 1999
23.42.0

IFF-99-22-080
Lüttgens G.
Photoelektronenspektroskopie an kleinen massenselektierten Germanium-
Oxidclusteranionen
DPG-Frühjahrstagung in Heidelberg 1999
16.03.1999
3.20.0

IFF-99-22-081
Messerschmidt U.1; Bartsch M.1; Geyer B.1; Häussler D.1; Feuerbacher M. and Urban K.
1 Max-Planck-Institut für Mikrostrukturphysik, Weinberg 2, 06120 Halle/Saale,
Germany
Microprocesses of the plastic deformation of icosahedral Al-Pd-Mn single quasicrystals
ICQ7 Stuttgart 1999, in press
23.55.0

IFF-99-22-082
Messerschmidt U.1; Geyer B.1; Bartsch M.1; Feuerbacher M.; Urban K.
1 Max-Planck-Institut für Mikrostrukturphysik, Weinberg 2, 06120 Halle/Saale,
Germany
The Activation Parameters and the Mechanisms of Plastic Deformation of Al-Pd-Mn Single Quasicrystals
Mat. Res. Soc. Symp. Proc. Vol. 553, 319-324 (1999)
23.55.0

IFF-99-22-083
Müller-Krumbhaar H.
Strukturbildung bei Benetzung
DFG-Seminar, Bad Honnef, 18.10.1999
23.15.0

IFF-99-22-084
Neeb M.
Photoelectron spectra of metal cluster anions reacted with Benzene
Clustertreffen, Sassnitz, Rügen
28.09.99
3.20.0

IFF-99-22-085
Neeb M.
Zeitaufgelöste 2-Photonen-Photoelektronenspektroskopie an massenselektierten Metallclusteranionen
DFG-Antragskolloquium, Schwerpunktprogramm "Femtosekunden-Spektroskopie elementarer Anregungen in Atomen, Molekülen und Clustern, Bad Honnef
15.11.1999

IFF-99-22-086
Nie X.; Blügel S.
Investigation of chemical Trends of the Magnetocrystalline Anisotropy for Magnetic Monolayers
44th Annual Conference on Magnetism and Magnetic Materials, San Jose, CA
17.11.1999

IFF-99-22-087
Persson B.
Brittle Fracture
APS Meeting, 21-25.3.1999, Atlanta, USA
23.20.0

IFF-99-22-088
Persson B.
Layering transition in molecular thin lubrication films
APS Meeting, 21-25.3.1999, Atlanta, USA
23.20.0

IFF-99-22-089
Pontius N.
Mehrphotonen-Photoemission aus kleinen Übergangsmetallclustern mit Femtosekundenlaserpulsen
DPG-Frühjahrstagung in Heidelberg 1999
16.03.1999
3.20.0

IFF-99-22-090
Prager M.
The layout of the backscattering spectrometer for the FRM-2
National Institute of Standards and Technology, Washington
am 16.04.99
23.89.1

IFF-99-22-091
Prager M.; Kirstein O.; Kozielewski T.; Richter D.
The backscattering spectrometer for the FRM-II reactor in Munich
NOP 99, Villigen, Schweiz 25.11. - 27.11.99
23.89.1

IFF-99-22-092
Rotenberg E.1, Theis W.2, Barman S.R.3, Paggel J.J.4, Horn K.5, Ebert Ph. Urban K.
1 Advanced Light Source, Lawrence Berkely Lab, Berkeley CA
2 FB Physik, Freie Universität Berlin, Berlin
3 IUC-DAEF. Indore, Indien
4 FB Physik, Philipps-Universität Marburg

5 Fritz-Haber-Institut der MPG, Berlin
Band-like valence states in i-AlPdMn Quasicrystals?
American Physical Society Centennial Meeting, Atlanta, Georgia, March 20-26, 1999.
23.55.0

IFF-99-22-093
Rotenberg E.1, Theis W.2, Barman S.R.3, Paggel J.J.4, Horn K.5, Ebert Ph., and Urban K.6
1 Advanced Light Source, Lawrence Berkely Lab, Berkeley CA
2 FB Physik, Freie Universität Berlin, Berlin
3 IUC-DAEF. Indore, Indien
4 FB Physik, Philipps-Universität Marburg
5 Fritz-Haber-Institut der MPG, Berlin
Elektronische Struktur von i-AlPdMn-Quasikristallen.
Frühjahrstagung des Arbeitskreises Festkörperphysik bei der DPG, Münster, Germany, 22.-26.3.1999.
23.55.0

IFF-99-22-094
Rotenberg E.1; Theis W2.; Barman S.R3.; Paggel J.J4.; Horn K.5; Ebert Ph.6 and Urban K.6
1 Advanced Light Source, Lawrence Berkely Lab, Berkeley CA
2FB Physik, Freie Universität Berlin, Berlin
3 IUC-DAEF. Indore, Indien
4 FB Physik, Philipps-Universität Marburg
5 Fritz-Haber-Institut der MPG, Berlin
6 Institut für Festkörperforschung, Forschungszentrum´Jülich
Photoemission study of dispersive states in i-Al-Pd-Mn.
7th International Conference on Quasicrystals (ICQ7), Stuttgart, Germany, Sept. 20-24, 1999.
23.55.0

IFF-99-22-095
Rotenberg E.1; Theis W2.; Barman S.R3.; Paggel J.J4.; Horn K.5; Ebert Ph.; Urban K.
1 Advanced Light Source, Lawrence Berkely Lab, Berkeley CA
2 FB Physik, Freie Universität Berlin, Berlin
3 IUC-DAEF. Indore, Indien
4 FB Physik, Philipps-Universität Marburg
5 Fritz-Haber-Institut der MPG, Berlin
Photoemission study of dispersive states in i-AlPdMn
ICQ7 Stuttgart 1999, in press
23.55.0

IFF-99-22-096
Rottländer P.; Kohlstedt H.; Girgis E.; de Gronckel H.; Schelten, J.; Grünberg P.
Ferromagnetische Tunnelkontakte mit UV-unterstützter Oxidation der Barriere
DPG-Frühjahrstagung in Münster 1999
24.03.1999
3.20.0

IFF-99-22-097
Rottländer P.; Kohlstedt H.; Grünberg P.
Barrier Formation by Ultraviolet light assisted Oxidation for Magnetic Tunnel Junctions
44th Annual Conference on Magnetism and Magnetic Materials, San Jose, CA
17.11.99
3.42.0

IFF-99-22-098
Schall P.; Feuerbacher M.; Messerschmidt U.1 and Urban K.
1 Max-Planck-Institut für Mikrostrukturphysik, Weinberg 2, 06120 Halle/Saale,
Germany
Dislocation structure and density in deformed Al-Pd-Mn single quasicrystals
ICQ7 Stuttgart 1999, in press
23.55.0

IFF-99-22-099
Schober H.
Diffusion and relaxations in liquid and amorphous CuZr
Seventh International Workshop on Disordered Systems, Molveno, Trento, Italien, 02.03.1999
23.30.0

IFF-99-22-100
Schroeder K.; Blügel S.
Diffusion und Einbau von Ge- und Si-Adatomen auf As-terminiertem Si(111): ein Vergleich
DPG-Frühjahrstagung, Münster
März 1999
23.20.0

IFF-99-22-101
Schwahn D.
Möglichkeiten der Neutronenkleinwinkelstreuung gezeigt am Beispiel der Synthese von TiO2 Kolloiden in einem mizellaren Kern
Kolloquium zum DFG-Schwerpunktprogramm "Prinzipien der Biomineralisation" in Bonn am 20.10.99
23.30.0

IFF-99-22-102
Schwahn D.
Phasenverhalten einer binären Polymermischung nach Zugabe des entsprechenden Diblockcopolymers - Experimente mit der Neutronenstreuung
Frühjahrstagung des Fachverbandes Polymerphysik der DPG in Leipzig am 03.03.99
23.30.0

IFF-99-22-103
Schwahn D.
Phasenverhalten einer binären Polymermischung nach Zugabe des entsprechenden Diblockcopolymers-Experimente mit der Neutronenstreuung
Deutsche Neutronenstreutagung 1999 in Potsdam am 26.05.99
23.30.0

IFF-99-22-104
Schwahn D.; Mortensen K.1; Frielinghaus H.1; Almdal K.1
1Risø National Laboratory, Roskilde, Denmark
3d-Ising and Lifshitz Critical Behavior in a Mixture of a Polymer Blend and a Diblock Copolymer
2nd European Conference on Neutron Scattering, Budapest am 03.09.99
23.30.0

IFF-99-22-105
Schweika W.
Feinstruktur der diffusen Streuung in CuAu Legierungen und Fermiflächeneffekte
Münster, DPG-Tagung, 22.03.1999
23.55.0, 23.89.1

IFF-99-22-106
Schweika W.
Oberflächeninduzierte Ordnungsphänomene in Legierungen des Cu3 Au-Typs - eine Monte Carlo Studie
Münster, DPG-Tagung, 22.03.1999
23.15.0

IFF-99-22-107
Schütz, G.
Lattice gas approach to the relaxation of entangled DNA
III Escola Brasileira de Probabilidade, Mambucaba (Brasilien), Konferenzbeitrag
5. 8. 1999

IFF-99-22-108
Schütz, G.
Relaxation of entangled DNA
Renoutre de Physique Statistique, Paris, Konferenzbeitrag
27. 1. 1999

IFF-99-22-109
Settels A.

Defektkomplexe in Si und Ge: Elektronenstruktur, Gitterrelaxationen und Elektrische Feldgradienten
Arbeitstreffen "Forschung mit nuklearen Sonden und Ionenstrahlen", Berlin, 06.10.-08.10.1999
23.20.0

IFF-99-22-110
Settels A.
Different Methods for Lattice Relaxations within the KKR-Formalism
TMR-Midterm Review, Aussois, Frankreich, 27.03.-01.04.1999
23.20.0

IFF-99-22-111
Settels A.
Vergleich verschiedener Verfahren zur Berücksichtigung von Gitterverschiebungen
DPG-Frühjahrstagung, Münster, 22.03.-26.03.1999
23.20.0

IFF-99-22-112
Spettmann R.1; Schroeder K.; Blügel S.; Entel P.1
1Theor. Tieftemperaturphysik, Gerhard Mercator Universität, GH Duisburg
Elektronische Struktur von Si(111): Sn (sqrt (3) x (sqrt(3))
DPG Frühjahrstagung Münster, 22.03.1999
23.42.0

IFF-99-22-113
Spettmann R.1; Schroeder K.; Blügel S.; Entel P.1
1Universität Duisburg
Elektronische Struktur von Si(111): Sn-
DPG-Frühjahrstagung, Münster
März 1999
23.20.0

IFF-99-22-114
Ullmaier H.
Status des Projekts Europäische Spallationsquelle ESS
Sitzung des Komitees für die Forschung mit Neutronen, 19.02.1999, Jülich
23.60.0

IFF-99-22-115
Ullmaier H.
The European Spallation Neutron Source ESS
4th Internat. Workshop on Advanced Cold Moderators (AcoM IV), 25.02.1999, Jülich
23.60.0

IFF-99-22-116
Ullmaier H.
The Project European Spallation Neutron Source
Besuch der Parlamentarier der Nordatlantischen Versammlung, 02.03.1999, Jülich
23.60.0

IFF-99-22-117
Urban K.
A new way towards higher resolution: Spherical aberration correction
Int. Symp. On Advanced Materials and Electron Microscopic Techniques for the Third Millenium, Hokkaido University 1998, Journal of Microscopy, in press (1999)
23.42.0

IFF-99-22-118
Urban K.
Plasticity of quasicrystals and related intermetallic phases
Int. Conf. on Rapidly Quenched and Metastable Metals, Bangalore, 1999, in press
23.42.0

IFF-99-22-119
Urban K.
Spherical aberration corrected transmission electron microscopy
Congress of Latin American Electron Microscopy Societies, Porlamar, Venezuela, 1999, in press.
23.42.0

IFF-99-22-120
Urban K.
Spherical aberration corrected transmission electron microscopy
Congress of the Int. Mat. Res. Soc. Beijing 1999
23.42.0

IFF-99-22-121
Wischnewski A.
Reptation in polyethylene-melts with different molecular weights
2nd European Conference on Neutron Scattering (ECNS'99) in Budapest, Ungarn, 03.09.99
23.30.0

IFF-99-22-122
Wortmann D.
Theorie der Rastertunnelmikroskopie von metallischen Oberflächenlegierungen
Seminar des Zentrums für Mikrostrukturforschung, Universität Hamburg
19.10.1999
3.20.0

IFF-99-22-123
Yu H.1; Jiang S.-C.1; Ebert Ph.; Wang X.-D.1; Shih C. K.1
1 Dept. of Physics, University of Texas, Austin
Enhanced interlayer mass transport and dynamics of film smoothening on a symmetry-broken Ag(111) surface
American Vacuum Society 46th International Symposium, Seattle, Washington, October 25-29, 1999.
23.55.0

IFF-99-22-124
Yurechko M.; Grushko B.
Investigation of Al-Pd-Co alloy system.
Frühjahrstagung des Arbeitskreises Festkörperphysik bei der DPG, Münster, Germany, 22-26.3.1999
23.55.0

IFF-99-22-125
Yurechko M.; Grushko B.
Study of Al-Pd-Co alloy system.
ICQ7 Stuttgart 1999, in press
23.55.0

List of references

Abbas B.	IFF-99-22-001		
Allgaier J.	IFF-99-22-046		
Antons A.	IFF-99-22-002		
Bechthold P.S.	IFF-99-22-065		
Berger R.	IFF-99-22-002		
Bihlmayer G.	IFF-99-22-005	IFF-99-22-070	IFF-99-22-071
	IFF-99-22-072	IFF-99-22-073	
Blügel S.	IFF-99-22-002	IFF-99-22-005	IFF-99-22-006
	IFF-99-22-007	IFF-99-22-008	IFF-99-22-009
	IFF-99-22-042	IFF-99-22-043	IFF-99-22-044
	IFF-99-22-045	IFF-99-22-070	IFF-99-22-071
	IFF-99-22-072	IFF-99-22-073	IFF-99-22-086
	IFF-99-22-100	IFF-99-22-112	IFF-99-22-113
Borbely S.	IFF-99-22-011	IFF-99-22-069	
Brener E.	IFF-99-22-035		
Bürgler D.E.	IFF-99-22-012		
Carsughi F.	IFF-99-22-014		
Chen J.	IFF-99-22-013	IFF-99-22-014	
Dallmeyer, A.	IFF-99-22-016		
Derz H.	IFF-99-22-014		
Divin Y.	IFF-99-22-018	IFF-99-22-019	IFF-99-22-020
Eberhardt W.	IFF-99-22-065		
Ebert Ph.	IFF-99-22-022	IFF-99-22-023	IFF-99-22-024
	IFF-99-22-025	IFF-99-22-047	IFF-99-22-066
	IFF-99-22-067	IFF-99-22-092	IFF-99-22-093
	IFF-99-22-094	IFF-99-22-095	IFF-99-22-123
Eisebitt S.	IFF-99-22-026		
Faley M.	IFF-99-22-027	IFF-99-22-028	
Faley M.I.	IFF-99-22-029	IFF-99-22-030	
Feuerbacher M.	IFF-99-22-004	IFF-99-22-017	IFF-99-22-031
	IFF-99-22-041	IFF-99-22-062	IFF-99-22-063
	IFF-99-22-081	IFF-99-22-082	IFF-99-22-098
Girgis E.	IFF-99-22-096		
Goerigk G.	IFF-99-22-032	IFF-99-22-033	
Gronckel de H.	IFF-99-22-096		
Grushko B.	IFF-99-22-003	IFF-99-22-010	IFF-99-22-017
	IFF-99-22-021	IFF-99-22-023	IFF-99-22-034
	IFF-99-22-036	IFF-99-22-066	IFF-99-22-067
	IFF-99-22-124	IFF-99-22-125	
Grünberg P.	IFF-99-22-012	IFF-99-22-096	IFF-99-22-097
Gutheim F.	IFF-99-22-035		
Harris J.	IFF-99-22-037	IFF-99-22-038	IFF-99-22-039
Haubold H.-G.	IFF-99-22-040		
Heggen M.	IFF-99-22-041		
Heiderich M.	IFF-99-22-011		

Heinze S.	IFF-99-22-042	IFF-99-22-043	IFF-99-22-044
	IFF-99-22-045		
Hiller P.	IFF-99-22-040		
Jia C.L.	IFF-99-22-020		
Jones R.	IFF-99-22-048	IFF-99-22-049	IFF-99-22-050
	IFF-99-22-051	IFF-99-22-052	IFF-99-22-053
	IFF-99-22-054	IFF-99-22-055	
Jung P.	IFF-99-22-056	IFF-99-22-057	
Jungbluth H.	IFF-99-22-040		
Karl A.	IFF-99-22-058		
Kehr, K.	IFF-99-22-059		
Kirstein O.	IFF-99-22-060	IFF-99-22-061	IFF-99-22-091
Klein H.	IFF-99-22-031	IFF-99-22-041	IFF-99-22-062
	IFF-99-22-063		
Klingeler R.	IFF-99-22-064	IFF-99-22-065	
Kluge F.	IFF-99-22-023	IFF-99-22-024	IFF-99-22-066
	IFF-99-22-067		
Kluge M.	IFF-99-22-068		
Kohlstedt H.	IFF-99-22-096	IFF-99-22-097	
Koizumi S.	IFF-99-22-069		
Kozielewski T.	IFF-99-22-061	IFF-99-22-091	
Kurz Ph.	IFF-99-22-005	IFF-99-22-070	IFF-99-22-071
	IFF-99-22-072	IFF-99-22-073	
Lentzen M.	IFF-99-22-074		
Liebsch A.	IFF-99-22-075		
Liu C.	IFF-99-22-057		
Lustfeld H.	IFF-99-22-076		
Luysberg M.	IFF-99-22-077	IFF-99-22-078	IFF-99-22-079
Lüttgens G.	IFF-99-22-080		
Müller-Krumbhaar H.	IFF-99-22-035	IFF-99-22-083	
Neeb M.	IFF-99-22-065	IFF-99-22-084	IFF-99-22-085
Nie X	IFF-99-22-009	IFF-99-22-086	
Persson B.	IFF-99-22-087	IFF-99-22-088	
Pontius N.	IFF-99-22-089		
Poppe U.	IFF-99-22-020	IFF-99-22-027	IFF-99-22-028
	IFF-99-22-029	IFF-99-22-030	
Pott G.	IFF-99-22-014		
Prager M.	IFF-99-22-061	IFF-99-22-090	IFF-99-22-091
Richter D.	IFF-99-22-046	IFF-99-22-061	IFF-99-22-091
Rottländer P.	IFF-99-22-096	IFF-99-22-097	
Schall P.	IFF-99-22-031	IFF-99-22-041	IFF-99-22-062
	IFF-99-22-098		
Schelten, J.	IFF-99-22-096		

Schliefer F.	IFF-99-22-057		
Schober H.	IFF-99-22-099		
Schroeder K.	IFF-99-22-002	IFF-99-22-100	IFF-99-22-112
	IFF-99-22-113		
Schwahn D.	IFF-99-22-001	IFF-99-22-011	IFF-99-22-015
	IFF-99-22-069	IFF-99-22-101	IFF-99-22-102
	IFF-99-22-103	IFF-99-22-104	
Schweika W.	IFF-99-22-105	IFF-99-22-106	
Schütz, G.	IFF-99-22-107	IFF-99-22-108	
Settels A.	IFF-99-22-109	IFF-99-22-110	IFF-99-22-111
Simon M.	IFF-99-22-024	IFF-99-22-025	
Soltner H.	IFF-99-22-027	IFF-99-22-028	
Steinbrecher J.	IFF-99-22-035		
Ullmaier H.	IFF-99-22-014	IFF-99-22-114	IFF-99-22-115
	IFF-99-22-116		
Urban K.	IFF-99-22-004	IFF-99-22-017	IFF-99-22-023
	IFF-99-22-024	IFF-99-22-025	IFF-99-22-027
	IFF-99-22-028	IFF-99-22-029	IFF-99-22-030
	IFF-99-22-031	IFF-99-22-041	IFF-99-22-062
	IFF-99-22-063	IFF-99-22-066	IFF-99-22-067
	IFF-99-22-074	IFF-99-22-081	IFF-99-22-082
	IFF-99-22-092	IFF-99-22-093	IFF-99-22-094
	IFF-99-22-095	IFF-99-22-098	IFF-99-22-117
	IFF-99-22-118	IFF-99-22-119	IFF-99-22-120
Vad Th.	IFF-99-22-040		
Willner L.	IFF-99-22-001	IFF-99-22-046	
Wischnewski A.	IFF-99-22-121		
Wortmann D.	IFF-99-22-122		
Yurechko M.	IFF-99-22-124	IFF-99-22-125	

Posters

IFF-99-23-001
Abbas B.
Thermische Fluktuationen der Zusammensetzung in einer binären Polymermischung und dem entsprechenden Diblockcopolymers als Funktion der Temperatur und des Druckes
Deutsche Neutronenstreutagung in Potsdam; 25.05. - 27.05.99
23.30.0

IFF-99-23-002
Abbas B.
Thermische Fluktuationen der Zusammensetzung in einer binären Polymermischung und dem entsprechenden Diblockcopolymers als Funktion der Temperatur und des Druckes
Frühjahrstagung der DPG in Leipzig; 01.03. - 03.03.99
23.30.0

IFF-99-23-003
Alefeld B.; Dohmen L.; Heidemann A.1
1ILL, Grenoble, France
GaAs as a Backscattering Crystal
Villigen, Switzerland, PSI, NOP99-Conference, 25. - 27.11.1999
23.89.1

IFF-99-23-004
Alefeld B.; Dohmen L.; Richter D.; Brückel Th.
X-Ray Space Technology for Focusing Small Angle Neutron Scattering and Neutron Reflectometry
Villigen, Switzerland, PSI, NOP99-Conference, 25. - 27.11.1999
23.89.1

IFF-99-23-005
Allen C.W.1; Schroeder H.; Hiller J.M.1
1Madison Area Techn. Coll., Madison
In situ study of dislocation behaviour in columnar of Al thin films on Si-substrate during thermal cycling
MRS Fall Meeting 1999, Boston, Symp. V "Thin Films - Stresses and Mechanical Properties VIII, 30.11.1999-12-19
23.42.0

IFF-99-23-006
Antons A.; Berger R.; Blügel S.; Schroeder K.
Ab initio investigation of ad-atom diffusion at surfaces
European Research Conference on Dynamical Processses at Surfaces, Lenggries
19. - 23.09.1999
23.20.0

IFF-99-23-007
Antons A.; Berger R.; Blügel S.; Schroeder K.
Ab-intio Untersuchungen der Adatom Diffusion auf Si(111) (3x3)
DPG-Frühjahrstagung, Münster, 22.03.1999
23.42.0

IFF-99-23-008
Antons A.; Berger R.; Blügel S.; Schroeder K.
Ab-intio Untersuchungen der Adatom Diffusion auf Si(111) (3x3)
European Research Conference on Dynamical Process at Surfaces, Lenggries, 19.-23.09.1999
23.42.0

IFF-99-23-009
Asada T.1; Blügel S.; Bihlmayer G.; Abt R.
1Faculty of Engineering, Shizuoka University, Hamamatsu, Japan
First Principles Investigation of the Stability of 3d Monolayer/Fe(001) against Bilayer Formation
44th Annual Conference on Magnetism and Magnetic Materials, San Jose, CA
16.11.1999
3.20.0

IFF-99-23-010
Attenkofer K.1; Caliebe W.; Chatterji T.2; Richter R.1
1University, Würzburg
2ILL, Grenoble, France
Magnetism Probed with Synchrotron Radiation Methods
Hamburg, HASYLAB, Users' Meeting, 29.01.1999
23.20.0, 23.89.1

IFF-99-23-011
Beiner M.1; Kahle S.; Meissner M.2; Hempel E.1; Donth E.1
1Fachbereich Physik, Universität Halle
2HMI in Berlin
Zusammenhang von Tieftemperatur-Wärmekapazität und Kooperativität des Glasübergangs
DPG-Frühjahrstagung in Leipzig vom 01.03.99-03.03.99
23.30.0

IFF-99-23-012
Berger R.; Blügel S.; Antons A.; Kromen Wi.; Schroeder K.
A Parallelized ab intio Molecular Dynamics Code for the Investigation of Atomistic Growth Processes
NIC-Workshop "Molecular Dynamics on parallel Computers", FZ Jülich, 08.02.-10.02.1999
23.42.0

IFF-99-23-013
Dallmeyer A.
Electronic structure of epitaxial fcc-Mn films
DPG-Frühjahrstagung in Münster
März 1999
23.20.0

IFF-99-23-014
Eisebitt S.; Wirth I.; Kann G.; Eberhardt W.
Electronic structure of single wall carbon nanotubes in buckypaper
XIII International Winterschool on Electronic Properties of novel Materials - Science and Technology of Molecular Nanostructures, Kirchberg, Tirol
März 1999
23.20.0

IFF-99-23-015
Emtsev V.V.1; Ehrhart P.; Poloskin D.S.1; Dedek U.
1 IOFFE Institut, St. Petersburg, Russia
Electron irradiation of heavily doped silicon: group-III impurty ion pairs
20th Int. Conf. Defects in Semiconductors, ICDS-20, Berkeley, CA, 26.07.-30.07.1999-12-19
23.55.0

IFF-99-23-016
Endo H.; Allgaier J.; Monkenbusch M.; Richter D.; Jakobs B.1; Sottmann T.1; Strey R.1
1Institut für Physikalische Chemie, Köln
PEP-PEO block copolymers as efficiency booster for microemulsions: a SANS investigation of the role of the block copolymer
73. ACS Colloid and Surface Science Symposium, MIT, Cambridge, Massachusetts, USA, 13.07.99 - 16.07.99
23.30.0

IFF-99-23-017
Endo H.; Allgaier J.; Monkenbusch M.; Richter D.; Jakobs B.1; Sottmann T.1; Strey R.1
1Institut für Physikalische Chemie, Köln
PEP-PEO block copolymers as efficiency booster for microemulsions: a SANS investigation of the role of the block copolymer
Conference of the European Colloid and Interface Society, Dublin, Irland, 12.09.99 - 17.09.99
23.30.0

IFF-99-23-018

Goerigk G.; Williamson D. L.1
1Colorado School of Mines, Department of Physics, USA
Nanostructural Characterization of a-SiGe:H Alloys by Anomalous Small-Angle X-Ray Scattering
Hamburg, HASYLAB, Users' Meeting, 29.01.1999
23.89.1

IFF-99-23-019
Heinrich M.; Pyckhout-Hintzen W.; Richter D.; Straube E.1
1Martin-Luther-Universität, Fachbereich Physik, Halle
A SANS study of quenched H-polymer melts under strain
Frontiers in SAXS/SANS workshop in Grenoble, France; 12.02.99 - 13.02.99
23.30.0

IFF-99-23-020
Heinrich M.; Pyckhout-Hintzen W.; Richter D.; Straube E.1
1Martin-Luther-Universität, Fachbereich Physik, Halle
A SANS study of quenched H-polymers under strain
DPG-Frühjahrstagung in Leipzig vom 01.03. - 03.03.99
23.30.0

IFF-99-23-021
Heinrich M.; Pyckhout-Hintzen W.; Richter D.; Straube E.1
1Martin-Luther-Universität, Fachbereich Physik, Halle
Frühjahrstagung der Deutschen Physikalischen Gesellschaft in Leipzig; 01.03.99 - 03.03.99
23.30.0

IFF-99-23-022
Heinze S.; Asada T.1; Blügel S.
1Faculty of Engineering, Shizuoka University, Hamamatsu, Japan
Ab initio Calculations of STM and STS on Magnetic thin Films: Mn and Cr on Fe(001)
44th Annual Conference on Magnetism and Magnetic Materials, San Jose, CA
18.11.1999
3.20.0

IFF-99-23-023
Hempel E.1; Kahle S.; Donth E.1
1Fachbereich Physik, Universität Halle
Charakteristische Länge und Kooperativität des dynamischen Glasübergangs in einem breiten Fragilitätsbereich
Frühjahrstagung in Leipzig vom 01.03.99-03.03.99
23.30.0

IFF-99-23-024
Hupfeld D.; Schweika W.; Strempfer J.1; Caliebe W.; Mattenberger K.2; McIntyre G.3; Brückel Th.
1APS at ANL, Ames, USA
2ETH, Laboratorium für Festkörperphysik, Zürich, Switzerland
3ILL, Grenoble, France
Element-specific magnetic order and competing interactions in GdxEu1-xS
Plymouth, USA, Gordon research conference on x-ray physics, 25. - 30.07.1999
23.89.1

IFF-99-23-025
Jung P.; Klein H.; Chen J.
A comparison of defects included in helium implanted (- and (-SiC
9th Int. Conf. on Fusion Reactor Materials, 12.10.1999, Colorado Springs, USA
23.80.5

IFF-99-23-026
Kahle S.; Schröter E.1; Hempel E.1; Donth E.1
1Fachbereich Physik, Universität Halle
Temperaturabhängigkeit der Kooperativität in der Crossover Region des dynamischen Glasübergangs von Benzoin isobutylether
DPG Frühjahrstagung in Leipzig vom 01.03.-03.03.99
23.15.0

IFF-99-23-027
Karl A.; Eisebitt S.; Freiwald M.; Scherer R.; Eberhardt W.
Soft X-ray emission and resonant inelastic soft X-ray scattering on InP
HASYLAB Annual Users Meeting 1999, Hamburg
29.01.1999
3.20.0

IFF-99-23-028
Karl A.; Eisebitt S.; Scherer R.; Eberhardt W.; Weidinger A.1; Hirsch A.2
1Hahn-Meitner-Institut, Berlin
2Universität Erlangen
Electronic structure of (C59N)2 studied locally at the Nitrogen site by soft x-ray emission and resonant inelastic scattering
18th International Conference on X-ray and Inner-shell Processes, Chicago, IL
23. - 27.08.1999
23.20.0

IFF-99-23-029
Kentzinger E.; Rücker U.; Caliebe W.; Goerigk G.; Werges F.; Nerger S.; Voigt J.; Schmidt W.; Alefeld B.; Fermon C.1; Brückel Th.
1DRECAM/SPEC, CEA Saclay, Gif sur Yvette, France
Structural and magnetic characterization of Fe/(-Mn thin films
Budapest, Hungary, ECNS '99 Conference, 01.09.1999
23.89.1

IFF-99-23-030
Kirstein O.; Grimm H.; Prager M.; Kozielewski T.
Designstudien zum Rückstreuspektrometer für den FRM-2
Verbundtreffen in Potsdam am 26.05.99
23.89.1

IFF-99-23-031
Kirstein O.; Prager M.;Johnson M.R.; Combet J.
Ammonia group rotation in Zn(NH3)4I2
QAMS '99, Krakow, Polen 26.09. - 30.09.99
23.15.0

IFF-99-23-032
Klingeler R.
Mass spectra of metal-doped carbon and fullerene clusters Mx@Cn<120 (M = Sc, Y, La, Ca, Ce; x = 1,2)
Clustertreffen, Sassnitz, Rügen
26.09. - 01.10.99
23.20.0

IFF-99-23-033
Kluge M.
Diffusion in unterkühlten Schmelzen und Gläsern aus Cu33 Zr67
DPG-Frühjahrstagung, Münster, 22.03.-26.03.1999
23.30.0

IFF-99-23-034
Kluge M.
Diffusion mechanisms in liquid and amorphous Cu33 Zr67
Summerschool "Physics of Glasses: Structure and Dynamics", Universität Montpellier, 10.05.-22.05.1999
23.30.0

IFF-99-23-035
Kluge M.
Diffusion mechanisms in under-cooled binary liquids of Cu33 Zr67
NIC-Workshop "Molecular Dynamics on Parallel Computers", FZ Jülich, 08.02.-10.02.1999
23.30.0

IFF-99-23-036
Kohlstedt H.; de Gronckel H.; Schmitz R.
Oxidation Methods and Analytical Studies of the Structure of Magnetic Tunnel Junctions

44th Annual Conference on Magnetism and Magnetic Materials, San Jose, CA
15.11.99
3.42.0

IFF-99-23-037
Kromen W.; Berger R.; Antons A.; Schroeder K.; Blügel S.
EStCoMMP, a parallelized (ab initio) molecular dynamics code for the investigation of atomistic growth processes
European Research Conference on Dynamical Processses at Surfaces, Lenggries
19. - 23.09.1999
23.20.0

IFF-99-23-038
Köbler U.
Modifizierte Bloch Exponenten für halbzahlige und ganzzahlige Spinquantenzahlen
Potsdam, Deutsche Neutronenstreutagung 1999, 25.05.1999
23.15.0

IFF-99-23-039
Lüttgens G.; Ponitius N.; Friedrich C.; Bechthold P.S.; Neeb M.; Eberhardt W.
Photoelectron spectra of benzene-adsorbed metal cluster anions
Gordon Conference on Photoions, Photoionization and Photodetachment, Plymouth State College, New Hampshire, USA
18.07.1999
3.20.0

IFF-99-23-040
Lüttgens G.; Pontius N.; Friedrich C.; Bechthold P.S.; Neeb M.; Eberhardt W.
Photoelectron spectroscopy of Benzene-adsorbed metal cluster anions
Clustertreffen, Sassnitz, Rügen
26.09. - 01.10.99
23.20.0

IFF-99-23-041
Morenzin J.; Schlebsuch C.; Kessler B.; Eberhardt W.
Charge Transfer and relaxation dynamics of excited electronic states in organic photoreceptor materials with and without C60
XIII International Winterschool on Electronic Properties of novel Materials - Science and Technology of Molecular Nanostructures, Kirchberg, Tirol
März 1999
23.20.0

IFF-99-23-042
Nie X.; Heinze S.; Weinert M.1; Blügel S.
1Brookhaven National Laboratory, Upton, USA
Magnetic surfaces under static external electric fields
211. WE-Heraeus Seminar (Magnetic Nanostructures), Physikzentrum Bad Honnef
04. - 06.01.1999
23.20.0

IFF-99-23-043
Pontius N.; Bechthold P.S.; Neeb M.; Eberhardt W.
Time-resolved photoelectron spectra of Pt3- using femtosecond laser pulses
Gordon Conference on Photoions, Photoionization and Photodetachment, Plymouth State College, New Hampshire, USA
18.07.1999
3.20.0

IFF-99-23-044
Pontius N.; Bechthold P.S.; Neeb M.; Eberhardt W.
Ultrafast hot-electron dynamics observed in Pt3- using time-resolved photoelectron spectroscopy
Clustertreffen, Sassnitz, Rügen
26.09. - 01.10.99
23.20.0

IFF-99-23-045
Prager M.
Schiebel P.1; Prager M.; Ritter H.2; Ihringer J.1; Prandl W.1
1Institut für Kristallographie, Universität Tübingen
2Institut Laue-Langevin, Grenoble
Phase transition in partially deuterated (NX4PdCl6(X= H1-yDy) studied by inelastic neutron scattering and diffraction methods
Verbundtreffen in Potsdam am 26.05.99
23.15.0

IFF-99-23-046
Prager M.'
The thermal time-of-flight spectrometer SV29 at FZ-Jülich: focusing in space and time
Neutron Optics '99 in Villigen am 28.11.99
23.89.1

IFF-99-23-047
Prager M.; Grimm H.; Parker S.F.1; McGrady S.2
1Rutherford-Appleton Laboratories, Chilton, United Kingdom
2Kings College, London
Rotational potentials of bridging and terminal methyl groups in trimethylaluminum-dimers
2nd European Conference on Neutron Scattering in Budapest (ECNS'99) am 03.09.99
23.15.0

IFF-99-23-048
Pyckhout-Hinten W.; Westermann S.; Botti A.; Urban V.1; Richter D.; Straube E.2
1ESRF in Grenoble
2Martin-Luther-Universität, Fachbereich Physik, Halle
Studies of reinforcement by SANS
Gordon Research Conference on elastomers, networks and gels in New Hamp vom 18.07. - 23.07.99
23.30.0

IFF-99-23-049
Rottländer P.; Kohlstedt H.; Girgis E.; de Gronckel H.; Schelten J.; Grünberg P.
TMR structures with barriers produced by UV oxidation
DPG-Frühjahrstagung in Münster
23.03.1999
3.42.0

IFF-99-23-050
Rücker U.
Charakterisierung von dünnen (-Mn-Schichten mit Streumethoden
Münster, DPG-Tagung, 23.03.1999
23.89.1

IFF-99-23-051
Rücker U.; Alefeld B.; Bergs W.; Kentzinger E.; Brückel Th.
The new polarized neutron reflectometer in Jülich
Villigen, Switzerland, NOP99-Conference, 25. - 27.11.1999
23.89.1

IFF-99-23-052
Rücker U.; Bergs W.; Alefeld B.; Kentzinger E.; Brückel Th.
The new polarized neutron reflectometer in Jülich
Budapest, Hungary, ECNS '99 Conference, 01.09.1999
23.89.1

IFF-99-23-053
Schroeder H.; Allen C.W.1; Hiller J.M.2
1 ANL, Argonne, USA
2 Madison Area Techn. Coll., Madison, USA
In situ study of dislocation behaviour in columnar of Al thin films on Si-substrate during thermal cycling
MRS Fall Meeting 1999, Boston Symposium V "Thin Films - Stresses and Mechancial Properties VIII", 30.11.99
23.42.0

IFF-99-23-054

Schweika W.
Einfluß des Magnetismus auf die chemische Ordnung und Nahordnung in Fe Al Legierungen
Potsdam, Deutsche Neutronenstreutagung N99, 25.05.1999
23.55.0

IFF-99-23-055
Schweika W.
Strukturfaktoren von polyalkylmethacrylaten als Beispiel für Seitenkettenpolymere
Potsdam, Deutsche Neutronenstreutagung N99, 26.05.1999
23.30.0, 23.89.1

IFF-99-23-056
Schätzler R.
Instrumentierung am FRJ-II in Jülich
Deutsche Neutronenstreutagung 1999, Potsdam, 25.-27.05.1999
23.89.1

IFF-99-23-057
Schütz, G.
Dynamical Theory of Steady-State Selection in Open Driven Diffusive Systems
Traffic and Granular Flow, Konferenzbeitrag, 28. 9. 1999

IFF-99-23-058
Spatschek R.; Brener E.; Müller-Krumbhaar H.
Oberflächeninstabilitäten von Rissen
DPG-Frühjahrstagung, Münster, 22.03.-26.03.1999
23.15.0

IFF-99-23-059
Willner L.; Poppe A.; Allgaier J.; Monkenbusch M.; Richter D
Micellarization of Amphiphilic PEP-PEO Block Copolymers
Gordon Research Conference on Polymers in Oxford; 04.07. - 08.07.99
23.30.0

IFF-99-23-060
Willner L.; Poppe A.; Allgaier J.; Stellbrink J.; Lindner P.1; Richter D.
1Institut Laue-Langevin, Grenoble
Aggregation Behavior of Amphiphilic PEP-PEO Block Copolymers
Polymer & Materials Research Symposium in Bayreuth; 11.04 - 13.04.99
23.30.0

IFF-99-23-061
Wirth I.; Kann G.; Eisebitt S.; Eberhardt W.
Elektronische Struktur von Kohlenstoffnanoröhren in "Buckypaper"
DPG-Frühjahrstagung in Münster
24.03.1999
3.20.0

IFF-99-23-062
Wortmann D.
Scanning tunneling microscopy of magnetic surface alloys
5th Workshop Full-Potential LAPW calculations with the WIEN97 code, Wien
09.04.1999
3.20.0

IFF-99-23-063
Yan S.-S.; Schreiber R.; Grünberg P.
Noncollinear Coupling in Fe/Mn/Fe Trilayers and ist Dependence on Growth Conditions
44th Annual Conference on Magnetism and Magnetic Materials, San Jose, CA
17.11.1999-09-01
3.42.0

IFF-99-23-064
Zeiske Th.
Structure and magnetism of Ho0.2Ca0.8MnO3
Budapest, Hungary, ECNS '99 Conference, 01. - 04.09.1999
23.89.1

IFF-99-23-065
Zorn, R.
Absence of ageing effect in the vibrational density of states of glass-forming polybutadiene
Sonderforschungsbereich 262, Workshop Aging Phenomena in Glassy Systems, Mainz, 03.12.99
23.15.0

List of references

Abbas B.	IFF-99-23-001	IFF-99-23-002	
Abt R.	IFF-99-23-009		
Alefeld B.	IFF-99-23-003	IFF-99-23-004	IFF-99-23-029
	IFF-99-23-051	IFF-99-23-052	
Allgaier J.	IFF-99-23-016	IFF-99-23-017	IFF-99-23-059
	IFF-99-23-060		
Antons A.	IFF-99-23-006	IFF-99-23-007	IFF-99-23-008
	IFF-99-23-012	IFF-99-23-037	
Bechthold P.S.	IFF-99-23-039	IFF-99-23-040	IFF-99-23-043
	IFF-99-23-044		
Berger R.	IFF-99-23-006	IFF-99-23-007	IFF-99-23-008
	IFF-99-23-012	IFF-99-23-037	
Bergs W.	IFF-99-23-051	IFF-99-23-052	
Bihlmayer G.	IFF-99-23-009		
Blügel S.	IFF-99-23-006	IFF-99-23-007	IFF-99-23-008
	IFF-99-23-009	IFF-99-23-012	IFF-99-23-022
	IFF-99-23-037	IFF-99-23-042	
Botti A.	IFF-99-23-048		
Brener E.	IFF-99-23-058		
Brückel Th.	IFF-99-23-004	IFF-99-23-024	IFF-99-23-029
	IFF-99-23-051	IFF-99-23-052	
Caliebe W.	IFF-99-23-010	IFF-99-23-024	IFF-99-23-029
Chen J.	IFF-99-23-025		
Dallmeyer A.	IFF-99-23-013		
Dedek U.	IFF-99-23-015		
Dohmen L.	IFF-99-23-003	IFF-99-23-004	
Eberhardt W.	IFF-99-23-014	IFF-99-23-027	IFF-99-23-028
	IFF-99-23-039	IFF-99-23-040	IFF-99-23-041
	IFF-99-23-043	IFF-99-23-044	IFF-99-23-061
Ehrhart P.	IFF-99-23-015		
Eisebitt S.	IFF-99-23-014	IFF-99-23-027	IFF-99-23-028
	IFF-99-23-061		
Endo H.	IFF-99-23-016	IFF-99-23-017	
Freiwald M.	IFF-99-23-027		
Friedrich C.	IFF-99-23-039	IFF-99-23-040	
Girgis E.	IFF-99-23-049		
Goerigk G.	IFF-99-23-018	IFF-99-23-029	
Grimm H.	IFF-99-23-030	IFF-99-23-047	
Grünberg P.	IFF-99-23-049	IFF-99-23-063	
Heinrich M.	IFF-99-23-019	IFF-99-23-020	IFF-99-23-021
Heinze S.	IFF-99-23-022	IFF-99-23-042	
Hupfeld D.	IFF-99-23-024		
Jung P.	IFF-99-23-025		
Kahle S.	IFF-99-23-011	IFF-99-23-023	IFF-99-23-026

	IFF-99-23-012	IFF-99-23-037	
Schweika W.	IFF-99-23-024	IFF-99-23-054	IFF-99-23-055
Schätzler R.	IFF-99-23-056		
Schütz, G.	IFF-99-23-057		
Spatschek R.	IFF-99-23-058		
Stellbrink J.	IFF-99-23-060		
Voigt J.	IFF-99-23-029		
Werges F.	IFF-99-23-029		
Westermann S.	IFF-99-23-048		
Willner L.	IFF-99-23-059	IFF-99-23-060	
Wirth I.	IFF-99-23-014	IFF-99-23-061	
Wortmann D.	IFF-99-23-062		
Yan S.-S.	IFF-99-23-063		
Zeiske Th.	IFF-99-23-064		
Zorn R.	IFF-99-23-065		
de Gronckel H.	IFF-99-23-036	IFF-99-23-049	

Patents

Patents granted

IFF-99-31-001
Althaus M.,; Küssel E.; Sonnenberg K.:
Verfahren und Vorrichtung zur Gewinnung rißfreier Kristalle
EP: 0760024 (07.07.99) (CH, DE, FR, GB, NL)
PT 1.1209
23.42.0

IFF-99-31-002
Blügel S.; Nie X.:
Elektrisches Feld für Ummagnetisierung eines dünnes Films
DE: 19841034 (06.08.99)
PT 1.1610
23.20.0

IFF-99-31-003
Divin Y.Y.; Seo J.W.; Poppe U.:
Schichterfolge mit wenigstens einer epitaktischen nicht c-Achsen orientierten Schicht aus einer mit Hochtemperatursupraleitern kristallographisch vergleichbaren Struktur
DE: 19648234 (08.07.99)
PT 1.1333a
23.42.0

IFF-99-31-004
Ghosh I.; Klein N.; Poppe U.:
Abstimmbarer Hochraumresonator
DE: 19841078 (12.10.99)
PT 1.1617
23.42.0

IFF-99-31-005
Hojczyk R.; Jia C.L.; Poppe U.:
Schichtenfolge mit einem hochtemperatursupraleitenden Material und deren Verwendung
DE: 19634645 (24.06.99)
PT 1.1386
23.42.0

IFF-99-31-006
Klein N.; Dähne U.; Tellmann N.:
Verfahren zur Qualitätsbestimmung eines einzelnen supraleitenden Filmes und Vorrichtung zur Durchführung dieses Verfahrens
EP: 0580836 (13.01.99) (DE, FR, GB, NL)
PT 1.1117
23.42.0

IFF-99-31-007
Poppe U.; Schubert J.; Evers W.;
Verfahren zur Herstellung dünner Schichten aus oxydischem Hochtemperatur-Supraleiter
JP: 2868526 (25.12.98)
PT 1.889
23.42.0

IFF-99-31-008
Speier W.; Szot K.:
ABO_3 Perowskit mit Stufe
DE: 19808778 (01.06.99)
PT 1.1563
23.42.0

List of references

Althaus M.	IFF-99-31-001
Blügel S.	IFF-99-31-002
Dähne U.	IFF-99-31-006
Divin Y.Y.	IFF-99-31-003
Evers W.	IFF-99-31-007
Ghosh I.	IFF-99-31-004
Hojczyk R.	IFF-99-31-005
Jia C.L.	IFF-99-31-005
Klein N.	IFF-99-31-004 IFF-99-31-006
Küssel E.	IFF-99-31-001
Nie X.	IFF-99-31-002
Poppe U.	IFF-99-31-003 IFF-99-31-004 IFF-99-31-005 IFF-99-31-007
Schubert J.	IFF-99-31-007
Seo J.W.	IFF-99-31-003
Sonnenberg K.	IFF-99-31-001
Speier W.	IFF-99-31-008
Szot K.	IFF-99-31-008
Tellmann N.	IFF-99-31-006

Patents applied for

IFF-99-32-001
Allgaier J.; Richter D.; Willner L.; Strey R.; Jakobs B.; Sottmann T.:
Verfahren zur Effiziensteigerung von Tensiden bei simultaner Unterdrückung lamellarer Mesophasen sowie Tenside, welchen ein Additiv beigefügt ist
PCT: PCT/DE99/02748 (26.08.99) (EP,US,JP)
PT 1.1605 G
23.15.0

IFF-99-32-002
Baldus O.; Waser R.; Krasser W.:
Lasersystem mit steuerbarer Pulsdauer
DE: 199 (.12.99)
PT 1.1754
23.42.0

IFF-99-32-003
Baldus O.; Waser R., Krasser W.:
Verfahren zur Herstellung einer kristallisierten keramischen Schicht durch Laser-Annealing
DE 199 (.12.99)
PT 1.1755
23.42.0

IFF-99-32-004
Blügel S.; Nie X.:
Elektrisches Feld für Ummagnetisierung eines dünnen Films
PCT: PCT/DE99/02840 (08.09.99) (EP,US,JP)
PT 1.1610
23.20.0

IFF-99-32-005
Dohmen L.; Alefeld B.:
Geschwindigkeitsselektor zur Monochromatisierung eines Neutronenstrahls
DE: 19904562.3 (04.02.99)
PT 1.1656
23.89.1

IFF-99-32-006
Eberhardt W.; Morenzin J.:
Markierungseinrichtung
PCT: PCT/EP 99/08433 (03.11.99) (EP,US,JP)
PT 1.1633
23.42.0

IFF-99-32-007
Gosh I.; Klein N.; Poppe U.
Abstimmbarer Hohlraumresonator,
PT 1.1617
23.42.0

IFF-99-32-008
Grossmann M. 1; Hoffmann S.; Slowak R.1; Waser, R.
1 Institut für Werkstoffe der Elektrotechnik
Keramischer Mehrlagen-Dünnschichtkondensator
PT 1.1560
Deutsche Patentanmeldung 198 06 002.5
23.42.0

IFF-99-32-009
Hoffmann S.; Waser R.; Slowak R.1; Liedtke R.1
1 Institut für Werkstoffe der Elektrotechnik, RWTH Aachen
Dünnschichtkondensator
Deutsche Patentanmeldung 199 42 341.5

IFF-99-32-010
Kohlstedt H.H.
Speicherkondensator
Deutsche Patentanmeldung 199 32 844.7
23.42.0

IFF-99-32-011
Kohlstedt, H.H.; Rottländer P.
Verfahren zur Herstellung eines magnetischen Tunnelkontaktes sowie magnetischer Tunnelkontakt
DE 199 38 215.8
23.42.0

IFF-99-32-012
Mantl S.; Zhao Q.T.; Kappius L.; Antons A.:
Verfahren zur Herstellung von Nanostrukturen in dünnen Filmen
PCT: PCT/DE99/03683 (18.11.99) (EP,US,CA,JP,KR)
PT 1.1626
29.87.0

IFF-99-32-013
Rickes J.; Tiedke S.1
1 Institut für Werkstoffe der Elektrotechnik, RWTH Aachen
Ein-/Ausleseverfahren zur Speicherung/Ausgabe eines Signalmusters unter Verwendung eines dynamischen Halbleiterspeichers
Deutsche Patentanmeldung 199 40 923.4
23.42.0

IFF-99-32-014
Schornstein S.; Klein N.; Ghosh I.:
Mehrpol–Bandpaßfilter mit elliptischer Filtercharakteristik
PCT: PCT/DE99/01447 (12.05.99) (EP,US,CA,RU,JP)
PT 1.1596
23.42.0

IFF-99-32-015
Sonnenberg K.; Küssel E.; Bünger Th.; Flade T.; Weinert B.; Fa. Freiberger:
Vorrichtung zur Herstelung von Einkristallen
DE: 19912484.1 (19.03.99)
PT 1.1680 G
23.42.0

IFF-99-32-016
Sonnenberg K.; Küssel E.; Bünger Th.; Flade T.; Weinert B.; Fa. Freiberger:
Verfahren und Vorrichtung zur Herstellung von Einrkristallen
DE: 19912486.8 (19.03.99)
PT 1.1681 G
23.42.0

IFF-99-32-017
Speier W.; Szot K.:
ABO_3-Perowski mit Stufe
PCT: PCT/DE99/00587 (25.02.99) (EP,US,JP)
PT 1.1563
23.32.0

IFF-99-32-018
Szot K., Speier W.1
1 Institut für Chemische Analysen
Teleskopartiger Mikromanipulator mit Piezomaterialien
Deutsche Patentanmeldung 199 16 277.8-15

IFF-99-32-019
Waser R.; Baldus O.; Hoffmann S.; Schuster A.:
Verfahren zur Herstellung einer oder mehrer kristallisierter keramischer Dünnschichten sowie Bauelement mit einer solchen Schicht
PCT: PCT/DE 99/00478 (15.02.99) (EP,US,JP,KR)
PT 1.1557
23.42.0

IFF-99-32-020
Zimmermann E.; Faley M.; Poppe U.
Magnetflußsensor mit schleifenförmigem Magnetfeldleiter sowie dessen Herstellung
PT 1.1674
23.42.0

List of references

Allgaier J.	IFF-99-32-001		
Alefeld B.	IFF-99-32-005		
Antons A.	IFF-99-32-012		
Baldus O.	IFF-99-32-002	IFF-99-32-003	IFF-99-32-019
Blügel S.	IFF-99-32-004		
Dohmen L.	IFF-99-32-005		
Eberhardt W.	IFF-99-32-006		
Faley M.	IFF-99-32-020		
Gosh I.	IFF-99-32-007	IFF-99-32-014	
Hoffmann S.	IFF-99-32-008	IFF-99-32-009	IFF-99-32-019
Jakobs B.	IFF-99-32-001		
Klein N.	IFF-99-32-007	IFF-99-32-014	
Kohlstedt H.H.	IFF-99-32-010	IFF-99-32-011	
Krasser W.	IFF-99-32-002	IFF-99-32-003	
Küssel E.	IFF-99-32-015	IFF-99-32-016	
Morenzin J.	IFF-99-32-006		
Nie X.	IFF-99-32-004		
Poppe U.	IFF-99-32-007	IFF-99-32-020	
Richter D.	IFF-99-32-001		
Rickes J.	IFF-99-32-013		
Rottländer P.	IFF-99-32-011		
Schornstein S.	IFF-99-32-014		
Schuster A.	IFF-99-32-019		
Sonnenberg K.	IFF-99-32-015	IFF-99-32-016	
Sottmann T.	IFF-99-32-001		
Strey R.	IFF-99-32-001		
Szot K	IFF-99-32-017	IFF-99-32-018	
Waser R.	IFF-99-32-002 IFF-99-32-009	IFF-99-32-003 IFF-99-32-019	IFF-99-32-008
Willner L.	IFF-99-32-001		

SS 99, Neutronenphysikalischs Praktikum, Sept. '99
23.30.0

IFF-99-04-025
Richter D.
Atomkerne als Festkörpersonden
WS 98, 30. IFF Ferienkurs: Magnetische Schichtsysteme, 04.03.99
23.30.0

IFF-99-04-026
Richter D.
Dynamik Weicher Materie
SS 99, Neutronenphysikalisches Praktikum, Sept. '99
23.30.0

IFF-99-04-027
Richter D.
Korrelationsfunktionen
SS 99, Neutronenphysikalisches Praktikum, Sept. '99
23.30.0

IFF-99-04-028
Richter D.
Struktur und Dynamik fester Ionenleiter
SS 99, Forschungspraktikum in Münster
23.30.0

IFF-99-04-029
Richter D.
Über die Bedeutung der Forschung mit Neutronen
SS 99, Neutronenphysikalisches Praktikum, Sept. '99
23.89.1

IFF-99-04-030
Richter D.
Polymerdynamik
SS 99, DPG-Sommerschule Soft Condensed Matter am 27.09.99 in Bad Honnef
23.30.0

IFF-99-04-031
Schober T.
Untersuchung von Materialien mit Elektronen- und Röntgenstrahlen
RWTH Aachen, WS 1999/2000
23.42.0

IFF-99-04-032
Schroeder H.
Neue Materialien und Bauelemente für die Informationstechnik I
RWTH Aachen, WS 1999/2000
23.42.0

IFF-99-04-033
Schroeder H.
Theoretische Metallkunde I
RWTH Aachen, WS 1999/2000
23.42.0

IFF-99-04-034
Schroeder H.
Theoretische Metallkunde I
RWTH Aachen, WS 98/99
23.42.0

IFF-99-04-035
Schroeder K.
Atomarer Magnetismus und Austauschwechselwirkung
30. IFF-Ferienkurs "Magnetische Schichtsysteme in Forschung und Anwendung", FZ Jülich, 01.03.1999
23.42.0

IFF-99-04-036
Schroeder K.
Computeranwendungen in der Festkörperphysik
Seminar RWTH Aachen, SS1999
23.42.0

IFF-99-04-037
Schwahn D.
Kleinwinkelstreuung und Reflexion mit Neutronen
SS 99, Neutronenphysikalisches Praktikum, Sept. '99
23.30.0

IFF-99-04-038
Schwahn D.
Weiche Materie - Struktur
SS 99, Neutronenphysikalisches Praktikum, Sept. '99
23.30.0

IFF-99-04-039
Schweika, W.
Schichtpräparation mit Sputterverfahren
WS 98/99, RWTH Aachen und IFF-Ferienkurs, V1
1.2 FKF

IFF-99-04-040
Schütz, G.
Einführung in die Polymerphysik
Universität Bonn, Wintersemester 1999/2000

IFF-99-04-041
Schütz, G.
Stochastische Vielteilchensysteme
Universität/Gesamthochschule Essen, Sommersemester 1999

IFF-99-04-042
Sturm K.
Elektronentheorie
WS 98/99, 30. IFF-Ferienkurs "Magnetische Schichtsysteme", 01-12.03.1999

IFF-99-04-043
Sturm K.
Elektronische Anregungen im Festkörper
SS 99, Universität Düsseldorf, V 2

IFF-99-04-044
Urban K.; Luysberg M.; Ebert Ph.; Klein N.
Experimentalphysikseminar "Die Physik und Technik der Nanostrukturen"
WS 98/99
23.42.0
3.55.0

IFF-99-04-045
Urban K.; Luysberg M.; Ebert Ph.; Thust A.; Klein N.
Experimentalphysikseminar "Physik der Nanostrukturen"
SS 1999
23.42.0
3.55.0

IFF-99-04-046
Waser R.
Vorlesung Werkstoffe der Elektrotechnik
Sensoren und Sensormeßtechnik I+II
RWTH Aachen

IFF-99-04-047
Waser, R.; Ehrhart P.; Hoffmann S.; Kohlstedt H.H.; Schroeder, H.
Neue Materialien und Bauelemente für die Informationstechnik I
RWTH Aachen, WS 1999/2000
23.42.0

Lecture

Lecture courses

IFF-99-04-001
Baumgarten L.
Winkelaufgelöste Photoemission zur Bandstrukturbestimmung in Festkörpern
IFF-Ferienschule 1999
05.03.1999
3.20.0

IFF-99-04-002
Bechthold P.S.
Cluster und Clustermaterie
SS 1999

IFF-99-04-003
Blügel S.
Theorie der magnetischen Anisotropie
IFF-Ferienschule 1999
03.03.1999
3.20.0

IFF-99-04-004
Brückel, Th.
Beugungsmethoden zur Untersuchung von Dünnschichtsystemen
WS 98/99, RWTH Aachen und IFF-Ferienkurs, V2
1.2 FKF

IFF-99-04-005
Brückel, Th., Eberhardt, W.
WS 99/00, IFF-Ferienschule: Von neV bis fsec: Dynamik der kondensierten Materie
V 40 / Ü 10

IFF-99-04-006
Brückel, Th.; Capellmann, H.; Schweika, W.; Zeiske, Th.
WS 98/99, Seminar: Aktuelle Aspekte des Festkörpermagnetismus
TÜ 2

IFF-99-04-007
Brückel, Th.; Schweika, W.; Zeiske, Th.
WS 99/00, Ferienschule (Praktikum) über Neutronenstreuung
TV 10 / TÜ 30

IFF-99-04-008
Carbone C.
Photoemission from magnetic films
IFF-Ferienschule 1999
05.03.1999
3.20.0

IFF-99-04-009
Dederichs P.H.
Computeranwendungen in der Festkörperphysik
Seminar RWTH Aachen, SS 1999
23.20.0

IFF-99-04-010
Dederichs P.H.
Magnetismus und Magnetoelektronik
RWTH Aachen, SS 1999
23.20.0

IFF-99-04-011
Dederichs P.H.
Spinabhängiges Tunneln
30. Ferienkurs des IFF: "Magnetische Schichtsysteme", FZ Jülich, 09.03.1999
23.20.0

IFF-99-04-012
Eberhardt W.; Grünberg P.; Bürgler D.
Oberseminar: "Magnetische Schichtsysteme in Forschung und Anwendung"
WS 99/00

IFF-99-04-013
Ehrhart P.
Präparation dünner Schichten: Molekularstrahlepitaxie
30. IFF-Ferienkurs "Magnetische Schichtsysteme in Forschung und Anwendung", 01.03.1999
23.42.0

IFF-99-04-014
Ehrhart P.; Lüth H.1; Mantl S.1
1 Institut für Schicht- und Ionentechnik
Physik moderner Halbleiterbauelemente
RWTH Vorlesung SS 99
23.42.0

IFF-99-04-015
Eisebitt S.
Zirkulardichroismus in der Rumpfabsorption
IFF-Ferienschule 1999
09.03.1999

IFF-99-04-016
Eisenriegler E.
Kritisches Verhalten begrenzter Systeme
SS 99, Universität Düsseldorf, V 2

IFF-99-04-017
Grimm H.
Kristallspektrometer: das Dreiachsen- und das Rückstreuspektrometer
SS 99, Neutronenphysikalisches Praktikum, Sept. '99
23.30.0

IFF-99-04-018
Grünberg P.
Zwischenschichtaustauschkopplung: Phänomenologische Beschreibung, Materialabhängigkeit
IFF Ferienschule 1999
03.03.1999
3.42.0

IFF-99-04-019
Lustfeld H.
Wavelets in der Physik mit Beispielen in C++
WS 99/00, Universität Duisburg, V 2, Ü 1

IFF-99-04-020
Monkenbusch M.
Flugzeitspektrometer
SS 99, Neutronenphysikalisches Praktikum, Sept. '99
23.30.0

IFF-99-04-021
Monkenbusch M.
Flugzeitspektrometer und Neutronenspinechospektrometer, NSE
SS 99, Neutronenphysikalisches Praktikum, Sept. '99
23.89.1

IFF-99-04-022
Müller-Krumbhaar H.
Computeranwendungen in der Festkörperphysik
Seminar RWTH Aachen, SS 1999
23.15.0

IFF-99-04-023
Müller-Krumbhaar H.
Praktisches Rechnen für Naturwissenschaftler
RWTH Aachen, WS 98/99
23.15.0

IFF-99-04-024
Prager M.
Translations- und Rotationsdynamik

List of references

Baumgarten L.	IFF-99-04-001		
Bechthold P.S.	IFF-99-04-002		
Blügel S.	IFF-99-04-003		
Brückel, Th.	IFF-99-04-004	IFF-99-04-005	IFF-99-04-006
	IFF-99-04-007		
Bürgler D.	IFF-99-04-012		
Capellmann, H.	IFF-99-04-006		
Carbone C.	IFF-99-04-008		
Dederichs P.H.	IFF-99-04-009	IFF-99-04-010	IFF-99-04-011
Eberhardt W.	IFF-99-04-005	IFF-99-04-012	
Ebert Ph.	IFF-99-04-044	IFF-99-04-045	
Ehrhart P.	IFF-99-04-013	IFF-99-04-014	IFF-99-04-047
Eisebitt S.	IFF-99-04-015		
Eisenriegler E.	IFF-99-04-016		
Grimm H.	IFF-99-04-017		
Grünberg P.	IFF-99-04-012	IFF-99-04-018	
Hoffmann S.	IFF-99-04-047		
Klein N.	IFF-99-04-044	IFF-99-04-045	
Kohlstedt H.H.	IFF-99-04-047		
Lustfeld H.	IFF-99-04-019		
Luysberg M.	IFF-99-04-044	IFF-99-04-045	
Monkenbusch M.	IFF-99-04-020	IFF-99-04-021	
Müller-Krumbhaar H.	IFF-99-04-022	IFF-99-04-023	
Prager M.	IFF-99-04-024		
Richter D.	IFF-99-04-025	IFF-99-04-026	IFF-99-04-027
	IFF-99-04-028	IFF-99-04-029	IFF-99-04-030
Schober T.	IFF-99-04-031		
Schroeder H.	IFF-99-04-032	IFF-99-04-033	IFF-99-04-034
	IFF-99-04-047		
Schroeder K.	IFF-99-04-035	IFF-99-04-036	
Schwahn D.	IFF-99-04-037	IFF-99-04-038	
Schweika, W.	IFF-99-04-006	IFF-99-04-007	IFF-99-04-039
Schütz, G.	IFF-99-04-040	IFF-99-04-041	
Sturm K.	IFF-99-04-042	IFF-99-04-043	
Thust A.	IFF-99-04-045		
Urban K.	IFF-99-04-044	IFF-99-04-045	
Waser R.	IFF-99-04-046	IFF-99-04-047	
Zeiske, Th.	IFF-99-04-006	IFF-99-04-007	

List of references

Bechthold P.S.	IFF-99-05-002
Blügel S.	IFF-99-05-001
Eberhardt W.	IFF-99-05-002
Neeb M.	IFF-99-05-002
Pontius N.	IFF-99-05-002
Wirth I.	IFF-99-05-003

Internal reports

IFF-99-05-001
Blügel S.
Theorie der magnetischen Anisotropie und Magnetostriktion
In: Magnetische Schichtstrukturen in Forschung und Anwendung, Jülich: 30. Ferienkurs des Instituts für Festkörperforschung 1999
23.20.0

IFF-99-05-002
Pontius N.; Bechthold P.S.; Neeb M.; Eberhardt W.
Infinity - Der Pumplaser der Wahl für nachverstärkende fs-Systeme
Laserline, Coherent (Deutschland) GmbH, 01/1999
23.20.0

IFF-99-05-003
Wirth I.
Jül-3619
Rastertunnelmikroskopie und Rastertunnelspektroskopie an einwandigen Kohlenstoff-Nanoröhren
23.20.0

Seminar Theorie/Neutronenstreuung: Aspekte des Glasübergangs, IFF, Jülich am 08.06.99
23.15.0

Internal seminars

IFF-99-06-001
Brückel Th.
Elastische Streuung an Vielteilchensystemen
Institut für Festkörperforschung, Neutronenpraktikum 1999, 29.09.1999
23.89.1

IFF-99-06-002
Brückel Th.
Komplementarität von Neutronen- und Synchrotron-Röntgenstreuung in der Festkörperforschung
Auditorium der Zentralbibliothek, IFF-Kolloquium, 15.01.1999
23.89.1

IFF-99-06-003
Brückel Th.
Magnetische Streuung und Polarisationsanalyse
Institut für Festkörperforschung, Neutronenpraktikum 1999, 29.09.1999
23.89.1

IFF-99-06-004
Brückel Th.
Streumethoden zur Untersuchung von Dünnschichtsystemen- Teil I und Teil II
Auditorium der Zentralbibliothek, IFF-Ferienschule "Magnetische Schichtsysteme", 05.03.1999
23.89.1

IFF-99-06-005
Brückel Th.
Streuung unter streifendem Einfall
Institut für Festkörperforschung, Neutronenpraktikum 1999, 30.09.1999
23.89.1

IFF-99-06-006
Conrad H.
Neutronenquellen - Von Radium-Beryllium zur Spallationsneutronenquelle -
Institut für Festkörperforschung, Neutronenpraktikum 1999, 29.09.1999
23.89.1

IFF-99-06-007
Haubold H.-G.
In situ Untersuchungen von Oberflächenreaktionen auf Elektrokatalysatoren
Institut für Festkörperforschung, Seminar, 25.01.1999
23.89.1

IFF-99-06-008
Hauck J.; Mika K.
Die Muster des W. Ostwald und die Adsorbatstrukturen
10. Wolfgang-Ostwald-Kolloquium der Kolloid-Gesellschaft: Adsorption an Nanopartikeln, FZ Jülich, 02.12.1999
23.15.0

IFF-99-06-009
Hupfeld D.
Untersuchung magnetischer Ordnungsphänomene in GdxEu1-xS mit resonanter Röntgenbeugung
IFF-Hörsaal, Informationstagung aus Anlaß der 14. Sitzung des Wissenschaftlichen Beirats des IFF, 22.04.1999
23.89.1

IFF-99-06-010
Kahle S.
Dielectric Spectroscopy at Dynamic Glass Transition
Theoretikerseminar 'Kehr' in Jülich am 11.05.99
23.15.0

IFF-99-06-011
Kahle S.
Vergleich zwischen inkohärenter Neutronenstreuung und dielektrischer Spektroskopie am Polyvinylacetat
Joint Soft Matter Seminar in Jülich am 16.12.99
23.30.0

IFF-99-06-012
Kluge M.
Theorien zum Glasübergang
Seminar "Aspekte des Glasübergangs", IFF, FZ Jülich, 27.04.1999
23.30.0

IFF-99-06-013
Plakhty V.
Spin Chirality and Polarised Neutrons
Institut für Festkörperforschung, 10.11.1999
23.89.1

IFF-99-06-014
Schober H.
Computersimulation
Seminar zum Glasübergang, IFF, FZ Jülich, 15.06.1999
23.30.0

IFF-99-06-015
Schroeder H.
Leckstromeigenschaften elektrokeramischer Dünnschichten
Seminar des Instituts für Werkstoffe der Elektrotechnik der RWTH Aachen, 27.10.1999
23.42.0

IFF-99-06-016
Schweika W.
Schichtpräparation mit Sputterverfahren
Auditorium der Zentralbibliothek, IFF-Ferienschule "Magnetische Schichtsysteme", 01.03.1999
23.89.1

IFF-99-06-017
Waser R.
Chancen und Perspektiven elektrokeramischer Materialien in der Informations- und Sensortechnik
IFF-Kolloquium, 05.02.1999

IFF-99-06-018
Zeiske Th.
Magnetismus und magnetische Neutronenstreuung
Institut für Festkörperforschung, Neutronenpraktikum 1999, 01.10.1999
23.89.1

IFF-99-06-019
Zeller R.
Bandmagnetismus
30. Ferienkurs des IFF: "Magnetische Schichtsysteme", FZ Jülich, 02.03.1999
23.20.0

IFF-99-06-020
Zorn R.
Magnetometrie
30. Ferienkurs des IFF, Jülich am 01.03.99
23.15.0

IFF-99-06-021
Zorn R.
Neutron Scattering Experiments on a Confined Glass-Forming Liquid
Mitarbeiterseminar Neutronenstreuung, IFF, Jülich am 27.05.99
23.15.0

IFF-99-06-022
Zorn R.
Non-Gaussianity in Simulations, Neutron Scattering, and Theoretical Models

List of references

Brückel Th.	IFF-99-06-001 IFF-99-06-002 IFF-99-06-003 IFF-99-06-004 IFF-99-06-005
Conrad H.	IFF-99-06-006
Haubold H.-G.	IFF-99-06-007
Hauck J.	IFF-99-06-008
Hupfeld D.	IFF-99-06-009
Kahle S.	IFF-99-06-010 IFF-99-06-011
Kluge M.	IFF-99-06-012
Mika K.	IFF-99-06-008
Plakhty V.	IFF-99-06-013
Schober H.	IFF-99-06-014
Schroeder H.	IFF-99-06-015
Schweika W.	IFF-99-06-016
Waser R.	IFF-99-06-017
Zeiske Th.	IFF-99-06-018
Zeller R.	IFF-99-06-019
Zorn R.	IFF-99-06-020 IFF-99-06-021 IFF-99-06-022

Institute for Solid State Research (IFF)

Research Center Jülich GmbH

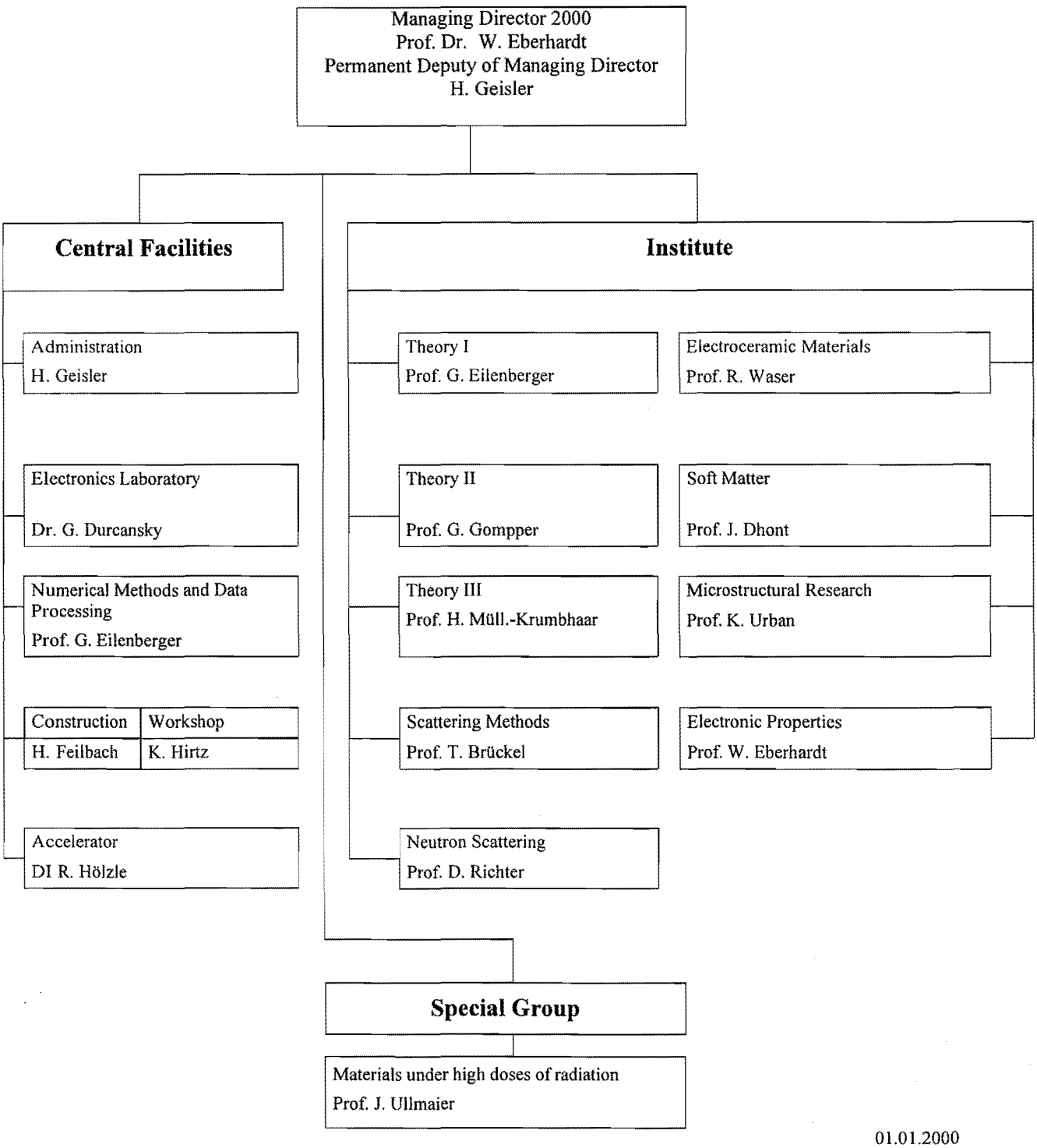

01.01.2000

Scientific Advisory Board 2000

The 2000 meeting of the Scientific Advisory Board will take place on the 13th/14th April. Currently, the board consists of the following members:

Dr. C. **Carlile**, ISIS Rutherford Laboratory, UK

Prof. R. **Dronskowski**, RWTH Aachen

Prof. H. **Eschrig**, IFW Dresden, **Vice chairman**

Prof. W.M. **Finnis**, Queen's University of Belfast, UK

Prof. U. **Gösele**, MPI Halle/Saale

Prof. S. **Hess**, TU Berlin

Dr. J. **Joosten**, DSM Research, Geleen, NL

Prof. H. **Lüth**, Forschungszentrum Jülich, ISI

Prof. H. **Micklitz**, Universität zu Köln

Prof. W. **Press**, Universität Kiel

Dr. J. **Rieger**, BASF, Ludwigshafen

Prof. J. **Schnakenberg**, RWTH Aachen, **Chairman**

Prof. L. **Singheiser**, Forschungszentrum Jülich, IWV2

Prof. U.W. **Suter**, ETH Zürich, Switzerland

Dr. H. **Thomann**, Siemens AG München

Prof. E. **Umbach**, Universität Würzburg

Prof. P. **Wyder**, Centre National de la Recherche Scientifique (MPI), Grenoble, France

Personnel 1999/2000

Staff members (centrally financial)	
- **Scientific Staff**	**86**
including those funded externally	16
- **Technical Staff**	**41**
including those funded externally	5
Post-doc (HGF)	**9**
Staff members of service-groups	**39**
Administrations incl. Secretaries	**18**
Graduate students	**52**
including those funded externally	14
Diploma students	**17**
Trainees	**22**
Guests Scientists staying for two weeks or longer	**74**
Invited lectures	**113**

IFF-Scientists Teaching at Universities

Lecturer:	University:
Dr. A. Baumgärtner	Duisburg
Dr. P.S. Bechthold	Köln
Dr. S. Blügel	Aachen
Prof. Th. Brückel	Aachen
Prof. U. Buchenau	Düsseldorf
Prof. P. Dederichs	Aachen
Prof. W. Eberhardt	Köln
Dr. P. Ehrhart	Aachen
Prof. G. Eilenberger	Köln
Prof. E. Eisenriegler	Düsseldorf
Prof. P. Grünberg	Köln
Prof. K. Kehr	Köln
Dr. N. Klein	Aachen
Dr. H. Lustfeld	Duisburg
Prof. H. Müller-Krumbhaar	Aachen
Prof. D. Richter	Münster
Prof. T. Schober	Aachen
Dr. H. Schroeder	Aachen
Prof. K. Schroeder	Aachen
Dr. G. Schütz	Bonn
Dr. W. Schweika	Aachen
Prof. K. Sturm	Düsseldorf
Prof. H. Ullmaier	Aachen
Prof. K. Urban	Aachen
Prof. R. Waser	Aachen
Prof. H. Wenzl	Aachen
Dr. R. Zorn	Münster

IFF Scientists on leave 1999

Dr. I. Cabria Alvaro	University Munich, Germany
Dr. W. Caliebe	HASYLAB at DESY, Hamburg, Germany
Dr. G. Goerigk	HASYLAB at DESY, Hamburg, Germany
Dr. D. Hupfeld	APS Argonne, USA
Dr. R. Lässer	Forschungszentrum Karlsruhe, Germany
Dr. M. Ohl	ILL Grenoble, France
Dr. W. Schmidt	ILL Grenoble, France
Dr. A. Scholl	Lawrence Berkeley Laboratory, USA
Dr. G. Schütz	University Essen, Germany
Dr. O. Seeck	HASYLAB at DESY, Hamburg, Germany
Dr. J. Stellbrink	University of Edinburgh, UK

List of IFF-Scientists

(G: Guests; GS: Graduate students)

Abbas, B.	(Neutron Scattering, GS)
Alaga-Bogdanovic, M.	(Theory III,GS)
Alefeld, B.	(Scattering Methods)
Allgaier, J.	(Neutron Scattering)
Ambaye, H.	(Theory II, GS)
Antons, A.	(Theory III, GS)
Arbe, A.	(Neutron Scattering, G)
Arons, R.R.	(Electroceramic Materials)
Babik, W.	(Scattering Methods, GS)
Baldus, O.	(Electroceramic Materials, GS)
Baumgarten, L.	(Electronic Properties)
Baumgärtner, ,A.	(Theory II)
Bechthold, P.S.	(Electronic Properties)
Bellini, V.	(Theory III, GS)
Bene, J.	(Theory I, G)
Berger, R.	(Theory III, GS)
Biermann, S.	(Theory I, GS)
Bihlmayer, G.	(Electronic Properties)
Blügel, S.	(Electronic Properties)
Bohn, H.G.	(Electroceramic Materials)
Borbely, S.	(Neutron Scatteirng, G)
Botti, A.	(Neutron Scattering, GS)
Brener, E.	(Theory III)
Bringer, A.	(Theory I)
Brückel, Th.	(Scattering Methods)
Buchenau, U.	(Neutron Scattering)
Burkhardt, T.	(Theory II, G)
Bürgler, D.	(Electronic Properties)
Byloss, C.	(Scattering Methods, G)
Caliebe, W.	(Scattering Methods)
Carbone, C.	(Electronic Properties)
Chen, J.	(Microstructure Research, G)
Chen, J.	(Special Group)
Chirotov, V.	(Microstructure Research, GS)
Clarke, S.	(Electronic Properties)
Colmenero, J.	(Neutron Scattering, G)
Conrad, H.	(Scattering Methods)
Cramm, S.	(Electronic Properties)

Dallmeyer, A.	(Electronic Properties; GS)
Dederichs, P.H.	(Theory III)
Dhont, J.	(Soft Matter)
Divin, Y.	(Microstructure Research)
Dürr, H.	(Electronic Properties)
Eberhardt, W.	(Electronic Properties)
Ebert, Ph.	(Microstructure Research)
Ehrhart, P.	(Electroceramic Materials)
Eilenberger, G.	(Theory I)
Eisebitt, S.	(Electronic Properties)
Eisenriegler, E.	(Theory I)
Endo, H.	(Neutron Scattering, GS)
Evers, W.	(Microstructure Research)
Faley, M.	(Microstructure Research)
Fetters, L.-J.	(Neutron Scattering, G)
Feuerbacher, M.	(Microstructure Research)
Fitsilis, F.	(Electroceramic Materials, GS)
Ganster, R.	(Electroceramic Materials)
Goerigk, G.	(Scattering Methods)
Goldstein, R.	(Scattering Methods, GS)
Gompper, G.	(Theory II)
Graf, K.-H.	(Microstructure Research)
Grimm, H.	(Neutron Scattering)
Grünberg, P.	(Electronic Properties)
Grushko, B.	(Microstructure Research)
Gutheim, F.	(Theory III, GS)
Harris, J.	(Theory I)
Hartmann, M.	(Theory III, GS)
Haubold, H.-G.	(Scattering Methods)
Hauck, J.	(Soft Matter)
He, Zhi.Y.	(Special Group, GS)
Heinrich, M.	(Neutron Scattering)
Hoffmann, S.	(Electroceramic Materials)
Hoffmann, S.	(Neutron Scattering, GS)
Höhler, H.	(Theory III, GS)
Hupfeld, D.	(Scattering Methods)
Istomin, K.	(Scattering Methods, GS)
Jahnen, B.	(Microstructure Research, GS)
Jia, C.L.	(Microstructure Research)
Jones, R.O.	(Theory I)
Jung, P.	(Special Group)

Kahle, St.	(Neutron Scattering)
Kann, G.	(Electronic Properties, GS)
Karl, A.	(Electronic Properties, GS)
Kaya, H.	(Neutron Scattering, GS)
Kehr, K.	(Theory II)
Kentzinger, E.	(Scattering Methods)
Kessler, B.	(Electronic Properties)
Kesternich, W.	(Special Group)
Kienle, D.	(Theory III, GS)
Kirstein, O.	(Neutron Scattering)
Klingeler, R.	(Electronic Properties, GS)
Kluge, F.	(Microstructure Research, GS)
Kluge, M.	(Theory III, GS)
Köbler, U.	(Scattering Methods)
Kohlstedt, H.H.	(Electroceramic Materials)
Koizumi, S.	(Neutron Scatteirng, G)
Koza, Z.	(Theory II, G)
Krasser, W.	(Electroceramic Materials)
Kreitschmann, M.	(Neutron Scattering)
Krenzlin, M.	(Theory II, GS)
Kromen, Wi.	(Theory III, GS)
Kuanr, B.	(Electronic Properties, G)
Kurz, P.	(Electronic Properties, GS)
Lei, Ch.	(Microstructure Research, GS)
Lentzen, M.	(Microstructure Research, GS)
Leube, W.	(Neutron Scattering)
Lichtenstein, A.	(Theory I, G)
Liebsch, A.	(Theory I)
Lin, J.-H.	(Theory II, GS)
Link, S.	(Electronic Properties, GS)
Liu, C.	(Special Group, G)
Lustfeld, H.	(Theory I)
Lüttgens, G.	(Electronic Properties, GS)
Luysberg, M.	(Microstructure Research)
Maaßen, R.	Theory I, GS)
Maiti, K.	(Electronic Properties, G)
Malagoli, M.	(Electronic Properties, GS)
Marton, K.	(Neutron Scattering, G)
Merkes, R.	(Special Group, GS)
Meuffels, P.	(Electroceramic Materials)
Mihailescu, M.	(Neutron Scattering, GS)

Monkenbusch, M.	(Neutron Scattering)
Montes, H.	(Neutron Scattering, G)
Morenzin, J.	(Electronic Properties)
Mueller, R.	(Scattering Methods)
Murthy, K.P.N.	(Theory II, G)
Müller-Krumbhaar, H.	(Theory III)
Mussawisade, K.	(Theory II, GS)
Neeb, M.	(Electronic Properties)
Nerger, S.	(Scattering Methods, GS) (since 01.06.1999)
Nie, X.	(Electronic Properties, G)
Noack, M.	(Materials Development)
Nonas, B.	(Theory III, GS)
Olligs, D.	(Electronic Properties, GS)
Ohly, Ch.	(Electroceramic Materials)
Olmstead, M.	(Electronic Properties, G)
Otterstedt, R.	(Electroceramic Materials)
Persson, B.N.J.	(Theory I)
Pigorsch, C.	(Theory II, G)
Pithan, Ch.	(Electroceramic Materials)
Plakthy, V.	(Scattering Methods, GS) (since 03.11.1999)
Pontius, N.	(Electronic Properties, GS)
Poppe, A.	(Neutron Scattering, GS)
Poppe, U.	(Microstructure Research)
Prager, M.	(Neutron Scattering)
Pyckhout-Hintzen, W.	(Neutron Scattering)
Regnery, St.	(Electroceramic Materials)
Reif, Th.	(Scattering Methods)
Richter, D.	(Neutron Scattering)
Rickes, J.	(Electroceramic Materials, GS)
Ritter, S.	(Electroceramic Materials)
Rosenfeld, R.	(Microstructure Research, GS)
Rottländer, P.	(Electronic Properties, GS)
Rücker, U.	(Scattering Methods)
Ryazonov, A.	(Special Group, G)
Rzehak, R.	(Theory III, GS)
Schäfer, P.	(Electroceramic Materials, GS)
Schall, P.	(Microstructure Research, GS)
Scherer, R.	(Electronic Properties, GS)
Schilling, T.	(Theory II, GS)
Schirmer, A.	(Scattering Methods)
Schliefer, F.	(Special Group, GS)

Schmidt, W.	(Neutron Scattering)
Schmitz, R.	(Electroceramic Materials, GS)
Schmitz, S.	(Electroceramic Materials, GS)
Schneider, St.	(Electroceramic Materials, GS)
Schober, H.	(Theory III)
Schober, T.	(Electroceramic Materials)
Schroeder, H.	(Electroceramic Materials)
Schroeder, K.	(Theory III)
Schütz, G.	(Theory II)
Schwahn, D.	(Neutron Scattering)
Schweika, W.	(Scattering Methods)
Seeck, O.	(Scattering Methods)
Settels, A.	(Theory III, GS)
Sonnenberg, K.	(Materials Development)
Spatschek, R.	(Theory III, GS)
Stellbrink, J.	(Neutron Scattering)
Stockmeyer, R.	(Neutron Scattering)
Straube, E.	(Neutron Scattering, G)
Sturm, K.	(Theory I)
Szot, K.	(Electroceramic Materials)
Thust, A.	(Microstructure Research)
Trinkaus, H.	(Theory III)
Ullmaier, H.	(Special Group)
Urban, K.	(Microstructure Research)
Vad, Th.	(Scattering Methods)
Voigt, J.	(Scattering Methods, GS)
Volokitin, A.	(Theory I, G)
Wang, Y.-G.	(Scattering Methods, GS)
Waser, R.	(Electroceramic Materials)
Willner, L.	(Neutron Scattering)
Wingbermühle, J.	(Electronic Properties, GS)
Winter, M.	(Microstructure Research, GS)
Wirth, I.	(Electronic Properties, GS)
Wischnewski, A.	(Neutron Scattering)
Yan, S.-S.	(Electronic Properties, G)
Yurechko, M.	(Microstructure Research, GS)
Zeiske, Th.	(Scattering Methods)
Zeller, R.	(Theory III)
Zilkens, C.	(Electronic Properties, GS)
Zorn, R.	(Neutron Scattering)

Guest Scientists

J.A. Abasolo-Hernandez	Instituto Politecnico Nacional, Mexico
Dr. S. Abdullaev	Bilkent University, Ankara, Turkey
Dr. M. Arbe	Universidad Pais Vasco, St. Sebastian, Spain
Prof. T. Asada	Shizouka University, Japan
Prof. P. Ballone	University Messina, Italy
Dr. G. Bihlmayer	University Vienna, Austria
DP A. Baranov	Moscow State University, Russia
Dr. J. Bene	Eötvös University Budapest, Hungary
Fr. Dr. C. Blaas	Technical University Vienna, Austria
Dr. S. Borbely	Hungarian Academy of Sciences, Budapest, Hungary
Prof. O. Braun	Institute of Kiew, Ukraina
Prof. T. Burkhardt	Temple University, Philadelphia, USA
DP C. Byloss	University Ferrara, Italy
Dr. I. Cabria Alvaro	University Santander, Spain
Fr. Dr. T. Cai	Ames Laboratory Iowa State University, USA
Dr. D. Caprion	University Montpellier II, France
Dr. S. Clarke	University of Wales, UK
Prof. J. Colmenero	University of San Sebastian, Spain
Dr. Y. Dai	Paul-Scherrer-Institute, Villigen, Switzerland
A. Dolzmann	University Passau, Germany
Dr. V. Drchal	Czech Academy of Sciences, Prague
Dr. H. Emmerich	University Magdeburg, Germany
Dr. M. Freyss	University Louis Pasteur, Strasbourg,, France
Dr. A. Garcia-Borques	Instituto Politecnico Nacional, Mexico
Dr. R. Gareev	Russian Academy of Sciences, Moskau, GUS
Prof. K. Hirai	University Nara, Japan
Dr. St. C. Hwang	University of California, Santa Barbara, USA
Dr. H. Ishida	University of Tokyo, Japan
Prof. Z. Jiao	University Zhejiang, China
Prof. E. Kats	Landau Institute for Theoretical Physics,Moskau, GUS
Dr. Z. Kaufmann	Eötvös University Budapest, Hungary
S. Koizumi	Japan Atomic Energy Resarch Institute, Tokai, Japan
Dr. Z. Koza	University Wroclaw, Polen
Prof. V.L. Kozub	Ioffe Institute, St. Petersburg, GUS
Prof. B. Kuanr	University of Delhi, Indien
M.Sc. C. Liu	The 4th Institute, Nuclear Power. Institute off China, Chengdu, China
Fr. Dr. C. Lopez	University Cuernavaca, Mexico
Dr. V.A. Luchnikov	Novosibirsk State University, GUS
Dr. W. Ma	Nanjing University, China

Dr. K. Maiti	IISC Bangalore, India
Prof. V. Marchenko	Academy of Sciences, Chernogolovka, Russia
Prof. H. Matsouka	Kyoto University, Japan
Dr. J. Matsui	Fukuoka University, Japan
Dr. P. Mavropoulos	University Athen, Greece
Dr. J.A. Maytorena Cordova	University Cuernavaca, Mexico
Prof. C. Misbah	Universite Joseph Fourier (CNRS), Grenoble, France
Fr. Dr. H. Montes	University Paris, France
Dr. K. Murthy	Indira Gandhi Centre for Atomic Reserarch, Kalpakkam, India
Dr. X. Nie	Massachusetts Inst. of Technology, Cambridge, USA
Fr. Prof. M. Olmstead	University of Washington, Seattle, USA
Dr. N. Papanikolaou	University Athens, Greece
Prof. K. Papathanassopoulos	University Patras, Greece
Dr. S. Perny	Thomson CSF-LCR, ENS Cachan, France
Dr. N. Pertsev	A.F. Ioffe Institute, St. Petersburg, GUS
Pigorsch, C.	Martin-Luther-University Halle-Wittenberg, Germany
Prof. V. Plakhty	St. Petersburg Nuclear Physics Institute, Gatchna, GUS
Dr. V. Popkov	Institute Low Temperature Physics, Kharkov, Ukraine
Prof. V.L. Popov	Russian Academy of Sciences, Tomsk, Russia
J. Santos	Physik-Department TU München, Garching, Germany
Dr. E. Shabalin	Joint Institute for Nuclear Research, Dubna, GUS
A. Smirnov	Joint Institute for Nuclear Research, Dubna, GUS
Prof. N. Stefanou	University Athens, Greece
Prof. E. Straube	University Merseburg, Germany
T. Sturm	University Passau
Dr. D. Temkin	I.P. Bardin Inst. Moskau, GUS
Dr. W. Temmerman	Daresbury Laboratory, Daresbury, GB
Dr. M. Vijayalakshmi	Indira Ghandi Centre, Kalpakham, Indien
Prof. A. Volokitin	Samara University, Samara, Russia
Dr. Y.-G. Wang	Sourtheast University, Nanjing, China
Prof. R. Wang	Department of Physics, Wuhan University, China
Dr. J. Wu	Chinese Academy of Sciences, Beijing, China
Dr. S. Yan	Physics Department, Shandong University, Jinan, China
DP J. Zabloudil	TU Wien, Austria
P. Zahn	University Dresden, Germany

Spring Schools of the IFF

Beginning in 1970, our institute has organized an annual two-week Spring School on modern topics in solid state physics.

The topics of the Spring Schools over the past 11 years were:

1990	Solid State research for Information Technology
1991	Physics of Polymers
1992	Synchrotron Radiation for investigating Condensed Matter
1993	Magnetism of Solids and Boundaries
1994	Complex Systems between Atoms and Solids
1995	Electroceramics – Basics and Applications
1996	Scattering Methods for investigating Condensed Matter
1997	Dynamics and Pattern Formation in Condensed Matter
1998	Physics of Nanostructures
1999	Magnetic Layer Structures
2000	fsec and neV: Dynamics of Condensed Matter

Spring School 2000 on "fs and neV: Dynamics in Condensed Matter"

This event was the 31th spring school offered by the IFF. It took place from 13. – 24. March 2000 and included the latest developments in the fields of spectroscopic investigations of the dynamics in condensed matter.

The following lectures were presented (in chronological order):

Th. Brückel, W. Eberhardt and R. Hölzle	Introduction
K. Sturm	Scattering of photons, neutrons and electrons by matter
M. Monkenbusch	Neutron Spectroscopy
W. Schweika	Sources and Properties of Neutron- and Synchrotron-Radiation
H. Conrad	The European Spallations Neutron Source ESS – Spallation Techniques
K. Schroeder	Elementary Excitations: Phonons, Magnons
P. Dederichs	Fundamentals of Electron Theory
P. Bechthold	Ultrashort Laser Pulses: Generation, handling
M. Neeb	Molecular Dynamics of Chemical Reactions on the femtosecond time scale – "The World's fastest Camera"
S. Blügel	The Quantum Hall Effect
N.M. Pyka	Lattice Dynamics of High T_c Superconductors
J. Tomkinson	Chemical Spectroscopy
Ch. Buchal	Electronic Relaxation in Semiconductors – Ultrafast Switches and Photodetectors
T. Schäpers	Ballistic Transport in Semiconductors
G. Gompper	Dynamics of membranes & complex fluids
D. Richter	Dynamics of Polymers
F. Sette	Inelastic X-Ray Scattering. A Spectroscopy Method to Study the Atomic Dynamics in Condensed Matter
J.R. Schneider	TESLA-FEL
H. Ibach	Surface-Phonons and localized Vibrations of Adsorbates
B. Persson	Sliding Friction
G. Grübel	X-Ray Photon Correlation Spectroscopy
B. Keimer	Magnetic Excitations in Correlated Electron-Systems
M. Enderle	Spin-Chains and Spin-Peierls-Systems
W. Wurth	Core Electron Relaxation
S. Eisebitt	Resonant Inelastic X-Ray Scattering: Measurements with an atomic stopwatch
G. Meier	Raman- and Brillouin-Scattering
P. Heitjans	NMR and beta-NMR
G. Gerber	Wavepacket Dynamics
R. Rüffer	Nuclear inelastic scattering

U. Buchenau	Relaxations in Glasses
G. Eckold	Chemical Reactions – Timeresolved Scattering Experiments
R. Zorn	Ionic Transport in Electrolytes
D. Bürgler	Magnetoelectronics I
P. Grünberg	Magnetoelectronics II
M. Aeschlimann	Electron Relaxation in Metals
H. Dürr	fsec-magnetism
U. Höfer	Time Resolved Spectroscopy of Image Potential States
B. Hillebrands	Dynamics of Magnetisation Processes

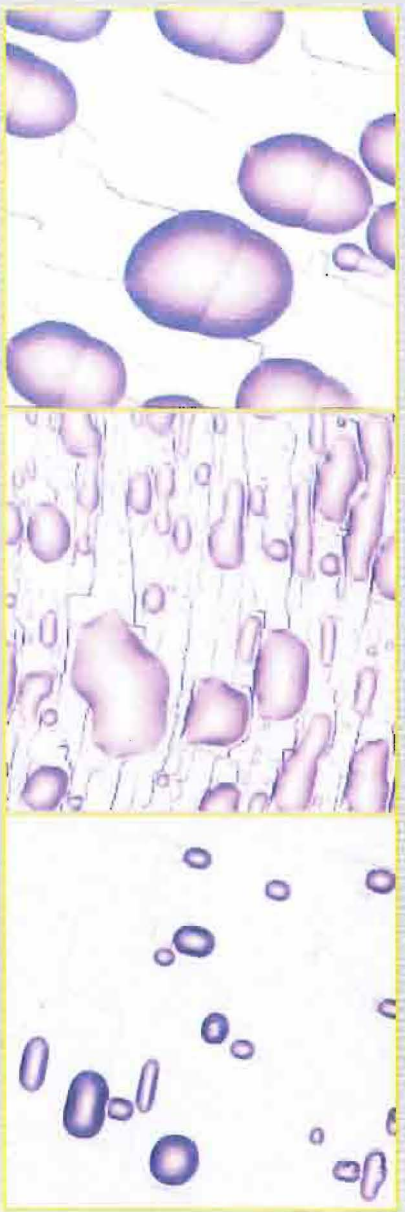

Topography of polished (100)-surfaces of various single crystals of $SrTiO_3$, obtained by AFM after thermal treatment at ambient pressure. All surfaces exhibit the same characteristics changes compared to the original surface prior to heat treatment, namely the formation of the step-like terraces and the appearance of the droplet-like features on top of the surface.

Forschungszentrum Jülich